Modulation of cell-mediated immunity by HIV-1 infection of macrophages

Lucy Caitríona Kiernan Bell

Division of Infection and Immunity

University College London

PhD Supervisor: Dr Mahdad Noursadeghi

A thesis submitted for the degree of

Doctor of Philosophy

University College London

August 2014

Declaration

I, Lucy Caitríona Kiernan Bell, confirm that the work presented in this thesis is my own. Where information has been derived from other sources, I confirm that this has been indicated in the thesis.

Abstract

Cell-mediated immunity (CMI) is central to the host response to intracellular pathogens such as *Mycobacterium tuberculosis* (Mtb). The function of CMI can be modulated by human immunodeficiency virus (HIV)-1 via its pleiotropic effects on the immune response, including modulation of macrophages, which are parasitized by both HIV-1 and Mtb. HIV-1 infection is associated with increased risk of tuberculosis (TB), and so in this thesis I sought to explore the host/pathogen interactions through which HIV-1 dysregulates CMI, and thus changes the natural history of TB.

Using an *in vitro* model of human monocyte-derived macrophages (MDMs), I characterise a phenotype wherein HIV-1 specifically attenuates production of the immunoregulatory cytokine interleukin (IL)-10 in response to Mtb and other innate immune stimuli. I show that this phenotype requires HIV-1 integration and gene expression, and may result from a function of the HIV-1 accessory proteins. I identify that the phosphoinositide 3-kinase (PI3K) pathway specifically regulates IL-10 production in human MDMs, and thus may be a target for HIV-1 to mediate IL-10 attenuation. I show that HIV-1 may attenuate IL-10 to maximise its own replication, and identify potential consequences of IL-10 attenuation for CMI.

By using the tuberculin skin test (TST) as a human challenge model, I evaluate HIV-1 modulation of CMI *in vivo* in active TB patients, and demonstrate IL-10 attenuation in this context. I identify a role for type I inteferons (IFNs) in HIV-1 anergy, and observe exaggerated T helper 2 responses associated with the immune reconstitution inflammatory syndrome (IRIS). To fully explore CMI *in vivo* by transcriptional profiling, I utilize the transcriptional heterogeneity of stimulated macrophages to develop a modular analysis strategy for transcriptional profiles, and apply this in the TST model.

My results delineate novel modulatory effects of HIV-1 on the function of CMI, and thus provide insights into immunopathogenesis in HIV-1/TB co-infection.

Acknowledgements

First and foremost I must acknowledge my supervisor, Dr Maddy Noursadeghi, whose zeal, support and advice has seen me through the challenges of the last four years, from scientific conundrums to experimental catastrophes. His unmitigated enthusiasm for discussing experiments and hypotheses has been invaluable for the research presented herein, and for stimulating my own enthusiasm for scientific endeavour. I must thank both Maddy and my secondary supervisor, Professor Benny Chain, for creating a supportive and stimulating environment in the lab, which has helped me learn how to be a scientist (I hope!). I have immensely enjoyed my time working with them, and have learned so much.

Secondly I have to thank everybody in the lab who has supported me over the course of this work. I must particularly mention Dr Gillian Tomlinson, whose own work formed the basis for much of mine, and whose patience guided me through my first months of lab work. Special thanks also go to Dr Nandi Simpson, Dr Rhia Kundu and Dr Theres Oakes, for saving me from many inept early moments. I must also thank Dr Elspeth Potton, Dr Jennifer Roe, Dr Rachel Byng-Maddick, Dr Gabriele Pollara and Jamie Heather, each of whom has contributed hugely to this work through our collaboration in the lab over the years – along with everyone else in the Noursadeghi and Chain groups, and in the Division of Infection and Immunity at UCL.

I would also like to acknowledge Professor Keertan Dheda and Dr Mellissa Pascoe at the University of Cape Town, Professor Greg Towers and Dr Jane Rasaiyaah at UCL, and Professor Robin May at the University of Birmingham, whose collaboration has been essential for the work I have presented here.

A huge thank you goes to the many blood donors who gave up 120ml of their circulating volume in the name of my experiments, and to all of the patients in London and Cape Town who participated in the TST study – this would not have been possible without their goodwill.

I would not have had the opportunity to do this work without the support of Professor Gordon Stewart and the UCL MB PhD programme. Professor Stewart has been a source of wisdom, guidance and humour, and I can't thank him enough for his support and belief in me. I would also like to thank Professor Ashley Moffatt at the University of

Cambridge, for being the first person to stimulate my interest in immunology, and for introducing me to the notion of mixing clinical medicine and basic science.

Very appreciative thanks go to Elspeth Potton, Ina Schim van der Loeff, Katharine Best and Gabriele Pollara for proof-reading various parts of this thesis in various unkempt forms.

I have to thank all of my friends for their support, which has sustained me throughout the last few years. Very special thanks have to go to Bryony Hopkinshaw and Victoria Sampson, who have been through the ups and downs with me, and who have listened to more scientific work crises than any friends should ever have to. Thanks also go to Becca Burrell, Ina Schim van der Loeff and Chris McKinnon, who have been a constant source of advice, coffee and pep talks during the busy final year of labwork and thesis-writing.

I would like to thank and acknowledge all of my family, who have been a tremendous source of love and support. My cousin Victoria Lennon has been a huge support in London, and has always been on hand with a G&T, a chat and even a spare bedroom in times of need. My grandparents Finella and David Wilson have provided invaluable support to me throughout my education, and many childhood conversations with Papa David, as well as with my uncle and godfather Thomas McErlean, may have helped ignite my enthusiasm for academia at an early age.

Lastly, I would like to thank my sisters Alice and Charlotte, and parents Bronagh and Hugh, whose love and support has been the greatest support and solace of all. Their belief in me has got me to where I am today, and their reassurance has got me through the most difficult times of all – I would like to dedicate this thesis to all of them.

Table of Contents

Table of figures

List of tables

Abbreviations

ABS	AB serum
AIDS	Acquired immunodeficiency syndrome
AIR	Anti-inflammatory response
AM	Alveolar macrophage
APC	Antigen-presenting cell
ART	Anti-retroviral therapy
ARV	Anti-retroviral
BCG	Bacilli Calmette-Guerin
BSA	Bovine serum albumin
BMDM	Bone marrow-derived macrophage
CAEV	Caprine arthritis encephalitis virus
cDC	Classical dendritic cell
cDP	Common dendritic cell precursor
cMoP	Common monocyte precursor
CLR	C-lectin type receptors
CMI	Cell-mediated immunity
CMV	Cytomegalovirus
CNS	Central nervous system
cGAS	Cyclic GMP-AMP synthase
Ct	Cycle threshold
DC	Dendritic cell
dH_2O	Deionised H_2O
DAMP	Danger-associated molecular pattern
DAPI	4',6-diamidino-2-phenylindole

DC	Dendritic cell
DMEM	Dulbecco’s modified eagle medium
DMSO	Dimethyl sulfoxide
DPBS	Dulbecco’s phosphate buffered saline
DTH	Delayed-type hypersensitivity
ECM	Extra-cellular matrix
EDTA	Ethylenediaminetetraacetic acid
ELISA	Enzyme-linked immunosorbant assay
ERK	Extracellular signal-regulated kinase
FACS	Fluorescence-activated cell sorting
FCS	Foetal calf serum
FDR	False detection rate
GALT	Gut-associated lymphoid tissue
GAPDH	Glyceraldehyde 3-phosphate dehydrogenase
GFP	Green fluorescent protein
GMP	Granulocyte-macrophage precursor
GM-CSF	Granulocyte-macrophage colony-stimulating factor
GO	Gene ontology
GSEA	Gene set enrichment analysis
GXM	Glucuronoxylomannan
H&E	Hematoxylin and eosin
HAART	Highly active anti-retroviral therapy
HIV	Human immunodeficiency virus
HRP	Horseradish peroxidase
HSC	Haematopoietic stem cell
HSV	Herpes simplex virus
IFN	Interferon

IGRA	Interferon gamma release assay
IκB	Inhibitor of κB
IL	Interleukin
IN	Integrase
iNOS	Inducible nitric oxide synthase
IRF	Interferon response factor
IRIS	Immune reconstitution inflammatory syndrome
KSHV	Kaposi's sarcoma herpes virus
LB	Lysogeny broth
LPS	Lipopolysaccharide
LTR	Long terminal repeat
MAC	*Mycobacterium avium* complex
MACS	Magnetic-activated cell sorting
MAPK/MAP kinase	Mitogen activated protein kinase
M-CSF	Macrophage colony-stimulating factor
MDM	Monocyte-derived macrophage
MDDC	Monocyte-derived dendritic cell
MDP	Macrophage and dendritic cell precursor
MDR	Multi-drug resistant
MHC	Major histocompatibility class
MMP	Matrix metalloproteinase
MOI	Multiplicity of infection
MP	Mononuclear phagocyte
MPS	Mononuclear phagocyte system
MSMD	Mendelian susceptibility to mycobacterial diseases
Mtb	*Mycobacterium tuberculosis*
$Mtb_{filtrate}$	*Mycobacterium tuberculosis* culture filtrate

mTOR	Mammalian target of rapamycin
NBF	Neutral buffered formalin
Nef	Negative regulatory factor
NES	Normalised enrichment score
NFκB	Nuclear factor κ-light-chain-enhancer of activated B cells
NK cell	Natural killer cell
NLR	NOD-like receptor
NOD	Nucleotide oligomerization domain
PAMP	Pathogen-associated molecular pattern
Pam_2CSK_4 / PCSK	Tripalmitoyl-S-glyceryl-L-Cys-Ser-Lys-Lys-Lys-Lys
PBL	Peripheral blood lymphocyte
PBMC	Peripheral blood mononuclear cell
PBS	Phosphate buffered saline
PC	Principal component
PCA	Principal component analysis
PCP	*Pneumocystis* pneumonia
pDC	Plasmacytoid dendritic cell
PDGF	Platelet-derived growth factor
PHA	Phytohaemagglutinin
PI3K	Phosphoinositide 3-kinase
PIC	Pre-integration complex
PPD	Purified protein derivative
PRR	Pattern recognition receptor
QFT	QuantiFERON-TB Gold
qRT-PCR	Quantitative real-time PCR
Rev	Regulator of Expression of Virion proteins
RLR	RIG-1-like receptors

Rin	RNA integrity
RNS	Reactive nitrogen species
ROS	Reactive oxygen species
rpm	Revolutions per minute
RPMI	Roswell Park Memorial Institute
RT	Reverse transcriptase
SDS	Sodium dodecyl sulfate
SDS-PAGE	Sodium dodecyl sulphate polyacrylamide gel electrophoresis
SEM	Standard error of the mean
SIV	Simian immunodeficiency virus
STAT	Signal transducer and activator of transcription
Tat	Transactivator of transcription
TB	Tuberculosis
TBE	Tris/borate/EDTA
TBS	Tris buffered saline
TF	Transcription factor
TFBS	Transcription factor binding site
TGF	Transforming growth factor
Th	T helper
TMB	3,3',5,5'-Tetramethylbenzidine
TNF	Tumour necrosis factor
TLR	Toll-like receptor
Treg	T regulatory
TST	Tuberculin skin test
UV	Ultra-violet
VLP	Virus-like particle

Vif	Viral infectivity factor
VL	Viral load
VMV	Visna-maedi virus
Vpr	Viral protein R
Vpu	Viral protein unique
Vpx	Viral protein X
WT	Wild-type
YPD	Yeast-peptone-dextrose
2FC	Two-fold change
4FC	Four-fold change

Publication

Part of the work presented in this thesis has been presented in the following publication:

Tomlinson, G.S.*****, **Bell, L.C.K**.*, Walker, N.F., Tsang, J., Brown, J.S., Breen, R., Lipman, M., Katz, D.R., Miller, R.F., Chain, B.M., Elkington, P.T.G., Noursadeghi, M., 2014. HIV-1 Infection of Macrophages Dysregulates Innate Immune Responses to Mycobacterium tuberculosis by Inhibition of Interleukin-10. J. Infect. Dis. 209, 1055–1065. doi:10.1093/infdis/jit621

***** indicates shared first authorship.

Chapter 1. Introduction

1.1 The cell-mediated immune system

1.1.1 Overview: the delayed-type hypersensitivity and cell-mediated immunity paradigm

The delayed-type hypersensitivity (DTH) reaction was first described in 1798 by Edward Jenner in his seminal studies of vaccination against smallpox, when he reported that individuals previously infected with cowpox had an accelerated reaction to injection with variolous matter derived from smallpox lesions (Allison, 1967). These reactions were evident as redness and induration at the injection site over 24–48 hours, and subsequently were found to occur in response to a range of pathogens or their products (Wing and Remington, 1977; Zinsser, 1921). Histological characterisation of the DTH reaction site showed capillary dilatation, endothelial swelling, and a perivascular infiltrate composed chiefly of lymphocytes and histiocytes, suggesting a cellular basis to this response (Allison, 1967).

By the 1960s, key criteria for defining a DTH reaction had been described (Humphrey, 1967). A gradual inflammatory response to a locally introduced antigen was typical, which did not resemble allergic hypersensitivity in terms of its gross or histopathological appearance. It was a distinct phenomenon from antibody-mediated immunity, as transfer of lymphoid cells, but not serum, from sensitized to unsensitised animals could render them hypersensitive (Chase, 1946). Importantly, the reaction was mediated locally by lymphocytes and activated macrophages, and was associated with resistance to pathogens that induced it (Wing and Remington, 1977). These observations led to its re-definition as cell-mediated immunity (CMI), to reflect more appropriately the functional importance of the phenomenon (Humphrey, 1967).

However, in the pre-pattern recognition and pre-lymphocyte subset era, many questions remained regarding what was described as a “complex, ill-defined and sometimes rather tiresome aspect of immunology” (Humphrey, 1967). Which “inherently hypersensitive” cells initiated the DTH reaction – the lymphocytes or the macrophages, or both (Dumonde, 1967)? Did lymphocytes make any antibody in the reaction (Gell, 1967), and did they secrete factors to activate the macrophages (Humphrey, 1967)? And what precisely were its relative contributions to pathology and protection (Humphrey, 1967)?

As a result of investigations in the intervening decades, CMI is now well-characterised at the cellular and molecular levels (**Figure 1.1**). A canonical primary CMI response is known to be initiated by phagocytes such as macrophages, which detect pathogens via pattern recognition receptors (Lemaitre et al., 1996; Medzhitov and Horng, 2009; Medzhitov et al., 1997) and become activated. These macrophages go on to present antigen and secrete cytokines such as interleukin (IL)-12 and IL-18 (Gracie et al., 2003; Hsieh et al., 1993), in order to activate $CD4^+$ T cells, the main lymphocyte effectors of CMI (Cher and Mosmann, 1987). Macrophage-derived IL-12 drives a polarised T-helper 1 (Th1) phenotype in $CD4^+$ T cells (Hsieh et al., 1993; Mosmann et al., 1986), inducing them to secrete interferon (IFN)γ and other cytokines, which then signal to macrophages in return, promoting their effector functions (Celada et al., 1984; Nathan et al., 1983; Pace et al., 1983). Macrophages and $CD4^+$ T cells may also co-ordinate with other effector cells of CMI, such as $CD8^+$ T cells and natural killer (NK) cells, which perform various cytotoxic functions and secrete further IFNγ (Kaufmann, 1995; Moretta et al., 2002). Activation of specific $CD4^+$ T cells via presentation of their cognate antigen leads to establishment of immunological memory for that antigen, the basis of the accelerated CMI response observed upon re-challenge in CMI (Bell et al., 1998). Together, these effector functions are thought to be critical in effective responses to many pathogens, as well as playing roles in the immune response to tumours, in transplant rejection and in chronic inflammatory conditions.

Thus, the clinical phenomenon of the DTH redness reaction first described by Jenner over 200 years ago is now known to result from a complex interplay of cells and secreted factors, which act together to cause inflammation and to co-ordinate a key arm of effective immunity.

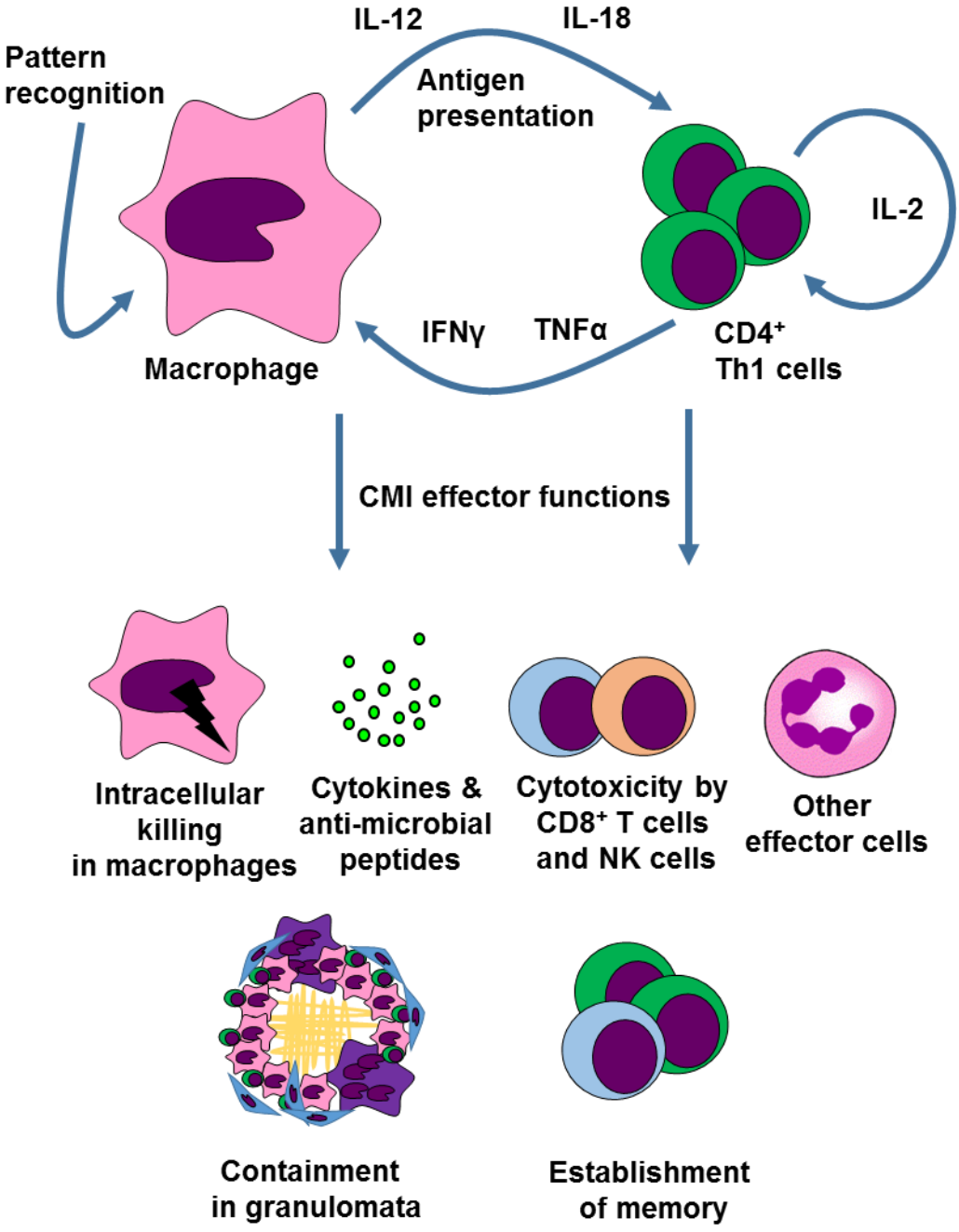

Figure 1.1: The cell-mediated immune response.

1.1.2 CMI and infectious diseases

CMI is central to the immune response to intracellular pathogens (Kaufmann, 1995). Classic experiments showed that transfer of lymphocytes from immunised to unimmunised animals could essentially vaccinate the latter (Lefford et al., 1973), demonstrating that cellular immunity was sufficient for protection against infection in some contexts. During early DTH research, it was noted that pathogens which were facultative intracellular parasites of macrophages, such as *Mycobacterium tuberculosis* (Mtb), *Brucella abortus*, *Listeria monocytogenes* and *Salmonella typhimurium*, were potent inducers of DTH responses (Mackaness, 1967). These pathogens induced a highly activated anti-bacterial phenotype in macrophages, termed “acquired cellular resistance”, which conferred time-limited non-specific protection against other intracellular infections (Mackaness, 1964).

Subsequent characterisation of CMI (**Figure 1.1**) has elucidated the effector functions which confer this potent restrictive ability. For bacterial or fungal pathogens, key responses may be direct macrophage-mediated killing, and anti-microbial peptide secretion (Flannagan et al., 2009; Izadpanah and Gallo, 2005). For viruses, cytotoxic activity and induction of anti-viral type I IFN responses are thought to be critical (Stetson and Medzhitov, 2006). In chronic infections, pathogens may be contained in a granuloma, which is essentially a mature focus of CMI made up of activated macrophages, $CD4^+$ T cells and other effector cells (Ulrichs and Kaufmann, 2006).

Deficiencies in components of the CMI response can lead to uncontrolled infections by intracellular pathogens in mouse models and in humans, and so CMI is suggested to be essential for protection against these pathogens (**Table 1.1**). In humans, CMI is observed to be particularly important in protection against mycobacteria, as a range of genetic deficiencies in CMI components such as IL-12 and IFNγ signalling cause Mendelian susceptibility to mycobacterial diseases (MSMD), in which patients present with severe infections caused by both weakly virulent mycobacteria and virulent mycobacteria such as Mtb (Al-Muhsen and Casanova, 2008).

The importance of CMI in the immune response to Mtb is also highlighted by the increased risk of tuberculosis (TB) in HIV-1^+ patients, who for a number of reasons may have compromised CMI responses. Both Mtb and HIV-1 are pathogens which directly parasitize macrophages, a central cellular effector of CMI. The interaction between macrophages, HIV-1, Mtb and the other immune mediators of CMI therefore

represents a complex set of host/pathogen interactions, which is likely to play a significant role in the diseases caused by these two critical global pathogens.

In the introduction to this thesis, I will explore this set of host-pathogen interactions, by introducing the role of macrophages in CMI, exploring HIV-1 and TB pathogenesis, and then examining the potential role of macrophages in CMI dysregulation in HIV-1/TB co-infection. I will also describe the function of the immunoregulatory cytokine IL-10, which has been shown to be dysregulated in the responses of HIV-1-infected macrophages to TB (Tomlinson et al., 2014). I will lastly discuss the use of transcriptional profiling for exploring immune responses to tuberculosis *in vivo*, and novel methods which could be utilized in this context to further understand the function of CMI in the host response to Mtb.

CMI component	Mouse	Reference	Human	Reference
IFNγ	IFNγ or IFNγ receptor −/−: increased suscepibility to Mtb, BCG and *Salmonella typhimurium*	Dalton *et al.* (1993); Hess *et al.* (1996); Flynn *et al.* (1993); Cooper *et al.* (1993)	Autoantibodies to IFNγ associated with increased risk of mycobacterial disease	Browne *et al.* (2012)
			IFNγ receptor genetic deficiency in children with disseminated mycobacterial infections	Jouanguy *et al. (* 1995); Newport *et al. (* 1995); Dorman & Holland (1998)
TNFα	TNFR p55−/−: increased suscepibility to *Listeria monocytogenes*	Pfeffer *et al.* (1993)	Patients treated with monoclonal antibodies to TNFα for auto-inflammatory conditions have increased risk of tuberculosis	Keane *et al.* (2001)
IL-12	IL-12 −/−: increased susceptibility to BCG	Wakeham *et al.* (1998)	IL-12 receptor genetic deficiency in patients with mycobacterial infections	Altare *et al.* (1998)
			IL-12 p40 deficiency in a child with disseminated BCG and *Salmonella* infection	Altare *et al.* (1998)
STAT1 (IFNγ signalling)	STAT1 −/−: increased susceptibility to *L. monocytogenes* and vesicular stomatitis virus	Meraz *et al.* (1996)	Heterozygous STAT1 mutation associated with mycobacterial disease	Dupuis *et al.* (2001)
$CD4^+$ T cells	Mice depleted of CD4+ T cells succumb more rapidly to Mtb infection	Leveton *et al.* (1989)	CD4+ T cell depletion in HIV-1 infection associated with increased risk of mycobacterial disease, cryptococcosis, herpesvirus infections	Moore *et al.* (1996)
T-bet (Th1 signature transcription factor)	T-bet −/−: increased susceptibility to Mtb and *S. typhimurium*	Sullivan *et al.* (2005); Ravindran *et al.* (2005)		

Table 1.1: Deficiencies in components of CMI and risk of intracellular infections in mouse models and human disease.

1.2 The role of macrophages in CMI

1.2.1 The mononuclear phagocyte system

CMI responses are mediated via the co-ordinated function of $CD4^+$ T cells and macrophages (**Figure 1.1**). Macrophages are a member of the mononuclear phagocyte system (MPS), which also includes monocytes and dendritic cells. To explore the functions of macrophages in mediating CMI, it is critical to understand their relationships with the other MPS cell types, as a group of phagocytic sentinel cells with diverse roles in homeostasis, inflammation and immunity (Chow et al., 2011a)

The first description of phagocytic cells was made by Elie Metchnikoff in 1892, and his work subsequently provided many insights into their functions: that phagocytosis is an active defence mechanism; that phagocytes could provide "natural immunity" via their responses to pathogens; that phagocytes could actively move towards inflammatory foci; and that phagocyte activation could enhance their microbicidal capabilities (Gordon, 2008). Subsequent work demonstrated shared characteristics of different tissue-resident phagocyte populations, leading to their common classification as macrophages (Guilliams et al., 2014), and also showed that peripheral blood monocytes could differentiate into macrophages *in vitro* and *in vivo* (Carrel and Ebeling, 1926; Ebert and Florey, 1939; van Furth and Cohn, 1968). Monocytes and macrophages were thus classified together as the MPS (van Furth et al., 1972), along with dendritic cells (DCs) once identified (Steinman and Witmer, 1978; Steinman et al., 1974).

This original classification of the MPS was based on distinct functional characteristics of monocytes, macrophages or DCs, wherein monocytes were circulating precursor cells; macrophages were large vacuolar cells specialised for phagocytosis and clearance; and DCs were stellate cells optimised for activating T cells (Guilliams et al., 2014)**.** As such, this MPS classification was also based on the premise that macrophages and DCs were primarily derived from monocytes, and that recruitment of blood monocytes replenished tissue populations of these cells in the steady state (Ginhoux and Jung, 2014), but the ontogeny of mononuclear phagocytes (MPs) is now no longer considered to be interrelated in this manner.

Mononuclear phagocytes (MPs) are now thought to be derived from three sources (Ginhoux and Jung, 2014). Most tissue macrophages are thought to be self-renewing via proliferation, and to have embryological origins (Ginhoux et al., 2010; Guilliams et al., 2013; Hashimoto et al., 2013; Hoeffel et al., 2012; Schulz et al., 2012; Yona et al., 2013). DCs are derived from a common DC precursor in the bone marrow (the cDP; Naik et al., 2013; Schraml et al., 2013), and monocytes from a distinct common monocyte precursor (the cMoP; Hettinger et al., 2013), although both cells originate from the clonotypic source of all haematopoietic MPs, the macrophage dendritic cell precursor (MDP; Fogg et al., 2006). Cells derived from monocytes are found in tissues under some inflammatory conditions, but do not substantially contribute to tissue populations in homeostasis (Ginhoux and Jung, 2014). A new ontogeny-based classification for the MPS has been proposed in light of these findings, based on these three origins (embryologic, the cDP, or the cMoP; Guilliams et al., 2014). The current consensus on the ontogeny of the MPS is shown in **Figure 1.3**.

The majority of the evidence for MPS ontogeny is derived from mouse models (Guilliams et al., 2014), and so its relevance in humans is unconfirmed. Some evidence exists to support its application. Comparative gene expression analyses have demonstrated substantial homology between murine and human monocyte and DC subsets, indicating that there are cross-species phenotypic similarities in the MPS (Crozat et al., 2010; Ingersoll et al., 2010; Robbins et al., 2008). Some observations also support the concept of macrophage self-renewal in humans. After haematopoietic stem cell (HSC) transplant, recipient macrophages persist longer in the skin than recipient DCs which are rapidly replaced with donor cells (Haniffa et al., 2009); conversely, in a limb transplant, the donor macrophages persisted in the skin and were not replaced with recipient-derived cells (Kanitakis et al., 2011). Additionally, genetic conditions affecting haematopoiesis exist wherein there are deficiencies in monocytes and DCs but tissue macrophage populations are unaffected, suggesting that macrophages do not require mature haematopoiesis for maintenance (Bigley et al., 2011).

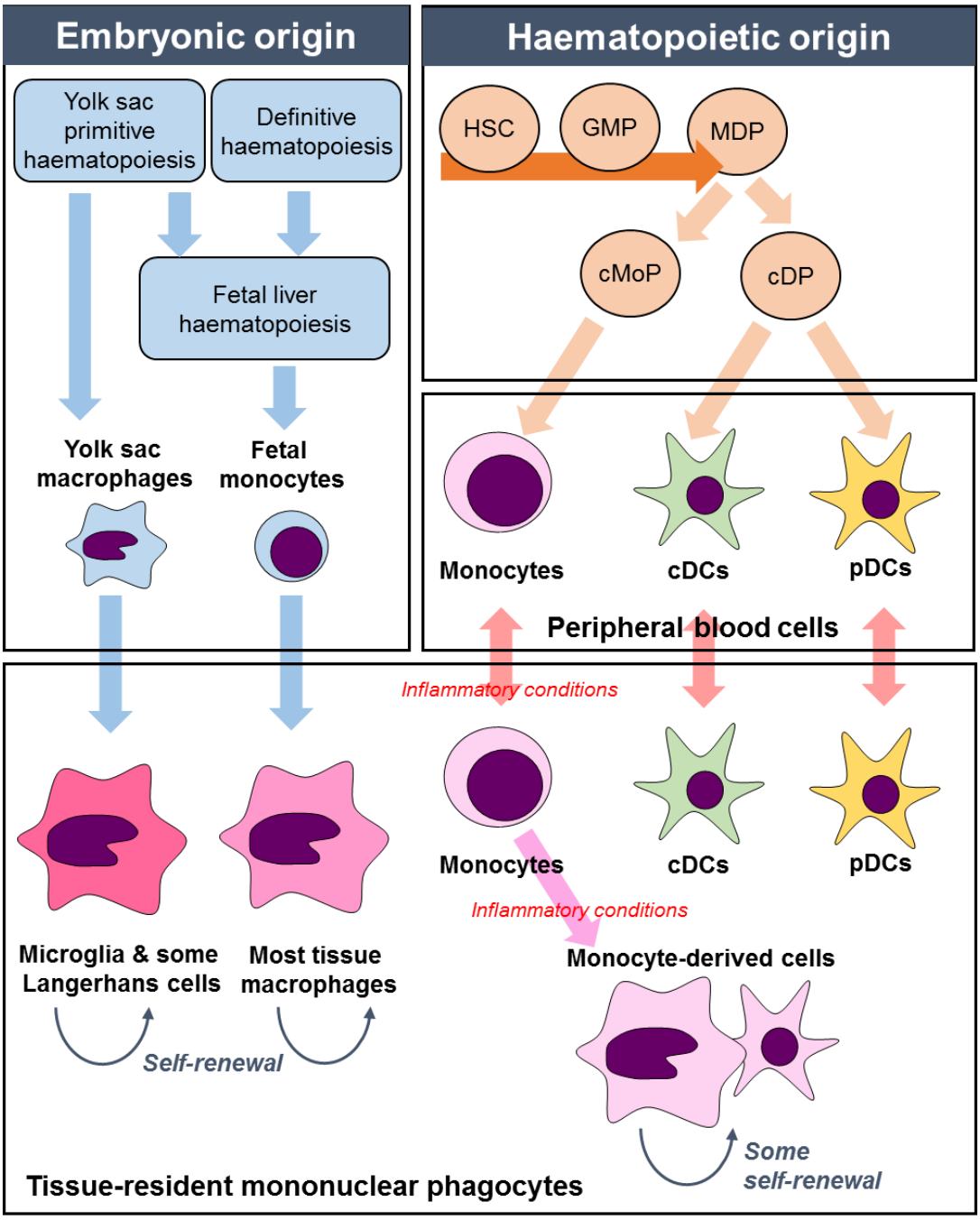

Figure 1.2: Ontogeny of mononuclear phagocytes.

Schematic of the development and ontogeny of the MPS based on current understanding. Adapted from diagrams in Guilliams *et al.* (2014) and Ginhoux and Jung (2014). Tissue macrophage ontogeny is purely embryological, while monocytes and DCs are derived from distinct mature haematopoietic precursor cells. Monocytes can differentiate into cells which infiltrate tissues and display macrophage- or DC-like properties. Macrophages and some monocyte-derived cells are capable of self-renewal. HSC, haematopoietic stem cell; GMP, granulocyte-macrophage precursor; MDP, macrophage and dendritic cell precursor; cMoP; common monocyte precurscor; cDP, common dendritic cell precursor; cDC, classical dendritic cell; pDC, plasmacytoid dendritic cell.

1.2.2 Monocytes and monocyte-derived cells

Monocytes are a short-lived cell population, with an estimated half-life of hours to days, which make up approximately 10% of the peripheral blood mononuclear cell (PBMC) population in humans (Ginhoux and Jung, 2014). Two major circulating subsets of monocytes have been identified in human (Ziegler-Heitbrock et al., 2010) and in mouse (Geissmann et al., 2003). Pro-inflammatory or classical monocytes ($Ly6C^{hi}$ in mouse and $CD14^{hi}$ in human) are rapidly recruited to tissues during inflammation, wherein they differentiate and perform effector functions (Shi and Pamer, 2011). Patrolling or non-classical monocytes ($Ly6C^{low}$ in mouse and $CD14^{low}$ in human) adhere and migrate along endothelial surfaces, from where they may also be recruited into tissues and undergo differentiation (Auffray et al., 2007); these cells have been described as “luminal blood macrophages” (Ginhoux and Jung, 2014). A third intermediate monocyte subset exists in humans, which may have inflammatory functions (Belge et al., 2002). The existence of these specialized subsets demonstrates that monocytes have specific functions beyond differentiation into macrophage and DC-like cells, such as patrolling of blood vessels (Auffray et al., 2007). They may also mediate specific functions in the tissues without further differentiating, such as carriage and presentation of antigen, and promoting angiogenesis (Avraham-Davidi et al., 2013; Jakubzick et al., 2013; Leirião et al., 2012)

Monocytes are no longer thought to contribute substantially to tissue macrophage populations in the steady-state (Ginhoux and Jung, 2014). However, after recruitment into tissues in inflammation, they can differentiate into cells with a spectrum of properties characteristic of macrophages and DCs, leading to the designations of monocyte-derived macrophages (MDMs) and monocyte-derived dendritic cells (MDDCs) (Shi and Pamer, 2011). Many *in vitro* evaluations of macrophages and DCs utilize this capacity of monocytes to differentiate, as the factors necessary to induce MDMs and MDDCs from monocytes *in vitro* have been established as macrophage colony stimulating factor (M-CSF; CSF1), or granulocyte-macrophage colony stimulating factor (GM-CSF; CSF2) and IL-4, respectively (Geissmann et al., 2010). Monocyte-derived cells may contribute to tissue MP populations in homeostasis in some tissues, for example in the gut and skin (Bogunovic et al., 2009; Tamoutounour et al., 2013; Varol et al., 2007) wherein inflammatory encounters may be more frequent (Ginhoux and Jung, 2014; Zigmond and Jung, 2013). At inflammatory foci, monocyte-

derived cells are postulated to mediate a range of DC and macrophage functions (Mildner and Jung, 2014; Wynn et al., 2013). It has been shown that MDDCs in murine skin are transcriptionally similar to resident classical DCs, supporting the hypothesis that they become phenotypically similar to resident cells – although this observation was made in steady-state rather than inflammatory conditions (Tamoutounour et al., 2013). The temporal nature of the contributions of MDMs and MDDCs have been investigated, and in some contexts, such as in the central nervous system, their seeding of tissues has been shown to be transient and resolve after inflammation (Ajami et al., 2011). In other contexts, such as MDM infiltration of atherosclerotic lesions, and MDDCs in a murine model of skin herpes simplex virus infection, they have been shown to persist and in some cases to proliferate *in situ* (Eidsmo et al., 2009; Robbins et al., 2008). It is suggested that the severity and nature of inflammation, and how it has affected resident MPs, may determine the persistence of monocyte-derived cells (Ginhoux and Jung, 2014).

Many effector functions of MPs have been elucidated using *in vitro* MDM and MDDC models. It is cognizant to consider how accurately these cells replicate *in vivo* tissue MPs. Early work noted that MDMs generated in whole blood cultures were "indistinguishable from tissue macrophages" (Carrel and Ebeling, 1926), and the morphological similarity of *in vitro* M-CSF-differentiated MDMs and *ex vivo* alveolar macrophages (AMs) has been noted (Tomlinson et al., 2012). Comparative gene expression profiling of M-CSF-differentiated MDMs and AMs showed that they were more similar to each other than to monocytes, DCs or macrophage-like cell lines, but were still transcriptionally distinct (Li et al., 2007; Tomlinson et al., 2012). As AMs are dependent on GM-CSF signalling for their development in addition to M-CSF (Guilliams et al., 2013; Shibata et al., 2001), and are phenotypically more similar to MDMs differentiated used GM-CSF (Akagawa et al., 2006), the described functional distinctions between MDMs and AMs may be predicated on inherent development differences, as opposed to global incongruities between MDMs and tissue macrophages. The substantial heterogeneity of tissue macrophage phenotypes (Davies et al., 2013) suggests it is unlikely that *in vitro* MDMs can precisely model all their highly specialised phenotypes. However, evidence for shared morphological and functional features, as well as a common developmental requirement for M-CSF, suggests MDMs are a reasonable reductionist model to study often inaccessible tissue macrophages *in vitro* (as well as presumably modelling *in vivo* MDMs), with the clear

caveat of any *in vitro* study, that the absence of the tissue microenvironment may influence functional insights.

1.2.3 Dendritic cells

DCs were identified by Steinman in 1972 as the critical accessory cell for initiating adaptive immune responses (Steinman and Witmer, 1978; Steinman et al., 1974). They are now known to be a distinct haematopoietic lineage derived from a dedicated precursor, the cDP (Naik et al., 2007; **Figure 1.3**) under the control of the cytokine Flt3L, with some input from M-CSF and GM-CSF for specific DC subsets (Schmid et al., 2010).

Several DCs subsets exist with specific phenotypes and functions (Satpathy et al., 2012). The original DC phenotype identified by Steinman is now held to be that of a classical DC (cDC), which are highly phagocytic and specialised for processing and presentation of antigen (Satpathy et al., 2012). A defining feature of cDCs is their ability to migrate from the periphery to secondary lymphoid organs wherein they present antigen and activate adaptive immune responses (Randolph et al., 2005), during which process they differentiate from an immature phagocytic phenotype to a mature phenotype specialised for antigen presentation (Pierre et al., 1997). A second subset, plasmacytoid DCs (pDCs), also arise from the cDP in the bone marrow, after which they are phenotypically and functionally divergent from cDCs (Satpathy et al., 2012). They are spherical rather than stellate, are not phagocytic, and do not efficiently present antigen; instead their primary function appears to be the ultra-fast production of type I IFN (Siegal et al., 1999).

Some controversy exists regarding the purpose behind classifying some cells as macrophages and some as DCs based on functional properties (Hume, 2008). The recent proposal that classification should be based on ontogeny may dispel these issues (Guilliams et al., 2014), but a key point is highlighted, which is that the functionality of different MPs clearly overlaps, with consequences for considering their specific roles in a CMI response. For example, although mature cDCs are specialised for antigen presentation, macrophages are also known to present antigen and prime T cells (Hume, 2008). Classical activation of macrophages via inflammatory stimuli may induce cDC-like characteristics, and differentiated inflammatory monocytes may also share similar phenotypic features (Mildner and Jung, 2014; Mosser and Edwards, 2008). Although mature cDCs, classically activated macrophages and mature

inflammatory monocytes do have key differences - such as their ontogeny, and their tendency to migrate (Murray and Wynn, 2011) – this functional convergence of different MPs upon an inflammatory T cell-priming phenotype suggests that they all may contribute to CMI responses. As macrophages are the primary targets for many of the intracellular pathogens which induce CMI responses, it seems likely that they are the critical MP functioning at the site of inflammation in this arm of immunity.

1.2.4 Embryologically-derived tissue macrophages

Macrophages are resident in tissues throughout the body and perform essential protective and homeostatic functions, including clearance of debris, immune surveillance, and co-ordination and resolution of inflammation (Davies et al., 2013). They are relatively long-lived cells with lifespans which may be in the region of months (Murphy et al., 2008). It is now known that the majority of tissue macrophages have embryological origins and are maintained by self-renewal throughout adult life (Ginhoux and Jung, 2014). This has been demonstrated by a range of studies in mouse models (Ginhoux et al., 2010; Guilliams et al., 2013; Hashimoto et al., 2013; Hoeffel et al., 2012; Naito et al., 1997; Schulz et al., 2012; Yona et al., 2013). Although there are some inconsistencies in these reports, the resultant consensus is that all tissue macrophages derive from fetal monocytes generated during early definitive haematopoiesis in the fetal liver, except microglia and some Langerhans cells, which derive from yolk sac macrophages generated during primitive haematopoiesis in the yolk sac (Ginhoux and Jung, 2014). As discussed in **section 1.2.2**, a minority of tissue macrophages are monocyte-derived.

Tissue macrophage development depends on CSFR1 signalling (Wynn et al., 2013). Many tissue macrophage populations are deficient in the M-CSF deficient mouse model (Witmer-Pack et al., 1993), but the phenotype of this mouse is less severe than that of the CSFR1-deficient mouse, which has additional deficiencies in microglia and Langerhans cells (Dai et al., 2002; Wynn et al., 2013) – indicating that a second CSFR1 ligand was involved in macrophage development. This was identified to be IL-34 (Greter et al., 2012; Wang et al., 2012). GM-CSF also contributes to macrophage development, specifically in terminal differentiation of AMs; the GM-CSF-deficient mouse has grossly normal haematopoiesis, but specific defects in lung homeostasis due to disrupted AM development (Dranoff et al., 1994; Guilliams et al., 2013; Shibata et al., 2001; Stanley et al., 1994), and human genetic defects in GM-CSF recapitulate this phenotype (Carey and Trapnell, 2010). Both M-CSF and GM-

CSF regulate macrophage biology post-developmentally; M-CSF, which is present in tissues under homeostasis, may influence macrophage survival and self-renewal, while GM-CSF, which is produced as part of the immune response, may induce inflammatory macrophage phenotypes (Wynn et al., 2013).

Populations of tissue macrophages (**Table 1.3**) display striking phenotypic diversity both between and within tissues, despite shared fetal origins and common growth factor requirements; this may result from differing interactions of populations with their tissue microenvironments (Davies et al., 2013; Hume, 2008; Wynn et al., 2013). Some macrophage functions are developmental or homeostatic, such those of osteoclasts, which co-ordinate bone remodelling, and liver Kupffer cells, which clear cell debris from the blood (Davies et al., 2013). However, many of their functions are those involved in immune responses and inflammation which are most integral to their role in CMI, which are discussed subsequently in **section 1.2.5**.

The diversity of macrophages has led to consideration of what fundamentally determines macrophage function. M-CSF-induced monocyte to MDM differentiation involves substantial changes in gene expression (Dong et al., 2013; Lehtonen et al., 2007; Liu et al., 2008), suggesting that transcriptional adaptations may partly determine macrophage cell state. The transcription factor (TF) PU.1 is a key regulator of myeloid cell fate (Mak et al., 2011), and PU.1 deficient mice have no macrophages from the yolk sac stage (Schulz et al., 2012), indicating that it is necessary for macrophage development. It is found to be associated with active transcriptional enhancers and may initiate nucleosome remodelling, suggesting that it may determine cell identity by instructing transcription (Ghisletti et al., 2010; Heinz et al., 2010). However, the PU.1-deficient mouse has multi-lineage defects in haematopoiesis (Anderson et al., 1998; Scott et al., 1994), and PU.1 expression also contributes to DC identity, so it cannot be considereda classic “lineage-specific” TF for macrophages (Bakri et al., 2005). A recent study confirmed that the substantial heterogeneity of tissue macrophages was evident at the transcriptional level, but also defined a core macrophage transcriptomic signature which distinguished macrophages from DCs (Gautier et al., 2012). This included genes classically involved in macrophage function such as *MR1*, *CD64* and *TLR4,* and up-regulated in monocytes *in vivo* during MDM differentiation. The TF C/EBPα was identified as a potential regulator of these genes, and has been suggested in other studies as an instructor of macrophage identity (Liu et al., 2008). Much remains to be clarified with regards to determinants of macrophage phenotype.

A recently defined tissue macrophage function is proliferation in order to self-renew in homeostasis (Davies et al., 2013). Macrophage proliferation may also occur in inflammation (Jenkins et al., 2011), where it may assist in replenishing tissue macrophage populations after inflammatory depletion (Davies et al., 2011). M-CSF is suggested to drive steady-state self-renewal, whereas proliferation in inflammation may require IL-4 (Jenkins et al., 2013, 2011). It has also been shown that proliferative capacity is controlled as part of an specific *in vivo* macrophage phenotype, which is lost when cells are cultured *ex vivo* (Rosas et al., 2014); highlighting the substantial contribution of the tissue microenvironment to macrophage function. Understanding the mechanisms by which tissue-specific signals control macrophage phenotypes may assist in developing tissue-specific *in vitro* models to study tissue macrophage function (Okabe and Medzhitov, 2014; Rosas et al., 2014).

Tissue	Macrophage type	Functions	References
Lung	Alveolar macrophages	Immune surveillance & homeostatic regulation, such as clearance of surfactant	Carey & Trapnell (2010); Westphalen et al. (2014)
	Interstitial macrophages	Regulation of DCs	Bedorot *et al.* (2009)
Liver	Kupffer cells	Clearance of debris from the blood - microorganisms, cells, RBCs	Bilzer *et al.* (2006)
	Motile liver macrophages	Immune surveillance	Klein *et al.* (2007)
CNS	Microglia	Immune surveillance & neuronal maintenance & remodelling	London *et al.* (2013)
	Perivascular and meningeal macrophages	Immune surveillance	Prinz *et al.* (2011)
Skin	Dermal macrophages	Immune surveillance	Chorro & Geissmann (2010)
	Langerhans cells	Immune surveillance & activation of T cells	Chorro & Geissmann (2010)
Bone	Osteoclasts	Bone resorption	Pollard (2009)
	Bone marrow macrophages	Support erythropoiesis & provide stem cell niche	Nagata (2007); Chow *et al.* (2011)
Gut	Intestinal macrophages	Regulation of gut homeostasis and inflammatory responses	Zigmond & Jung (2013)
Serosal surfaces	Peritoneal macrophages	Immune surveillance & homeostatic regulation	Cailhier *et al.* (2005)
	Pleural macrophages	Immune surveillance	Cailhier *et al.* (2006)
Spleen	Marginal zone macrophages	Immune surveillance	den Han & Kraal (2012)
	Metallophilic macrophages	Immune surveillance	den Han & Kraal (2012)
	Red pulp macrophages	Erythrocyte clearance & iron metabolism	Kohyama *et al.* (2009)
Lymph nodes	Subcapsular sinusoidal macrophages	Processing & presentation of antigen to B cells	Junt *et al.* (2007)
	Medullary macrophages	Induction of immune tolerance	Albacker *et al. (* 2013)
Blood	$CD14^{lo}$ monocytes ("luminal macrophages")	Surveillance & homeostasis of endothelial surfaces	Auffray *et al.* (2007); Ginhoux & Jung (2014)
Inflamed tissues	Monocyte-derived macrophages	Inflammatory & regulatory responses	Murray and Wynn (2013)

Table 1.2: Hetereogeneity and functions of tissue macrophages.

Adapted from Davies *et al.* (2013) and Murray & Wynn (2011). CNS, central nervous system.

1.2.5 Functions of macrophages in CMI

Tissue macrophages and MDMs perform key functions in mediating CMI. These range from initiation of the immune response via pattern recognition, to microbicidal effector functions and resolution of inflammation. Importantly, they also interact with the adaptive immune response (Davies et al., 2013; Murray and Wynn, 2011). The striking plasticity of macrophages is critical for their ability to carry out this array of roles, and both innate activation by microbes and adaptive modulation can contribute to their responsive functional heterogeneity.

1.2.6 Innate immune recognition by macrophages

The pattern recognition hypothesis for pathogen detection by sentinel cells was proposed by Janeway in 1989 and within ten years was proven by the discovery of toll-like receptors (TLRs; Lemaitre et al., 1996; Medzhitov et al., 1997), transmembrane proteins which bind conserved pathogen components designated as pathogen-associated molecular patterns (PAMPs). The function of germline-encoded pattern recognition receptors (PRRs) is now known to fundamentally underlie the initiation of the immune response to microbial infection in invertebrates and vertebrates (Medzhitov, 2009). In macrophages, PRR activation stimulates intracellular signalling cascades, which converge on transcriptional and non-transcriptional outputs manifest as macrophage activation and inflammatory responses (Taylor et al., 2005).

Ten TLRs have been characterised in mammals (Takeda et al., 2003). These are membrane-bound receptors found on the cell surface or in endosomes; the former mainly recognise microorganism membrane components, while the latter recognise pathogen-associated nucleic acid forms (Kawai and Akira, 2010). Many other PRR families are now also recognised. The C-lectin type receptors (CLRs) are also membrane-localised and recognise carbohydrate PAMPS; an archetypal CLR is dectin-1, which is important in fungal and mycobacterial recognition (Reid et al., 2009). Pattern recognition also occurs in the cytoplasm, where it is mediated by nucleotide oligomerization domain (NOD)-like receptors (NLRs; Chen et al., 2009), RIG-1-like receptors (RLRs; Loo and Gale, 2011) and a range of DNA sensors (Paludan and Bowie, 2013). The NLRs are divided into three sub-families: the NODs, the NLRPs (NLR, leucine-rich repeat and pyrin-domain-containing) and the IPAFs (ice protease-

activating factors). The NODs, which recognise bacterial peptidoglycans, mediate classical transcription-activating innate immune signalling, while the NLRPs and IPAFs recognise a range of substrates and form inflammasomes, discussed subsequently (Schroder and Tschopp, 2010). The RLRs are sensors for pathogen-associated RNA motifs, and along with sensors which sense pathogenic DNA, such as IFI16 and cyclic GMP-AMP synthase (cGAS), activate anti-viral responses primarily mediated by type I IFNs (Loo and Gale, 2011; Paludan and Bowie, 2013). In view of the focus on Mtb in this thesis**,** I have summarized the contributions of PRRs from several families to recognition of mycobacteria (**Table 1.3**). This example demonstrates the ability of macrophages, which express most known PRRs, to initiate immune responses to pathogens encountered extracellularly, in endosomes or in the cytoplasm.

Family	PRR	Location	Mycobacterial ligand	References
TLRs	TLR-2 or TLR-1/TLR-2	Cell surface	Phosphatidylmyoinositol mannosides (PIMs); cell wall	Gilleron *et al.* (2003)
			Lipoproteins; membrane and secreted	Ferwerda *et al.* (2005); Jung *et al.* (2006)
			Lipoarabinomannan (LAM); cell wall	Quesniaux *et al.* (2004)
	TLR-4	Cell surface	Lipoproteins; membrane and Heat shock proteins; cytoplasmic	Jung *et al.* (2006) Bulut *et al.* (2005)
	TLR-9	Endosomal	DNA	Kiemer *et al.* (2009)
	TLR-3	Endosomal	RNA	Bai *et al.* (2014)
CLRs	Mannose receptor (MR)	Cell surface	Mannosylated (man)-LAM; cell wall	Kang *et al.* (2005)
			PIMs; cell wall	Torrelles *et al.* (2006)
	DC-SIGN	Cell surface	Alpha-glucan; cell wall	Geurtsen *et al.* (2009)
			Man-LAM; cell wall	Maeda *et al.* (2003)
			PIMs; cell wall	Torrelles *et al.* (2006)
	Dectin-1		Beta-glucan; cell wall	Yadav & Schorey (2006); Rothfuchs *et al.* (2007)
NLRs	NOD2	Cytoplasm	Muramyl dipeptide; peptidoglycan; cell wall	Ferwerda *et al.* (2005); Coulombe *et al.* (2009)
	NLRP3	Cytoplasm	ESAT6; secreted	Mishra *et al.* (2010)

Table 1.3: Pattern recognition of Mtb.

Ligation of most membrane-bound PRRs, such as TLRs, causes intracellular domain conformational changes leading to recruitment of adaptor proteins such as MyD88, which activate intracellular signalling via enzymatic functions (Takeuchi and Akira, 2010). The archetypal pathways which are activated in this manner downstream of TLRs include the NFκB (nuclear factor kappa-light-chain-enhancer of activated B cells) pathway, the MAPK (mitogen-activated protein kinase) cascades, and interferon response factor 3 (IRF3) signalling (Takeuchi and Akira, 2010). TLR-induced NFκB pathway activation causes degradation of the inhibitor of κB (IκB), which retains NFκB TFs in the cytoplasm in the steady state, thus leading to their release and translocation to the nucleus where they induce innate inflammatory gene expression (Takeuchi and Akira, 2010). Concomitant activation of the MAPK cascade also leads to transcription factor activity, such as that of AP-1 and CREB (Dong et al., 2002).

Other PRRs stimulate similar signalling pathways to TLRs; e.g. the RLR RIG-1 (retinoic acid-inducible gene 1) activates NFκB via the adaptor IPS-1 (interferon-beta promoter stimulator 1) (Kawai and Akira, 2006), and CLRs recruit the tyrosine kinase Syk via which MAP kinases are activated, as well as stimulating calcium-signaling pathways to activate the TFs CREB and NFAT (Kelly et al., 2010). A major DNA sensing pathway is activated by the inherent enzymatic activity of the sensor, cGAS, which produces cyclic dinucleotides that act as second messengers to activate STING (stimulator of IFN genes), leading to IRF activation (Li et al., 2013). IRF3, which is also activated downstream of TLRs, then induces type I IFN transcription and thus stimulates innate antiviral responses (Burdette and Vance, 2013).

It has also been established that some innate immune responses are not powered by transcription, such as inflammasome activation (Strowig et al., 2012). Activation of the NLRP or IPAF NLRs causes their oligomerization via their NACHT domains, forming complexes termed inflammasomes which can activate caspase-1. Caspase-1 then enzymatically cleaves the pro-forms of two pro-inflammatory cytokines, pro-IL-1β and pro-IL-18, into their active forms which can be secreted. This process can also induce a form of inflammatory cell death termed pyroptosis (Rathinam et al., 2012). Many stimuli have been shown to activate inflammasomes, including microbial PAMPs, and also signals that communicate tissue damage termed danger-associated molecular patterns (DAMPs), such as urate crystals, β-amyloid and extracellular ATP (Schroder and Tschopp, 2010). The mechanisms by which these signals activate

inflammasomes are unclear, but may involve effects on membrane integrity, or the recently favoured hypothesis of mitrochondrial dysfunction and reactive oxygen species (ROS) generation (Schroder and Tschopp, 2010).

Other non-transcriptional innate immune signalling outputs have been described, which modulate the outcome of inflammatory gene expression programmes via mechanisms such as altering splicing, mRNA stability and translation (Carpenter et al., 2014). One example involves the phosphoinositide (PI)-3-kinase (PI3K)–mammalian target of rapamycin (mTOR) pathway, the activity of which was shown to be modulated in macrophages after bacterial infection, leading to alterations in the efficiency of translation of cytokine mRNAs, and resultant biasing of pro- or anti-inflammatory responses (Ivanov and Roy, 2013).

1.2.7 Macrophage effector functions

It has been long been established that during interactions with pathogens, macrophages assume a pro-inflammatory phenotype involving an increased microbicidal capacity (Unanue, 1976). It is now known that this is primarily induced by pattern recognition, which primes the macrophage for physiological adaptation to inflammation, and directs active anti-microbial functions. One potent macrophage effector function is secretion of cytokines: pleiotropic secreted proteins which act in an autocrine, paracrine and endocrine fashion. They signal via receptors on both immune and non-immune cells to stimulate outcomes such as leukocyte activation, increased vascular permeability and tissue adaptation to inflammation. It was first shown in the 1970s that factors secreted by macrophages could alter lymphocyte activity (Hoffmann and Dutton, 1971) and that macrophage activation modulated this secretion (Unanue, 1976). A range of macrophage-produced cytokines have now been characterised (**Table 1.4**). Macrophages are also able to secrete chemokines, molecules which are able to control the migration and positioning of leukocytes (Griffith et al., 2014), and so they also modulate inflammation by controlling the recruitment of other immune cells (Mantovani et al., 2004). Via the action of cytokines and chemokines, macrophages exert powerful effects on the quality of inflammation and the immune response.

Cytokine	Ascribed functions	References
TNFα	Broad range of inflammatory bioactivites, including co-ordination of the acute phase response, induction of intracellular killing in macrophages and induction of apoptosis	Wajant *et al.* (2003)
IL-6	Broad range of inflammatory bioactivities, including co-ordination of the acute phase response, stimulation of neutrophil production, and induction of monocyte recruitment	Scheller *et al.* (2011)
IL-1β	Broad range of inflammatory bioactivities, including increasing vascular adhesion, co-ordination of the acute phase response, activating and inducing survival of innate immune cells such as neutrophils, influencing polarisation of Th17 cells,	Dinarello (2009)
IL-12	Influences polarisation of Th1 cells	Hsieh *et al.* (1993)
IL-18	Influences polarisation of Th1 cells	Gracie *et al.* (2003)
IL-10	Immunomodulatory functions; contributes to resolution of inflammation	See **section 1.5**
IFNβ	Antiviral responses and immunosuppressive functions	Stetson & Medzhitov (2006); Gonzalez-Navajas *et al.* (2012)
IL-23	Influences polarisation of Th17 cells	Iwakura & Ishigame (2006)
TGFβ	Promotes resolution of inflammation and fibrosis; influences polarisation of Treg and Th17 cells	Lee *et al.* (2001); Murray & Wynn (2013)

Table 1.4: Cytokines secreted by macrophages.

In addition to regulating other cells, macrophages display direct anti-microbial activity via their potent phagocytic function and capacity for intracellular killing. Phagocytosis is initiated by binding of pathogens by receptors which can mediate ingestion, including scavenger receptors, complement receptors, lectins, integrins and Fc receptors (Stuart and Ezekowitz, 2005). The initiation of phagocytosis triggers a range of intracellular processes, including cytoskeletal rearrangements and membrane trafficking events involved in uptake, but also pro-inflammatory signalling, microbial killing pathways and in some cases apoptosis (Stuart and Ezekowitz, 2005). Phagocytosis essentially co-operates with pattern recognition to trigger anti-microbial defences (Underhill and Ozinsky, 2002); this is evidenced by observations that PRRs such as dectin-1 can mediate phagocytic uptake (Herre et al., 2004), but also in the recruitment of PRRs such as TLRs to phagosomes to facilitate microbial detection (Ozinsky et al., 2000; Underhill et al., 1999). Macrophages can also phagocytose fragments of apoptotic cells as a result of pro-phagocytic signals on the apoptotic cell surface (Flannagan et al., 2012).

Phagocytosis internalises micro-organisms in an early phagosome, which then undergoes a maturation process to mediate microbial killing (Stuart and Ezekowitz, 2005). This involves acidification and a series of fusion and fission events with other endosomal compartments, most importantly lysosomes, to form the phagolysosome (Flannagan et al., 2009). The phagolysosome is optimised for pathogen degradation, containing degradative enzymes such as hydrolases and proteases (Stuart and Ezekowitz, 2005). ROS are also generated to mediate killing, via the NADPH oxidase and mitochondrial pathways (Sakata et al., 1987; West et al., 2011). In humans, mutations in the genes encoding the subunits of the NADPH oxidase are associated with chronic granulomatous disease (CGD), a primary immunodeficiency characterised by recurrent bacterial and fungal infections, demonstrating the importance of this phagocytic killing pathway in pathogen control (Heyworth et al., 2003). Generation of reactive nitrogen species (RNS) by the action of inducible nitric oxide synthase (iNOS) is an accepted event in murine macrophages which contributes to host protection but evidence for this pathway in human macrophages is less clear (Aberdein et al., 2013). The importance of phagolysosomal killing is evident in the range of pathogens which have evolved to inhibit phagosomal maturation and function (Flannagan et al., 2009); as a result, alternative pathways of killing may be utilized, such as autophagic killing of Mtb (Gutierrez et al., 2004). In some contexts wherein the macrophage capacity for

phagolysosomal killing is exhausted, it has been shown that macrophage apoptosis may be utilized as an alternative microbial killing mechanism, for example in the response to *Streptococcus pneumonie* (Aberdein et al., 2013; Ali et al., 2003; Bewley et al., 2011; Dockrell et al., 2003, 2001).

Macrophages also co-ordinate tissue repair and resolution of inflammation. Acute inflammatory macrophage responses can be inherently tissue-damaging and contribute to disease, in addition to damage which may be caused directly by pathogens (Wynn et al., 2013). Chronic inflammation, which arises when the acute response is not appropriately resolved, is also a major driver of pathology in which macrophage function is implicated (Nathan and Ding, 2010). Therefore, the resolving functions of macrophages represent an important feedback mechanism by which they regulate immunopathogenic outcomes of their own function. Two specialised macrophage phenotypes mediate resolution, described as either pro-fibrotic macrophages, which are involved in wound-healing, or regulatory macrophages, which are involved in suppression of inflammation (Wynn and Ramalingam, 2012). The latter have also been referred to as “M2” or alternatively activated macrophages, and are proposed to represent a polarised macrophage phenotype in contrast to pro-inflammatory “M1” macrophages; however, the utility of these designations is a matter of debate, and is discussed subsequently in **section 1.2.9**.

The factors which induce these resolution phenotypes include the Th2 cytokines IL-4 and IL-13, IL-10, glucocorticoids, prostaglandins and apoptotic cells (Wynn et al., 2013). Pro-fibrotic macrophages secrete factors such as platelet-derived growth factor (PDGF) and transforming growth factor β (TGFβ), which mediate repair by inducing fibroblasts to synthesise collagen (Wynn and Ramalingam, 2012). They also secrete tissue inhibitors of metalloproteinases (TIMPs), which inhibit matrix metalloproteinase (MMP)-mediated degradation of the extra-cellular matrix (ECM) (Murray and Wynn, 2011). Although depletion studies have demonstrated the necessity of pro-fibrotic macrophages in repair (Duffield et al., 2005; Lucas et al., 2010), they have also alluded to their potentially pathogenic functions in causing fibrosis and scar formation in chronic inflammation (Wynn and Ramalingam, 2012). Regulatory macrophages contribute to the resolution of inflammation by producing factors which suppress pro-inflammatory responses, such as IL-10, which is discussed subsequently in **section 1.5**. Another suppressive factor produced is resistin-like molecule alpha (RELMα), which may contribute to the regulation of Th2-polarised immune responses (Nair et al., 2009).

1.2.8 Interactions of macrophages with the adaptive immune system

The crux of the CMI response is the collaboration between macrophages and $CD4^+$ T cells in the control of intracellular pathogens (**Figure 1.1**). Macrophages are thought to be less migratory than DC, and to persist in tissues after initiating inflammation (Murray and Wynn, 2011). Thus, their interactions with adaptive immune cells are subject to lymphocyte recruitment to the site of inflammation. The chemokine milieu produced by macrophages in acute inflammation may drive this, including factors such as CXCL9 and CXCL10, which are chemotactic for $CD4^+$ Th1 cells, $CD8^+$ cytotoxic cells and natural killer (NK) cells, and CCL17, which is chemotactic for Th2 cells (Griffith et al., 2014; Hardison et al., 2006; Katakura et al., 2004).

Once macrophages and adaptive immune cells are closely spatially related, several interactions may occur. The first set of interactions stem from the macrophage, and the most classic interaction in this regard is macrophage-driven activation of $CD4^+$ T cells. This is suggested to involve three signals from the macrophage or antigen presenting cell (APC): antigen presentation is signal 1, ligation of co-stimulatory receptors is signal 2, and secretion of modulatory cytokines is signal 3 (Curtsinger et al., 1999; Kapsenberg, 2003). The ability of macrophages to provide signal 3 is clear, as they secrete a range of cytokines which can modulate T cells (**Table 1.5**). They are also able to provide signal 1 and signal 2, as although they are not considered to be professional APCs like DCs, they do express major histocompatibility class (MHC) II and co-stimulatory molecules, and have the appropriate phagocytic and antigen processing capabilities to facilitate class II-restricted presentation to $CD4^+$ T cells (Hume, 2008). Investigations have demonstrated that macrophage-mediated antigen presentation to $CD4^+$ T cells can occur *in vitro* (Desmedt et al., 1998) and *in vivo* (Moser, 2001).

The cytokine-driven signal 3 produced by macrophages can alter the polarisation of the subsequent $CD4^+$ T cell response. Associations of different macrophage-derived cytokines with different polarised CD4+ T cell responses are shown in **Table 1.6**. Polarised $CD4^+$ T cell responses are can then feedback to macrophages to modulate their effector functions and hence produce further immune response adaptation, which again mainly occurs via cytokine signalling. IFNγ was the first lymphocyte-produced factor described which modulated macrophage function (Celada *et al.*, 1984; Fowles *et al.*, 1973; Mackaness, 1964; Nathan *et al.*, 1983, 1973; Pace *et al.*, 1983), and was found to induce a potently pro-inflammatory, microbicidal activated macrophage

response. Subsequently, the Th2-produced cytokines IL-4 and IL-13 were shown to induce a divergent form of macrophage activation: promoting endocytosis via mannose receptors, inducing expression of MHC class II molecules, and downregulating pro-inflammatory cytokine secretion (Doyle *et al.*, 1994; Stein *et al.*, 1992). These two macrophage phenotypes were respectively designated as classical and alternative activation of macrophages, and led to the development of the M1 vs. M2 macrophage polarisation concept, discussed subsequently in **section 1.2.9**. In addition to responding to IFNγ, IL-4 and IL-13, macrophages have been reported to alter their functions in response to other cytokines produced by $CD4^+$ T cells, demonstrating the diverse ways in which T cells and macrophages interact to mediate CMI. These are summarised in **Table 1.5**.

Polarised $CD4^+$ T cell response	Immune response	Macrophage-derived cytokines	References
Th1	CMI; IFNγ-producing; intracellular pathogens	IL-12, IL-18	Hsieh *et al.* (1993); Gracie *et al.* (2003)
Th2	Humoral immunity; IL-4/IL-13 producing; extracellular pathogens	IL-4	Pouliot *et al.* (2005); Mukhurjee *et al.* (2009)
Th17	IL-17 producing; extracellular bacteria and fungi	IL-23, IL-6, IL-1β, TGFβ	Langrish *et al.* (2005); Scheller (2011); Chung *et al.* (2009); Mangan *et al.* (2006)
Treg	Immunoregulation	IL-10, TGFβ	Horwitz *et al.* (2003); Chen *et al.* (2003)
Th9	IL-9 producing; immunity to nematodes	TGFβ, IL-4	Veldhoen *et al.* (2008)
Th22	IL-22 producing; skin immune responses	IL-6, TNFα	Duhen *et al.* (2009); Trifari *et al.* (2009)

Table 1.5: Induction of polarised $CD4^+$ T cell responses by macrophage-derived cytokines.

T-cell derived cytokine	T cell subset association	Reported effects on macrophages	References
IFNγ	Th1, Th17	Classical macrophage activation; induction of microbicidal killing and inflammation	Fowles *et al.* (1973); Nathan *et al.* (1983); Pace *et al.* (1983);
TNFα	Th1	Induction of microbicidal killing, effects on apoptosis pathways; regulation of cytokine secretion	Rojas *et al.* (1999); Munoz-Fernandez *et al.* (1992); Hodge-Dufour *et al.* (1998)
IL-4	Th2	Alternative macrophage activation; enhancement of phagocytosis & antigen presentation pathways, suppression of killing pathways	Stein *et al.* (1992); Martinez *et al.* (2009)
IL-13	Th2	Similar effects to IL-4	Doyle *et al.* (1994)
IL-17	Th17	Reported to induce an anti-apoptotic phenotype involved in resolution; other reports suggest induction of pro-inflammatory cytokines	Zizzo & Cohen (2013); Jovanovic *et al.* (1998)
IL-10	Tregs; most subsets under some conditions	Outlined in **section 1.5.3**	
TGFβ	Tregs	Activation of a specific gene expression programme which may be involved in Th2 responses and lipid metabolism	Gratchev *et al.* (2008)
IL-22	Th22, Th17	Induction of microbial killing; however also reported that macrophages may not express the IL-22R	Wolk *et al.* (2004); Dhiman *et al.* (2009)
IL-9	Th9	May induce inflammatory phenotypes	Nowak *et al.* (2009)

Table 1.6: Modulation of macrophages by different $CD4^+$ T cell subset-derived cytokines.

1.2.9 Macrophage functional plasticity

Macrophages are able to appropriately adapt their function in response to detection of a wide range of extracellular signals (Mosser and Edwards, 2008). As such, macrophages display substantial functional plasticity, in addition to phenotypic heterogeneity in different tissues. This plasticity of activation states has been a subject of intensive research, mainly using *in vitro* MDM models, and has provided many insights into the diverse ways in which macrophages may function during the immune response.

Stimulation of macrophages with either IFNγ or IL-4 and IL-13 produces distinct macrophage phenotypes which have been strongly associated with Th1 and Th2 immune responses, with demonstrations *in vitro* and *in vivo* that they are both provoked by these immune responses and played key roles in their outcomes (Mills *et al.*, 2000). A macrophage subset nomenclature was proposed to formalise this parallel with the type I *vs.* type II immune response paradigm, in which classically activated macrophages, which could also be induced by innate stimulation, became known as M1 macrophages and alternatively activated macrophages became known as M2 macrophages (Mills *et al.*, 2000). However, many other stimuli could clearly modulate macrophage biology, including cytokines such as IL-10 and TNFα, and other factors such as glucocorticoids and immune complexes (Mantovani *et al.*, 2004). Modifications of the nomenclature were proposed to incorporate this, such as division of macrophages into three functional subsets of host defence, wound healing and immune regulation (Mosser and Edwards, 2008), or sub-division of the M2 category into M2A, B and C sub-subsets, depending on which input stimuli were used to induce alternative activation (Mantovani *et al.*, 2004). Formulation of this classification was accompanied by research into the molecular mechanisms by which a macrophage becomes classically or alternatively activated, for example at the transcriptomic level (Martinez et al., 2006) or by identification of what are postulated to be subset signature transcription factors, such as IRF5 in M1 polarisation (Krausgruber *et al.*, 2011) and IRF4 (Satoh *et al.*, 2010) and PPAR-γ (Bouhlel *et al.*, 2007; Odegaard *et al.*, 2007) in M2 polarisation.

Throughout the characterisation of macrophage activation within the M1 *vs.* M2 framework, there was recognition that these phenotypes were an oversimplification,

and were actually likely to represent polarised extremes of a spectrum of phenotypes (Mantovani *et al.*, 2004; Biswas and Mantovani, 2010). Their existence *in vivo* as pure polarized subsets was questioned (Lawrence and Natoli, 2011), with the suggestion that it was more likely that mixed phenotypic populations were driven by multiple signals (Martinez and Gordon, 2014). It was also reported that activated macrophage phenotypes were in fact more labile and prone to temporal re-adaptations than a system describing polarised subsets might indicate (Biswas and Lopez-Collazo, 2009; Stout and Suttles, 2004; Stout *et al.*, 2005). Subsequently, a report evaluating human macrophages *in vitro* using a wide range of stimulation conditions, and transcriptional profiling of the activation states produced, showed that the M1 *vs.* M2 bipolarization model could be replaced with a complex spectral range of heterogeneous macrophage activation states (Xue *et al.*, 2014).

As a result, the concept of macrophage plasticity as a binary polarised system of classically and alternatively activated macrophages has been superseded by a paradigm in which macrophages are understood to be functionally dynamic, long-lived cells which are capable of switching their function between a complex array of "metastable" activation states appropriate to their microenvironment (Wynn *et al.*, 2013; Xue *et al.*, 2014). This plasticity is assumed to be primarily controlled at the transcriptional level, wherein the extracellular mediators inducing phenotypic adaptation activate intracellular signalling cascades via receptor ligation, converging on transcriptional outputs which reprogram the function of the cell (Lawrence and Natoli, 2011; Natoli and Monticelli, 2014).

Overall, it is clear that both autocrine and paracrine signals in CMI, generated by macrophages and T cells, can substantially affect the phenotype of both of these cell types as well co-ordinating other effector functions. Hence, the outcomes of CMI responses are likely to be determined stochastically by these signals, and an understanding of both macrophage biology and how it is modulated by these signals, and by pathogens such as HIV-1 and Mtb which can parasitize macrophages, is central to understanding the function of CMI.

1.3 HIV-1 infection and CMI

1.3.1 The human immunodeficiency virus

In the early 1980s, the first reports were made of a condition characterised by severe opportunistic infections, tumours and reduced $CD4^+$ T cell counts. Within four years this condition had been formalized in name as the acquired immunodeficiency syndrome (AIDS), and its causative agent identified: a retrovirus able to infect and cause cytopathic effect in T cells, now called human immunodeficiency virus 1 (HIV-1) (Barré-Sinoussi et al., 1983; Popovic et al., 1984). In the subsequent three decades, research has extensively characterised this infection and its pathogenesis. The cellular receptors for HIV-1 have been identified – the co-stimulatory molecule CD4 (Dalgleish et al., 1984; Maddon et al., 1986) in combination with a chemokine co-receptor (Alkhatib et al., 1996; Feng et al., 1996; Deng et al., 1996), which allows the virus to infect a range of cell types *in vivo*, including $CD4^+$ T cells and macrophages. The ability of HIV-1 to infect both of these central cellular players in CMI highlights the propensity of the virus to modulate this arm of immunity. CMI modulation represents a major pathway of viral pathogenesis, which is mediated through the direct effects of the virus on these cells and through its pleiotropic effects on the immune system more broadly. The aberrant effects of HIV-1 on CMI are evident in the increased risk of infection by intracellular pathogens in HIV-1^+ individuals, of which one the most striking examples is mycobacterial disease including TB.

1.3.2 Epidemiology, clinical course and treatment of HIV-1 disease

The global burden of the HIV-1 pandemic is substantial. In 2012, 35.3 million people globally were HIV-1^+, 2.3 million new HIV-1 infections occurred, and 1.6 million deaths were attributed to the virus (UNAIDS, 2013). This burden of infection is disproportionately found in sub-Saharan Africa, where more than 70% of new HIV-1 infections occurred in 2012 (UNAIDS, 2013). Two distinct epidemiological patterns of HIV-1 infection exist; firstly, countries in which infection is primarily found in particular at-risk groups, such as men who have sex with men (MSMs) or injecting drug users (Cohen et al., 2008). This is the primary pattern of disease in countries outside sub-Saharan Africa. Therein, the second epidemiological pattern is observed, in

generalised epidemics of HIV-1 infection which are self-sustaining throughout the whole population (Cohen et al., 2008).

The natural history and clinical manifestations of HIV-1 disease result from the immunopathogenic processes driven by the virus discussed subsequently in **section 1.3.6**). Many individuals (estimates range from 40–90%) experience an acute retroviral syndrome or seroconversion illness within 2–6 weeks of infection, due to the initial immune response to the virus, with archetypal symptoms of viral infection, such as fever, myalgia, rash, lymphadenopathy and headache (Kassutto and Rosenberg, 2004). The infection soon enters a phase of clinical latency, in which most individuals are asymptomatic and the plasma HIV-1 viral load (VL) is maintained at a lower set point (Levy, 2009). After approximately 5–10 years of untreated infection, late-stage HIV-1 disease is manifest in substantial loss of peripheral blood $CD4^+$ T cells and increased incidence of opportunistic infections, recognized clinically as AIDS (Cohen et al., 2008). Progression to AIDS can be prevented by effective anti-retroviral therapy (ART); however, it is now recognized that even treated HIV-1^+ individuals are at increased risk of non-AIDS-related chronic health complications, including cardiovascular disease, neurocognitive disease, liver and kidney disease, some cancers, and frailty (Deeks et al., 2013).

Notwithstanding non-AIDS related morbidity, the development of ART and the global expansion of access to anti-retrovirals (ARVs) is coincident with substantial reductions in HIV-1-associated mortality. The central principal of ART is the use of several ARVs in combination, to avoid the rapid development of drug resistance to single agents that occurs due to the rapid HIV-1 replication rate; this is termed highly active anti-retroviral therapy (HAART) (Cohen et al., 2008). Due to the robust efficacy of HAART in preventing progression to AIDS and reducing HIV-1-related mortality (The HIV-CAUSAL Collaboration, 2010), and recent demonstrations that it can also reduce transmission (Cohen et al., 2011a), it is now recommended that ART is initiated in all HIV-1^+ individuals with a $CD4^+$ T cell count of less than 500/mm^3 (WHO, 2013a).

1.3.3 HIV-1 virology

HIV-1 is spherical enveloped virus which is a member of the genus *Lentivirus*, part of the family *Retroviridae* (Fields Virology, 2007). It is a single-stranded positive-sense RNA virus, with genome of approximately 10kB (Ratner et al., 1985; Wain-Hobson et al., 1985) containing nine genes flanked by two long terminal repeats (LTR)

(Morrow et al., 1994). The gag gene encodes a polyprotein containing structural components of the virus; the pol gene encodes a polyprotein containing the viral enzymes, reverse transcriptase, integrase and protease; and the env gene encodes the viral glycoproteins gp120 and gp41 (Morrow et al., 1994). The six remaining genes – tat, rev, vpr, vpu, vif and nef – encode the viral accessory proteins which have a range of functions in replication and host cell manipulation (Morrow et al., 1994; Strebel, 2013). In the virion, two copies of the RNA genome are packaged in diploid form inside the viral core which has a characteristic conical structure in mature virions (Morrow et al., 1994). This is surrounded by the viral matrix, and lastly the lipid envelope, which contains the glycoproteins which determine the cellular tropism of the virus (Shioda et al., 1991). The virion also contains viral enzymes and various host factors which are either packaged or derived from the host membrane during the budding process (Morrow et al., 1994; Ott, 2008).

Phylogenetic analyses have determined that the closest ancestor of HIV-1 is simian immunodeficiency virus (SIV) cpz, a pathogenic lentivirus of chimpanzees, and HIV-1 is estimated to have transmitted to humans zoonotically within the last century (Gao et al., 1999; Keele et al., 2009; Korber et al., 2000). HIV-1 is formed of four genetic groups; M (major), O (outlier), N (non-M, non-O) and P; group M is the pandemic HIV-1 which accounts for ≥ 90% of infections globally (Hemelaar, 2012). Within group M, there is great genetic diversity, as a result of the inherent replicative properties of HIV-1 that confer a rapid evolutionary rate upon the virus (Rambaut et al., 2004). There are nine group M clades; clade B viruses predominate in Europe and the Americas, whereas clade C viruses are most common in sub-Saharan Africa (Hemelaar, 2012).

HIV-2, despite also being an aetiological agent of AIDS in humans, is less closely related to HIV-1 than SIVcpz, and its genome is only partially homologous to HIV-1 (de Silva et al., 2008). Its closest relation in the lentivirus family is the sootey mangabey virus SIVsm, from which a separate zoonotic transmission event is thought to have occurred (Gao et al., 1992). HIV-2 is less pathogenic than HIV-1, causing slower progression to AIDS and exhibiting reduced rates of transmission; its global distribution is mostly limited to west Africa (Gilbert et al., 2003; Marlink et al., 1994).

1.3.4 Interactions of HIV-1 with host cells: the viral lifecycle, host restriction and immune evasion

The HIV-1 replication strategy in host cells is described as follows (Fields Virology, 2007). HIV-1 enters cells by interaction of the viral envelope glycoproteins with the host glycoprotein CD4 and a chemokine receptor, leading to fusion of the viral and host membranes and release of the viral core into the cell. This core is made of capsid proteins and contains the HIV-1 RNA genome and the viral enzymes reverse transcriptase (RT), protease and integrase (IN), as well as tRNA primers for the process of reverse transcription, which takes place rapidly after entry to produce a double stranded DNA (dsDNA) copy of the viral genome. This initial RT complex then reassembles around the dsDNA genome to form the pre-integration complex (PIC), made up of both viral and host proteins, which is trafficked into the host cell nucleus for the process of integration into chromosomal DNA, facilitated by IN. The transport of the PIC through nuclear pores allows HIV-1 to effectively infect non-dividing cells, such as tissue macrophages, a feature shared with other lentiviruses. The integrated viral genome, termed the provirus, is used as the template for viral transcription under the control of the viral LTR and mediated by host RNA polymerase II and the viral transactivator protein Tat, along with cellular transcription factors. Viral transcripts are transported to the cytoplasm using both the host nuclear export systems and the viral protein Rev, and are translated into the polyproteins Gag and Gag-Pol, as well as accessory proteins and envelope proteins, or alternatively become nascent viral genomes. Viral proteins and genomic RNA dimers assemble at the plasma membrane and bud as an immature virion, which matures throughout the budding process as the protease enzyme cleaves the polyproteins to form a mature virion which is competent for infection of new host cells.

This strategy is broadly similar to most retroviruses, although the six HIV-1 accessory proteins provide additional functions which aid replication, infectivity and transmission. The transactivator protein Tat increases the efficiency of viral transcription by promoting the formation of a highly efficient RNA polymerase II complex, and the export protein Rev allows efficient shuttling of viral transcripts in spliced and unspliced forms. These two proteins are essential for viral infectivity, and deletion or mutation of their genes renders the virus non-infectious (Dayton et al., 1986; Terwilliger et al,. 1988). The remaining four accessory proteins - Vif, Vpr, Vpu and Nef - perform functions which maximise the efficiency of viral replication, but

deletion of these genes in many studied cell systems is not fully deleterious for viral replication. Vif interacts with the host restriction factor APOBEC3G to counteract the effects of this protein on the virus (Conticello et al., 2003). A range of functions have been ascribed to Vpr; it is suggested to be most important for replication in macrophage-lineage cells (Balliet et al,. 1994), and has been reported to influence viral and host gene expression, enhance nuclear import of the PIC, and interfere with the host cell cycle and apoptotic processes (Andersen & Planelles, 2005). It is not clear which, if any, of these is the dominant function of Vpr. The Vpu protein is unique to HIV-1 among lentiviruses, and has been implicated in enhancing release of virus by countering the host restriction factor tetherin (Neil et al., 2008), and causing degradation of CD4 in infected cells, the latter in order to prevent retention of the envelope glycoproteins in the cell (Dubé et al., 2010). The final accessory protein, Nef, has been shown to be important for pathogenesis *in vivo*, as individuals infected with Nef-mutated viruses progressing more slowly to AIDS (Kirchhoff et al., 1995). Several functions have been ascribed to Nef *in vitro*: altering cellular activation states, downregulating a range of cell surface molecules, and interacting with autophagy pathways, although exactly how these functions link to enhancement of infectivity *in vivo* is not understood (Roeth & Collins, 2006).

A common theme emerges that many HIV-1 accessory proteins act to antagonise or degrade host proteins which can inhibit viral replication; these proteins are termed restriction factors, and represent a cell-autonomous part of the innate immune system which acts to inhibit viral replication (Towers and Noursadeghi, 2014). These factors include APOBEC3G, which introduces mutations in viral DNA (Mangeat et al., 2003); TRIM5α, which mediates restriction by binding to the viral capsid (Stremlau et al., 2004); tetherin, which physically prevents viral budding from the plasma membrane (Neil et al., 2008); SAMHD1, which reduces intracellular nucleotide pools to reduce reverse transcription efficacy (Hrecka et al., 2011; Laguette et al., 2011), and Mx2, which restricts viral nuclear entry (Goujon et al., 2013; Kane et al., 2013). This system of cell-autonomous HIV-1 restriction is inducible by IFN responses, and so HIV-1 has evolved to avoid triggering IFN responses, by evading innate immune detection in the immune sentinel cells it infects, such as macrophages (Rasaiyaah et al., 2013; Tsang et al., 2009). The main step in the HIV-1 lifecycle at which pattern recognition might occur is after reverse transcription of viral RNA in the cytoplasm, as the resultant viral DNA could potentially trigger cytoplasmic DNA sensors such as cGAS and IFI16 (D. Gao et al., 2013; Towers and Noursadeghi, 2014).

HIV-1 utilizes cellular co-factors to prevent DNA sensor triggering and hence prevent restrictive IFN responses. These cofactors include TREX1, which degrades excess viral DNA products (Yan 2010), and cyclophilin A and CPSF6, both of which are recruited to the viral capsid and are necessary for evasion of IFN triggering (Rasaiyaah et al., 2013).

1.3.5 HIV-1 pathogenesis and antiviral immune responses

The pathogenesis of HIV-1 infection, and subsequent progression to AIDS, has been characterised via clinical observations and studies of SIV infection in primate models. The first event post-transmission is establishment of infection in small populations of founder cells – indicated from animal models to primarily be resting $CD4^+$ T cells, although myeloid cells may also be affected - in the mucosa, wherein virus infection and replication expands locally for the first week of infection. This is known as the “eclipse phase”, during which viraemia is not detectable (Cohen et al., 2011b). Infection then disseminates systemically to secondary lymphoid organs, manifesting within the second week post-infection as a high viraemia, as large numbers of target cells in these cell-rich tissues are infected (Haase, 2005). Pathological processes, including $CD4^+$ T cell depletion, start in secondary lymphoid organs during the initial first four weeks or “fast phase” of infection: memory $CD4^+$ T cells, and those in the gut-associated lymphoid tissue (GALT), are particularly affected (Cohen et al., 2011b). By week four, viraemia starts to decline as the infection enters its “slow phase”, as a result of the development of some immunity to the virus and potentially depletion of target cells for infection (Haase, 2010). The slow phase, characterised by a low steady state level of viral replication and resulting low set-point VL, continues for a number of years, which is clinically manifest as the latent phase until virus-driven depletion of the $CD4^+$ T cell population becomes profound and progression to AIDS occurs (Levy, 2009).

Throughout this process, an immune response is mounted, which may confer some control of the virus, but which also contributes to pathogenesis. An innate anti-viral immune response is evident early post-infection, in production of acute-phase proteins (Kramer et al., 2010) and an inflammatory cytokine storm (Stacey et al., 2009). This response is thought to be generated by the responses of cells such as pDCs, which may be able to detect HIV-1, unlike macrophages (Lepelley et al., 2011; Towers and Noursadeghi, 2014). This innate response importantly includes production of type I IFNs, which may confer some control of the virus in the acute phase (Towers and

Noursadeghi, 2014). This is evident in the observation that successful founder viruses have low propensity to trigger type I IFN responses (Salazar-Gonzalez et al., 2009). However, prolonged IFN signalling in HIV-1 infection is thought to contribute to disease pathogenesis as a part of chronic immune activation (discussed subsequently in **section 1.3.6**), as well as potentially contributing to immunosuppression and tolerance of the virus (González-Navajas et al., 2012; Towers and Noursadeghi, 2014). Strong evidence for this bimodal role of type I IFNs in mediating both protection and pathogenesis in lentiviral disease is provided in the macaque model of SIV infection (Sandler et al., 2014). HIV-1 specific T and B cell responses can also be measured *in vivo*, with a particularly strong $CD8^+$ T cell response evident (Cohen et al., 2011b). This adaptive response contributes to the decline in viral load after the initial fast phase (Haase, 2005), but fails to clear the virus. The replicative properties of HIV-1 make it unusually adapted for immune escape, and so these responses are ineffectual in the face of the constantly mutating viral quasispecies (Rambaut et al., 2004). Additionally, like the innate response, they may contribute to disease progression, via contributing to $CD4^+$ depletion via cytotoxicity, and potential involvement in chronic immune activation phenotypes (Levy, 2009).

1.3.6 Immune dysfunction in HIV-1 infection

The most apparent immune dysfunction in HIV-1 infection is the progressive loss of $CD4^+$ T cells. Several mechanisms have been suggested for how depletion occurs, and concomitantly why and when AIDS develops as a result of this (Levy, 2009). Early studies suggested that increased apoptosis was a major mechanism, and that reduction in thymic output might also contribute to the decrease in circulating numbers (Douek et al., 1998; Finkel et al., 1995; Meyaard et al., 1992). Recent investigations have demonstrated that pyroptosis of abortively infected $CD4^+$ T cells may account for the majority of cell death caused by the virus, and that apoptosis may only occur in a minority of productively infected cells (Doitsh et al., 2013, 2010). Pyroptosis is an inherently inflammatory form of cell death driven by the inflammasome, which in this case is triggered by the DNA sensor IFI16 detecting defective RT products in the T cell cytosol (Monroe et al., 2014). This leads to IL-1β release as well as cell death, and so the process may be propagated as inflammation attracts new target cells for infection and depletion (Doitsh et al., 2013). In terms of how depletion leads to progression to AIDS, a critical event may be loss of central memory $CD4^+$ T cells which normally act as a self-renewing source for effector memory $CD4^+$ T cells, as has been shown in the

macaque SIV model (Okoye et al., 2007). As well as depletion, HIV-1 infection is associated with changes in T cell function. These include gross alterations in the make-up of T cell subsets and increased basal rates of T cell activation (Douek et al., 2009). As ART can reverse these phenotypes, ongoing viral replication is implicated in their mechanism; however, they have not been shown to correlate with disease progression, and their contribution to pathogenesis is unclear (Douek et al., 2009).

In addition to its effects on the T cell compartment, HIV-1 is associated with other aberrant immune phenotypes, which may contribute to pathogenesis and impact on the function of CMI. The most striking of these is a state of chronic immune activation present in HIV-1^+ individuals throughout the slow phase of disease, characterised by ongoing leukocyte activation and hypercytokinaemia (Douek et al., 2009). This process correlates with disease progression and does not occur in long-term non progessors (individuals who remain chronically infected without progression to AIDS) and so is thought to be critical in pathogenesis (Deeks et al., 2004; Douek et al., 2009; Forsman and Weiss, 2008). This is supported by the observation that pathogenic lentiviruses are more likely to cause immune activation in their hosts than non-pathogenic lentiviruses (Evans and Silvestri, 2013; Forsman and Weiss, 2008). The inflammatory processes surrounding $CD4^+$ depletion, as well as anti-HIV-1 immune responses, may contribute to chronic immune activation (Douek et al., 2009). However, a specific mechanism involving HIV-1-mediated disruption of the gut mucosa has been suggested to play a role. The postulated process is as follows (Douek et al., 2009): massive loss of $CD4^+$ T cells in the GALT soon after infection causes immunodeficiency and inflammation within the mucosa. This causes fibrosis and structural abnormalities, along with dysbiosis of gut commensals. These combined immunological and structural insults to this important barrier tissue allow the translocation of microbial products from the gut flora into the bloodstream, activating innate immune cells and causing chronic immune activation. Evidence for this model comes from high levels of circulating LPS measured in HIV-1^+ individuals and in the SIV macaque model, which correlate with measures of immune activation (Brenchley et al., 2006).

Two consequences of chronic immune activation are suggested. Firstly, it may contribute to $CD4^+$ depletion, T cell dysfunction and viral replication (i.e. the processes which drive progression to AIDS) by providing a source of activated T cells for the virus to infect. This essentially establishes a vicious cycle, wherein viral replication leads to gut pathology, which drives immune activation, which then potentiates viral replication, etc (Douek et al., 2009). The second aberrant outcome is suggested to be the non-

AIDS-related chronic health complications observed in HIV-1$^+$ individuals. Chronic inflammation itself, and a hypercoagulable state produced by effects on the liver (Shen and Frenkel, 2004), are both drivers of tissue damage which may cause these conditions (Deeks et al., 2013). Immune activation may therefore be a major cause of HIV-1-related disease which is not reversible by ART, as although ART does effectively reduce immune activation, tissue damage as a result of chronic inflammation may have already occurred (Douek et al., 2009).

Another aberrant HIV-1-associated immune phenotype is the immune reconstitution inflammatory syndrome (IRIS), wherein after the commencement of ART there is a severe inflammatory exacerbation or unmasking of an underlying condition, most commonly TB, *Cryptococcus neoformans* infection or cytomegalovirus (CMV) retinitis, but also other herpesvirus infections and neoplastic syndromes (Lai et al., 2013). IRIS has a high incidence and mortality, which were estimated as 16% and 4.5% respectively in a meta-analysis (Müller et al., 2010). The mechanisms which underlie this pathology are not well understood. Although the term IRIS suggests that it results from reconstitution of the immune system and a recovered CD4$^+$ T cell count mediating exacerbated inflammation, it is accepted that this explanation is too simple. Most investigations exploring IRIS immunopathology have focussed on TB IRIS, which is either considered to be paradoxical (worsening of TB symptoms after commencing ARVs) or unmasking (presentation of TB after commencing ARVs) (Lai et al., 2013). In these studies, various phenotypes have been associated with IRIS, such as T cell expansions, hypercytokinaemia, innate dysfunctions and high rates of NK cell activation (**Table 1.7**). A common mechanism for IRIS in different infections was proposed by one study, in which expansions of polyfunctional (TNFα and IFNγ secreting) memory CD4$^+$ T cells were observed which were specific to the underlying co-infection (Mahnke et al., 2012). Altogether, these observations may assist in explaining the pathogenesis of IRIS, but they may also be phenomena resulting from the disease process rather than precipitating it, and the underlying cause-and-effect behind the syndrome is not yet clear (Chahroudi and Silvestri, 2012).

One suggested mechanism for IRIS, as well as for immune activation processes, involves HIV-1-triggered dysfunction of innate inflammatory cells such as macrophages (Lai et al., 2013). As macrophages are target cells for HIV-1, modulation of their function by the virus represents another potential aberrant immune phenotype associated with HIV-1. This is discussed subsequently in **section 1.3.9**.

The range of dysfunctional immune phenotypes found in HIV-1 infection are summarised in **Table 1.8**, including observed dysfunction of B cells, NK cells, neutrophils and pDCs (Fauci et al., 2005; Fitzgerald-Bocarsly and Jacobs, 2010; Kuritzkes, 2000; Moir and Fauci, 2008). HIV-1 has been associated with dysfunction of almost all components of the immune system in some context; however, cause-and-effect for these phenotypes are not clear, and whilst some of these are likely to be secondary to T cell dysfunction or chronic immune activation, conclusive evidence is lacking for their mechanisms. It is clear that the disease caused by HIV-1 is not only an immunodeficiency, but also an immunopathology, involving aberrant inflammatory phenotypes which may contribute substantially to pathogenesis. Dysregulated CMI responses could potentially result from many of these phenotypes; HIV-1 dyregulation of macrophages, as key CMI effector cells, may be a major contributor in this regard.

TB IRIS-associated phenotype	Reference
T cell-based	
Expansions of PPD//Mtb-specific Th1 cells	Bourgarit *et al.* (2006); Elliott *et al.* (2008)
Increased activation of circulating T cells	Antonelli *et al.* (2010)
Impaired T-regulatory cells	Seddiki *et al.* (2009)
Increased numbers of TCR+ γδ T cells	Bourgarit *et al.* (2009)
Cytokine dysregulation	
Increased cytokine release in heat-killed Mtb-stimulated IRIS patient PBMC & concomitant increased cytokines in serum	Takodera *et al.* (2011)
Innate responses	
Dysregulated complement component expression	Tran *et al.* (2013)
High CRP expression	Haddow *et al.* (2011)
High TLR-2 expression	Tan *et al.* (2011)
High rates of NK cell activation	Conradie *et al.* (2011)
High neutrophil counts and TNF at site of inflammation	Marais *et al.* (2013)
Humoral responses	
High expression of TB-specific anti-phenolic glycolipid antibody	Simonney *et al.* (2008)

Table 1.7: Immune phenotypes associated with TB-IRIS.

Table produced from the mechanisms for TB IRIS reviewed in Lai *et al.* (2013). In the studies presented, the comparator groups for TB IRIS patients include a range of controls (HIV-1 negative TB, HIV-1 non-IRIS TB, etc) and include both paradoxical and unmasking IRIS presentations.

Immune phenotype	Description	Suggested mechanisms
$CD4^+$ T cell depletion	Depletion of $CD4^+$ T cells, which occurs first in primary infection but then recovers, then progressively decreases over the clinically latent phase until progression to AIDS.	Pyroptosis & apoptosis of infected cells or bystander cells; killing by HIV-1-specific CD8+ T cells; impaired thymic function leading to reduced T cell production
T cell dysfunction	Gross alterations in T cell subset makeup; high basal rates of activation	Driven by viral replication; may be due to anti-HIV immune response, or be part of immune activation
Gut pathology	Preferential depletion of CD4+ T cells in the GALT, inflammatory damage to the gut epithelium, dysbiosis. Commences early post-transmission	Depletion of $CD4^+$ T cells as above, which leads to inflammation, damage & compromised immunity.
Chronic immune activation	Chronic lymphocyte activation & hypercytokinaemia throughout the clinically latent phase of infection.	Translocation of microbial components across the gut wall leading to dysregulated innate immune cell responses, as well as anti-HIV immune responses and inflammation resulting from $CD4^+$ cytotoxicity
Chronic IFN signalling	Elevated levels of type I IFN evidence systemically throughout disease which may be broadly immunosuppressive	Chronic anti-viral immune response
Macrophage dysfunction	See **section 1.3.8**	
B cell dysfunction	Hyperactivation and alterations in subpopulation frequencies, and decreases in memory B cell pools	Associated with chronic immune activation and effects on T cell compartment
NK cell dysfunction	Increased expression of inhibitory receptors, along with decreased capacity for cytotoxic responses and cytokine & chemokine production	Direct interactions of the virus with NK cells, or resulting from chronic immune activation
Neutrophil dysfunction	Reduced numbers, increased apoptosis, and deceased microbicidal abilities	Bone marrow dysfunction, treatment-related, aberrant cytokine regulation
pDC dysfunction	Chronic activation combined with reductions in numbers and altered functionality	Direct interactions of the virus with pDCs, or resulting from chronic immune activation
IRIS	Clinical exacerbation or unmasking of an infection or neoplasm after commencement of HAART	See **Table 1.7**

Table 1.8: Immune dysfunctions in HIV-1 infection

Table produced from mechanisms and references cited throughout **section 1.3.6.**

1.3.7 HIV-1-associated co-infections

The most apparent clinical manifestation of HIV-1 and AIDS are the co-infections which result from immunodeficiency. In the early era of AIDS, fungal *Pneumocystis* pneumonia (PCP) and neoplastic herpesvirus infection with Kaposi's sarcoma herpes virus (KSHV) were the most commonly observed conditions in the USA (Jaffe et al., 1983). Other fungal co-infections are caused by *C. neoformans* (Harrison, 2009) and *Candida albicans* (Imam et al., 1990), while infections with herpesviruses other than KSHV, such as CMV and herpes simplex virus (HSV) are also common (Jacobson et al., 1997; Siegal et al., 1981). Protozal co-infections are caused by *Cryptosporidium* and *Toxoplasma* (Antinori et al., 2004; Pozio et al., 1997), and invasive bacterial co-infections by non-typhoidal *Salmonella* spp. and *S. pneumoniae,* among others (Noursadeghi et al., 2006a). Finally, mycobacterial infections caused by both Mtb and non-tuberculous mycobacteria such as *Mycobacterium avium* complex (MAC) organisms contribute a significant burden of co-infections (De Cock et al., 1992; Karakousis et al., 2004).

Co-infections can be divided into two categories; those caused by pathogens which do not commonly cause disease in immunocompetent hosts, such as *Pneumocystis*, KSHV and *Cryptococcus* (typically designated as opportunistic infections), and those caused by pathogens which cause a burden of disease in healthy individuals, such as Mtb, HSV & CMV and bacterial infections. In the latter category, HIV-1$^+$ individuals may experience disease more frequently, more severely or in atypical presentations compared to healthy individuals. The risk of different co-infections varies with the degree of immunosuppression (shown in **Table 1.7**); typically, infections termed opportunistic only present at very low CD4$^+$ counts; this may be because these infections are directly controlled by CD4$^+$ T cells, or simply indicate that CD4$^+$ count is a powerful marker of disease progression. Risk of other conditions, such as TB (non-disseminated) and invasive bacterial infection, are higher in all HIV-1$^+$ individuals regardless of CD4$^+$ count (Noursadeghi et al., 2006a; Sonnenberg et al., 2005). This suggests that some inherent consequence of HIV-1 infection which is not necessarily involved in disease progression may contribute to risk in these settings. This is supported by the observation that risk of opportunistic infections decreases with HAART (Kaplan et al., 2000), whereas increased risk of TB and invasive bacterial

infections persists in ARV-treated individuals (Gupta et al., 2012; Noursadeghi et al., 2006a).

TB co-infection, in particular, causes a substantial burden of morbidity and mortality in HIV-1^+ individuals. Mtb is thought to be controlled by CMI (discussed in **section 1.4.3**), and like HIV-1, parasitizes macrophages. The interaction between Mtb, HIV-1 and macrophages may therefore be a key example of where dysregulation of CMI contributes to risk of co-infection in HIV-1^+ individuals, and this is discussed in the following sections describing HIV-1 infection of macrophages, tuberculosis, and HIV-1-associated TB.

HIV-1^+ group at risk	Infections	References
All HIV-1^+ individuals	Pulmonary TB, invasive bacterial infections	Gupta et al. (2012); Noursadeghi *et al.* (2006); Sonnenberg *et al.* (2005); Zumla *et al.* (2013)
CD4<200/mm^3	KSHV, cryptosporidium, PCP, atypical pulmonary or extrapulmonary TB	Crowe *et al.* (1994); Phair *et al.* (1990); Zumla et al. (2013)
CD4<100/mm^3	Disseminated MAC, HSV, toxoplasmosis, cryptococcosis, oesophageal candidiasis	Crowe *et al.* (1994); Chaisson *et al.* (1992)
CD4<50/mm^3	CMV retinitis, disseminated TB	Crowe *et al.* (1994); von Reyn *et al.* (2011); Zumla et al. (2013)

Table 1.9: HIV-1 associated co-infections.

1.3.8 HIV-1 infection of macrophages

All lentiviruses can infect cells of the macrophage lineage (Chapter 57, Fields Virology, 5th ed, Knipe 2007), and HIV-1 is no exception. It was determined soon after the isolation of HIV-1 that the virus could infect macrophages *in vitro* and *in vivo* (Gartner et al., 1986a; Ho et al., 1986), an infection which is permissible due to macrophage expression of CD4 and the chemokine receptor CCR5, as well as the ability of HIV-1 to evade innate immune detection in these cells (Towers and Noursadeghi, 2014). HIV-1 infection of macrophages is productive but not cytopathic (Cassol et al., 2006), and has been shown to occur *in vivo* in tissue macrophages (Cao et al., 1992; Jambo et al., 2014; Jarry et al., 1990; Koenig et al., 1986). Infection of monocytes *in vivo* is shown to be much less frequent (Spear et al., 1990) reflecting their lower expression of the CCR5 co-receptor (Naif et al., 1998; Tuttle et al., 1998). DCs are thought to be resistant to infection by HIV-1 *in vivo*, in part because of their lower expression of CD4 and CCR5 (Luban, 2012), but also due to expression of the restriction factor SAMHD1 (Laguette et al., 2011). Macrophage tropism may also be modulated by SAMHD1 restriction to some extent (Sunseri et al., 2011), and it is possible that macrophage-tropic HIV-1 strains have evolved to specifically avoid this restriction pathway (Towers and Noursadeghi, 2014).

Infection of macrophages by HIV-1 may be important for a number of reasons. Production of virus by macrophages may contribute considerably to viral production and burden, even if they are only infected at low levels (Eckstein et al., 2001). Macrophages may be infected early post-transmission, due to the fact that they are present at the initial site of infection in the mucosa (Margolis and Shattock, 2006) coupled with the preferential transmission of R5-tropic virus, which can infect macrophages (Zhu et al., 1993), although the observation that MDMs are poorly permissive *in vitro* to founder viruses means their role in early infection is not yet clarified (Li et al., 2010; Salazar-Gonzalez et al., 2009). Later in disease, macrophages form a long-lived reservoir of virus, capable of infecting $CD4^+$ T cells (Groot et al., 2008). This reservoir might be a privileged site in which the virus evades the immune system, in light of findings that virions are protected from neutralizing antibodies in macrophage intracellular compartments (Koppensteiner et al., 2012). Due to their relatively long life-spans, any consequences of macrophage infection are likely to be prolonged, and this covert reservoir may persist after HAART (Stevenson, 2003). It has

recently been reported that cell-to-cell spread of virus can continue after HAART (Sigal et al., 2011), which highlights the potential significance of this reservoir in HIV-1 persistence. Infection of macrophages might also contribute to HIV-1 pathology by causing bystander apoptosis of T cells (Badley et al., 2000) and neurons (Kaul et al., 2001), which may be due to increased expression of death receptor ligands such as Fas ligand on infected macrophages (Dockrell et al., 1998). Furthermore, it has been reported that macrophages harboring HIV-1 infection have altered functionality in a number of ways which may contribute to immunopathogenesis, discussed subsequently in **section 1.3.9.**

In addition to evidence demonstrating that HIV-1 infection of macrophages occurs *in vivo* and has functional consequences, a broader perspective on the significance of HIV-1 macrophage tropism exists. It is clear that infection of $CD4^+$ T cells is a central feature of HIV-1 pathogenesis, as this is the compartment wherein the vast majority of viral replication takes place *in vivo* (Towers and Noursadeghi, 2014). However, this infection is often abortive and cytopathic (Doitsh et al., 2013, 2010), whereas the virus appears to be more highly adapted to macrophages as a host cell, in which it does not trigger cell death or an IFN response and establishes a productive infection (Cassol et al., 2006; Tsang et al., 2009). As such, it has been proposed that the virus has specifically evolved to establish this quiet but productive infection in macrophages, suggesting that they may be a critical host cell for HIV-1 to maximise its own replication or persistence in some context (Towers and Noursadeghi, 2014).

Evidence from other animals also indicates that macrophages can drive lentiviral pathogenesis. Visna-maedi virus (VMV), which infects sheep, and caprine arthritis encephalitis virus (CAEV), which infects goats, are both retroviruses of the genus *Lentivirus,* like HIV-1 (Blacklaws, 2012). They present clinically as slowly progressing inflammatory conditions: VMV is characterised by chronic pulmonary inflammation, a wasting syndrome and neurological disease (Sigurdardottir and Thormar, 1964; Thormar, 2013), while CAEV presents with inflammatory arthritis and neurological disease (Narayan and Cork, 1985). Importantly, VMV and CAEV do not infect lymphocytes, but only cells of the monocyte/macrophage lineage (Anderson et al., 1983; Blacklaws, 2012; Narayan et al., 1982), suggesting that the inflammatory disease processes are purely driven by infection of these cells. Although their clinical courses are clearly distinct from HIV-1, it is speculated that shared clinical features (wasting and neurological involvement) may also be driven by macrophage infection in HIV-1 infection (Forsman and Weiss, 2008). These conditions also provide a proof of

principal, in terms of infected macrophages contributing to disease in lentiviral pathogenesis.

1.3.9 Modulation of macrophages by HIV-1

Due to the role of macrophages as key immune sentinel and effector cells (**section 1.2.5–1.2.9**), there has been considerable interest in assessing whether these functions are disrupted by HIV-1 infection, as this has the potential to contribute to HIV-1-associated immunopathogenesis (Noursadeghi et al., 2006a). Various investigations have been made into the function of MDMs and *ex vivo* tissue macrophages from HIV-1^+ individuals, reporting a range of phenotypes, such as impaired phagocytosis (Chaturvedi et al., 1995; Koziel et al., 1998; Torre et al., 2002; Wehle et al., 1993); conserved phagocytosis (Elssner et al., 2004; Gordon et al., 2001); impaired cytokine release (Gordon et al., 2005; Nicol et al., 2008; Tachado et al., 2005); increased cytokine release (Gordon et al., 2007; Millar et al., 1991; Trentin et al., 1992); and impaired apoptosis (Patel et al., 2009). However, as the burden of infection in monocytes and macrophages *in vivo* is not uniform, it is likely that many of the cells in these studies were not actually HIV-1-infected, and so it is difficult to assess whether these phenotypes are directly caused by the virus or result from indirect effects of the virus on the host immune response (Noursadeghi et al., 2006a).

Other studies have used *in vitro* models of HIV-1 infection in MDMs, *ex vivo* AMs or macrophage cell lines, to establish more conclusively that observed phenotypes result from HIV-1 infection. The range of described phenotypes is summarised in **Table 1.10**, and include effects on phagocytosis, microbicidal killing, autophagy, inflammatory responses and apoptosis. These phenotypes have the potential to contribute to disease, particularly in the context of opportunistic infections. However, due to the range of models used (different time-points, methods of MDM differentiation, HIV-1 strains used, etc), it is challenging to draw many overarching conclusions from this body of work. Identifying mechanisms for phenotypes in terms of their HIV-1 determinants may lend confidence; for example, it is reported that some inhibitory effects on phagocytosis are Nef-dependent (Mazzolini et al., 2010). Corroboration of phenotypes *in vivo* is also likely to be an important step in determining whether they contribute to disease, and recently developed methods for quantifying HIV-1 infection in *ex vivo* AMs from HIV-1^+ individuals has allowed specific assessment of their phagocytic function (Jambo et al., 2014).

Effects of HIV-1 accessory proteins in modulating signalling pathways involved in innate immunity have also been described, which could potentially contribute to HIV-1 dysregulation of macrophages; these include inhibition of NFκB signalling by Vpu and Vpr (Bour et al., 2001; Muthumani et al., 2005), and multifaceted effects on signalling and receptor expression by Nef (Aiken et al., 1994; Tachado et al., 2005; Vigerust et al., 2005). However, these effects have mainly been described in cell lines or in T cells, and their relevance to macrophage function, innate immune responses and particular HIV-1-dysregulated phenotypes remains to be assessed.

As it has been shown in two independent assessments that HIV-1 does not modulate the baseline transcriptome of macrophages (Maddocks et al., 2009; Noursadeghi et al., 2009), and it is known that it does not trigger innate immunity or cause baseline cytotoxicity in these cells (Cassol et al., 2006; Rasaiyaah et al., 2013), effects of the virus are likely to be evident in altered innate immune responses, rather than in changes in resting activity. A hypothesis for why the virus might act to alter innate immune signalling in macrophages is presented by the observation that these pathways can modulate HIV-1 replication via effects on viral transcription (Chen et al., 1997; Perkins et al., 1994, 1993; Williams et al., 2007). Therefore, it is possible that HIV-1 may have evolved to modulate inflammatory pathways to maximise its own replication; further evidence for this comes from studies using HIV-1/Mtb co-infected macrophages, discussed subsequently in **section 1.4.5**.

Clearly, if HIV-1 modulates macrophage function *in vivo* in the ways it has been described to *in vitro*, this may contribute to immune dysfunction in HIV-1 infection, and in particular affect CMI pathways in which macrophage function is integral. One scenario in which this would be likely to contribute is in TB, as CMI is critical in control and pathogenesis of Mtb, for which macrophages also act as host cells.

Phenotype	Experimental model	Reference
Uptake and microbicidal killing		
Increased intracellular growth of *Mycobacterium avium*	MDM infected with full-length HIV-1	Kallenius *et al.* (1992)
Impaired phagocytosis of *Candida albicans*	MDM infected with full-length HIV-1	Crowe *et al.* (1994)
Impaired phagocytosis and killing of *Toxoplasma gondii*	MDM infected with full-length HIV-1	Biggs *et al.* (1995)
Impaired phagosome-lysosome fusion	MDM infected with full-length HIV-1 or treated with gp120	Moorjani *et al.* (1996)
Impaired killing of *Cryptococcus neoformans*	*Ex vivo* AMs infected with full-length HIV-1	Ieong *et al.* (2000)
Increased intracellular growth of Mtb	MDM infected with full-length HIV-1	Imperiali *et al.* (2001)
Impaired complement-mediated phagocytosis	MDM infected with full-length HIV-1	Azzam *et al.* (2006)
Impaired intracellular killing of *Leishmania*	MDM infected with full-length HIV-1	Barreto-de-Souza *et al.* (2006)
Impaired FcR-mediated phagocytosis	MDM infected with full-length HIV-1	Leeansyah *et al.* (2007)
Interaction with autophagy pathways	MDM infected with full-length HIV-1	Kyei *et al.* (2009)
Impaired phagocytosis due to perturbations in endosomal remodelling	MDM infected with full-length HIV-1	Mazzolini *et al.* (2010)
Increased intracellular growth of mycobacteria	MDM infected with full-length HIV-1	Pathak et al. (2010)
Impaired phagocytosis	*Ex vivo* small AMs from HIV-1+ individuals confirmed to be infected with HIV-1 by FiSH	Jambo *et al.* (2014)
Inflammatory responses		
Impaired LPS-induced MAP kinase activation, NFκB binding to the IL-12p40 promoter & IL-12 production	Macrophage cell line infected with full-length HIV-1	Chambers *et al.* (2004)
Reduction in co-stimulatory molecule expression	MDM treated with HIV-1 Vpr	Muthumani *et al.* (2005)
Reduction in mannose receptor expression	MDM expressing HIV-1 Nef	Vigerust *et al.* (2005)
Impaired LPS-induced TNFα release	Macrophage cell line harbouring HIV-1 provirus	Tachado *et al.* (2005); Nicol *et al.* (2008)
Impairment of TNFα release and apoptosis in response to Mtb	Macrophage cell line harbouring HIV-1 provirus and *ex vivo* AMs infected with HIV-1	Patel *et al.* (2007)
Attenuation of classical NFκB signalling but broadly preserved downstream transcriptional response	MDM infected with full-length HIV-1	Noursadeghi *et al.* (2009)
Increased pro-inflammatory cytokine production in response to Mtb	MDM infected with full-length HIV-1	Pathak *et al.* (2010)
Activation of the inflammasome leading to IL-1β and IL-18 production	MDM cultured with plasma from viraemic HIV-1+ patients	Chattergoon *et al.* (2014)

Table 1.10: Reported effects of HIV-1 on macrophage innate immune responses.

1.4 Tuberculosis

1.4.1 Epidemiology, clinical course and treatment of TB

TB, the disease caused by Mtb, has been present in human populations for at least 2000 years (Russell, 2007; Zink et al., 2003). Advances in public health and antibiotic therapy throughout the 20th century reduced the mortality attributed to TB (Lawn and Zumla, 2011), but the global burden of TB disease remains substantial. In 2012, 8.6 million new cases of TB occurred worldwide, and 1.3 million deaths were attributed to the disease (WHO, 2013b). This burden is disproportionately found in low- and middle-income countries, but high TB incidence is also observed in urban centres in some high-income countries, including the UK (Abubakar et al., 2011; Hayward et al., 2003). The global distribution of the TB pandemic is co-incident with the HIV-1 pandemic, leading to a huge burden of morbidity and mortality associated with TB/HIV-1 co-infection in sub-Saharan Africa (Lawn and Churchyard, 2009).

Current estimates suggest that approximately 10% of individuals exposed to Mtb will develop active TB in their lifetime, whereas the remaining 90% either contain the pathogen as a latent infection, or potentially clear the infection, although the latter scenario may be difficult to conclusively prove (O'Garra et al., 2013). Two billion individuals worldwide are estimated to have latent TB (Zumla et al., 2013). Within the 10% of exposed individuals who develop active TB, half are estimated to do so within 18 months of exposure; designated as primary progressive disease (Zumla et al., 2013). The remainder initially contain the infection latently, and then go on to develop active disease due to reactivation (Zumla et al., 2013).

Mtb transmission occurs via the respiratory route, and the majority of TB disease is pulmonary, with archetypal symptoms including cough, increased sputum production, fever, weight loss, night sweats and haemoptysis (Zumla et al., 2013), along with pulmonary features evident on chest X-ray such as lung lesion cavitation and thoracic lymphadenopathy (O'Garra et al., 2013). Extra-pulmonary presentations of TB are also relatively common, enumerating 10-42% of patients depending on the at-risk group. The manifestations of extra-pulmonary disease can be extremely varied and preclude simple diagnosis; in fact, diagnosis of TB is often challenging, due to sharing of cardinal clinical features with other diseases such as sarcoidosis and cancer (O'Garra et al., 2013). Microbiological confirmation forms the backbone of diagnosis,

although the challenges inherent in culturing the bacterium also present difficulties (Lawn and Zumla, 2011; Zumla et al., 2013).

Current standard care for drug-sensitive active TB is quadruple antibiotic therapy with isoniazid, rifampin, ethambutol, and pyrazinamide (Zumla et al., 2013). The emergence of multi-drug resistant (MDR)-TB, enumerating approximately 5% of cases annually (WHO, 2013b), has meant that an additional 17 anti-microbial agents are used therapeutically (Zumla et al., 2013). Immunotherapy for TB has previously been evaluated, but has not been cemented as a therapeutic option, with a need for further assessment in randomised controlled trials (Uhlin et al., 2012). Treatment targeting active TB immunopathology is commonly used in one context, wherein corticosteroids are used as adjunctive treatment for TB meningitis (Thwaites et al., 2004). Increasing interest in host-directed immunotherapy exists, after it was demonstrated that the outcome of corticosteroid therapy in TB meningitis was dependent on host genotype (Tobin et al., 2012).

The bacilli Calmette-Guerin (BCG) vaccine for TB has been available for nearly 100 years, but its efficacy varies between groups and wanes over time (Lawn & Zumla 2011). It may be effective in preventing disseminated disease in infants, but its value is limited in preventing adult pulmonary infection (Colditz et al., 1994; Trunz et al., 2006). The first TB vaccine efficacy trial since BCG, which tested the vaccine-modified Vaccinia virus Ankara expressing antigen 85A (MVA85A), reported no protective effect after promising results in pre-clinical studies (Tameris et al., 2013). When considering the complexity of the immune response to Mtb, in that immunocompetent individuals with latent TB develop an immune response which is protective in preventing active disease, but the development of active TB in other individuals involves an immune response which causes immunopathology (discussed in **section 1.4.3**), the challenges are clear for developing a vaccine which can induce an immune response with this critical balance between protection and pathogenesis (Andersen and Woodworth, 2014).

1.4.2 Mtb and parasitism of macrophages

In 1882, Robert Koch identified the infective aetiological agent of tuberculosis, the tubercle bacillus, by staining fine rod-like bacilli in tuberculous material from infected animals (Sakula, 1982). This agent, known now as *Mycobacterium tuberculosis*, is an aerobic, acid-fast, non-motile, unencapsulated bacterium which replicates slowly and has a lipid-rich cell wall characteristic of mycobacteria (Lawn and Zumla, 2011). Mtb is a facultative intracellular pathogen, and its primary host cell is the macrophage (Russell et al., 2010). Macrophage uptake of Mtb is the initial host-pathogen interaction that occurs after aerosol Mtb transmission, when alveolar macrophages internalise inhaled bacilli (Russell et al., 2010). This occurs by phagocytosis mediated via receptors such as scavenger, complement and mannose receptors (Schäfer et al., 2009). This host-driven process is rapidly hijacked by the pathogen: Mtb arrests maturation of the phagosome, hence preventing early macrophage-mediated killing and limiting the hostility of the intracellular environment (Russell, 2007).

Mtb then persists within the early endosomal system in macrophages, wherein it can access nutrients for growth (Russell et al., 2010). Despite phagosome arrest, macrophage activation can deliver Mtb to bactericidal environments and lead to killing (Russell, 2007). In humans, autophagy pathways may be critical for this process, in which arrested phagosomes are targeted via the autophagosome to acidified lysosomes, wherein the bacterium can be degraded by acidification, antimicrobial peptides and hydrolases (Alonso et al., 2007; Gutierrez et al., 2004; Russell et al., 2010). Activation of macrophages by TLR ligands and IFNγ may activate or enhance autophagy (Delgado et al., 2008; Singh et al., 2006). The importance of intracellular killing of Mtb in human macrophages is also demonstrated by the association of CGD (in which NADPH oxidase mutations lead to impaired respiratory burst killing in phagocytes) and predisposition to TB (Bustamante et al., 2011; Lee et al., 2008).

Mtb parasitism of macrophages may cause cell death, and it is apparent that macrophage cell death occurs in TB pathogenesis, as dead or dying macrophages are observed *in vivo* within granulomata (Ramakrishnan, 2012). However, the contribution of different cell death pathways to this remains ill-defined. Some evidence indicates that Mtb is anti-apoptotic in macrophages, diverting the cell to death by necrosis (Gan et al., 2008), and that this process is associated with virulence (Velmurugan et al.,

2007). Mtb may also directly induce necrosis (Divangahi et al., 2009). Conversely, some reports show that Mtb and other mycobacteria promote macrophage apoptosis (Davis and Ramakrishnan, 2009; Keane et al., 1997). Which of these pathways is more advantageous for the bacterium is not clear. Necrosis may confer more benefit, as uncontrolled intracellular replication followed by cell lysis promotes extracellular propagation of high bacillary loads, whereas apoptosis may be a form of innate defence and reduce Mtb viability (Behar et al., 2011; Keane et al., 2000). However, apoptosis has been shown to facilitate transmission to new host macrophages as a result of phagocytosis of apoptotic fragments containing viable bacilli (Davis and Ramakrishnan, 2009). The association between active TB and necrotic phenotypes in granulomata (Ramakrishnan, 2012) suggests that necrosis may be a particularly host-detrimental process.

1.4.3 TB pathogenesis and the immune response

It is known that the immune system, and in particular CMI, is important in protection against TB. Many known TB risk factors demonstrate the importance of CMI in protecting against TB disease. Firstly, the existence of MSMD conditions, in which patients have genetic mutations in CMI effectors such as IFNγ, the IFNγ receptor and IL-12 (see **table 1.1**). Although these conditions have mainly been described to confer susceptibility to less virulent non-tuberculous mycobacteria, they have also been shown to be associated with severe tuberculosis in some patients with mutations in IL-12p40, IL-12Rβ1 and IFNGR1 (Abel et al., 2014; Boisson-Dupuis et al., 2011; de Beaucoudrey et al., 2010; Dorman et al., 2004; Picard et al., 2002; Sasaki et al., 2002). Thus, MSDM highlights the importance of these effectors of CMI in the response to TB. Further evidence is provided by some polymorphisms in genes related to CMI components which are associated with increased TB risk, such as *IL12B1*, *IFNG* and *MBL* (Lawn and Zumla, 2011; Maartens and Wilkinson, 2007).

Some iatrogenic TB risk factors also demonstrate the protective role of the immune response in TB, such as the increased risk of active TB in patients on anti-TNFα antibody therapy (Keane et al., 2001) or corticosteroids (Lawn and Zumla, 2011). However, the most clear example of immune dysfunction increasing TB risk is observed in HIV-1 infection, which is the strongest single risk factor for active TB (Walker et al., 2013). As HIV-1 is characterised by immune defects, this strongly indicates that alterations in the immune response impact on both TB risk and the natural history of the condition, and so in some capacity the immune response must be

protective. However, it is also clear that we do not yet understand the correlates of immune protection in TB, and precisely what components of immunity mediate protection (O'Garra et al., 2013). This is complicated by the fact that the pathogenesis of TB disease is driven by the immune response; the hallmark of disease is the caseating granuloma, a classic focus of CMI (Dannenberg, 1994; Dannenberg et al., 1968), and immune-mediated tissue destruction is strongly implicated in active disease (Elkington et al., 2011).

The archetypal drivers of CMI, Th1-polarised $CD4^+$ T cells, are suggested to be necessary for protection against Mtb, due to studies of their deficiency in mouse models (Leveton et al., 1989) and their depletion in HIV-1^+ individuals. However, whether they are sufficient for protection is unclear, and the effector functions they utilise to mediate this protection are not defined (Sakai et al., 2014). For example, the contribution of IFNγ production by $CD4^+$ T cells is unclear, as it has not been found to correlate with BCG-induced immune protection against Mtb (Kagina et al., 2010), and protection mediated by $CD4^+$ T cells was independent of IFNγ in a mouse model (Gallegos et al., 2011). IFNγ may also be produced by cytotoxic $CD8^+$ T cells, and this may contribute to protection (Tascon et al., 1998). Overall, the relative contributions of $CD4^+$ and $CD8^+$ T cells to anti-mycobacterial immunity via CMI remain unclear. The fact that most individuals exposed to TB, including those with active disease, develop a TB-specific Th1 response as evidenced by positive IFNγ release assays (IGRAs) and tuberculin skin tests (TSTs) also demonstrates that although a Th1 response is necessary for protection against TB due to risk factors as discussed above, it is not sufficient for protection, as active disease occurs in its presence.

This has raised the question of what other immune components contribute to protection. A range of cytokine signalling axes which can modulate the function of CMI have been implicated in this. An overarching theme is observed with regard to these cytokines modulating CMI to produce a balanced inflammatory response which can induce protection without immunopathogenesis. This is exemplified by investigations into the role of TNFα in the zebrafish *M. marinum* model, in which it is demonstrated that either too little or too much production of TNFα can drive disease, whereas the "just-right" amount of TNFα is protective (Roca and Ramakrishnan, 2013; Tobin et al., 2012) – a so-called "Goldilocks effect" (Andersen and Woodworth, 2014). The downstream effects of either low or high TNFα result in macrophage necrosis and uncontrolled extracellular replication of bacteria (Roca and Ramakrishnan, 2013), and

the potential relevance of this phenotype to human TB has been confirmed via genetic studies of homologues of implicated factors (Tobin et al., 2012).

TNFα dysregulation in this zebrafish model is caused by various eicosanoid lipid mediators (Tobin et al., 2012). The anti-mycobacterial functions of the cytokine IL-1β (Fremond et al., 2007) have also been shown to be mediated by eicosanoid induction. Again, counter-regulation of pro- and anti-inflammatory pathways is found to be key in this mechanism, as these lipid mediators act by limiting the anti-inflammatory effects of another group of cytokines, type I IFNs (Mayer-Barber et al., 2014). Signatures of type I IFN responses, and by implication their immunosuppressive functions (Guarda et al., 2011; Reboldi et al., 2014), have been described to distinguish active TB from latent controlled infection in peripheral blood gene expression profiles (Berry et al., 2010), lending support to the hypothesis that they are host-detrimental in mycobacterial infection (Teles et al., 2013). In this regard, they have been strongly associated with the anti-inflammatory cytokine IL-10 and are suggested to induce its expression (Teles et al., 2013), although this is yet to be conclusively demonstrated. The role of IL-10 in the response to tuberculosis is a matter of some investigation and is discussed subsequently in **section 1.5.4**.

Overall, these investigations have begun to describe a system in which the protective immune response to Mtb involves a CMI response driven by $CD4^+$ T cells and IFNγ, in the context of a cytokine and lipid mediator mileu which appropriately regulates the burden of inflammation caused by this response, while also ensuring it can mediate protection against the pathogen – a balanced inflammatory response. Dysfunction of CMI, due to deficiency or aberrant immunoregulation, is then suggested to lead to active TB, by disrupting this balance with consequences for bacterial growth and immunopathology.

Studies of the site of TB disease in granulomata have lent support to this concept. The granuloma is driven by CMI, and is implicated in both containment of Mtb and in immunopathology (Russell et al., 2009). Contexts in which well-formed granuloma are not generated are associated with severe disseminated TB, such as in immunosuppressed HIV-1^+ individuals (Lawn and Zumla, 2011), or TNFα-deficient mouse models (Bean et al., 1999), showing that the CMI response in TB granuloma can contribute to protection. However, inappropriate inflammation, such as that causing macrophage cell death by necrosis (Roca and Ramakrishnan, 2013) may lead to instability of the granuloma and thus compromise protection; clinical observations

indicate that necrosis and liquefaction in granulomata are associated with active TB (Ramakrishnan, 2012). Dysregulated inflammation at the site of disease may also contribute to tissue destruction and cavitation, for example by production of matrix metalloproteinases (Elkington et al., 2011).

Studies in the macaque Mtb infection model have also demonstrated that the CMI response in granulomata can contribute to active disease, by demonstrating the heterogeneity of granulomata *in vivo*. Animals with both latent and active infection were shown to have a spectrum of lesion types, from healed fibrous sterile lesions, to caseating lesions with high bacillary burdens (Lin et al., 2014, 2009). However, in animals with active disease, there were more caseating granulomata with extensive tissue pathology (Lin et al., 2014). This indicated that the granulomatous CMI response had the potential to contain bacteria and sterilize sites of disease in all animals, but that stochastic degenerative events in individual granulomata caused some animals to develop active disease.

It can be assumed that the nature of the immune response contributes to these stochastic determinants of granuloma degeneration, and resulting active disease, and that risk factors such as HIV-1 which dysregulate CMI increase the likelihood that the immune response at the site of TB disease will not be appropriately balanced to mediate microbial killing without exacerbated inflammation. Considering the nature of TB disease in HIV-1^+ individuals lends support to this, as the natural history of TB is drastically altered by HIV-1 co-infection.

1.4.4 HIV-1 and TB

TB co-infection is the leading cause of death in HIV-1^+ individuals (UNAIDS, 2013). Globally, the incidence of active TB in HIV-1^+ individuals is approximately twenty times greater than in HIV-1^- individuals (Lawn and Churchyard, 2009), and risk is increased in all HIV-1^+ patients, including those with preserved $CD4^+$ counts (Sonnenberg et al., 2005). HIV-1 co-infection severely alters the natural history of TB. Although HIV-1^+ individuals with preserved $CD4^+$ counts may present with typical pulmonary TB, those with $CD4^+$ counts of less than 200/mm^3 often have atypical presentations of pulmonary TB and extra-pulmonary manifestations (Zumla et al., 2013). Individuals with severely depleted $CD4^+$ counts (<50/mm^3) often present with disseminated TB disease, characterised by a non-specific febrile illness with

widespread organ involvement and mycobacteraemia (Domoua et al., 1995; Elliott et al., 1993; Gilks et al., 1990; von Reyn et al., 2011).

In addition to aberrant clinical phenotypes, the underlying pathology of TB may be altered in HIV-1$^+$ individuals. Radiological features of pulmonary TB have been reported to be different, with less consolidation, apical involvement and bronchopulmonary spread, but higher rates of pleural effusions and lymphadenopathy (Lawn et al., 1999). Tissue pathology studies have also described altered phenotypes, particularly in severely immunosuppressed patients where granulomata are often absent or poorly formed (Lawn and Zumla, 2011). Other observations from the site of disease in HIV-1$^+$ individuals, when compared to HIV-1$^-$ individuals, have shown increased granuloma necrosis and polymorphonuclear cell infiltration (de Noronha et al., 2008); increased TNFα levels and necrosis in pleural granulomata (Bezuidenhout et al., 2009); increased rates of apoptosis in cells from pleural fluid (Hirsch et al., 2001); and a paucity of inflammation accompanied by many extracellular bacilli in tuberculous lymphadenitis biopsies (Nambuya et al., 1988). Although TB tissue pathology may not be atypical in relatively immunocompetent HIV-1$^+$ individuals (Walker et al., 2013), there is clearly a spectrum of pathology associated with HIV-1 that illustrates potent dysregulation of anti-mycobacterial immune responses by the virus.

This poses the question of which of the immune responses that are affected by HIV-1 mediate these effects on TB natural history? CD4$^+$ depletion does correlate with increased rates of atypical TB presentation (Zumla et al., 2013), and the extent of initial CD4$^+$ depletion by SIV correlates with the time to TB reactivation in the macaque model of SIV/TB co-infection (Diedrich et al., 2010; Mattila et al., 2011). Low numbers of CD4$^+$ cells are observed at the site of disease in HIV-1+ patients, indicating that systemic depletion does translate into differences in *in situ* CMI responses (Law et al., 1996). Additionally, Mtb-specific T cells may be preferentially depleted by HIV-1 due to their higher CCR5 expression, meaning that TB risk would be hypersensitive to CD4$^+$ loss (Geldmacher et al., 2012, 2010).

However, the increased risk of TB in HIV-1$^+$ individuals before CD4$^+$ depletion has strongly indicated that other changes in immune function may also contribute to disease risk. One hypothesis is that T cell function is altered in a way that compromises TB protection (O'Garra et al., 2013), and investigations have shown that the frequency of polyfunctional mycobacteria-specific T cells (i.e. those producing

IFNγ, TNFα and IL-2) are lower in the lungs of HIV-1$^+$ individuals compared to healthy individuals, although this study was not performed in patients with active TB (Kalsdorf et al., 2009). Another report in HIV-1$^+$ individuals with ongoing active TB showed increased numbers of polyfunctional T cells at the site of disease (Matthews et al., 2012), and no consensus has yet emerged about the contribution of T cell functionality.

An alternative hypothesis is that dysfunction of HIV-1-infected macrophages contributes to increased TB risk, and this is further discussed in **section 1.4.5**. Other proposed mechanisms include dysregulation of MMPs in HIV-1$^+$ individuals causing tissue damage, although observations that MMP levels are lower in the sputum of HIV-1$^+$ active TB patients do not support this suggestion (Walker et al., 2012). Finally, the increased rates of HIV-1 replication which are observed at the site of TB disease (Lawn et al., 2001; Nakata et al., 1997) has suggested that a direct effect of viral replication *in situ* may exacerbate immunopathology (Diedrich and Flynn, 2011), although the mechanisms by which this would compromise control are unclear.

No all-encompassing theory of how HIV increases TB risk has yet emerged. It is likely that several factors contribute to this interaction (Diedrich and Flynn, 2011), and the diversity of clinical presentations & pathology observed in HIV-1/TB co-infection may reflect the diverse effects of HIV-1 on the immune response (Walker et al., 2013). The fact that HIV-1 is the strongest known risk factor for TB suggests that the parts of the immune system which are dysregulated by HIV-1, including those involved in mediating CMI, are essential for protection against active TB. Increased understanding of how HIV-1 modulates CMI is therefore critical for understanding HIV-1/TB co-infection pathogenesis. The role of macrophages, as a host cell for both HIV-1 and Mtb infection, may be critical in this.

1.4.5 Macrophages, HIV-1 and Mtb

Both HIV-1 and Mtb parasitize macrophages *in vivo* as a niche for growth and persistence which may contribute to disease. It is possible that co-infection of macrophages by both pathogens may take place *in vivo*, particularly in the respiratory tract wherein both may infect AMs. This has posed the question of whether the increased risk of TB in HIV-1$^+$ individuals may result from dysregulation of macrophage/Mtb interactions by HIV-1 co-infection. As discussed in **section 1.3.9**, HIV-1 infection of macrophages may result in a range of dysregulated phenotypes, including some involving Mtb. These include increased intracellular growth of Mtb in

HIV-1 infected MDMs (Imperiali et al., 2001; Pathak et al., 2010), which may be due to effects of HIV-1 on autophagic pathways which are critical in macrophage control of TB (Gutierrez et al., 2004; Kyei et al., 2009). Exaggerated pro-inflammatory responses and dysregulation of apoptosis have also been reported in HIV-1/Mtb co-infected macrophages (Patel et al., 2007; Pathak et al., 2010).

HIV-1 replication is also reported to be modulated in co-infected macrophages, although there has been some controversy about whether Mtb promotes viral replication (Honda et al., 1998; Hoshino et al., 2004, 2002; Toossi et al., 1997) or inhibits it (Goletti et al., 2004; Weiden et al., 2000). Reports from sites of TB disease *in vivo* in co-infected individuals have shown high levels of HIV-1 (Collins et al., 2002b; Lawn et al., 2001; Nakata et al., 1997), and a mechanism involving Mtb activation of the transcription factor NFAT and subsequent transactivation of the HIV-1 LTR has been described (Ranjbar et al., 2012); these observations support the concept that HIV-1 replication increases in co-infected macrophages, although this is likely to vary with temporal and Mtb-strain-specific conditions (Ranjbar et al., 2009).

Previous work in our group has investigated the consequences of HIV-1/Mtb co-infection of macrophages, using a well-characterised *in vitro* MDM model in which confluent HIV-1 infection can be established (Noursadeghi et al., 2009). This work has found that expression of the anti-inflammatory cytokine IL-10 in response to Mtb is attenuated in HIV-1 infected macrophages, potentially as a result of attenuated signalling through MAP kinase pathways (Tomlinson et al., 2014) – a previously unreported phenotype. This deficiency in IL-10 was associated with exaggerated and sustained pro-inflammatory macrophage responses to Mtb. These *in vitro* data were mirrored by identification of lower levels of IL-10 and higher levels of pro-inflammatory IL1β in respiratory samples from HIV-1 infected patients with pulmonary TB in comparison to non-tuberculous respiratory infections, suggesting that the same immunological phenotype may occur *in vivo*.

Attenuation of IL-10 by HIV-1 might be caused by a novel host/virus interaction affecting common macrophage IL-10 induction pathways, and so this observation might also be applicable in responses to other co-infecting pathogens. IL-10 is known to have a range of potent immunomodulatory functions (described further in **section 1.5**), and so this phenotype may have consequences which contribute to dysregulation of CMI and immunopathogenesis in HIV-1/TB co-infection. Therefore, further characterisation of this phenotype and its consequences, and identifying the

mechanism by which HIV-1 causes IL-10 attenuation merits further investigation, which may also provide insight into the regulation of IL-10 responses in macrophages.

1.5 Interleukin-10

1.5.1 The IL-10 and IL-10 receptor family

Although most cytokines induce pro-inflammatory or immune-activating processes, several have been identified that have anti-inflammatory activities which are essential for producing a balanced immune response capable of pathogen clearance with limited immunopathology. Among these, interleukin-10 (IL-10) is considered to be non-redundant in the initial anti-inflammatory component of the immune response (Iyer and Cheng, 2012). IL-10 is a homodimeric secreted protein produced by immune cells, which mediates potent negative regulation of immune responses by gene-specific transcriptional repression and up-regulation of factors that modulate immune signalling pathways (Iyer and Cheng, 2012; Moore et al., 2001). It was first identified as a factor produced by Th2 $CD4^+$ T cells, which was capable of suppressing Th1 responses, and was subsequently found to be produced by other cells including B cells, mast cells and macrophages, and to be broadly suppressive with regard to many cell types (O'Garra & Murphy, 2009).

The human IL-10 protein is relatively highly conserved, with 73% homology to mouse IL-10, and has an α-helical bundle structure classic of many cytokines including IFNs (Moore et al., 2001). The secreted IL-10 homodimer signals via a receptor complex made up of IL-10R1 and IL-10R2, of which IL-10R1 is the ligand-binding subunit with some signalling activity, and IL-10R2 purely functions in signalling (Moore et al., 2001). As IL-10R2 is constitutively expressed in most cells, IL-10R1 expression determines IL-10 responsiveness (Moore et al., 2001). IL-10R1 is expressed on most haematopoietic cells at relatively low levels, but most highly on macrophages and DCs, and its expression can be regulated by cellular activation (Murray, 2006; Tan et al., 1993). Expression on fibroblasts and in intestinal epithelium has also been observed (Denning et al., 2000; Weber-Nordt et al., 1994). Binding of IL-10 to its receptor complex initiates a cascade of signalling: the receptor-associated kinases JAK1 and TYK2 are phosphorylated and activated, leading to recruitment and phosphorylation of STAT3 (Carey et al., 2012; Finbloom and Winestock, 1995; Riley et al., 1999; Rodig et al., 1998; Weber-Nordt et al., 1996). Activated STAT3 homodimerises and translocates to the nucleus (Pranada et al., 2004) wherein initiates transcription to mediate the

downstream functions of IL-10 (described subsequently in **section 1.5.3**). It should also be noted that seven other cytokines, along with IL-10, form the IL-10 cytokine superfamily; these cytokines generally signal via other receptors and have a range of divergent effects on immunity and inflammation (Commins et al., 2008).

1.5.2 Regulation of IL-10 production

IL-10 can be produced by many immune cells *in vivo*, but T cell subsets and MPs such as monocytes, macrophages and cDCs are the main cell types involved (Murray, 2006). Most $CD4^+$ T helper subsets can produce IL-10 in some contexts, and this is thought to be partly regulated by subset-specific signals (Cretney et al., 2011; Saraiva and O'Garra, 2010; Saraiva et al., 2009; Shoemaker et al., 2006). A central role for ERK signalling has been suggested (Saraiva et al., 2009), but the mechanisms controlling production in T cells are not well delineated (Iyer and Cheng, 2012). However, IL-10 induction pathways in macrophages and other MPs downstream of pattern recognition have been extensively described, and are thought to involve an array of transcriptional and post-transcriptional regulatory mechanisms (summarised in **Figure 1.3**).

TLR-2 and dectin-1 are central PRRs in IL-10 induction (Kelly et al., 2010; Moreira et al., 2008; Netea et al., 2004), and have been shown to be synergistic in this regard (Ferwerda et al., 2008). TLR-3, TLR-4, TLR-9 and NOD2 stimulation have also been shown to induce macrophage IL-10 production (Boonstra et al., 2006; Moreira et al., 2008). PRR stimulation activates complex arrays of signalling pathways (**section 1.2.6**), and accordingly IL-10 is regulated via several axes. The MAPK cascades via p38 and ERK are thought to be critical (Chanteux et al., 2007; Elcombe et al., 2013; Ma et al., 2001; Yi et al., 2002), and both signalling strength through this pathway and negative regulation of its activity contribute to fine-tuning of IL-10 production (Chi et al., 2006; Kaiser et al., 2009; Saraiva and O'Garra, 2010). MAPKs, along with NFκB signalling (Banerjee et al., 2006; Gringhuis et al., 2007), calcium-burst signalling downstream of dectin-1, CaM kinase II and Pyk2 (Kelly et al., 2010), and some PI3K-stimulated pathways (Hu et al., 2006), activate a range of transcription factors which may influence IL-10 transcription. These include Sp1, IRFs, CREB, C/EBP, c-MAF and NFκB; which of these are necessary and sufficient for IL-10 transcription is still not clarified, although Sp1 is suggested to have a critical role (Brightbill et al., 2000). Regulation at this level may be highly stimulus-specific (Saraiva and O'Garra, 2010). Chromatin remodelling at the IL-10 locus may also influence IL-10 transcription; this

has been shown to occur at the IL-10 locus downstream of LPS stimulation of macrophages (Saraiva et al., 2005), and histone modifications of the locus also contribute to control of expression (Cheng et al., 2014; Villagra et al., 2009). Active negative regulation of IL-10 transcription has been demonstrated: suppression by factors including CIITA, STAT1 and BCL-6 has been demonstrated, but whether all these pathways operate in macrophages is not clear (Saraiva and O'Garra, 2010). The IκB protein BCL-3 has been shown to negative regulate IL-10 expression in murine macrophages, via regulation of the initiation of IL-10 transcription (Riemann et al., 2005).

Post-transcriptional mechanisms also contribute to regulation of macrophage IL-10 production. Like many other cytokines, IL-10 mRNA has destabilizing motifs in the 3' untranslated region (Powell et al., 2000) and is a target for the RNA-degradation mediator, tristetraprolin (Stoecklin et al., 2008). IL-10 regulation by miRNAs, which act on mRNA to increase degradation or prevent translation, has also been demonstrated downstream of TLR-2 and TLR-4 signalling (Xie et al., 2014). Finally, mechanisms acting on translation have been described. The activity of the PI3K pathway, mediated by Akt and ultimately through mTOR, has been reported to determine the magnitude of IL-10 production via global effects on the efficiency of translation; this allows distinct regulation of anti-inflammatory IL-10 production vs. pro-inflammatory cytokine production in a phenomenon termed "cytokine biasing" (Ivanov and Roy, 2013; Weichhart et al., 2008).

Another line of evidence suggests that there may be indirect control of IL-10 production in the innate immune response, via PRR-induced type I IFN production which feeds back to induce IL-10 in a circuit which may also involve the production of IL-27 (Chang et al., 2007; Iyer and Cheng, 2012). However, other reports suggest that type I IFNs can inhibit IL-10 production (Lin et al., 2013), and so this mechanism is not yet clarified. However, it is representative of the complex molecular mechanisms which control IL-10 expression in macrophages. This complexity is likely to be linked to the fine balance which is required in its expression, owing to the potency of its suppressive functions.

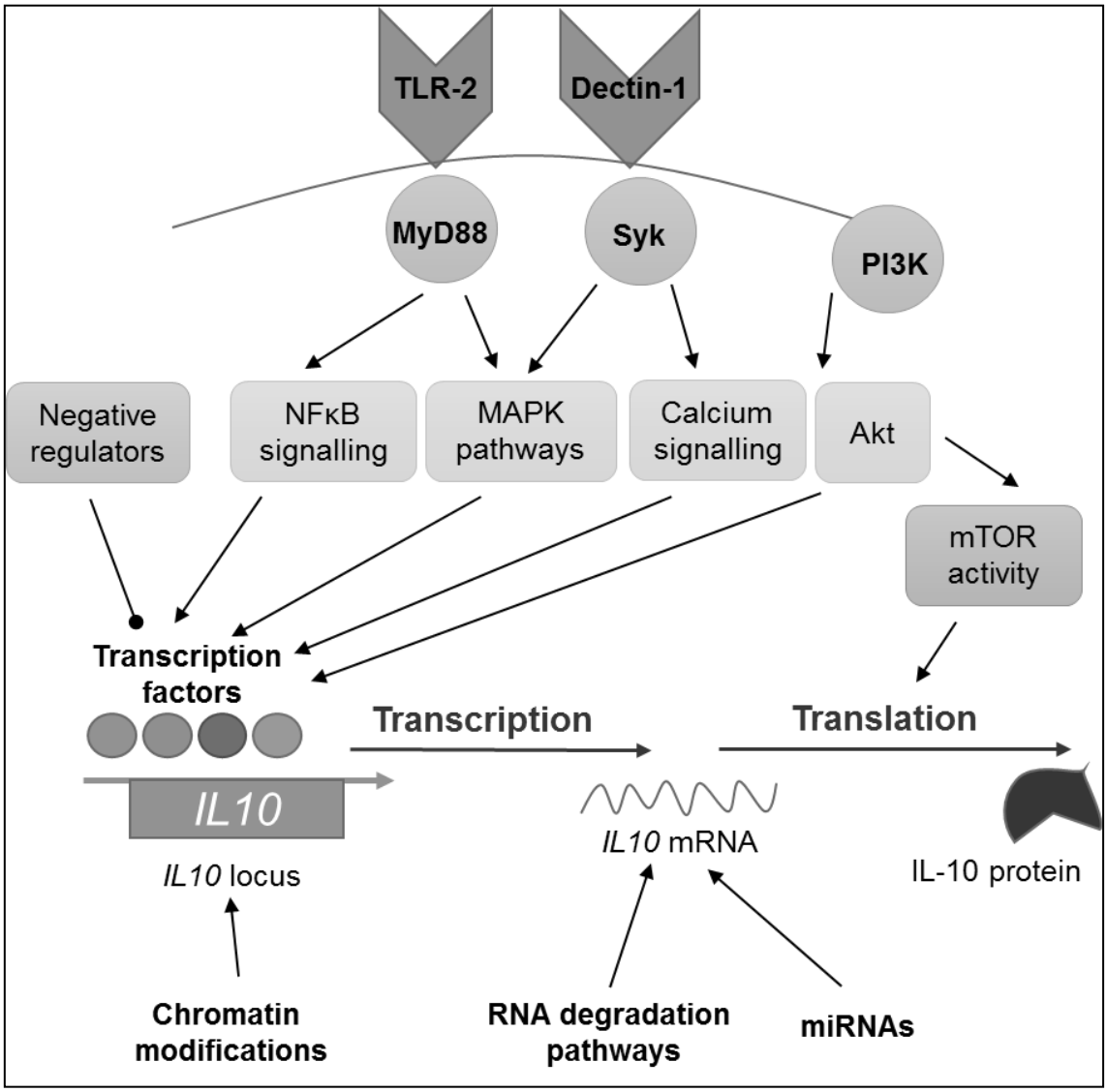

Figure 1.3: Regulation of IL-10 expression in macrophages.

1.5.3 Functions of IL-10

IL-10 signalling activates the transcription factor STAT3, which has been shown to be essential for all described functions of IL-10 (Williams et al., 2004; Williams et al., 2007). The main targets for IL-10 signalling are the MPs: macrophages, DCs and monocytes, which express the highest amounts of IL10R1 (Murray, 2006), although most other immune cells may respond to IL-10 in some context (Iyer and Cheng, 2012). IL-10 signalling may occur in a paracrine or an autocrine fashion; autocrine signalling in macrophages downstream of PRR activation has suggested to be an important auto-regulatory axis (Lang et al., 2002c; Murray, 2006).

The downstream functions of IL-10/STAT3 signalling have been termed the “anti-inflammatory response” (AIR), and it has been shown in macrophages that the overall outcome of the AIR is selective inhibition of transcription of components of the inflammatory response (Murray, 2005). However, STAT3 is a positive transcriptional regulator, and mediates the AIR in macrophages indirectly by inducing the transcription of “AIR factors”: various transcription factors and signalling modulators which then exert the AIR (Hutchins et al., 2012). Some AIR factors have been identified via gene expression studies of IL-10 stimulated cells (Antoniv et al., 2005; Hutchins et al., 2012; Park-Min et al., 2005; Stumpo et al., 2003), and include molecules such as SOCS3, which regulates pro-inflammatory cytokine signalling (Berlato et al., 2002; Niemand et al., 2003; Yasukawa et al., 2003); BCL3, which limits the production of TNFα via NFκB signalling suppression (Kuwata et al., 2003; Wessells et al., 2004); Zfp36, which targets TNFα mRNA for degradation (Gaba et al., 2012; Schaljo et al., 2009); and Nfil3, while regulates IL-12 expression (Kobayashi et al., 2011). Suppression of NFκB signalling and potent inhibitory effects on TNFα production are common themes of the AIR (Chan et al., 2012; Driessler et al., 2004; Smallie et al., 2010). However, the suppressive effects of IL-10 are not uniform across the entire pro-inflammatory response; a study in mouse macrophages showed that IL-10 negatively regulated approximately 15–20% of the response to LPS (Lang et al., 2002a). The significance of which components of the inflammatory response are regulated by IL-10, and which are not, is not yet clarified (Murray, 2006), and limited data exists investigating the intricacies of this pathway in human macrophages.

Various cellular phenotypes have been described which result from these molecular mechanisms of IL-10 signalling. Macrophages and other APCs, as well as being subject to inflammatory response auto-regulation, are suggested to take on an anti-inflammatory phenotype (variously described as M2, alternatively activated or regulatory; Mantovani *et al.*, 2004). These effects of IL-10 on APCs lead to inhibition of Th1-polarised responses (Fiorentino et al., 1991, 1991) and may act to promote resolution of inflammation (Ogawa et al., 2008). In T cells, IL-10 signalling may directly suppress Th1 effector functions such as IFNγ production, but this mechanism is less clear than its indirect modulation of Th1 responses via APCs (Del Prete et al., 1993; Redford et al., 2011). Despite its original description as a Th2 factor, IL-10 has also been shown to suppress Th2-driven responses in some contexts (Grunig et al., 1997). Induction of a Treg phenotype is another described function of IL-10 (Horwitz et al., 2003), which may potentiate regulatory function via the production of further IL-10. The overall effects of IL-10 on B cells and NK cells are less clear; it has been shown to modulate activation of these cells in some reports (Go et al., 1990; Itoh and Hirohata, 1995; Shibata et al., 1998; Stacey et al., 2011). Another key cellular phenotype controlled by IL-10 is apoptosis. Its anti-apoptotic functions have been described both *in vitro* and *in vivo* (Eslick et al., 2004; Geng et al., 2000; Penttilä et al., 2008; Zhou et al., 2001), and it may act either directly, or indirectly via TNFα regulation, to mediate these (Cyktor and Turner, 2011).

The potent effects of IL-10 on a range of immune cells suggest its signalling may have significant consequences for disease and inflammation. Many studies of physiological IL-10 function have been performed in mouse models of IL-10 deficiency, signalling blockade, or supplementation, and examples of phenotypes observed in these models are presented in **Table 1.11**. The baseline phenotype of the IL-10 deficient mouse model is severe spontaneous enterocolitis, and the important role of IL-10 in maintaining gut homeostasis has recently been attributed to its effects on gut-resident macrophages (Kühn et al., 1993; Shouval et al., 2014; Zigmond et al., 2014). Various models using inflammatory and infectious challenges have elucidated the importance of IL-10 in limiting immunopathology, as deficient mice are hypersusceptible to endotoxin-induced shock, contact hypersensitivity, and succumb rapidly in some infections due to exacerbated inflammation in the absence of IL-10 regulation (Berg et al., 1995a, 1995b; Gazzinelli et al., 1996; Hunter et al., 1997; Li et al., 1999). However, in some contexts IL-10 is shown to limit control of infections due to its suppressive effects on microbicidal functions; this is most clear in the context of

persistant viral infections (Brooks et al., 2006; Ejrnaes et al., 2006), but also in bacterial infections such as *Salmonella enterica* serotype Typhimurium and *Yersinia pestis* (Lokken et al., 2014; Sing et al., 2002). The discovery of functional viral IL10 homologues supports the concept that IL10 expression may confer an evolutionary advantage to pathogens in some contexts (Ouyang et al., 2013). An overall picture of the role of IL-10 in infections has emerged wherein IL-10 exerts regulation which must be limited to allow pathogen clearance, but sufficient to prevent immunopathology (Couper et al., 2008). It is suggested that features of particular infections determine the net outcome of its signalling; for pathogens which induce lots of inflammation, IL-10 signalling may be critical in preventing disease, but for persistent pathogens which have adapted to avoid killing, IL-10 signalling may exacerbate disease by further preventing microbicidal functions (Cyktor and Turner, 2011).

In humans, the precise role of IL-10 in regulating inflammation is not as well elucidated as in mice. Its homeostatic role in the gut is clear, as IL-10 receptor mutations have been found in patients with spontaneous severe inflammatory bowel disease (Glocker et al., 2009). IL-10 polymorphisms, including promoter haplotypes which influence levels of gene expression, have been described which contribute to the risk or severitiy of inflammatory and infectious diseases such as graft vs. host disease, hepatitis C virus and community-acquired pneumonia (Edwards-Smith et al., 1999; Gallagher et al., 2003; Lin et al., 2003; Paladino et al., 2006), and treatment of patients with HCV with recombinant IL-10 was shown to limit the tissue damage caused by chronic inflammation (Nelson et al., 2000) – again suggesting that IL-10 limits damaging immunopathology in humans as well as in mice.

The potential role of IL-10 in regulating CMI is clear from its described effects in modulating macrophage and T cell function, and this is supported by the observation that infections by intracellular pathogens such as *Listeria monocytogenes*, *Salmonella enterica* serotype Typhimurium, *Toxoplasma gondii* and *Toxoplasma cruzii* have altered phenotypes in mouse models in the context of IL-10 deficiency (**Table 1.11**). Inhibition of macrophage IL-10 production by HIV-1 (**section 1.3.9**) may therefore have substantial consequences for the regulation of CMI, and pathology caused by intracellular pathogens such as Mtb.

Mouse model	Phenotype	Reference
IL-10 −/−	Spontaneous chronic enterocolitis	Kuhn *et al.* (1993)
	Excessive inflammation & death after *Trypanosoma cruzi* infection, but improved parasite clearance	Hunter *et al.* (1997); Holscher *et al.* (2000)
	Excessive inflammation & death after *Toxoplasma gondii* infection	Gazzinelli *et al.* (1996)
	Excessive inflammation & death after *Listeria monocytogenes* meningoencephalitis	Deckert *et al.* (2001)
	Increased morbidity and mortality in malaria infection but improved parasite clearance	Li *et al.* (1999)
	Protection against *Yersinia pestis* infection	Sing *et al.* (2002)
	Hypersensitive to endotoxin-induced shock	Berg *et al.* (1995a)
	Exaggerated contact hypersensitivity response	Berg *et al.* (1995b)
	Impaired resolution of lung inflammation	Aggarwal *et al.* (2014)
Neutralization of IL-10 via antibody	Improved control of *Salmonella typhimurium* co-infection during malaria infection	Lokken *et al.* (2014)
Blockade of IL-10 signalling by neutralising antibody to IL-10R	Increased inflammation but improved parasite control in *Leishmania* infection	Gonzalez-Lombana *et al.* (2013)
	Resolution of chronic viral infections	Ejrnaes *et al.* (2006); Brooks *et al.* (2006)
IL-10 −/−: macrophage/neutrophil-specific	Enhanced inflammatory response to LPS	Siewe *et al.* (2006)
IL-10 −/−: T cell-specific	Excessive inflammation & death after *Trypanosoma cruzi* infection, but protected from LPS and skin irritant hypersensitivity	Roers *et al.* (2004)
IL-10 supplementation to WT	Protection from endotoxin-induced shock	Howard *et al.* (1993)
	Protection from acute induced pancreatitis	Kusske *et al.* (1996)

Table 1.11: Effects of IL-10 on infection and inflammation in mouse models.

1.5.4 The role of IL-10 in tuberculosis

The role of IL-10 in regulating TB disease has been extensively researched (Redford et al., 2011). The known functions of IL-10 in regulating Th1 responses and macrophage microbicidal functions could clearly impact on control of Mtb; however, it also regulates the inflammation associated with TB immunopathology, suggesting that the contribution of IL-10 to TB disease may be dichotomous. Accordingly, investigations of TB in mouse models have described a spectrum of phenotypes, from those in which IL-10 deficiency improves control of TB with reduced bacterial loads in deficient mice (Beamer et al., 2008; Redford et al., 2010; Turner et al., 2002), to those in which it is unaffected (Jung et al., 2003; North, 1998), to those in which it exacerbates immunopathology (Higgins et al., 2009). Different inbred mouse strains are known to have different inherent susceptibilities to Mtb, which may somewhat account for this range of observations (Redford et al., 2011). As such it is difficult to draw any overall conclusions from this body of work, except from the broad observation that dysregulation of IL-10 can compromise TB control or cause immunopathology in a context-dependent manner. Differences between human and mouse TB, such as the inability to establish latent infection also make it difficult to extrapolate from this model to human disease (Flynn, 2006).

IL-10 is thought to contribute to human TB, as it can be measured at the site of disease in active TB patients (Barnes et al., 1993). Studies of IL-10 function in active TB patient PBMC have shown that it can inhibit proliferation and IFNγ production by T cells (Gong et al., 1996; Zhang et al., 1994). Although this demonstrates the potentially suppressive role of IL-10 in TB, it does not provide insight into the potential function of IL-10 at the site of disease, in which its roles in regulating resolution, tissue damage and apoptosis could be critical. One study has reported that a polymorphism that increases the risk of pulmonary TB also increases IL-10 levels, providing some indication that it may compromise protection (Awomoyi et al., 2002); however, a metaanalysis of the contribution of IL-10 polymorphisms to risk of TB showed no overall effect (Pacheco et al., 2008).

Overall, the postulated function of IL-10 in human TB is mainly still derived from knowledge about its functions and how these impact on the immune response to TB. As described above, its inhibitory effects on the Th1 axis of immunity have the potential

to compromise protection. However, as IL-10 is a potent regulator of TNFα responses and apoptosis (Cyktor and Turner, 2011), it seems likely that it may also feed into the TNFα-balance and cell death determinants of TB immunopathology (as discussed in **section 1.4.3**), and again may be subject to a "Goldilocks effect" in terms of too much or too little IL-10 being damaging. However, this hypothesis has not been formally demonstrated. It has also been shown that IL-10 may inhibit phagolysosome maturation in Mtb-infected human macrophages (O'Leary et al., 2011), suggesting that it may also impact on macrophage parasitism by the pathogen.

The role of IL-10 in regulating the immune response to TB is clearly complex. This is a scenario in which there is substantial host-damaging inflammation, which IL-10 can regulate, but also in which the pathogen persists and subverts killing, which IL-10 may compromise. In terms of the effects of HIV-1-mediated IL-10 attenuation for HIV-1-associated mycobacterial disease, existing knowledge about the role of IL-10 mainly indicates that this phenotype has the potential to dysregulate host immunity, but the precise downstream consequences are not clear and merit further investigation. It should also be noted that due to systemic immune dysfunction in HIV-1 infection, the consequences of IL-10 inhibition may have context-specific effects, as the normal role of IL-10 in the immune system is likely to be altered by concurrent HIV-1 infection. Notwithstanding the complexity of these interactions, investigation of the consequences of this potent mechanism of CMI dysregulation by HIV-1 is likely to provide valuable insights into pathogenesis in HIV-1/TB co-infection.

1.6 Investigating immune responses using transcriptional profiling

1.6.1 Using transcriptional profiling to understand immune responses in tuberculosis *in vivo*

Of the various –omics technologies, transcriptomics or transcriptional profiling, in which the expression of thousands of transcripts is measured simultaneously in one sample, has perhaps been used most widely to gain biological insights. The main advantage of transcriptional profiling, as with other –omics technologies, is that it can provide systems-level insights into biology, with resolution of these systems at the molecular level. For investigating cells, transcriptional profiling can provide a broad impression of cell state; at the tissue level, it can be used to assess the overall activity of tissues in homeostasis and disease. Key insights using transcriptional profiling of tissues have been made in a range of human diseases, including cancer and autoimmune conditions (Chaussabel et al., 2008; Rhodes et al., 2005).

As a major human disease in which the immune response remains poorly understood, TB is a clear candidate for systems-level analysis via transcriptional profiling. To date, this has mainly been performed using peripheral blood samples from active TB patients and appropriate comparator groups (latent TB, healthy individuals, etc). Evaluating the blood is suggested to be a suitable method, as it contains immune effector cells which may traffic from the site of disease (Berry et al., 2013), and various insights have indeed been gained from these studies. Dominant IFN signatures driven by neutrophil and monocyte activity in the peripheral blood have been identified, which are specifically associated with active TB as opposed to latent disease (Berry et al., 2010; Maertzdorf et al., 2012; Ottenhoff et al., 2012). These signatures may have diagnostic and therapeutic utility, as they can differentiate TB from some other conditions, and may correlate with the resolution of disease throughout chemotherapy (Bloom et al., 2013, 2012; Cliff et al., 2013).

However, there are arguably major limitations in studying TB in the peripheral blood. The site of disease is known to be crucial in determining disease outcome in TB (Lin et al., 2014), and although the blood transcriptome may reflect activity at the disease site (as the signatures seen resolve with recovery from active disease; Berry et al., 2013), it

clearly has a very different cellular and structural milieu. Regardless of whether the blood is an appropriate tissue to study, transcriptional profiling of the site of disease would certainly provide further insights into mechanisms of pathogenesis, as it has in other settings such as leprosy and transplantation (Cantu et al., 2013; Teles et al., 2013). However, the site of disease in TB usually has limited accessibility, and so collecting appropriate samples for this purpose may be challenging. It may be even more challenging to obtain samples which can be robustly evaluated comparatively (i.e. to assess the effect of HIV-1 co-infection on TB) which are appropriately controlled in terms of time of disease, site of disease and other aspects of disease heterogeneity.

An approach recently developed by our group to assess anti-mycobacterial immune responses *in vivo* in humans may assist in overcoming these various limitations, by using the TST, a classic model of CMI/DTH, as a standardised human challenge model, from which RNA samples can be collected and assessed by transcriptional profiling. Using this method in healthy individuals has provided a proof-of-concept that it can characterise CMI *in vivo* in an inflamed site, and provide molecular-level insights into the anti-mycobacterial immune response (Tomlinson et al., 2011). As a tissue model which contains macrophages and infiltrating T cells, it is arguable that it provides a stronger surrogate for the site of TB disease than the peripheral blood, although clearly aspects of pulmonary inflammation may not be replicated here. However, this method provides an attractive option for performing comparative studies of immune responses to tuberculosis *in vivo* in particular groups of patients, for example those with HIV-1 co-infection.

1.6.2 Transcriptional profiling analysis

To gain reliable insights into biological systems by using transcriptional profiling, it is clear that robust analysis methods are required. Traditional methods include feature selection analysis, in which statistical testing and fold-change difference cut-offs are used to identify differences in transcript levels across gene expression profiles. This method is crucial for generating lists of differentially expressed transcripts, but does not provide any inherent systems-level insights. These are generally gained by further downstream assessments using bioinformatics methods such as pathway, gene ontology or transcription factor binding site enrichment analyses.

In addition to these supervised methods of exploring transcriptomic data, unsupervised clustering methods, such as principal component analysis (PCA), can provide powerful insights. PCA is a unsupervised exploratory statistical method which can be used to assess variance across a large data set in such a way that retains more information than simple hierarchical clustering (Chain et al., 2010; Ringnér, 2008). It identifies directions (components) across which the variation in the data is maximal. Each sequential principal component (PC) identified by the PCA algorithm describes variation in a new direction, which is uncorrelated to the previous components identified. PCA can thus be used to gain an impression of the overarching patterns of variation within a set of gene expression datasets, by describing multiple distinct relationships between samples. The PCA algorithm output assigns each sample a numerical value within each identified component (a PC score). This simplifies visualisation of the highly multidimensional data, as each sample can be represented by a single PC score for each component, rather than by using the many thousands of expression values which contribute to this (Ringnér, 2008).

The power of PCA lies in its ability to deconvolute highly multidimensional gene expression data into a restricted set of components which can be used for simple cross-sample comparisons. Another method of gene expression data deconvolution is modular analysis, which is a powerful method for assessing the activation of pathways of biological interest in gene expression profiles.

1.6.3 Modular analysis of transcriptomic data

Modular analysis, in which the expression of defined sets of genes of interest is measured as a unified variable, has been widely used in recent years for analysis of transcriptomic data, initially in the fields of cancer biology and diabetes, and subsequently in immunology (Chaussabel et al., 2008; Li et al., 2014; Rhodes et al., 2005; Segal et al., 2003). It is postulated to be an intuitive systems-based approach for exploring gene expression datasets (Chaussabel and Baldwin, 2014), and may be superior to traditional methods such feature selection for a number of reasons. It does not rely as heavily on user-selected cut-offs or ranking methods (Chaussabel and Baldwin, 2014), and by defining *a priori* gene sets of interest, it may be less subject to bias than *post hoc* assessments of functional enrichment (Mootha et al., 2003). It may also be less susceptible to confounding by multiple testing (Subramanian et al., 2005) or cross-platform transcriptomic comparisons – i.e. those in which compared datasets are generated using different platforms – as measuring sets of genes is presumably

less likely to be affected by statistical noise or technological differences than assessment of a single transcript (Chaussabel and Baldwin, 2014). The overarching advantage of modular analysis may be the increased power of assessing gene expression changes at the level of sets of genes, rather than at the level of single genes, which seems plausible when biological systems are considered at the pathway level (Subramanian et al., 2005).

Two principal methods of generating modules have been employed. Firstly, data-driven modules, which use the expression values in a collection of transcriptome datasets of interest to build co-clustering networks of transcript correlations. Sets of transcripts which behave in a similar way in that particular setting are extracted from the network in an unsupervised manner to construct repertoire of modules, which can then be functionally explored and defined as being associated with particular functional axes – relying on the premise that co-clustering will be driven by functional associations (Chaussabel and Baldwin, 2014). The activity of these modules can then be assessed in similar types of datasets to those used to generate the module. Limitations of this method lie in the ability of the investigator to associate a given module with a plausible function, which is somewhat reliant on individual expertise and/or the availability of appropriate bioinformatics tools, and also the assumption that co-correlation of transcriptomic data will provide superior functional insight than purely providing an assessment of differential cell numbers within the source dataset. Data-driven modules have been employed extensively for analysis of peripheral blood transcriptomic data, where they have provided valuable insights into disease phenotypes, including in TB (Berry et al., 2010; Bloom et al., 2013).

The second method of module generation can be described as hypothesis-driven. In this method, the modular activity that the user wishes to assess is defined *a priori* – for example, the activity of a particular cytokine or the phenotype of a specific cell. There are two options for deriving such a module; (a) to use a curated gene list from a bioinformatics source which pertains to the module of interest, or (b) to use experimental transcriptomic data, either from curated gene expression data repositories or generated independently, to build a stimulus/cell-specific gene list. Both methods have been used successfully to gain specific biological insights (Cantu et al., 2013; Mootha et al., 2003; Rhodes et al., 2005; Teles et al., 2013). As this is a supervised method, there is a considerable degree of user determination in setting the parameters for what genes should make up a module. For the bioinformatics approach, this relates to the resources selected to obtain gene lists. For the transcriptome-derived

approach, there is firstly the question of what experimental setup will provide the most appropriate data for module derivation. There are then multiple options for extracting a gene list from the dataset, pertaining to statistical or fold-change thresholds, correlation analyses and specificity filters. For testing specific hypotheses, this module generation approach is arguably superior to data-driven modules, as it provides an increased degree of confidence that a module is strongly associated with the context of interest, rather than requiring external verification of the module's nature. Furthermore, although data-driven modules can provide valuable insight into a particular system, the unsupervised approach used may mean that a desired module is not generated and so that particular pathway cannot be assessed in that system.

A reliable modular analysis method also relies on selecting an appropriate measurement for evaluation of whether expression of a module is enriched in a dataset of interest in comparison to control or other datasets. Similarly to generating modules, multiple strategies have been developed to do this. The simplest of these are the most intuitive methods, in which the mean or median expression value of the genes making up the module is calculated in the sample of interest, which is then used as a module score which can be used for between-group comparisons (Chaussabel and Baldwin, 2014). This strategy has been used most often for assessing data-driven module expression within the framework of the system used to generate the modules, with the assumption that the inherently co-correlated nature of the sets of genes within each module mean that assessing them as essentially a single variable is justified (Chaussabel and Baldwin, 2014).

Assessing the expression of hypothesis-driven modules has generally been performed using more complex techniques, perhaps owing to a lower level of prior confidence that a module which is generated entirely independently from the system in which it is to be assayed will have specificity for phenotypes within that system. One of the most widely used methods in this regard is gene set enrichment analysis (GSEA), the development of which helped to pioneer the concept of assessing hypothesis-driven modules (Mootha et al., 2003; Subramanian et al., 2005). GSEA uses an algorithm which determines a list of ranked gene expression differences between the transcriptomes of two phenotypes of interest, e.g. a disease state and a control, and then assesses where the members of the module gene set lie in this ranked list; if they tend to occur towards one or other end of the list, then the module is assessed as significantly enriched in that phenotype in comparison to the other (Subramanian et al., 2005).

This approach essentially produces a gene-set level statistic by the sum of the gene-level statistics (Alavi-Majd et al., 2014), and variations on this univariate testing approach have been developed using different statistical tests and assumptions about dataset distribution (Dinu et al., 2007; Luo et al., 2009; Irizarry et al., 2009). Multivariate approaches which incorporate the correlation structures of gene sets into the testing algorithm have also been developed (Tsai and Chen, 2009). A gold standard for hypothesis-driven module enrichment analysis is yet to emerge (Hung et al., 2012), and it is suggested that the most appropriate analysis method to use depends on the distribution of the dataset to be assessed (Alavi-Majd et al., 2014), or that use of multiple methods to widely explore datasets and confirm enrichment may be most appropriate (Glazko and Emmert-Streib, 2009).

As macrophages are highly responsive to many different signals and stimuli, and their plasticity is evident transcriptionally (discussed in **section 1.2.9**), they may be an appropriate cell type to use as a barometer for different functional axes in transcriptional profiles, by deriving hypothesis-driven modules from gene expression profiles of differentially stimulated macrophages. Data-driven modules derived from macrophage gene expression profiles have already been successfully used to gain insights in macrophage heterogeneity and *in vivo* disease processes (Xue et al., 2014), indicating that they may indeed be an appropriate source of gene expression data for modular assessments. Modules derived from macrophages may be particularly appropriate for the analysis of CMI *in vivo*, due to the central role of macrophages in CMI, and assessment of immune responses in TB may be one example of where such modules might have utility.

1.7 Summary and research objectives

Macrophages are critical effector cells of CMI, the function of which is central to determining protection and pathogenesis in active TB. HIV-1 infection is associated with aberrant immune phenotypes which modulate the function of CMI, and also significantly alters the natural history of TB. HIV-1 infection and modulation of macrophages, which are also the host cell for Mtb, may be a major contributor to these complex host/pathogen interactions. Recent observations in our group have shown that production of the critical immunomodulatory cytokine IL-10 is attenuated in HIV-1 infected macrophages in the response to Mtb. As IL-10 has potent modulatory effects

on CMI, this phenotype is highly likely to have consequences for TB control and pathogenesis, which may contribute to the increased risk of TB in HIV-1 infection. As such, investigation of the mechanism and consequences of this phenotype are merited.

A central feature of macrophage function, which is likely to impact on CMI, is their responsive plasticity to different stimuli. In particular, their responses to different T cell subset cytokines may determine the quality of a CMI response. As their plasticity is controlled transcriptionally, macrophage heterogeneity represents an opportunity for development of modular tools for transcriptional profiling analysis, by using gene expression profiles from differentially stimulated macrophages to derive specific modules of interest. Such tools would clearly have potential applications for gaining insights into the function of CMI in HIV-1/TB co-infection at the systems level, wherein transcriptional profiling may assist in elucidating complex immune phenotypes in this host/pathogen interaction. Using the TST as a human challenge model in HIV-1− and HIV-1+ patients represents an opportunity to do this in a controlled and highly comparative manner.

My broad research objectives for this thesis are as follows, with specific objectives expanded upon in each chapter.

1. To investigate the mechanisms and consequences of attenuation of IL10 responses by HIV-1 in monocyte derived macrophages (**Chapter 3** and **Chapter 4**).

2. To investigate MDM molecular heterogeneity in response to differentially polarised T cell responses and cytokines, and to use this data to develop modular tools for investigation of *in vivo* gene expression datasets (**Chapter 5**).

3. To investigate CMI responses *in vivo* in HIV-1 infected patients with TB by using the TST as a human challenge model (**Chapter 6**).

Chapter 2. Materials & Methods

2.1 Buffers, solutions and media

2.1.1 Buffers and solutions

Buffer or solution	Composition
Phosphate buffered saline (PBS)	**10×**: 80g NaCl, 2g KCl, 14.4g Na_2HPO_4, 2.4g KH_2PO_4, pH adjusted to 7.4 and made up to 1l with deionised H_2O (dH_2O) **1×**: 10× diluted 1 in 10 with dH_2O
PBS-Tween	1× PBS with 0.05% vol/vol Tween-20 (Fisher Scientific)
Tris buffered saline (TBS)	**10×**: 24.23g Tris-base, 80.06g NaCl, pH adjusted to 7.6 and made up to 1l with dH_2O **1×**: 10× diluted 1 in 10 with dH_2O
TBS-Tween	1× TBS with 0.05% vol/vol Tween-20
Tris/borate/EDTA (TBE)	**10×**: 108g of Tris-base, 55g of boric acid, 7.5 g of EDTA disodium salt, made up to 1l with dH_2O **1×**: 10× diluted 1 in 10 with dH_2O
SDS-PAGE MES running buffer	Proprietary (Novex; Life Technologies)
Western blotting transfer buffer	Proprietary (Novex; Life Technologies) with 10% methanol (Sigma-Aldrich)
Western blotting blocking buffer	TBS-Tween, 5% weight/vol bovine serum albumin (BSA), 0.45μM filtered
Western blotting antibody buffer	TBS-Tween, 5% weight/vol BSA, 0.45μM filtered
ELISA blocking buffer	PBS-Tween, 1% weight/vol BSA, 0.45μM filtered
Cell freezing buffer	FCS, 10% dimethyl sulfoxide (DMSO)
25% sucrose buffer for ultracentrifugation	25% weight/vol sucrose in sterile DBPS, 0.22μM filtered
Magnetic-activated cell sorting (MACS) buffer	1x PBS with 0.5%BSA and 2mM EDTA

Table 2.1: Buffers and solutions.

2.1.2 Cell culture media

Cell type		Medium
Primary human PBMC		Roswell Park Memorial Institute (RPMI)-1640 with L-glutamine (GIBCO, Invitrogen), supplemented with 5% heat-inactivated (56°C, 30 minutes) filtered (0.45μM filter units; Corning) pooled human type AB serum (ABS) (Sigma-Aldrich)
Primary human monocytes		RPMI-1640 with L-glutamine supplemented with 10% heat-inactivated autologous serum
Primary human MDMs		
	Differentiation media	RPMI-1640 with L-glutamine supplemented with 10% heat-inactivated autologous serum and M-CSF (20ng/ml; R&D Systems)
	Maintenance media	RPMI-1640 with L-glutamine supplemented with 5% heat-inactivated filtered pooled human ABS
Primary human MDDCs		
	Differentiation media	RPMI-1640 with L-glutamine supplemented with 10% heat-inactivated autologous serum, IL-4 (50ng/ml; Peprotech) and GM-CSF (100ng/ml; Peprotech)
	Maintenance media	RPMI-1640 with L-glutamine supplemented with 5% heat-inactivated filtered pooled human ABS
HEK293T cells		Dulbecco's Modified Eagle's Medium (DMEM) with 2 mM L-glutamine (Invitrogen) supplemented with 10% foetal calf serum (FCS) (Biosera)
NP-2 cells		DMEM (Invitrogen) supplemented with 5% FCS, puromycin (1μg/ml; Sigma-Aldrich) and geneticin (G418; 100μg/ml; Sigma-Aldrich)

Table 2.2: Cell culture media.

All plastic used for tissue culture was obtained from TPP. All cultures were incubated at 37°C, 5% CO_2 except where stated otherwise.

2.2 Isolation and culture of primary human cells

This healthy volunteer study was approved by the joint University College London/University College London Hospitals National Health Service Trust Human Research Ethics Committee, and written informed consent was obtained from all participants.

2.2.1 Isolation of PBMC

Blood samples of up to 120ml were obtained from healthy volunteers. Blood was collected into heparinised syringes, mixed in a 1:1 ratio with sterile Dulbecco's phosphate buffered saline containing Ca and Mg - DPBS with Ca, Mg - (Gibco, Life Technologies), layered in a 2:1 ratio over density gradient media (Lymphoprep, Axis-Shield), and centrifuged at 800*g* for 20 minutes with minimum brake, in order to separate the peripheral blood mononuclear cell fraction (PBMC) from erythrocytes and granulocytes. The PBMC layer was removed using a Pasteur pipette and centrifuged for 10 minutes at 800*g*. PBMC were subsequently washed three times in DPBS with Ca, Mg, for 5 minutes at 400*g*. PBMC were counted and resuspended at 6.25 x 10^5/ml in PBMC medium (see **Table 2.2**).

Blood samples for autologous serum were collected concurrently with blood samples for cell isolation, into unheparinised syringes. Serum was isolated from whole blood using serum separation tubes (Starstedt) which were centrifuged for 10 minutes at 1000*g*. Serum was aspirated using a Pasteur pipette and heat-inactivated at 56° for 30 minutes.

2.2.2 Differentiation and culture of monocyte-derived macrophages

For differentiation of MDMs, monocytes were selected by adhesion as follows. PBMC were seeded at 2×10^6/cm^2 in appropriate tissue culture plates and incubated for 1 hour at 37°C, 5% CO_2, to allow the monocytic fraction to adhere. Non-adherent cells, which were peripheral blood lymphocytes (PBLs), were then removed and adherent peripheral blood monocytes were washed 3 times with DPBS with Ca, Mg. Adherent monocytes were cultured for 3 days in MDM differentiation medium (see **Table 2.2**), after which they were washed to remove remaining non-adherent cells, followed by 3 further days of culture in MDM differentiation medium without M-CSF supplementation. This method typically yields 1×10^5 MDM/cm^2 with less than 5% lymphocyte

contamination (Noursadeghi et al., 2009). From 6 days post-isolation, MDMs were used for experiments, and were maintained in culture for up to 4 weeks in macrophage maintenance medium (see **Table 2.2**). Media was replaced every 3–4 days.

In this MDM model, M-CSF was selected as the macrophage differentiation factor as opposed to GM-CSF, for several reasons. M-CSF has been shown *in vivo* to be necessary for the development and homeostatic maintenance of many tissue macrophage populations, whereas GM-CSF primarily plays a role in terminal differentiation of AMs and under inflammatory conditions (Wynn et al., 2013). Hence, M-CSF differentiated MDMs may be a reasonable *in vitro* model for a resting tissue macrophage. Additionally, in the experience of our laboratory, M-CSF differentiated MDMs are much more permissive for infection by full-length HIV-1 (without VSV-G pseudotyping or Vpx-mediated relief of SAMHD1 restriction), meaning that this MDM model is practically more suited for some of the experiments conducted using these viruses.

For some experiments wherein MDMs were to be compared to monocytes and monocyte-derived DCs, monocytes isolated by MACS (**section 2.2.3**) were used for MDM differentiation as above. MDMs were also differentiated by this method using GM-CSF (20ng/ml; Peprotech) instead of M-CSF.

2.2.3 Isolation and culture of monocytes

Periphal blood monocytes were isolated from PBMC by MACS using a CD14 positive selection kit (Miltenyi Biotec) according to the manufacturer's instructions. Monocytes were resuspended in monocyte medium (see **Table 2.2**) at 1×10^6 cells/ml and seeded in appropriate tissue culture plates. Monocytes were used for experiments within 48 hours of isolation.

2.2.4 Differentiation and culture of monocyte-derived DCs

Peripheral blood monocytes, isolated by CD14 positive selection MACS, were differentiated into MDDCs by resuspension at 1×10^6 cells/ml in MDDC differentiation media (see **Table 2.2**)**.** Cells were differentiated over 4 days, after which they were used for experiments, and were maintained in MDDC maintenance media (see **Table 2.2**).

2.3 Cell line culture

2.3.1 HEK293T cell culture

Human embryonic kidney 293T (HEK-239T) cells, which were used for virus production, were cultured at 37°C, 10% CO_2 in HEK293T media (see **Table 2.2**), and were passaged 1:4 three times per week using trypsin/EDTA (GIBCO, Invitrogen). Frozen stocks were maintained in cell freezing buffer stored in liquid nitrogen.

2.3.2 NP2 cell culture

NP2 cells are an astrocytoma cell line stably transduced to express the HIV-1 co-receptors CD4 and CXCR4 (NP2-X4) or CD4 and CCR5 (NP2-R5), which were used for HIV-1 titrations. NP2 cells were cultured in NP2 media, which is DMEM supplemented with 5% FCS and antibiotic selection (100µg/ml G418 and 1µg/ml puromycin) to maintain expression of the HIV-1 co-receptors. The cells were passaged 1:10 once a week.

2.4 HIV-1 strains and HIV-1 based vectors

All full-length HIV-1 strains were used in Category 3 laboratories using appropriate safety precautions. VSV-G-pseudotyped HIV-1 strains with *env* deletions, VLPs and lentiviral vectors were used in Category 2 laboratories using appropriate safety precautions.

2.4.1 Production of HIV-1 Ba-L

The CCR5- and thus macrophage-tropic HIV-1 strain Ba-L (Gartner et al., 1986b) was produced by propagation of infectious stocks in PBL and MDM cultures. Non-adherent PBLs from MDM preparations were cultured for 3 days in RPMI-1640 with 20% FCS and 0.5g/ml phytohaemagglutinin (PHA; Sigma-Aldrich) to generate activated T cells. These cells were then inoculated with HIV-1 Ba-L, using a multiplicity of infection (MOI) of 1, and subsequently cultured in RPMI 1640 with 20% FCS and 20 U/ml IL-2 (PeproTech). At 3- to 4-day intervals, the cell culture supernatants were collected and additional PHA-stimulated PBMC were added to maintain the cell density at $1x10^6$/ml. Cell culture supernatants containing PBMC-derived HIV-1 were filtered through 0.45µm filters (Millipore) and used to inoculate 6-day-old MDM cultures

overnight (MOI of 1), refreshing the medium on the following day. Culture supernatants from infected MDM, containing MDM-derived HIV-1 Ba-L, were collected at weekly intervals, centrifuged at 400*g* for 5 min and 0.45μm filtered to remove cellular debris. Virus was purified and concentrated from supernatants as below (**section 2.4.4**).

2.4.2 Production of HIV-1 and lentiviral vectors from molecular clones

Full-length, and Env-deleted single-round HIV-1 strains with a range of mutations, were generated by transfection of producer cells with molecular clones. The range of molecular clones used in this thesis, and details of their derivations, are listed in **Table 2.3**.

To generate the R9ΔenvΔvif and R9ΔenvΔvpr molecular clones as described in **Table 2.3**, I performed molecular cloning. All enzymes and buffers used in this process were obtained from Promega, and plasmid preparation and transformations were as detailed below. Ligations were performed at 4°C overnight. Clones were verified by sequencing (performed by the Wolfson Institute for Biomedical Research Scientific Support Services) using primers obtained from Sigma-Aldrich. All plasmids were prepared for transfections by transformation of HB101 competent *Escherichia coli* with 1μl of plasmid DNA at 42°C for 45 seconds, followed by plating of bacteria onto lysogeny broth (LB) agar (Invitrogen) plates with the appropriate selection antibiotic. Plates were incubated overnight at 37°C. Single colonies were picked and inoculated into starter cultures of 5ml LB (Invitrogen) with appropriate selection antibiotic, which were incubated for 8 hours at 37°C on a shaker. One millilitre of starter culture was inoculated into 100ml of media as above and incubated on a shaker overnight at 37°C to grow bacteria for plasmid purification, which was performed using a Qiagen Plasmid Midikit (Qiagen). Plasmid concentration and purity was determined using a NanoDrop spectrophotomer. All plasmids were routinely checked by restriction digests and TBE agarose gel electrophoresis.

Transient transfection of plasmids into subconfluent HEK-239T producer cells was performed to produce viruses, using Fugene-6 transfection reagent (Roche) and OptiMEM media (GIBCO, Life Technologies). Fugene-6 (18μl per 10cm^2 tissue culture dish) was mixed with OptiMEM (200μl per dish) and left for 5 minutes, followed by addition of plasmid DNA as detailed below. This mixture was incubated for 20 minutes after which it was added dropwise to cells. Media was changed the following day, and supernatants were collected to harvest virus on the subsequent 2 days.

Full-length HIV-1 clones were generated by transfection of 3.5µg of plasmid DNA per 10cm^2 dish of HEK293T cells. Env-deleted viruses were vesicular stomatitis virus G protein (VSV-G) pseudotyped, and so were co-transfected with pMDG, a VSV-G expression vector (Naldini et al., 1996). Three micrograms of Env-deleted virus plasmids and 1ug of pMDG were used for these transfections per 10cm^2 dish of HEK293T cells. Gag-Luc-GFP and HR'-based lentiviral vector were co-transfected with the packaging plasmid p8.91 (Zufferey et al., 1997) and pMDG. 1.5ug of virus/vector plasmid, 1ug of p8.91 and 1ug of pMDG were used for these transfections per 10cm^2 dish of HEK293T cells.

2.4.3 Production of Vpx virus-like particles (Vpx VLPs)

To express the SIV and HIV-2 protein Vpx, which can increase the efficiency of macrophage lentiviral transduction by overcoming SAMHD1-medated restriction (Berger et al., 2011; Hrecka et al., 2011; Laguette et al., 2011), VSV-pseudotyped Vpx virus-like particles (Vpx VLPs) were produced as follows. The plasmid pSIV3$^+$, a SIVmac Gag-Pol expression vector which includes the gene for Vpx (Nègre et al., 2000), was co-transfected with pMDG, without any genome plasmid, into HEK293T cells as above. pSIV3$^+$ was used at 3µg, and pMDG at 1µg, per 10cm^2 dish of HEK293T cells.

2.4.4 Virus purification by ultracentrifugation

To purify and concentrate virus, filtered culture supernatants were layered over 25% sucrose buffer cushions and ultracentrifuged in sterilised ultracentrifuge tubes (Beckman-Coulter) for 2 hours at 23000 rpm, 4°C, to remove soluble contaminants. Ultracentrifugation was performed using a Sorvall Sure-Spin 630 rotor. Viral pellets were resuspended in MDM maintenance media, aliquoted and stored in liquid nitrogen.

Virus	Details and references
Full-length HIV-1	
NL4.3 BaL	NL4.3 BaL was provided by Dr Jane Rasaiyaah (UCL). The full-length X4-tropic HIV-1 clone NL4.3 was modified by cloning in the Env gene from R5-tropic HIV-1 BaL, to render NL4.3 R5-tropic in order to infect MDMs (Rasaiyaah *et al.*, 2013).
NL43 BaL ΔIN	NL4.3 BaL ΔIN was provided by Dr Jane Rasaiyaah (UCL). A mutation in integrase, D116N, was introduced to NL4.3 BaL by site-directed mutagenesis (Rasaiyaah *et al.*, 2013).
Env-deleted HIV-1	
R9Δenv	The R9Δenv molecular clone was provided by Dr Elspeth Potton (UCL). This virus is a derivative of the R9 BaL full-length HIV-1 clone (Saphire *et al.*, 2002) with a 445bp deletion in Env.
R9ΔenvΔnef	The R9ΔenvΔnef molecular clone was provided by Dr Elspeth Potton (UCL). A fragment from a full-length HIV-1 NL4.3 clone with a premature stop codon in Nef (Schindler *et al.*, 2006) provided by Professor Frank Kirchoff (University of Ulm) was cloned into R9Δenv to produce R9ΔenvΔnef.
R9ΔenvΔvif	To create a Vif-defective virus in the R9 background, a fragment from the Vif-defective virus VH17 (Simon *et al.*, 1995) which has nonsense mutations in Vif (provided by Professor Mike Malim, KCL) was cloned into R9Δenv using the *Spe*I and *Sal*I restriction sites.
R9ΔenvΔvpr	To create a Vpr-defective virus in the R9 background, a full-length HIV-1 NL4.3 molecular clone with a mutation in the start codon of Vpr (provided by Dr Jane Rasaiyaah, UCL) was used. NL4.3 and R9 are essentially equivalent, as although R9 was based on an NL4.3/HXB2 hybrid, all HXB2 sequence has been removed in subsequent modifications (Saphire *et al.*, 2002). Accordingly, the NL4.3Δvpr clone was modified by cloning in the R9Δenv *Bam*HI–*Sal*I fragment which contains the truncated Env sequence, to produce R9ΔenvΔvpr.
Gag-Luc-GFP	The Gag-Luc-GFP molecular clone was provided by Professor Greg Towers (UCL). This clone is a derivative of pLAI (Peden *et al.*, 1991), a HIV-1 clone with a 500bp deletion in Env, based on the original LAI HIV-1 isolate. The gene for luciferase is cloned in frame in Gag and GFP is cloned in place of Nef. This construct therefore encodes the accessory genes Tat, Rev, Vpu, Vpr and Vif and a gag luciferase fusion protein. The Gag-Pol sequence downstream of luciferase is out of frame.
Lentiviral vector	
HR'-based	The pHR' vector plasmid (Naldini *et al.*, 1996), expressing eGFP under the control of the CMV promoter, was used to generate lentiviral vector particles expressing GFP only as a transgene.

Table 2.3: HIV-1 molecular clones and lentiviral vectors.

2.4.5 Virus titrations

HIV-1 strains were titrated on the NP2 cell line (**section 2.3.2**) as previously described (Noursadeghi et al., 2009). NP2/CD4/CCR5 cells were seeded 24 hours prior to titrations, to allow for attachment to the tissue culture plastic as well as for expression of the receptors required for HIV-1 infection. Cells were inoculated for 2 hours at 37°C with serial log-fold dilutions of viral stocks, using duplicate wells. The inoculum was then removed and the media replaced. Infection was detected after 72 hours by p24 immunostaining (**section 2.8.1**). P24-positive cells were counted using an AID Viruspot reader, and titres calculated from the lowest dilution with positive cells, in which the number of positive cells was verified by manual counting using the light microscope. Titration values were calculated as infectious units per ml.

Integrase-deficient HIV-1, Gag-LucGFP, lentiviral vectors and Vpx VLPs, which could not be titrated by p24-gag staining, were titrated by measuring the amount of reverse transcriptase in the viral sample a reverse transcriptase (RT) assay colorimetric kit (Roche) according to the manufacturer's instructions. One nanogram of RT correlates to 1×10^6 infectious units in this assay.

2.5 *Cryptococcus neoformans* strains and culture

2.5.1 *C. neoformans* strains

C. neoformans strains used are shown in **Table 2.4.** All strains were provided by Professor Robin May, University of Birmingham.

2.5.2 *C. neoformans* culture

All strains were propagated on yeast-peptone-dextrose (YPD) agar (Sigma-Aldrich) plates. Stocks of *C. neoformans* were stored at −80° in glycerol stocks, using a microbank bacterial and fungal preservation system (Fisher Scientific). Beads from microbanks were added to agar plates and incubated for up to 48 hours at 25–30°C. Fungal lawns were re-streaked onto a fresh plate to give stock plates for experiments, which were incubated similarly. Stock plates were stored at 4°C for up to 2 weeks before re-streaking. For experiments, YPD broth (Sigma-Aldrich) was inoculated from fungal lawns, and *C. neoformans* yeasts were cultured in suspension for 16–24 hours at 20rpm in a microbial incubator at 25–30°C. These cultures were centrifuged at

6000*g* for 2 minutes to pellet yeast cells, which were then resuspended in sterile DPBS for counting by haemocytometer.

***C. neoformans* strain**	**Details**	**Serotype**	**Reference**
H99	WT laboratory-propagated strain; *C. neoformans* type strain	A	Perfect *et al.* (1980); Perfect *et al.* (1993)
Cap59	Unencapsulated derivative of H99	A	Nelson *et al.* (2001)
B3501	WT laboratory-propagated strain	D	Kwon-Chung (1976)
Cap67	Unencapsulated derivative of B3501	D	Jacobson *et al.* (1982)
H99-GFP5	H99 expressing GFP	A	Voelz *et al.* (2010)

Table 2.4: *Cryptococcus neoformans* strains.

2.6 Cell culture infections and stimulations

2.6.1 Infection with HIV-1 and viral vectors

MDMs were inoculated with Ba-L at an MOI of 3–5 in a minimal cell culture volume, followed by an overnight incubation, after which inoculums were removed and maintenance media refreshed. Infected MDMs were kept in culture for a further seven days, to allow spreading propagation of virus to establish uniform infection of the culture, before use in experiments.

MDMs were inoculated with NL4.3 Ba-L WT or ΔIN at an MOI of 15 in a minimal cell culture volume, followed by an overnight incubation, after which inoculums were removed and maintenance media refreshed. Infected MDMs were kept in culture for a further 14 days, to allow spreading propagation of virus to establish uniform infection of the culture, before use in experiments.

MDMs, MDDCs and monocytes were inoculated with VSV-G pseudotyped HIV-1 strains at an MOI of 3–5 in a minimal cell culture volume, and were co-transduced with Vpx VLPs at 2ng RT/ml. Inoculums were removed after an overnight incubation

and normal maintenance media was refreshed. Infected cells were kept in culture for at least 24 hours before use in experiments.

MDMs were inoculated with the lentiviral vector HR' and HIV-1 GagLucGFP at 7ng RT/ml in a minimal cell culture volume, and were co-transduced with Vpx VLPs at 2ng RT/ml. Inoculums were removed after an overnight incubation and normal maintenance media was refreshed. Infected cells were kept in culture for at least 24 hours before use in experiments.

For all experiments in which Vpx VLPs were used, uninfected wells were also transduced with Vpx VLPs at 2ng RT/ml as a control. Success of HIV-1 infection was routinely verified in experiments using p24 immunostaining of paired wells (see **section 2.8.1**).

2.6.2 *C. neoformans* infection

C. neoformans yeasts from liquid cultures were resuspended at the appropriate MOI (10–100; indicated in figure legends) in MDM maintenance media, and incubated with MDMs for 4 hours, after which MDMs were washed thoroughly using DPBS to eliminate extracellular yeasts. Infected MDMs were maintained for up to 24 hours.

2.6.3 Innate immune stimuli and cytokines

MDMs were incubated with innate immune stimuli and recombinant human cytokines as shown in **Table 2.5.**

MDMs were also stimulated with Mtb culture supernatant. To generate this, *M.tuberculosis* H37Rv was cultured in Middlebrook 7H9 medium (BD Biosciences) supplemented with 10% ADC enrichment medium, 0.2% glycerol (AnalaR, VWR) and 0.02% Tween-80 (Sigma-Aldrich). Mtb culture filtrate was generated by centrifugation of cultures at an OD_{600nm} of 0.6 at 15000*g* for five minutes followed by filtration through a 0.2µm Anopore filter (Whatman), and this was used to stimulate MDMs.

Reagent	Concentration for use	Manufacturer
Innate immune stimuli		
Ultrapure lipopolysaccharide (LPS) from *Escherichia coli* O111:B4	100ng/ml	Invivogen
Pam3-Cys-Ser-Lys4 (Pam_3CSK_4)	100ng/ml	Axis-Shield
Zymosan from *Saccharomyces cerevisiae* cell wall	0.4mg/ml	Invivogen
Curdlan (β-1,3-glucan from *Alcaligenes faecalis*)	0.1mg/ml	Wako Chemicals
Recombinant human cytokines		
IL-10	10ng/ml	eBioscience
TNFα	10ng/ml	eBioscience
IFNγ	10ng/ml	Peprotech
IFNα (clinical grade)	200IU/ml	Teva
IFNβ (clinical grade)	200IU/ml	Merck Serono
IL-4	10ng/ml	Peprotech
IL-13	10ng/ml	eBioscience
TGFβ	10ng/ml	Peprotech

Table 2.5: Innate immune stimuli and cytokines.

2.6.4 Blockade of cytokine signalling

To block IL-10 signalling in innate immune responses, MDMs were preincubated with neutralising antibodies to IL-10 (clone JES3-9D7, 5ug/ml, eBioscience) and the IL-10 receptor (clone 3F9, 10ug/ml, BD Biosciences) for 2 hours prior to innate immune stimulation, and throughout the stimulation conditions.

To block type I IFN signalling in innate immune responses, MDMs were preincubated with neutralising antibody to the type I IFN receptor IFNBAR2 (clone MMHAR-2, 1ug/ml, PBL Assay Science) for 2 hours prior to innate immune stimulation, and throughout the stimulation conditions.

2.6.5 Chemical inhibitors and drugs

MDMs were incubated with chemical inhibitors and drugs as detailed in **Table 2.6**. Cells were pre-incubated with inhibitors for 2 hours before experiments, and throughout the experiment as appropriate. Conditions without inhibitors were controlled by the addition of the appropriate carrier. For experiments using indinivir sulphate, MDMs were pre-incubated for 3 days prior to assays.

Inhibitor/drug	Target	Carrier	Concentration for use	Manufacturer
SB203580	p38 MAP kinase	DMSO	10µM	Calbiochem
PD98059	MEK (and downstream ERK1/2 MAP kinase)	DMSO	10µM	Calbiochem
UO126	MEK1 (and downstream ERK1/2 MAP kinase)	DMSO	10µM	Calbiochem
AG17	Pyk2	DMSO	10µM	Calbiochem
KN93	CaM kinase II	DMSO	10µM	Calbiochem
LY294002	PI3K	DMSO	10µM	Calbiochem
Triciribine	Akt	DMSO	20µM	Calbiochem
Rapamycin	mTOR	DMSO	200nM	Sigma-Aldrich
Actinomycin D	RNA polymerase II	DMSO	10ug/ml	Sigma-Aldrich
Indinivir sulphate	HIV-1 protease	H_2O	10µM	Centre for AIDS reagents, NIBSC

Table 2.6: Chemical inhibitors and drugs.

2.7 PBMC migration assays

PBMC were isolated from healthy donor blood samples as above, and resuspended at 5×10^6 cells/ml in PBMC media. Five hundred microliters of MDM-conditioned media (described below) or control media was placed into the lower chamber of 5µm-pore polycarbonate transwells (Costar). One hundred microliters of the PBMC suspension was transferred into the top chamber of transwells, and incubated for 3 hours at 37°C for migration to occur. Transwells were gently lifted out of the lower chamber and the undersurface was rinsed twice with trypsin-EDTA and incubated for a further 10 minutes to remove adherent cells. Transwells were removed and the migrated cells were fixed by addition of PFA to the lower chamber suspension to a final concentration of 1% and incubation for 15 minutes. Cells were then stained with fluorochrome-conjugated antibodies to CD14 and CD3, to delineate monocytes and T cells respectively (both antibodies from BD Biosciences) and acquired on a FACS Calibur flow cytometer to quantify migrated cells. Fluorescent beads (Flow-Check Fluorospheres; Beckman Coulter) were added to all samples to standardise acquisition. Migration indices were calculated as follows to quantify the migration of

different cell populations: the absolute numbers of cells recruited, for the cell population of interest, were normalised as a ratio to the absolute number of that cell population in an input PBMC sample.

MDM-conditioned media, which was generated by stimulation of MDMs in conditions described in figure legends, was pooled from 4 donors, diluted 1 in 10 in macrophage maintenance media and 0.45μM filtered before use.

2.8 Quantification of HIV-1 p24

2.8.1 Intracellular HIV-1 p24 staining

Immunostaining of cells for HIV-1 p24 was performed as follows. Cells were fixed with ice cold acetone (Sigma-Aldrich) and methanol (Sigma-Aldrich) in a 1:1 ratio for 30 minutes at room temperature, followed by three washes with PBS. The primary antibody (mouse anti-p24, clone EVA365/366, NIBSC) diluted 1 in 50 in PBS with 1% FCS was added. After incubation for 2 hours at room temperature, cells were washed 3 times with PBS and the secondary antibody, goat anti-mouse Ig β-galactosidase conjugate (Southern Biotechnology Associates) diluted 1 in 40 in PBS with 1% FCS was applied and incubated for 1 hour at room temperature. Cells were washed three times in PBS, and pre-mixed β-galactosidase substrate, X-gal, at 20mg/ml (Fermentas) was added in X-gal solution (PBS containing 3 mmol/l potassium ferricyanide, 3 mmol/l potassium ferrocyanide and 1 mmol/l magnesium chloride), followed by incubation overnight at 37°C. p24-positive cells, stained blue, were quantified as infected cells per field using an AID Viruspot reader.

2.8.2 HIV-1 p24 ELISA

HIV-1 p24 enzyme-linked immunosorbant assay (ELISA) was used to quantify HIV-1 in cell culture supernatants. Plates, antibodies and standards were from the p24 ELISA kit version 9.2, AIDS and Cancer Virus Programme, National Cancer Institute, Frederick. Cell culture supernatants were diluted 1 in 10 in RPMI-1640 with 1% BSA and 0.2% Tween-20. Lysing solution, which was 10% Triton-X-100 (Sigma-Aldrich) in Milli-Q H_2O (Millipore UltraPure Water Purification System), was added in a 1:10 ratio. Samples were incubated for 1 hour at 37°C for HIV-1 lysis. Recombinant protein standards were prepared by making two-fold dilutions in the appropriate cell culture medium. Standards and samples were added in duplicate or triplicate to pre-blocked

plates coated with anti-p24 capture antibody and incubated at 37°C for 2 hours, followed by washing three times with PBS-Tween (see **Table 2.1**). The biotinylated detection antibody was prepared 1 in 150, in 0.45µm filtered RPMI-1640 with 10%FCS and 2% normal mouse serum (NMS) (Sigma-Aldrich), added to wells and incubated for 1 hour at 37°C. Wells were washed as above and the avidin-horseradish peroxidase (HRP) conjugate, diluted 1 in 100 in 0.45µm filtered RPMI-1640 with 2% NMS, 5% normal goat serum (NGS) (Sigma-Aldrich) and 0.01% Tween-20, was added to wells and incubated for 1 hour at 37°C. Wells were washed as above, the HRP substrate, 3,3',5,5'-tetramethylbenzidine (TMB) in solution was applied and the reaction was allowed to develop in the dark. When the reaction had reached an appropriate stage, it was stopped using 1N hydrochloric acid (Sigma-Aldrich). The resulting colorimetric product was quantified at OD_{450nm} using a Thermo Scientific Multiskan FC, and the standard values used to construct a standard curve, from which p24 concentrations in the samples were calculated. Co-efficients of variation (CV) were calculated for replicate wells and samples with %CV greater than 20% were re-assayed.

2.9 RNA isolation from cultured cells

RNA was isolated by lysis of cells using RLT buffer (Qiagen) as per the manufacturer's instructions. Extraction was performed using a Qiagen RNeasy Kit (Qiagen) as per the manufacturer's instructions. For downstream processing, RNA was subject to DNase treatment using a TURBO DNA-free kit (Ambion, Life Technologies) as per the manufacturer's instructions to remove contaminating genomic DNA. When RNA was used for microarray analysis, RNA quality and quantity was checked using RNA Nanochips (Agilent) and an Agilent 2100 Bioanalyzer.

2.10 Quantitative real-time PCR measurements of gene expression

DNase-treated RNA was used as the template to make first strand cDNA, using qScript cDNA Mastermix (Quanta Biosciences), which contains appropriate buffer, dNTPs, MgCl2, primers, RNase inhibitor protein, qScript reverse transcriptase and stabilizers. Quantitative real-time PCR (qRT-PCR) for genes of interest was performed using TaqMan inventoried assays (Applied Biosystems, Invitrogen), shown in **Table 2.7**, and 2× TaqMan Gene Expression Mastermix (Applied Biosystems, Invitrogen), using

an AB7500 Fast RT-PCR System. Expression levels of target genes were normalised using a Δ cycle threshold (Ct) calculation, to that of glyceraldehyde 3-phosphate dehydrogenase (GAPDH), which was amplified and detected using primer and probe sequences (**Table 2.8**) as previously reported (Tsang et al., 2009). GAPDH primers and probes were obtained from Sigma-Aldrich. TaqMan assays use FAM as the dye, and GAPDH probes were also used with FAM.

Gene	Applied Biosystems Assay ID
IL10	Hs00961622_m1
IL6	Hs00985639_m1
TNFA	Hs00174128_m1
IL1B	Hs01555410_m1
IFI16	Hs00194261_m1
HIV-1 LTR	Pa03453409_s1

Table 2.7: Applied Biosystems Taqman qRT-PCR assays.

	Sequence (5'–3')
GAPDH forward primer	GGC TGA GAA CGG GAA GCT T
GAPDH reverse primer	AGG GAT CTC GCT CCT GGA A
GAPDH probe	TCA TCA ATG GAA ATC CCA TCA CCA

Table 2.8: GAPDH primer and probe sequences.

2.11 Cytokine ELISAs

To measure cytokine secretion from cells, ELISAs were performed as follows. Cell culture supernatants were collected during experiments, centrifuged for 2 minutes at 12000*g* to remove cell debris, and stored at −80°C. Antibodies, standards and detection reagents from Ready-Set-Go ELISA kits (eBioscience) were used, and 100µl volumes of all reagents was used per well. Antibodies, sample dilution factors and upper concentrations of standards are summarised in **Table 2.9** and buffers used are shown in **Table 2.1**. Flat-bottomed polystyrene 96-well plates (Nunc) were coated with the primary capture antibody at 1µg/ml in PBS and incubated overnight at 4°C. The capture antibody was flicked out, and blocking buffer was applied for 2 hours at room

temperature. A range of standards were prepared from recombinant proteins by doubling dilutions in sample buffer, which was the appropriate cell culture medium. Sample dilutions were also made in sample buffer. The blocking buffer was flicked out and the plate was washed three times with PBS-Tween and blotted dry. Standards and samples were applied to wells, in duplicate or triplicate as appropriate, leaving duplicate blank wells. This was incubated at room temperature for 2 hours or at 4°C overnight. Samples and standards were flicked out and the plate washed as above. The biotinylated secondary detection antibody was applied at 1µg/ml in PBS-Tween, incubated for 1 hour at room temperature, flicked out, and washed as above. The avidin-HRP conjugate was applied at 1µg/ml in PBS-Tween, for 30 minutes at room temperature, flicked out, and washed as above. TMB was added and the reaction was developed and assessed as detailed in **section 2.8.2, pg. 27**.

Cytokine	Capture antibody clone	Detection antibody clone	Highest standard used (pg/ml)	MDM culture supernatant dilution factor
IL-10	JES3-9D7	ES3-12G8	4000	1:2
IL-6	MQ2-13A5	MQ2-39C3	4000	1:5
TNFα	MAb1	MAb11	4000	1:5

Table 2.9: ELISA antibodies, standards and dilutions.

2.12 SDS-PAGE and western blotting

Cell lysates were collected in sodium dodecyl sulfate (SDS) sample buffer (Novex, Life Technologies), containing protease and phosphatase inhibitor cocktails (Pierce), and were homogenised by boiling at 103°C for 5 minutes and subsequent sonication at 40 Hz using an ultrasonic processor (Jencons Scientific). Proteins were separated by SDS polyacrylamide gel electrophoresis (SDS-PAGE) using 4−12% Bis-Tris polyacrylamide gels (Novex, Life Technologies) in MES running buffer (Novex, Life Technologies) using an XCell SureLock electrophoresis system (Novex, Life Technologies). PageRuler protein marker (Fermentas) was used as a size reference. Protein transfer onto Hybond nitrocellulose membranes (Amersham, GE Healthcare)

was performed in transfer buffer (Novex, Life Technologies), also using the XCell SureLock electrophoresis system with the blot module.

Buffers used for western blotting are shown in **Table 2.1** and antibodies are shown in **Table 2.10**. Membranes were blocked on a shaker for 1 hour at room temperature, and washed three times in TBS-Tween for five minutes on a shaker. Membranes were sequentially immunoblotted with primary antibodies overnight at 4°C, and HRP-conjugated secondary antibodies for one hour at room temperature, with washing as above between each step. Immediately before detection, membranes were washed twice in TBS without Tween. Detection was performed using ECL Prime (Amersham, GE Healthcare) according to the the manufacturer's instructions, and chemiluminescence was visualized using the FluorChem FC2 imaging system (Alpha Innotech). Images were acquired and analysed for densitometry using AlphaView software v3.03 (Alpha Innotech).

Target	Species	Clone	Dilution	Manufacturer
Primary antibodies				
HIV-1 gag/p24	Mouse	E365/366	1:1000	NIBSC
HIV-1 Vif	Mouse	#319	1:500	NIH AIDS Reagent Program
HIV-1 Nef	Rabbit	Polyclonal	1:200	NIH AIDS Reagent Program
β-actin	Mouse	AC-15	1:10000	Abcam
Akt	Rabbit	C67E7	1:1000	Cell Signaling
Phospho Akt (Ser473)	Rabbit	9271	1:1000	Cell Signaling
Secondary antibodies				
Anti-rabbit HRP conjugate	Swine	Polyclonal	1:3000	DAKO
Anti-mouse HRP conjugate	Goat	Polyclonal	1:3000	DAKO

Table 2.10: Western immunoblotting antibodies.

2.13 Microscopy

2.13.1 *C. neoformans* uptake assay

Confocal immunofluorescence microscopy was used to analyse MDM uptake of *C. neoformans*. For this purpose, MDMs were cultured in 96-well tissue culture-treated confocal plates (Perkin-Elmer). Three replicate wells were used per condition. After experiments, MDMs were fixed using 4% paraformaldehyde (Sigma-Aldrich) for 30 minutes at 4°C, and washed with ice-cold PBS. Cells were blocked using 10% normal goat serum (Sigma-Aldrich) in PBS for 1 hour at room temperature. Intracellular *C. neoformans* was visualised by use of a GFP-expressing strain (H99-GFP5). Extracellular *C. neoformans* was counterstained using a monoclonal antibody to glucuronoxylomannan, a component of the *C. neoformans* capsule (mouse; clone 18B7; used at 1.98 µg/ml; provided by Arturo Casadevall, Albert Einstein School of Medicine, New York) and goat anti-mouse conjugated to Alexa Fluor 555 (Molecular Probes; Life Technologies), both applied for 1 hour at room temperature with 3 washes in PBS between incubations. MDM nuclei were stained for 5 minutes at room temperature with 4',6-diamidino-2-phenylindole (DAPI; Cell Signaling) at 2 µg/ml in PBS. Confocal microscopy was performed using the PerkinElmer Opera LX microscope and images were analysed using IMAGEJ, in collaboration with Dr Janos Kristin-Vizi, Laboratory for Molecular and Cellular Biology, University College London.

2.13.2 NFκB translocation assay

Confocal immunofluorescence microscopy was used to quantify nuclear translocation of NFkB RelA as previously described (Tsang et al., 2009). For this purpose, MDMs were cultured in 96-well tissue culture-treated confocal plates (Perkin-Elmer). Three replicate wells were used per condition. Cells were fixed and blocked as above (section **2.13.1**). Cells were permeablised using 0.1% Triton-X-100 (Sigma-Aldrich) in PBS. The primary antibody NFκB p65 (RelA) (rabbit; clone C-20; Santa Cruz Biotechnology) was applied at 1 in 100 in blocking buffer for 1 hour at room temperature. Wells were washed 3 times with PBS, and the secondary antibody (goat anti-rabbit conjugated to Alexa Fluor 488; Molecular Probes, Life Technologies) was applied at 1 in 250 in 1 in 100 in blocking buffer for 1 hour at room temperature. Wells were washed as above, and then stained with CellMask HCS Orange reagent for 30 minutes at room temperature to delineate the cytoplasm (1 in 20000 of stock in PBS;

Molecular Probes, Life Technologies) and DAPI to delineate the nucleus, as above. Cells were imaged using a Hermes WiScan Cell Imaging System (IDEA Biomedical) on the 10× objective, with 100% coverage and 100% density of each well imaged to acquire images of approximately 5×10^4 cells/well. Images were analysed using Wiscan software (IDEA Biomedical), to quantify the nuclear:cytoplasmic ratio of average RelA fluorescence intensity, per well. Ratios were compared over time-courses to analyse nuclear translocation.

2.14 Tuberculin skin tests

The study was approved by the research ethics committees of all sites and institutions involved, and informed written consent was obtained from all participants.

2.14.1 TST injection and sample collection

TSTs were performed by intradermal injection of 2U purified protein derivative (PPD) (Serum Stratens Institute) into the proximal third of the volar aspect of the forearm. A subset of patients received saline injections (clinical grade saline, from local clinical sites) as a control cohort. TSTs were assessed at 48 hours and two 3mm punch skin biopsies were collected from the marked injection site which were collected into either RNAlater reagent (Sigma-Aldrich) for RNA isolation, or 4% neutral buffered formalin (NBF; LabSource) for adjunctive histological analysis. All TSTs and biopsies were performed by trained clinical staff. Until processing, samples in RNAlater were stored at −80°C and samples in 4%NBF were stored at room temperature.

2.14.2 Histological assessment of TST biopsy samples

After fixation in 4%NBF, biopsies were embedded in paraffin (performed by the Department of Pathology, Groote Schuur Hospital, Cape Town, South Africa), sectioned and mounted on slides, and stained with haemotoxylin and eosin (performed by the University College London Hospital histopathology department). Digital images were acquired with an AxioScan Z1 slide scanner (Zeiss) and are presented without any subsequent processing. All histological assessments were performed by a histopathologist blinded to concomitant clinical information.

2.14.3 RNA isolation from TST biopsy samples

Biopsy samples were transferred into QIAzol reagent (Qiagen) and were disrupted using a homogeniser (Omni International). RNA was purified from homogenised samples using the Lipid Tissue RNeasy kit (Qiagen) according to the manufacturer's instructions. RNA was subject to DNase treatment using a TURBO DNA-free kit (Ambion, Life Technologies) as per the manufacturer's instructions to remove contaminating genomic DNA. RNA quality and quantity was checked using RNA Nanochips (Agilent) and an Agilent 2100 Bioanalyzer.

2.15 RNA isolation from peripheral blood samples

Blood samples for RNA isolation were collected into Tempus RNA blood tubes (Life Technologies) and were stored at −80°C until processing. RNA processing of blood samples was performed by Dr Jennifer Roe and Dr Gabriele Pollara, UCL Division of Infection and Immunity. RNA was purified using a Tempus Spin RNA Isolation Kit (Ambion; Life Technologies) and globin mRNA was eliminated using a GlobinClear kit (Life Technologies) both according to the manufacturer's instructions. RNA was subject to DNase treatment using a TURBO DNA-free kit (Ambion, Life Technologies) as per the manufacturer's instructions to remove contaminating genomic DNA. RNA quality and quantity was checked using RNA Nanochips (Agilent) and an Agilent 2100 Bioanalyzer.

2.16 QuantiFERON-TB Gold assays

Blood samples for QuantiFERON-TB Gold (QFT) assays were collected into QFT assay blood tubes (Qiagen) and processed according to the manufacturer's instructions to isolate plasma samples. Plasma samples were stored at −80°C until processing. IFNγ in plasma samples was measured using the QFT ELISA kit according to the manufacturer's instructions.

2.17 Transcriptional profiling by cDNA microarray

2.17.1 Microarray methodology

The quantity and quality of all RNA samples was checked using RNA Nanochips (Agilent) and the Agilent 2100 Bioanalyzer prior to processing for microarray analysis.

Only RNA samples with an RNA integrity value (Rin) of greater than 6 were used for microarrays. The Agilent Low RNA Input Linear Amplification Kit was used to generate amplified cDNA and subsequently labelled cRNA, according to the manufacturer's instructions. Successful purification, labelling and intensity and cRNA concentration were verified using a NanoDrop ND-1000 UV-VIS Spectrophotometer (Thermo Scientific). Equal concentrations of Cy5-labelled and Cy3-labelled cRNA samples were mixed and hybrised to Agilent 8×60k whole genome cDNA microarrays, according to the manufacturer's instructions. Array images were acquired with a dual-laser G2565BA microarray scanner (Agilent) and signal data was collected and processed using Agilent Feature Extraction software (v10.7.1.1).

2.17.2 Microarray data analysis

Raw microarray signal data were processed, $\log_2$ transformed, and subjected to local regression (LOESS) normalisation to a baseline derived from gene expression data of the appropriate cell type or tissue, using the agilp R package (Chain, 2012; Chain et al., 2010; available at http://www.bioconductor.org/packages/release/bioc/html/agilp.html) in R v3.0.2 (http://www.r-project.org/). This process also averages duplicate probe signal data. Normalised $\log_2$ transformed gene expression data was used for all subsequent analyses. Within datasets, data cleaning was performed before clustering, statistical and bioinformatics analyses, by removing data from any microarray probe for which signal never exceeded the baseline background signal in any sample, and for which signal never varied by more than two-fold between any two samples.

Euclidean distance hierarchical clustering and statistical analyses of microarray data were performed using MultiExperiment Viewer (MeV) v4.9.0 (http://www.tm4.org/mev.html). For experimental MDM gene expression data, significant differences in gene expression between groups were assessed by paired t-tests with a Welch's correction for unequal variance, or unpaired tests where samples were not derived from shared paired healthy donors. For clinical sample data, I assumed data were not normally distributed, so elected to use non-paramteric tests and thus assessed significant differences in gene expression between groups by Wilcoxon rank sum tests. For both tests, a *P* value of <0.05 was considered significant. The generated lists of significantly differently expressed genes were then subject to a two-fold change cut-off between groups to produce gene lists for downstream

bioinformatics analyses. These approaches have been used extensively in published data from our group (Chain et al., 2010; Le Bert et al., 2011; Rasaiyaah et al., 2013; Tomlinson et al., 2014, 2012, 2011; Tsang et al., 2009).

Bioinformatic analyses were performed using publicly available online tools. All gene lists submitted for bioinformatics analyses were restricted to genes for which annotation with a RefSeq accession number was available, and any duplicate genes (by Gene Symbol) were removed. InnateDB (www.innatedb.com; Breuer et al., 2013) was used to perform gene ontology (GO) and pathway enrichment analyses, using the recommended default settings to identify significantly enriched GO terms and pathways (a hypergeometric algorithm with a significance level of Benjamini-Hochberg correction-adjusted $P<0.05$). InnateDB integrates GO term and pathway annotation information from several publicly available databases, and the databases used for particular analyses are indicated in the relevant figure legends. GO and pathway enrichment analysis results are presented as network visualisations which were generated using Gephi v0.8.2 (https://gephi.github.io/). Transcription factor binding site (TFBS) enrichment analysis was performed using oPOSSUM-3 human single site analysis (Kwon et al., 2012; http://opossum.cisreg.ca), which compares the rate of occurrence of a TFBS in the submitted set of genes to the expected rate estimated from the pre-computed background set, by describing the normal approximation to the binomial distribution and determining how many standard deviations away from this the gene-list rate of occurrence lies: the Z-score is equal to this number of standard deviations. A Z score of greater than 10 is commonly accepted as significant.

Clustering analysis of microarray gene expression data was also performed by principal component analysis (PCA), in R v3.0.2 using a package provided by Professor Benjamin Chain. Modular analysis strategies were also used for microarray data analysis purposes, and are discussed and outlined in **Chapter 4**.

2.18 Statistical analysis of experimental data

Statistical tests used for analyses of experimental data are indicated in the relevant figure legends, and were performed using GraphPad Prism v6.0. =

Chapter 3. Results 1. Attenuation of IL-10 responses by HIV-1 in human monocyte-derived macrophages

3.1 Background

Previous work has shown that HIV-1-infected MDMs display attenuated IL-10 responses to Mtb, which are associated with downstream exacerbated pro-inflammatory responses to Mtb (Tomlinson et al., 2014). IL-10 is a critical immunomodulatory cytokine, and so this phenotype may represent a novel host-virus interaction with physiologically significant consequences. Elucidation of the mechanism behind IL-10 attenuation is therefore merited, to characterize HIV-1 modulation of macrophage function, and to further understand CMI dysfunction in HIV-1 infection.

The initial observation, that full-length replication-competent HIV-1 can attenuate the MDM IL-10 response to Mtb, poses several questions. Is this phenotype Mtb-specific, or can HIV-1 also attenuate IL-10 expression induced by other innate immune stimuli? Does the phenotype require ongoing viral propagation with replicative virus, or can it result from macrophage-autonomous infection? As HIV-1 has been shown to modulate macrophage function in a number of ways (**Introduction, section 1.3.8**), it is possible that IL-10 attenuation represents further direct modulation by the virus; therefore, what are the viral determinants of the phenotype?

The pathways regulating IL-10 production in mononuclear phagocytes are complex and highly context-specific (**Introduction, section 1.5.2**). Exploring which host pathways are modulated by HIV-1 to produce specific attenuation of IL-10 while not affecting pro-inflammatory cytokines may assist in elucidating the mechanism behind the phenotype, and also provide insight into specific regulation of IL-10 responses.

I aimed to characterise the specificity of IL-10 attenuation, and the viral and host determinants of this phenotype, by evaluating the following questions:

1) Does HIV-1 attenuate IL-10 responses to innate immune stimuli other than Mtb in MDMs?
2) Is IL-10 attenuation by HIV-1 evident over the time-course of the innate immune IL-10 response in MDMs?

3) If IL-10 attenuation represents direct modulation of macrophage function by HIV-1, specific components of the viral lifecycle will be necessary and/or sufficient for the phenotype.
    a. Is viral entry necessary or sufficient to cause IL-10 attenuation?
    b. Is HIV-1 integration necessary or sufficient to cause IL-10 attenuation?
    c. Which expressed components of HIV-1 are necessary or sufficient to cause IL-10 attenuation?
4) Type I IFNs have been shown to be involved in regulating IL-10 responses. Is this evident in this MDM model, and does HIV-1 modulate this pathway?
5) Monocytes and DCs can also mount innate immune IL-10 responses. Are these affected by HIV-1?
6) IL-10 can be regulated by post-transcriptional mechanisms. Does HIV-1 alter IL-10 mRNA stability?
7) A range of innate immune signalling pathways have been implicated in regulating IL-10 transcription in macrophages.
    a. Which of these signalling pathways are important in MDM IL-10 responses?
    b. Are any of these signalling pathways modulated by HIV-1 infection?

3.2 Results

3.2.1 IL-10 attenuation by HIV-1 is not Mtb-specific

The effect of infection with full-length HIV-1 Ba-L on MDM IL-10 responses was assessed following stimulation with Mtb culture filtrate and a range of alternative innate immune stimuli, including those which have previously been reported to induce IL-10, or which share innate immune receptors for Mtb (**Table 3.1**). The primary cellular response to stimulation was initially assessed at four hours. In these experiments, *IL10* mRNA expression and IL-10 protein secretion were reduced in HIV-1 infected MDMs compared to uninfected MDMs in response to all stimuli (**Figure 3.1**). $Mtb_{filtrate}$, zymosan and curdlan induced the *IL10* mRNA responses of the greatest magnitude, which were statistically significantly attenuated by HIV-1 (**Figure 3.1a**). Pam_2CSK_4 and LPS induced smaller IL-10 responses, which were attenuated by HIV-1, but this did not reach statistical significance (**Figure 3.1a, b**).

These data suggest that HIV-1 inhibits IL-10 induction pathways which are conserved in the innate immune responses to different stimuli, and so this phenotype is not specific to Mtb. For further experiments evaluating the phenotype of IL-10 attenuation by HIV-1, I employed zymosan as a model inducer of IL-10 expression, which stimulates similar PRRs to Mtb (TLR-2 and dectin-1; **Table 3.1**).

Stimulus	Description	Receptor	Reference
$Mtb_{filtrate}$	Filtrate from *M. tuberculosis* 7H9 cultures	TLR-2, dectin-1, TLR-4, others	Tomlinson *et al.* 2014
Zymosan	Derivative of the cell wall of the fungus *Saccharomyces cerevisiae*	TLR-2, dectin-1	Gantner *et al.* 2004
Pam_2CSK_4	Synthetic diacylated lipopeptide	TLR-2/6	Long *et al.* 2009
Curdlan	β-1,3-glucan from *Alcaligenes faecalis*	Dectin-1	Goodridge *et al.* 2009
LPS	Ultra-pure lipopolysaccharide from *E. coli* O111:B4	TLR-4	Poltorak *et al.* 1998

Table 3.1: Innate immune stimuli used to induce IL-10 expression in MDMs.

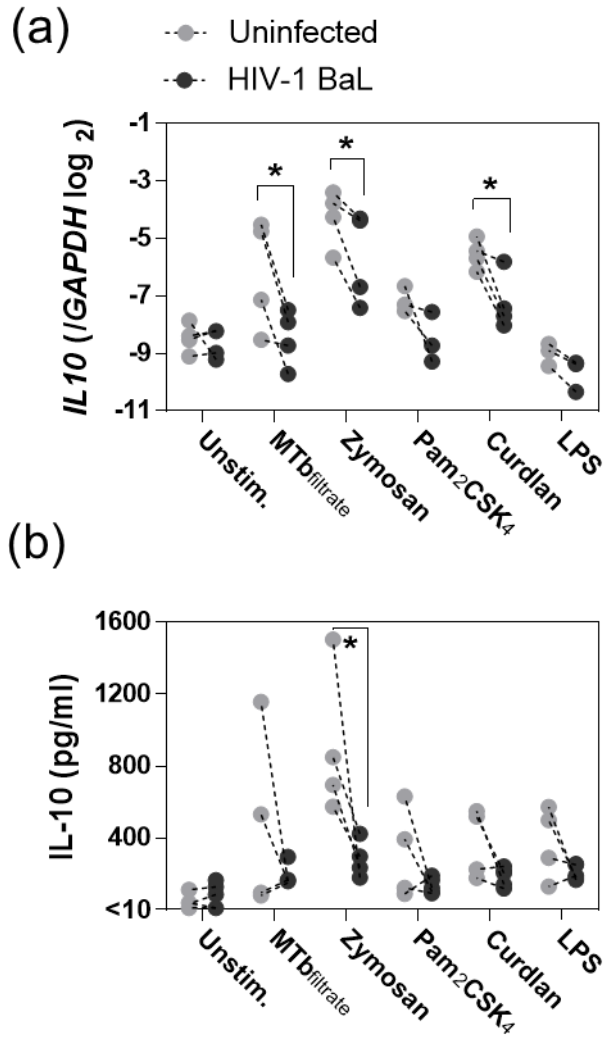

Figure 3.1: IL-10 attenuation by HIV-1 is not Mtb-specific.

MDMs were infected with HIV-1 (full-length strain Ba-L at an MOI of 3-5) for 1 week, and then stimulated for 4 hours with Mtb culture filtrate, zymosan (0.4mg/ml), Pam_2CSK_4 (100ng/ml), curdlan (0.1mg/ml) or LPS (100ng/ml). **(a)** *IL10* mRNA was measured 4 hours post-stimulation by qRT-PCR. HIV-1 infected MDMs expressed lower levels of *IL10* mRNA in comparison to uninfected MDMs in response to all stimuli, and a significantly lower level in response to Mtb filtrate, zymosan and curdlan **(b)** IL-10 protein secretion at 4 hours was measured by ELISA of culture supernatants. HIV-1 infected MDMs secreted lower levels of IL-10 in comparison to uninfected MDMs in response to all stimuli, and significantly lower levels in response to zymosan. * = $P<0.05$, paired t-test. Paired data points from the same experiment are indicated. Bars represent the mean result +/- SEM of 4 experiments. Each experiment employed MDMs from a single healthy blood donor, and a different donor was used for each experiment. Both *IL10* mRNA and IL-10 protein production varied up to fourfold between different healthy donors; this magnitude of variation was seen consistently across experiments.

3.2.2 A single-round model of HIV-1 infection can attenuate IL-10

Next, I investigated whether a single-round model of HIV-1 infection in MDM was sufficient to attenuate IL-10 responses. On one hand, this experiment would establish whether on-going viral propagation is necessary for the phenotype. More importantly, using this approach would also allow further experiments to investigate the virological determinants of IL-10 attenuation, as establishing confluent infection in a single round mitigates the deleterious effects of viral mutations or deletions in a spreading infection.

For this purpose, I used a HIV-1 clone (R9 Δenv) with a deletion in envelope which is produced as a VSV-G pseudotyped virus, and so can infect cells but is not capable of assembly, budding or propagation of infection (see **Methods section 2.4.2** for all details of viruses). It should be noted that VSV-G pseudotyped viruses use different receptors and potentially routes of entry to WT virus, and so the dynamics of this infection may differ from the full-length model.

Vpx VLPs were used to maximise infection efficiency in this model (described in **Methods section 2.4.3**). As use of Vpx VLPs involves entry of viral components into the cell, which are functional and mediate cellular modulation such as degradation of SAMHD1, it was possible that they had autonomous effects on IL-10 production, and so MDMs were transduced with Vpx VLPs alone and IL-10 transcription was measured. Vpx VLPs did not have any effect on IL-10 transcription autonomously, and so their use should not alter the phenotype of IL-10 attenuation (**Figure 3.2a**).

Confluent infection of MDMs was achieved using the single-round model of infection (**Figure 3.2b, c**). R9Δenv attenuated zymosan-induced *IL10* mRNA expression in MDMs at 4 hours post-stimulation, while *IL6* mRNA expression was unaffected (**Figure 3.2d**). Secretion of IL-10 at 4 hours was similarly attenuated while IL-6 was again unaffected (**Figure 3.2e**).

These results demonstrate that a single-round infection by HIV-1 can lead to IL-10 attenuation, similarly to full-length HIV-1. This suggests that ongoing viral propagation is not required for IL-10 attenuation, nor are the Env-derived proteins. This model was used to further investigate the virological determinants of IL-10 attenuation.

In all subsequent experiments using this model, control uninfected MDMs were transduced with Vpx VLPs.

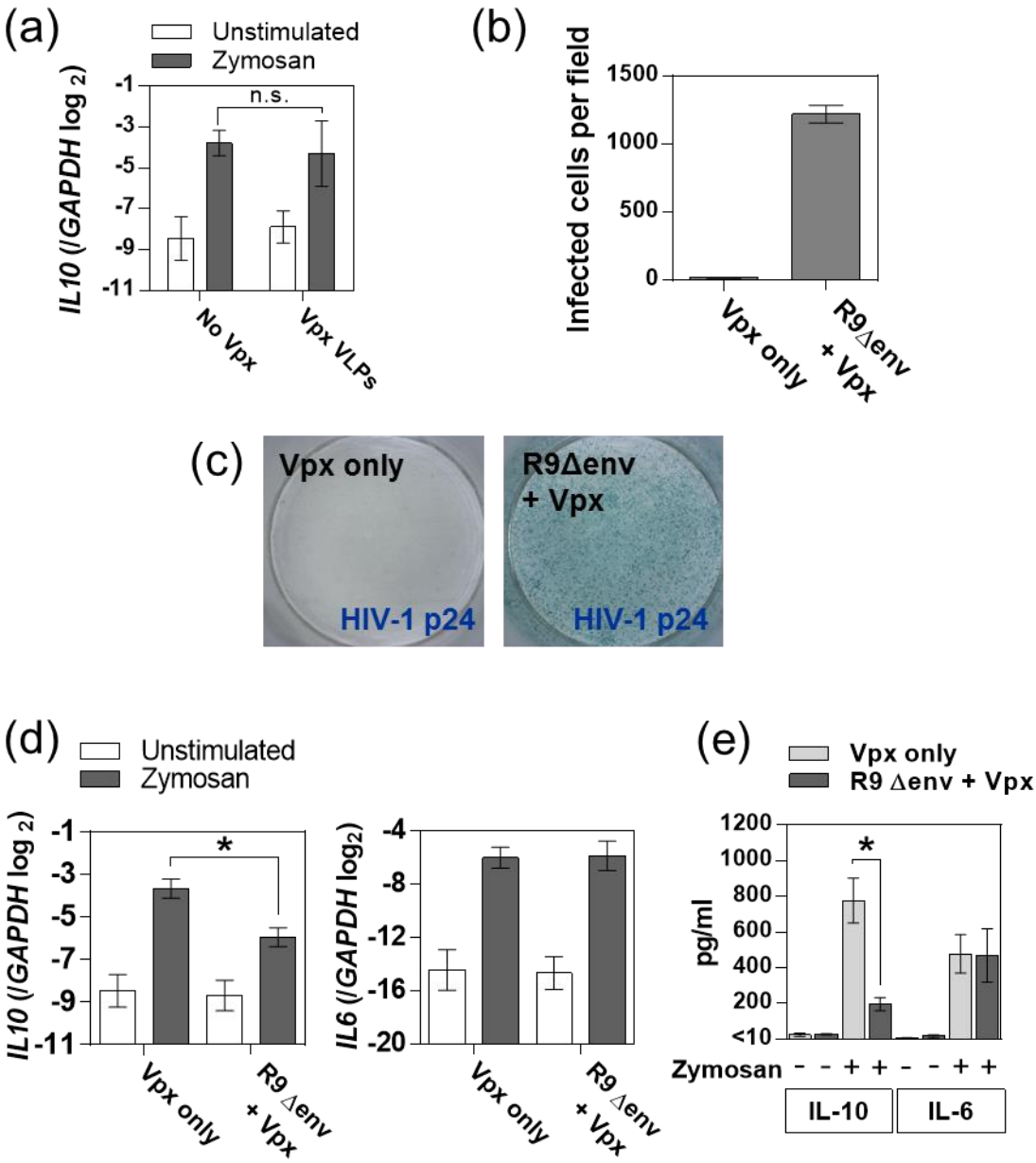

Figure 3.2: Single round infection by HIV-1 attenuates IL-10.

(a) MDMs were transduced with Vpx VLPs at 2ng RT/ml and stimulated 1 week subsequently with zymosan (0.4mg/ml) for 4 hours. Vpx-transduced MDMs and control MDMs expressed similar amounts of *IL10* mRNA. **(b)** HIV-1 p24 staining of Vpx-only transduced or single-round HIV-1 (R9Δenv, MOI of 3–5) plus Vpx transduced MDMs. **(c)** Representative images of p24 stains. **(d, e)** MDMs were infected and stimulated with zymosan as in (b). *IL10* mRNA expression and protein secretion were significantly attenuated in comparison to Vpx-only transduced MDMs. *IL6* mRNA expression and protein secretion were unaffected. mRNA expression was measured by qRT-PCR, and cytokine secretion was measured by ELISA of cell culture supernatants. ***** = $P<0.05$, n.s. = non-significant, paired t-test. Bars represent the mean result −/+ SEM of at least 3 experiments.

3.2.3 The time-course of the zymosan-induced IL-10 response and HIV-1 attenuation

To further evaluate the phenotype of IL-10 attenuation by HIV-1, I characterised the time-course of the zymosan-induced IL-10 response, and for comparison, the pro-inflammatory IL-6 and TNFα responses, and the effects of HIV-1 infection on these responses over a time-course of 1–72 hours. Induction of *IL10* mRNA expression in response to zymosan was evident from 3 hours and peaked at 6 hours, before returning to baseline levels by 24 hours (**Figure 3.3a**). Attenuation of this response by HIV-1 was evident across the time-course, and was statistically significant at 3–6 hours. It was also clear that although HIV-1 attenuated *IL10* mRNA expression, it did not entirely inhibit it, as some *IL10* mRNA expression was induced in HIV-1 infected MDMs over a similar time-course to uninfected MDMs (**Figure 3.3a**). *IL6* and *TNFA* mRNA expression in response to zymosan was not attenuated by HIV-1 at any time-point (**Figure 3.3b, c**).

Similar observations were made when measuring zymosan-induced cytokine secretion over this time-course. IL-10 protein secretion was detected from 3 hours, at which time IL-10 attenuation was already evident (**Figure 3.4a**). Peak levels of IL-10 were measurable in the MDM culture supernatants at 12 hours, and these then declined over the following 60 hours (**Figure 3.4a**). HIV-1 attenuation was evident across the time-course and was statistically significant at 3, 12 and 72 hours (**Figure 3.4a**). IL-6 and TNFα protein secretion was measured at 6, 24 and 72 hours, and was evident across the time-course for both cytokines, with no clear diminution of these responses over 72 hours, or as a result of HIV-1 infection (**Figure 3.4b, c**).

These results demonstrated that HIV-1 attenuated the innate immune IL-10 response to zymosan across the time-course of IL-10 production. They also confirmed that attenuation was specific to the IL-10 response and did not similarly affect pro-inflammatory cytokines.

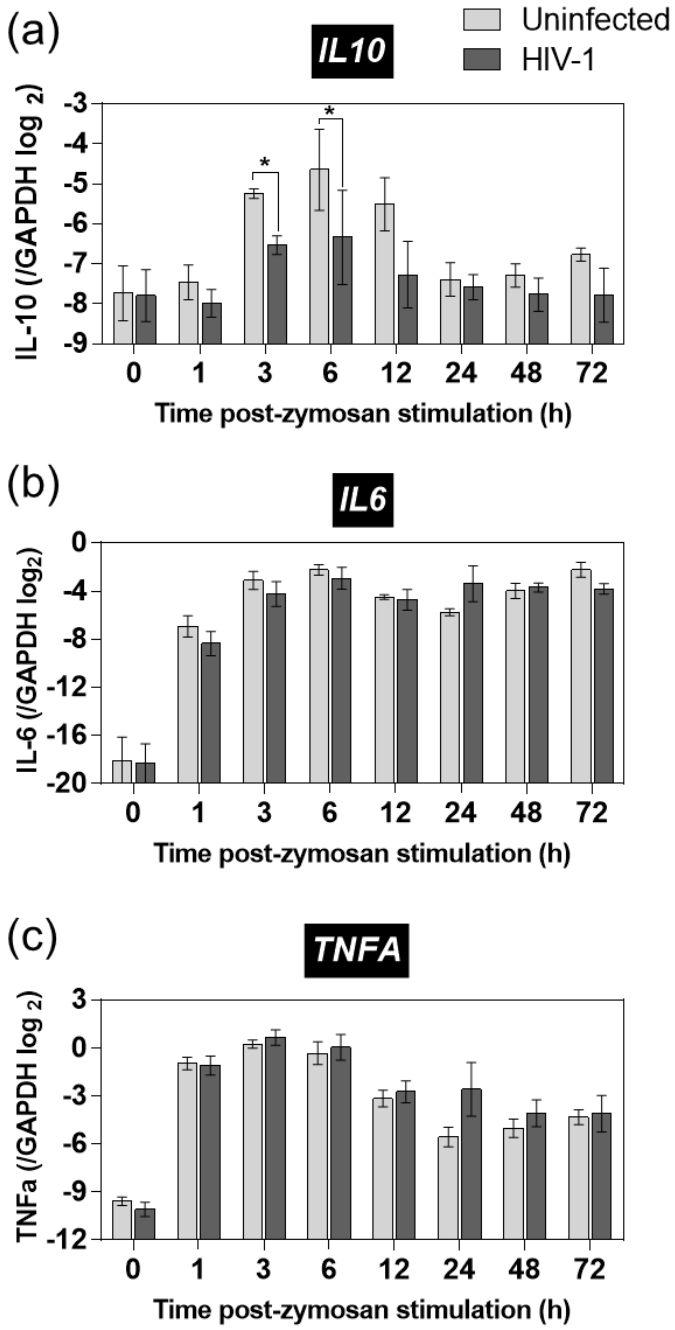

Figure 3.3: The time-course of zymosan-induced cytokine mRNA expression.

MDMs were infected with HIV-1 (R9Δenv at an MOI of 3–5, with Vpx VLPs at 2ng RT/ml) for 1 week and then stimulated with zymosan (0.4mg/ml) for 1–72 hours. Cytokine mRNA expression was measured by qRT-PCR. **(a)** *IL10* mRNA expression was significantly attenuated by HIV-1 at 3 and 6 hours post-stimulation. **(b)** *IL6* mRNA expression was not altered by HIV-1 at any time-point. **(c)** *TNFA* mRNA expression was not altered by HIV-1 at any time-point. ***** indicates $P<0.05$, paired t-test. Bars represent the mean −/+ SEM of at least 3 experiments.

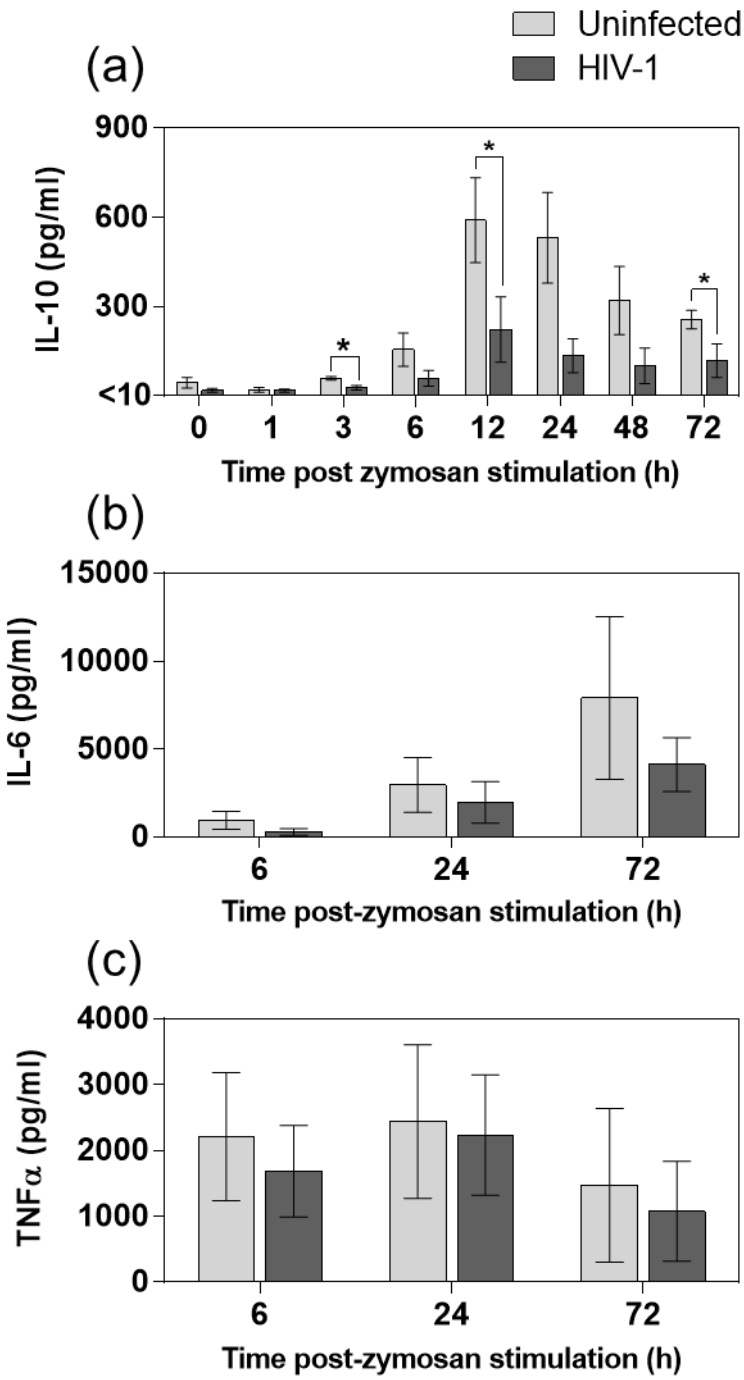

Figure 3.4: The time-course of zymosan-induced cytokine secretion.

MDMs were infected with HIV-1 and stimulated with zymosan as in **Figure 3.3**. Cytokine secretion was measured by ELISA of cell culture supernatants. **(a)** IL-10 secretion was significantly attenuated by HIV-1 at 3, 12 and 72 hours. **(b)** IL-6 secretion was not altered by HIV-1 at any time-point assessed. **(c)** TNFα secretion was not altered by HIV-1 at any time-point assessed. ***** indicates $P<0.05$, paired t-test. Bars represent the mean −/+ SEM of at least 3 experiments.

3.2.4 IL-10 attenuation is not affected by protease inhibitors

Infection with a single-round model of HIV-1 infection demonstrated that viral propagation is not necessary for IL-10 attenuation. Viral propagation can be also be prevented by ARVs, which inhibit parts of the viral lifecycle. To test whether IL-10 attenuation could persist in the context of ART, the protease inhibitor indinavir was supplemented into confluently HIV-1-infected MDM cultures, and IL-10 secretion in response to zymosan was measured.

The mechanism of action of protease inhibitors is shown in **Figure 3.5a.** Briefly, during budding, the HIV-1 particle undergoes a maturation process mediated by the viral protease, which is necessary for infection of new cells (Flexner, 1998). HIV-1 clones lacking the protease gene produce only immature non-infectious viral particles (Kohl et al., 1988), and protease inhibitors are understood to exert the same effect.

Addition of indinavir to infected MDMs led to a near-complete reduction in HIV-1 p24 measurable in the culture supernatant (**Figure 3.5b**), indicating that release of mature virus was abrogated. IL-10 protein secretion in response to zymosan was attenuated in infected MDMs supplemented with indinavir (**Figure 3.5c**). Indinavir alone had no effect on cytokine secretion, and secretion of IL-6, assessed for comparison, was unaffected in all conditions (**Figure 3.5d**). This supports conclusions made based on the single-round virus experiments; that viral propagation is not necessary for attenuation to occur. It also indicates that HIV-1 attenuation of macrophage IL-10 responses might persist in the context of anti-retroviral therapy, while a reservoir of non-productively infected macrophages remains.

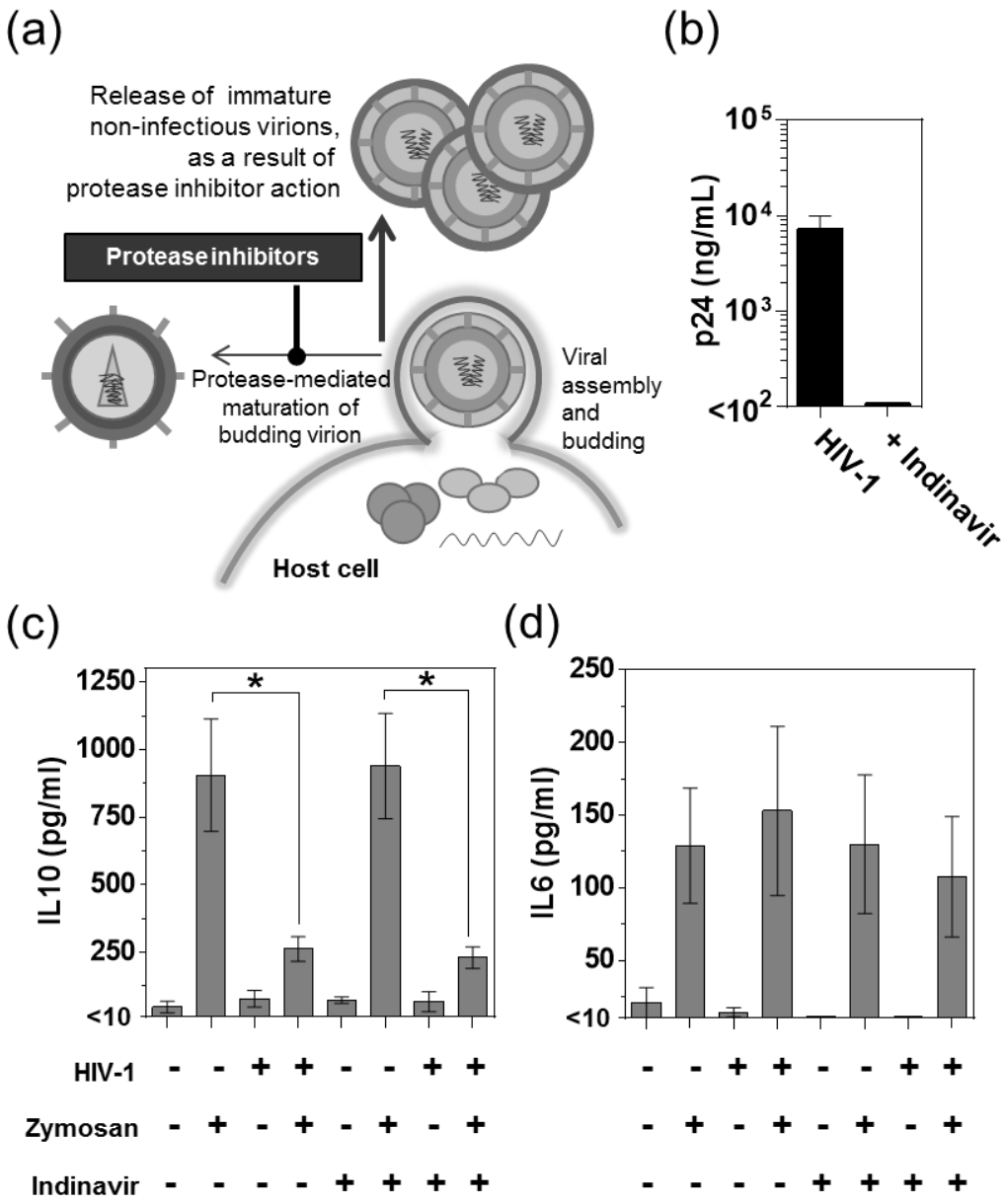

Figure 3.5: Inhibition of HIV-1 protease does not alter IL-10 attenuation by HIV-1.

(a) Schematic of the protease inhibitor mechanism of action. **(b)** MDMs were infected with HIV-1 for one week of spreading infection (full-length strain Ba-L, at an MOI of 3–5) and then were treated with the protease inhibitor indinavir sulphate at 10µM for 3 days prior to zymosan stimulation. Inhibition of mature virion production was assessed by p24 ELISA of cell culture supernatants. Indinavir sulphate treatment reduced p24 levels by 2 logs. **(c, d)** MDMs were stimulated with zymosan (0.4mg/ml) for 4 hours. IL-10 and IL-6 secretion were assessed by ELISA of cell culture supernatants. HIV-1 significantly attenuated IL-10 secretion, and this was not altered by indinavir treatment. Indinavir alone had no effect on IL-10 production. IL-6 secretion was not altered by HIV-1 infection or indinavir treatment. * indicates $P<0.05$, paired t-test. Bars represent the mean +/- SEM of 4 experiments.

3.2.5 HIV-1 entry is not sufficient for IL-10 attenuation

Treatment of viral particles with ultra-violet (UV) radiation dimerises viral nucleic acids, which are then non-replicable, rendering the virus non-infectious (Mohr et al., 2009). The consequences of UV treatment for HIV-1 are that the virus can enter the cell, but is unable to reverse transcribe or integrate its genome, and thus is unable to establish infection. UV-inactivated HIV-1 was used to assess whether viral entry was sufficient to cause IL-10 attenuation, or whether the presence of viable viral nucleic acid was necessary for the phenotype. No HIV-1 LTR transcript was detected in MDMs infected with UV-treated virus after 1 week (**Figure 3.6a**), and there was no attenuation of *IL10* mRNA expression in response to zymosan (**Figure 3.6b**). IL-10 protein secretion in response to zymosan was also reduced by HIV-1 but not by UV-treated HIV-1, although these differences did not reach statistical significance (**Figure 3.6d**). IL-6 responses were not affected (**Figure 3.6c, e**).

These data indicated that HIV-1 entry alone is not sufficient for IL-10 attenuation, but that carriage of viable viral genomes is required. I explored this observation further, by assessing the relationship between the timing of HIV-1 infection and the presence of the IL-10 attenuation phenotype (**Figure 3.7**). MDMs were infected with HIV-1 at 1 week, 24 hours or 4 hours before zymosan stimulation, or were infected at the same time as stimulation. MDMs which had been infected for 1 week or 24 hours pre-stimulation displayed statistically significantly attenuated *IL10* mRNA expression, whereas those which had been infected for 4 hours or simultaneously with stimulation did not (**Figure 3.7a**). The MDMs that were infected for 4 hours prior to stimulation, or that were simultaneously infected with stimulation, were within the first 8 hours of viral infection when they were assessed. Previous reports suggest that integration of the HIV-1 pro-virus will not have occurred in this timeframe (Mohammadi et al., 2013), and thus that nascent viral production will not have commenced. In-keeping with this hypothesis, detectable HIV-1 RNA levels decreased over this time-frame (4–8 hours) post-infection (**Figure 3.7b**), suggesting that *de novo* viral transcription from an integrated provirus had not yet occurred. These results indicated that early post-entry events are not sufficient for HIV-1 to attenuate IL-10 responses, but that subsequent steps in the viral life-cycle involving the viral genome may be necessary, such as integration of the HIV-1 provirus.

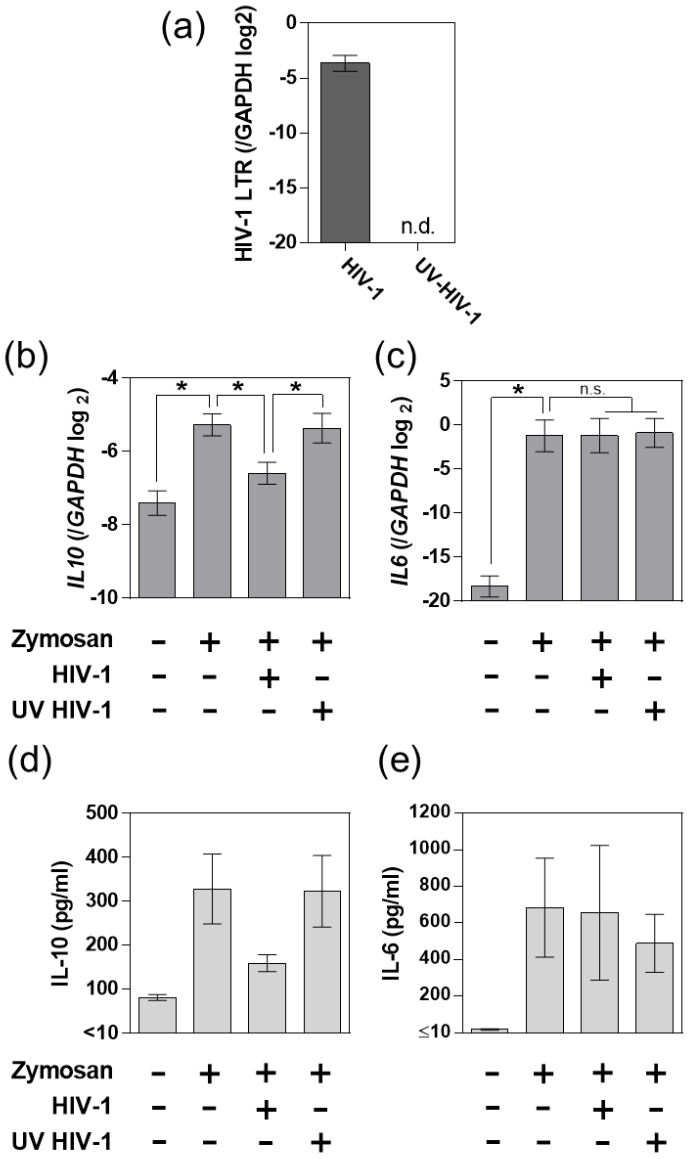

Figure 3.6: UV-inactivated HIV-1 does not attenuate IL-10.

MDMs were infected with HIV-1 (R9Δenv at an MOI of 3–5, with Vpx VLPs at 2ng RT/ml), or an equivalent inoculum in which HIV-1 was UV-inactivated (UV-C, 254nm, for 10 min). MDMs were stimulated with zymosan (0.4mg/ml) for 4 hours at 1 week post-infection. mRNA expression was measured by qRT-PCR and secretion was measured by ELISA of cell culture supernatants. **(a)** HIV-1 RNA was measured by qRT-PCR for the HIV-1 LTR. No HIV-1 RNA was detectable in MDMs infected with UV-inactivated HIV-1. **(b)** HIV-1, but not UV-inactivated HIV-1, significantly attenuated *IL10* mRNA expression in response to zymosan. **(c)** *IL6* mRNA expression was not altered by HIV-1 infection. **(c)** HIV-1, but not UV-inactivated HIV-1, reduced IL-10 secretion in response to zymosan. **(d)** IL-6 secretion was not altered by HIV-1 infection. ***** indicates $P<0.05$, paired t-test. n.d., not detectable. Bars represent the mean −/+ SEM of 4 experiments.

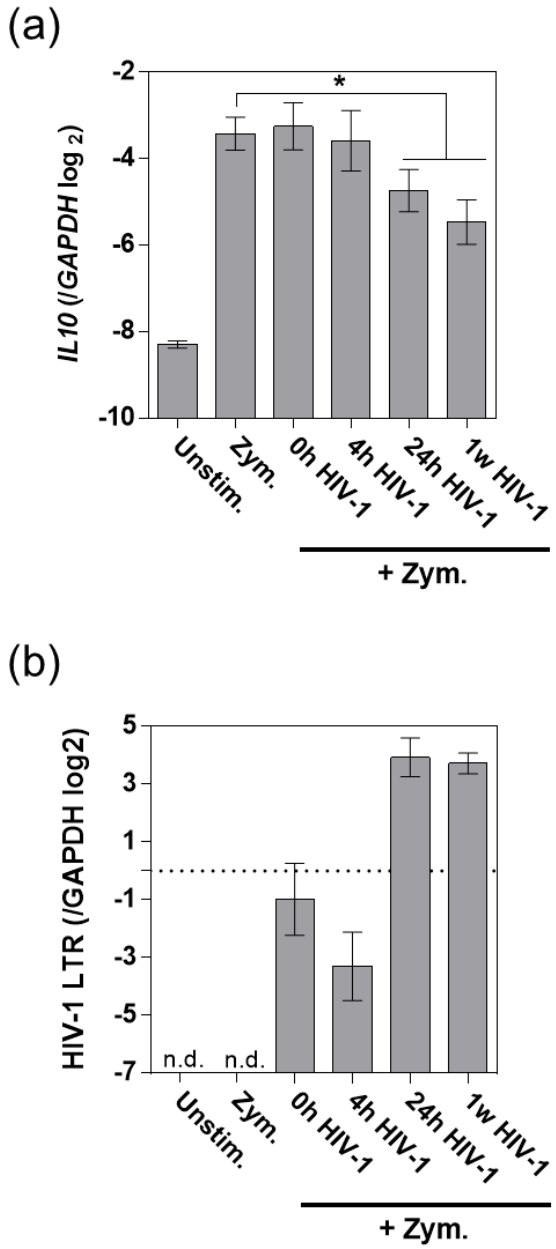

Figure 3.7: The timing of IL-10 attenuation post-infection indicates that early post-entry events are not sufficient.

MDMs were infected with HIV-1 (R9Δenv at an MOI of 3–5, with Vpx VLPs at 2ng RT/ml) and then stimulated for 4 hours with zymosan (0.4mg/ml) at the indicated times (0h, 4h, 24h, 1 week) post-HIV-1 infection **(a)** *IL10* mRNA expression was measured by qRT-PCR. Expression was significantly attenuated at 24h and 1 week post-HIV-1 infection, but not 4h post-infection or when zymosan and HIV-1 were added simultaneously. **(b)** HIV-1 transcript in MDMs measured by qRT-PCR for the HIV-1 LTR. Viral RNA was detectable at 4 hours post-infection (the 0h HIV-1 condition, as all conditions have 4 hours of zymosan stimulation after the infection), which dropped approximately fourfold after 8 hours of infection, before rising >100-fold 28 hours post-infection and remaining stable at this level for 1 week. ***** indicates $P<0.05$, paired t-test. n.d., not detectable. Bars represent the mean −/+ SEM of 4 experiments.

3.2.6 Integration by HIV-1 is necessary but not sufficient for IL-10 attenuation

Once HIV-1 enters the cell, the RNA viral genome is reverse transcribed into a DNA copy by the viral reverse transcriptase. This DNA is then integrated into the host cell genome to form the HIV-1 provirus by the action of the viral integrase. To establish if these events in the viral lifecycle are necessary for IL-10 attenuation, a full-length HIV-1 clone with a mutation in the integrase active site was employed (Rasaiyaah et al., 2013), which is capable of cell entry and reverse transcription but not integration (see **Methods section 2.4.2** for details of this virus). MDMs were infected with this virus (HIV-1ΔIN) or its WT parent virus. Confluent infection with the WT virus was confirmed at 2 weeks post-infection by HIV-1 p24 staining of MDM cultures (**Figure 3.8a, b**). MDMs infected with HIV-1ΔIN were negative for HIV-1 p24, confirming that this virus could not establish replicative infection (**Figure 3.8a, b**). IL-10 secretion in response to zymosan was statistically significantly attenuated by WT HIV-1 but not by HIV-1ΔIN (**Figure 3.8c**), suggesting that integration is necessary for IL-10 attenuation to occur.

Insertion of viral DNA into the host genome has an inherent mutagenic potential, and can lead to dysregulation of expression of host genes (Cavazza et al., 2013). Proviral integration itself may thus have consequences for cell function, irrespective of the transcription and production of new viral components. IL-10 attenuation may therefore be a consequence of integration itself. To assess whether integration was sufficient to cause IL-10 attenuation, I employed a HIV-1 based viral vector (HR') carrying a genome with just the GFP gene, and no HIV-1 components other than the viral LTRs (see **Methods section 2.4.2** for details). The absence of mature HIV-1 proteins expressed after infection with this virus was confirmed by negative HIV-1 p24 staining of transduced cells (**Figure 3.9a, c**). Successful integration of the sequence carried by HR' was confirmed by measuring transcription from the HIV-1 LTR, which was present, albeit at lower levels than with single-round HIV-1 (**Figure 3.9b**).

HR'-transduced cells did not exhibit attenuated IL-10 responses at the level of mRNA expression or protein secretion, in comparison to single-round HIV-1, which statistically significantly attenuated both (**Figure 3.9c, e**). *IL6* mRNA expression was not affected by either virus (**Figure 3.9d**). This suggests that integration alone is not sufficient for IL-10 attenuation, but that it is necessary for the provirus to express HIV-1 genes.

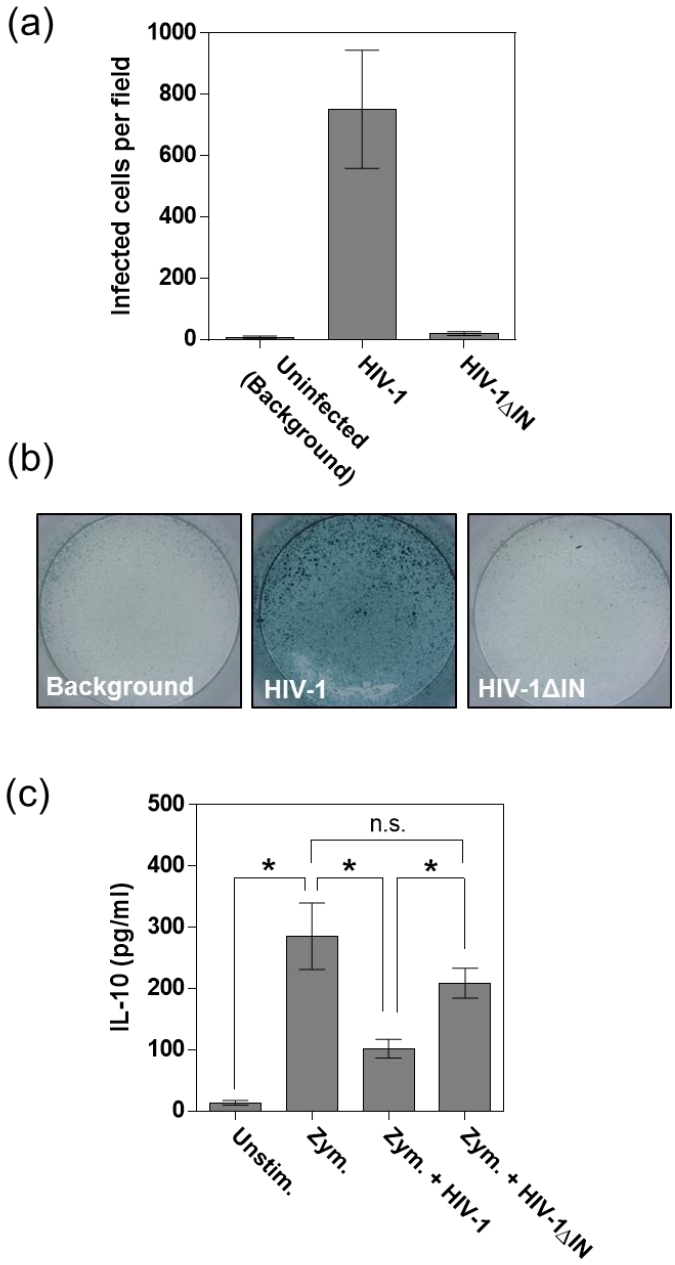

Figure 3.8: An integrase mutant of HIV-1 does not attenuate IL-10.

MDMs were infected with HIV-1 (full length strain NL4.3 BaL, MOI of 15) or an integrase deficient (ΔIN) mutant (NL4.3 BaLΔIN – D116N) for 2 weeks of spreading infection. **(a)** Cultures were stained for HIV-1 p24 to enumerate infected cells. HIV-1 p24 staining of cells infected with the ΔIN mutant did not significantly exceed background levels. **(b)** Representative images of HIV-1 p24 staining (blue). **(c)** MDMs were stimulated with zymosan (0.4mg/ml) and IL-10 secretion was measured by ELISA of cell culture supernatants. HIV-1 significantly attenuated IL-10 secretion in comparison to uninfected MDMs or MDMs infected with the ΔIN mutant. HIV-1ΔIN did not attenuate IL-10 secretion. ***** indicates $P<0.05$, paired t-test. n.s., not significant. Bars represent the mean −/+ SEM of 4 experiments.

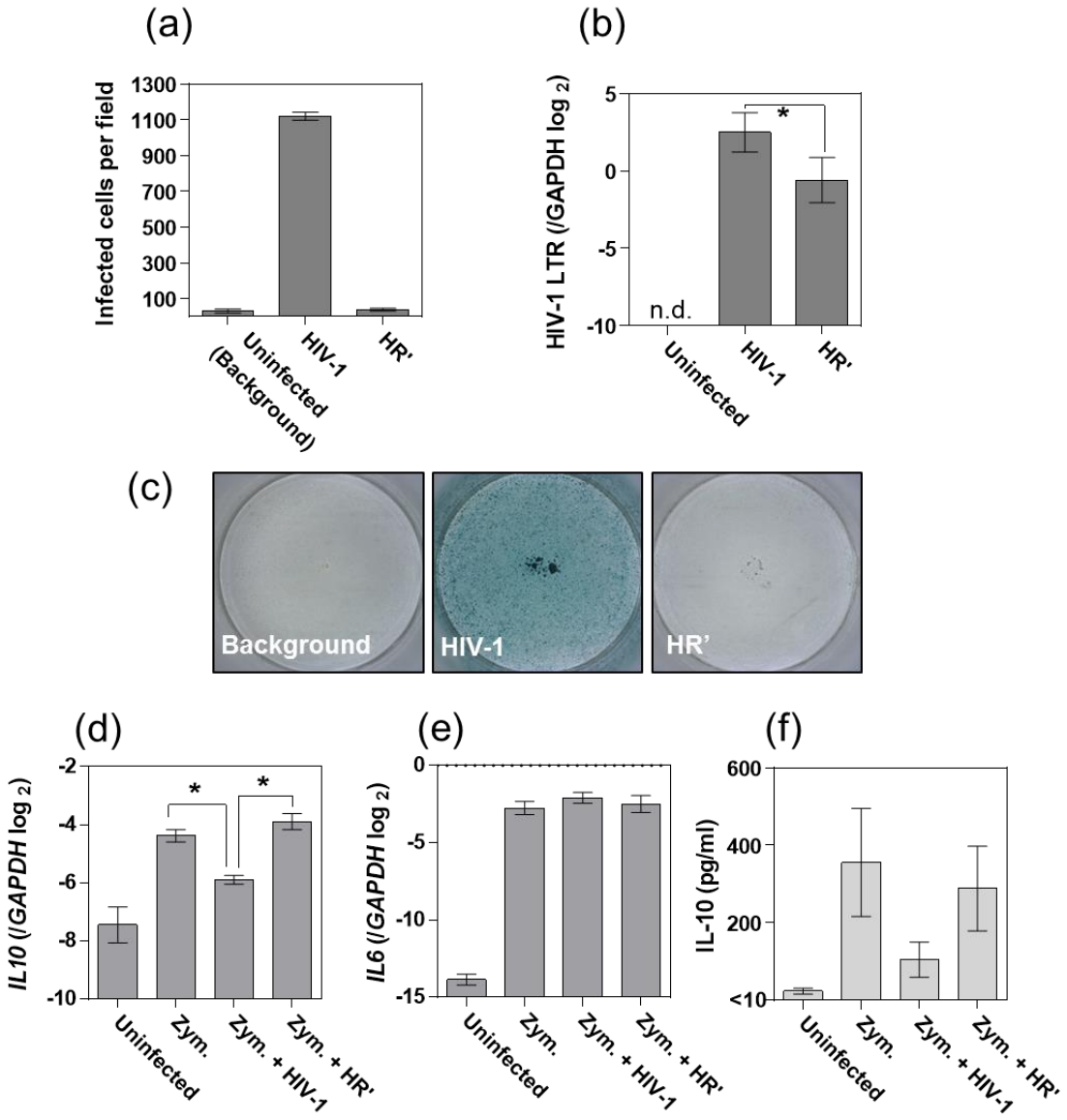

Figure 3.9: A HIV-1-based lentiviral vector does not attenuate IL-10.

MDMs were infected with HIV-1 (R9Δenv at an MOI of 3–5, with Vpx VLPs at 2ng RT/ml), or a HIV-1-based viral vector (HR') carrying only the eGFP gene under the control of the CMV promoter (7ng RT/ml with Vpx VLPs at 2ng RT/ml). MDMs were stimulated with zymosan (0.4mg/ml) for 4 hours at 1 week post-infection. mRNA expression was measured by qRT-PCR and secretion was measured by ELISA of cell culture supernatants. **(a)** Cultures were stained for HIV-1 p24 to enumerate infected cells. Staining of cells infected with HR' did not significantly exceed background levels. **(b)** HIV-1 transcript was measured by qRT-PCR for the HIV-1 LTR, and was detectable in cells infected with HIV-1 or HR', but was significantly less in those infected with HR'. **(c)** Representative images of HIV-1 p24 staining (blue). **(d)** HIV-1, but not HR', significantly attenuated *IL10* mRNA expression in response to zymosan. **(e)** *IL6* mRNA expression was not affected. **(f)** HIV-1, but not HR', reduced IL-10 secretion in response to zymosan. ***** indicates $P<0.05$, paired t-test. n.d., not detectable. Bars represent the mean −/+ SEM of 3 experiments.

3.2.7 HIV-1 Gag-Pol is not necessary for IL-10 attenuation

As integration of a provirus containing HIV-1 genetic material was necessary for IL-10 attenuation, I next investigated which HIV-1 gene products were necessary for this phenotype. The single-round virus, deleted in *env,* suggested that the Env-derived viral glycoproteins gp120 and gp41 were not necessary for attenuation. To assess whether components of the HIV-1 *gagpol* coding region, wherein the viral capsid and enzymes are encoded, were necessary for IL-10 attenuation, a mutant clone of HIV-1 (GagLucGFP) was used. In this virus, Gag-Pol expression is disrupted by cloning of the luciferase gene into this region (see **Methods section 2.4.2** for details). Infectious particles are produced using a separate Gag-pol expressor packaging plasmid.

Deficiency of HIV-1 capsid protein expression using GagLucGFP was confirmed by the absence of HIV-1 p24 staining in infected MDMs (**Figure 3.10a, c**), which also confirms the absence of immature HIV-1 gag p55. Transcription from the integrated provirus was confirmed by measurement of HIV-1 LTR transcript (**Figure 3.10b**). Expression of viral accessory proteins in the absence of HIV-1 capsid expression in GagLucGFP infection was confirmed by western immunoblotting for HIV-1 gag p55 and p24 and the accessory protein Vif (**Figure 3.10d**). The absence of viral enzymes was confirmed by an RT-ELISA of concentrated supernatants from HEK293T cells transfected with GagLucGFP plasmid with or without a Gag-Pol expressor plasmid. This showed that no RT was detectable in the latter condition (**Figure 3.10e**).

IL10 mRNA expression in response to zymosan was reduced in MDMs infected with both WT HIV-1 and GagLucGFP, but this did not reach statistical significance in either condition (**Figure 3.11a**). However, IL-10 secretion was statistically significantly reduced by both WT HIV-1 and GagLucGFP (**Figure 3.11c**). *IL6* mRNA expression was not affected by either virus (**Figure 3.11b**). These results suggest that Gag-Pol expression is not necessary for IL-10 attenuation, and thus that the viral components encoded in this region – capsid proteins, integrase, reverse transcriptase and protease – are not necessary for this phenotype.

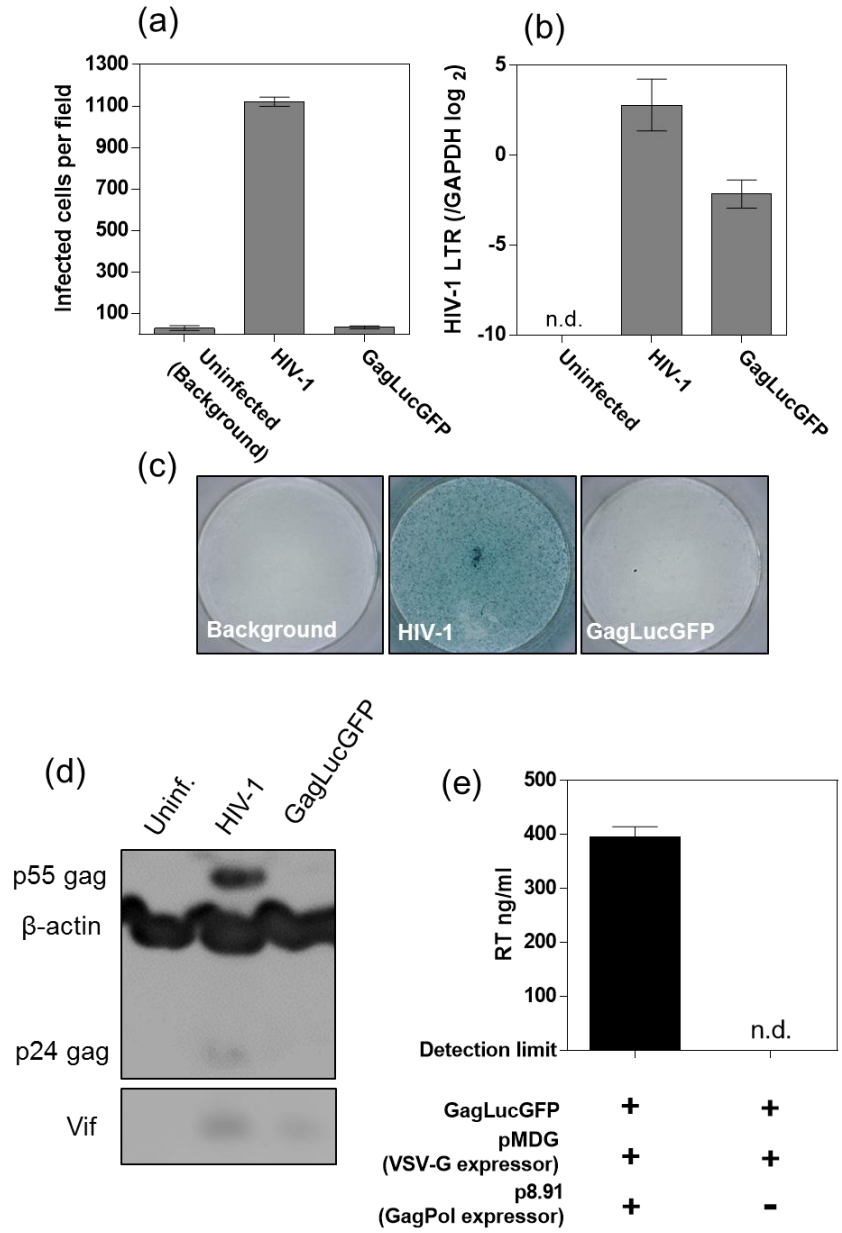

Figure 3.10: Infection using GagLucGFP, a HIV-1 mutant which does not express Gag-Pol.

MDMs were infected with HIV-1 (R9Δenv at an MOI of 3–5, with Vpx VLPs at 2ng RT/ml), or a HIV-1 mutant with the luciferase gene cloned into the GagPol coding sequence to disrupt it (GagLucGFP; at 7ng RT/ml with Vpx VLPs at 2ng RT/ml). Assessments were made 1 week post-infection. **(a)** Cultures were stained for HIV-1 p24 to enumerate infected cells. Staining of cells infected with GagLucGFP did not significantly exceed background levels. **(b)** HIV-1 RNA was measured by qRT-PCR for the HIV-1 LTR, and was detectable in cells infected with HIV-1 or GagLucGFP, but was less in those infected with GagLucGFP. **(c)** Representative images of HIV-1 p24 staining (blue). **(d)** Western immunoblotting for HIV-1 proteins. Capsid proteins p55 gag and p24 were detectable in cells infected with HIV-1, but not GagLucGFP. The HIV-1 accessory protein Vif was detectable in both infections. β-actin was used as a loading control. **(e)** Supernatants from HEK293T cells transiently transfected with the indicated plasmids were concentrated by ultracentrifugation and HIV-1 RT was measured by an RT ELISA. RT was not detectable in supernatants derived from GagLucGFP transfection unless a Gag-Pol expression plasmid (p8.91) was also transfected, indicating lack of functional RT in GagLucGFP. n.d., not detectable. Bars represent the mean −/+ SEM of 3 experiments.

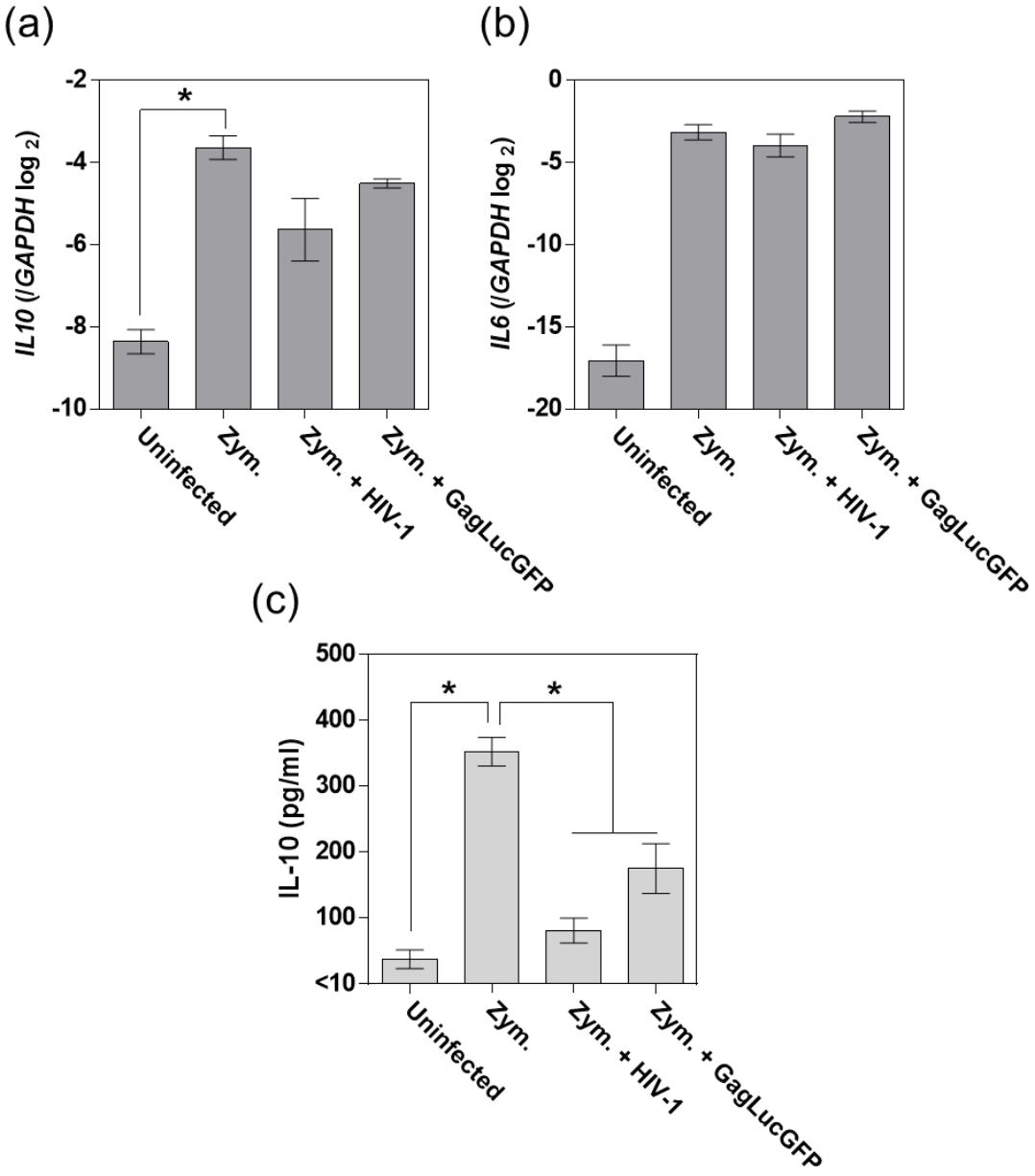

Figure 3.11: The HIV-1 mutant GagLucGFP attenuates IL-10.

MDMs infected as in **Figure 3.10** were stimulated with zymosan (0.4mg/ml) for 4 hours. **(a)** *IL10* mRNA expression was measured by qRT-PCR, and was significantly induced by zymosan. HIV-1 and GagLucGFP both reduced *IL10* mRNA expression but this was not significant. **(b)** *IL6* mRNA expression was not altered by either virus. **(c)** IL-10 secreted by MDMs was measured by ELISA of cell culture supernatants. HIV-1 and GagLucGFP significantly attenuated IL-10 secretion in response to zymosan. There was no significant difference between levels of IL-10 secreted by HIV-1 infected or GagLucGFP infected MDMs. ***** indicates $P<0.05$, paired t-test. Bars represent the mean −/+ SEM of 3 experiments.

3.2.8 The HIV-1 accessory proteins Nef, Vif and Vpr are not individually necessary for IL-10 attenuation

HIV-1 Gag-Pol and Env expression were shown not to be necessary for IL-10 attenuation but the role of the other six HIV-1 proteins in the mechanism of this phenotype remained to be explored. The viral regulatory proteins are Tat and Rev, which transactivate viral transcription and co-ordinate viral RNA transport respectively. As a result, Tat and Rev are difficult to assess in isolation via deletion, as their function is necessary for expression of all HIV-1 genes. The other four accessory proteins are non-essential for infection of cells by HIV-1, but provide functions which enhance replication such as counteracting host restriction factors (Strebel, 2013). The consequences of their loss-of-function can thus be assessed using a high-efficiency single-round model of infection such as the one presented in **Figure 3.2**. Using this model, the consequences of the loss-of-function of these proteins for propagation of infection are mitigated by achieving confluent infection of the culture in a single transduction.

To assess the role of accessory proteins in IL-10 attenuation, deleterious mutations in the genes encoding for the accessory proteins Vif, Nef and Vpr were cloned into the R9Δenv single-round infection background (see **Methods section 2.4.2** for details of mutants). Establishment of confluent infection in MDM cultures using these mutants was confirmed by HIV-1 p24 staining (**Figure 3.12a, c**), and they also displayed similar levels of viral transcript as the WT virus (**Figure 3.12b**). Deletions of Vif and Nef were confirmed by western blotting (**Figure 3.13**); suitable antibody reagents to confirm the Vpr deletion were not identified.

All mutants tested statistically significantly attenuated *IL10* mRNA expression in response to zymosan (**Figure 3.14a**), while *IL6* mRNA expression was unaffected (**Figure 3.14b**). IL-10 protein secretion was also significantly attenuated by all mutants (**Figure 3.14c**), excepting the HIV-1Δvif mutant, which non-statistically significantly attenuated IL-10 secretion. This suggests that the HIV-1 accessory proteins Nef, Vif and Vpr are not necessary for IL-10 attenuation.

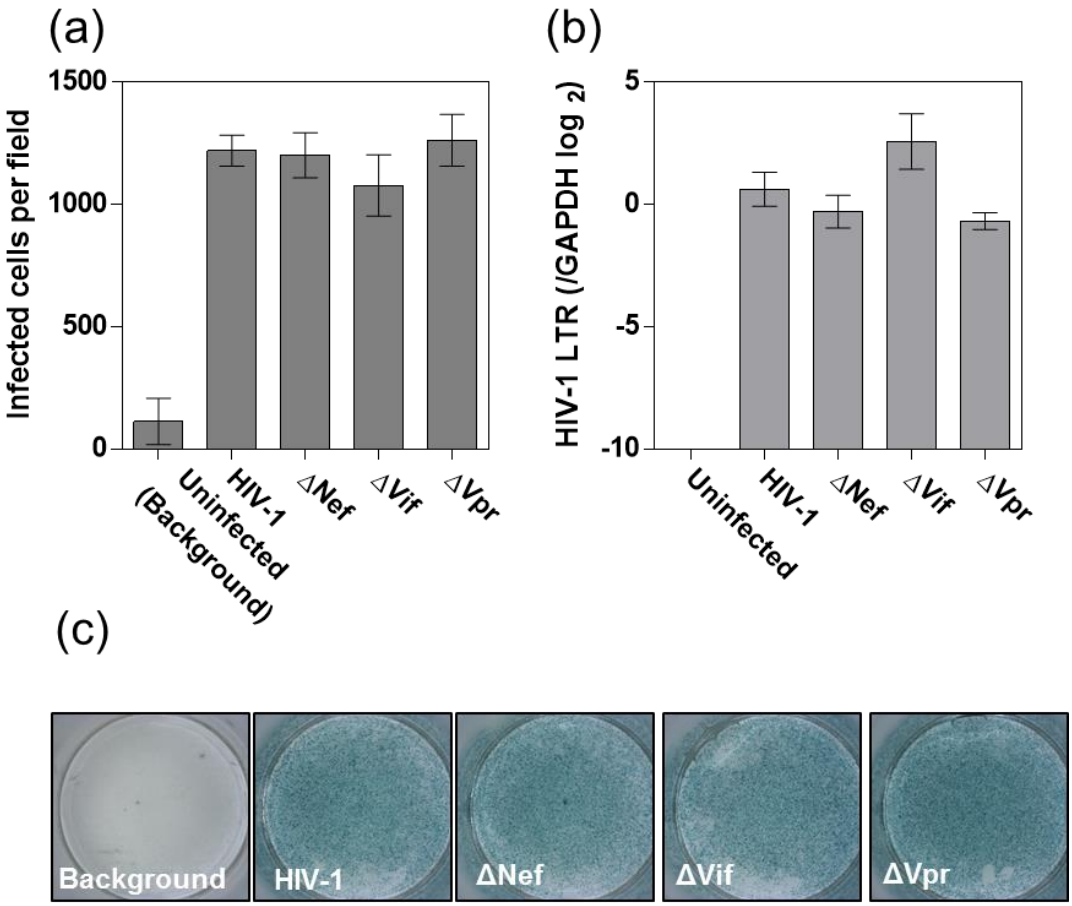

Figure 3.12: Infection with HIV-1 clones with mutations in the accessory genes Nef, Vif and Vpr.

MDMs were infected with HIV-1 clones with mutations in the accessory genes Nef, Vif and Vpr. These mutants were all in the single-round infection R9Δenv background and were used at an MOI of 3–5, with Vpx VLPs at 2ng RT/ml. Assessments were made 1 week post-infection. **(a)** Cultures were stained for HIV-1 p24 to enumerate infected cells. Staining of cells infected with deletion mutants was equivalent to that with WT virus. **(b)** HIV-1 RNA was measured by qRT-PCR for the HIV-1 LTR, and was equivalent in cells infected with deletion mutants to that with WT virus. **(c)** Representative images of HIV-1 p24 staining (blue). Bars represent the mean −/+ SEM of at least 3 experiments.

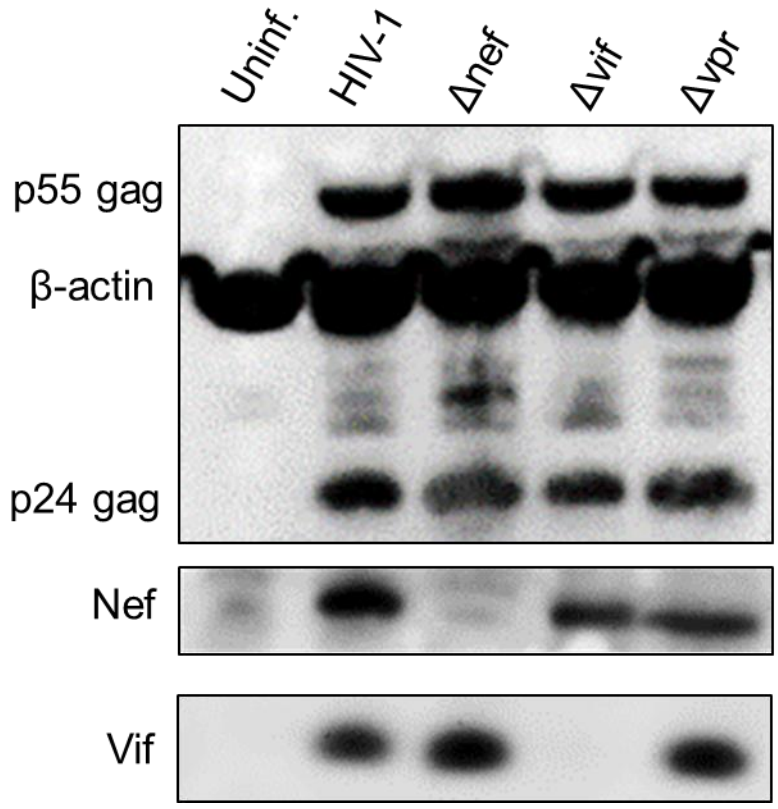

Figure 3.13: Confirmation of HIV-1 accessory protein deletions by western blotting.

MDMs were infected with HIV-1 clones with mutations in the accessory genes Nef, Vif and Vpr as in **Figure 3.12.** Western immunoblotting for Nef and Vif was performed to confirm deletions. Immunoblotting for HIV-1 p55 gag and p24 was performed to confirm HIV-1 infection, and β-actin was used as a loading control.

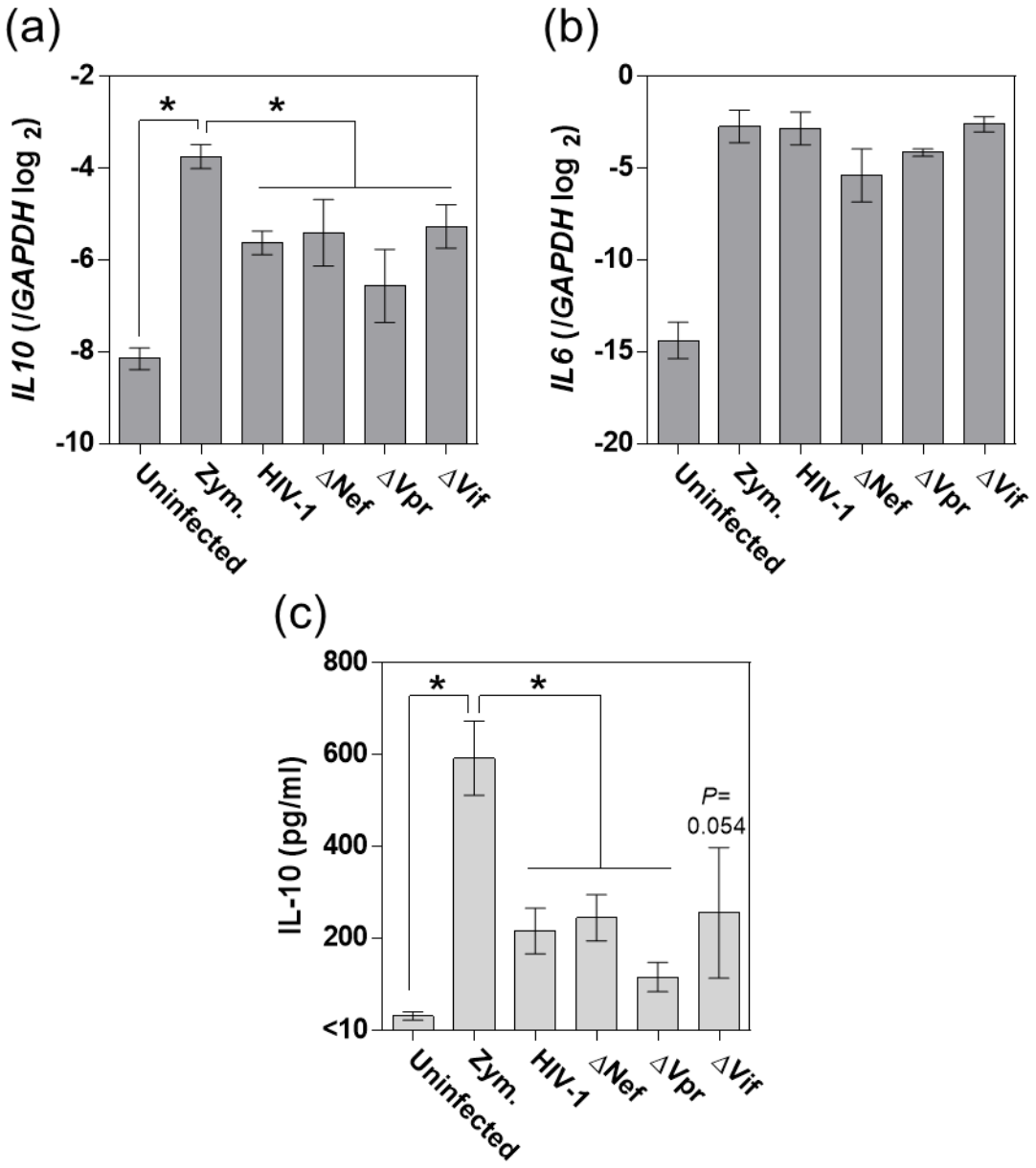

Figure 3.14: HIV-1 clones with mutations in the accessory genes Nef, Vif and Vpr attenuate IL-10.

MDMs infected as in **Figure 3.12** were stimulated with zymosan (0.4mg/ml) for 4 hours. mRNA expression was measured by qRT-PCR and secretion was measured by ELISA of cell culture supernatants. **(a)** *IL10* mRNA expression was significantly attenuated by WT HIV-1 and all mutants. **(b)** *IL6* mRNA expression was not affected by any virus used. **(c)** IL-10 secreted by MDMs was significantly attenuated by WT HIV-1 and all mutants tested, except HIV-1Δvif, in which secretion was non-significantly reduced (*P*=0.054). ***** indicates *P*<0.05, paired t-test. Bars represent the mean −/+ SEM of at least 3 experiments.

3.2.9 Type I IFN does not induce IL-10 in human MDMs

Recently, investigations of type I IFN responses in mycobacterial infection have suggested that they may exert an immunosuppressive effect by inducing IL-10 expression in monocytes and macrophages (Mayer-Barber et al., 2011; McNab et al., 2013; Teles et al., 2013). Corroboration of this observation in human MDMs, and investigation of whether HIV-1 could attenuate such a pathway, may provide insight into both the mechanism and the stimulus-specificity of IL-10 attenuation. Therefore, I sought to test whether induction of IL-10 expression by type I IFNs in human MDMs occurs, and if so, whether this can be attenuated by HIV-1 infection.

Stimulation of MDMs for 24 hours with either IFNα or IFNβ did not induce IL-10 mRNA expression or protein secretion (**Figure 3.15a, b**). This phenotype was not affected by HIV-1 infection. Type I IFN responses in MDMs at this time-point were confirmed by measuring mRNA of a prototypic IFN responsive gene, *IFI16* (Trapani et al., 1994), which was induced by both IFNα and IFNβ (**Figure 3.15c**). These data suggest that type I IFNs do not induce IL-10 responses over this time-course in M-CSF differentiated human MDMs, although they do induce other gene expression changes.

In mouse models, it has been reported that type I IFNs may be involved in inducing IL-10 expression in the context of innate immune stimulation, wherein LPS-induced IFNβ acts on macrophages in an autocrine fashion to mediate the LPS-induced IL-10 response (Chang et al., 2007). To test whether this mechanism played a role in zymosan-induced IL-10 responses and attenuation of these by HIV-1, MDMs were stimulated with zymosan in the presence of neutralising antibody to the β chain of the IFNα/β receptor (anti-IFNAR2), a method which has been shown to effectively neutralise type I IFN responses in MDM cultures (Rasaiyaah et al., 2009). Anti-IFNAR2 supplementation had no effect on zymosan-induced IL-10 mRNA expression or protein secretion, or HIV-1 attenuation thereof (**Figure 3.16**), suggesting that type I IFN does not contribute to this phenotype.

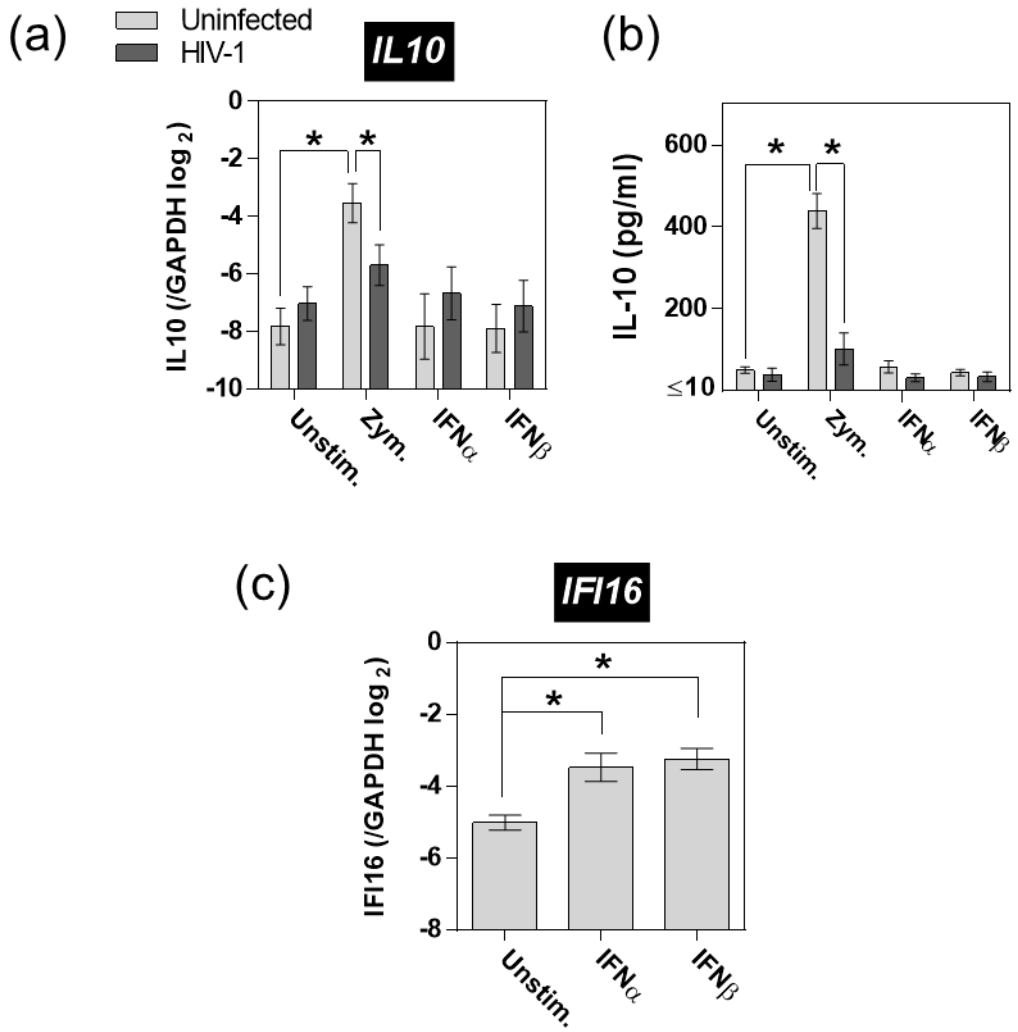

Figure 3.15: Type I IFNs do not induce IL-10 production in human MDMs.

MDMs were infected with HIV-1 (R9Δenv at an MOI of 3–5, with Vpx VLPs at 2ng RT/ml) for 1 week, and stimulated with zymosan (Zym., 0.4mg/ml) for 4 hours, or either IFNα or IFNβ (200IU/ml) for 24 hours. **(a)** *IL10* mRNA expression was measured by qRT-PCR. Zymosan induced *IL10* mRNA expression, which was attenuated in HIV-1 infected MDMs. IFNα and IFNβ did not induce *IL10* mRNA expression. **(b)** *IL10* protein secretion was measured by ELISA of cell culture supernatants. Zymosan induced *IL10* secretion, which was attenuated in HIV-1 infected MDMs. IFNα and IFNβ did not induce IL-10 secretion. **(c)** *IFI16* mRNA expression was measured by qRT-PCR. Both IFNα and IFNβ induced *IFI16* mRNA expression. ***** indicates $P<0.05$, paired t-test. Bars indicate the mean +/- SEM of at least 3 experiments.

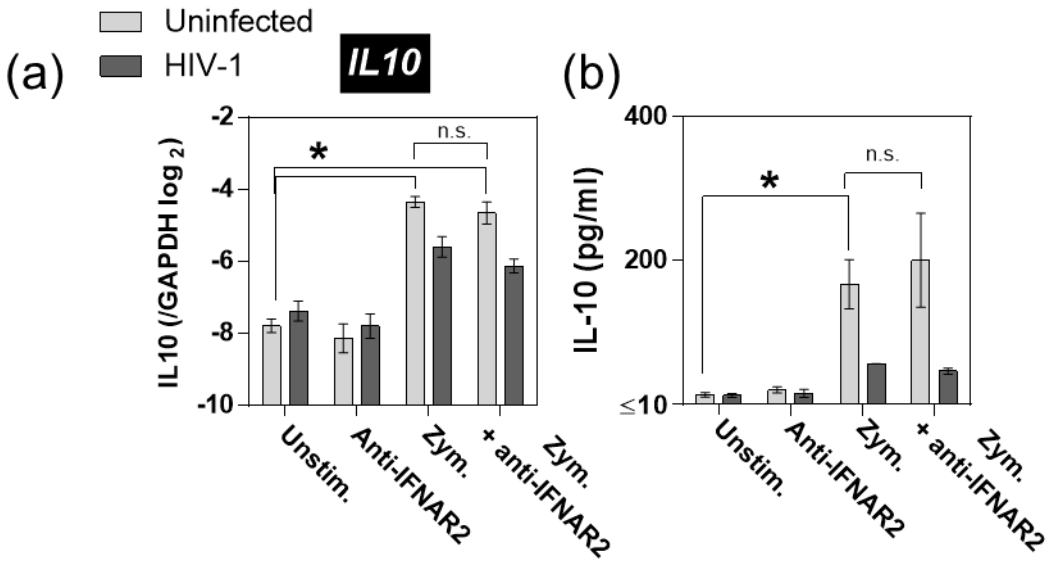

Figure 3.16: Type I IFNs do not contribute to zymosan-induced IL-10 responses.

MDMs were infected with HIV-1 (R9Δenv at an MOI of 3–5, with Vpx VLPs at 2ng RT/ml) for 1 week, and stimulated with zymosan (Zym., 0.4mg/ml) for 4 hours, with or without neutralising antibody to the β chain of the IFNα/β receptor (anti-IFNAR2, 1μg/ml). **(a)** IL-10 mRNA expression was measured by qPCR. Zymosan induced IL-10 mRNA expression, and this was attenuated by HIV-1. This phenotype was not altered by anti-IFNAR2 supplementation. **(b)** IL-10 secretion was measured by ELISA of cell culture supernatants. Zymosan induced IL-10 secretion, and this was attenuated by HIV-1. This phenotype was not altered by anti-IFNAR2 supplementation. * indicates $P<0.05$, paired t-test. Bars indicate the mean +/- SEM of at least 3 experiments.

3.2.10 IL-10 attenuation by HIV-1 is context-specific

IL-10 can be produced by cells of the mononuclear phagocyte system other than macrophages, such as monocytes and DCs (Saraiva and O'Garra, 2010). Therefore, in order to assess the cell specificity of IL-10 attenuation by HIV-1, I tested the effect of HIV-1 infection on innate immune IL-10 responses in peripheral blood monocytes, MDMs differentiated with GM-CSF rather than M-CSF, and MDDCs differentiated with IL-4 and GM-CSF. This may provide insight into the mechanism of IL-10 attenuation, as different signalling pathways are thought to be involved in the induction of IL-10 responses in different myeloid cells (Saraiva and O'Garra, 2010), as well as determining the context-specificity of this phenotype.

All cell types were infected using the single-round (R9Δenv with Vpx VLPs) model of HIV-1 infection, thus overcoming post-entry restrictions that have previously been reported in monocytes, GM-CSF differentiated MDM or MDDC. After 24 hours of infection, cells were stimulated with either zymosan, as an innate immune inducer of IL-10, or IFNβ, to assess whether type I IFNs induce IL-10 in cell types other than macrophages. HIV-1 transcription could be measured in all cell types 24 hours post-infection, suggesting that the virus had successfully integrated and was transcribing in all contexts tested (**Figure 3.17a**). *IL10* mRNA expression was induced by zymosan in monocytes, M-CSF MDMs and MDDCs, but not in GM-CSF MDMs (**Figure 3.17b**). HIV-1 statistically significantly attenuated this response in M-CSF MDMs only (**Figure 3.17b**). Significant induction of *IL10* mRNA expression by IFNβ was not observed in any cell type. *TNFA* mRNA expression was measured to assess pro-inflammatory responses, and occurred in response to zymosan in all cell types. This was unaffected by HIV-1 infection (**Figure 3.17b**).

Zymosan induced IL-10 protein secretion in monocytes and M-CSF MDMs (**Figure 3.18a**). IL-10 protein secretion was also evident in MDDCs, but this experiment was not adequately powered to reach statistical significance, and GM-CSF MDMs did not secrete IL-10 under any condition (**Figure 3.18a**). HIV-1 infection significantly attenuated IL-10 protein secretion in M-CSF MDMs (**Figure 3.18a**), in-keeping with previous data (**Figure 3.1**). In monocytes, HIV-1 infection was associated with reduced zymosan-induced IL-10 secretion, but this did not reach statistical significance (**Figure 3.18a**).

Induction of IL-10 by type I IFN was only observed in MDDCs, which secreted IL-10 after stimulation with IFNβ; however, this failed to reach statistical significance (**Figure 3.18a**). Cellular responses to IFNβ were confirmed by measuring *IFI16* mRNA expression, which was induced by IFNβ in all cell types (**Figure 3.18b**).

These results demonstrate striking cell-type specificity, in both the magnitude of IL-10 responses to zymosan and in the effect of HIV-1 infection on these. Considering the fact that equivalent levels of HIV-1 infection and pro-inflammatory cytokine responses are observed in all cell types tested, these results strongly suggest that innate immune IL-10 responses are differentially regulated in each cell, and consequently that there is a context-specific effect of the virus in exerting IL-10 attenuation.

Any role for type I IFN in inducing IL-10 responses is not demonstrated by these experiments. IFNβ does not induce IL-10 in human monocytes over 24 hours (**Figure 3.17b, Figure 3.18a**) as previously reported (Teles et al., 2013). The only context tested in which any IL-10 is produced in response to IFNβ is a secretory response in MDDCs, but that did not reach significance (**Figure 3.18a**), and *IL10* gene expression is not induced by IFNβ in these cells (**Figure 3.17b**).

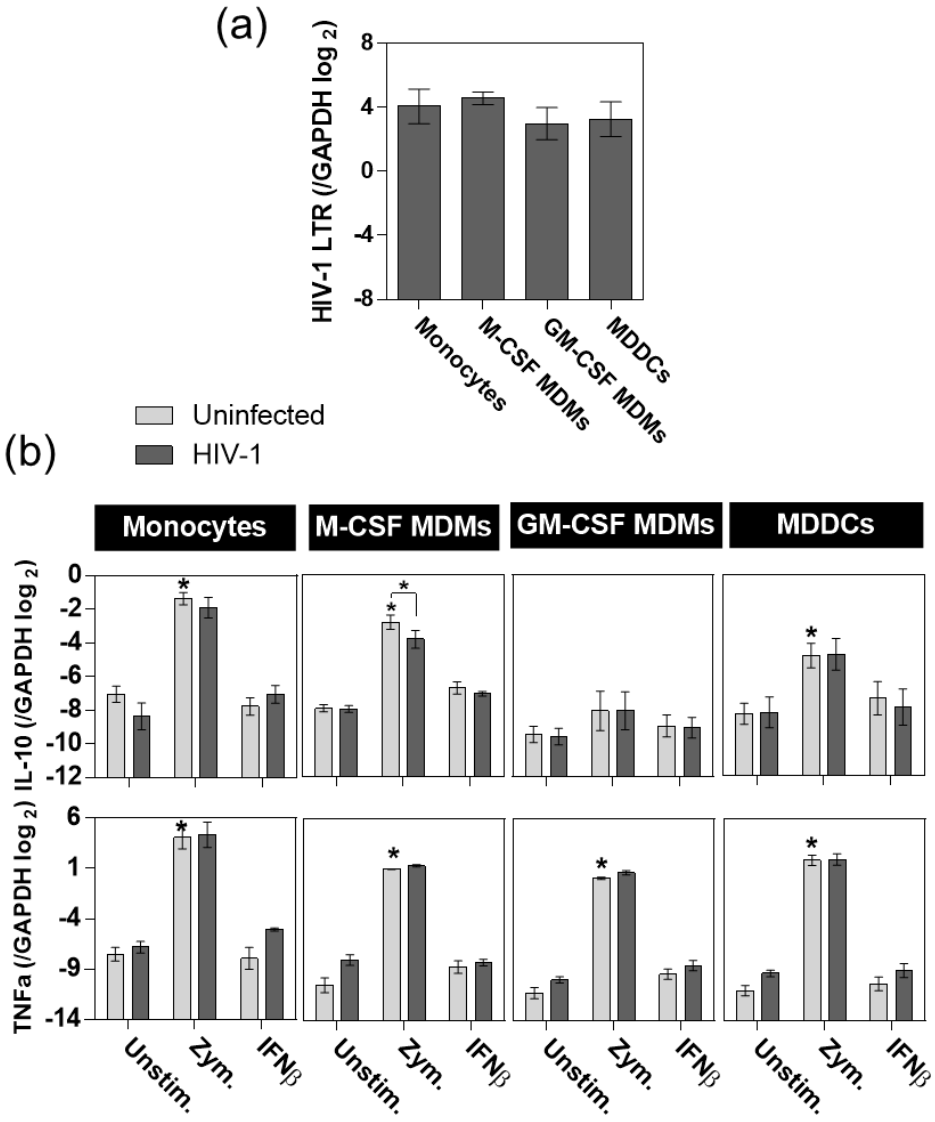

Figure 3.17: IL-10 transcription and HIV-1 attenuation in mononuclear phagocytes.

Monocytes were isolated from peripheral blood by $CD14^+$ positive selection, and either infected with HIV-1 directly *ex vivo* (R9Δenv at an MOI of 3–5, with Vpx VLPs at 2ng RT/ml), or differentiated into MDMs with either M-CSF (20ng/ml) or GM-CSF (20ng/ml), or into MDDCs with IL-4 (50ng/ml) and GM-CSF (100ng/ml). MDMs and MDDCs were differentiated for 6 days and then infected with HIV-1 as above. **(a)** HIV-1 transcription in different cell types was measured by qRT-PCR for the HIV-1 LTR. No HIV-1 transcript was detectable in uninfected cells. **(b)** After 24 hours of HIV-1 infection, each cell type was stimulated with zymosan (Zym., 0.4mg/ml) for 4 hours or IFNβ (200IU/ml) for 24 hours. *IL10* and *TNFA* mRNA expression were measured by qRT-PCR. *IL10* mRNA expression in response to zymosan occurred in monocytes, MDDCs and M-CSF differentiated MDMs, and this was attenuated by HIV-1 infection in the latter. *TNFA* mRNA expression in response to zymosan occurred in all cell types. IFNβ did not induce *IL10* or *TNFA* mRNA expression in any cell type. ***** indicates $P<0.05$, paired t-test; * above bars indicates difference from unstimulated cells, and * above brackets indicates difference between the relevant bars.

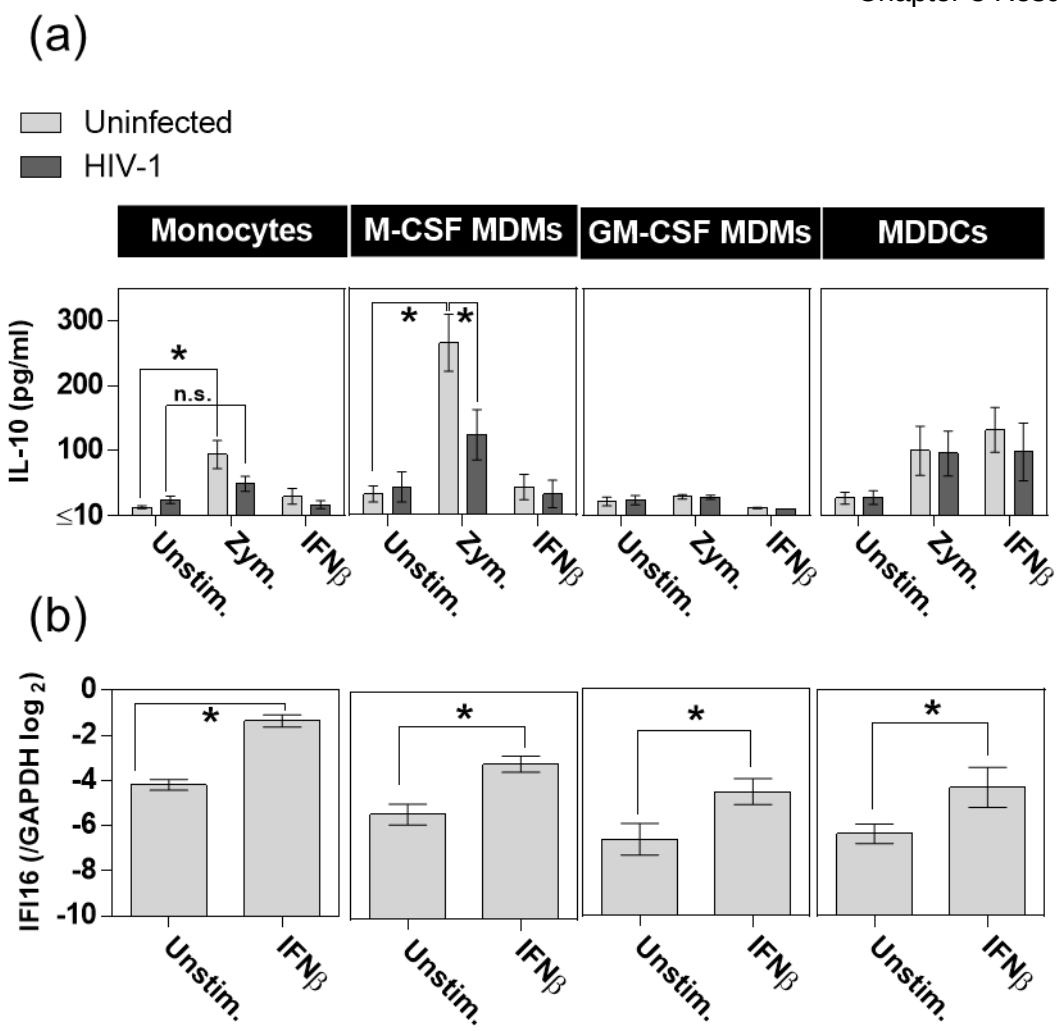

Figure 3.18: IL-10 secretion, HIV-1 attenuation and IFN responses in mononuclear phagocytes.

For details of cell differentiation, HIV-1 infection and stimulation, please see **Figure 3.17** legend. **(a)** IL-10 protein secretion was measured by ELISA of cell culture supernatants. Secretion of IL-10 in response to zymosan occurred in monocytes and M-CSF differentiated MDMs, and this was attenuated by HIV-1 infection in the latter. Significant induction of IL-10 secretion did not occur in HIV-1 infected monocytes. IL-10 secretion was observed in response to zymosan and IFNβ in MDDCs, but this was not significant in comparison to unstimulated MDDCs. **(b)** *IFI16* mRNA expression was measured by qRT-PCR, and occurred in response to IFNβ in all cell types. ***** indicates $P<0.05$, paired t-test. Bars indicate the mean +/- SEM of at least 3 experiments.

3.2.11 HIV-1 does not accelerate IL-10 mRNA decay

In addition to being controlled transcriptionally, inflammatory responses can also be regulated by effects on mRNA stability and decay (Hao and Baltimore, 2009), for example by the activity of RNA-degrading enzymes, or via the action of micro-RNAs. The molecular details of some of these mechanisms have been elucidated for pro-inflammatory cytokines such as IL-6 (Iwasaki et al., 2011) and TNFα (Carballo et al., 1998) and also for IL-10 (Stoecklin et al., 2008; Teixeira-Coelho et al., 2013). I therefore sought to test the hypothesis that reduction of *IL10* mRNA levels observed in the context of HIV-1 infection could be due to accelerated *IL10* mRNA decay. This hypothesis might underpin the observation that some induction of *IL10* mRNA by zymosan was still evident in HIV-1 infected MDM.

To measure cytokine mRNA decay rates, an inhibitor of transcription, actinomycin D, was employed. Actinomycin D prevents any new transcription by inhibiting RNA polymerase II (Sobell, 1985), and so sequential measurements of mRNA levels after its addition can be used to plot the rate of mRNA decay. MDMs with and without HIV-1 infection were stimulated with zymosan for 3 hours, after which actinomycin D was added. Measurements of mRNA levels were then made over the following 3 hours.

As expected, less *IL10* mRNA was induced by zymosan in HIV-1 infected MDMs (**Figure 3.19a**). Decay of *IL10* mRNA clearly occurred over 3 hours in both unstimulated and zymosan-stimulated cells, and this was shown to be statistically significant by two-way ANOVA (**Figure 3.19a**). *IL10* mRNA decay rates appeared similar in HIV-1 infected MDMs (**Figure 3.19a**). Decay rates were quantified by fitting a one-phase decay curve and measuring the mRNA half-life (**Table 3.2**). The half-lives calculated for *IL10* mRNA were longer in HIV-1 infected MDMs, suggesting that the mRNA was in fact more stable in this context, rather than less stable. This suggests that HIV-1 does not attenuate IL-10 by accelerating the rate of *IL10* mRNA decay.

The effects of HIV-1 on pro-inflammatory cytokine mRNAs were also measured. Statistically significant decay over this time-course was detected for *TNFA* mRNA in unstimulated and zymosan-stimulated MDMs, and for *IL1B* mRNA in unstimulated MDMs (**Figure 3.19b, c**). *IL1B* and *IL6* mRNA in zymosan-stimulated MDMs did not show statistically significant decay rates, potentially reflecting increased stability of these mRNAs due to activation of inflammatory signalling (**Figure 3.19c, d**, Hao and

Baltimore, 2009)**).** HIV-1 did not accelerate any cytokine mRNA decay rates, but in fact stabilised all cytokine mRNAs measured, as quantified by one-phase decay half-lives. These were increased for all mRNAs measured, or in some cases could no longer be calculated as decay curves could no longer be fitted to the data (**Table 3.2**).

These results demonstrate that HIV-1 does not attenuate IL-10 responses by modulating cytokine mRNA decay pathways. However, they do strongly suggest that cytokine mRNA is differentially regulated in HIV-1 infected MDMs, as all cytokine mRNAs tested were found to be more stable in this context.

	IL-10		TNFα		IL-1β		IL-6
	Unstim.	Zym.	Unstim.	Zym.	Unstim.	Zym.	Zym.
Uninfected	26.25	19.7	22	37.45	48.18	n/a	34.32
HIV-1	105.8	n/a	57.44	386.3	877.4	n/a	n/a

Table 3.2: Cytokine mRNA half-lives calculated from one phase decay curves.

Half-lives for cytokine mRNAs were calculated from fitted one-phase decay curves using GraphPad Prism 6. Where significant decay curves could not be fitted, suggesting that mRNA did not decay, half-lives are not presented (indicated by n/a). Zymosan stimulation increased the half-life of *TNFA* mRNA and prevented decay of *IL1B* mRNA. HIV-1 infection increased half-lives or prevented decay for all cytokine mRNAs measured. Data are derived from the results of 3 experiments.

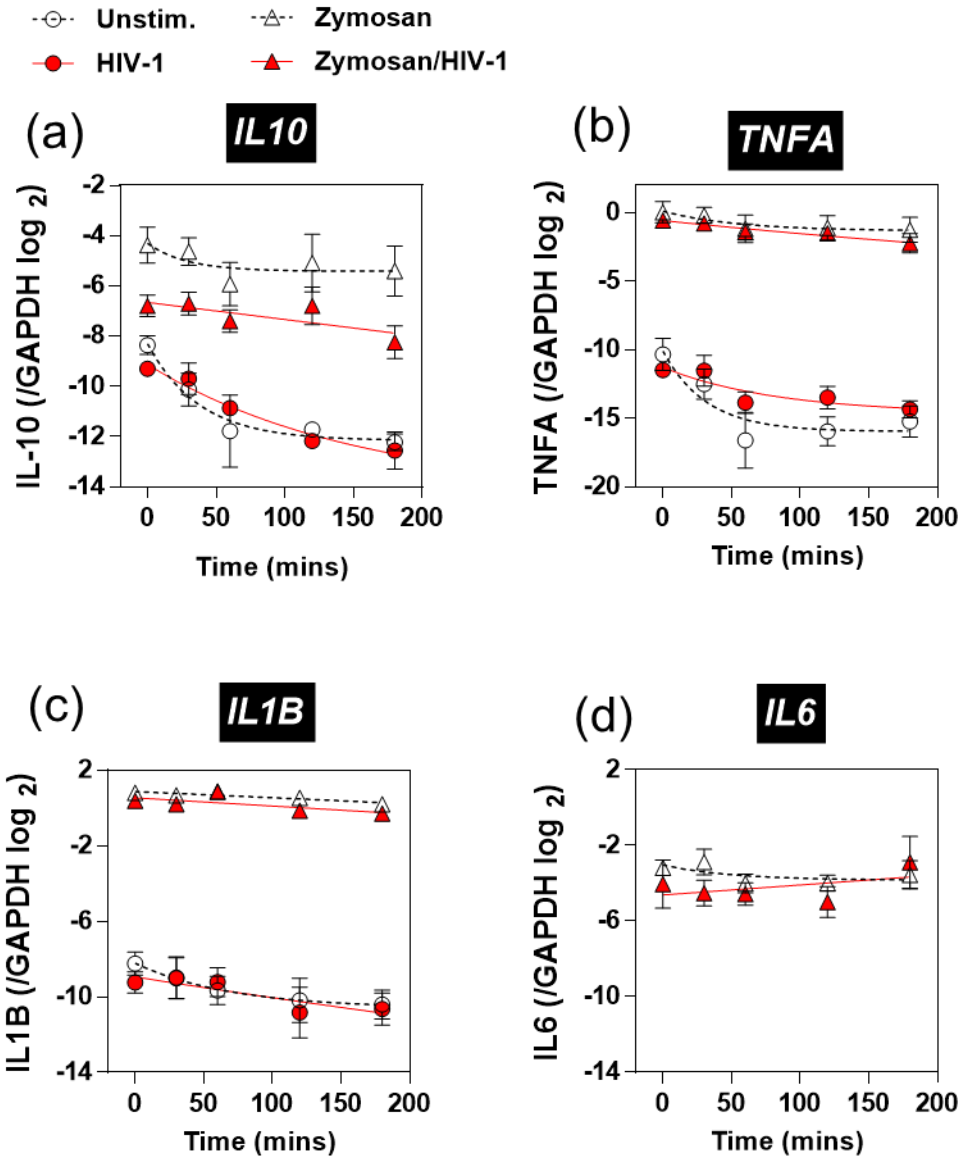

Figure 3.19: HIV-1 does not accelerate cytokine mRNA decay.

MDMs were infected with HIV-1 (R9Δenv at an MOI of 3–5, with Vpx VLPs at 2ng RT/ml) for 1 week and then stimulated with zymosan (0.4mg/ml) for 3 hours, at which time actinomycin D (an RNA polymerase II inhibitor) was added to cultures at 10ug/ml to inhibit further transcription. RNA samples were collected at 0, 30, 60, 120 and 180 minutes post-actinomycin D addition. Levels of cytokine mRNA at each time-point were measured by qRT-PCR. One-phase decay curves were fitted to data using GraphPad Prism 6. Symbols show mean mRNA level −/+ SEM at each time-point and lines show one-phase decay curves. The X-axis shows time post-actinomycin D addition. Statistical assessment was performed by two-way ANOVA, with $P<0.05$ used to determine significance. **(a)** *IL10* mRNA measurements and decay curves. Significant decay of *IL10* mRNA was observed across this time-course in all conditions. **(b)** *TNFA* mRNA measurements and decay curves. Significant decay of *TNFA* mRNA was observed across this time-course in all conditions. **(c)** *IL1B* mRNA measurements and decay curves. Significant decay of *IL1B* mRNA was observed across this time-course in unstimulated MDMs, with and without HIV-1 infection. **(d)** *IL6* RNA mRNA measurements and decay curves. No significant decay of *IL6* mRNA was detected across this time-course in any condition. *IL6* RNA was not detected in unstmulated MDMs. RNA half-lives, calculated from one-phase decay curves, are presented in **Table 3.2**. Data are derived from the results of 3 experiments.

3.2.12 HIV-1 does not attenuate zymosan-induced NFκB translocation

HIV-1 did not modulate IL-10 mRNA post-transcriptionally by accelerating its decay. It also did not act at the level of receptor signalling, as attenuation was observed downstream of multiple PRRs (**Figure 3.1**). This indicates that that the mechanism of attenuation involves the signalling pathways controlling IL-10 transcription downstream of PRR signalling.

Diminution of the activity of a signalling pathway, rather than complete inhibition, would account for the observed incomplete inhibition of IL-10 transcription. Previous investigations have shown that LPS-induced NFκB pathway activation is attenuated in HIV-1 infected MDMs (Noursadeghi et al., 2009). The NFkB pathway has been implicated in the control of IL-10 responses in macrophages (Saraiva and O'Garra, 2010), but NFkB attenuation was not previously observed to be associated with IL-10 attenuation (Noursadeghi et al., 2009). However, LPS is not a strong inducer of IL-10 responses in M-CSF differentiated MDMs (**Figure 3.1b**), and so significant IL-10 attenuation may simply not have been evident in that context. I investigated NFκB activation in response to zymosan, which does induce substantial IL-10 responses in MDMs.

NFκB activation was measured by assessing nuclear translocation of the RelA subunit of NFκB, quantified as a nuclear/cytoplasmic ratio of this protein. Induction of translocation by zymosan from 30−120 minutes was statistically significant by two-way ANOVA, and equivalent in uninfected and HIV-1 infected MDMs (**Figure 3.20**). This suggests that attenuation of NFκB signalling is not the mechanism of IL-10 attenuation in HIV-1 infected MDMs, as no clear attenuation occurs during stimulation with a strong inducer of IL-10.

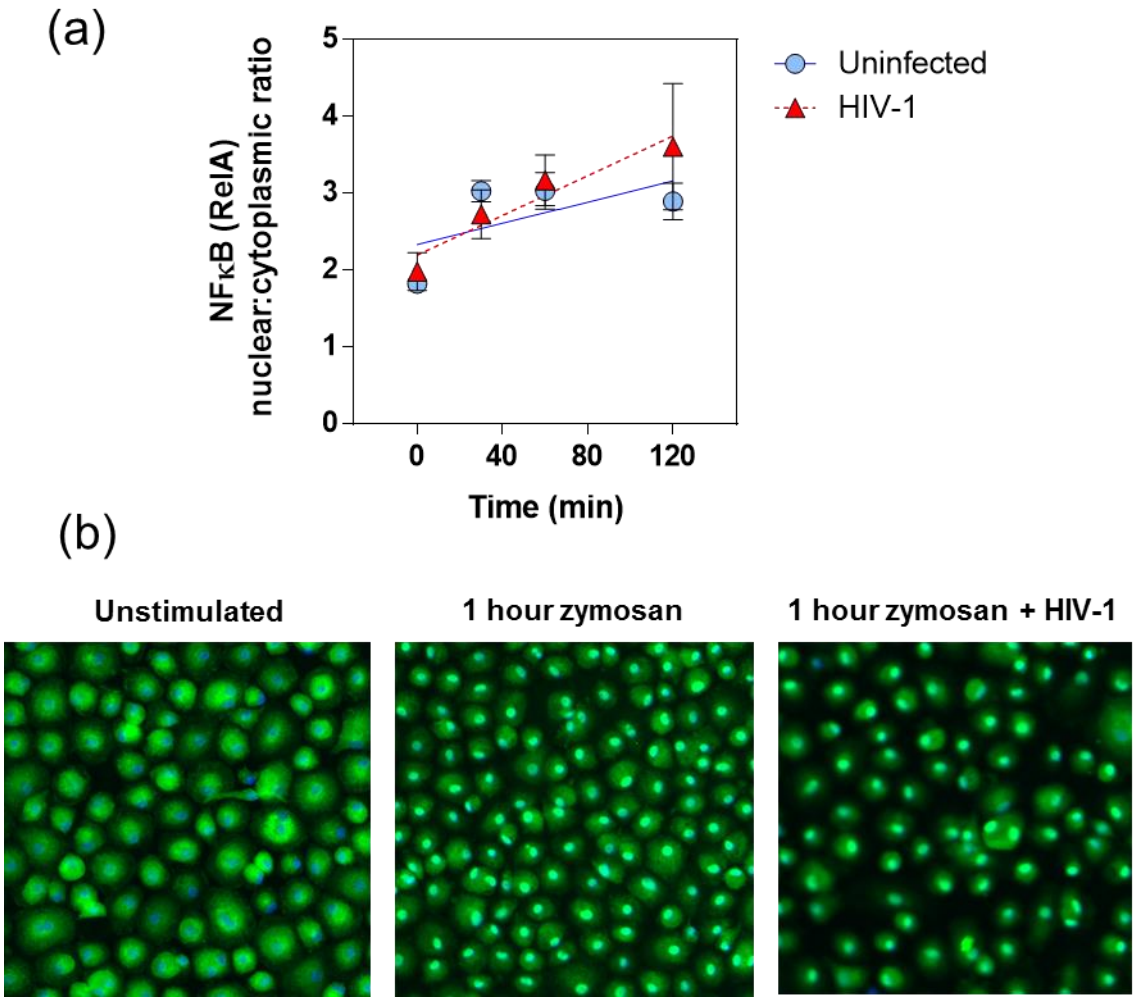

Figure 3.20: HIV-1 does not alter zymosan-induced NFκB translocation.

MDMs were infected with HIV-1 (R9Δenv at an MOI of 3–5, with Vpx VLPs at 2ng RT/ml) for 1 week and then stimulated with zymosan (0.4mg/ml) for 0–120 minutes. **(a)** Activation of the NFκB pathway was measured by quantitative imaging analysis of nuclear translocation of NFκB (RelA), assessed as a ratio of nuclear:cytoplasmic intensity of RelA immunofluorescence staining. Nuclear localisation of RelA significantly increased with time (P=0.0054, two-way ANOVA) but this was not affected by HIV-1. Symbols represent mean values −/+ SEM from 4 experiments. Lines show linear regression, fitted using GraphPad Prism 6. **(b)** Representative images of the NFκB translocation assay. Nuclei are stained blue with DAPI and NFκB RelA is stained green. Nuclear NFκB is evident in the right-hand panels of zymosan-stimulated MDMs (green nuclear staining).

3.2.13 Inhibition of IL-10 induction pathways identifies the PI3K pathway as a specific regulator of anti-inflammatory cytokines

In addition to the NFκB pathway, multiple other signalling pathways downstream of PRRs have been shown to contribute to IL-10 expression in mononuclear phagocytic cells. Activation of the MAP kinase cascades (Chanteux et al., 2007; Ma et al., 2001b; Yi et al., 2002) and PI3K signalling (Bai et al., 2014; Hu et al., 2006) are suggested to play critical roles. Calcium-burst stimulated signalling via CaM kinase II and Pyk2 is also thought to contribute, downstream of dectin-1 (Kelly et al. 2010).

I aimed to identify which of these pathways were involved in controlling IL-10 production in M-CSF differentiated MDMs, in order to highlight candidate pathways on which HIV-1 might exert its effects. Small molecule inhibitors of these pathways were used to this effect. MDMs were pre-incubated with inhibitors of p38 and ERK MAP kinases, PI3K, CaM kinase II or Pyk2, prior to stimulation with Mtb culture filtrate or zymosan. Secretion of IL-10, and for comparison, IL-6, were measured at 4 hours.

Inhibition of p38 MAP kinase, PI3K or Pyk2 reduced IL-10 secretion in response to Mtb culture filtrate (**Figure 3.21a**) or zymosan (**Figure 3.21b**). However, inhibiting p38 MAP kinase or Pyk2 also led to reduced IL-6 secretion in response to these stimuli (**Figure 3.21c, d**). As HIV-1 does not attenuate production of IL-6, this suggests that the virus does not act via these pathways to exert specific attenuation of IL-10. However, inhibition of PI3K did not reduce IL-6 secretion in response to these stimuli (**Figure 3.21c, d**), highlighting it as a candidate molecule involved in specific regulation of IL-10 but not of pro-inflammatory cytokines.

Activation of the PI3K signalling pathway begins with recruitment of PI3K to the intracellular regions of activated receptors, including PRRs (Weichhart and Säemann, 2008), where it is activated and catalyses the phosphorylation of phosphatidylinositol-4,5-trisphosphate (PIP_2) to phosphatidylinositol-3,4,5-trisphosphate (PIP_3) (Liu et al., 2009). PIP_3 then acts as a second messenger to activate downstream targets, the most critical of which is the serine/threonine kinase Akt (Liu et al., 2009). Akt acts as the main mediator of the functional effects of PI3K activation by phosphorylating a range of further targets (Liu et al., 2009). One key target of Akt is mTOR, a high molecular weight kinase which controls protein synthesis pathways (Liu et al., 2009). It has previously been highlighted that the PI3K-Akt-mTOR pathway might play a role in

differential regulation of the anti-inflammatory IL-10 response versus pro-inflammatory responses, in a review of the function of this pathway in innate immune cells (Weichhart and Säemann, 2008). A recent study further explored this mechanism in mouse bone marrow-derived macrophages (BMDMs), and showed that mTOR activity specifically controlled anti-inflammatory and pro-inflammatory responses (termed "cytokine biasing") by controlling the efficiency of translation of cytokine mRNAs (Ivanov and Roy, 2013).

I tested whether the PI3K-Akt-mTOR pathway was involved in differential control of anti-inflammatory and pro-inflammatory responses in M-CSF differentiated human MDMs, using specific inhibitors of PI3K, Akt and mTOR, and measuring cytokine mRNA and protein expression in response to zymosan. Inhibition of any of these molecules led to a statistically significant reduction in *IL10* mRNA expression in response to zymosan (**Figure 3.22a**), while *IL6* and *TNFA* mRNA expression were unaffected (**Figure 3.22b, c**). Similarly, at the level of protein expression, inhibition of PI3K or mTOR led to a statistically significant reduction in IL-10 secretion, and inhibition of Akt substantially reduced IL-10 secretion although this did not reach statistical significance (**Figure 3.22d**). Again, IL-6 and TNFα were unaffected (**Figure 3.22e, f**).

These results confirm that the PI3K-Akt-mTOR pathway specifically controls the anti-inflammatory IL-10 response, and not the pro-inflammatory cytokines TNFα and IL-6, in human MDMs. The effects of inhibiting this pathway phenotypically copies the effect of HIV-1 on cytokine responses to zymosan, and thus highlights a strong candidate for where HIV-1 may exert its effects to mediate IL-10 attenuation.

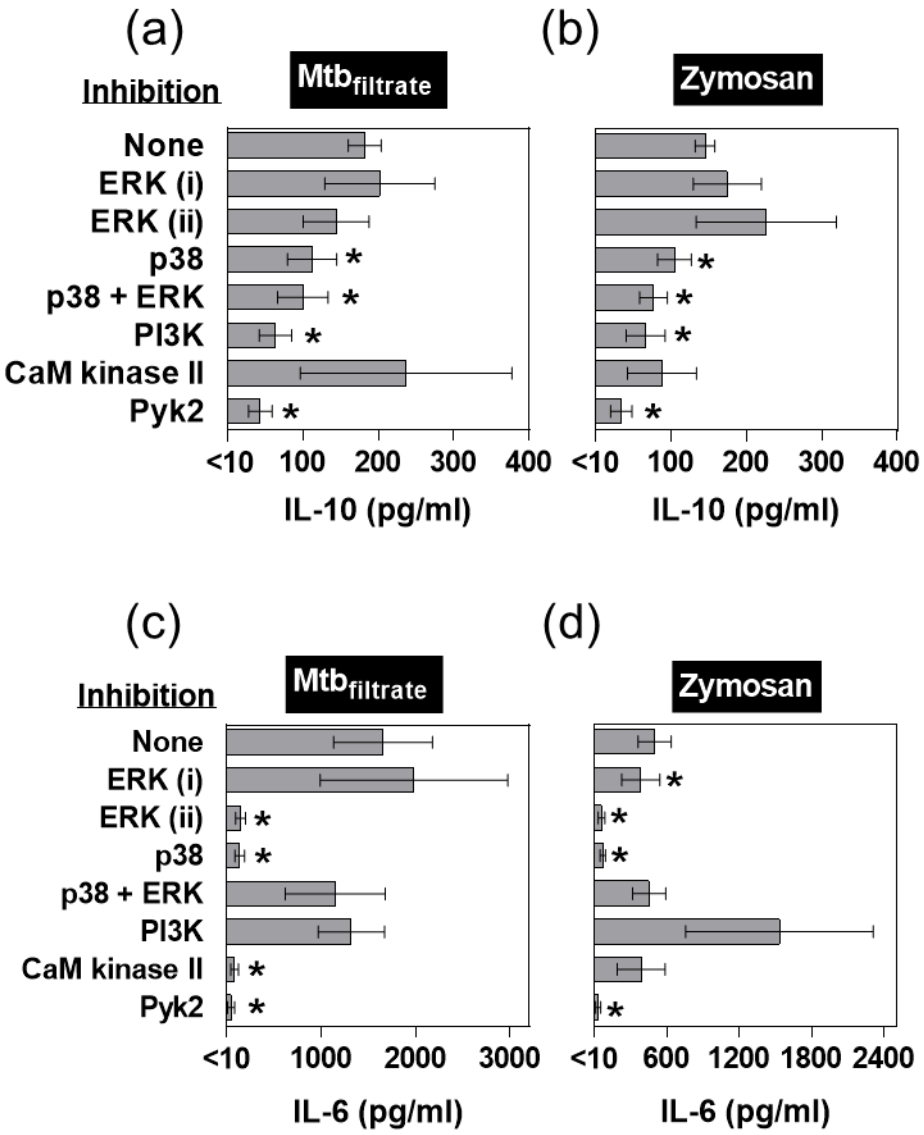

Figure 3.21: Inhibition of innate immune signalling pathways inhibits IL-10 and IL-6 responses.

MDMs were pre-incubated with small molecule inhibitors of ERK1/2 MAP kinase (i: PD98059 or ii: U0126), p38 MAP kinase (SB203580), p38 and ERK1/2 combined (PD98059 and SB 203580), PI-3 kinase (LY294002), CaM kinase II (KN93) or Pyk2 (AG17), all at 10μM, for 2 hours before stimulation with Mtb culture filtrate or zymosan (0.4mg/ml) for 4 hours. Cytokine secretion was measured by ELISA of cell culture supernatants. **(a)** IL-10 secretion in response to $Mtb_{filtrate}$ was significantly reduced by inhibition of p38, p38 and ERK combined, PI-3 kinase or Pyk2. **(b)** IL-10 secretion in response to zymosan was significantly reduced by inhibition of p38, p38 and ERK combined, PI-3 kinase or Pyk2. **(c)** IL-6 secretion in response to $Mtb_{filtrate}$ was significantly reduced by inhibition of ERK, p38, CaM kinase II or Pyk2. **(d)** IL-6 secretion in response to zymosan was significantly reduced by inhibition of ERK, p38 or Pyk2. ***** indicates $P<0.05$, paired t-test. Bars represent the mean −/+ SEM of 4 experiments.

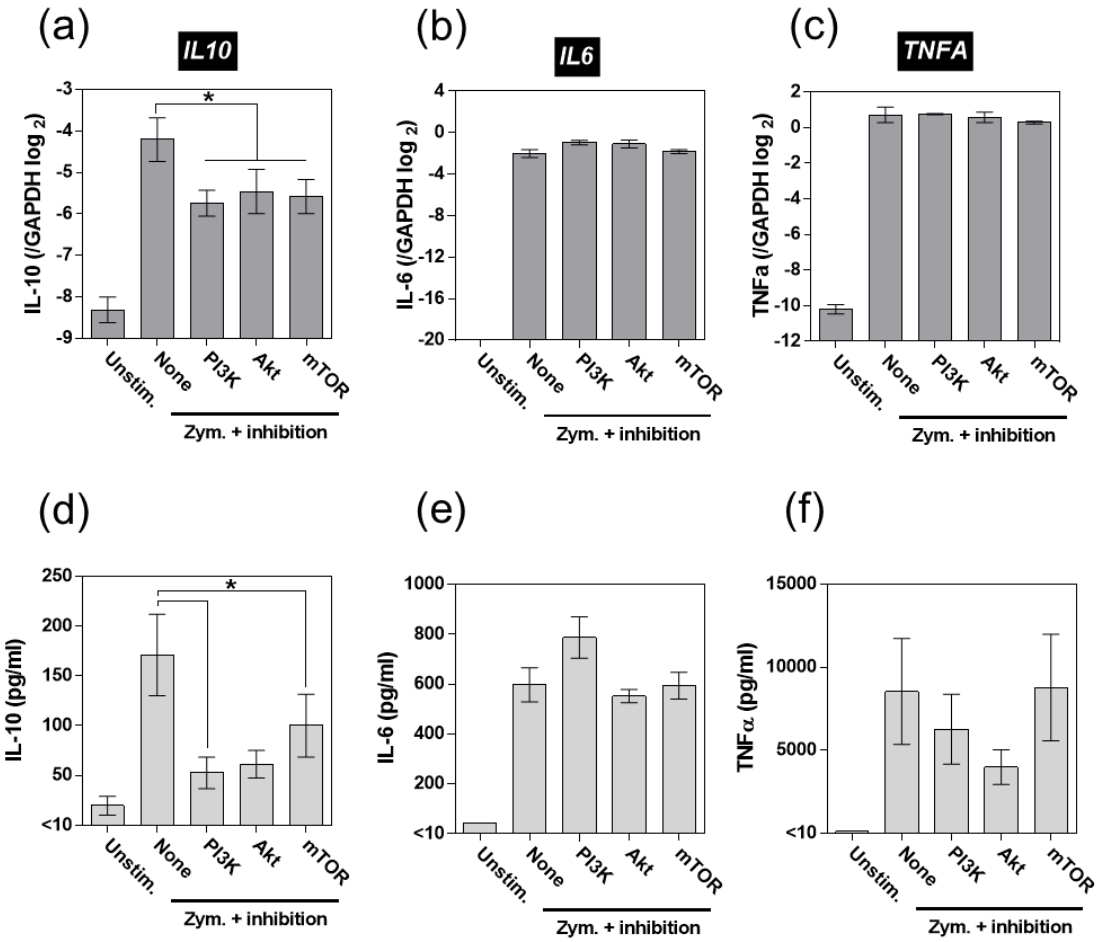

Figure 3.22: Inhibition of the PI3K pathway specifically inhibits IL-10 but not pro-inflammatory cytokine responses.

MDMs were pre-incubated with small molecule inhibitors of PI3K (LY294002, 10μM), Akt (triciribine, 20μM) or mTOR (rapamycin, 200nM), all at 10μM, for 2 hours before stimulation with zymosan (0.4mg/ml) for 4 hours. Cytokine mRNA expression was measured by qRT-PCR and secretion was measured by ELISA of cell culture supernatants. **(a)** *IL10* mRNA expression in response to zymosan was significantly reduced by inhibition of PI-3 kinase, Akt or mTOR. **(b, c)** *IL6* and *TNFA* mRNA expression in response to zymosan were not affected by any inhibitor. **(d)** IL-10 secretion in response to zymosan was reduced by Akt inhibition and significantly reduced by PI-3 kinase and mTOR inhibition. **(e, f)** IL-6 and TNFα secretion were not affected by any inhibitor. ***** indicates $P<0.05$, paired t-test. Bars represent the mean −/+ SEM of 3 experiments.

3.2.14 Levels of Akt and its phosphorylation are not altered by HIV-1

As the PI3K-Akt-mTOR pathway was a strong candidate for where HIV-1 might act to exert IL-10 attenuation, I further investigated this pathway in HIV-1 infected MDMs. Akt is essentially the central hub of this signalling pathway: it is recruited to the membrane by PI3K-produced PIP_3, where it undergoes a conformational change which facilitates its activation via phosphorylation, after which it phosphorylates a range of downstream targets (Liu et al., 2009). Assessment of Akt activation may therefore help identify if HIV-1 modulates the upstream membrane-proximal section of this signalling pathway involving PI3K, PIP_3 and Akt, or the downstream components such as mTOR and other Akt targets. Control of total Akt levels by its ubiquitination and subsequent targeting for degradation has been reported as a regulatory mechanism for this pathway (Ivanov and Roy, 2013). It has also previously been reported that phosphorylation of Akt may be reduced in HIV-1 infected M-CSF differentiated human MDMs (Huang et al., 2006).

I assessed total Akt levels and Akt phosphorylation in response to 5–120 minutes of zymosan stimulation in uninfected and HIV-1 infected MDMs. Total levels of Akt were unaffected by HIV-1 infection, suggesting that ubiquitin-targeted degradation of Akt also does not play a role in this phenotype (**Figure 3.23**); however, the bands for total Akt for donors 2 and 3 were highly dense and may have been saturated, meaning that assessing the dynamic range of density of these bands may not have been optimal. Akt phosphorylation was present at baseline, and was increased by zymosan stimulation over this time-course, but this was not affected by HIV-1 infection (**Figure 3.23, 3.24**). These results suggest that HIV-1 does not attenuate IL-10 by degrading Akt, or modulating its activation via phosphorylation at its Ser473 residue. This suggests that if HIV-1 does modulate the PI3K-Akt-mTOR pathway in order to attenuate IL-10, it may act downstream of Akt, potentially at the level of mTOR activation. It is also possible that an aspect of Akt activation which has not been assessed is affected, such as its localisation, or phosphorylation at its second activation residue, Tyr308.

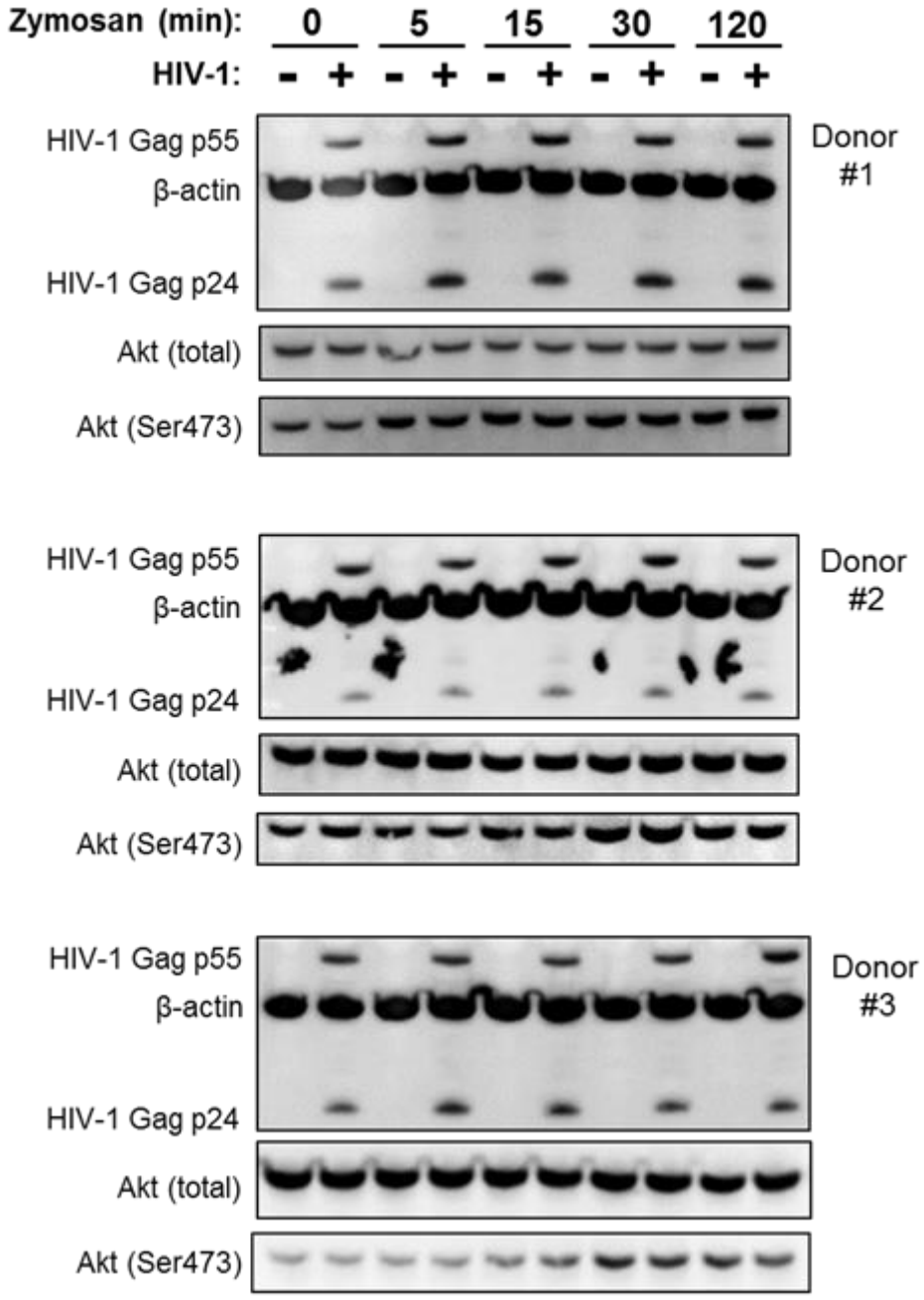

Figure 3.23: Levels of total Akt and Akt phosphorylation in response to zymosan are not altered by HIV-1.

MDMs were infected with HIV-1 (R9Δenv at an MOI of 3–5, with Vpx VLPs at 2ng RT/ml) for 1 week and then stimulated with zymosan (0.4mg/ml) for 0–120 minutes. Cell lysates were collected and Akt phosphorylation (Ser473) was assessed by Western immunoblotting. Total Akt levels were also measured for comparison. β-actin levels were measured to confirm equivalent loading. HIV-1 Gag p55 and p24 were measured to confirm HIV-1 infection. Western blots from 3 independent experiments are presented.

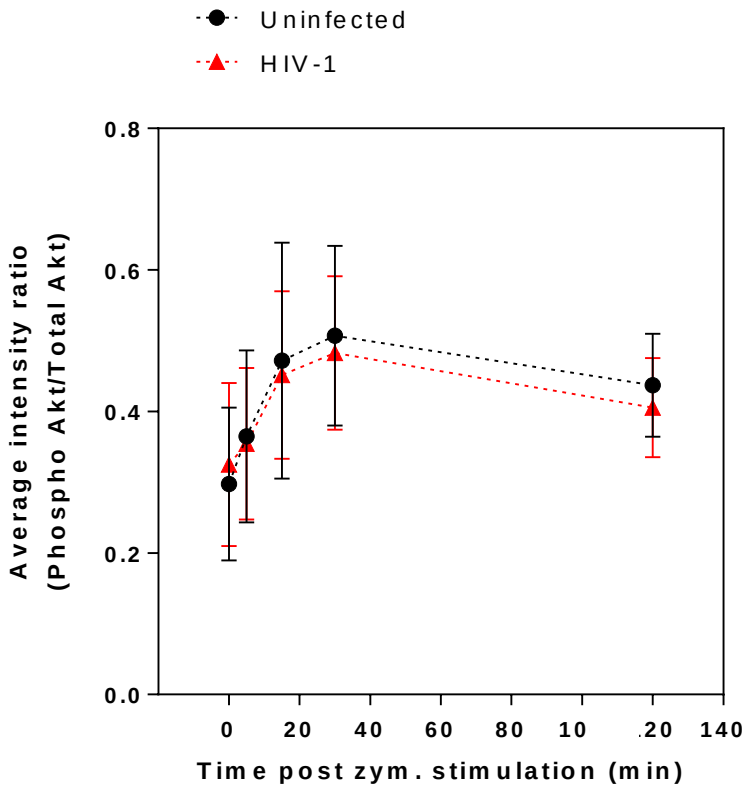

Figure 3.24: Densitometry of Akt phosphorylation in response to zymosan.

Densitometry calculations were performed with AlphaViewer software on the Western blots presented in **Figure 3.23**. The average intensity of the phosphorylated (Ser473) Akt bands was normalised to the average intensity of the total Akt bands, to quantify relative levels of Akt phosphorylation. Akt phosphorylation was significantly induced over time (*P*= 0.0429, two-way ANOVA), but this was not altered in HIV-1 infection. Symbols represent mean values −/+ SEM from 3 experiments.

3.3 Chapter discussion

In this body of work, I aimed to characterise HIV-1 mediated attenuation of macrophage IL-10 responses, in terms of viral and host determinants, and to identify a potential mechanism for this phenotype. I found that IL-10 attenuation was not limited to Mtb responses, but occurred downstream of other IL-10-inducing innate immune stimuli, and was evident across the time-course of the innate immune IL-10 response. Viral propagation was not required, as IL-10 was attenuated by a single-round HIV-1 infection or in the presence of protease inhibitor inhibition of mature virion production. Viral entry was not sufficient for IL-10 attenuation to occur, nor was integration. My results indicate that transcription of HIV-1 genes, and specifically accessory proteins, were necessary for this phenotype.

The host determinants of IL-10 attenuation were also delineated. Type I IFNs did not induce IL-10 responses in mononuclear phagocytes, and played no evident role in HIV-1 attenuation of IL-10. Attenuation was highly cell type-specific, as HIV-1-infected monocytes and DCs did mount innate immune IL-10 responses but these were not attenuated by HIV-1. Suppression of *IL10* mRNA by HIV-1 was demonstrated to be due to modulation of pre-transcriptional regulatory pathways, as *IL10* mRNA decay was not potentiated by the virus. Investigation of which signalling cascades controlled IL-10 production in MDMs highlighted the PI3K pathway as a key regulator of the anti-inflammatory cytokine response. Exploration of the effects of HIV-1 on this pathway suggested that any modulation of its activity by the virus occurs downstream of the activation of the kinase Akt.

HIV-1 attenuated IL-10 responses downstream of a range of innate immune stimuli, such as zymosan, curdlan and Pam_2CSK_4. This suggested that IL-10 attenuation may be relevant to infection with pathogens other than Mtb which stimulate TLR-2 or dectin-1. To assess whether this phenotype is relevant in further contexts, challenge with ligands or pathogens which stimulate other PRRs may be informative. For example, IL-10 responses have been reported downstream of TLR-3 (Bai et al., 2014). It is clear that the attenuating effect of HIV-1 is most apparent in the context of stimuli such as Mtb and zymosan, which induce the most substantial macrophage IL-10 responses. When considering host immune adaptation to pathogens, it might be that when a large IL-10 response is requisite for an effective response, the attenuating

effect of HIV-1 is at its greatest and most subversive for normal host immunity. As such, the significance of this phenotype *in vivo* is likely to display pathogen specificity, in relation to their propensity to induce IL-10.

These results also provide insight into the mechanism by which HIV-1 attenuates IL-10: it must act downstream of receptor ligation, as multiple receptors are implicated in this phenotype. Further mechanistic insight is provided by the demonstration that a single-round Env-deleted HIV-1 can attenuate IL-10 (**Figure 3.2**), as this shows that Env-derived proteins, viral assembly and budding are not causative in this phenotype. I further confirmed this observation via protease inhibitor supplementation of HIV-1 infected MDM cultures, in which context IL-10 attenuation was still evident (**Figure 3.5**).

These experiments demonstrate that non-productively infected MDMs exhibit attenuated IL-10 responses, and that ongoing viral propagation is not necessary for this phenotype. This is of particular significance when considering that macrophages may form a long-lived reservoir of HIV-1 infection during anti-retroviral therapy; these experiments suggest that IL-10 attenuation might persist in such a context, and that it might contribute to immune dysfunction which occurs during HAART, such as IRIS. It is interesting to note that some of the co-infections most commonly associated with IRIS are with Mtb or fungal pathogens (Lawn et al., 2008), which are indicated to be strong innate immune producers of IL-10 responses in macrophages, using Mtb culture filtrate, or the fungal cell wall derivative zymosan (**Figure 3.1**).

Investigation of the viral determinants of IL-10 attenuation clearly showed that viral entry was not sufficient for attenuation to occur. This suggests that the component of HIV-1 which mediates attenuation is not present in the virion in sufficient quantities to mediate its effects. Viral integration was necessary for attenuation, but was not sufficient, as an empty viral vector did not cause attenuation. This experiment indicates that the various consequences of integration itself, such as insertional mutagenesis, do not cause IL-10 attenuation, but that HIV-1 genetic material is necessary for attenuation. It has not formally been demonstrated in this set of experiments that viral transcription from the integrated HIV-1 provirus is necessary for attenuation; it may be difficult to test this question specifically, as inhibitors of HIV-1 transcription generally also have off-target effects on host transcription (Baba, 2004). HIV-1 clones deleted for the viral transactivator Tat, in which viral transcription is instead controlled by doxycycline responsive Tet-on elements, may be potential tools in this regard (Das et al., 2011).

It is difficult to envisage a viral function that results purely from the presence of HIV-1 genetic material without its transcription, out-with mutagenic consequences of the event of integration, which has already been eliminated as a sufficient mechanism. Consequently, the most likely hypothesis is that viral transcription, and production of new viral components, is necessary for IL-10 attenuation. I therefore investigated which components of the virus may be necessary. As previously discussed, Env-derived proteins and the viral protease have been shown not to be involved.

I tested the role of the remaining Gag-Pol proteins by using a virus in which no mature Gag-Pol-derived proteins are expressed, as the luciferase gene is cloned in-frame into Gag. This virus also lacks Env and expresses GFP in place of Nef. Resultingly, only the viral accessory proteins Tat, Rev, Vif, Vpr and Vpu are expressed. However, it was still capable of attenuating zymosan-induced IL-10 production – suggesting that one or more of the aforementioned accessory proteins are causative in this phenotype. It also remains possible that immature sections of Gag, which are still expressed as part of the Gag-Luciferase fusion protein expressed here, are involved. To clarify this, it may be necessary to construct and test a virus which expresses only Gag-Pol and no accessory proteins.

The necessity of various HIV-1 accessory proteins was further investigated using deletion mutants, showing that Nef, Vif and Vpr are not autonomously necessary for IL-10 attenuation. This leaves Vpu, Tat and Rev as candidates for this mechanism. Testing a Vpu deletion mutant in the same manner as Nef, Vif and Vpr is a simple subsequent experiment. However, Tat and Rev cannot be similarly assessed via deletion, as their functions are necessary for all efficient viral RNA production. As Tat in particular may be a strong candidate for mediating the phenotype, as it is a modulator of transcription, a priority for future experiments should be designing strategies for testing its role. The aforementioned doxycycline-inducible Tat mutants are an option for testing this, or expressing either Tat or Rev in isolation may demonstrate if either is sufficient to cause this phenotype. It also remains possible that IL-10 attenuation is a consequence of a redundant function of the accessory proteins, in which case single expression vectors should cause the phenotype. As the HIV-1 accessory proteins have a range of functions (see **Introduction section 1.3.4**), there is no single clear potential mechanism for how one of them might act to attenuate IL-10. However, the functions of Vpu and Vif in mediating host interactions are by degrading host proteins (Conticello et

al., 2003; Dubé et al., 2010) suggest that degradation of a host factor involved in IL-10 regulation is a potential mechanism.

A final potential mechanism to consider is that IL-10 attenuation does not involve viral proteins, but is due to a viral mRNA species, such as a microRNA. It has been shown that HIV-1 encodes microRNA species, and that these can regulate host gene expression (Narayanan et al., 2011; Ouellet et al., 2013; Schopman et al., 2012). MicroRNAs regulate gene expression post-transcriptionally by binding to mRNAs, preventing their translation or targeting them for degradation (Fabian et al., 2010). As the effect of HIV-1 on IL-10 is to reduce transcript levels, the former mechanism is unlikely, and the latter mechanism is refuted by later experiments showing that HIV-1 does not accelerate IL-10 mRNA decay. This suggests the action of viral miRNAs is not likely to be causative in mediating attenuation.

Further insights into the mechanism of IL-10 attenuation were made by investigating the host determinants of this phenotype. Various publications have described that induction of IL-10 by type I IFNs in macrophages and monocytes is a critical mechanism by which these cytokines exert immunosuppressive effects which may be relevant in protection against mycobacteria (Mayer-Barber et al., 2011; McNab et al., 2013; Teles et al., 2013). In my experiments, no significant IFN-mediated IL-10 induction was evident in human MDMs, DCs or monocytes (**Figure 3.15, Figure 3.18**), nor was type I IFN found to contribute to zymosan-induced IL-10 (**Figure 3.16**), as has been reported for LPS-induced IL-10 (Chang et al., 2007). There may be several reasons for these discrepancies with published reports: substantial evidence is derived from mouse models of Mtb infection (Chang et al., 2007; Guarda et al., 2011; Mayer-Barber et al., 2014, 2011; McNab et al., 2013), and so this may reflect differences between the murine and human immune systems. Additionally, several murine studies use surrogate methods to demonstrate induction of IL-10 by type I IFN, such as suppressed IL-10 responses in the context of *IFNAR1* knock-out (Mayer-Barber et al., 2011; McNab et al., 2013), or IL-10 production downstream of an inducer of type I IFN such as pICLC (Mayer-Barber et al., 2014, 2011), and do not show direct induction of IL-10 as a result of type I IFN signalling.

Previous reports in the human system also have some key differences from the experiments presented here. These include showing induction of IL-10 by type I IFNs in whole PBMC (Aman et al., 1996; Rudick et al., 1996) rather than specifically in mononuclear phagocytic cells; induction in monocytes only during synergistic

stimulation with LPS (Aman et al., 1996); or drawing conclusions from increased serum IL-10 in multiple sclerosis patients treated with IFNβ (Rep et al., 1999; Rudick et al., 1996). Additionally, the Interferome 3.0 database does not identify IL-10 as a type I IFN target gene (http://interferome.its.monash.edu.au/interferome; Rusinova et al., 2013).

This review of the literature, in conjunction with the experimental data presented here, strongly suggests that although type I IFNs have clearly been shown to exert immunosuppressive functions (Mayer-Barber et al., 2014) and may indeed contribute to IL-10 responses in an indirect manner, they do not directly induce IL-10 production from resting human mononuclear phagocytes. Their well-characterised immunosuppressive effects on IL-1β production, via which pathway they have been postulated to regulate anti-mycobacterial responses, have recently been shown to be controlled by a pathway which does not implicate IL-10 (Reboldi et al., 2014). A single published report shows direct induction of IL-10 in human monocytes after stimulation with IFNβ (Teles et al., 2013), and there are no clear differences between that experimental setup and the one presented here. Reductionist experiments, such as using an IL-10 promoter-reporter system in an IFNAR-expressing cell line, may assist in further clarifying this issue. Overall, these experiments demonstrate that type I IFN does not directly induce macrophage IL-10 responses, and so further insights into HIV-1 attenuation of IL-10 cannot be gained via investigation of this pathway.

The cell type specificity of IL-10 responses and attenuation was also investigated. It was observed that HIV-1-mediated attenuation of zymosan-induced IL-10 specifically occurred in M-CSF differentiated MDMs and not in other IL-10-producing mononuclear phagocytes, such as monocytes or MDDCs (**Figure 3.17, Figure 3.18**). This suggests that IL-10 attenuation is a context-specific phenomenon. Macrophages differentiated with GM-CSF did not express IL-10 in response to zymosan, despite expressing a pro-inflammatory cytokine, TNFα; it is possible that the *IL10* locus is closed in these cells and as such *IL10* expression is not inducible. This observation is interesting when considering that the major roles of GM-CSF in regulating macrophage biology are thought to be during inflammation or differentiation of alveolar macrophages. The absence of production of an anti-inflammatory cytokine may fit with the former scenario, but as AMs are suggested to produce IL-10 *in vivo*, the relevance to the latter scenario is less clear.

The largest IL-10 responses evident in the different cell types tested were found in the cells in which HIV-1 significantly attenuated IL-10: the M-CSF differentiated

MDMs. This again suggests that the attenuating effect of HIV-1 is at its greatest and most potent in the context of large IL-10 responses which are generated by specific cell types in response to specific pathogens. If these responses are a host-evolved protective mechanism, then this suggests that modulation by HIV-1 may certainly have pathogenic consequences. This leads to consideration of how the demonstrated context-specificity of this phenotype might be relevant *in vivo*; which *in vivo* mononuclear phagocyte is the *in vitro* M-CSF differentiated MDM an appropriate model of? Are they an appropriate *in vitro* model of alveolar macrophages (AMs), which are presumably the most relevant cells for this phenotype in HIV-1/Mtb co-infection? A previous investigation showed that this MDM model is morphologically and transcriptionally more similar to AMs than to DCs and monocytes, but that AMs had a heightened pro-inflammatory bias compared to MDMs (Tomlinson et al., 2012). It is also clear that AM development is dependent on GM-CSF signalling (Bonfield et al., 2003; Guilliams et al., 2013), which may suggest that GM-CSF differentiated MDMs are a more appropriate model of AM. AM, however, have been shown to produce IL-10, although less than M-CSF differentiated MDM (Hoppstädter et al., 2010). Further experiments assessing this phenotype using *ex vivo* isolated tissue mononuclear phagocytes, such as alveolar macrophages or Langerhans cells, including from HIV-1 positive patients, may be informative.

To establish the temporal dynamics of MDM cytokine responses and HIV-1 modulation of these, I investigated zymosan-induced expression of *IL-10* mRNA and IL-10 protein, and of pro-inflammatory cytokines for comparison, over a time-course in uninfected and HIV-1 infected MDMs (**Figure 3.3, Figure 3.4**). The dynamics of the IL-10 response were clearly differentiated from that for the pro-inflammatory cytokines IL-6 and pro IL-1β. *IL10* mRNA expression took longer to develop, and this was also a self-limited response which returned to baseline after 24 hours, whereas the pro-inflammatory cytokines were expressed rapidly after stimulation and these responses persisted to 72 hours. This raises two hypotheses about the specific regulation of IL-10 responses in MDMs, which may provide insight into how HIV-1 attenuates these responses; firstly, is it a secondary response gene in the innate immune response (Medzhitov and Horng, 2009), as would be suggested by a delay in its transcription post-stimulation? Chromatin remodelling of the *IL10* locus has been shown to play a role in LPS-induced IL-10 expression (Saraiva et al., 2005), which would support this suggestion. And secondly, do negative feedback loops exist to limit its expression? IL-

10 is suggested to be negatively regulated by a range of transcription factors (Saraiva and O'Garra, 2010), and whether HIV-1 modulates these pathways merits investigation.

Homeostatic control of IL-10 is also known to be mediated post-transcriptionally via destabilizing motifs in the 3' untranslated region of the mRNA (Powell et al., 2000). It is also a target for the RNA-degrading enzyme tristetraprolin (Stoecklin et al., 2008). HIV-1 might attenuate IL-10 responses by accelerating decay of *IL10* mRNA, leading to lower measurable levels of the cytokine mRNA at any single time-point. I investigated the rate of IL-10 mRNA decay, and found that it was not accelerated by HIV-1 infection. In fact, HIV-1 was associated with increased stability of all cytokine mRNAs measured; an interesting observation which may be informative when considering modulation of the PI3K-mTOR pathway by HIV-1 as a potential mechanism of attenuation, discussed subsequently.

It is also possible that an effect of the virus on the IL-10 locus, e.g. in terms of its histone modifications and availability for transcription, is involved. However, as some IL-10 transcription is detectable in HIV-1 infected MDMs, this seems less likely, indicating that the virus acts pre-transcriptionally to attenuate IL-10. I therefore investigated the signalling pathways involved in inducing IL-10 transcription in macrophages. Although attenuation of the NFκB pathway has previously been demonstrated in HIV-1 infected MDMs (Noursadeghi et al., 2009), this was not evident downstream of zymosan stimulation, and so did not present a strong candidate for the host determinant of this phenotype. Investigation of which innate immune pathways were involved in specific regulation of IL-10 and not pro-inflammatory cytokine responses in MDMs identified the PI3K pathway as a clear candidate target for HIV-1, as inhibition of this pathway pheno-copied the effects of HIV-1 on IL-10.

A number of previous reports have highlighted the PI3K pathway as a positive regulator of IL-10 in both human and murine macrophages, including in responses to mycobacteria (Bai et al., 2014; Fallah et al., 2011; Foey et al., 2001; Hu et al., 2006). One key report using mouse BMDMs demonstrated that this pathway was critical in establishing the phenomenon of "cytokine biasing", wherein the cytokine response to pathogenic strains of *Legionella* was dominated by pro-inflammatory transcripts and displayed a lack of IL-10, while non-pathogenic strains did induce IL-10 (Ivanov and Roy, 2013). This was controlled by degradation of Akt during infection with the pathogenic bacteria, which led to lower levels of mTOR activity, thus reducing the efficiency of cellular translation. The mRNAs of pro-inflammatory cytokines, which were

in higher abundance, were then preferentially translated in comparison to low abundance IL-10 transcripts (Ivanov and Roy, 2013).

If this mechanism also occurs in human macrophages, it is clearly a strong candidate for how HIV-1 might cause IL-10 attenuation; perhaps the virus essentially induces a “cytokine biasing” phenomenon, causing the macrophage to react to stimuli as though they had increased pathogenicity. The levels of IL-10 transcript which are induced in response to innate immune stimulation are generally of lower abundance than pro-inflammatory transcripts (**Figure 3.19, Figure 3.22**), which would support this possibility. However, these is clearly a discrepancy here, as the mechanism described by Ivanov and Roy (2013) takes place at the level of protein production, while the phenotype caused by HIV-1 attenuates IL-10 transcription. In addition, inhibiting mTOR in human MDMs inhibited IL-10 transcription as well as protein secretion (**Figure 3.22**), and as it is well-established that mTOR regulates proteins via translation and not transcription, this observation requires further exploration. It is possible that inhibitory effects on transcription due to mTOR inhibition represent negative feedback effects from its effects on translation, wherein reduced levels of IL-10 protein (or another anti-inflammatory factor) feedback to impact on IL-10 transcription. The observation that HIV-1 increases all cytokine mRNA stability (**Figure 3.19**) is also interesting to consider in this regard; if the virus reduces mTOR activity and translational efficiency by affecting the PI3K pathway, perhaps mRNAs are more stable as a result due to less traffic through the translation pathway.

Although how the PI3K-Akt-mTOR pathway specifically regulates the IL-10 response in human MDMs is not entirely clarified, I made preliminary assessments of its activity in HIV-1 infected MDMs. Previous reports linking HIV-1 to this pathway have suggested that Nef activates PI3K in order to downregulate MHC class I molecules and modulate apoptosis (Hung et al., 2007; Linnemann et al., 2002; Swann et al., 2001; Wolf et al., 2001). It has also been shown that Env-derived gp120 or Tat can activate this pathway (Deregibus et al., 2002; François and Klotman, 2003). An up-regulatory effect on this pathway would be unlikely to explain the IL-10 attenuation phenotype, and in any case the relevance of these reports to MDM biology is not entirely clear, as they are mainly made using T cells, or transformed cell lines which often have inherent PI3K pathway dysfunction (Astoul et al., 2001). Akt is a central hub of the PI3K pathway, and has been implicated in the phenomenon of cytokine biasing, and so it was selected as a focus for investigation. However, HIV-1 was not shown to have any

effect on its total levels or on Ser473 phosphorylation. This suggests that the virus does not modulate the activity of this pathway at this level, or further upstream; the most informative subsequent experiments, therefore, should be to investigate activation of mTOR and other downstream targets of Akt in HIV-1 infected MDMs. Localisation of Akt, which also plays a role in its activation, should also be assessed.

In summary, I have shown that HIV-1 mediates innate immune IL-10 attenuation in macrophages in a highly context-specific manner, and that this is likely to be due to an as-yet unidentified function of a viral accessory protein. The most promising candidate host pathway that might be affected by the virus is the PI3K-Akt-mTOR pathway, which appears to play a key role in specifically regulating IL-10, and hence potentially producing the phenomenon of cytokine biasing. HIV-1 might act downstream of Akt to modulate this pathway and hence dysregulate IL-10 production in macrophages. Further exploration of the activity of this pathway in MDMs, and of the virological determinants of this phenotype, may fully chararactise this novel host-virus interaction which has the potential to impact substantially on the function of the immune response.

Chapter 4. Results 2. The consequences of IL-10 attenuation for HIV-1 replication and the immune response

4.1 Background

HIV-1 attenuates macrophage IL-10 responses to Mtb and other innate immune stimuli. My investigation into the mechanism of this phenotype has shown that it is a consequence of integration by HIV-1 and is dependent on expression of viral accessory proteins. The host pathways affected by the virus may involve the specific regulation of the anti-inflammatory cytokine response differentially from the pro-inflammatory cytokine response, and the PI3K pathway is a strong candidate in this regard.

The ability of HIV-1 to specifically inhibit macrophage production of IL-10, which has well-established immunomodulatory and anti-inflammatory functions, raises several questions about the consequences of this phenotype. Firstly, does it have consequences for the virus? HIV-1 appears to have evolved to cause this phenotype, as it is indicated to be due to the function of viral proteins expressed in the macrophage. This raises the teleological question of whether IL-10 attenuation confers any advantage to the virus; can IL-10 modulate HIV-1 replication, or alter cellular permissivity to HIV-1 infection?

The previously characterised potent functions of IL-10 suggest that its attenuation by HIV-1 is also likely to have consequences for the host immune response. The contexts in which this phenotype might play an immunopathological role must be considered. Mtb is clearly one example of a clinically important co-infecting pathogen that induces a strong macrophage IL-10 response which HIV-1 can attenuate. However, as this phenotype is not Mtb-specific, are there other pathogens which may be affected by it? Exploring whether other co-infecting pathogens induce IL-10 responses in MDMs may help elucidate the importance of this phenotype for immunopathology *in vivo* in HIV-1 positive patients.

The potential mechanisms of immunopathology which IL-10 attenuation might trigger also clearly merit investigation. In a previous investigation within our group, IL-10 attenuation was associated with exaggerated downstream pro-inflammatory

responses in HIV-1/Mtb co-infected macrophages (Tomlinson et al., 2014). This included exaggerated production of pro-inflammatory cytokines which IL-10 normally acts to suppress, such as TNFα, IL-1β and IL-23. These results indicated that autocrine IL-10 signalling in macrophage inflammatory responses could potently affect macrophage function. Further understanding of how IL-10 modulates macrophage function and macrophage-generated inflammatory processes may provide further insight into how HIV-1 might impact on inflammatory responses to co-infecting pathogens, and thus the prospective immunopathological consequences of this phenotype *in vivo*.

I therefore aimed to explore the potential consequences of IL-10 attenuation for the virus and the host immune response, with the following objectives:

1) To explore whether IL-10 modulates HIV-1 replication in human macrophages, in order to determine whether the virus might attenuate IL-10 to promote its own replication.
2) To identify whether IL-10 attenuation is present in macrophage responses to clinically important co-infecting pathogens other than Mtb, by evaluating the macrophage response to *Cryptococcus neoformans* and the effect of HIV-1 on this.
3) To explore how IL-10 modulates macrophage transcriptional responses, in the following contexts:
    a. The effects of IL-10 on gene expression in unstimulated MDMs.
    b. The effects of IL-10 on IFNγ-induced gene expression in MDMs.
    c. The role of IL-10 in modulating the pro-inflammatory transcriptional response to zymosan.
4) To explore how attenuation of IL-10 modulates cell recruitment to inflammatory foci.

4.2 Results

4.2.1 IL-10 inhibition may confer a replicative advantage on HIV-1 in inflammation

I aimed to identify why HIV-1 attenuates IL-10 by exploring the consequences of this phenotype for the virus. The simplest hypothesis is that IL-10 is detrimental to viral replication, and so the virus has evolved to suppress IL-10 to avoid these detrimental effects. It has previously been shown that IL-10 can suppress HIV-1 replication in macrophages (Tanaka et al., 2005; Wang and Rice, 2006). Conversely, innate immune signalling via the NFκB pathway (Pazin et al., 1996; Perkins et al., 1993; Williams et al., 2004; Williams et al., 2007), and pro-inflammatory cytokines (Poli et al., 1994, 1990) can induce HIV-1 replication. The effect of IL-10 on HIV-1 replication in the context of an inflammatory response has not specifically been addressed. To investigate this, I sought to supplement deficient IL-10 production in HIV-1-infected MDMs stimulated with zymosan, by addition of recombinant IL-10 four hours after zymosan stimulation.

72 hours post-zymosan stimulation, HIV-1 release and transcription were measured, and were significantly increased above levels in unstimulated MDMs (**Figure 4.1**). Supplementation of IL-10 significantly suppressed zymosan-induced HIV-1 transcription (**Figure 4.1b**) and showed a trend to suppression of zymosan-induced HIV-1 release at this time point (**Figure 4.1a**), although this effect fell short of statistical significance. The outcome of 72 hours of IL-10 supplementation on viral replication in unstimulated MDMs was also assessed, and no effect was seen on either viral transcription or release (**Figure 4.2a, b**). To investigate the effect of IL-10 on macrophage permissivity to HIV-1 infection, MDMs were pre-treated with IL-10 prior to HIV-1 infection. This had no impact on the number of cells which were infected by HIV-1 when measured at 3 days post-infection (**Figure 4.2c**). These results indicate that IL-10 can inhibit zymosan-induced viral replication in MDMs, but has no effect on the baseline level of HIV-1 replication in unstimulated MDMs, or on the permissivity of unstimulated MDMs to HIV-1 infection.

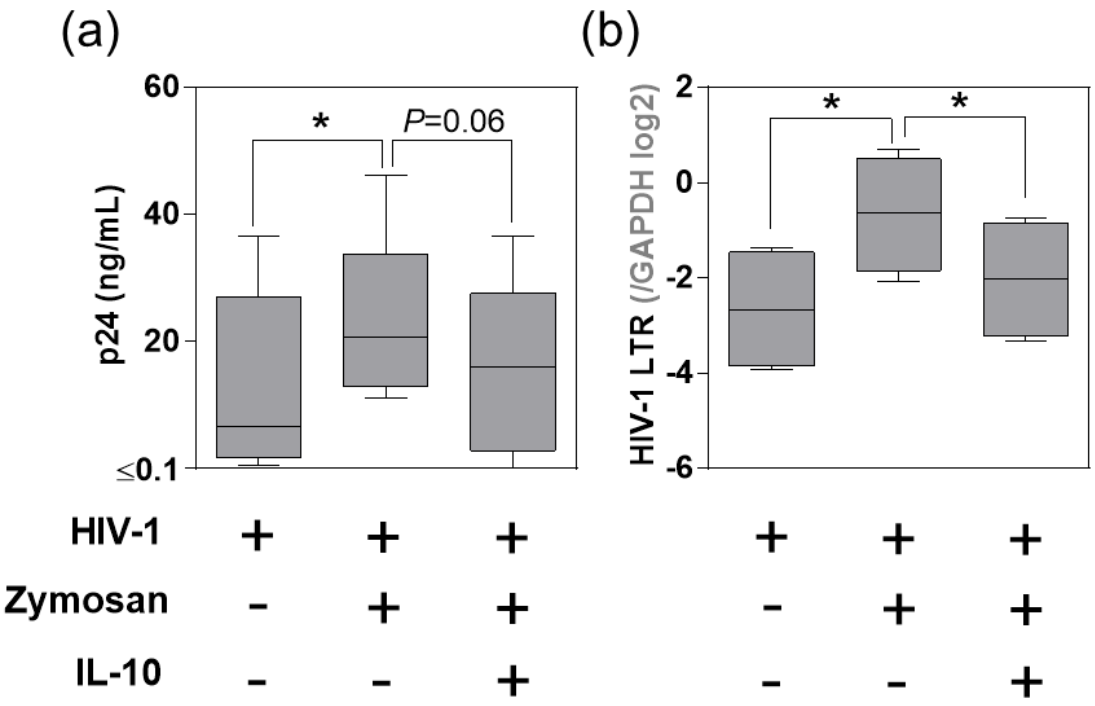

Figure 4.1: IL-10 suppresses zymosan-induced HIV-1 replication.

MDMs were infected with HIV-1 (full-length strain Ba-L, at an MOI of 3–5) for 1 week of spreading infection, and then stimulated with zymosan (0.4mg/ml). 4 hours later, recombinant IL-10 (10ng/ml) was supplemented into the culture. Viral release and transcription were measured 72 hours post-supplementation. **(a)** Viral release was measured by HIV-1 p24 ELISA of cell culture supernatants. Zymosan induced significantly higher levels of HIV-1 release compared to unstimulated MDMs, and IL-10 supplementation suppressed this. **(b)** Viral transcription was measured by qRT-PCR for the HIV-1 LTR. Zymosan induced significantly higher levels of HIV-1 transcript compared to unstimulated MDMs, and this was significantly suppressed by IL-10 supplementation. * indicates $P<0.05$, paired t-test. Box-and-whisker plots indicate the median and range of at least 3 experiments.

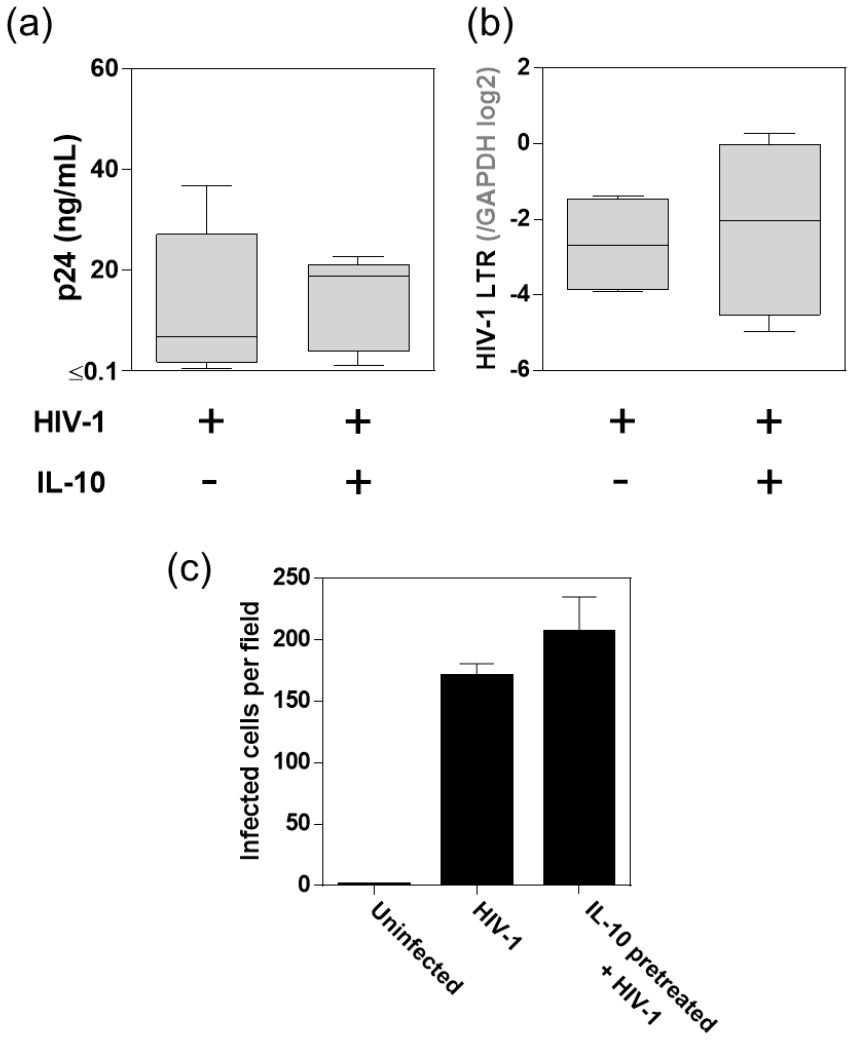

Figure 4.2: IL-10 does not modulate HIV-1 replication in resting MDMs, or alter MDM permissivity to HIV-1.

MDMs were infected with HIV-1 (full-length strain Ba-L, at an MOI of 3–5) for 1 week of spreading infection, and then supplemented with recombinant IL-10 (10ng/ml). **(a)** Viral release was measured at 72 hours by HIV-1 p24 ELISA of cell culture supernatants. IL-10 supplementation had no effect on HIV-1 release. **(b)** Viral transcription was measured at 72 hours by qRT-PCR for the HIV-1 LTR. IL-10 supplementation had no effect on HIV-1 transcription. **(c)** MDMs were pre-incubated with recombinant IL-10 (10ng/ml) for 24 hours prior to infection with HIV-1 (full-length strain Ba-L, at an MOI of 3-5). At 72 hours, MDMs were fixed and stained for HIV-1 p24 to measure the number of HIV-1 infected MDMs in the culture. IL-10 pre-treatment had no effect on the numbers of MDMs infected. Box-and-whisker plots indicate the median and range of at least 3 experiments. Bars indicate the mean +/- SEM of at least 3 experiments.

4.2.2 Macrophage responses to *Cryptococcus neoformans*

Having shown that IL-10 attenuation was not Mtb-specific (**section 3.2.1**), I aimed to establish whether HIV-1 attenuation of IL-10 might have immunopathological consequences in the response to a pathogen other than Mtb. Zymosan, a particulate innate immune stimulus which is a derivative of the cell wall of the fungus *Saccharomyces cerevisiae* (Gantner et al., 2003), induced substantial IL-10 responses in human MDMs (**Figure 3.1**), as has been previously reported (Kelly et al., 2010). Therefore, I aimed to test if a clinically important fungal pathogen in HIV-1^+ patients also induces IL-10 responses in human MDMs, and whether HIV-1 infection attenuates these responses.

Cryptococcus neoformans is a fungal species which commonly causes disseminated infections associated with meningoencephalitis in HIV-1 positive patients with AIDS (Harrison, 2009). *C. neoformans* can be manipulated in culture (Sabiiti et al., 2012), directly infects macrophages (Vecchiarelli et al., 1994), and the major component of its capsule, glucuronoxylomannan (GXM), has been shown to be a potent inducer of IL-10 expression (Monari et al., 2006; Vecchiarelli et al., 1996). Therefore, it provided an appropriate candidate pathogen with which to test IL-10 attenuation by HIV-1 in the context of a fungal infection. To characterise infection by *C. neoformans* in this MDM model, MDM uptake of *C. neoformans* at 4 hours post-infection was measured by confocal microscopy using a GFP-expressing *C. neoformans* WT strain, H99-GFP (**Figure 4.3a**). Using an MOI of 10, intracellular fungal burden at 4 hours was approximately 0.1 cryptococci per MDM (**Figure 4.3b**), indicating that approximately 10% of MDMs were infected, although heterogeneity in fungal burden may exist at the single cell level. Co-infection of MDMs with HIV-1 did not affect uptake of *C. neoformans* (**Figure 4.3b**).

Macrophage inflammatory responses to *C. neoformans*, in the presence and absence of pre-existing HIV-1 infection, were assessed by measuring changes to selected cytokine mRNA expression in MDMs at 4h and 24h post-infection. In these experiments, zymosan was used as a positive control for induction of cytokine gene expression. Two WT laboratory-propagated strains of *C. neoformans* of different serotypes, H99 and B3501, did not induce IL-10, TNFα or IL-1β mRNA expression at 4 or 24 hours post-infection, irrespective of co-existing HIV-1 infection (**Figure 4.4**). The

C. neoformans capsule is suggested to be its major virulence factor and may mask immunogenic PAMPs in the cell wall, or be directly immunosuppressive (Monari et al., 2006; Vecchiarelli et al., 1996, 1995; Zaragoza et al., 2009). Isogenic unencapsulated mutants of the H99 and B3501 WT strains exist, which have mutations in enzymes involved in capsule production or trafficking (all *C. neoformans* strains used are detailed in **Methods section 2.5**). These mutants, Cap59 (H99) and Cap67 (B3501) were used to infect MDMs, to assess whether cytokine gene expression could be induced by *C. neoformans* when the capsule was absent. At 24 hours post-infection, these strains induced expression of mRNA for the pro-inflammatory cytokines IL-1β and TNFα (**Figure 4.4**). *IL10* mRNA expression was not induced at any time-point, and consequently no modulation by HIV-1 was observed.

To further assess whether *C. neoformans* could induce an IL-10 response in MDMs, secretion of IL-10 protein was measured at 4 and 24 hours post-infection with WT strains or unencapsulated mutants. No IL-10 secretion was evident at 4 hours in response to any *C. neoformans* strain (**Figure 4.5a**). At 24 hours post-infection with unencapsulated strains, IL-10 secretion was observed in 3 of 6 experiments, and this was reduced in paired HIV-1 co-infected MDMs, although these data were insufficient to reach statistical significance (**Figure 4.5b**). *C. neoformans* WT strains did not induce IL-10 secretion at 24 hours (**Figure 4.5b**).

Previous investigators have reported that macrophages and monocytes can produce pro-inflammatory and IL-10 responses to *C. neoformans* in various *in vitro* models (Delfino et al., 1997; Levitz et al., 1994; Oliveira et al., 2010; Vecchiarelli et al., 1996). The non-immunogenicity of *C. neoformans* in this MDM model was investigated. The MOI employed was not shown to be limiting, as an eight-fold increase in MOI did not induce IL-10 or IL-6 secretion (**Figure 4.6a**). In animal models of *C. neoformans* infection, the innate immune adaptor MyD88, which transduces TLR signals to activate the NFκB pathway, has been shown to be essential for protection against *C. neoformans* (Biondo et al., 2005; Yauch et al., 2004). Additionally, the *C. neoformans* capsule has been shown to induce NFκB activation, as assessed by nuclear translocation, in human PBMC (Shoham et al., 2001). I assessed NFκB nuclear translocation in response to a WT strain of *C. neoformans* in this MDM model. In comparison to LPS stimulation as a positive control, *C. neoformans* did not induce NFκB translocation (**Figure 4.6b, c**), suggesting that MDMs do not respond to *C. neoformans* via this archetypal innate immune signalling pathway.

Taken together, these data show that M-CSF-differentiated MDMs do not mount a classical transcriptional innate immune response to *C. neoformans*, despite internalising the pathogen. The absence of NFκB pathway activation suggests that they might not detect *C. neoformans* by classical pattern recognition. As such, whether HIV-1 could attenuate IL-10 responses to *C. neoformans* could not be evaluated, and the effects of the phenotype of IL-10 attenuation in HIV-1/*C. neoformans* co-infection could not be explored using this experimental model.

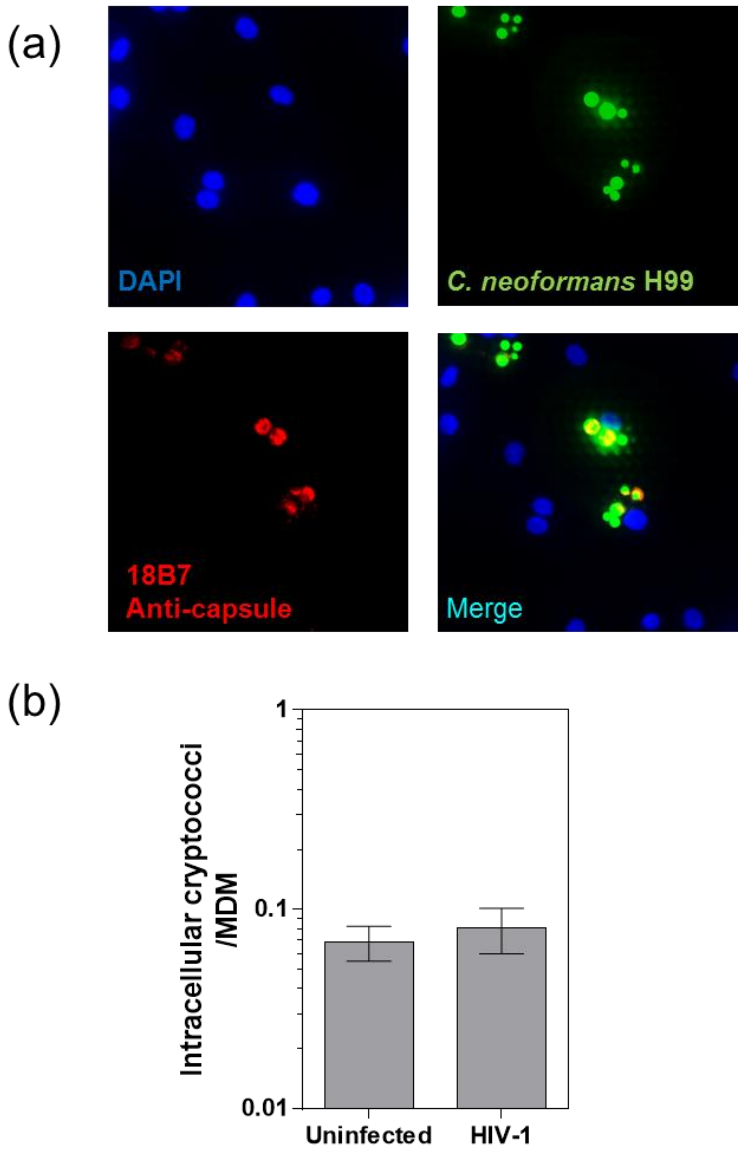

Figure 4.3: Uptake of *C. neoformans* to human MDMs.

MDMs were infected with HIV-1 (R9Δenv at an MOI of 3–5, with Vpx VLPs at 2ng RT/ml) for 1 week, and then infected with GFP-expressing *C. neoformans* strain H99-GFP at an MOI of 10. Four hours post-infection, MDMs were washed to remove extracellular yeasts. Cells were fixed and uptake was assessed by confocal microscopy. Non-internalised *C. neoformans* was excluded by counterstaining with an antibody (18B7) to the GXM component of the capsule. MDMs were enumerated by staining of nuclei with DAPI. **(a)** Representative images of the DAPI nuclear stain; GFP-expressing cryptococci; counterstaining of external cryptococci with 18B7; and a merged image demonstrating extracellular cryptococci (yellow) and intracellular cryptococci (green). **(b)** MDMs and intracellular cryptococci were enumerated, and expressed as a ratio of intracellular cryptococci per MDM over the whole culture. Bar represents the mean +/- SEM of 3 experiments. Confocal imaging and analysis was carried out in collaboration with Dr. Janos Kristin-Vizi, LMCB, UCL.

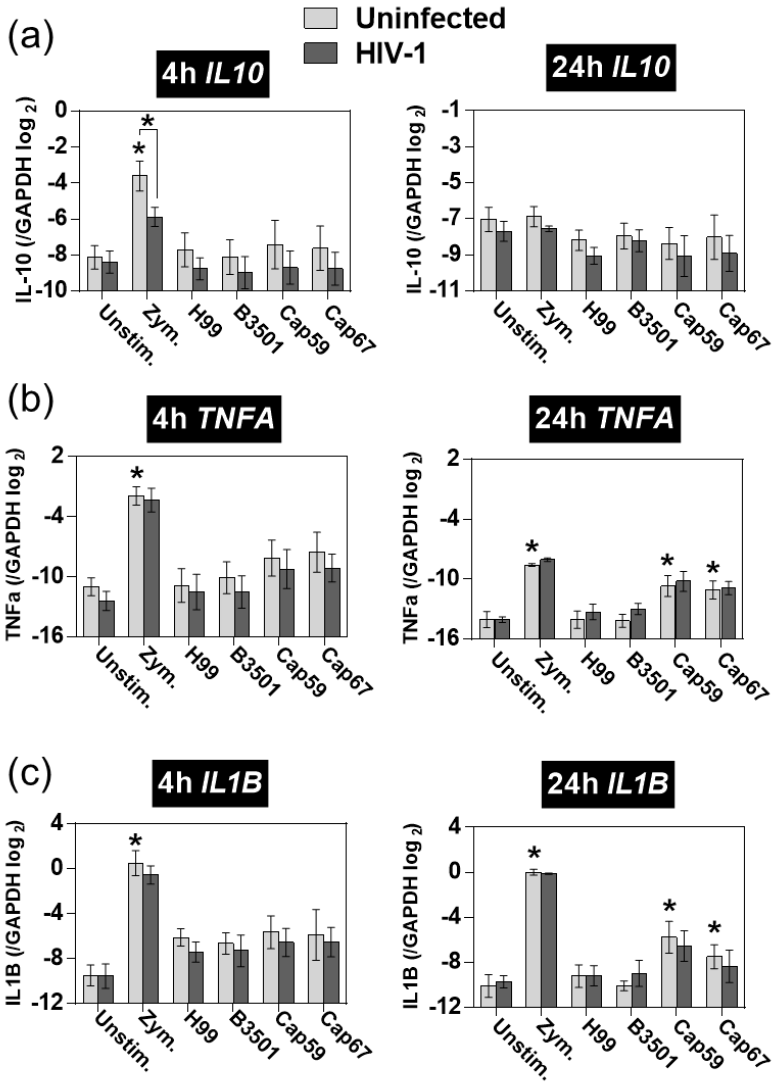

Figure 4.4: Expression of cytokine mRNA by MDMs in response to *C. neoformans* in HIV-1 co-infection.

MDMs were infected with HIV-1 (R9Δenv at an MOI of 3–5, with Vpx VLPs at 2ng RT/ml) for 1 week, and then infected with WT *C. neoformans* strains H99 or B3501, their isogenic unencapsulated mutants Cap59 or Cap67 (all at an MOI of 10), or stimulated with zymosan (Zym.; 0.4mg/ml). Cytokine mRNA expression at 4 and 24h was measured by qRT-PCR. Significant (P<0.05, paired t-test) differences in mRNA expression from unstimulated MDMs are indicated by * above bars, and significant differences in mRNA expression between uninfected and HIV-1 infected cells are indicated by * above brackets. **(a)** *IL10* mRNA was expressed at 4h in response to zymosan but not *C. neoformans* strains, and was not expressed at 24h in response to any stimulus. HIV-1 attenuated IL-10 mRNA expression. **(b)** *TNFA* mRNA was expressed at 4h and 24h in response to zymosan and at 24h in response to unencapsulated *C. neoformans.* **(c)** *IL1B* mRNA was expressed at 4h and 24h in response to zymosan and at 24h in response to unencapsulated *C. neoformans.* Bars represent mean -/+ SEM of at least 3 experiments.

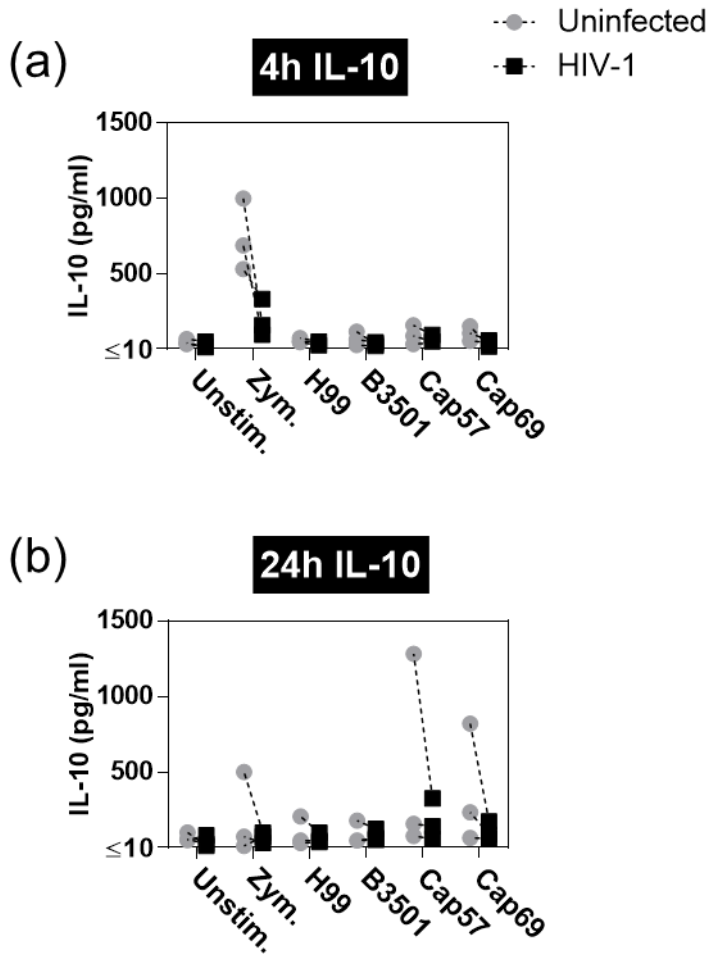

Figure 4.5: MDM secretion of IL-10 in response to *C. neoformans* in HIV-1 co-infection.

MDMs were infected with HIV-1 (R9Δenv at an MOI of 3–5, with Vpx VLPs at 2ng RT/ml) for 1 week, and then infected with WT C. neoformans strains H99 or B3501, their isogenic unencapsulated mutants Cap59 or Cap67 (all at an MOI of 10), or stimulated with zymosan (Zym., 0.4mg/ml). IL-10 secretion at 4h and 24h was measured by ELISA of cell culture supernatants. **(a)** IL-10 secretion at 4h. IL-10 was secreted in response to zymosan, but not in response to *C. neoformans* strains. IL-10 secretion was reduced in HIV-1 infected MDMs, but this was non-significant. **(b)** IL-10 secretion at 24h. In 3 of 6 experiments, IL-10 was secreted at 24h in response to unencapsulated mutants of *C. neoformans*, and this was attenuated by HIV-1 co-infection. Significant differences between groups were not observed. Paired results from the same experiment are indicated.

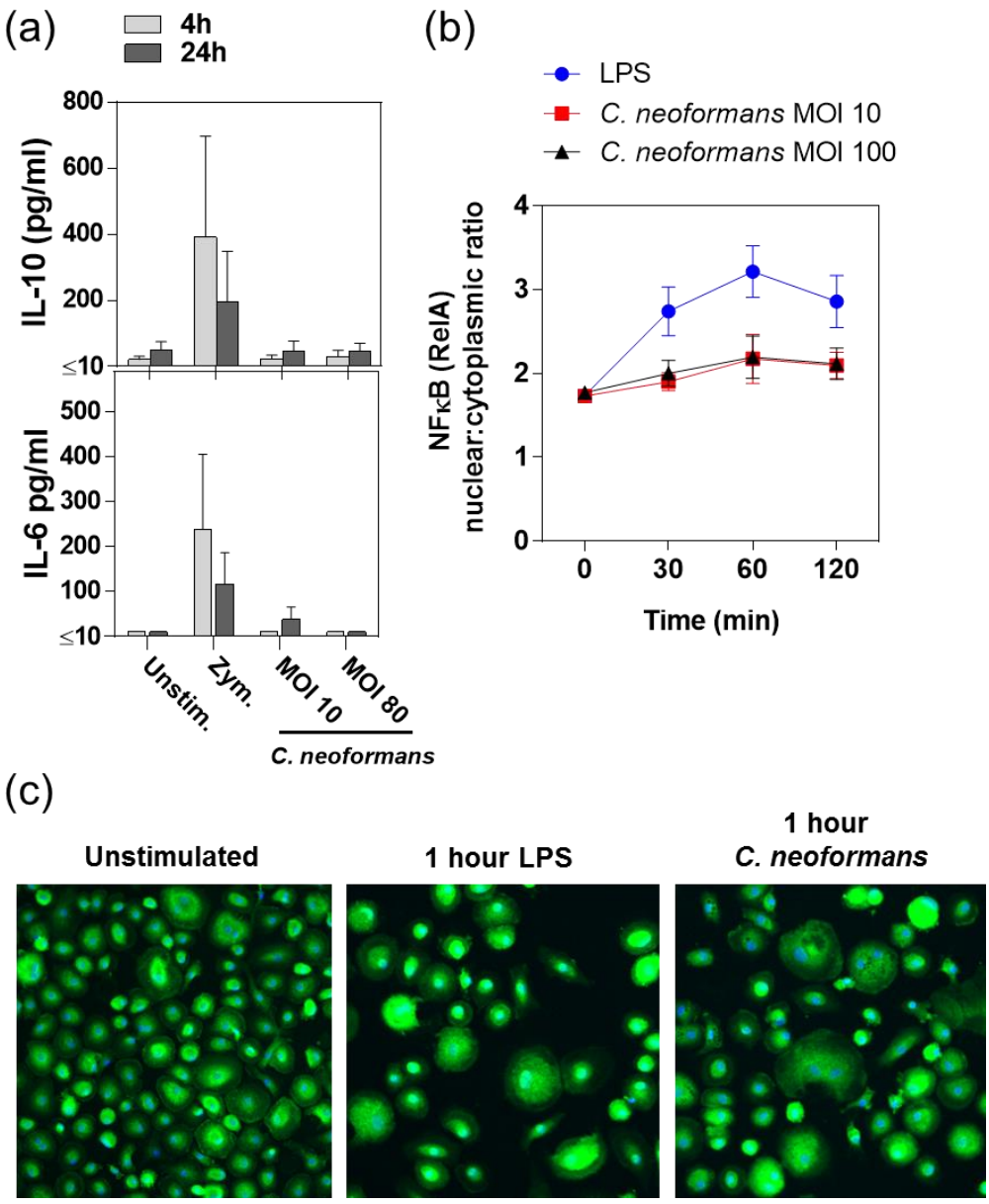

Figure 4.6: Non-immunogenicity of *C. neoformans*.

(a) MDMs were infected with *C. neoformans* WT strain H99 at an MOI of 10 or 80, or stimulated with zymosan (Zym., 0.4mg/ml). IL-10 and IL-6 secretion at 4h and 24h was measured by ELISA of cell culture supernatants. Both cytokines were secreted in response to zymosan at 4h and 24h, but not in response to *C. neoformans* at either MOI or timepoint. **(b)** MDMs infected with *C. neoformans* WT strain H99 at an MOI of 10 or 100, or stimulated with LPS at 10ng/ml. Activation of the NFκB pathway was measured by quantitative imaging analysis of nuclear translocation of NFκB (RelA), assessed as a ratio of nuclear: cytoplasmic intensity of RelA staining. LPS stimulation induced translocation of NFκB (*P*=<0.0001, 0 mins vs. 30 mins or 120 mins, two-way ANOVA). *C. neoformans* did not induce NFκB translocation at either MOI used at any time point (*P*>0.05, two-way ANOVA). Bars represent mean -/+ SEM of at least 3 experiments. **(c)** Representative images of the NFκB translocation assay. Nuclei are stained blue with DAPI and NFκB RelA is stained green. Nuclear NFκB is evident in the middle panel of LPS-stimulated MDMs (green nuclear staining).

4.2.3 The transcriptional response to IL-10 in human MDMs

Previous investigations showed that attenuated IL-10 responses in HIV-1/Mtb co-infected macrophages were associated with exaggerated downstream pro-inflammatory macrophage responses (Tomlinson et al., 2014), and it is well described that IL-10 induces an anti-inflammatory response in macrophages, which includes cytokine suppression (Murray, 2005). Accordingly, IL-10 supplementation of co-infected MDM cultures reversed the HIV-1 associated exaggerated inflammatory phenotype (Tomlinson et al., 2014). Further understanding the function of IL-10 in macrophage-driven immune responses may delineate potential outcomes of HIV-1-mediated IL-10 attenuation as well as the role of IL10 in the context of an inflammatory response. As macrophages express the IL-10 receptor (Moore et al., 2001), macrophage IL-10 production can lead to autocrine IL-10 signalling and modulation of macrophage function (Murray, 2006). To investigate this, MDMs were stimulated with recombinant IL-10 for 24 hours, and changes in gene expression were assessed by genome-wide transcriptional profiling. IL-10 induced the expression of 47 genes in resting MDMs (**Figure 4.7a**). TFBS enrichment analysis of these genes using oPOSSUM-3 (Kwon et al., 2012; http://opossum.cisreg.ca) corroborated that they could be regulated by IL-10. Binding sites for STAT3, the major downstream mediator of IL-10 signalling (L. Williams et al., 2004), were highly enriched (**Figure 4.7b**). IL-10 did not cause any substantial suppression of gene expression in resting MDMs (**Figure 4.7a**).

The function of the IL-10-induced genes was investigated by GO enrichment analysis using the web-tool InnateDB (Breuer et al., 2013; http://www.innatedb.com). This analysis was visualised as a network of enriched GO terms and associated genes (**Figure 4.7c**). IL-10 induced expression of genes involved in the innate immune response, inflammation and apoptosis. Some of these encoded for molecules with the potential to alter macrophage function, including signalling molecules such as SOCS3 and JAK3, and receptors such as IgG F_C receptors and the IL-7 receptor. Secreted molecules were also highlighted, including the chemokine CCL18, and members of S100 protein family, which can be secreted and play immunomodulatory roles (Donato et al., 2013). IL-10 also induced expression of the genes encoding pro-IL-1β and the complement factor C1S. These results show that IL-10 modulates macrophages by inducing gene expression and thus potentially altering functionality, consistent with previous reports (Antoniv et al., 2005; Park-Min et al., 2005; Stumpo et al., 2003).

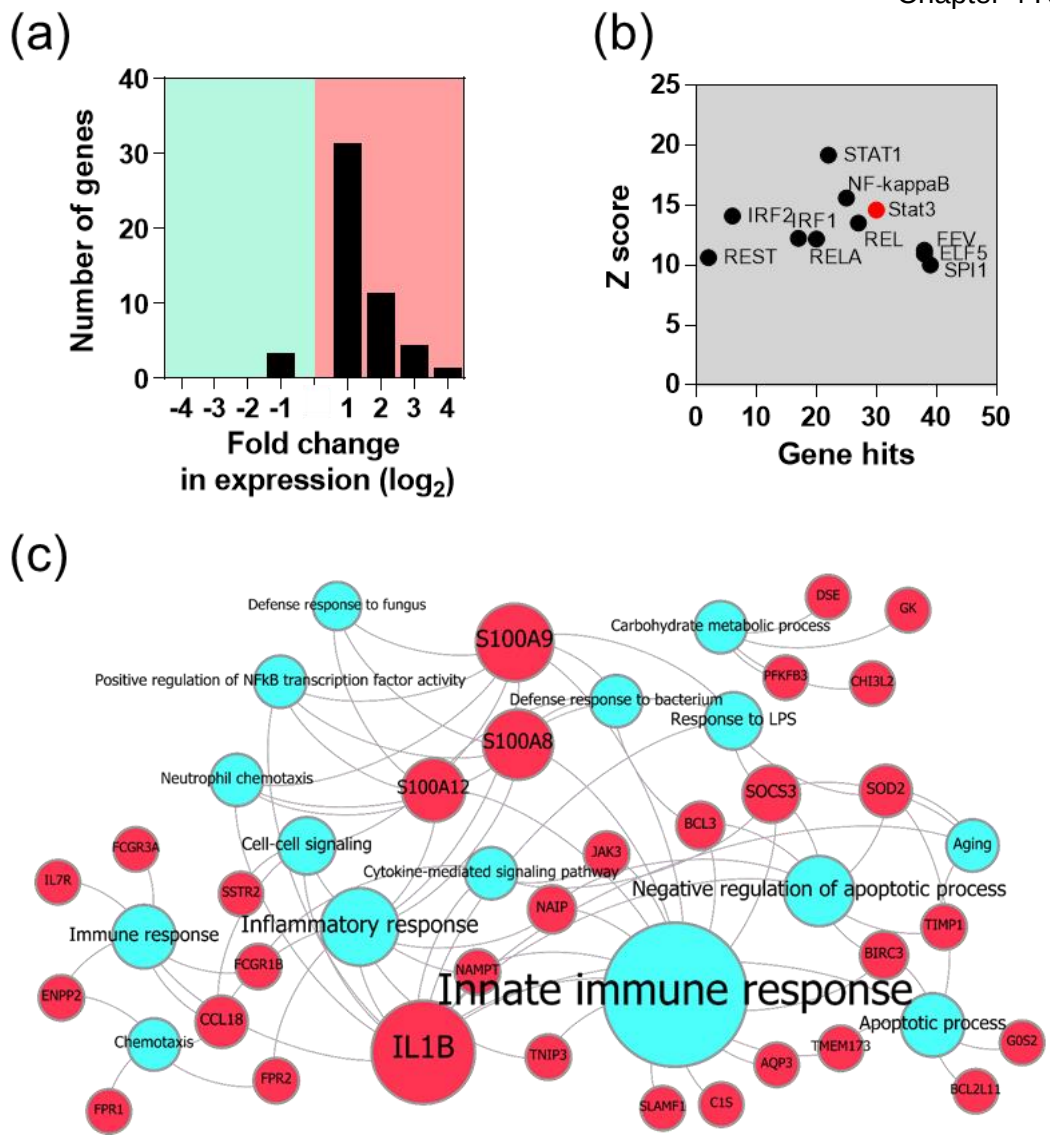

Figure 4.7: The MDM transcriptional response to IL-10.

MDMs were stimulated for 24h with recombinant IL-10 (10ng/ml). RNA was collected and genome-wide transcriptional profiling by microarray was performed. Significant gene expression changes induced by IL-10 were identified by t-test (P<0.05) and a twofold change threshold in comparison to unstimulated MDMs. **(a)** Frequency distribution of IL-10-induced changes in gene expression, presented as fold-change increases/decreases. **(b)** Genes up-regulated by IL-10 were subjected to transcription factor binding site (TFBS) enrichment analysis using oPOSSUM-3. The sequence 5000bp up/downstream of each gene was analysed. Significance of TFBS frequency compared to background was assessed by the Z-score statistic, which was considered significant when ≥10. The X axis lists the number of genes enriched for a TFBS, and the Y axis displays the Z score. **(c)** Network visualisation of InnateDB gene ontology (GO) enrichment analysis of IL-10-induced genes. Enrichment assessment was performed using a hypergeometric algorithm, and filtered to biological process GO terms with a significance level of P<0.05 (Benjamini-Hochberg correction-adjusted). The top 15 enriched GO terms by gene count are shown. GO terms are in blue and genes are in red. Node size is determined by number of connections. All data presented are derived from the mean results of 3 independent experiments.

4.2.4 IL-10 pre-treatment does not inhibit the transcriptional response to IFNγ in human MDMs

As well as negatively regulating the innate inflammatory response (Lang et al., 2002b), IL-10 is also suggested to suppress functions of adaptive immunity (Hutchins et al., 2013). The ability of adaptive immune $CD4^+$ Th1 cells to activate macrophages via IFNγ is a key interface of CMI. I tested whether IL-10 could modulate this interface by altering macrophage responses to IFNγ.

MDMs were pre-treated with IL-10 for 24 hours prior to IFNγ stimulation. The response to IFNγ was assessed by genome-wide transcriptional profiling. In both the presence and absence of IL-10 pre-treatment, IFNγ up-regulated the expression of hundreds of genes in MDMs (**Figure 4.8a, b**). IL-10 modulation of this response was assessed by comparing gene expression in the two MDM conditions, and specifically testing for significant differences in gene expression in the IFNγ response gene list (**Figure 4.8c**). The IFNγ response was highly conserved in the presence of IL-10 pre-treatment, with only four statistically significant changes of ≥two-fold in transcription (**Figure 4.8c**), which were either in genes independently inducible by IL-10 (*JAK3*, *SOCS3*), or were in uncharacterised loci.

These results demonstrate that IL-10 priming of macrophages does not alter their transcriptional response to IFNγ.

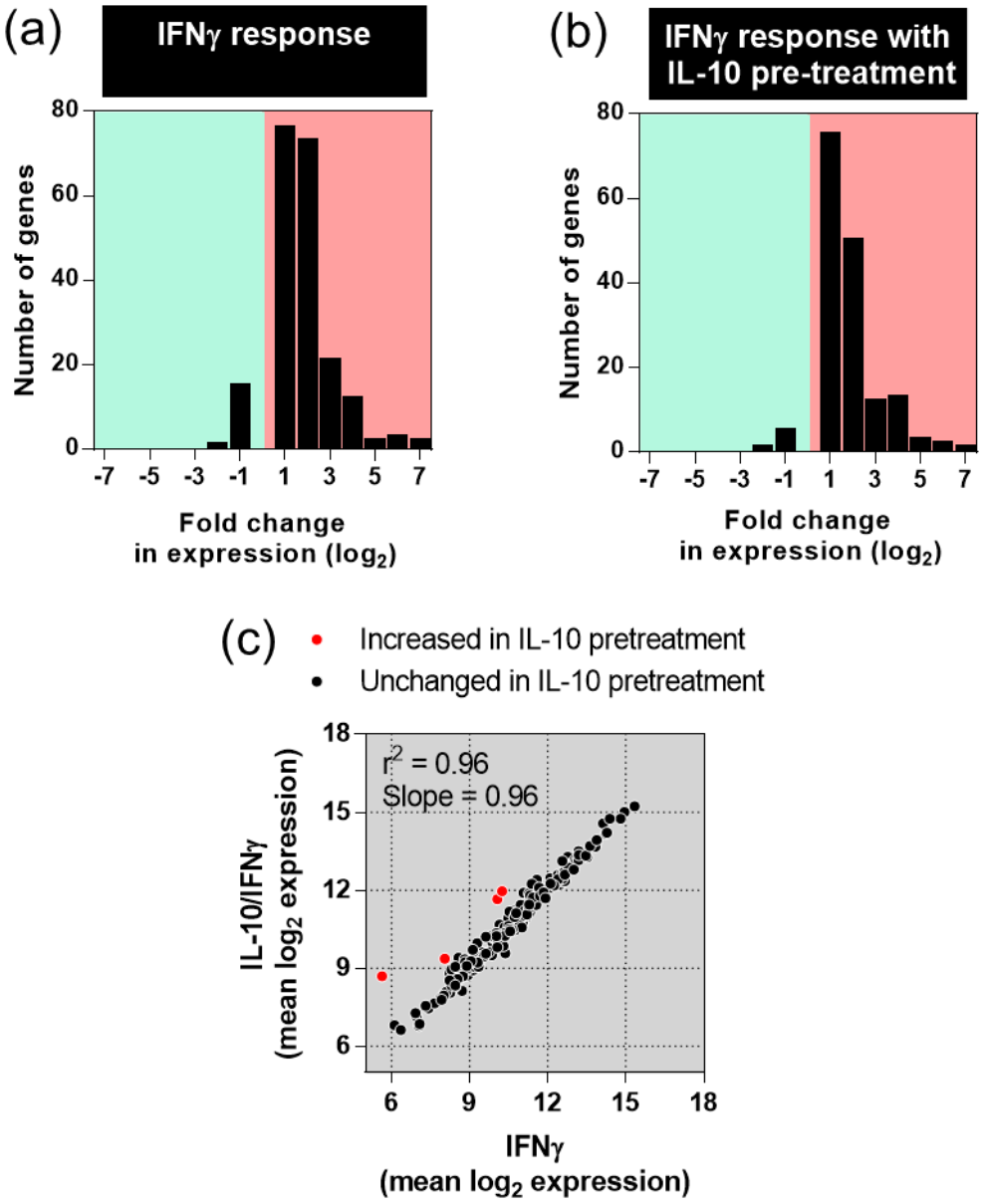

Figure 4.8: IL-10 pre-treatment does not inhibit the MDM transcriptional response to IFNγ.

MDMs were pre-treated for 24 hours with recombinant IL-10 (10ng/ml) and then stimulated for 4 hours with recombinant IFNγ (10ng/ml). RNA was collected and genome-wide transcriptional profiling was performed by microarray. Significant gene expression differences were identified by t-test ($P<0.05$) and a twofold change threshold. **(a)** Frequency distribution of IFNγ-induced changes in gene expression in comparison to unstimulated MDMs, presented as fold-change increases or decreases. **(b)** Frequency distribution as in (a) but for IL-10 pre-treated MDMs. **(c)** XY plot comparing mean expression of all genes induced in MDMs stimulated with with IFNγ, or IFNγ with IL-10 pretreatment. Linear regression showed a significant positive correlation and covariance between the two conditions. Highlighted genes showed significantly higher expression in IL-10 pretreated MDMs. All data presented are the mean results of 3 independent experiments.

4.2.5 IL-10 deficiency in inflammation dysregulates macrophage gene expression

As the primary function of IL-10 is thought to be regulation of immune and inflammatory responses, I assessed the role of IL-10 in the context of an inflammatory response. MDMs were stimulated with zymosan in the presence or absence of neutralising antibodies to IL-10 and the IL-10 receptor, in order to block zymosan-induced autocrine IL-10 signalling, and thus assess the consequences of IL-10 deficiency in the inflammatory response. A similar exercise has been carried out in LPS-stimulated murine BMDMs from IL-10 deficient mice (Lang et al., 2002a), but the role of IL-10 in regulating the inflammatory response of human macrophages to a strong IL-10 inducer, such as zymosan, has not previously been assessed. The MDM response to 24 hours of zymosan stimulation was measured by genome-wide expression profiling. Zymosan caused up- and down-regulation of the expression of hundreds of genes (**Figure 4.9a**), and IL-10 blockade magnified this response (**Figure 4.9b**).

These transcriptional response were explored using the unsupervised exploratory statistical method of PCA. PCA is described in **Introduction section 1.6.2**. Briefly, it can be used to assess variance across a large data set by identifying multiple directions (termed components) across which the variation in the data is maximal (Chain et al., 2010; Ringnér, 2008). Each sample in such a dataset can be represented by its value within each component (a PC score), rather than by using the many thousands of expression values which contribute to this (Ringnér, 2008), and thus these scores can be used to visualise relationships within the dataset in multiple different dimensions. PC scores for the major component describing the zymosan response were significantly increased in the presence of IL-10 neutralisation (PC1; **Figure 4.9c**). PC scores for components describing further aspects of the zymosan response were, conversely, attenuated by IL-10 neutralisation (PC2–4; **Figure 4.9c**). This suggests that blocking IL-10 function in the innate inflammatory response leads to both induction and suppression of components of gene expression.

To identify which genes were involved in this dysregulated phenotype, the lists of genes up-regulated by zymosan were compared in the presence or absence of IL-10 neutralisation (**Figure 4.10a**). As suggested by PCA, IL-10 blockade produced further increases in gene expression, while other gene expression increases were no longer evident (**Figure 4.10a**). Directly comparing the expression of all genes up-regulated in

either condition showed a significant positive correlation and covariance of the overall response. However, statistically significant differences in expression of ≥two-fold as a result of IL-10 neutralisation could be identified (**Figure 4.10b**): 117 genes were further increased in expression, while 45 genes were attenuated in expression, representing dysregulation of 17.4% of the response to zymosan.

The 117 zymosan-induced genes which are further increased in expression as a result of IL-10 neutralisation (**Figure 4.10b**) are ostensibly negatively regulated by IL-10 in the context of an innate immune inflammatory response, as IL-10 blockade leads to their up-regulation. The function of these genes was investigated by GO enrichment analysis using InnateDB, and the results of this were visualised as a network of enriched GO terms and associated genes (**Figure 4.11**). IL-10 exerted negative regulatory effects on genes encoding for innate immune signalling components, such as the NFκB pathway mediators RelA and IRAK1, and mediators and regulators of cytokine signalling such as JAK2, STAT5a and SOCS1. Regulation of apoptosis by IL-10 was also highlighted, as well as negative regulation of cytokines and secreted factors, such as IL-12 p40, CCL22, M-CSF and GM-CSF.

A similar analysis was performed for the 45 genes for which expression was attenuated as a result of IL-10 neutralisation (**Figure 4.10b**), which are postulated to be positively regulated by IL-10, as IL-10 blockade leads to their inhibition. A network for the GO enrichment analysis for these genes is presented in **Figure 4.12.** This analysis demonstrates that in the context of inflammation, IL-10 induced changes in gene expression with potential functions in modulating the innate immune response, in addition to suppressive effects. Many of the gene induction effects of IL-10 described in resting MDMS (**Figure 4.7**) were evident here, such as induction of JAK3 and SOCS3, S100 proteins, C1S and chemokines.

A large component of the response to zymosan was not affected by autocrine IL-10 signalling as assessed by IL-10 blockade (**Figure 4.10**). To investigate the functional characteristics of the non-IL-10-regulated response, the most highly zymosan-upregulated genes (≥16-fold increase in expression) for which expression was not significantly altered by IL-10 blockade were selected, and assessed by GO enrichment analysis. The results of this analysis are presented in a network in **Figure 4.13**. This analysis suggests that IL-10 does not regulate the expression of many molecules considered to be part of the type I IFN and antiviral responses, such as CXCL9 and members of the IFITM (IFN-induced transmembrane protein) and ISG (IFN

stimulated gene) families. Some genes which IL-10 had been shown to regulate in other contexts, such as *IL23A* and *IL1B* (**Figure 4.7;** Tomlinson et al., 2014), were not regulated by IL-10 in this setting, perhaps reflecting some context-specificity of the function of IL-10.

To gain insight into the mechanisms by which IL-10 regulated gene expression in inflammation, TFBS enrichment analysis was performed on genes increased in expression (**Figure 4.14a**), attenuated in expression (**Figure 4.14b**) or conserved in expression (**Figure 4.14c**) in IL-10 blockade. It should be noted that identification of TFBS enrichment in this analysis does not definitively indicate that the TF in question is regulating the genes concerned in this particular experiment, as the majority of genes will be regulated by many TFs in different contexts, and hence will contain binding sites for many TFs. Additionally, the presence of a TFBS does not indicate whether the associated TF is positively or negatively regulating gene expression, both of which are possible. However, the analysis provides insight into the potential list of TFs which may regulate these groups of genes in either a positive or negative fashion.

Many TFBSs were significantly enriched in the group of genes postulated to be negatively regulated by IL-10 (**Figure 4.14a**). This included binding sites for STAT3, the primary transcriptional mediator of IL-10 signalling; however, this was one of the least significantly enriched TFBSs identified, with sites in less than half of the genes assessed. However, many other TFs were identified in this analysis, and previous reports have described that the IL-10-induced AIR involves STAT3 inducing expression of a secondary wave of transcription factors, the AIR factors, which then co-ordinate the AIR by exerting inhibitory effects on transcription (Hutchins et al., 2012; Murray, 2005). The multiplicity of TFBSs highlighted in this gene list, including many known innate immune mediators such as NFκB and MZFs, thus supports the suggestion that negative regulation by IL-10 may mainly be controlled indirectly by other TFs downstream of STAT3, which alter the outcome of innate immune signalling pathways.

Assessment of the genes postulated to be positively regulated by IL-10 showed no significant TFBS enrichment (**Figure 4.14b**; no TFBS has a Z score ≥10). Stat3 binding sites were identified in >50% of these genes, but this was not statistically significant. The presence of STAT3 binding sites nonetheless suggests that some of these genes may be directly positively regulated by IL-10 signalling. However, it may also be possible that these genes are indirectly regulated by IL-10. Overall, assessments of these gene lists are concordant with the hypothesis that IL-10

signalling involves a limited primary response mediated by STAT3, which then produces functional outcomes via secondary responses and feedback loops mediated via other TFs. TFBS enrichment analysis of the genes which were identified as not regulated by IL-10 (**Figure 4.13**) shows significant enrichment for NFκB binding sites only (**Figure 4.14c**). IRF1 and IRF2 binding sites are also identified in many of these genes, although are not enriched to a level of statistical significance; however, this lends support to the hypothesis that this gene list is highly enriched for features of type I IFN responses, further indicating that this axis of innate immunity is not regulated by IL-10.

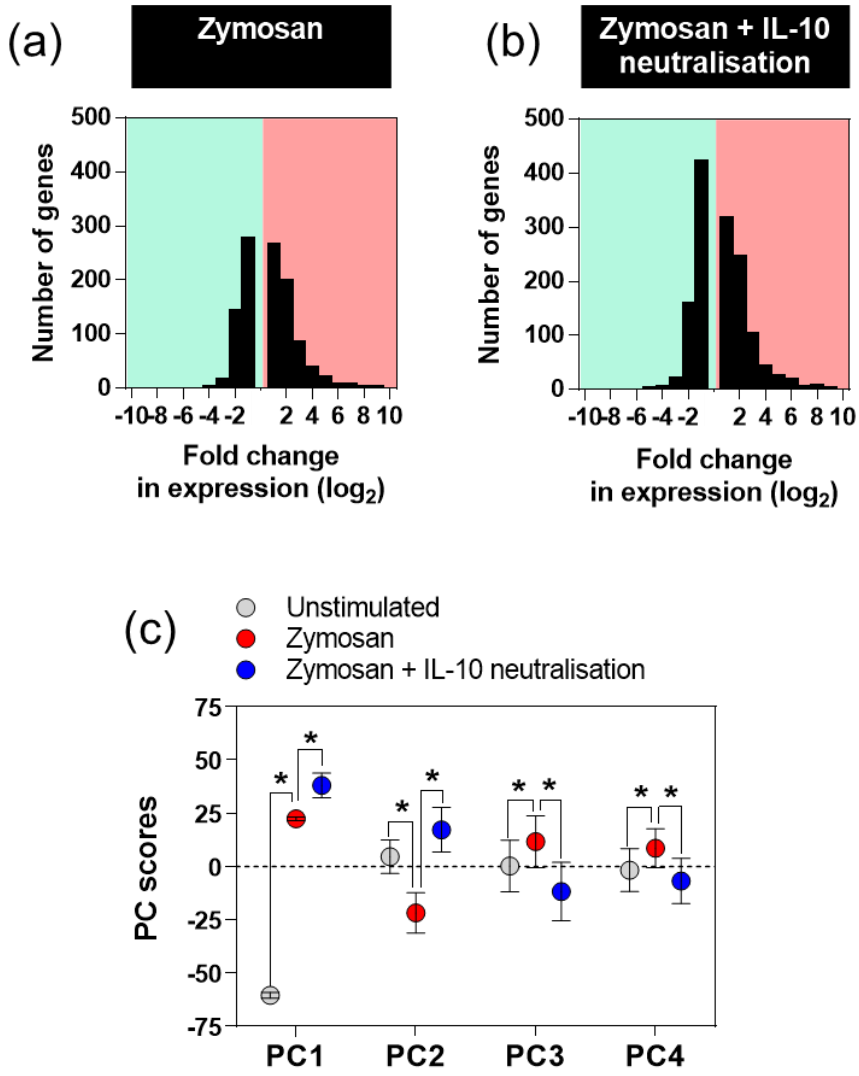

Figure 4.9: Neutralisation of IL-10 alters the zymosan-induced inflammatory response in MDMs.

MDMs were stimulated with zymosan (0.4mg/ml) for 24 hours in the presence of neutralising antibodies to IL-10 (5ug/ml) and to the IL-10 receptor (10ug/ml). RNA was collected and genome-wide transcriptional profiling was performed by microarray. Significant gene expression differences were identified by t-test (P<0.05) and a twofold change threshold. **(a)** Frequency distribution of zymosan-induced changes in gene expression in comparison to unstimulated MDMs, presented as fold-change increases or decreases. **(b)** Frequency distribution as in (a) but for MDMs stimulated with zymosan with IL-10 neutralisation. **(c)** PCA of zymosan-stimulated MDMs −/+ IL-10 neutralisation. The first four principal components showed significant differences in PC score between unstimulated MDMs and zymosan-stimulated MDMs. PC1 scores were significantly increased by IL-10 neutralisation, while PC2–4 scores were significantly decreased by IL-10 neutralisation. * indicates P<0.05, paired t-test. Symbols represent mean −/+ SEM. All data presented are the mean results of 3 independent experiments.

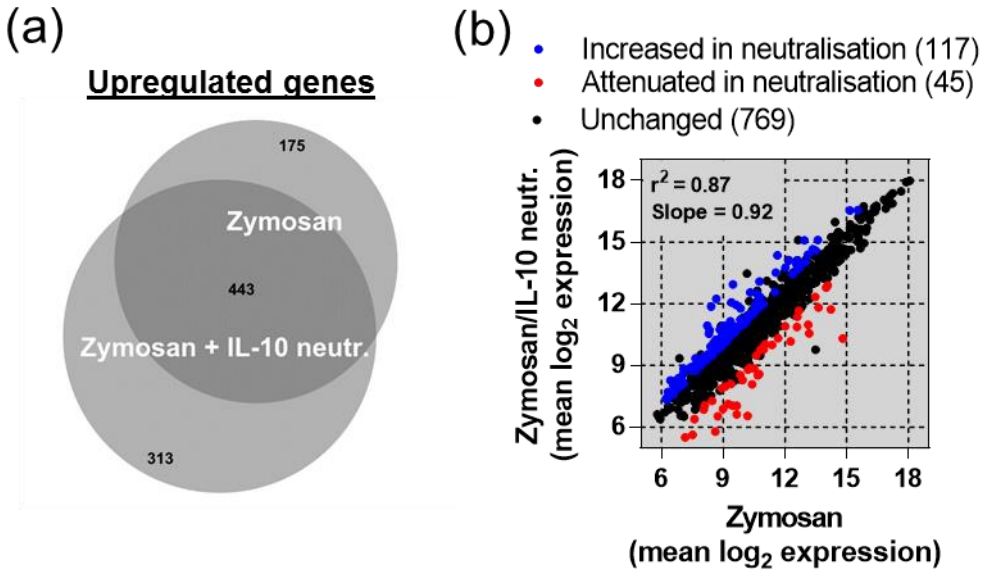

Figure 4.10: Identification of zymosan-induced gene expression changes which are dysregulated by IL-10 neutralisation.

(a) Venn diagram of genes which are upregulated in MDMs by zymosan stimulation −/+ IL-10 neutralisation. **(b)** XY plot comparing mean expression of all genes upregulated in MDMs stimulated with zymosan stimulation −/+ IL-10 neutralisation. Linear regression showed a significant positive correlation and covariance between the two conditions. Highlighted genes showed significantly different (≥two-fold higher or lower) expression in the presence of IL-10 neutralisation. Numbers in brackets indicate numbers of genes. All data presented are the mean of 3 independent experiments.

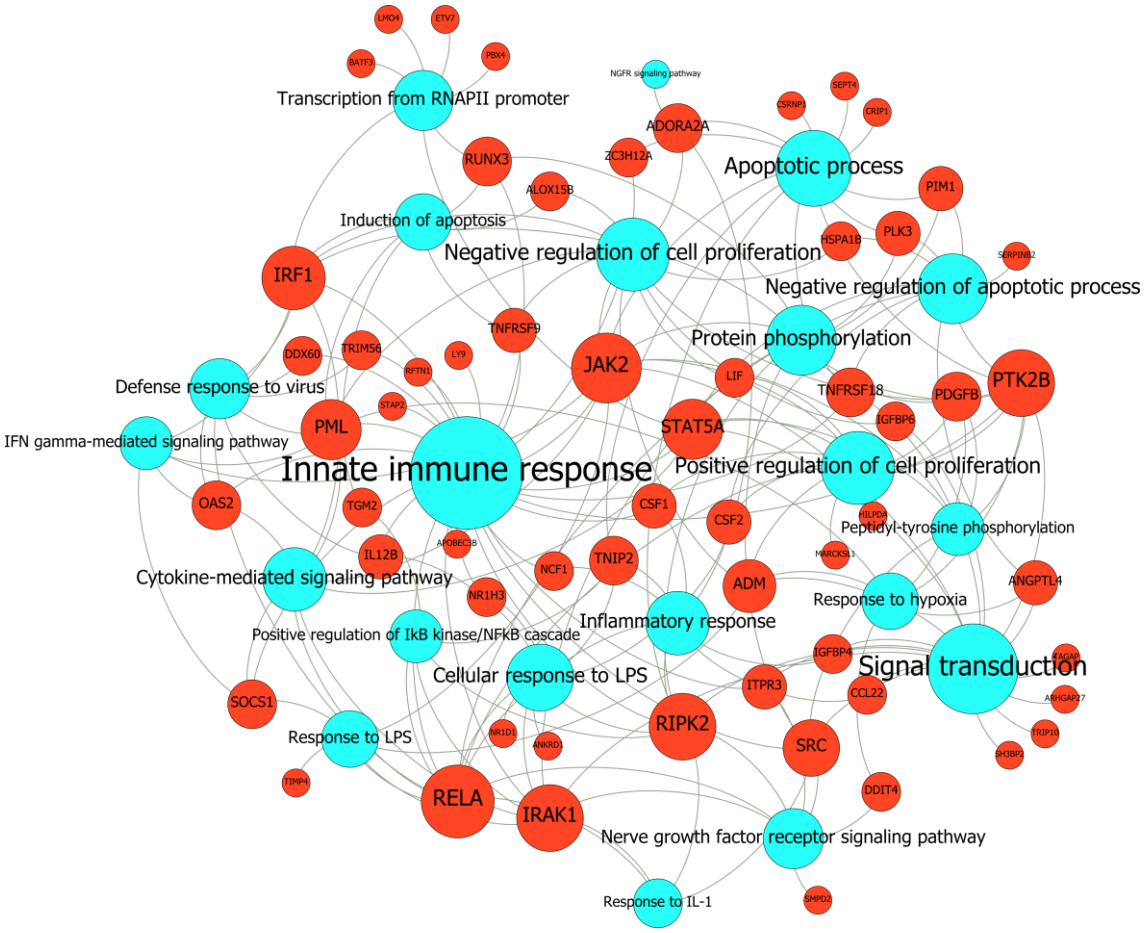

Figure 4.11: Genes which are negatively regulated by IL-10 in zymosan stimulation of MDMs.

IL-10 neutralisation significantly increased the expression of 117 genes which are usually upregulated in the MDM response to zymosan (**Figure 4.10b**), suggesting that these genes were negatively regulated by IL-10. InnateDB (Breuer et al., 2013; http://www.innatedb.com) GO enrichment analysis was performed for this gene list and the results of this analysis are visualised as a network. Enrichment assessment was performed using a hypergeometric algorithm, and filtered to biological process GO terms with a significance level of $P<0.05$ (Benjamini-Hochberg correction-adjusted). The top 20 enriched GO terms by gene count are shown. GO terms are in blue and genes are in red. Node size is determined by number of connections. All data presented are derived from the mean results of 3 independent experiments.

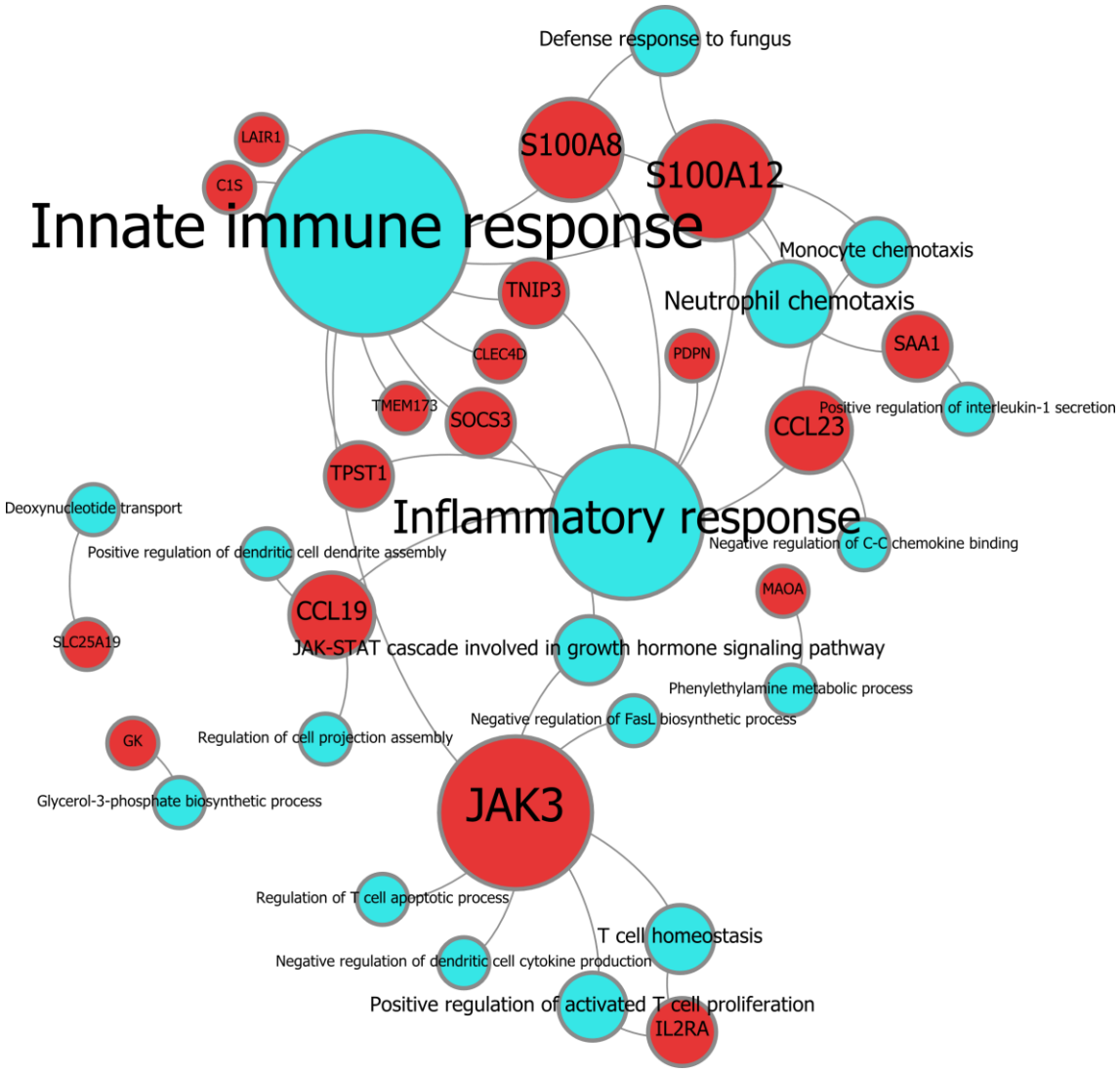

Figure 4.12: Genes which are positively regulated by IL-10 in zymosan stimulation of MDMs.

IL-10 neutralisation significantly attenuated the expression of 45 genes which are usually upregulated in the MDM response to zymosan (**Figure 4.10b**), suggesting that these genes were positively regulated by IL-10. InnateDB (Breuer et al., 2013; http://www.innatedb.com) GO enrichment analysis was performed for this gene list and the results of this analysis are visualised as a network. Enrichment assessment was performed using a hypergeometric algorithm, and filtered to biological process GO terms with a significance level of $P<0.05$ (Benjamini-Hochberg correction-adjusted). All enriched GO terms are shown. GO terms are in blue and genes are in red. Node size is determined by number of connections. All data presented are derived from the mean results of 3 independent experiments.

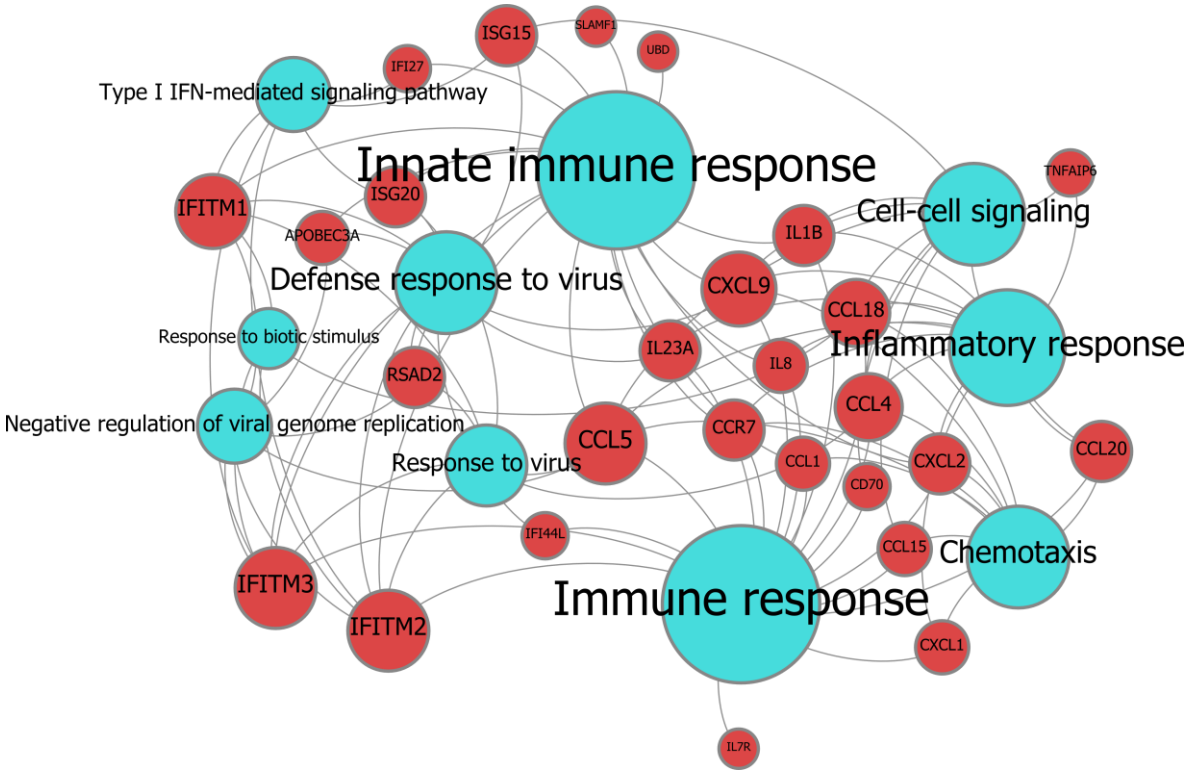

Figure 4.13: Genes which are not regulated by IL-10 in zymosan-stimulated MDMs.

A large proportion of the gene expression response to zymosan in MDMs was not affected by IL-10 neutralisation (769 of 915 genes; **Figure 4.10b**). To gain insight into the function of these non-IL-10 regulated components of the innate immune response, the most highly zymosan-inducible genes (≥16-fold increase in expression) were selected and InnateDB (Breuer et al., 2013; http://www.innatedb.com) GO enrichment analysis was performed for this gene list. Enrichment assessment was performed using a hypergeometric algorithm, and filtered to biological process GO terms with a significance level of $P<0.05$ (Benjamini-Hochberg correction-adjusted). The 10 most highly enriched GO terms are shown. GO terms are in blue and genes are in red. Node size is determined by number of connections. All data presented are derived from the mean results of 3 independent experiments.

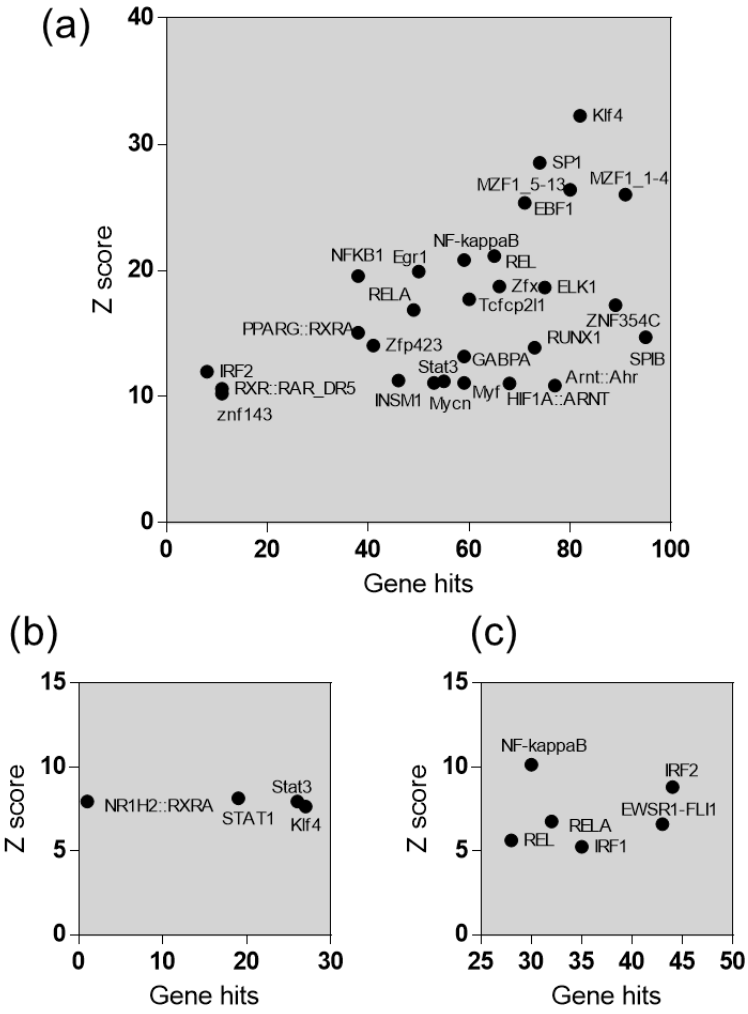

Figure 4.14: TFBS enrichment analyses of IL-10 regulated genes in zymosan-stimulated MDMs

To gain insight into transcriptional regulation of the genes which were differentially expressed in zymosan stimulation −/+ IL-10 neutralisation, TFBS enrichment analysis was performed using oPOSSUM-3 (Kwon et al., 2012; http://opossum.cisreg.ca). The sequence 5000bp up/downstream of each gene was analysed. Significance of TFBS frequency compared to background was assessed by the Z-score statistic, which was considered significant when ≥10. The X axis lists the number of genes enriched for a TFBS, and the Y axis displays the Z score. **(a)** TFBS enrichment analysis for genes further up-regulated as a result of IL-10 neutralisation (**Figure 4.10b**; **Figure 4.12**). **(b)** TFBS enrichment analysis for genes which were attenuated in expression as a result of IL-10 neutralisation (**Figure 4.10b**; **Figure 4.13**). **(c)** TFBS enrichment analysis for genes which were conserved in IL-10 neutralisation (**Figure 4.13**). All data presented are derived from the mean results of 3 independent experiments.

4.2.6 IL-10 deficiency in inflammation modulates cell recruitment

Neutralisation of IL-10 in the MDM response to zymosan dysregulated expression of a range of secreted factors, including cytokines and chemokines (**Figure 4.11, 4.12**). This suggested that a deficiency in autocrine IL-10 signalling in macrophages might impact on the function of other cells which are responsive to these factors. One candidate pathway which may be affected is the recruitment of other leukocytes to an inflammatory focus generated by the macrophage. A previous investigation of dysregulated inflammatory responses in HIV-1/Mtb co-infected macrophages demonstrated that expression of the chemokines CCL20, CCL3, CCL3L3 and CCL5 in response to Mtb was potentiated by HIV-1 co-infection, and that this may be a result of IL-10 attenuation (Tomlinson et al., 2014).

I aimed to investigate whether IL-10 deficiency in macrophage-generated inflammation altered cellular recruitment. A transwell experiment was used to model recruitment to an inflammatory focus (**Figure 4.15a**). Conditioned media generated by zymosan stimulation of macrophages in the presence or absence of IL-10 neutralisation was placed in the lower chamber, and PBMC were placed in the upper chamber. After 3 hours of migration, cells in the lower chamber were collected and stained for CD3 and CD14 to quantify T cells and monocytes respectively, using flow cytometry.

To quantify the migration of different cell populations, a migration index was used. The absolute numbers of cells recruited, for each cell population of interest, were normalised as a ratio to the absolute number of that cell population in an input PBMC sample. The acquisition of all samples, including the input sample, was standardised using beads spiked into equivalent volumes of fixed cell suspensions. Migration indices for conditioned media of interest were compared to the migration index for control non-conditioned media, to identify differential recruitment generated by macrophage responses.

The PBMC migration index was statistically significantly increased using conditioned media generated by MDMs with IL-10 neutralisation, regardless of zymosan stimulation (**Figure 4.15b**). The $CD3^+$ migration index suggests that increased numbers of T cells are recruited using zymosan-stimulated conditions (**Figure 4.15c**), and this was significantly increased further by IL-10 neutralisation (**Figure 4.15c**). The $CD14^+$ monocyte migration index was significantly increased by IL-10 neutralisation

alone (**Figure 4.15d**). Assessing modulation of $CD14^+$ cell migration in the context of zymosan stimulation may be confounded by the fact that fewer monocytes migrated using zymosan-conditioned media (**Figure 4.15d**), which may be due to inflammatory mediator-induced increases in monocyte adhesion (Gerszten et al., 1999; Imhof and Aurrand-Lions, 2004; Jiang et al., 1992) meaning they adhere within the upper chamber and to the upper surface of the transwell, preventing migration. No differential recruitment was observed for the $CD3^-CD14^-$ cell population (**Figure 4.15e**).

These results suggest that deficiency of IL-10 can impact on cellular recruitment to a macrophage-generated inflammatory focus. Most strikingly, T cell recruitment is clearly potentiated by neutralisation of IL-10 in zymosan-stimulated MDMs. Monocyte recruitment may also be affected, as resting MDMs with IL-10 neutralisation appear to recruit increased numbers of monocytes; however, further assessment is merited to clarify whether this also occurs in the presence of inflammation. The $CD3^-CD14^-$ population is made up of several cell types, including B cells, NK cells and $CD14^-$ mononuclear myeloid cells, and so although no gross differential recruitment was shown in this experiment, further assessment may be necessary to delineate any differential regulation as a result of IL-10 deficiency.

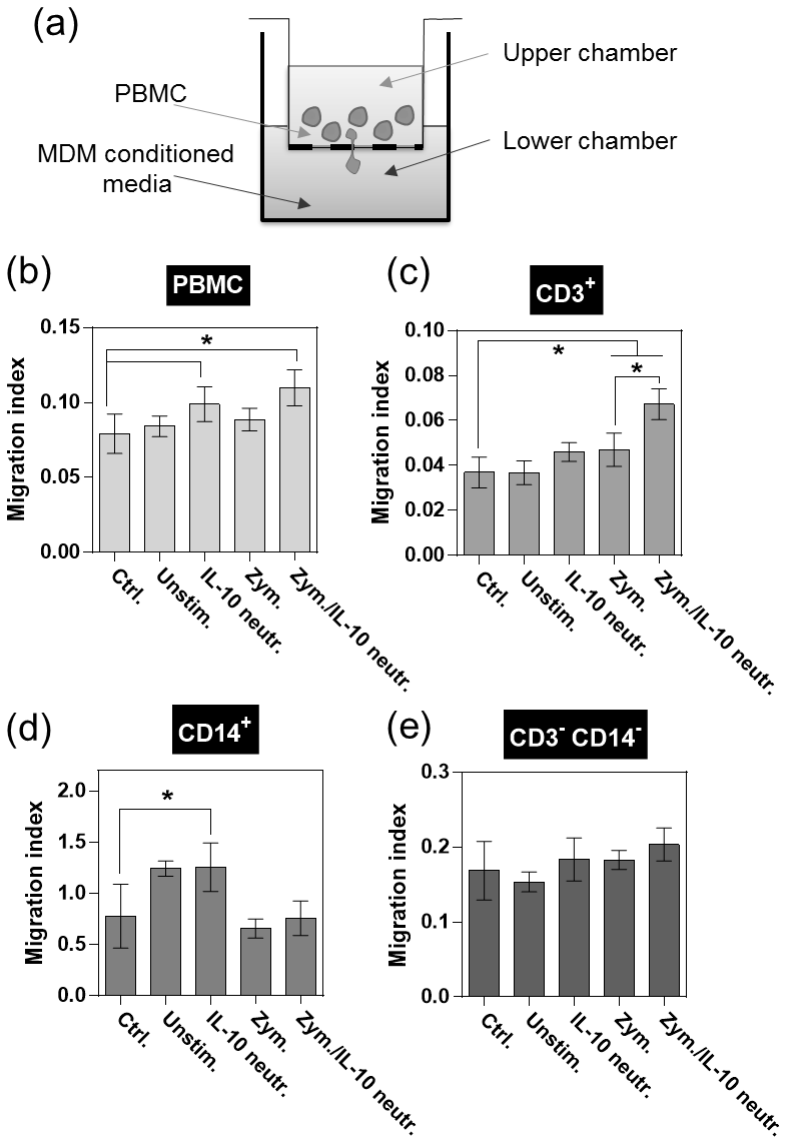

Figure 4.15: IL-10 neutralisation modulates recruitment of PBMC.

(a) Schematic of transwell experimental model. Conditioned media generated from stimulation of MDMs with zymosan −/+ IL-10 neutralisation (pooled from 4 donors) was placed in the lower chamber of the transwell. PBMC from a healthy donor were placed in the upper chamber and allowed to migrate for 3 hours. Recruited cells were stained and analysed by flow cytometry. Migration indices were calculated for each cell population by normalising the absolute number of recruited cells to the absolute number in an input PBMC sample. Sample acquisition was standardised using beads. Control (ctrl) indicates unconditioned media in the lower chamber. **(b)** PBMC migration was significantly increased by conditioned media generated with IL-10 neutralisation −/+ zymosan stimulation. **(c)** $CD3^+$ (T cell) migration was significantly increased by zymosan-stimulated conditioned media, and addition of IL-10 neutralisation significantly increased $CD3^+$ migration above zymosan alone. **(d)** $CD14^+$ (monocyte) migration was significantly increased by conditioned media generated with IL-10 neutralisation without zymosan stimulation. **(e)** $CD3^-$ $CD14^-$ cell migration index. No conditioned media altered migration. ***** indicates $P<0.05$, paired t-test. Bars show mean −/+ SEM of 4 independent experiments.

4.3 Chapter discussion

I aimed to explore the consequences of IL-10 attenuation for viral replication, and for the host immune response, in terms of the pathogens affected and the functional outcomes of innate immune IL-10 deficiency.

To understand the consequences of IL-10 attenuation by HIV-1 in MDMs, I assessed whether this phenotype provided the virus with a replicative advantage. IL-10 supplementation inhibited zymosan-induced viral replication and release in MDMs (**Figure 4.1**), and did so at the level of virus transcription, corroborating previously published work suggesting this to be the case in other systems (Tanaka et al., 2005; Wang and Rice, 2006). This gives a strong indication of why restricting IL-10 transcription might provide an advantage to the virus, and thus why HIV-1 has evolved this function. This enhancement of HIV-1 replication by zymosan, or other stimuli which activate dectin-1, has not previously been observed. Mtb has been shown to enhance HIV-1 replication in macrophages, but TLR-2 rather than dectin-1 stimulation has been the primary pathway implicated in this mechanism (Falvo et al., 2011; Ranjbar et al., 2012). Establishing whether specific stimulation of dectin-1 can directly enhance HIV-1 replication is of interest, as it would provide insight into the dynamics of viral replication during fungal co-infections in which dectin-1 is a major PRR. Stimulation of MDMs with curdlan, a specific dectin-1 ligand, may provide insight into this interaction.

IL-10 supplementation did not affect HIV-1 replication in non-stimulated macrophages, nor was IL-10 found to modulate macrophage permissivity to HIV-1 infection (**Figure 4.2**). However, as IL-10 is less likely to be produced by macrophages in the resting state, and thus to elicit a response in these cells, this situation may be less relevant than the interplay between HIV-1, IL-10 and macrophages in the context of macrophage activation. In this model, macrophages are reservoirs of latent HIV-1 infection, which begins to replicate during activation by a pathogen, at which time there is accumulation of other macrophages and T cells, i.e. an appropriate time for viral propagation between cells. IL-10 can suppress viral replication and limit the inflammatory response, so it is advantageous to the virus to inhibit IL-10 production in order to amplify the inflammatory environment and to maximise viral replication and transmission to new host cells. Importantly, several studies have identified increased HIV-1 replication *in vivo* at the site of TB disease, i.e. an inflammatory environment, indicating that these interactions may be relevant to co-infection pathogenesis (Collins

et al., 2002b; Garrait et al., 1997; Lawn et al., 2001; Nakata et al., 1997). Testing the effects of IL-10 supplementation on cell-to-cell spread of virus may provide further insight into this hypothesis, by determining if IL-10 attenuation by HIV-1 augments transmission between macrophages or from macrophages to T cells.

To investigate whether HIV-1 attenuated IL-10 responses to a pathogen other than Mtb, the opportunistic pathogenic fungus *C. neoformans* was investigated. Uptake of *C. neoformans* to MDMs was confirmed, albeit at relatively low levels, and this was not affected by HIV-1 co-infection (**Figure 4.3**). However, inflammatory responses to *C. neoformans* were not evident, except in response to unencapsulated *C. neoformans* mutants, where some pro-inflammatory cytokine expression, and IL-10 secretion (non-significantly in a subset of donors), was measured at 24 hours (**Figure 4.4, Figure 4.5**). The non-immunogenicity of *C. neoformans* was further confirmed by the lack of NFκB activation in response to this pathogen (**Figure 4.6**). As such, the existence or relevance of attenuated MDM IL-10 responses to *C. neoformans* could not be assessed.

C. neoformans is known to be a relatively non-immunogenic organism (Vecchiarelli et al., 1995). However, as healthy individuals (who do not commonly experience cryptococcal disease) generate protective immune responses to *C. neoformans*, as evident by detectable antibody responses in most individuals by early childhood (Abadi and Pirofski, 1999; Goldman et al., 2001), presumably an innate response must occur *in vivo* in order for an adaptive response to be provoked. It is also clear that this innate response is likely to be generated by alveolar macrophages, as transmission of *C. neoformans* infection occurs via the respiratory tract, and so alveolar macrophages are assumed to be the primary host cell for the fungus (McQuiston and Williamson, 2011). It may be that this model of M-CSF differentiated MDMs does not effectively model the *in vivo* sentinel cell, alveolar macrophage or otherwise, which detects *C. neoformans*, and indeed other reports describing innate responses have used different cellular models, such as PBMC (Levitz et al., 1994; Walenkamp et al., 1999) *ex vivo* alveolar macrophages (Vecchiarelli et al., 1994), DCs (Lupo et al., 2008; Vecchiarelli et al., 1995) or monocytes (Delfino et al., 1997; Vecchiarelli et al., 1995). Further experiments using these cells may allow assessment of whether HIV-1 infection of the mononuclear phagocyte sentinel cell modulates the innate response to *C. neoformans*, as well as assessing other aspects of this host-pathogen interaction such as phagocytosis, killing and inflammasome activation. In terms of further

identification of pathogens for which HIV-1-mediated IL-10 attenuation may be relevant, the agents of other clinically important fungal co-infections are candidates, such as *Candida albicans* and *Pneumocystic jirovecii*.

The consequences of IL-10 attenuation for the function of the immune response were explored in a set of experiments investigating regulation of macrophage function by IL-10 signalling. Stimulation of resting MDMs with recombinant IL-10 for 24 hours induced modest gene expression changes (**Figure 4.7**), in comparison to the magnitude of gene expression changes induced by another cytokine which can modulate macrophage function, IFNγ (**Figure 4.8**). This gene expression response was concordant with known functions of IL-10, such as modulation of apoptotic pathways (Balcewicz-Sablinska et al., 1999, 1998; Eslick et al., 2004; Rojas et al., 1999; Zhou et al., 2001). Many gene expression changes identified have also been reported by other investigators as effects of IL-10 on macrophages or monocytes, such as induction of SOCS3, IL7R, CD163, C1S, IL1B and CCL18 (Antoniv et al., 2005; Teles et al., 2013; Williams et al., 2002). Many of these genes encode for proteins with functions which are not classically immunosuppressive or anti-inflammatory, and which have functions other than mediating inhibition of transcriptional responses, which is suggested to the main mechanism of IL-10/STAT-3 induced AIR factors (Hutchins et al., 2012; Murray, 2006, 2005). This demonstrates that IL-10 signalling in macrophages can modulate function, as well as having directly suppressive effects on pro-inflammatory responses. For example, the induction of signalling molecules such as SOCS3 and JAK3 could modulate subsequent responses to innate immune stimuli and cytokines, IL1B and C1S are potentially involved in inflammation, and CCL18 is chemotactic for Th2 cells (Griffith et al., 2014).

As this gene expression profile represents the outcome 24 hours post-IL-10 signalling, it may include both genes induced directly by IL-10 via STAT3 signalling, and secondary waves of response coordinated via indirect pathways, particularly as it is suggested that STAT3 mainly acts to induce the expression of transcription factors (Hutchins et al., 2012). That it might include both responses is supported by the observation that it includes previously identified secondary STAT3 effectors, such BCL3 and BATF (Hutchins et al., 2012), but also clearly includes many genes with divergent functions. Additionally, TFBS enrichment analysis only identifies STAT3 binding sites in a subset of the genes (**Figure 4.7b**).

The effects of IL-10 pre-treatment on the MDM response to IFNγ was measured, to assess whether IL-10 could modulate this key interaction in the cell-mediated immune response. No significant impact of IL-10 pretreatment was apparent (**Figure 4.8**). This is consistent with some published reports, including in the mouse model of Mtb, wherein it has been shown that macrophage-derived IL-10 modulates the immune response to Mtb by pathways which do not involve the Th1 response (Schreiber et al., 2009). However, there is a prevalent concept within the field that IL-10 can negatively regulate protective IFNγ responses and that this is a pathway by which it could compromise protection in TB infection (O'Garra et al., 2013). This may still occur indirectly, due to IL-10 regulation of the innate response leading to less Th1 polarisation (Fiorentino et al., 1991, 1991). It is also possible that *post hoc* signalling by IL-10 might modulate the IFNγ response. The former scenario is supported by subsequent experiments assessing the effect of IL-10 blockade on leukocyte recruitment, in which IL-10 neutralisation potentiates T cell recruitment, suggesting that IL-10 normally acts to inhibit macrophage/T cell interactions.

However, this experiment strongly indicates that IL-10 does not directly suppress the macrophage response to IFNγ, and this is supported by the observation that IL-10 does not induce expression of the major intracellular negative regulatory of IFNγ signalling, SOCS1 (Carey et al., 2012). In fact, IL-10 negatively regulates SOCS1 in a subsequent experiment assessing the effects of IL-10 via its blockade (**Figure 4.11**). The main negative regulator induced by IL-10 in these experiments is SOCS3 (**Figure 4.7, Figure 4.12**), the main function of which is in negative regulation of innate inflammatory IL-6 signalling (Carey et al., 2012). These divergent effects of IL-10 on regulatory pathways controlling either adaptive or inflammatory signalling may indicate that its main direct function in human macrophages is to regulate the innate response, via which it may then exert indirect effects on adaptive immunity.

Assessment of the role of IL-10 in the innate immune response was further extended by specifically investigating its role in inflammation, by blockade of autocrine IL-10 signalling during zymosan stimulation of MDMs (**Figure 4.9–Figure 4.14)**. Some of the genes shown to be induced by IL-10 in resting MDMs are also highlighted here, such as SOCS3, C1S and S100 proteins, showing that in the context of inflammation, IL-10 still induces particular phenotypic changes in macrophages, as well as exerting suppressive effects. Its suppressive role is strongly evident in this context: IL-10 negatively regulated approximately 20% of the MDM response to zymosan, consistent

with the reported magnitude of its role in regulating the LPS response in murine BMDMs (Lang et al., 2002b). It is also clear from this experiment, similarly to the previous investigation of the murine LPS response, that the regulatory effects of IL-10 on gene expression are greater in magnitude in the context of innate activation of macrophages than in resting macrophages, supporting the concept that the major role of IL-10 is to modulate inflammation.

Many of the genes affected by IL-10 neutralisation in this experiment may have roles in cell-autonomous macrophage functions, highlighting potential dysregulated macrophage phenotypes which might result from HIV-1 mediated IL-10 attenuation in the innate immune response. These include the previously discussed dysregulation of SOCS proteins. Expression of SOCS1, which regulates IFNγ signalling, was induced as a result of IL-10 blockade, while the IL-6 signalling regulator SOCS3 was suppressed (**Figure 4.11, Figure 4.12**; Carey et al., 2012). If corroborated in HIV-1 infected MDMs, this suggests that IL-10 attenuation might cause hyper-responsiveness to inflammatory IL-6 signalling and hypo-responsiveness to adaptive IFNγ signalling. Assessing responses of HIV-1 infected MDMs to these cytokines may be informative, as well as testing the response of HIV-1 infected MDMs to type I IFNs or co-infecting viruses, as these latter pathways were highlighted by exploration of the component of the innate immune response which was not regulated by IL-10. Finally, the role of IL-10 in modulating apoptosis was emphasized in these experiments, and as a result assessments of dysregulation of apoptosis in HIV-1 infected MDMs are clearly merited.

As well as indicating macrophage-autonomous functions which are modulated by IL-10 neutralisation and hence also potentially by HIV-1 attenuation of IL-10, this experiment also identifies many factors secreted by MDMs which are dysregulated as a result of IL-10 blockade, including the genes encoding for IL-12 p40, M-CSF, GM-CSF and a number of chemokines. This suggests that autocrine IL-10 signalling in macrophages can indirectly regulate the function of other cells via these factors, thus identifying candidate pathways by which the IL-10 attenuation phenotype might impact on the downstream immune response. One such pathway, regulation of chemotaxis, is discussed subsequently. Other strong candidates for investigation including assessing the effect of HIV-1 infected macrophages on T cell polarisation, as IL-12, the major inducer of Th1 polarisation, is dysregulated. Exploring the effects of these cells on monocyte differentiation is also merited, due to the demonstrated dysregulation of M-CSF and GM-CSF.

The effects of innate immune IL-10 deficiency on chemotaxis were investigated by testing recruitment of leukocytes to an inflammatory focus, via modelling this interaction in a transwell experiment (**Figure 4.15**). Conditioned media from zymosan-stimulated MDMs was shown to induce T cell migration, and IL-10 neutralisation was capable of significantly increasing this (**Figure 4.15c**). This could potentially be due to absence of negative regulation by IL-10 of the T cell chemotactic factor CCL22 (**Figure 4.11**; Griffith et al., 2014). Assessment of whether HIV-1-mediated IL-10 attenuation produces the same phenotype is warranted, as if HIV-1 uses macrophage IL-10 deficiency to potentiate T cell recruitment in inflammation, this would support the concept that HIV-1 produces this phenotype in order to maximise its own propagation. The previous investigation of dysregulated responses in HIV-1/Mtb co-infected macrophages did not identify CCL22 dyregulation, but did demonstrate exaggerated production of the T cell chemotactic factor CCL20 (Griffith et al., 2014; Tomlinson et al., 2014), also supporting further investigation of this phenotype. Blockade of different chemokines with neutralising antibodies within this experimental setup may also help identify the specific mechanisms by which IL-10, and possibly HIV-1, lead to downstream modulation of leukocyte recruitment.

These alterations in cellular recruitment due to IL-10 deficiency also have the potential to change the quality of the inflammation generated; for example by leading to polarised T cell phenotypes. As such, further work defining the phenotype of these recruited T cells is merited: firstly, whether they are $CD4^+$ or $CD8^+$, and secondly, whether there is differential polarisation within the $CD4^+$ population: CCL22, discussed above, is postulated to be associated with specific recruitment of Th2 cells (Griffith et al., 2014).

In these experiments, monocyte recruitment was found to be abrogated in the presence of conditioned media from zymosan-stimulated MDMs (**Figure 4.15d**), and as such the effect of IL-10 neutralisation on modulating their recruitment could not be assessed. This absence of migration may be due to increased monocyte adhesion in the upper chamber of the transwell setup, as monocyte adhesion can be induced by various inflammatory mediators that are likely to be generated by zymosan stimulation of MDMs (Gerszten et al., 1999; Imhof and Aurrand-Lions, 2004; Jiang et al., 1992).

In summary, the phenotype of IL-10 attenuation may have substantial consequences for both viral replication and for the host immune response. Inflammation represents a valuable opportunity for the virus to maximise its own

replication, both within macrophages and by inducing recruitment of new target cells for infection. Suppressing innate immune IL-10 production allows HIV-1 to potentiate its own replication in the context of inflammation. As IL-10 has a multitude of modulatory and suppressive effects, this host-virus interaction may impact on the immune response in a number of ways. Further exploring the functions of macrophage-produced IL-10 and dysregulated responses of HIV-1 infected macrophages may provide insight into the immunopathology of HIV-1 associated co-infections, and the role of macrophages in these.

Chapter 5. Results 3. Derivation of transcriptional modules reflecting macrophage heterogeneity

5.1 Background

Macrophages are tissue-resident sentinel cells which are also involved in regulation and repair processes, and so must continuously respond to changes in the homeostasis of their environment (Wynn *et al.*, 2013), via a wide variety of potential inputs. Each of these inputs requires the macrophage to alter its function appropriately, and therefore functional plasticity and subsequent phenotypic heterogeneity are central tenets of macrophage biology (Lawrence and Natoli, 2011). This plasticity is assumed to be primarily controlled at the transcriptional level, wherein the extracellular mediators inducing macrophage phenotypic adaptation activate intracellular signalling cascades via receptor ligation, converging on transcriptional outputs which reprogram the function of the cell (Lawrence and Natoli, 2011; Natoli and Monticelli, 2014). Hence, genome-wide transcriptional profiling, has been widely employed to characterise the molecular detail of macrophage activation states (Beyer et al., 2012; Lacey et al., 2012; Martinez et al., 2006; Nau et al., 2002; Xue et al., 2014).

As macrophages are critical co-ordinators of the immune response in the tissue microenvironment, most evidently in the context of CMI, assessment of their phenotype can potentially provide insight into the overarching phenotype of an immune response. I aimed to use the functional heterogeneity of macrophage phenotypes as a window for assessing immune responses *in vivo*, through investigating macrophage plasticity in human MDMs by transcriptional profiling, and subsequently using these datasets to analyse *in vivo*-derived gene expression profiles. To make this link between macrophage transcriptomes and *in vivo* gene expression profiles, I chose to use MDM gene expression data to develop a modular strategy for transcriptional analysis.

Modular analysis of gene expression data is a method by which the expression of a set of genes that define a particular functional response, cell type or pathway is quantified as a single variable for comparative assessments (reviewed fully in **Introduction section 1.6.3**). For example, to measure IFNγ activity, the expression of all genes induced by IFNγ is integrated to quantify as a single IFNγ score. There are several clear advantages provided by modular transcriptomic analyses. Firstly, in identifying a particular biological process of interest, assaying a set of genes as

opposed to a single gene is likely to provide superior specificity; a single gene is more likely to act as a false positive than is a combined set of genes. Secondly, the power available to assess the bioactivity of a particular stimulus is increased by measuring a larger set of genes as a proxy, as it does not rely on the ability to measure any single particular molecule. Finally, in assessing gene expression profiles derived from complex *in vivo* samples, which are likely to contain multiple signatures of parallel functional processes, modular analysis may be a particularly valuable method for deconvoluting genome-wide data into its component, functionally informative parts.

Two principal methods of generating modules currently exist. Firstly, data-driven modules, an unsupervised method in which co-clustering networks of transcript correlations are built and used to identify a repertoire of modules each of which is made up of co-correlated genes. Modules can then be assigned particular functional or cellular labels by *post hoc* assessments (Chaussabel and Baldwin, 2014). The second method can be described as hypothesis-driven, in which the modular activity that the investigator wishes to assess is defined *a priori* – for example, the activity of a particular cytokine or the phenotype of a specific cell – and a gene set is constructed for this module from bioinformatics sources or experimentally generated transcriptomic data (Subramanian et al., 2005). Multiple strategies have also been developed to quantify enrichment of module expression in transcriptomic datasets. These include simple methods, in which the mean or median expression value of the module gene set is calculated in the sample of interest, which is then used as a module score which can be used for between-group comparisons (Chaussabel and Baldwin, 2014). More complex techniques for assessing enrichment involve statistical algorithms such as GSEA (Mootha et al., 2003; Subramanian et al., 2005). A gold standard for module enrichment scoring is yet to emerge (Hung et al., 2012). The most appropriate analysis method to use is likely to depend on the distribution of the dataset to be assessed (Alavi-Majd et al., 2014), and use of multiple methods to widely explore datasets and confirm enrichment may be most appropriate (Glazko and Emmert-Streib, 2009).

I aimed to use macrophage heterogeneity, a powerful gauge of the function of the immune response, to develop hypothesis-driven modules for stimuli of interest, in order to facilitate downstream analyses of *in vivo*-derived gene expression profiles. In order to do this, I aimed to explore macrophage plasticity via transcriptional profiling, to develop and optimise gene expression profiles from these data, and to identify

appropriate methods for assessing enrichment of these modules in downstream applications. The specific objectives of this investigation were as follows:

(a) To use transcriptional profiling to characterise MDM responses to signature cytokines produced by different T cell subsets: IFNγ, or TNFα (Th1), IL-4 and IL-13 combined (Th2) or TGFβ and IL-10 combined (Treg), to explore adaptive immune modulation of macrophage plasticity in different types of polarised immune response.

(b) To use this dataset to generate hypothesis-driven modules, which are optimised for detection of stimulus-specific effects in gene expression datasets.

(c) To use the optimised modular generation pipeline to produce modules for other stimuli of interest, from appropriate MDM transcriptomic datasets: differential IFN responses, immuno-regulatory IL-10 responses, and specific innate immune stimuli.

(d) To identify an appropriate method for quantifying enrichment of these modules in *in vivo*-derived gene expression profiles.

5.2 Results

5.2.1 MDM transcriptional responses to cytokines associated with differentially polarised T cell responses

Whole genome transcriptional profiling of unstimulated MDMs revealed gene expression levels above that of the genome-wide median for the receptors for all signature cytokines associated with differentially polarised T cell responses (**Figure 5.1a**). TGFβ receptor type 1 (*TGFBR1*) expression was lower than that of the other receptors, but still above the background level of detectable expression (**Figure 5.1a**). Interestingly, TGFβ receptor type 2 (*TGFBR2*) which was highly expressed, can function as a homodimeric receptor (Derynck and Feng, 1997). These data suggest that our model of MDM express the full complement of receptors necessary to respond to the canonical T cell cytokines.

To assess macrophage responses to cytokines, human MDMs were stimulated with IFN γ, TNFα, IL-4 & IL-13 combined or TGFβ & IL-10 combined, all at 10ng/ml for 24 hours, and genome-wide transcriptional profiling was performed by microarray. Significant transcriptional expression changes in comparison to unstimulated MDMs were identified, and are shown as frequency distributions of increased and decreased fold changes in gene expression (**Figure 5.1b**). All four conditions were associated with hundreds of up- and down-regulatory changes in gene expression, with IFNγ being associated with the greatest magnitude and numbers of changes (**Figure 5.1b**).

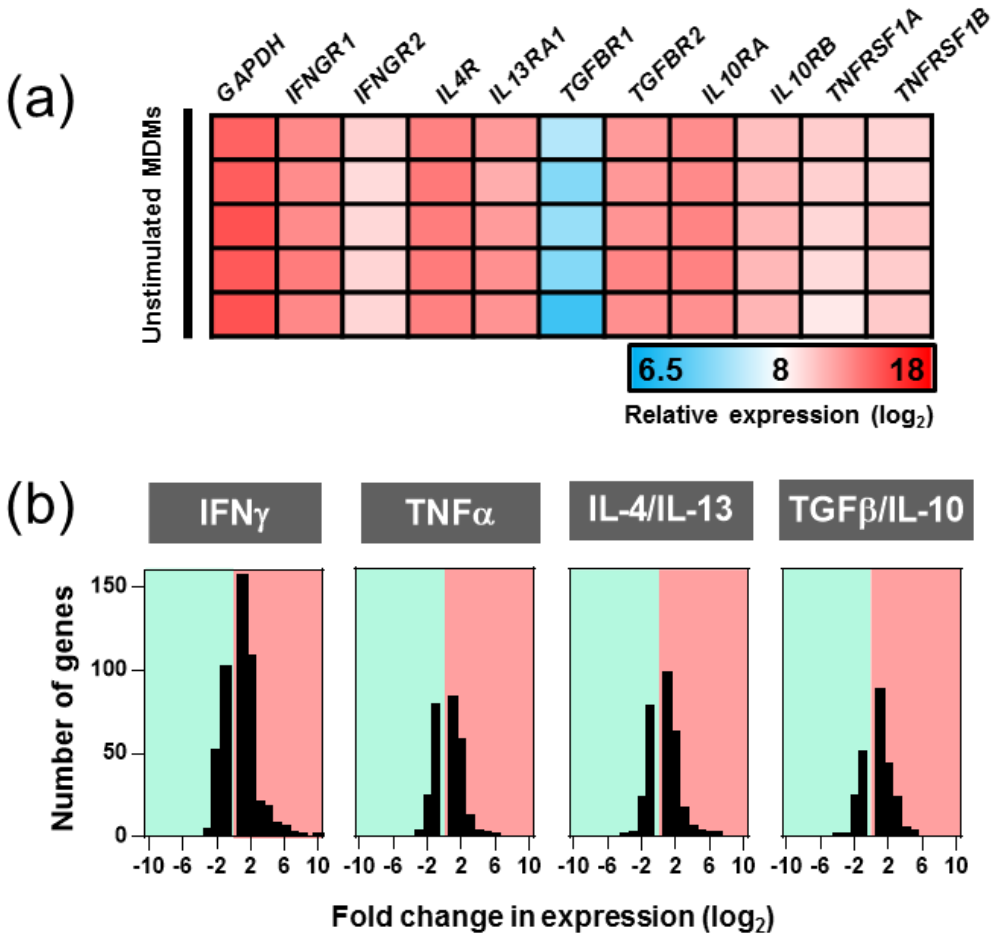

Figure 5.1: Transcriptional responses of MDMs to cytokines produced by differentially polarised T cell responses.

(a) Gene expression matrix for cytokine receptor genes in unstimulated MDMs from five healthy donors. Data is presented as normalised microarray expression values, where 6.5 is the lowest detectable expression, 18 is the highest and 8 is the median. *GAPDH* is shown as a reference housekeeping gene. **(b)** Human MDMs were stimulated with recombinant cytokines for 24 hours at 10ng/ml. RNA was collected and transcriptional profiling performed by microarray. Significant gene expression changes (≥two-fold, $P<0.05$) from unstimulated MDMs were identified by t-test with a Welch's approximation. All ≥two-fold increases and decreases in gene expression are displayed as frequency distributions of numbers of changes induced in each condition. Gene lists are filtered to remove any duplicate genes which might be present due to representation of the same gene by multiple probes on the microarray. Results represent mean gene expression values for at least three individual healthy donor MDMs for each condition.

5.2.2 Functional investigation of MDM transcriptional responses to cytokines associated with differentially polarised T cell responses

I explored the transcriptional changes induced by each cytokine using a bioinformatics approach. Firstly, in order to investigate the potential regulation of each up-regulated or down-regulated gene list, TFBS enrichment analysis was performed using oPOSSUM-3 (Kwon et al., 2012; http://opossum.cisreg.ca). Diverse arrays of transcription factors were enriched in these gene lists, representing potentially complex programs of cytokine-induced or cytokine-suppressed transcriptional changes (**Figure 5.2–5.5**). These included transcription factors known to be activated by these cytokines, such as NFκB in TNFα-induced genes (**Figure 5.3**) and STAT1 in IFNγ-suppressed genes (**Figure 5.2a**). The latter observation may reflect direct transcriptional suppression mediated by STAT1, as has been reported in the murine system (Begitt et al., 2014).

Exploration of the functional characteristics of the gene lists was performed via pathway enrichment analysis using the web tool InnateDB, a manually curated knowledge database for the innate immune response, which integrates interaction & pathway information from several public databases (Breuer et al., 2013; http://www.innatedb.com; **Figure 5.2–5.5**). The results of this analysis were visualised as networks of enriched pathways and associated genes. All gene lists were enriched for multiple pathways. Some of these were confirmatory with regards to the assumed effects of the cytokines. IFN signalling pathways were enriched in IFNγ-up-regulated genes (**Figure 5.2b**). Inflammatory pathways, such as complement activation, were enriched in genes down-regulated by the regulatory cytokines TGFβ and IL-10 (**Figure 5.5c**). Common themes of cytokine-mediated MDM activation were also evident. Chemokine activity was enriched in genes up-regulated by TNFα, IL-4 and IL-13, or TGFβ and IL-10 (**Figure 5.3–5.5**). Arachidonic acid metabolism was enriched in genes down-regulated by TNFα, or by IL-13 and IL-13 (**Figure 5.3, 5.4**).

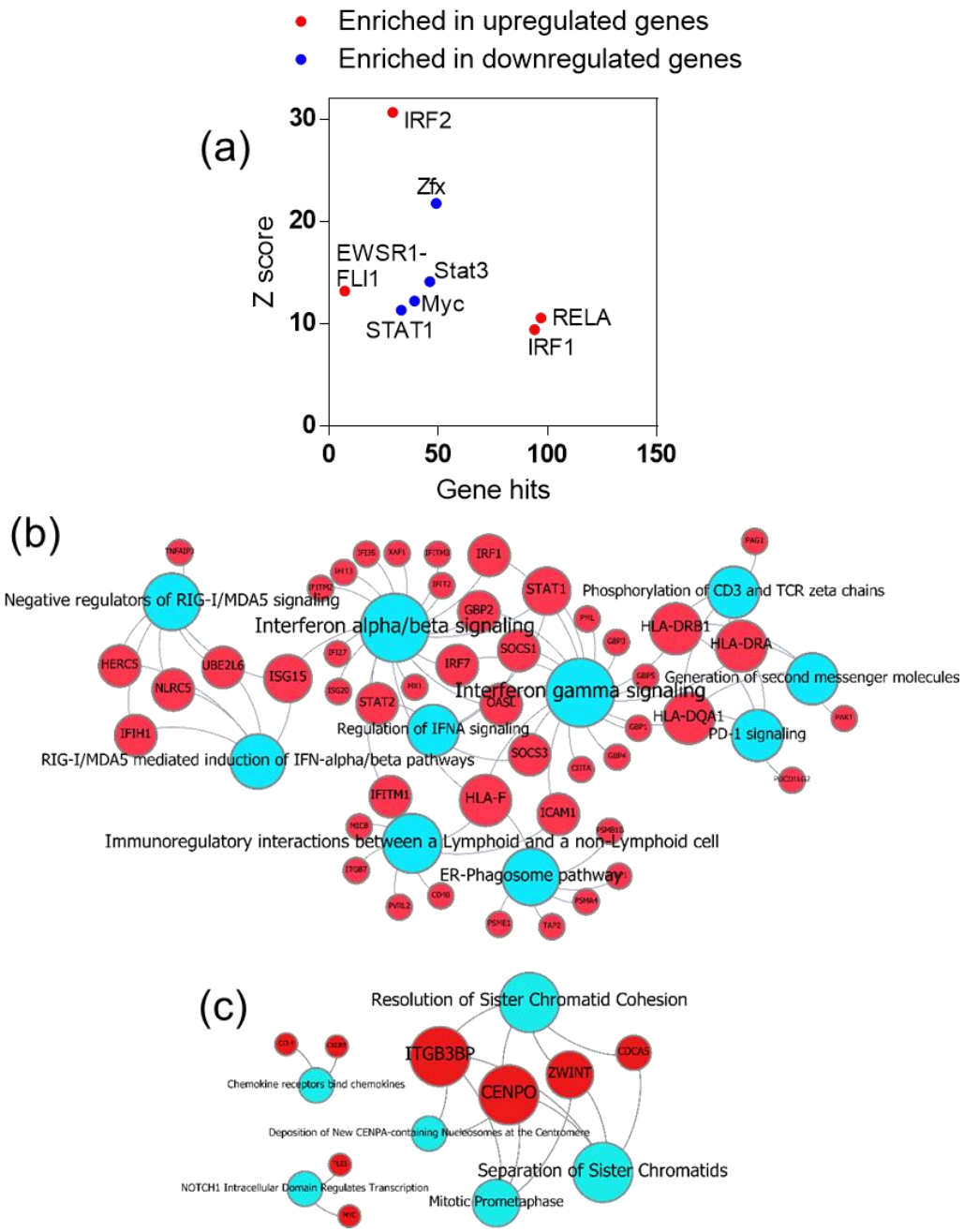

Figure 5.2: MDM transcriptional response to IFNγ.

Human MDMs were stimulated with recombinant IFNγ for 24 hours at 10ng/ml. RNA was collected and transcriptional profiling performed by microarray. Significant gene expression changes (P<0.05) from unstimulated MDMs were identified by t-test with a Welch's approximation. **(a)** Lists of genes up-regulated or down-regulated (≥two-fold) by IFNγ were subjected to TFBS enrichment analysis using oPOSSUM-3. Significance of the frequency of TFBS occurrence in gene lists compared to background was assessed by the Z-score statistic, with a score greater than 10 used as a significance threshold. **(b, c)** Network visualisations of InnateDB pathway enrichment analysis for genes up-regulated (b) or down-regulated (c) by IFNγ. Enrichment assessment was performed using a hypergeometric algorithm and filtered to Reactome-curated pathways with a significance level of P<0.05 (Benjamini-Hochberg correction-adjusted. Gene nodes are in red and pathway nodes are in blue. Node size is determined by the number of connections.

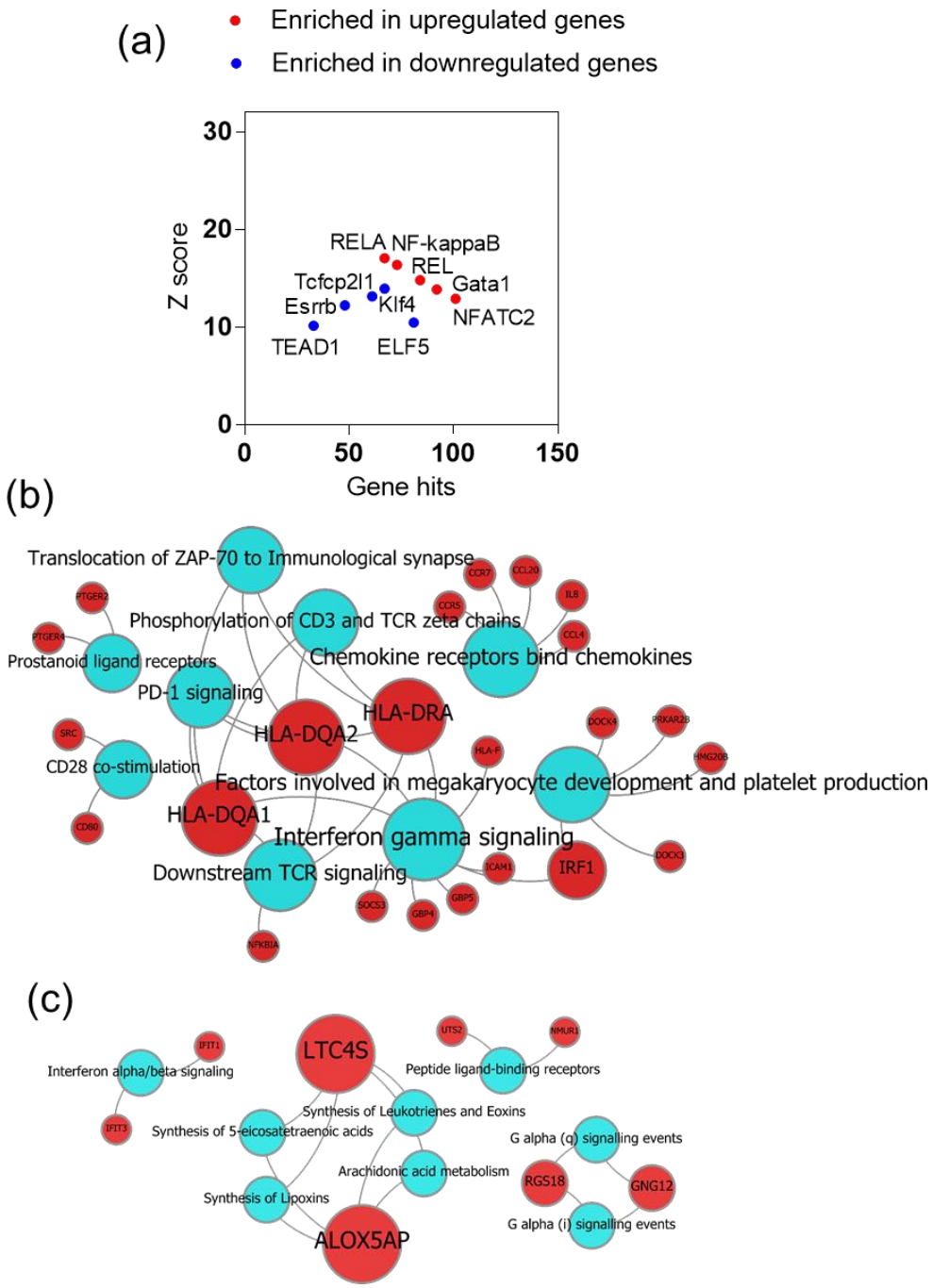

Figure 5.3: MDM transcriptional response to TNFα.

Human MDMs were stimulated with recombinant TNFα for 24 hours at 10ng/ml. RNA was collected and transcriptional profiling performed by microarray. Significant gene expression changes (P<0.05) from unstimulated MDMs were identified by t-test with a Welch's approximation. **(a)** Lists of genes up-regulated or down-regulated (≥twofold) by TNFα were subjected to TFBS enrichment analysis using oPOSSUM-3. Significance of the frequency of TFBS occurrence in gene lists compared to background was assessed by the Z-score statistic, with a score greater than 10 used as a significance threshold. **(b, c)** Network visualisations of InnateDB pathway enrichment analysis for genes up-regulated (b) or down-regulated (c) by TNFα. Enrichment assessment was performed using a hypergeometric algorithm and filtered to Reactome-curated pathways with a significance level of P<0.05 (Benjamini-Hochberg correction-adjusted. Gene nodes are in red and pathway nodes are in blue. Node size is determined by the number of connections.

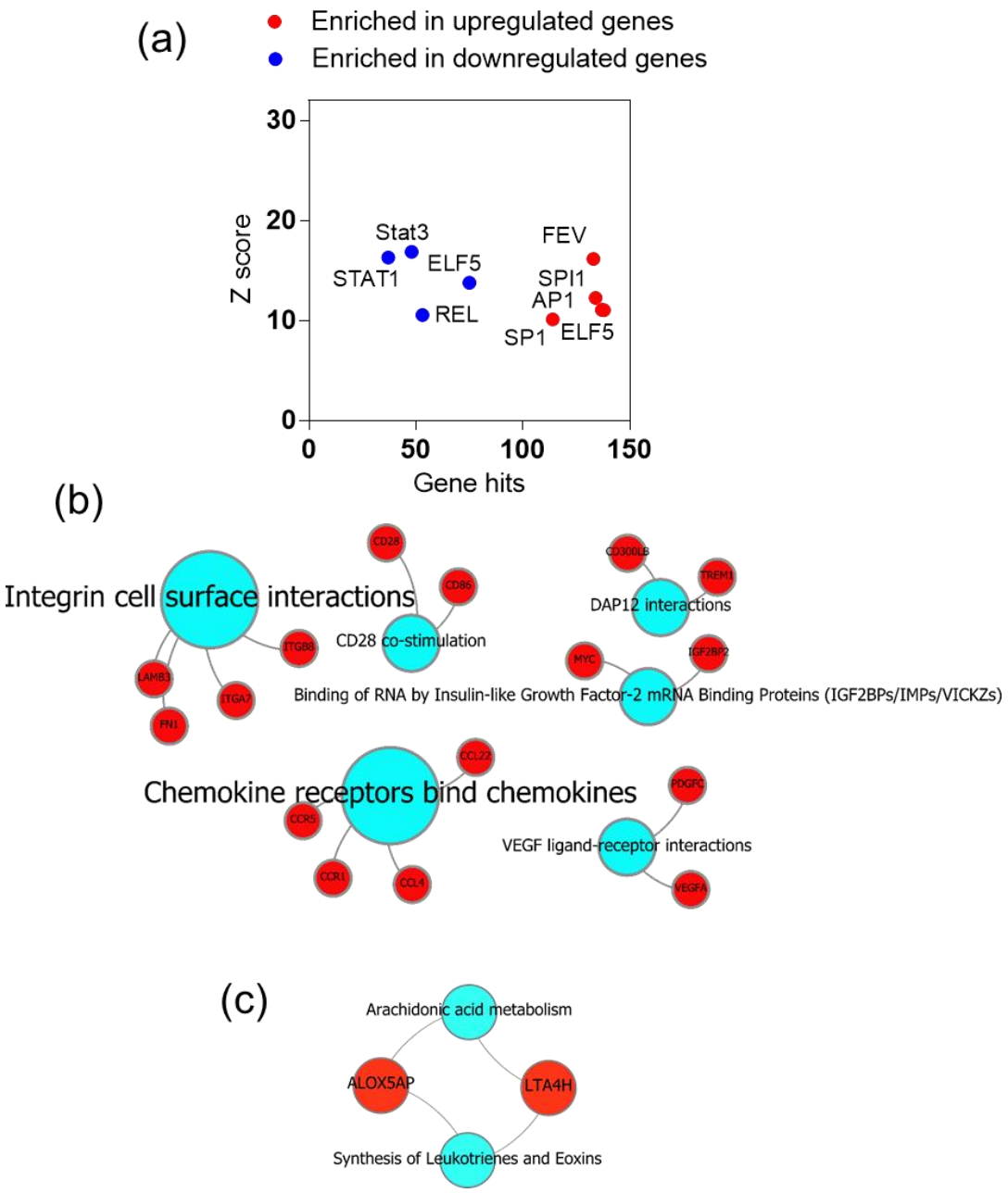

Figure 5.4: MDM transcriptional response to IL-4 and IL-13.

Human MDMs were stimulated with recombinant IL-4 and IL-13 for 24 hours at 10ng/ml. RNA was collected and transcriptional profiling performed by microarray. Significant gene expression changes (P<0.05) from unstimulated MDMs were identified by t-test with a Welch's approximation. **(a)** Lists of genes up-regulated or down-regulated (≥twofold) by IL-4 and IL-13 were subjected to TFBS enrichment analysis using oPOSSUM-3. Significance of the frequency of TFBS occurrence in gene lists compared to background was assessed by the Z-score statistic, with a score greater than 10 used as a significance threshold. **(b, c)** Network visualisations of InnateDB pathway enrichment analysis for genes up-regulated (b) or down-regulated (c) by IL-4 and IL-13. Enrichment assessment was performed using a hypergeometric algorithm and filtered to Reactome-curated pathways with a significance level of P<0.05 (Benjamini-Hochberg correction-adjusted. Gene nodes are in red and pathway nodes are in blue. Node size is determined by the number of connections.

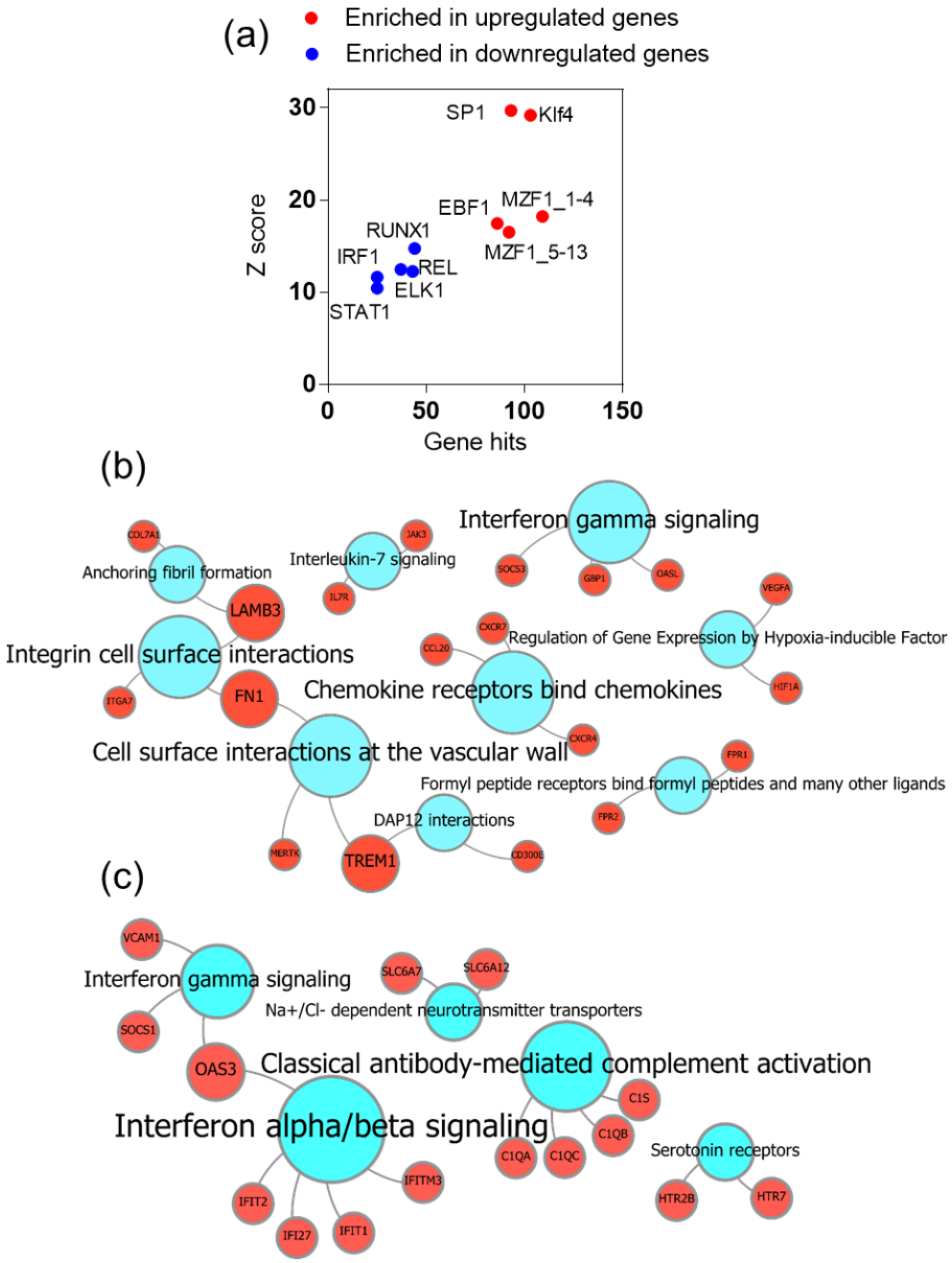

Figure 5.5: MDM transcriptional response to TGFβ and IL-10.

Human MDMs were stimulated with recombinant TGFβ and IL-10 for 24 hours at 10ng/ml. RNA was collected and transcriptional profiling performed by microarray. Significant gene expression changes (P<0.05) from unstimulated MDMs were identified by t-test with a Welch's approximation. (a) Lists of genes up-regulated or down-regulated (≥twofold) by TGFβ and IL-10 were subjected to TFBS enrichment analysis using oPOSSUM-3. Significance of the frequency of TFBS occurrence in gene lists compared to background was assessed by the Z-score statistic, with a score greater than 10 used as a significance threshold. (b, c) Network visualisations of InnateDB pathway enrichment analysis for genes up-regulated (b) or down-regulated (c) by TGFβ and IL-10. Enrichment assessment was performed using a hypergeometric algorithm and filtered to Reactome-curated pathways with a significance level of P<0.05 (Benjamini-Hochberg correction-adjusted. Gene nodes are in red and pathway nodes are in blue. Node size is determined by the number of connections.

5.2.3 Exploring the stimulus specificity of MDM transcriptional responses

PCA is an unsupervised exploratory statistical method which can be used to assess variance across a large data set in such a way that retains more information than simple hierarchical clustering, described in **Introduction section 1.6.2.**

PCA was used to explore the transcriptional responses of MDMs to different T cell subset-derived cytokines. The outcome of the PCA is shown in **Figure 5.6(a)**, and demonstrates that the dataset is highly multidimensional, with 80% of the variance explained by seven PCs. A matrix of the PC scores for these components for each stimulated MDM condition is shown in **Figure 5.6(b)**. Negative and positive signs in PC scores do not represent any inherent increase or decrease in gene expression, but are arbitrarily assigned in order to centre each PC on zero. Visualisation of PC scores in geometric space is shown for PC1 and PC2, or PC3 and PC4, in **Figure 5.6(c)**. Assessment of these PCA plots and the PC score matrix shows that most PC directions are associated with more than one condition (displayed in network form in **Figure 5.6d**). This analysis demonstrates that the transcriptional programs induced by these cytokines in MDMs have many overlapping features, although a subset of responses to each stimulus may in fact be unique and specific, e.g. the positive direction of PC3 for IL-4 and IL-13; the positive direction of PC2 for TNFα; and the negative direction of PC3 for TGFβ and IL-10.

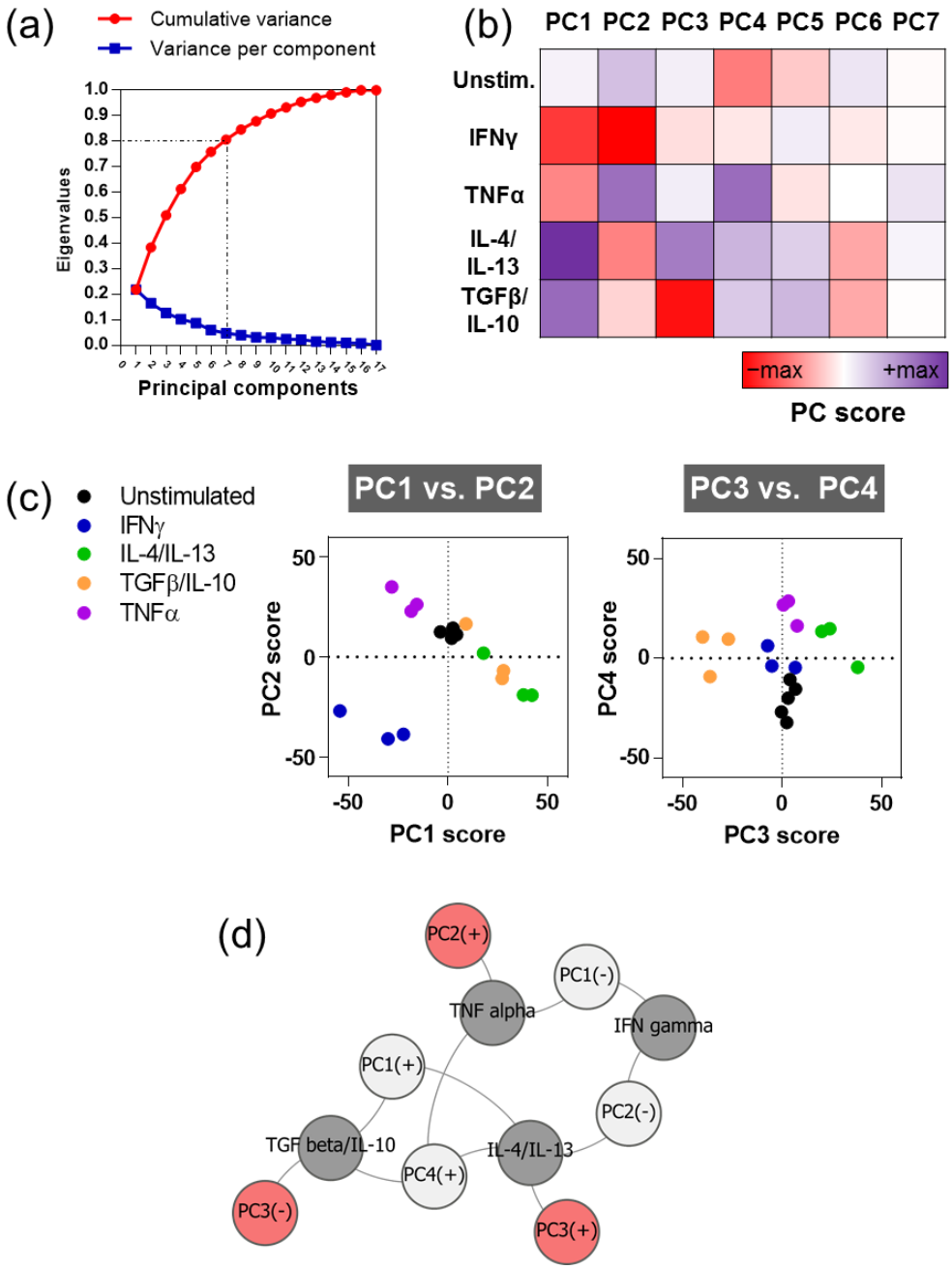

Figure 5.6: Exploring the stimulus-specificity of MDM transcriptional responses to cytokines using principal component analysis.

Principal component analysis (PCA) of gene expression data from MDMs stimulated with IFNγ, TNFα, IL-4 and IL-13 or TGFβ and IL-10. **(a)** Plot demonstrating the variance (determined by eigenvalues) attributable to each principal component (PC), autonomously (blue) or cumulatively (red). The dashed box shows selection of components which describe approximately 80% of the variance in the dataset, for which principal component scores (PC scores) for each MDM condition are shown in the matrix in **(b)**. Values shown are the median of at least three independent MDM transcriptomes for each condition. **(c)** PC score plots for PC1 and PC2, or PC3 and PC4. Each symbol represents a separate MDM transcriptome. **(d)** Network map of relationships of different PC directionss to stimulation conditions. PC directions which are uniquely associated with one stimulus are shown in red.

5.2.4 Identifying appropriate measurements of module expression and enrichment

I explored the transcriptional responses of MDMs to cytokines associated with particular polarised T cell responses and showed that these cytokines induced many gene expression changes in MDMs (**Figure 5.1**), which were associated with particular functional outcomes (**Figure 5.2–5.5**), including responses which were either shared between stimuli or were stimulus-specific (**Figure 5.6**). I then used these gene expression data sets to develop a pipeline for generating gene expression modules optimised for detecting stimulus-specific transcriptional responses, for subsequent use in detecting the effects of these stimuli in *in vivo* gene expression datasets. I aimed to derive modules of optimal specificity, which were powered to detect the specific activity of a particular stimulus, while also having adequate sensitivity to detect this activity in a potentially noisy *in vivo* setting. I also aimed to ensure that the modules contained enough genes to retain the advantages of using a gene list strategy (discussed in **section 5.1**).

In order to derive and optimise modules, I first identified an appropriate measurement of module expression in a gene expression dataset, as using such a measurement would be critical in assessing module specificity. Three measurements of central tendency of module gene list expression were considered for this purpose: the mean, the median and the geometric mean. These will respectively assume that the data in question is parametric, is non-parametric (which is likely for complex gene expression data), or that the different parameters contributing to the data may have different distributions (which is also likely, as expression of different genes may vary over different ranges).

For this exercise, I used a preliminary module in which high *a priori* confidence was held, due to the potent functional effects of the stimulus in question: an IFNγ module, made up of genes significantly ($P<0.05$) up-regulated by ≥twofold by IFNγ. The mean, median and geometric mean expression for this module were assessed in unstimulated MDMs and cytokine-stimulated MDMs, as a test group of gene expression datasets. All three measurements proved to be discriminatory with regard to differential modular expression: the IFNγ module was only highly expressed in IFNγ-stimulated MDMs (**Figure 5.7a–c**). There were no clear major differences between the three measurements in their quantitative or discriminatory capacities, as they produced similar overall expression patterns (**Figure 5.7a–c**). However, it was considered that

the geometric mean was the most appropriate measurement of central tendency due to the nature of the data, so this measurement was carried forward for further use.

Methods for assessing enrichment of modular expression, as quantified by geometric mean, were then tested, to establish a system for assigning "module enrichment scores" to different samples for comparative analyses. Firstly, enrichment with regard to the genome-wide gene expression level was measured, wherein the geometric mean of genome-wide expression was calculated and used as the denominator in a ratio for normalisation to produce module scores (**Figure 5.7d**). In this method, if the module enrichment score is >0, this indicates that the expression of the module is above the genome-wide geometric mean, as the scale used in these assessments is a $\log_2$ scale, wherein a ratio of 0 indicates equivalence and a ratio of 1 indicates a twofold difference. This assessment is suitable for measuring enrichment, as it can be assumed that the expression of a randomly selected set of genes would approximate to the genome-wide geometric mean; thus expression above this level for a module gene set shows that the expression of that module is non-random and enriched. It can also control for any variation in genome-wide gene expression between samples. In this dataset, this appeared to be an appropriate method for scoring enrichment, as IFNγ-stimulated MDMs had the highest enrichment scores of all MDMs tested (**Figure 5.7d**).

Although this is a powerful method for assessing enrichment, the most interesting and relevant differences biologically are likely to be those quantified in comparison to control samples. In these test datasets, the unstimulated MDMs were the appropriate control, and so a second set of module enrichment scores was calculated, wherein the denominator was the median of the measured module expression values (geometric means) for the control group of unstimulated MDMs (**Figure 5.7e**). This again appeared to be an appropriate method for scoring enrichment, as the highest scores produced were for IFNγ-stimulated MDMs (**Figure 5.7e**). It is also possible to perform statistical testing of module expression when control data are available, by comparison of module expression values between the group of interest and the control group. Therefore, in future assessments of module enrichment, I aimed to use normalisation to control data where it was available, as this is the most biologically relevant comparison. Where control data is not available, comparison with the genome-wide geometric mean, as described above, is an appropriate alternative.

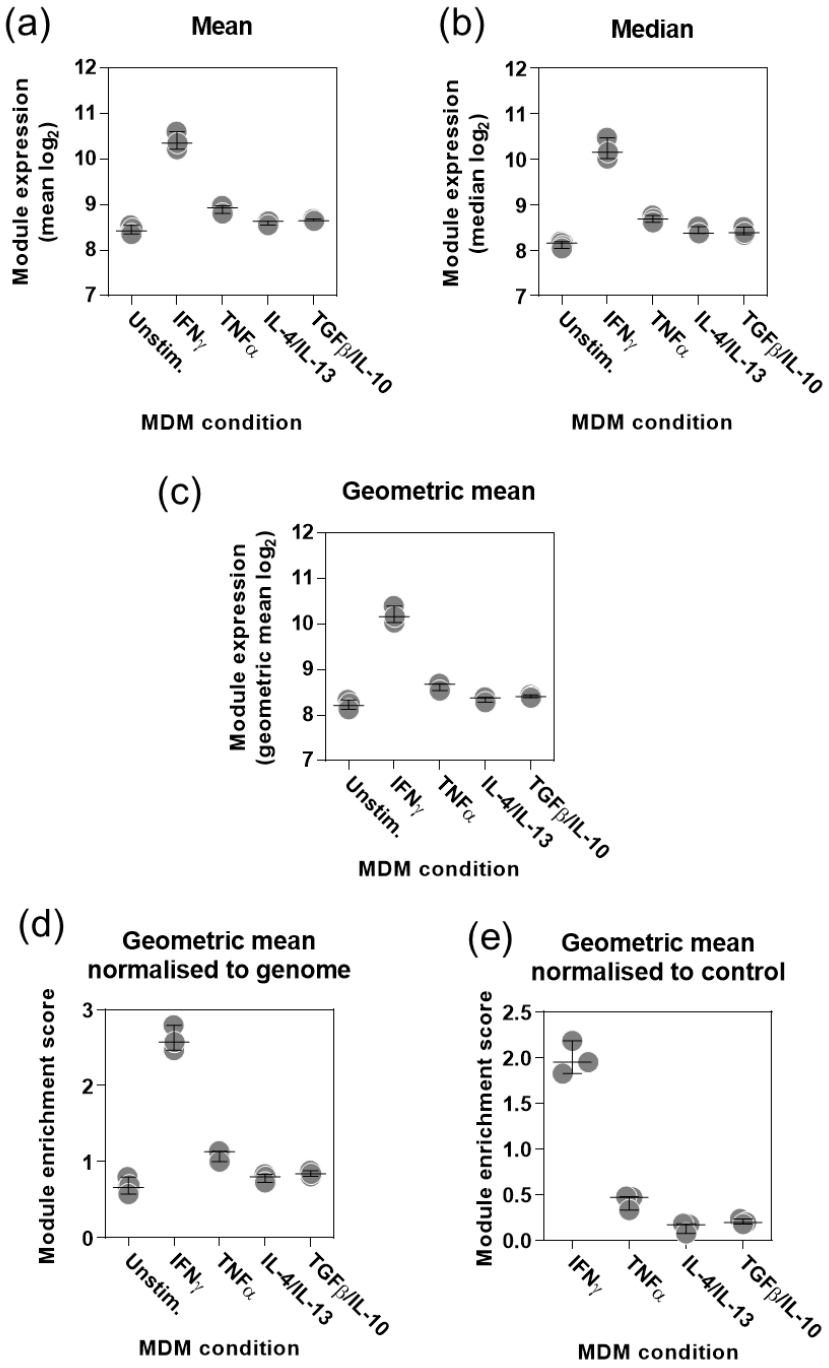

Figure 5.7: Methods of quantifying module expression and module enrichment.

To identify an appropriate measurement of module gene set expression, a test exercise was carried out. Expression of an IFNγ module was assessed in unstimulated and cytokine-stimulated MDMs. Three measures of central tendency were assessed: mean **(a)**, median **(b)**, and geometric mean **(c).** For all measurements, the IFNγ module was most highly expressed in IFNγ-stimulated MDMs. Geometric mean was selected as the most appropriate measurement. Using geometric mean module expression, two methods for quantifying module enrichment were assessed. **(d)** Enrichment scores were calculated as module expression normalised by a ratio to the geometric mean expression for the entire genome. **(e)** Enrichment scores were calculated as module expression normalised by a ratio to the median value for module expression in a control sample group: in this case, unstimulated MDMs. Each symbol shows a separate MDM transcriptome. Lines and error bars indicate median and range.

5.2.5 Developing modules from T cell subset-derived-cytokine-stimulated MDMs

After selecting appropriate methods for measuring module expression and enrichment, I then developed a pipeline for deriving optimally specific modules using the cytokine-stimulated MDM datasets discussed in sections **5.2.1–5.2.3**. The gene lists derived in the analysis presented in **Figure 5.1**, of genes significantly (P<0.05) up-regulated by ≥two-fold by each stimulus, were used as the initial modules, shown in **Table 5.1**. I aimed to ensure that these modules had adequate sensitivity for detecting the effects of these stimuli in potentially noisy *in vivo* settings, by selecting a twofold change cut-off and hence only including genes which are highly up-regulated by the cytokines.

I then went on to assess the specificity of these modules via two approaches: firstly identifying any cross-over in the module gene lists via Venn diagrams, and secondly measuring the module enrichment scores in all cytokine-stimulated MDMs, with the hypothesis that an optimally specific module should only be highly expressed in MDMs stimulated with the module-specific stimulus. These assessments are presented as matrices, wherein rows represent modules and columns represent MDM transcriptomes for the conditions indicated. The two module enrichment scores described in **section 5.2.5** and **Figure 5.7**, by either normalisation to the genome-wide geometric mean or the median control geometric mean, were used.

The specificity of this set of modules was not optimal (**Figure 5.8**). For example, high expression of the TNFα module was evident in IFNγ-stimulated MDMs and TGFβ/IL-10 stimulated MDMs (**Figure 5.8a**). A Venn diagram demonstrated that there was considerable cross-over between module gene lists (**Figure 5.8c**).

I hypothesised that further restricting the modules to genes up-regulated by ≥four-fold by each stimulus might improve specificity. The derivation of these modules is shown in **Table 5.2** and the specificity assessment (performed as for the twofold change modules) is shown in **Figure 5.9**. Some specificity issues were still evident with these modules, with cross-enrichment of modules observed in differential conditions. Additionally, some cross-over between the module gene lists was still identified by Venn diagram (**Figure 5.9c**).

I performed a final filtering step to further improve specificity, in which any gene which was up-regulated more than twofold by any other stimulus was removed from

the fourfold change gene lists (**Table 5.3**), to produce completely unique gene lists. Module specificity was further improved by this filter (**Figure 5.10**), evident in the minimal enrichment detected for all modules in MDMs not stimulated with the module-specific cytokine, and approximately eight-fold higher enrichment scores in the specifically stimulated MDMs in comparison to controls. These modules were employed for downstream analyses, and the pipeline used for their development was used to derive modules for other stimuli of interest (**sections 5.2.6–5.2.8**).

Stimulus	T-test, p<0.05 filter	2FC filter
IFNγ	1693	315
TNFα	1460	157
IL-4/IL-13	1435	190
TGFβ/IL-10	1084	161

Table 5.1: Development of T cell-subset-derived-cytokine modules – twofold change modules.

Numbers in each column represent the number of genes selected by that stage of filtering. 2FC, twofold change.

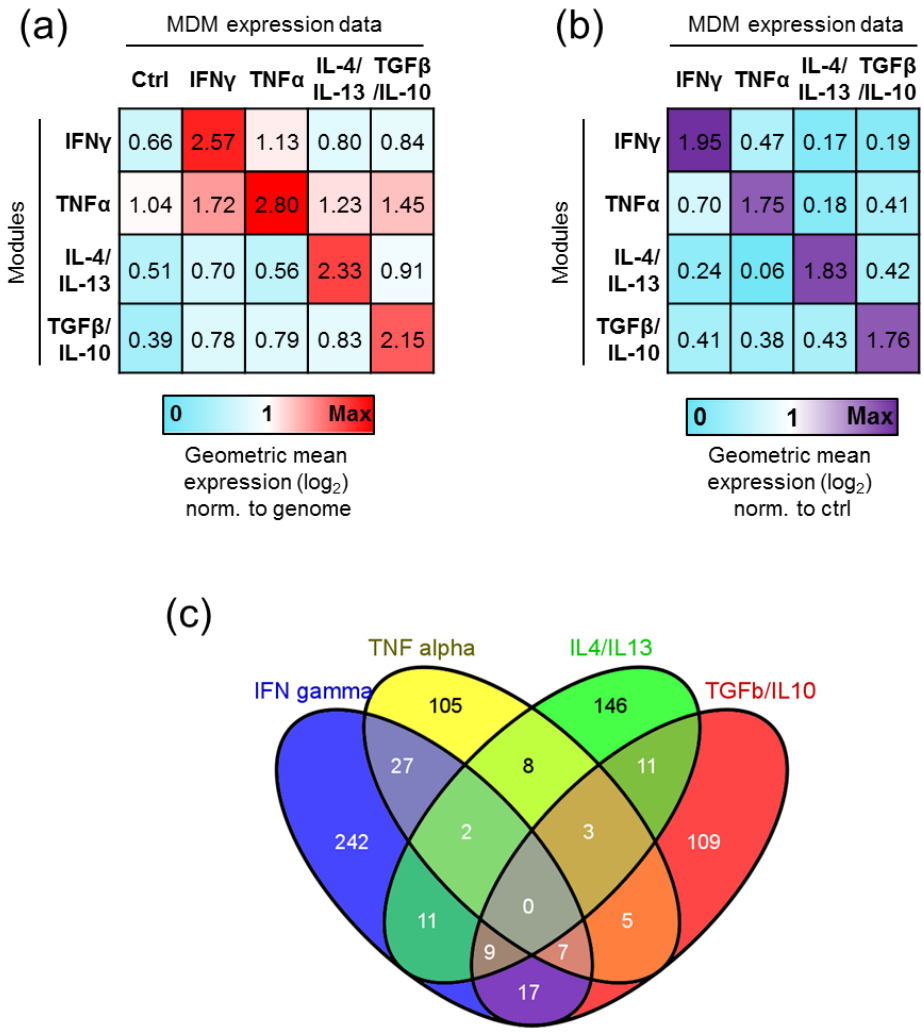

Figure 5.8: Assessing specificity of T cell-subset-derived-cytokine modules – twofold change modules.

Matrices are presented showing module enrichment scores in the MDM transcriptomes used for module derivation, as an assessment of module specificity. Modules are in rows and MDM transcriptomes are in columns. Ctrl indicates unstimulated MDMs. All values presented are the medians of module enrichment scores in at least three independent MDM datasets for each condition. **(a)** Matrix of module expression presented as the geometric mean of the expression values for the genes making up the module, normalised to the genome-wide geometric mean expression for the same sample. Max on the colour scale is the maximum value for this dataset. **(b)** Matrix of module expression presented as the geometric mean of the expression values for the genes making up the module, normalised to the same measure of modular expression in the control samples. Max on the colour scale is the maximum value for this dataset. **(c)** Venn diagram depicting the shared genes between the four module gene lists. Numbers represent the number of twofold change-induced genes shared between/unique to module gene lists.

Stimulus	T-test, p<0.05 filter	2FC filter	4FC filter
IFNγ	1693	315	93
TNFα	1460	157	34
IL-4/IL-13	1435	190	51
TGFβ/IL-10	1084	161	42

Table 5.2: Development of T cell-subset-derived-cytokine driven modules – fourfold change modules.

Numbers in each column represent the number of genes selected by that stage of filtering. 2FC, twofold change; 4FC, fourfold change.

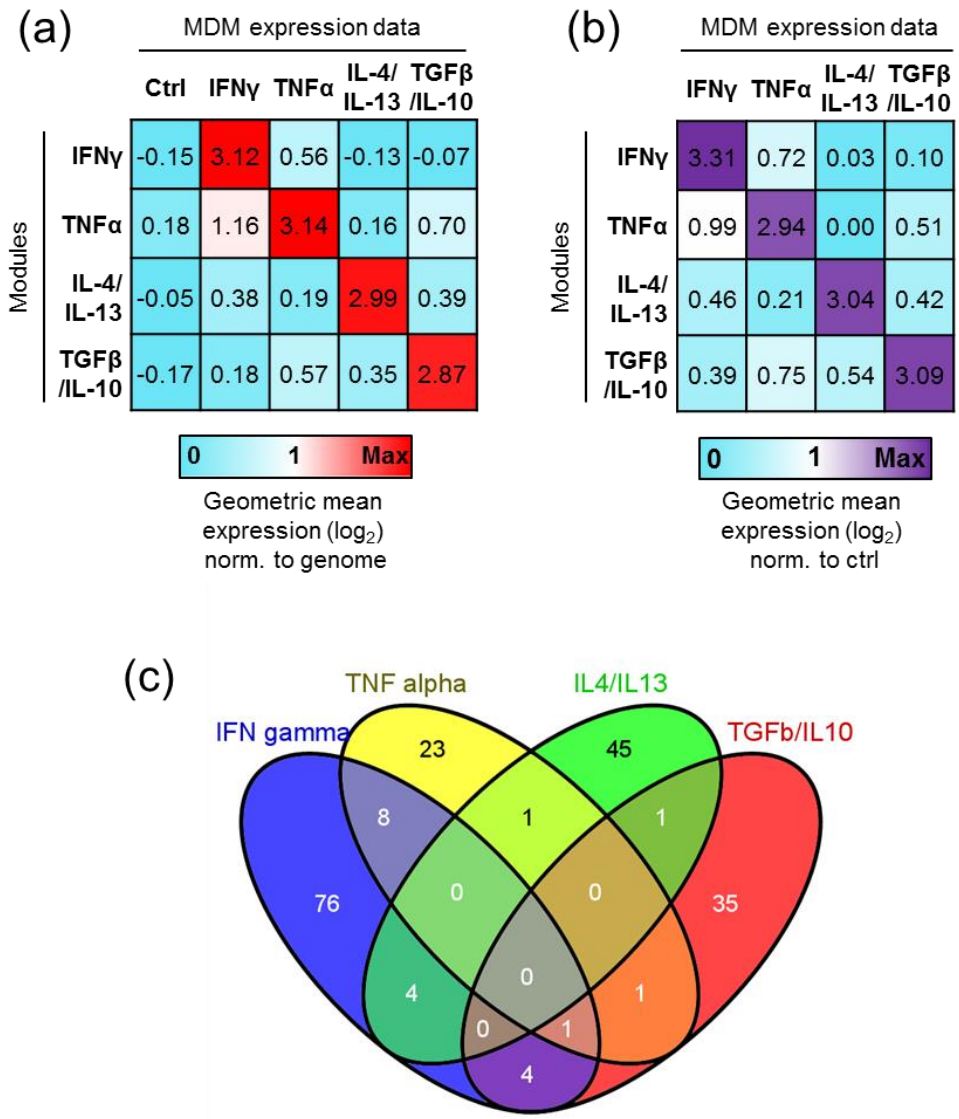

Figure 5.9: Assessing specificity of T cell-subset-derived-cytokine modules – fourfold change modules.

Matrices are presented showing module enrichment scores in the MDM transcriptomes used for module derivation, as an assessment of module specificity. Modules are in rows and MDM transcriptomes are in columns. Ctrl indicates unstimulated MDMs. All values presented are the medians of module enrichment scores in at least three independent MDM datasets for each condition. **(a)** Matrix of module expression presented as the geometric mean of the expression values for the genes making up the module, normalised to the genome-wide geometric mean expression for the same sample. Max on the colour scale is the maximum value for this dataset. **(b)** Matrix of module expression presented as the geometric mean of the expression values for the genes making up the module, normalised to the same measure of modular expression in the control samples. Max on the colour scale is the maximum value for this dataset. **(c)** Venn diagram depicting the shared genes between the four module gene lists. Numbers represent the number of twofold change-induced genes shared between/unique to module gene lists.

Stimulus	T-test, p<0.05 filter	2FC filter	4FC filter	Specificity filter
IFNγ	1693	315	93	65
TNFα	1460	157	34	16
IL-4/IL-13	1435	190	51	32
TGFβ/IL-10	1084	161	42	27

Table 5.3: Development of T cell-subset-derived-cytokine driven modules – specific fourfold change modules.

Numbers in each column represent the number of genes selected by that stage of filtering. The specificity filter represents the removal of any gene which features in the 2FC gene list for more than one condition. 2FC, twofold change; 4FC, fourfold change.

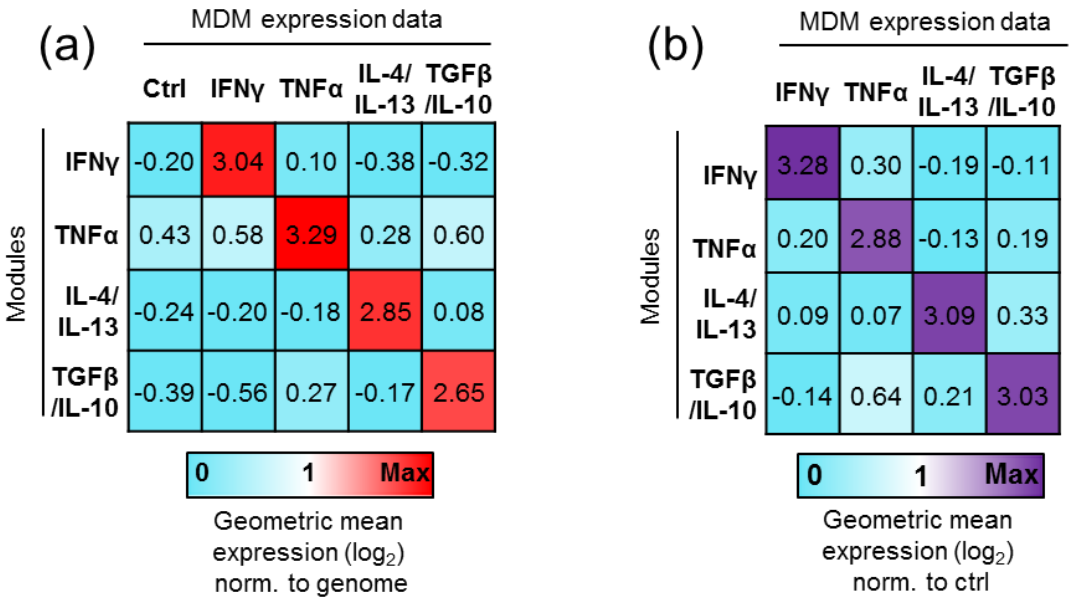

Figure 5.10: Assessing specificity of T cell-subset-derived-cytokine modules – unique fourfold change modules.

Matrices are presented showing module enrichment scores in the MDM transcriptomes used for module derivation, as an assessment of module specificity. Modules are in rows and MDM transcriptomes are in columns. Ctrl indicates unstimulated MDMs. All values presented are the medians of module enrichment scores in at least three independent MDM datasets for each condition. **(a)** Matrix of module expression presented as the geometric mean of the expression values for the genes making up the module, normalised to the genome-wide geometric mean expression for the same sample. Max on the colour scale is the maximum value for this dataset. **(b)** Matrix of module expression presented as the geometric mean of the expression values for the genes making up the module, normalised to the same measure of modular expression in the control samples. Max on the colour scale is the maximum value for this dataset.

5.2.6 Development of differential IFN pathway modules

Type I and type II IFNs induce complex programs of gene expression which share many features, but are known to be functionally distinct (Schneider et al., 2014). Recently there has been interest in the impacts that these differential functional effects might have on anti-mycobacterial immunity (Teles et al., 2013). I developed modules for measuring the specific activity of type I or type II IFNs using the pipeline developed in **section 5.2.5**. The gene expression dataset available for this purpose was derived from MDMs stimulated for 4 hours with either IFNβ (type I IFN), or IFNγ (type II IFN) (Tsang et al., 2009). Derivation of these modules is presented in **Table 5.4**. Although assessment of the crossover between the two-fold and four-fold change gene lists for both IFNs showed considerable overlap (**Figure 5.11**), an arguably adequate degree of specificity was achieved (**Figure 5.12**), wherein each IFN module was enriched by ≥twofold in its matched IFN-stimulated MDM dataset in comparison to the non-matched dataset.

As an additional quality control step, *post hoc* bioinformatic verification of module gene list function was carried out using InnateDB pathway analysis. This suggested that adequate specificity had been achieved, as each module gene list was highly enriched for its respective IFN signalling pathway (**Table 5.5**).

Stimulus	T-test, p<0.05 filter	2FC filter	4FC filter	Specificity filter
Type I IFN	3524	630	181	108
Type II IFN	1373	226	71	24

Table 5.4: Development of IFN pathway modules – specific fourfold change modules.

Numbers in each column represent the number of genes selected by that stage of filtering. The specificity filter represents the removal of any gene which features in the 2FC gene list for more than one condition. 2FC, twofold change; 4FC, fourfold change.

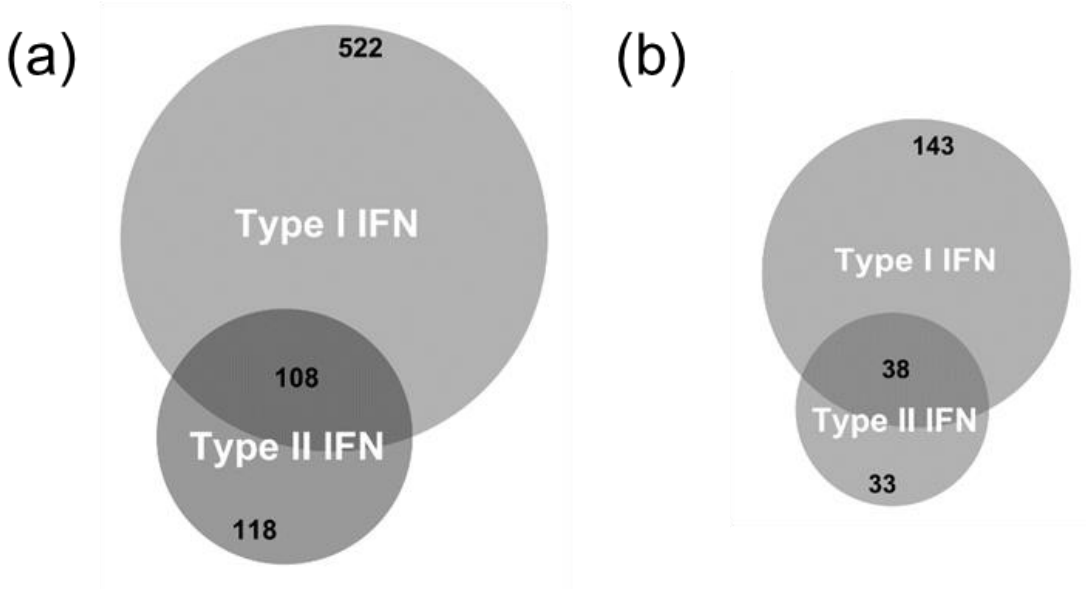

Figure 5.11: **Venn diagrams of cross-over between IFN-induced gene lists.**

Venn diagrams depicting shared genes between the IFN-induced gene lists. Numbers represent the number of genes shared between/unique to gene lists.
(a) Two-fold change gene lists. **(b)** Four-fold change gene lists.

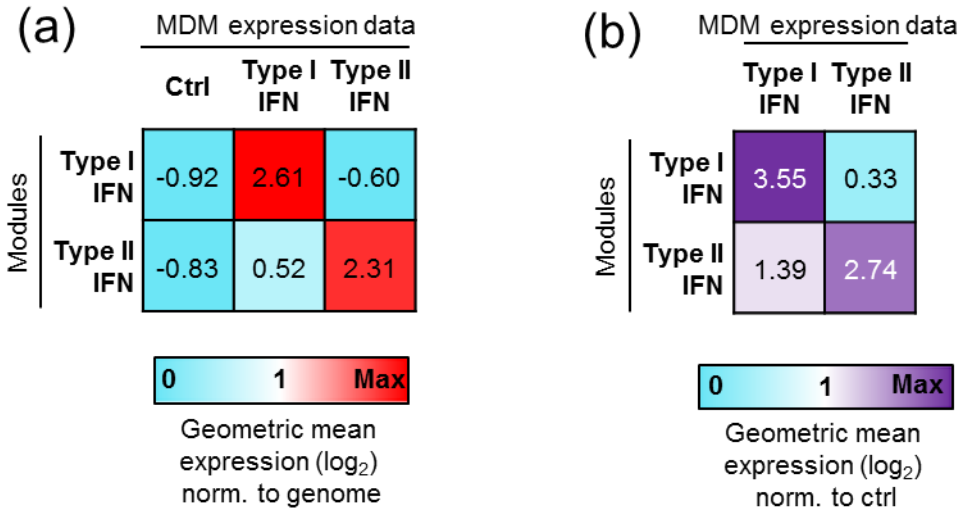

Figure 5.12: Assessing specificity of IFN pathway modules – specific fourfold change modules.

Matrices are presented showing module enrichment scores in the MDM transcriptomes used for module derivation, as an assessment of module specificity. Modules are in rows and MDM transcriptomes are in columns. Ctrl indicates unstimulated MDMs. All values presented are the medians of module enrichment scores in at least three independent MDM datasets for each condition. **(a)** Matrix of module expression presented as the geometric mean of the expression values for the genes making up the module, normalised to the genome-wide geometric mean expression for the same sample. Max on the colour scale is the maximum value for this dataset. **(b)** Matrix of module expression presented as the geometric mean of the expression values for the genes making up the module, normalised to the same measure of modular expression in the control samples. Max on the colour scale is the maximum value for this dataset.

Module	Pathway Name	Source Name	Pathway *P* value (corrected)
Type I IFN	**Interferon alpha/beta signaling**	REACTOME	1.90E-08
	Scavenging of Heme from Plasma	REACTOME	2.75E-06
	Nicotinate Nicotinamide metabolism	INOH	9.76E-04
Type II IFN	Chemokine signaling pathway	KEGG	2.70E-06
	Interferon gamma signaling	REACTOME	9.72E-06
	IL23-mediated signaling events	PID NCI	1.40E-04

Table 5.5: Bioinformatic verification of IFN pathway modules.

InnateDB pathway enrichment analysis (Breuer et al., 2013; http://www.innatedb.com) for module gene lists. Enrichment assessment was performed using a hypergeometric algorithm and filtered to pathways with a significance level of $P<0.05$ (Benjamini-Hochberg correction-adjusted). The three most highly enriched pathways, their sources and corrected *P* values for enrichment significance are shown for each module.

5.2.7 Development of IL-10 modules

Gene expression profiling had demonstrated a detectable but limited transcriptional response in MDMs to specific stimulation with IL-10 for 24 hours (**Chapter 4, section 4.2.3**). I developed a module from this dataset using a less stringent pipeline than the one described in **section 5.2.5**. A two-fold change filter was used, as few genes were up-regulated by more than four-fold by IL-10, and a specificity filtration step with comparisons to gene lists from other stimuli was not employed. This strategy was used in order to develop a module which was highly sensitive for detecting the subtle autonomous effects of IL-10, even if some specificity was compromised as a result. A module of 47 genes was derived (**Table 5.6**).

An alternative IL-10 module was also developed from an independent dataset: gene expression data from MDMs stimulated for 24 hours with an inflammatory stimulus (zymosan) in the presence of neutralising antibodies to IL-10 and the IL-10 receptor (i.e. an inflammatory scenario in which IL-10 activity is known to be deficient) (**Chapter 4, section 4.2.5**). In this case, the module gene list was generated by testing for significant gene expression differences between MDMs stimulated with zymosan and MDMs stimulated with zymosan in the presence of IL-10 neutralisation. A two-fold change filter was then applied, to select genes for which expression was decreased in IL-10 neutralisation, i.e. those which are usually positively regulated by IL-10. This yielded a module of 49 genes (**Table 5.6**). Comparison of this gene list with the directly-induced IL-10 module revealed some overlap (**Figure 5.13**), lending confidence to the hypothesis that these genes are regulated by IL-10.

Module gene list specificity was assessed by Venn diagram comparison with the T cell-subset-derived cytokine modules (excepting the TGFβ/IL-10 combined module, with which overlap would be expected). Both IL-10 modules had minimal overlap with these gene lists (**Figure 5.14a, b**). A formal assessment of specificity demonstrated that the IL-10 module was highly enriched in IL-10 stimulated MDMs, with a reasonably high degree of specificity, but that the zymosan/IL-10 neutralisation module was not enriched as highly or specifically (**Figure 5.14c, d**). I performed bioinformatic verification of these modules by oPOSSUM TFBS enrichment analysis (**Figure 5.15**). Significant enrichment of binding sites for STAT3, the downstream mediator of IL-10 signalling, was found in the IL-10 module gene list (Williams et al.,

2004; **Figure 5.15a**). STAT3 binding sites were also identified in the majority of genes in the zymosan/IL-10 neutralisation module, but this enrichment was not significant (**Figure 5.15b**).

Due to the low sensitivity and specificity of the zymosan/IL-10 neutralisation module in the initial set of analyses, I performed further evaluations of these modules. Enrichment scores for both modules were significantly higher in IL-10 stimulated MDMs than in MDMs stimulated with other cytokines (**Figure 5.16a, b**). Correlation and covariance of the two module scores were assessed across all cytokine-stimulated MDMs. They were found to strongly correlate (r^2=0.82) and have significant covariance (*P*<0.0001), but the zymosan/IL-10 neutralisation module scores were much lower for each sample (slope = 0.58; **Figure 5.16c**). This suggested that the zymosan/IL-10 neutralisation module could specifically detect the effect of IL-10, but that it was less sensitive than the IL-10 module.

I hypothesised that the zymosan/IL-10 neutralisation module might be more sensitive to detect the effects of IL-10 in the context of an inflammatory stimulus, as it was generated from such a condition. Correlation and covariance of module scores were assessed between the two modules in innate immune-stimulated MDMs, and were found to strongly correlate (r^2=0.93) and have significant covariance (*P*<0.0001), with a slope of close to 1 (**Figure 5.16d**). Both modules were most highly enriched in MDMs stimulated with Mtb, which has been shown to be most potent inducer of IL-10 of the four stimuli tested (Tomlinson et al., 2014; **Figure 5.16d**). A formal specificity assessment of modular enrichment in innate immune-stimulated MDMs also demonstrated that the zymosan/IL-10 neutralisation module was highly enriched in these datasets, and in particular in Mtb-stimulated MDMs (**Figure 5.17**). These analyses suggest that the zymosan/IL-10 neutralisation module is most sensitive for detecting the effect of IL-10 in an inflammatory context. Therefore, it may have utility in assessing IL-10 function in inflammatory *in vivo* samples.

Stimulus	T-test, p<0.05 filter	2FC filter
IL-10	274	47
Zymosan + IL-10 neutralisation	374	49

Table 5.6: Development of IL-10 modules – twofold change modules.

Numbers in each column represent the number of genes selected by that stage of filtering. 2FC, twofold change.

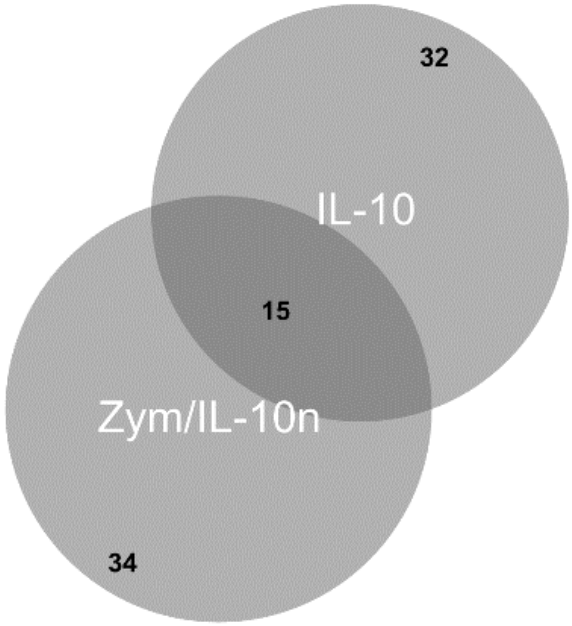

Figure 5.13: Venn diagram of cross-over between IL-10 module gene lists.

Venn diagrams depicting shared genes between the IL-10 module gene lists. Numbers represent the numbers of genes shared between/unique to gene lists. Zym/IL-10n; zymosan + IL-10 neutralisation

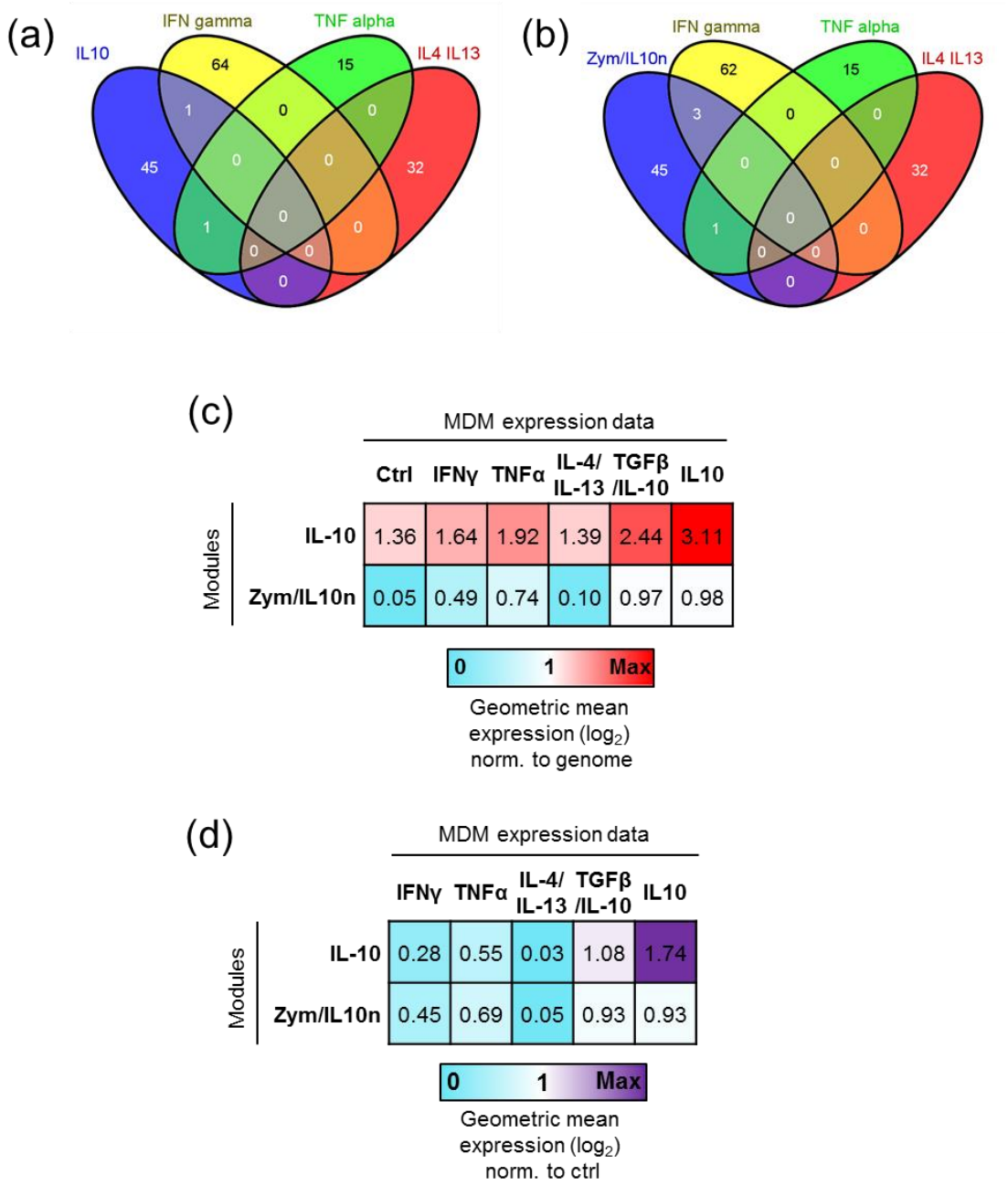

Figure 5.14: Assessing specificity of IL-10 modules – twofold change modules.

(a, b) Venn diagrams depicting shared genes between the IL-10 module gene lists and other cytokine-induced modules; **(a)** IL-10; **(b)** zymosan + IL-10 neutralisation. Numbers represent the numbers of genes shared between/unique to gene lists. **(c)** Matrix of module expression presented as the geometric mean of the expression values for the genes making up the module, normalised to the genome-wide geometric mean expression for the same sample. Max on the colour scale is the maximum value for this dataset. **(d)** Matrix of module expression presented as the geometric mean of the expression values for the genes making up the module, normalised to the same measure of modular expression in the control samples. Max on the colour scale is the maximum value for this dataset.

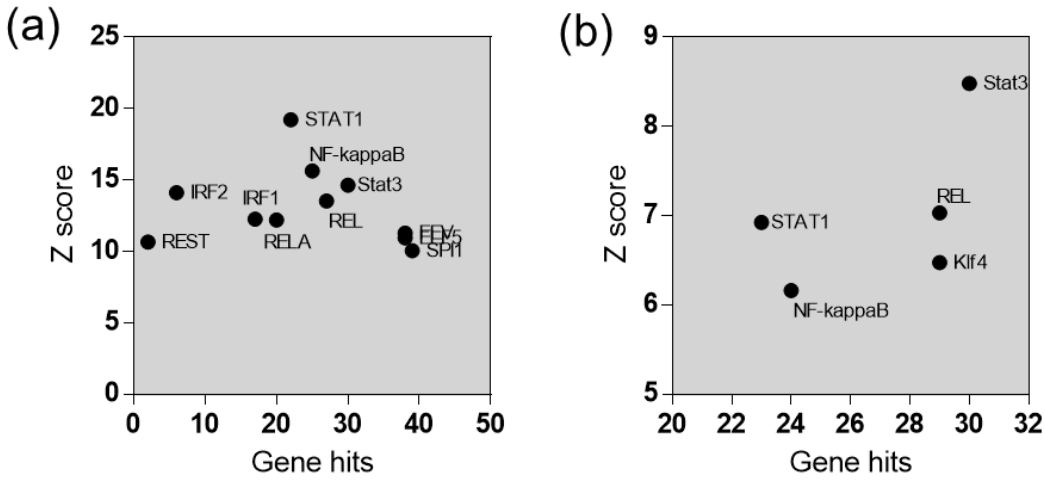

Figure 5.15: Bioinformatic verification of IL-10 modules by TFBS enrichment analysis.

Module gene lists were subjected to TFBS enrichment analysis using oPOSSUM-3 (Kwon et al., 2012; http://opossum.cisreg.ca). Significance of the frequency of TFBS occurrence in gene lists compared to background was assessed by the Z-score statistic, with a score greater than 10 used as a significance threshold. Results of this analysis are shown for the IL-10 module **(a)** and the zymosan/IL-10 neutralisation module **(b)**. All significantly enriched TFBSs in the sequence region 5000bp upstream/downstream of each gene are shown. The X axis lists the number of genes enriched for a TFBS, and the Y axis displays significance by Z score.

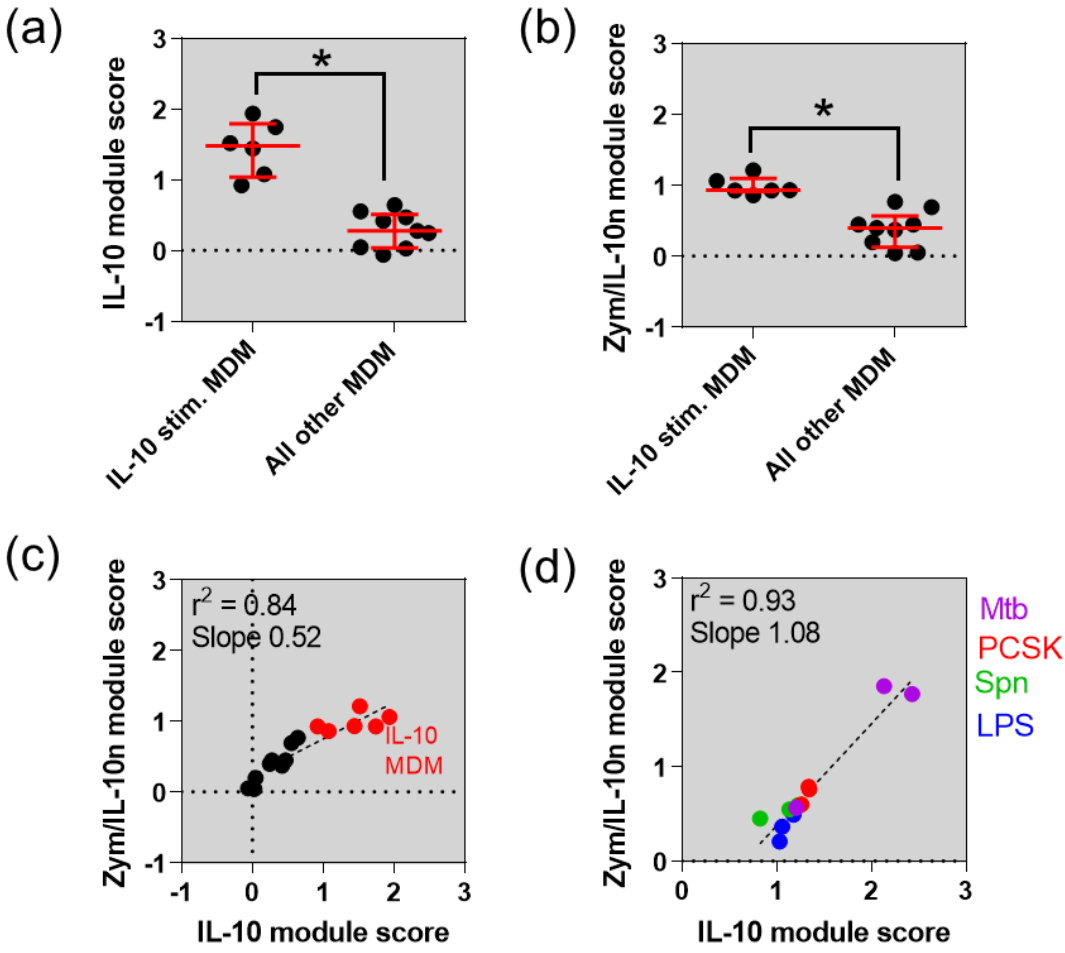

Figure 5.16: Further investigations of specificity and comparability of IL-10 modules.

(a) Comparison of the geometric mean of module expression in the dataset of interest normalised to the geometric mean of module expression in control MDMs (module score) of the IL-10 module in IL-10 stimulated MDMs versus all other cytokine-stimulated MDMs. * represents $P<0.05$, Mann-Whitney test. **(b)** Comparison of the zymosan/IL-10 neutralisation module scores in IL-10 stimulated MDMs versus all other cytokine-stimulated MDMs. * represents $P<0.05$, Mann-Whitney test. **(c)** Comparison of IL-10 module scores versus zymosan + IL-10 neutralisation module scores in IL-10 stimulated MDMs (red symbols) and other cytokine-stimulated MDMs (black). **(d)** Comparison of IL-10 module scores versus zymosan + IL-10 neutralisation module scores in the indicated innate immune stimulated MDMs. Dashed lines represent linear regressions and descriptive statistics for correlation (r^2) and covariance (slope) are presented within the plots. All slopes presented were significantly non-zero ($P<0.05$). Fitting and statistical analyses were performed using GraphPad Prism 6.0.

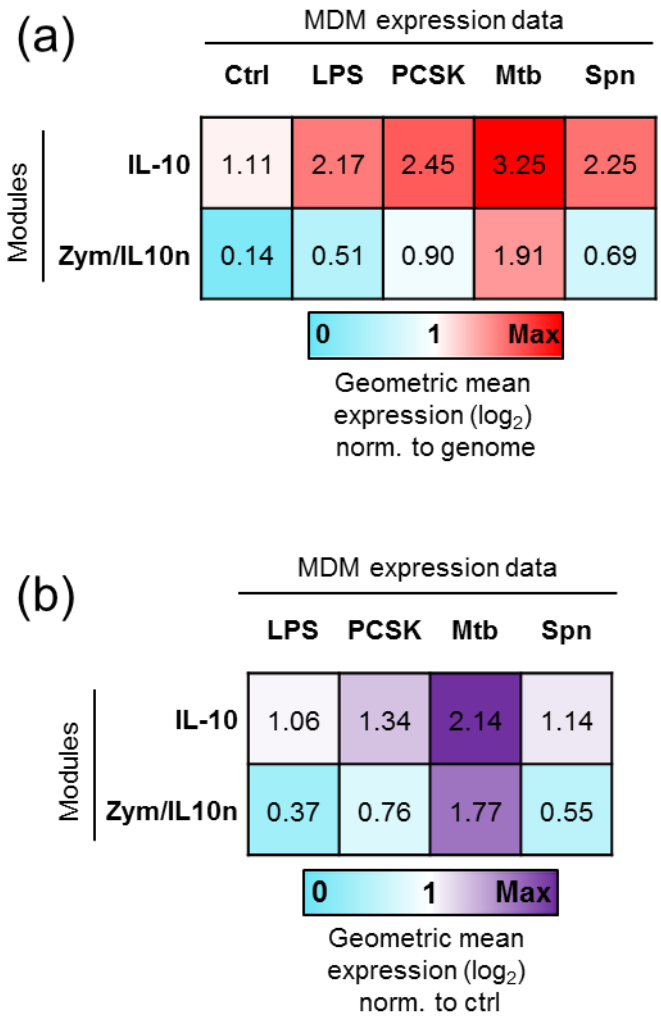

Figure 5.17: Assessing enrichment of IL-10 modules in innate immune-stimulated MDMs.

Matrices are presented showing module enrichment scores in the MDM transcriptomes used for module derivation, as an assessment of module specificity. Modules are in rows and MDM transcriptomes are in columns. Ctrl indicates unstimulated MDMs. All values presented are the medians of module enrichment scores in at least three independent MDM datasets for each condition. **(a)** Matrix of module expression presented as the geometric mean of the expression values for the genes making up the module, normalised to the genome-wide geometric mean expression for the same sample. Max on the colour scale is the maximum value for this dataset. **(b)** Matrix of module expression presented as the geometric mean of the expression values for the genes making up the module, normalised to the same measure of modular expression in the control samples. Max on the colour scale is the maximum value for this dataset.

5.2.8 Development of innate immune stimulus-driven modules

Using the module development pipeline outlined in **section 5.2.5**, I developed modules specific to the effects of a selection of innate immune stimuli, with the aim of being able to assess specific stimulation of inflammatory pathways within *in vivo* gene expression samples. These were derived from transcriptomic datasets generated in previous investigations, in which MDMs were stimulated for 4 hours with different innate immune stimuli or pathogens: LPS, a TLR4 ligand; PCSK, a TLR2 ligand; Mtb; or *S. pneumoniae* (Spn) (Noursadeghi et al., 2009; Tomlinson et al., In press, 2014). The derivation pipeline for these modules is shown in **Table 5.7**.

Cross-over between the two-fold-change and four-fold-change induced gene lists for these stimuli was assessed by Venn diagram and was found to be considerable (**Figure 5.18**). Specificity assessments demonstrated that these modules were most highly expressed in their matched MDM datasets (**Figure 5.19**). However, some lack of specificity was demonstrated: for example, expression of the PCSK module was enriched in LPS-stimulated MDMs, and cross-enrichment of the PCSK and Mtb modules was observed in their respective MDM datasets. It is probable that these stimuli activate conserved innate signalling pathways, and so the differential transcriptomes of innate stimuli may be fairly limited. Further improvements in specificity may, therefore, be difficult to achieve. With regard to the cross-enrichment of Mtb and PCSK modules, it should be noted that Mtb is known to stimulate TLR-2 (Means et al., 1999; Reiling et al., 2002), and this cross-enrichment may be expected.

Stimulus	T-test, p<0.05 filter	2FC filter	4FC filter	Specificity filter
LPS	3341	556	121	39
PCSK	3158	628	108	12
Mtb	2645	292	103	19
Spn	3140	403	67	19

Table 5.7: Development of innate immune stimulus-driven modules – specific fourfold change modules.

Numbers in each column represent the number of genes selected by that stage of filtering. The specificity filter represents the removal of any gene which features in the 2FC gene list for more than one condition. 2FC, twofold change; 4FC, fourfold change.

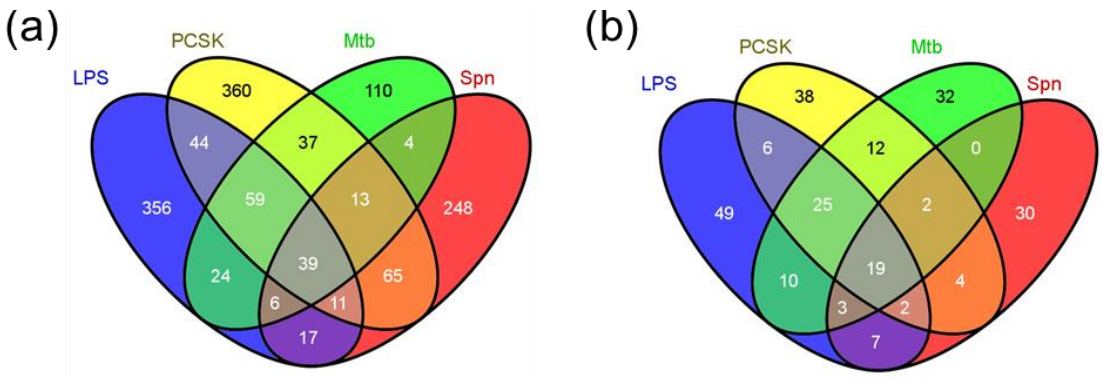

Figure 5.18: Venn diagrams of cross-over between innate immune stimulus-induced gene lists.

Venn diagrams depicting shared genes between the innate immune stimulus-induced gene lists. Numbers represent the numbers of genes shared between/unique to gene lists. **(a)** Two-fold change gene lists. **(b)** Four-fold change gene lists.

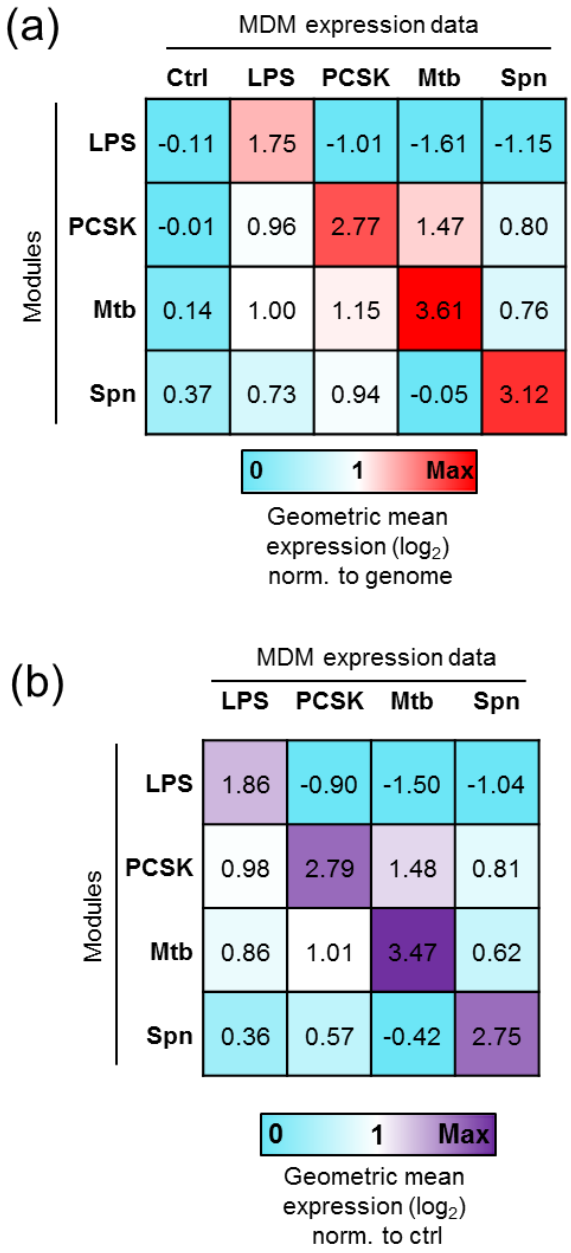

Figure 5.19: Assessing specificity of innate immune stimulus-driven modules – specific fourfold change modules.

Matrices are presented showing module enrichment scores in the MDM transcriptomes used for module derivation, as an assessment of module specificity. Modules are in rows and MDM transcriptomes are in columns. Ctrl indicates unstimulated MDMs. All values presented are the medians of module enrichment scores in at least three independent MDM datasets for each condition. **(a)** Matrix of module expression presented as the geometric mean of the expression values for the genes making up the module, normalised to the genome-wide geometric mean expression for the same sample. Max on the colour scale is the maximum value for this dataset. **(b)** Matrix of module expression presented as the geometric mean of the expression values for the genes making up the module, normalised to the same measure of modular expression in the control samples. Max on the colour scale is the maximum value for this dataset.

5.2.9 Assessing modular enrichment in *in vivo* gene expression datasets

As an initial test exercise to evaluate the ability of the modules developed in **sections 5.2.5–5.2.8** to detect immune biological activities in *in vivo* samples, I analysed module enrichment scores in gene expression profiles from tuberculin skin test (TST) biopsies obtained from healthy volunteers (Tomlinson et al., 2011). As these gene expression profiles had already been investigated via bioinformatic and comparative methods, this meant that the function of these modules could be tested in a context where some *a prior* hypotheses existed. For example, enrichment for IFNγ or type II IFN signalling was expected, as was differential modular enrichment between positive and negative TST biopsies, or between biopsies collected at 6 hours and 48 hours post-TST.

I calculated module enrichment scores using the module geometric mean expression normalised to the genome-wide geometric mean expression, as an appropriate control dataset for normalisation was not available in this dataset. Each set of modules developed proved to be quantitative and discriminatory in this dataset (**Figure 5.20**). The IFNγ module was the most highly expressed in the 48 hour positive TSTs in comparison to the other cytokine modules, but was not highly expressed in the 6 hour TST biopsies (**Figure 5.20a**), which is consistent with findings from bioinformatic assessments of this data (Tomlinson et al., 2011). This was also confirmed when using the specific IFN modules, wherein the type II IFN module was more highly enriched in 48 hour TST biopsies than the type I IFN module (**Figure 5.20b**). The differential enrichment measured for the IFN modules also suggested that they were able to discriminate between these two closely related immune responses. The IL-10 modules were also enriched in the TST samples, consistent with recognized IL-10 responses in anti-mycobacterial immune responses (**Figure 5.20c**; Redford et al., 2011). Additionally, the two different IL-10 modules were enriched to a similar degree in this dataset, supporting the hypothesis that the zymosan/IL-10 neutralisation module is able to detect IL-10 activity in the context of inflammation, such as in the TST. Finally, the highest enrichment for the innate immune stimulus modules was for the Mtb-specific or PCSK (TLR-2)-specific modules, suggesting that specific anti-mycobacterial innate responses could be measured in the TST using these modules.

Many published methods exist for quantifying modular enrichment in gene expression datasets (Ackermann and Strimmer, 2009). These include simple methods such as the one used here, in which a measure of central tendency of the expression

values of the module is used as a single measurement of module expression. More complex methods are also used, such as the GSEA algorithm, which has been widely used for previous modular analysis exercises (Mootha et al., 2003; Subramanian et al., 2005). This method is designed to detect differences in module enrichment between two groups of gene expression samples, as it involves ranking all genes in a dataset in order of their difference between the compared two groups. I tested GSEA as an alternative method of module enrichment scoring in the TST dataset, using the T cell subset cytokine-driven modules (**Figure 5.21**). GSEA produces a normalised enrichment score (NES) for each module, and a recommended statistic used to assess the significance of the NES, which is the false detection rate (FDR) q-value.

The quantitative power of GSEA was assessed by comparison of the 48 hour TST samples with the 6 hour TST samples (**Figure 5.21a**, **b).** This detected enrichment of the IFNγ and TNFα modules in the positive TST samples (**Figure 5.21a**), but assigned a marginally higher NES to the TNFα module than the IFNγ module, although the geometric mean scoring method used shown the IFNγ module to be expressed at a considerably higher (>two-fold) level (**Figure 5.20a**). The IL-4/IL-13 and TGFβ/IL-10 modules were not scored as significantly enriched in this comparison (**Figure 5.21a**), although the previous assessment had indicated some enrichment of the latter in the same samples (**Figure 5.20a**). No modules were assessed as enriched in the negative TST samples (**Figure 5.21b**), although again, some had been assessed as enriched using the alternative method (**Figure 5.20a**). These observations suggested that GSEA might be less sensitive and quantitative for assessment of modular enrichment than using a geometric mean-derived module score.

The discriminatory power of GSEA was assessed by comparisons between the 48 hour positive TSTs and the 48 hour negative TSTs. Significant enrichment of the TNFα module in the 48 hour positive TST in comparison to the 48 hour negative TST was identified (**Figure 5.21c**), suggesting that this method might have some utility for discriminating differential enrichment between groups of samples.

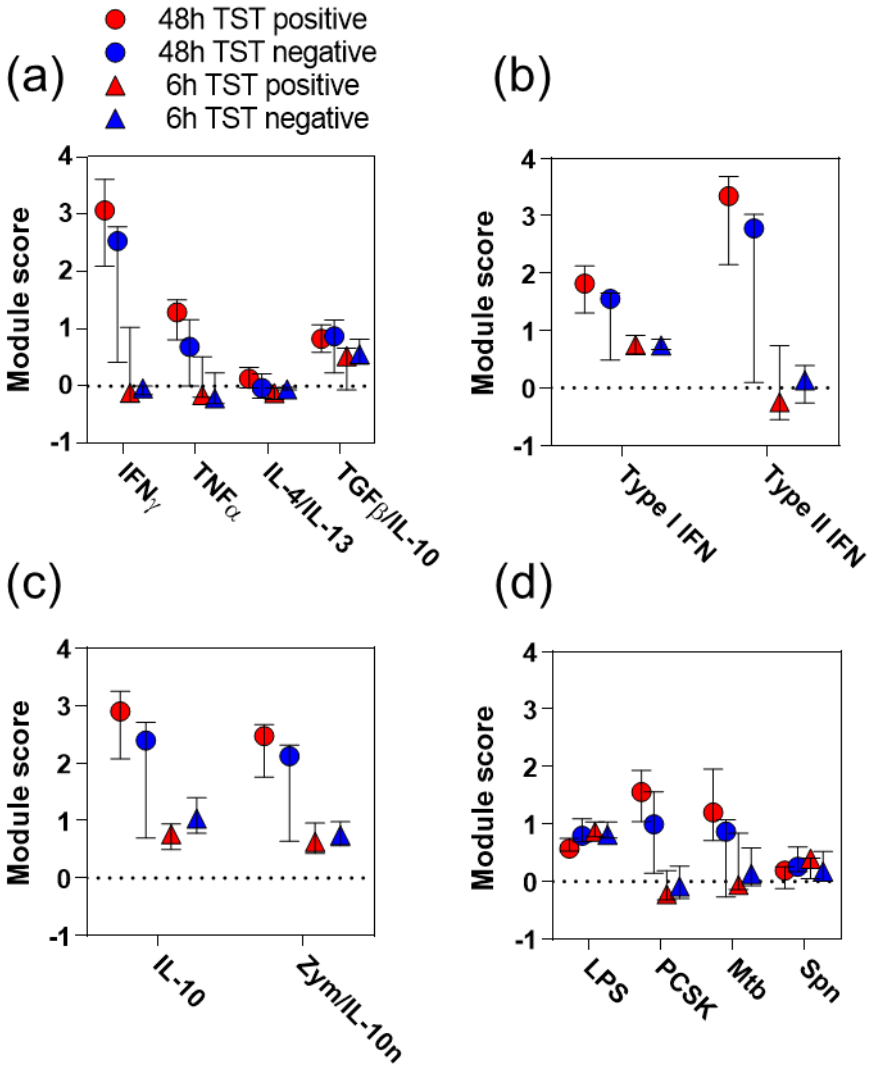

Figure 5.20: Testing module enrichment in *in vivo* gene expression datasets.

A test dataset of *in vivo* gene expression profiles, generated from TST biopsies obtained from healthy volunteers, was used to evaluate module enrichment in *in vivo* samples. Module enrichment scores were calculated as module expression normalised by a ratio to the geometric mean expression for the entire genome. **(a)** Module enrichment score in the indicated TST groups for T cell subset-derived cytokine modules. **(b)** Module enrichment score in the indicated TST groups for specific IFN modules. **(c)** Module enrichment score in the indicated TST groups for IL-10 modules. **(d)** Module enrichment score in the indicated TST groups for innate immune stimulus modules. Symbols and error bars represent median −/+ range for at least 4 samples in each group.

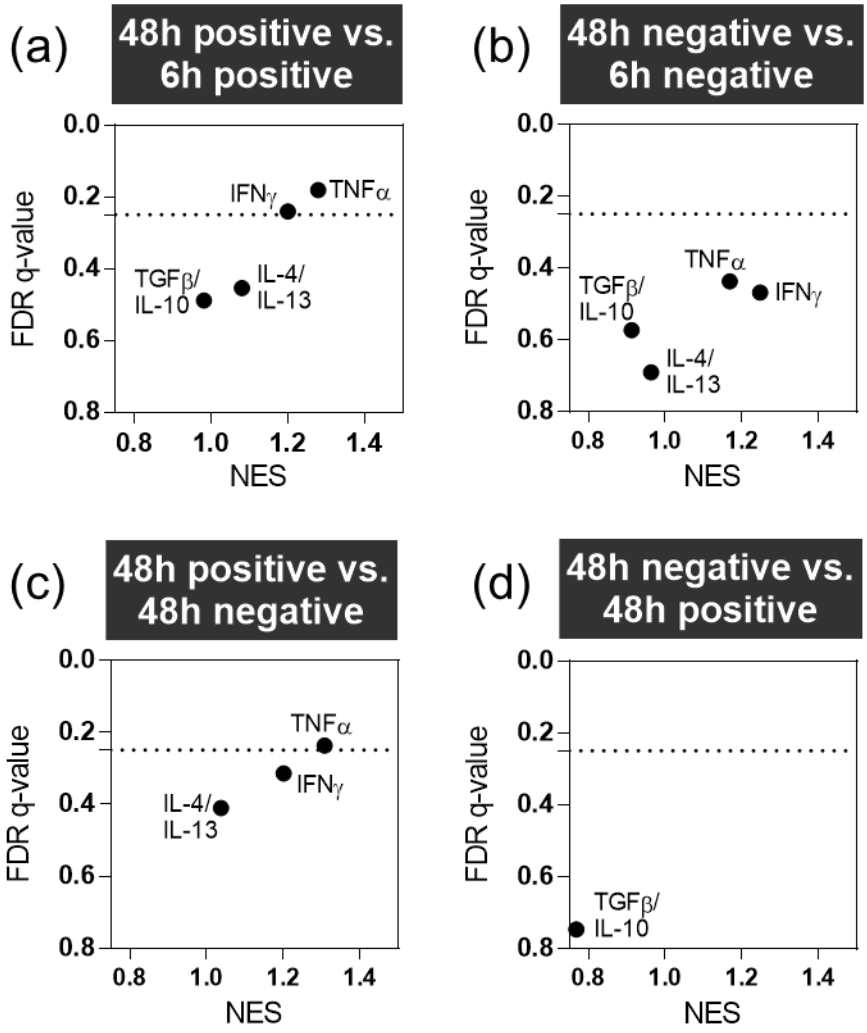

Figure 5.21: Using gene set enrichment analysis to quantitate modular expression and enrichment in *in vivo* gene expression samples.

Modular enrichment analysis between groups of TST biopsies performed using the gene set enrichment analysis (GSEA) algorithm. The normalised enrichment scores (NES) are shown on the X axes and measurement of statistical significance (FDR q-value) is shown on the Y axis. The dashed line indicates the threshold of statistical significance recommended for use for this algorithm. **(a)** Comparison of 48 hour positive biopsies with 6h positive biopsies. (b**)** Comparison of 48 hour negative biopsies with 6h negative biopsies. **(c, d)** Comparison of 48 hour positive biopsies with 48h negative biopsies; three modules were assessed as enriched in the positive group **(c)** and one module was assessed as enriched in the negative group **(d)**.

5.3 Chapter discussion

5.3.1 Insights into macrophage plasticity from transcriptional profiling

Macrophage plasticity, which is thought to be primarily controlled at the transcriptional level, is central to the function of these key sentinel cells of the immune system. I aimed to use gene expression profiling of human MDMs to understand this plasticity. I then aimed to utilise the multidimensional power of this data for evaluating immune responses *in vivo*, by deriving gene expression modules from MDMs stimulated with different factors of interest for use in assessing *in vivo* transcriptomic datasets.

Human MDMs were shown to express cell-surface receptors for cytokines associated with differentially polarised T cell responses (**Figure 5.1a**), for IFNγ, TNFα, IL-4, IL-13, TGFβ and IL-10. Stimulation of MDMs with these cytokines induced hundreds of gene expression changes (**Figure 5.1b**). This illustrated the potent role of transcriptional reprogramming in cytokine-driven macrophage activation, and confirmed that human macrophages can be functionally modulated by polarised T cell responses beyond the Th1 and CMI paradigm, as previously suggested (Mosser and Edwards, 2008). One potential caveat of this approach is that using cytokines in combination (IL-4 and IL-13, and TGFβ and IL-10) means that the unique effects of these cytokines cannot be teased out; however, while not using an absolutely reductionist approach means that some direct mechanistic insight may be lost, this method may better simulate polarised inflammatory responses *in vivo* where multiple cytokines are likely to be acting in tandem.

TFBS analysis of the cytokine-regulated gene lists revealed enrichment for sets of transcription factors which may be downstream of signalling by these cytokines. This included enrichment for some factors previously shown to be associated with these stimuli, such as NFκB in TNFα up-regulated genes (Aggarwal, 2003; **Figure 5.3a**). Strikingly, many of the canonical transcription factors which are activated by these cytokines were not shown to be enriched in the up-regulated gene lists. For example, STAT1 TFBS were not enriched in the IFNγ-induced genes (Platanias, 2005), STAT6 was not enriched in the IL-4-induced genes (Takeda et al., 1996) and SMADs were not enriched in the TGFβ-induced genes (Derynck and Feng, 1997; **Figure 5.2a, 5.4a, 5.5a**). However, as these gene expression profiles represent the MDM transcriptome

after 24 hours after cytokine stimulation, it is possible that the primary transcriptional responses mediated by these signature transcription factors were no longer evident.

Pathway enrichment analysis of cytokine-regulated gene lists provided insight into the functional outcomes of cytokine signalling in macrophages. Some specific effects of the cytokines were confirmed, such as IFN signalling pathway enrichment in the IFNγ-stimulated MDMs (**Figure 5.2b**). Novel pathways downstream of these cytokines were also identified. For example, TGFβ and IL-10 induced expression of genes enriched for integrin pathways, vascular wall interactions, fibrin formation and hypoxia-inducible factor 1α (HIF1α)-regulated gene expression. This included expression of the potent angiogenic factor vascular endothelial growth factor A (*VEGFA*; Nagy et al., 2007; **Figure 5.5d**). This might reflect the role of macrophages in structural aspects of inflammatory resolution induced by these regulatory cytokines. Further experiments are required to evaluate whether these *in silico* analyses are associated with significant functional effects.

Common themes of macrophage transcriptional responses to cytokines were identified in the bioinformatic assessment of these gene lists, such as chemokine activity and integrin interactions (**Figure 5.2–5.5**). The multidimensional relationships between the gene expression programmes were evaluated using the exploratory statistical technique of PCA. This demonstrated that the data was highly multi-dimensional, and that many patterns of variation in gene expression were shared between the different stimulation conditions (**Figure 5.6**). This analysis alludes to the multi-dimensional spectral nature of macrophage activation programmes, as described in previous reports (Xue et al., 2014). Further analysis of the PCA results, focussing in particular on the genes which are most associated with various PC deviations, may assist in identifying novel functional hubs of macrophage activation.

5.3.2 Development of gene expression modules for analysis of microarray data

I aimed to utilize macrophage transcriptional heterogeneity for evaluation of immune responses *in vivo*, by developing gene expression modules from MDM gene expression datasets. The data-driven module generation method has provided valuable insights in a number of previous studies (Berry et al., 2010; Li et al., 2014; Obermoser et al., 2013; Xue et al., 2014), but as it is inherently reliant on the structure of the input data, the range of modules generated may not include those relating to pathways of interest if they are not variably expressed in the datasets used. This then

precludes assessment of those pathways in downstream analyses. As a major aim of the exercise in constructing modules was the ability to assess pathways and phenotypes of interest in a range of potential downstream contexts, I chose to use the hypothesis-driven method of module generation, in which the function that the user wishes to assess is defined *a priori*.

Module gene lists for this purpose can be derived from bioinformatic databases, published data or publicly accessible array data repositories, but in this context I chose to derive these modules using in-house-generated rather than independent datasets. This was to maximise confidence that the baseline cellular phenotype in the datasets was consistent, so that any differential effects seen were specifically due to the stimulation conditions used rather than any extraneous contextual differences. This does not preclude using published datasets to derive modules for comparative and verification purposes, which may in fact add value to such an exercise and can be used for validation. As this is a supervised method, there is a considerable degree of user determination in setting parameters for extracting a gene list from a dataset, pertaining to statistical or fold-change thresholds, correlation analyses and specificity filters. Consensus for a method of deriving such a module has not yet emerged (Bild and Febbo, 2005).

I first evaluated how module expression should be quantified in a dataset of interest, and how enrichment of this expression should be measured for comparisons to other datasets. Three measurements of central tendency of modular gene list expression values were tested: mean, median and geometric mean. Each provided broadly similar approximations of module expression (**Figure 5.7a–c**). Although selection of one above the other may therefore be arbitrary, geometric mean was felt to provide the most accurate measurement of central tendency in terms of the nature of the data, so this was used for further assessments. Two strategies for quantifying enrichment of expression were then tested: using either the geometric mean of the genome-wide gene expression or the module expression in a control sample as a denominator for producing an enrichment score (**Figure 5.7d, e**). Both methods produced discriminatory measurements of enrichment. However, the latter strategy has the advantage of allowing statistical testing of modular enrichment, i.e. in comparison to control data. This illustrates the importance of identifying or obtaining appropriate control datasets for such analyses, as it eliminates the inherent assumptions present in

the genome-wide normalisation method with regards to the baseline expression of a module.

I then used the gene expression profiles of MDMs stimulated with different T cell subset-derived cytokines to develop a pipeline for module generation. Firstly, significant gene expression differences from unstimulated MDMs were identified by t-tests with a Welch approximation. As an FDR algorithm was not used, it may be suggested that high rate of false positive identification will occur. However, as the subsequent steps in the pipeline involve applying fold-change filters to select for gene expression changes which are within a biologically plausible range of interest, any false positives (which are unlikely to exceed these thresholds if they are background noise) should be eliminated.

Two-fold change and four-fold change filters were applied to these gene lists to derive modules (**Table 5.1**, **5.2**) which were then subjected to tests of specificity (**Figure 5.8, 5.9**). Although these modules were highly sensitive in detecting the effects of the stimulus of interest (suggesting that the t-test and fold-change approach used was competent for identifying the effects of these stimuli), their specificity was poor, as modular enrichment could be detected in some non-stimulus-specific contexts. The fact that non-specificity becomes an issue is not surprising when the PCA of the source data is considered (**Figure 5.6)**, as the macrophage transcriptional responses to cytokines clearly share many overlapping features.

I therefore applied an additional filter to improve specificity, in which any gene up-regulated by more than two-fold by any of the other cytokines tested was eliminated from the four-fold change gene lists (**Table 5.3**). This improved module specificity (**Figure 5.10**), and so this pipeline was used to develop further modules for specific IFN pathways and innate immune stimuli. Although this is an arguably rigorous strategy to select the highly specific effects of a stimulus, to construct a stimulus-specific module, it is possible that there may still be confounders present. For example, genes which are just below the two-fold threshold of induction by one stimulus will not be filtered out of other gene lists, and thus may contribute to some residual non-specificity. However, as gene expression measurements are essentially continuous variables, which vary in multiple contexts, developing completely stimulus-specific modules of sufficient gene numbers for usage may not be possible. Overall, there is a trade-off to be made between developing highly stimulus-specific modules, and developing modules which are sensitive to detect activation of a pathway of interest. Aiming to be

entirely reductionist, and eliminating any gene from a module which is potentially regulated by another stimulus, may prevent valuable insights being made into inherently noisy biological systems *in vivo.* As long as modules are adequately tested and validated, and used appropriately in conjunction with other analysis methods, then low-level risk of non-specificity such as described above, may be acceptable.

Modules for detecting the function of IL-10 were derived using a less stringent pipeline than the other cytokine modules, using a two-fold change threshold and no specificity filter. The autonomous effects of IL-10 in up-regulating gene expression appear to be subtle, perhaps reflecting its immunomodulatory rather than immunostimulatory function. As such, IL-10 induced insufficient numbers of genes by more than four-fold to use the initial strategy. To maximise confidence using this less stringent approach, two IL-10 modules were developed from different gene expression datasets in parallel, and their specificity to detect the activity of IL-10 was extensively validated (**Figure 5.14, Figure 5.16**), which suggested that they would still have reasonable utility in this regard.

5.3.3 Measuring enrichment of gene expression modules in gene expression profiles from *in vivo* samples

Lastly, I validated whether the modules developed could detect enrichment of the immune response pathways of interest in *in vivo* samples, using a previously published dataset of TST biopsies (Tomlinson et al., 2011). This analysis suggested that the modules were quantitative and discriminatory in detecting the effects of the stimuli of interest in an *in vivo* setting. The enrichment results produced corroborated published analyses of this data, and also provided evidence for activity of factors such as IFNγ, TNFα, IL-10 and type I IFN at the site of inflammation in *in vivo* human anti-mycobacterial immune responses.

These enrichment scores were based on measuring the geometric mean of module expression. For comparative purposes, I tested the GSEA algorithm as a more complex method of assessing modular enrichment. This produced different results to a certain extent, which seemed to be less quantitative and sensitive for detecting module expression than the geometric mean-based analyses (**Figure 5.21**). Some discriminatory capacity was demonstrated in comparing highly expressed modules in similar samples (**Figure 5.21c**). An inherent limitation of the GSEA algorithm is that it does not produce a range of module enrichment scores for a group of tested samples,

but alternatively produces an average enrichment value for the entire group. This means that the heterogeneity of a given dataset cannot be assessed (Chaussabel and Baldwin, 2014). It also only allows comparative assessments of enrichment between two samples, which may also limit its utility.

Overall, using the geometric mean of the module gene list to measure expression and enrichment appeared to be a sufficiently sensitive, discriminatory and quantitative strategy, and may be especially so when appropriate comparative control data is available, wherein statistical testing can be performed (as discussed above in **section 5.3.2**). GSEA may have some utility as an adjunctive strategy for comparing expression of modules between highly similar groups of samples. Reviews of module enrichment assessment strategies have suggested that the most appropriate analysis method to use depends on the distribution of the dataset to be assessed (Alavi-Majd et al., 2014), or that use of multiple methods to widely explore datasets and confirm enrichment may be most appropriate (Glazko and Emmert-Streib, 2009). Thus, using both geometric mean expression and GSEA may maximise confidence in the results of modular analysis exercises.

Chapter 6. Results 4. Modulation of anti-mycobacterial cell-mediated immunity by HIV-1 *in vivo* assessed in a human challenge model

6.1 Background

6.1.1 Cell-mediated immunity, HIV-1 and tuberculosis

CMI is the process by which T cells and macrophages functionally collaborate to kill and control intracellular pathogens (Kaufmann, 1999; Wing and Remington, 1977). HIV-1 impacts on many functions of the immune system, which is evident in the depletion of the circulating $CD4^+$ T cell pool, chronic immune activation and compromise of the gut-associated lymphoid tissues (Levy, 2009), among other phenomena (reviewed in **Introduction section 1.3.6**). CMI in particular may be at risk of modulation by HIV-1, as the virus directly infects both $CD4^+$ T cells (Spear et al., 1990) and macrophages (Noursadeghi et al., 2006b).

Mtb, which also replicates within macrophages, is the prototypic example of a pathogen that is thought to be controlled by CMI (Dannenberg, 1989), and the human TB granuloma can be described as a mature focus of CMI, wherein macrophages and T cells are spatially and functionally coordinated in order to exert this control (Ulrichs and Kaufmann, 2006). The major functional axes of CMI, such as IFNγ, IL-12 and STAT1 signalling, are known from human genetic studies to be essential for control of mycobacterial infections (Altare et al., 1998a; Dorman and Holland, 1998; Dupuis et al., 2001; Newport et al., 1996). Recent work in non-human primates has shown that host/pathogen interactions in individual granulomata are critical in determining the course of TB disease (Lin et al., 2014), indicating the importance of an effective localised CMI response in Mtb containment.

The effects of HIV-1 on CMI may therefore have major consequences for immune control of Mtb. *In vivo*, HIV-1 co-infection has profound effects on TB infection; it is associated with substantial increases in the incidence and mortality of active TB (Corbett et al., 2006), and with differences in disease presentation such as disseminated infections (Schutz et al., 2010) and immune reconstitution inflammatory syndromes (IRIS; Lawn et al., 2008). $CD4^+$ T cell depletion by HIV-1 is assumed to contribute to these changes in TB natural history (Geldmacher et al., 2012). However,

TB risk is increased in all HIV-1$^+$ patients including those without substantial CD4$^+$ T cell loss (Gupta et al., 2012; Sonnenberg et al., 2005), and so other HIV-1-associated immune dysfunction may also contribute. Investigating how HIV-1 modulates anti-mycobacterial CMI *in vivo* may aid our understanding of TB pathogenesis in HIV-1/TB co-infection.

6.1.2 Using the tuberculin skin test as an *in vivo* challenge model to study CMI in HIV infection

I sought to describe the effects of HIV-1 on CMI responses to mycobacteria *in vivo*. Previous studies of active TB *in vivo* have identified phenotypes in the peripheral blood (Antonelli et al., 2010; Berry et al., 2010), which has provided insight into the systemic immune response, but does not characterise the function of CMI at the site of inflammation. Others have explored samples obtained from the site of disease (Matthews et al., 2012; Mwandumba et al., 2008); this latter approach affords a valuable opportunity to study CMI *in situ*, but might be prone to confounding by time of sampling and disease heterogeneity. To study CMI at the site of inflammation *in vivo* using a controlled approach, I employed the tuberculin skin test (TST) as a standardised challenge model, which as a DTH reaction is a classic *in vivo* model of anti-mycobacterial CMI (Scheynius et al., 1982).

The TST is performed via an intradermal injection of tuberculin, also known as purified protein derivative (PPD), which is a sterilized precipitated filtrate of Mtb cultures (Magnusson and Bentzon, 1958). This elicits a localised inflammatory reaction, manifest as erythema and induration, over 24–48 hours in mycobacterial antigen-sensitized individuals. HIV-1 infection is known to be associated with increased incidence of TST anergy, i.e. clinical TST non-responsiveness as measured by induration (Markowitz et al., 1993), including in individuals who are epidemiologically highly likely to have been exposed to mycobacteria (Rangaka et al., 2007). TST anergy has been shown to correlate with HIV-1 disease progression (Graham et al., 1992), although some reports suggest that compromised skin DTH in HIV-1 infection may not correlate with disease markers (Okulicz et al., 2012).

The TST has previously been used to investigate CMI *in situ* via histological methods. This demonstrated a cellular infiltrate composed of CD4$^+$ T cells, CD8$^+$ T cells and APCs (Poulter et al., 1982; Scheynius et al., 1982), showed the presence of cytokines at the inflammatory site (Chu et al., 1992; Fullmer et al., 1987), and outlined

the contribution of different APC subsets to the reaction (Bond et al., 2012). The effects of HIV-1 have also previously been investigated using TST histology, in studies showing that DC recruitment to the TST is correlated to the magnitude of T cell recruitment in HIV-1^{+} individuals (Liang et al., 2013), and that the make-up of cellular infiltrates in TSTs in these individuals may be altered compared to HIV-1 negative (HIV-1^{-}) individuals (Sarrazin et al., 2009).

I aimed to use the TST as a challenge model to understand the effects of HIV-1 on anti-mycobacterial CMI *in vivo* with molecular resolution, by genome-wide transcriptional profiling of RNA collected from TST biopsies. This approach was previously validated in healthy individuals, in which TST transcriptional profiling was used to distinguish molecular signatures of polarised T cell and innate immune responses in the positive TST. Furthermore, this method was used to demonstrate immune responses in TST negative (TST^{-}) individuals, which were present but quantitatively less than in TST positive (TST^{+}) individuals – demonstrating that the transcriptomic approach added value, and may be more sensitive than clinical and histological assessments (Tomlinson et al., 2011). It also demonstrated that CMI responses in this setting showed no major systematic confounding by ethnicity (Tomlinson et al., 2011). I have now used TST gene expression profiling to characterise anti-mycobacterial CMI at the site of inflammation in patients with active TB and HIV-1 co-infection, and have identified diverse ways in which HIV-1 dysregulates this immune response *in vivo*.

6.2 Study outline

Patients with active TB, with or without HIV-1 co-infection, were recruited from clinical sites in London (UK) and Cape Town (South Africa) within the first month of TB chemotherapy. This patient cohort and time point was chosen in order to minimise inter-subject variability in mycobacterial exposure, as patients without active TB may have latent or undiagnosed TB, particularly in a high transmission setting in Cape Town, and distinguishing these groups clinically may not be possible. HIV-1 status was confirmed by routine clinical testing. Microbiological TB diagnosis was confirmed by smear, culture or GeneXpert MTB/RIF in >90% of enrolled patients, with the remainder of TB diagnoses being made on a clinical basis (see **Appendix II** for case by case clinical details). The study design and sample collection protocol is outlined in **Figure 6.1(a)**, and inclusion and exclusion criteria are shown in **Table 6.1**.

TSTs were performed by intradermal injection of 2U PPD into the proximal third of the volar aspect of the forearm. A subset of patients received saline injections as a control cohort. TSTs were assessed at 48 hours and two 3mm punch skin biopsies were collected from the marked injection site (**Figure 6.1b**). The biopsies were collected into either RNAlater reagent for RNA isolation, or 4% neutral buffered formalin for adjunctive histological analysis. A positive TST was defined clinically as an induration of ≥10mm at 48 hours, which is indicated to be an appropriate cut-off for this cohort (Cobelens et al., 2006). All TSTs, TST assessments and biopsies were performed by experienced TB clinical research staff. Blood samples for clinical measurements, PBMC, RNA and DNA were also collected from all individuals before TSTs were performed, as outlined in **Figure 6.1(a)**. A time-point of 48 hours was chosen for assessments, as in the previous proof-of-concept study, both innate and adaptive components of the immune response were evident at this time-point in both TST^+ and TST^- individuals, and differences between groups were also evident. Thus, using this time-point should allow assessment of the overall CMI response in the different groups of interest.

The study was approved by the research ethics committees of all sites and institutions involved, and informed written consent was obtained from all participants.

Inclusion criteria	Exclusion criteria
Active TB confirmed by microbiological and/or clinical diagnosis	Neoplastic disease
Within the first 4 weeks of anti-TB therapy	AIDS defining disease other than tuberculosis or KSHV infection
> 16 years of age	Hepatitis B/C co-infection
	Immunomodulatory therapy (e.g. interferon)
	Immunization within preceding 2 weeks
	Existing paradoxical reaction to anti-tuberculosis treatment
	Previous keloid formation

Table 6.1: Inclusion and exclusion criteria.

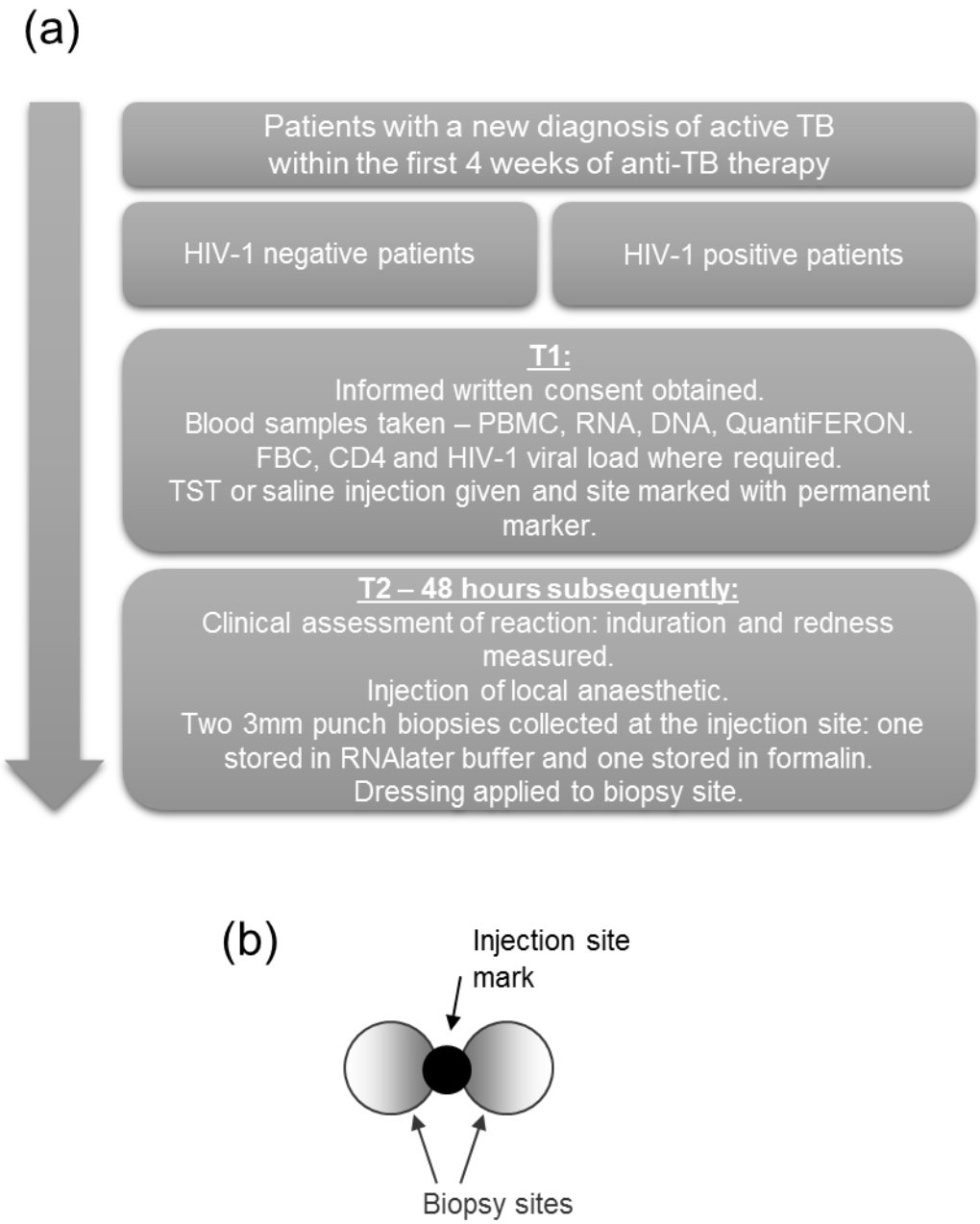

Figure 6.1: TST human challenge model study design.

(a) **Flowchart outlining the study design.** (b) **Diagram demonstrating collection of skin biopsies; the injection site was marked with permanent marker, and two biopsies were collected directly adjacent to this mark, of which one was used for expression profiling and one for complementary histological assessments.**

6.3 Cohort description

Characteristics of the recruited cohort are shown in **Table 6.2**. Fifty patients with active TB were recruited. Forty-two received TSTs and eight received control saline injections (see **Appendix II** for case-by-case demographic and clinical information table).

HIV-1$^-$ patients were recruited from Cape Town and London. The Cape Town cohort were predominantly black African and had pulmonary TB, while the London cohort were a mix of ethnicities and had extra-pulmonary disease. This may reflect the distinct epidemiological settings of the two groups: a high transmission setting with predominantly primary infection in Cape Town (Verver et al., 2004), and a low transmission setting with predominantly reactivation of latent disease in London (Kruijshaar and Abubakar, 2009). The Cape Town cohort included two patients with MDR TB. All HIV-1$^-$ patients were TST$^+$, and median induration did not differ between London and Cape Town cohorts (**Table 6.2**). The London and Cape Town HIV-1$^-$ cohorts were combined as a single group for all subsequent analyses.

All HIV-1$^+$ patients were recruited in Cape Town. In comparison to the equivalent HIV-1$^-$ Cape Town cohort, this group of patients included more females and had a higher incidence of extra-pulmonary disease, as might be expected for a HIV-1$^+$ South African cohort (Abdool Karim et al., 2009; Schutz et al., 2010). Consistent with previous reports, HIV-1 infection was associated with a higher incidence of clinically anergic TSTs (**Table 6.2**; Markowitz et al., 1993; Rangaka et al., 2007)**.** HIV-1$^+$ patients were divided into three groups for subsequent analyses: those who were TST$^-$ (anergic), TST$^+$, or classified as undergoing an unmasking IRIS, which was defined in this instance as presentation with active TB within 2–8 weeks of commencing ARVs, consistent with published case definitions of this condition (Haddow et al., 2009; Meintjes et al., 2008a). All patients in the IRIS group were TST$^+$. Of note, these patients had some of the greatest induration reactions of all HIV-1$^+$ TST$^+$ patients.

The TST$^-$ HIV-1$^+$ group of patients had a lower median CD4$^+$ count than TST$^+$ HIV-1$^+$ patients (28 vs. 214; **Table 6.2**). More TST$^+$ patients were on ARVs than TST$^-$ patients (55.56% vs. 35.71%; **Table 6.2**), and median length of ARV use was also higher (123 weeks vs. 0.7 weeks; **Table 6.2**). I specifically evaluated the correlation

between HIV-1 disease markers and TST induration. Within the HIV-1$^+$ cohort, induration was significantly but weakly positively correlated with CD4$^+$ count (**Figure 6.2a**), although the CD4$^+$ count ranges in TST$^+$ and TST$^-$ patients overlapped (**Table 6.2**), suggesting that there is not a direct linear relationship between these variables. HIV-1 viral loads, where available, did not correlate with TST induration (**Figure 6.2b**). These findings are consistent with previous reports, in demonstrating that HIV-1 seropositivity is associated with a high incidence of TST anergy, and that although this does correlate with CD4$^+$ count, anergy is still observed among patients with CD4$^+$ counts ≥200 CD4$^+$ cells mm^{-3}, and positive TSTs are observed among patients with CD4$^+$ counts ≤200 CD4$^+$ cells mm^{-3} (Markowitz et al., 1993; Selwyn et al., 1992).

The group of patients who received saline control injections was made up of three HIV-1$^-$ patients and five HIV-1$^+$ patients. The characteristics of this group were comparable to the groups which received TSTs (**Table 6.2**).

To assess TB antigen reactivity directly in T cells, IFNγ release assays (IGRAs) were used, in which peripheral blood mononuclear cells are mixed with TB-specific antigens and IFNγ release is measured. The QuantiFERON-TB Gold In-Tube test was used in this instance. This test uses the Mtb antigens ESAT-6, CFP-10 and TB7.7, which are mixed with whole blood *ex vivo*. IFNγ release is measured after 24 hours by ELISA, and compared to baseline IFNγ levels, and release induced by a positive control mitogen, to determine whether the test is positive, negative or indeterminate. QuantiFERON tests were performed on all patients recruited from sites in Cape Town. HIV-1$^+$ individuals had a high incidence of negative or indeterminate QuantiFERON results, despite being Mtb antigen-exposed as a result of having active TB (**Figure 6.2c**). Positive tests were more frequent in groups with higher CD4$^+$ counts when patients were stratified as such (**Figure 6.2d**) as previously reported (Leidl et al., 2010).

TST and IGRA responses were compared by correlating induration with TB antigen-elicited IFNγ release, and weak positive correlations were observed for both HIV-1$^-$ and HIV-1$^+$ groups (**Figure 6.2e**). Some TST$^+$ individuals had negative or indeterminate QuantiFERON results, and vice versa, particularly in the HIV-1$^+$ group; this discordance is consistent with previous reports (Luetkemeyer et al., 2007; Rangaka et al., 2007).

In addition to the five groups of patients recruited in this cohort, subsequent analyses also made comparisons with gene expression profiles from TSTs obtained

from healthy individuals in a previous study (Tomlinson et al., 2011). The definitions of all groups which were analysed are presented in **Table 6.3**.

Characteristics	HIV-1 negative			HIV-1 positive				Saline controls
	All	Cape Town	London	All	TST negative (anergic)	TST positive (non-IRIS)	TST positive (IRIS)	(3 HIV-1 negative, 5 HIV-1 positive)
n	16	9	7	26	14	9	3	8
Age (years)	38 (25–71)	35 (27–66)	44 (25–71)	37.5 (19–64)	36.5 (26–58)	40 (23–64)	37 (19–50)	42 (29–54)
Sex								
Male (%)	62.50	66.67	57.14	38.46	50.00	33.33	0.00	62.50
Female (%)	37.50	33.33	42.86	61.54	50.00	66.67	100.00	37.50
Ethnicity								
White (%)	12.50	11.11	14.29	0.00	0.00	0.00	0.00	0.00
Black (%)	62.50	88.89	28.57	96.15	92.86	100.00	100.00	75.00
Coloured (%)	0.00	0.00	0.00	3.85	7.14	0.00	0.00	25.00
Asian (%)	25.00	0.00	57.14	0.00	0.00	0.00	0.00	0.00
Site of TB disease								
Pulmonary (%)	56.25	100.00	0.00	84.62	71.43	100.00	100.00	87.50
Extra-pulmonary (%)	43.75	0.00	100.00	15.38	28.57	0.00	0.00	12.50
MDR TB (%)	12.50	22.22	0.00	0.00	0.00	0.00	0.00	0.00
Time on TB treatment when recruited (days)	11.5 (1–32)	6 (1–28)	26 (11–32)	10 (1–28)	9 (1–28)	15 (2–28)	10 (3–13)	3.5 (1–13)
CD4 count (mm^{-3})	N/A	N/A	N/A	73.5 (2–511)	28 (2–207)	214 (34–511)	279 (128–507)	105 (46–412)
HIV-1 viral load (log_{10} copies ml^{-2})	N/A	N/A	N/A	5.15 (1.70–6.34)	5.27 (2.09–6.34)	5.22 (1.70–6.02)	1.81 (1.70–5.31)	4.82 (1.70–5.89)
ARV use (%)	N/A	N/A	N/A	50.00	35.71	55.56	100.00	40.00
Time on ARVs before TB diagnosis (weeks)	N/A	N/A	N/A	3.7 (0–311)	0.7 (0–24)	123 (0–311)	3.7 (2–6.6)	2–6.6
TST reaction								
Induration (mm)	21 (12–28)	20 (12–25)	25.5 (13–28)	0 (0–26)	0.00	16 (10–24)	24 (21–26)	N/A
Redness (mm)	22 (12–50)	20 (12–27)	30 (15–50)	0 (0–38)	0 (0–15)	17 (0–38)	28 (26–29)	N/A
IGRA response (QuantiFERON)								
Positive (%)	88.89	88.89	N/A	53.85	35.71	77.78	66.67	75.00
Indeterminate (%)	11.11	11.11	N/A	30.77	50.00	11.11	0.00	25.00
Negative (%)	0.00	0.00	N/A	15.38	14.29	11.11	33.33	0.00

Table 6.2: Demographic and clinical characteristics of the study cohort.

Data presented in the format x (y–z) represents median (interquartile range).

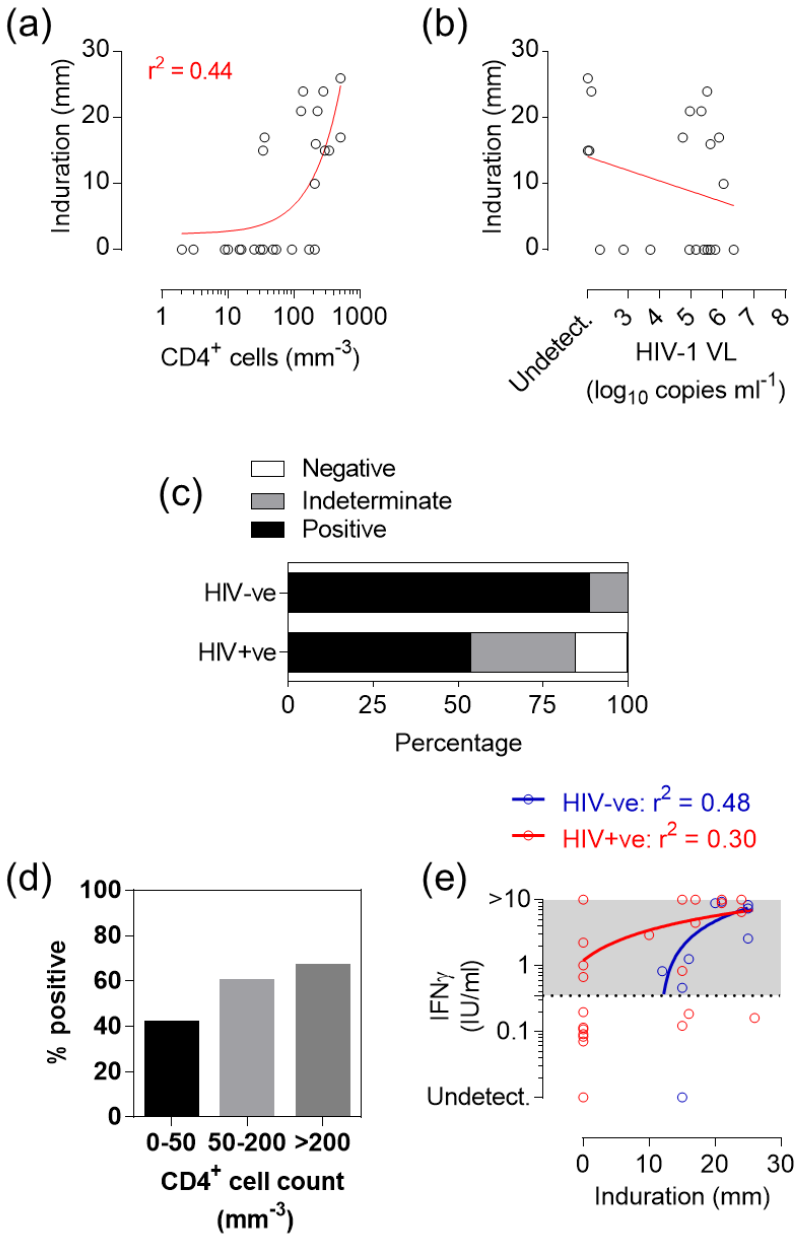

Figure 6.2: TST responses and IGRAs.

(a) Correlation of TST induration with CD4⁺ cell counts for HIV-1⁺ individuals. Linear regression showed a weak but significant positive correlation. **(b)** Correlation of TST induration with viral loads (where available) for HIV-1⁺ individuals. Linear regression was was non-significant. **(c)** QuantiFERON (IGRA) test responses. **(d)** QuantiFERON test positivity (% of indicated group) in HIV-1⁺ patients stratified by CD4⁺ cell count. **(e)** Correlation of induration with IFNγ release elicited by TB antigens in QuantiFERON tests, in HIV-1⁻ and HIV-1⁺ patients. Weak but significant positive correlations were observed for both groups. The dashed horizontal line indicates the level required for a positive result; subjects below this line had negative or indeterminate results. IU, international units. Red/blue lines indicate medians or linear regressions for all plots.

Group	*n*	TB disease status	HIV-1 status	TST response	Notes	Source
A	16	Active TB	Negative	Positive		This study
B	14	Active TB	Positive	Anergic	Termed TST anergic as opposed to TST negative, as patients have confirmed active TB so should have Mtb antigen memory, but do not react.	This study
C	9	Active TB	Positive	Positive		This study
D	3	Active TB	Positive	Positive	Unmasking IRIS patients; presentation with active TB within 2–8 weeks of commencing ARV therapy.	This study
E	5	Healthy (latent TB, or previous exposure to mycobacteria)	Negative	Positive		Tomlinson *et al.* (2011)
F	5	Healthy (uninfected)	Negative	Negative	Termed TST negative, as no TST response in healthy individuals with no clear risk factor for anergy suggests no Mtb exposure.	Tomlinson *et al.* (2011)
G (Saline)	8	Active TB	Negative (3) / Positive (5)	N/A		This study

Table 6.3: Study group definitions for subsequent analyses.

6.4 Histological assessments

Histological assessments of inflammation were made using biopsies from this recruited cohort (groups A, B, C, D, G, **Table 6.3**). Hematoxylin and eosin (H&E) stained sections were scored by a histopathologist blinded to concomitant clinical information and TST/saline status. Inflammation was scored from 0 (no inflammation) to 3. **Figure 6.3(a)** shows the relationship between histological inflammation score and clinical induration in each group, which demonstrates that although histological inflammation was detected in some clinically negative TSTs or saline control samples, there was mainly concordance between TST positivity and higher histological inflammation scores. No difference in median histological inflammation score was found between positive TSTs from HIV-1$^-$ patients or HIV-1$^+$ patients.

Where present, the cellular composition of the inflammatory infiltrate in the TST biopsies was assessed. This was largely composed of lymphocytes and histiocytes (APCs), which were reported to make up the majority of the cellular influx in all cases, consistent with previous studies (Poulter et al., 1982; Scheynius et al., 1982). The median ratio of lymphocytes to histiocytes was higher in positive TSTs from HIV-1$^-$ patients in comparison to HIV-1$^+$ patients, although this difference was not statistically significant (**Figure 6.3b**; Mann-Whitney test, P=0.1049). The distribution of the inflammatory infiltrate was also assessed, and found to have a predominantly perivascular distribution in all groups, which is again consistent with previous reports assessing TST reactions at this time-point (**Figure 6.3c**; Gibbs et al., 1984).

Representative images of H&E stains from each group for each inflammatory score (where applicable) are shown in **Figure 6.4**.

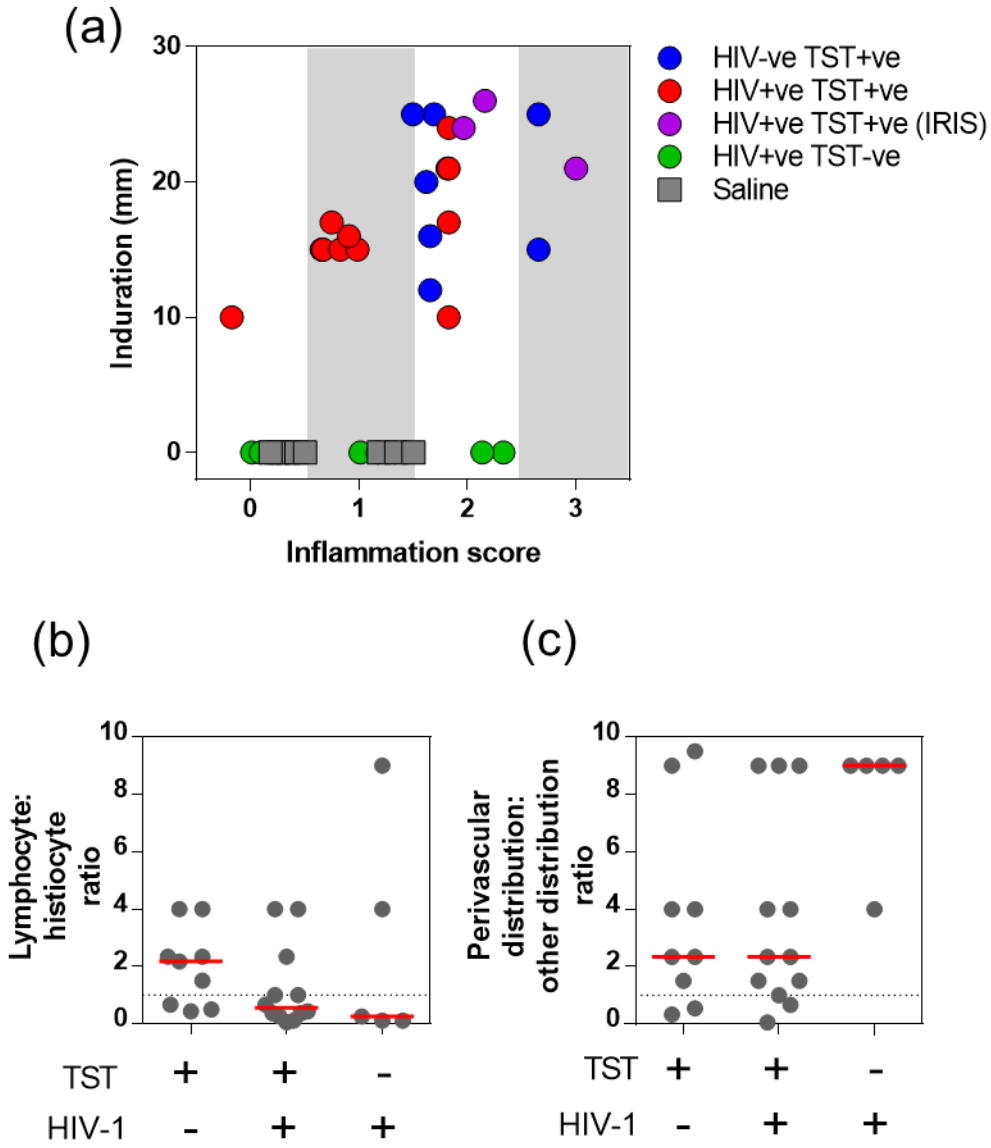

Figure 6.3: Histological assessment of TST and saline biopsies.

Biopsies were formalin fixed, paraffin embedded, sectioned and stained with H&E to delineate the inflammatory infilitrate. All quantitative assessments were performed by an assessor blinded to clinical information. **(a)** Inflammatory infilitrate grading on a 0 (no inflammation) to 3 scale. Each symbol represents an individual TST. **(b)** Composition of cellular infilitrate, where present, as assessed by a lymphocyte:histiocyte ratio. Each symbol represents an individual TST. Red lines indicates medians per group. **(c)** Distribution of cellular infilitrate, where present, as assessed by a perivascular:other distribution ratio. Each symbol represents an individual TST. Red lines indicates medians per group.

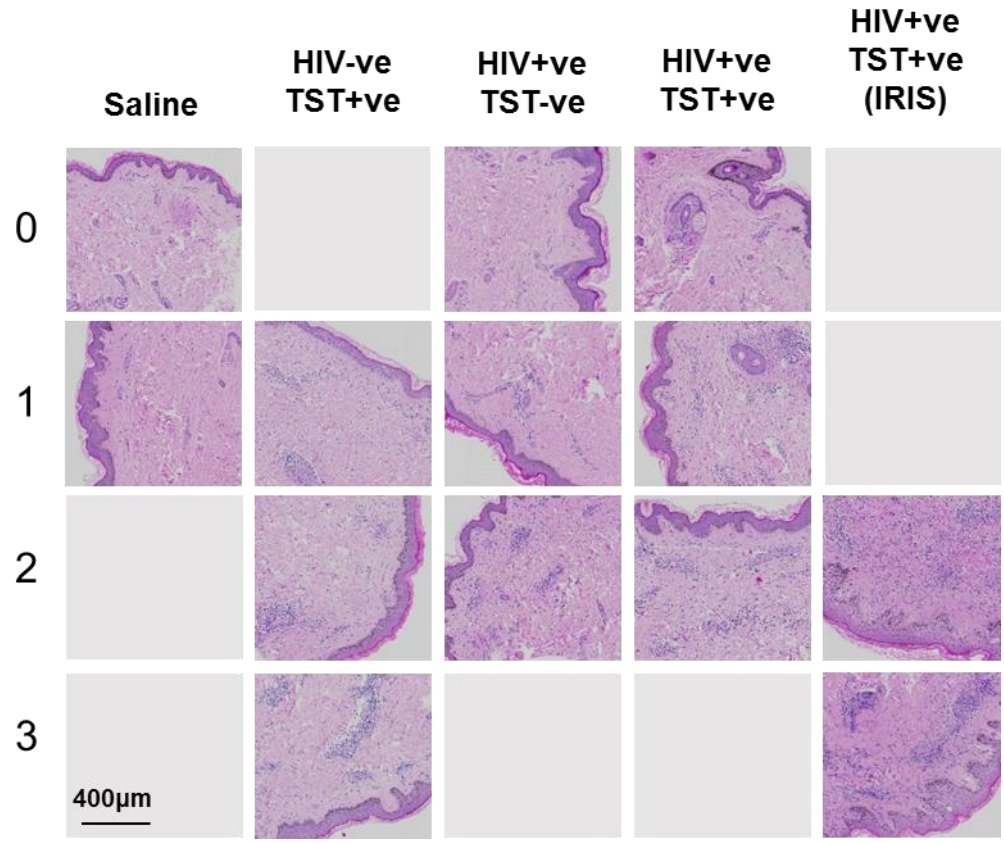

Figure 6.4: Representative H&E stains of TST and saline biopsies.

Representative images from each group for each inflammatory score (indicated by the left-hand column of numbers). Paraffin embedding of biopsies was performed by Groote Schuur Hospital (Cape Town) Department of Pathology. Sectioning and H&E staining were performed by the University College London Hospital (UCLH) histopathology department. With thanks, histopathology assessments and scoring were performed by Dr Alan Ramsay, UCLH Department of Pathology.

6.5 Gene expression profiling of TSTs

6.5.1 Saline injection gene expression profiles

Biopsies were collected from the site of saline control injections performed on eight active TB patients, in order to establish a baseline from which induction of gene expression in TSTs could be investigated (group G, **Table 6.3**). Three patients were HIV-1$^-$ and five were HIV-1$^+$. Before gene expression profiles from these biopsies were used as a pooled group, the characteristics of the samples in the HIV-1$^-$ and HIV-1$^+$ groups were compared, to assess whether any systematic differences existed that could confound their use as a common baseline.

No difference between the groups was found upon histological inflammation scoring of biopsies (**Figure 6.5a**). Hierarchical clustering of gene expression profiles also did not discriminate HIV-1$^-$ and HIV-1$^+$ samples (**Figure 6.5b**). Specific assessment of significant differences between the groups in genome-wide gene expression identified only 11 genes for which median expression differed by two-fold between the HIV-1$^-$ and HIV-1$^+$ saline groups, all of which were expressed more highly in HIV-1$^-$ samples (**Figure 6.5c**).

PCA was used to explore the multidimensional relationships of variance within the entire dataset. The two highest PCs showed clustering of saline biopsies, with again no distinction observed between HIV-1$^-$ and HIV-1$^+$ saline biopsies **(Figure 6.6**).

The clustering analyses and the minimal level of between-group differences in gene expression indicated that there was no systematic difference between the groups of saline biopsies. They were subsequently used as a common baseline for all gene expression analyses.

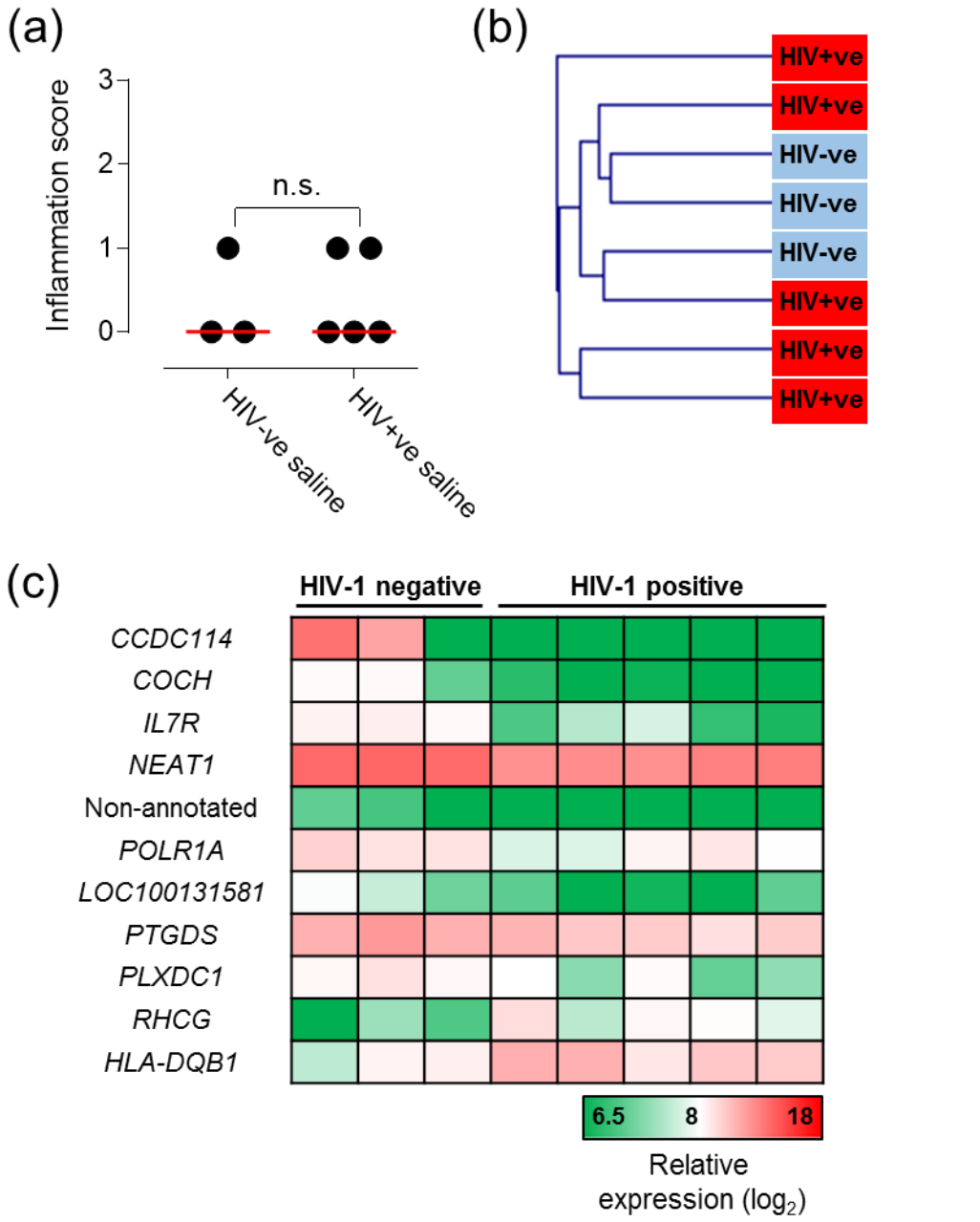

Figure 6.5: Comparing HIV-1⁻ and HIV-1⁺ saline control samples.

(a) Histological inflammation scoring of HIV-1⁻ and HIV-1⁺ saline injection biopsies. There was no significant difference in scores between the two groups (Mann-Whitney test). Red lines indicate medians. **(b)** Hierarchical clustering of gene expression profiles from HIV-1⁻ and HIV-1⁺ saline injection biopsies using a Euclidean distance metric, average linkage clustering and optimised sample leaf order. **(c)** Heatmap of saline biopsy gene expression of 11 genes for which median expression was significantly different (Wilcoxon rank test, $P<0.05$) by at least two-fold between HIV-1⁻ and HIV-1⁺ saline injection biopsies. Data is presented as normalised microarray expression values.

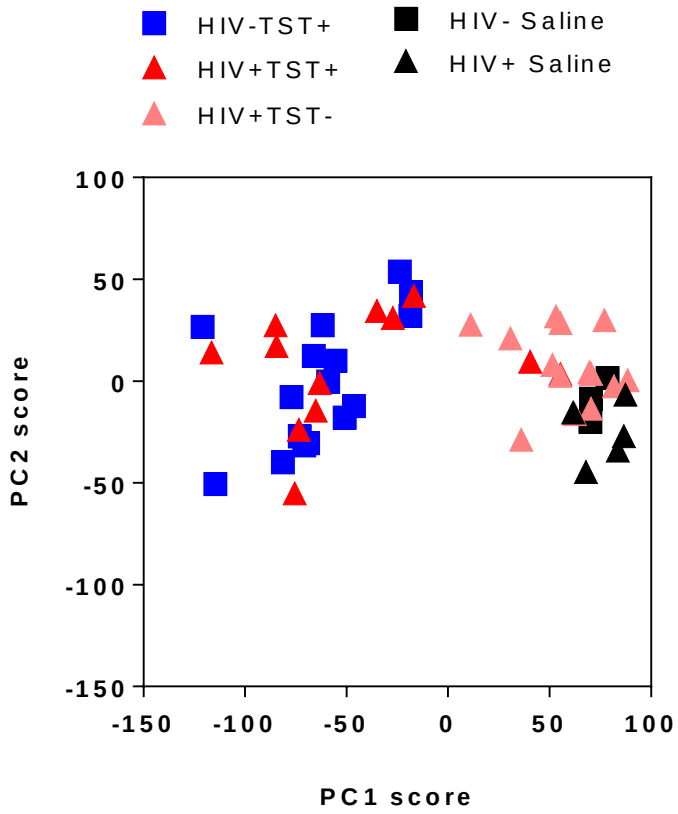

Figure 6.6: Principal component analysis of TST and saline biopsy gene expression profiles.

Principal component analysis was performed on genome-wide expression profiles from TST or saline biopsies from the indicated groups. Principal component (PC) scores for the two highest PCs, PC1 and PC2, are shown. Each symbol represents a distinct biopsy gene expression profile.

6.5.2 The TST in HIV-1⁻ patients with active TB induces innate & adaptive-associated gene expression with evidence for cell recruitment and immunoregulatory processes

The TST transcriptional response in active TB was characterised by comparing gene expression profiles of TST biopsies from HIV-1⁻ active TB patients to saline controls (groups A and G in **Table 6.3**). Statistically significantly increased expression of 1725 genes was found in the TST (**Figure 6.7a**). Transcription factor binding site (TFBS) enrichment analysis of this gene list using oPOSSUM-3 (Kwon et al., 2012; http://opossum.cisreg.ca) indicated that these genes were regulated by multiple immune response signalling pathways (**Figure 6.7b**). These included innate immune NFκB and IRF2 signalling, adaptive immune STAT1 signalling and regulatory cytokine signalling via STAT3.

The functional characteristics of the TST gene expression profile were explored by InnateDB pathway enrichment analysis (Breuer et al., 2013; http://www.innatedb.com; **Figure 6.7c**). This showed enrichment for innate pathways such as phagocytosis and type I IFN signalling, and adaptive pathways such as type II IFN signalling and T cell receptor (TCR) signalling. Pathways involved in the interface between innate and adaptive immunity were also enriched, such as antigen presentation and immunoregulatory interactions, as were pathways involved in cellular recruitment to inflammatory foci, such as chemokine activity and integrin activation.

These bioinformatic analyses were complemented by assessing the TST using independently derived gene expression modules (see **Chapter 5** & **Appendix I** for further description) constructed to detect specific cell types (**Figure 6.8a**; with thanks to Dr Gabriele Pollara; see **Appendix I** for description), or specific cytokine- or innate stimulus-induced functional signatures (generated in **Chapter 5**; **Figure 6.8b** and **6.6c** respectively). Statistically significant enrichment in comparison to the saline control baseline was observed for all cell types, but B cell, macrophage and DC-specific modules were only very modestly enriched above salines (**Figure 6.8a**). The modest increase observed in enrichment in the macrophage-specific module, despite evidence of many histiocytes on histology, may be because these histiocytes are infilitrating monocytes which have not yet completely differentiated into MDMs; the monocyte-specific signature enrichment corroborates this hypothesis.

The IFNγ, TNFα, IL-4/IL-13 and TGFβ/IL-10 modules generated in **Chapter 5** from stimulated MDMs can be compared quantitatively, as the gene sets for each had similar overall module expression values in MDMS stimulated with the relevant cytokines; suggesting that no module is biased towards more highly-expressed genes (see **pg. 228**). The most highly significantly enriched cytokine module was specific for IFNγ activity, followed by TNFα – cytokines known to be critical in CMI and anti-mycobacterial responses. Significant but lesser enrichment was observed for activity of the Th2 cytokines IL-4 and IL-13, and the regulatory cytokines TGFβ and IL-10 (**Figure 6.8b**). Innate stimulus modules specific to PCSK (a TLR-2 ligand) or Mtb were significantly enriched in TSTs, while those specific to another pathogen, Spn or LPS (a TLR-4 ligand), were not enriched above saline controls (**Figure 6.8c**) - suggesting that the inflammation generated in the TST exhibits specificity for Mtb-induced innate inflammatory respnses.

These analyses demonstrated that molecular assessment of the TST in active TB, via bioinformatic and modular characterisation of gene expression profiles, can provide qualitative and quantitative insights into multiple components of the CMI response in site of inflammation samples from patients with active TB.

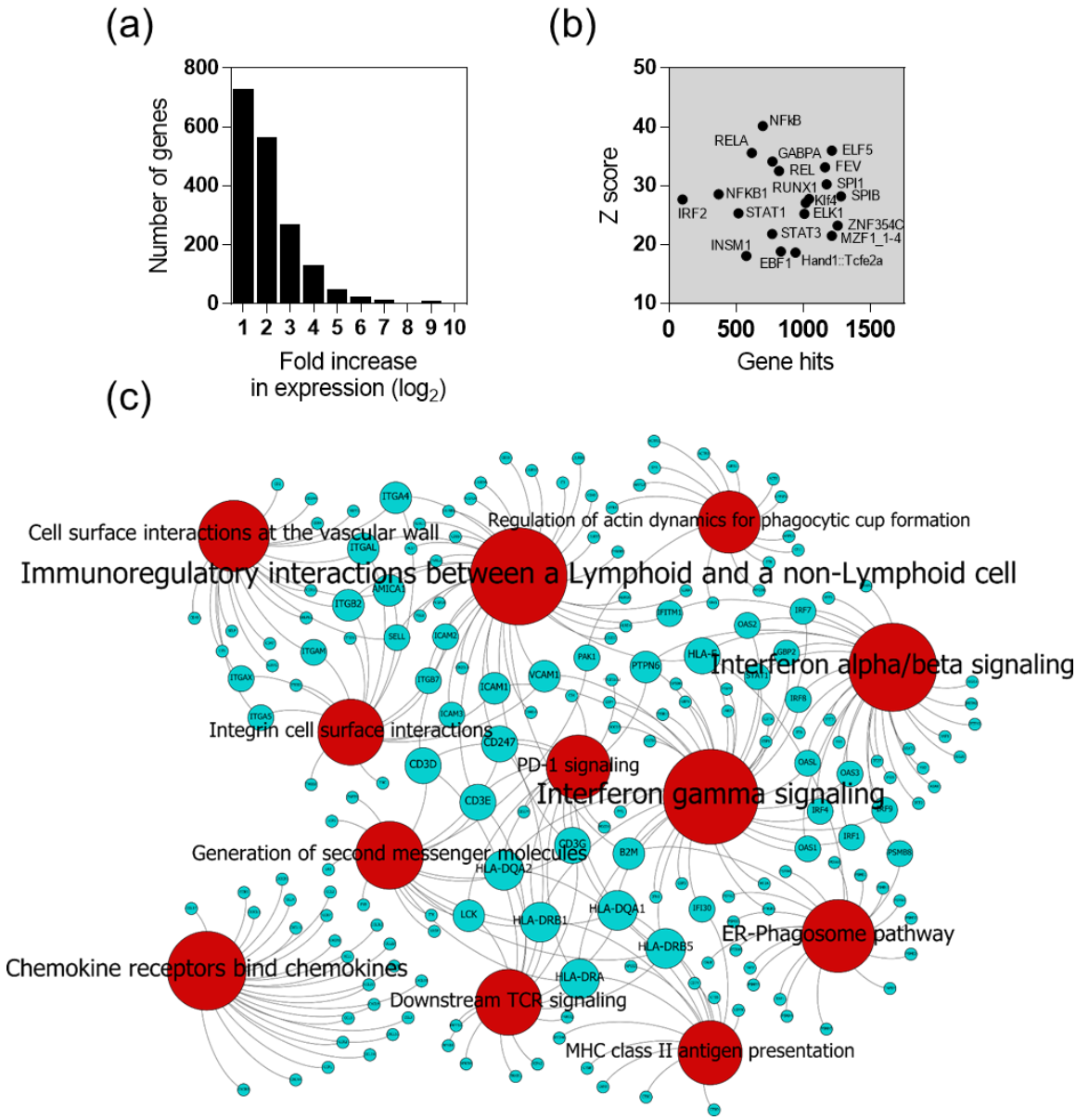

Figure 6.7: TST gene expression profiling in HIV-1⁻ patients with active TB.

(a) Frequency distribution of genes for which median expression was significantly increased (Wilcoxon rank test, *P*<0.05) by at least two-fold in HIV-1⁻ TSTs compared to saline controls. **(b)** oPOSSUM transcription factor binding site (TFBS) enrichment analysis of 5000bp upstream/downstream of the 1725 genes presented in (a). The X axis lists the number of genes enriched for a TFBS, and the Y axis displays significance by Z score. **(c)** Network visualisation of InnateDB (Reactome) pathway enrichment analysis of the 1725 genes. The 12 enriched pathways with the highest numbers of genes identified are shown, all of which were significantly enriched in this gene set (corrected *P*<0.05). Red nodes, pathways; blue nodes, genes; node size is correlated to number of network connections.

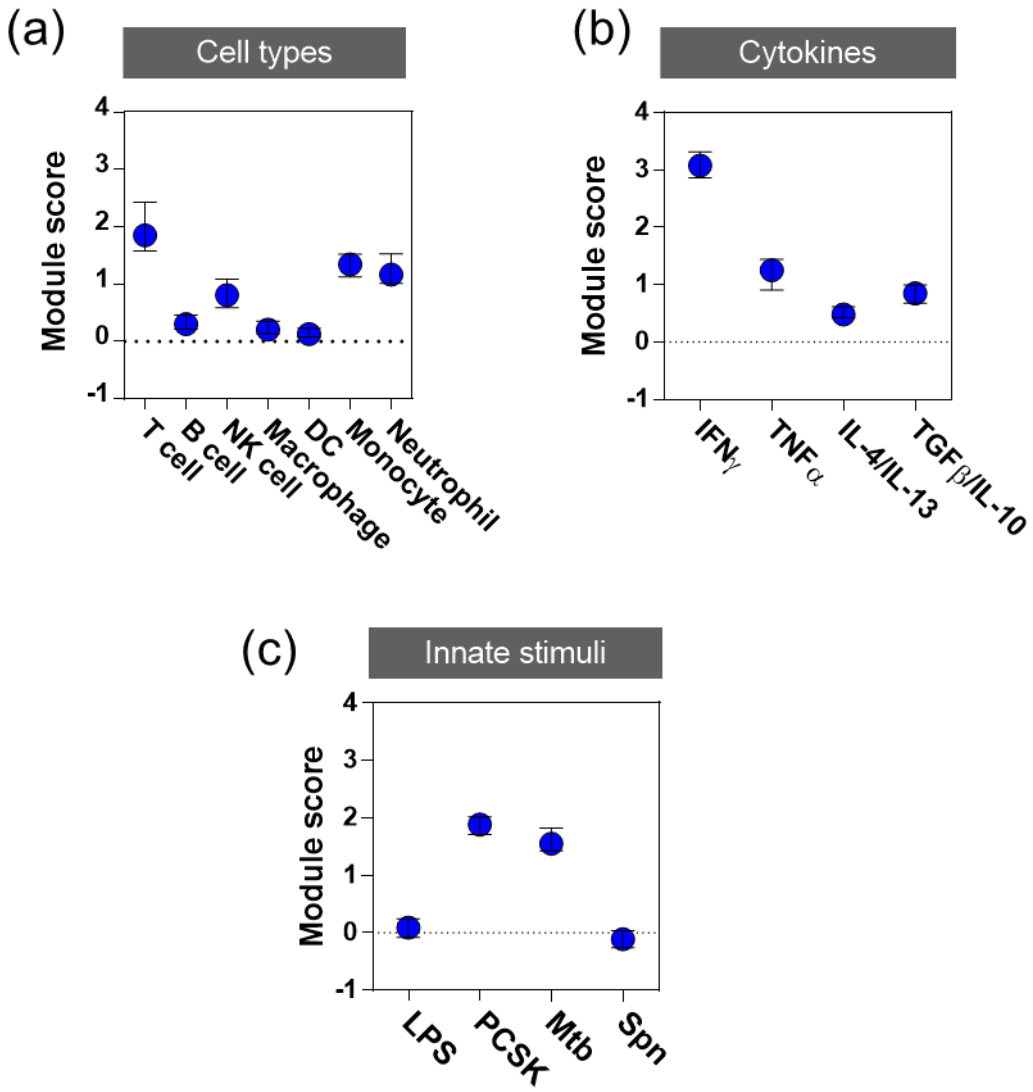

Figure 6.8: Modular analysis of the TST in HIV-1⁻ patients with active TB.

Modular analysis of TST gene expression profiles from HIV-1⁻ TST⁺ (active TB) samples. Module score represents the geometric mean expression of the module gene set in each TST gene expression profile, normalised to the saline control baseline, which is the median of the geometric mean module expression in all saline samples. Symbols represent group median module score and error bars represent interquartile range. The statistical significance of modular enrichment above the saline baseline was assessed using a Mann-Whitney test for differences in module expression between all TSTs and all salines (P<0.05). **(a)** All modules were significantly enriched above salines. **(b)** All modules were significantly enriched above salines. **(c)** PCSK and Mtb modules were significantly enriched above salines.

6.5.3 The molecular detail of the TST response is not systematically altered by active TB disease

Active TB infection is associated with significant changes to the peripheral blood transcriptome (Berry et al., 2010). To assess if active TB also altered or confounded the TST response, I compared TST^+ gene expression profiles from $HIV\text{-}1^-$ patients with active TB to TST^+ gene expression profiles from healthy individuals generated in an earlier study (Tomlinson et al., 2011; groups A and E in **Table 6.3**). Previous analysis of the healthy individual TST^+ gene expression profiles showed similar global functional enrichment results to the active TB profiles (**Figure 6.7**), such as T cell activation, chemokine activity and innate immune pathways (Tomlinson et al., 2011).

Comparison of genes which were increased in expression in either TST^+ group showed a substantial degree of overlap (**Figure 6.9a**). Directly comparing the expression of all these genes showed a significant positive covariance and correlation between active TB patients and healthy individuals (**Figure 6.9b**). I identified statistically significant differences in gene expression of more than two-fold between the groups (**Figure 6.9b**). 356 genes were increased in healthy individuals in comparison to active TB patients, and 156 genes were increased in active TB patients in comparison to healthy individuals (in total, <25% of the integrated gene set). The 25 most highly increased genes in active TB patients are shown in **Figure 6.9c**, and include immune response factors such as the antimicrobial peptides *DEFB4A* and *PI3*, and the matrix metalloproteinase *MMP1*. Pathway enrichment analysis of the gene list increased in active TB showed enrichment for Src signalling, integrin activation, vascular wall interactions and complement pathway activation (**Figure 6.9c**). Fewer pathways were enriched in the gene list increased in healthy individuals, and reflected mRNA processing and splicing (data not shown).

Modular enrichment analysis of the gene expression profiles showed similar enrichment in the two groups for all modules tested (**Figure 6.10a, b, c**), except for the T cell-specific module, which was statistically significantly more highly enriched in healthy individual TST^+ profiles (**Figure 6.10a**).

Overall, these gene expression analyses suggested that substantial components of the TST response in active TB are shared with the TST response in

healthy individuals, and so employing the TST as a challenge model in active TB patients is not likely to be systematically confounded by attendant active disease. In fact, as active disease is associated with some functionally enriched alterations in gene expression, this may add value to an exercise in investigating inflammation in active TB specifically.

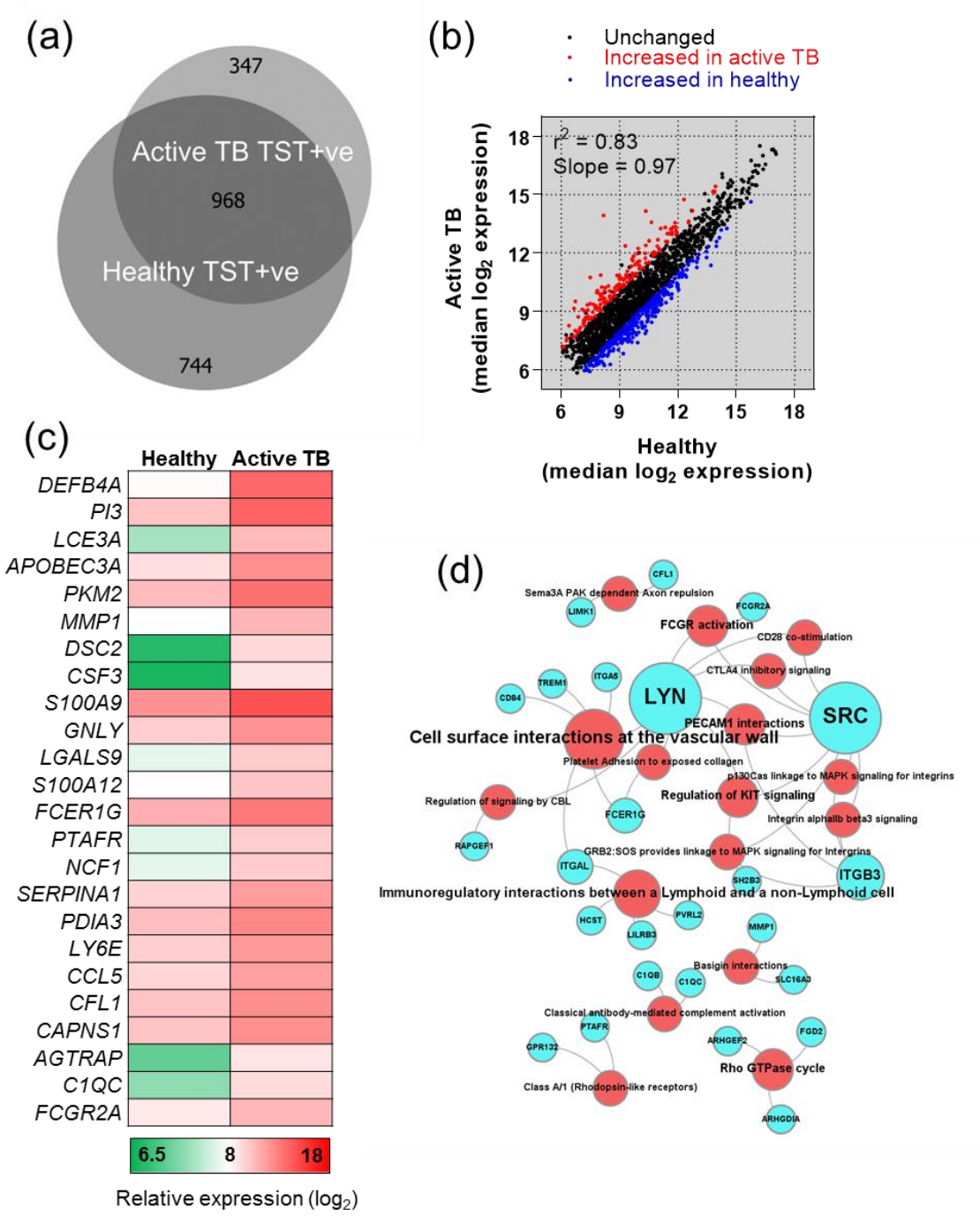

Figure 6.9: Comparing active TB and healthy individual TST⁺ gene expression profiles.

(a) Venn diagram of the overlap between genes significantly induced in active TB TST⁺ vs. healthy individual TST⁺ samples (both in comparison to saline controls). **(b)** XY plot comparing median expression of all genes induced in either active TB or healthy TST⁺ samples. Linear regression showed a significant positive correlation and covariance between the two groups. Highlighted genes are significantly (P<0.05, Wilcoxon rank test) expressed ≥two-fold in one group compared to the other. Data are normalised microarray expression values. **(c)** Matrix showing the top 25 genes with significantly increased expression in active TB patient TSTs compared to healthy individuals. Data are normalised microarray expression values. **(d)** Network visualisation of InnateDB (Reactome) pathway enrichment analysis of genes upregulated in active TB TST⁺ profiles compared to healthy individuals. All significantly (corrected P<0.05) enriched pathways are shown. Red nodes, pathways; blue nodes, genes; node size is correlated to number of network connections.

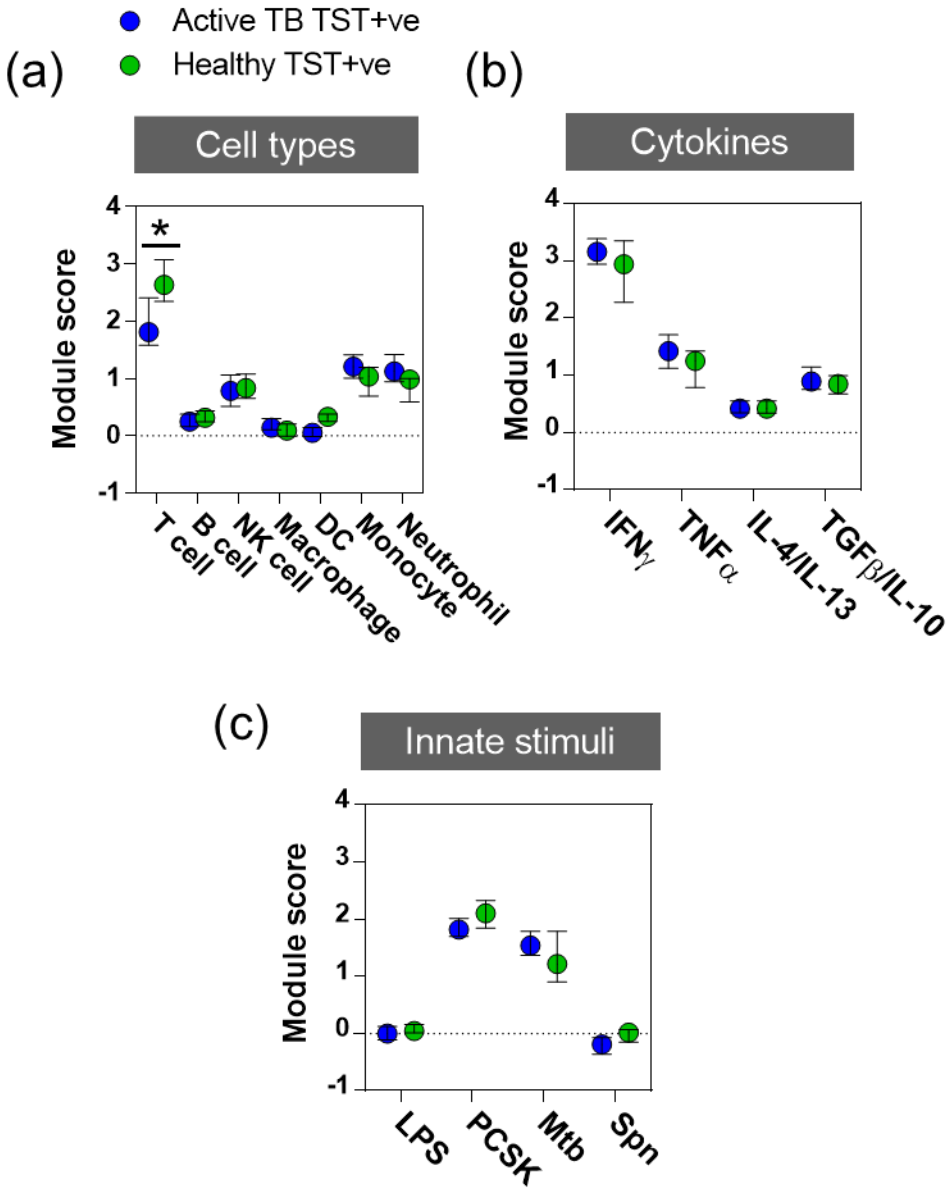

Figure 6.10: Modular analysis of TST⁺ gene expression profiles from HIV⁻ active TB patients and healthy individuals.

Modular analysis of TST gene expression profiles from HIV-1⁻ TST⁺ (active TB) and HIV-1⁻ TST⁺ (healthy individual) samples. Module score represents the geometric mean expression of the module gene set in each TST gene expression profile, normalised to the saline control baseline, which is the median of the geometric mean module expression in all saline samples. Symbols represent group median module score and error bars represent interquartile range. The statistical significance of modular enrichment above the saline baseline was assessed using a Mann-Whitney test for differences in module expression between all TSTs and all salines (P<0.05). Mann-Whitney tests were also used to test for significant differences in module score between groups (* indicates P<0.05 between indicated groups). **(a)** All cell type modules were significantly enriched above salines. The T cell module score was significantly increased in healthy individuals. **(b)** All cytokine modules were significantly enriched above salines. **(c)** PCSK and Mtb modules were significantly enriched above salines.

6.5.4 Relative preservation of type I IFN responses in anergic TSTs from HIV-1$^+$ active TB patients

In HIV-1$^+$ patients with anergic TST responses, biopsies collected from the marked TST injection site at 48 hours were assessed for differences in gene expression in comparison to saline controls (groups B and G in **Table 6.3**). Expression of 98 genes was statistically significantly increased in these samples despite the absence of a clinical reaction (**Figure 6.11a**), almost all of which were also increased in expression in the HIV-1$^-$ TST$^+$ samples (**Figure 6.11b**). Directly comparing the expression of all genes induced in either group showed a significant positive correlation, but with a substantially reduced covariance (**Figure 6.11c**), demonstrating significantly attenuated enrichment of TST-associated gene expression in in HIV-1 anergy. This detectable but attenuated anergic TST response was further evident when comparing induction of gene expression in each group above saline (**Figure 6.11d**). Importantly, this analysis suggests that the detectable response is not purely made up of genes which are the most highly expressed in TST$^+$ samples, but are instead distributed across the spectrum of gene expression levels.

Pathway enrichment analysis of the HIV-1$^+$ anergic response gene list demonstrated enrichment for both type I and type II IFN signalling, with the most significant enrichment detected for the former (**Figure 6.12a**). Directly comparing how many genes from the Reactome biological pathway database (http://www.reactome.org/) IFN pathway gene lists were expressed in each group showed a change in bias from type II IFNs towards type I IFNs in HIV-1$^+$ anergic samples (**Figure 6.12b**). TFBS enrichment analysis of the anergic response gene list also reflected the relative dominance of innate type I IFN activity in these samples, with highly significant enrichment detected for IRF2 and NFκB TFBS (**Figure 6.12c**).

To further characterise IFN activity in these samples, and in particular to distinguish type I and type II signatures which have substantial functional overlap, modular enrichment analysis was performed using modules specific to type I and type II IFNs developed in **Chapter 5, section 5.2.6** (**Figure 6.13a**). Both modules were statistically significantly enriched above saline in all TSTs. Type II IFN activity was significantly more highly enriched in comparison to type I IFN in all TST$^+$ samples, regardless of HIV-1 status. In the HIV-1$^+$ anergic TSTs, both modules were less highly

enriched than in TST$^+$ samples. However, a differential pattern of enrichment was observed: type I and type II IFN activity were enriched to a similar degree, indicating relative preservation of the type I IFN response in these samples. The resulting alteration in balance between the two IFN pathways was evident when the type I and type II module scores were expressed as a ratio. Significantly increased type I IFN/type II IFN ratios were observed in HIV-1$^+$ anergic TST biopsies, in comparison to either HIV-1$^-$ or HIV-1$^+$ TST$^+$ samples (**Figure 6.13b**).

Assessment of the panel of cell type, cytokine and innate stimulus-specific modules in HIV-1$^+$ anergic TSTs showed that enrichment of all modules was either absent or substantially attenuated in comparison to HIV-1$^-$ TST$^+$ biopsies (**Figure 6.13c, d, e**). Detectable responses above the saline baseline included IFNγ cytokine activity (**Figure 6.13d**), consistent with some type II IFN activity identified in the specific IFN analysis. TLR-2 specific responses induced by PCSK were also detectable (**Figure 6.13e**).

These results indicated that immune responses were evident at the site of mycobacterial challenge in clinically anergic TSTs from HIV-1$^+$ active TB patients, and that these were characterised by a relatively preserved type I IFN response.

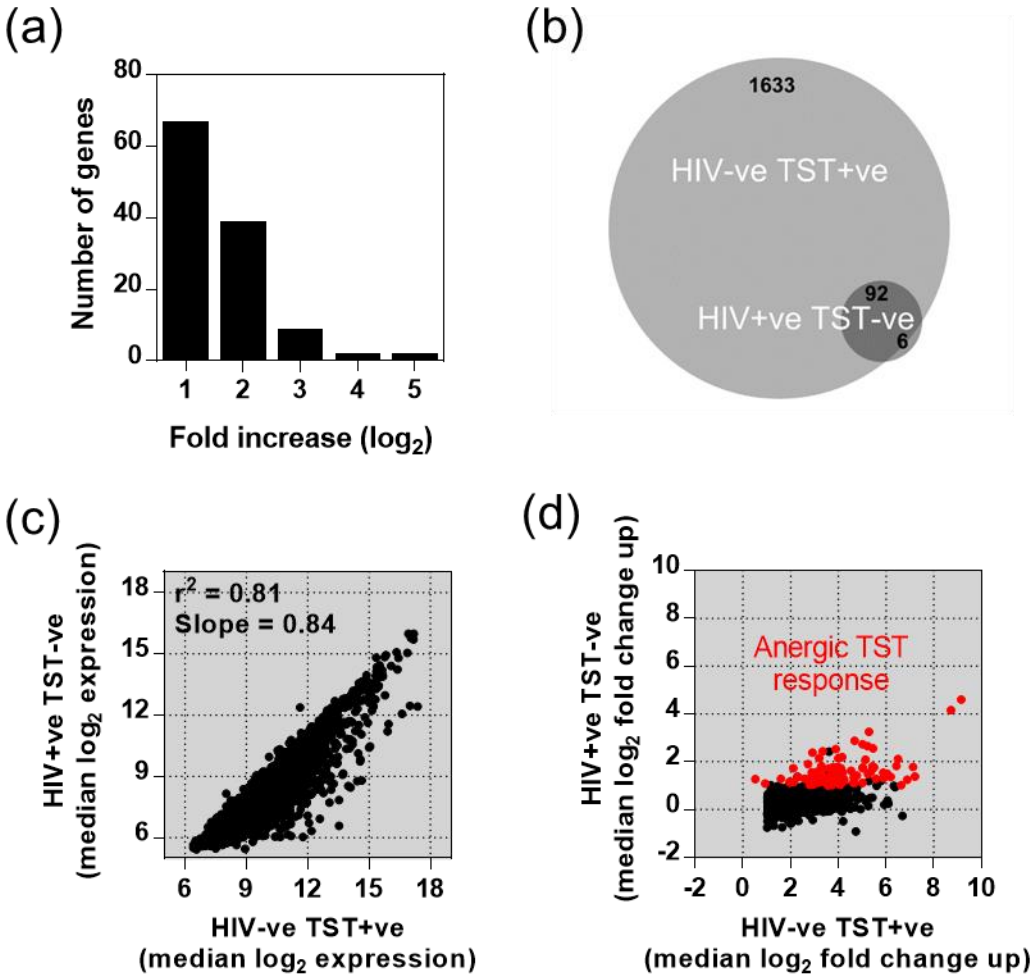

Figure 6.11: Gene expression profiling of anergic TSTs from HIV-1$^+$ active TB patients.

(a) Frequency distribution of 98 genes for which median expression was significantly increased by at least two-fold in HIV-1$^+$ anergic TSTs compared to saline controls. **(b)** Venn diagram demonstrating the overlap between genes significantly induced in active TB HIV-1$^-$ TST$^+$ vs. HIV-1$^+$ anergic samples (both in comparison to saline controls). **(c)** XY plot comparing median expression of all genes induced in either HIV-1$^-$ TST$^+$ or HIV-1$^+$ anergic samples. Linear regression showed a significant positive correlation between the two groups, but with a slope of substantially <1, suggesting reduced expression in HIV-1$^+$ anergic samples. Data presented are normalised microarray expression values. **(d)** XY plot comparing median fold-change induction compared to saline controls of all genes induced in either HIV-1$^-$ TST$^+$ or HIV-1$^+$ anergic samples. The 98 significantly induced genes in the latter are highlighted in red.

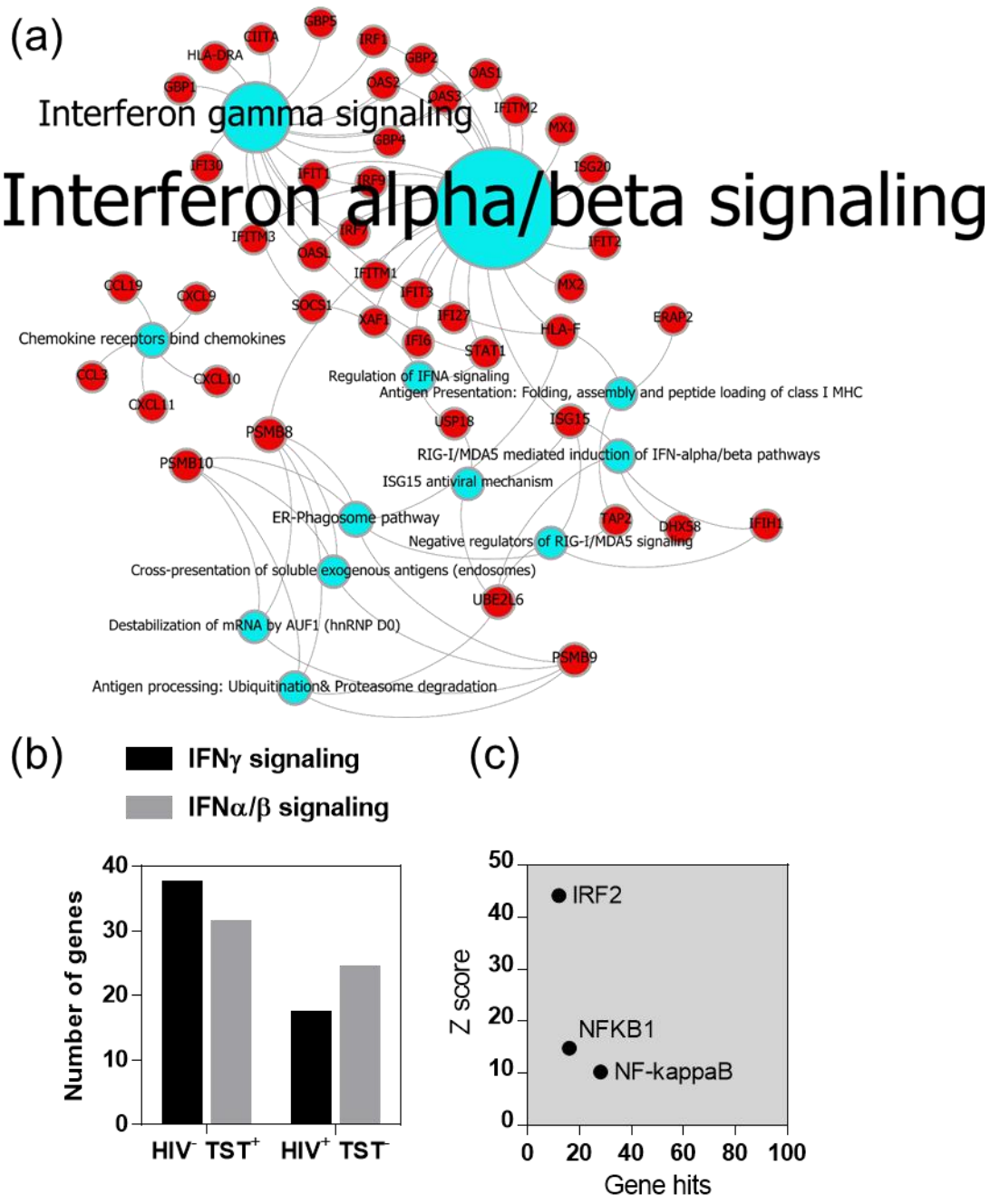

Figure 6.12: Bioinformatic analyses of the HIV-1$^+$ anergic TST response shows enrichment for IFN signalling pathways.

(a) Network visualisation of InnateDB (Reactome) pathway enrichment analysis of the 98 induced genes. The 12 enriched pathways with the highest numbers of genes identified are shown, all of which were significantly enriched in this gene set (corrected *P*<0.05). Red nodes, pathways; blue nodes, genes; node size and labelling are correlated to the number of network connections. **(b)** Comparison of numbers of genes from Reactome IFN pathways expressed in HIV-1$^-$ TST$^+$ and HIV-1$^+$ anergic samples. **(c)** oPOSSUM TFBS enrichment analysis of 5000bp upstream/downstream of the induced 98 genes. The X axis lists the number of genes enriched for a TFBS, and the Y axis displays significance by Z score.

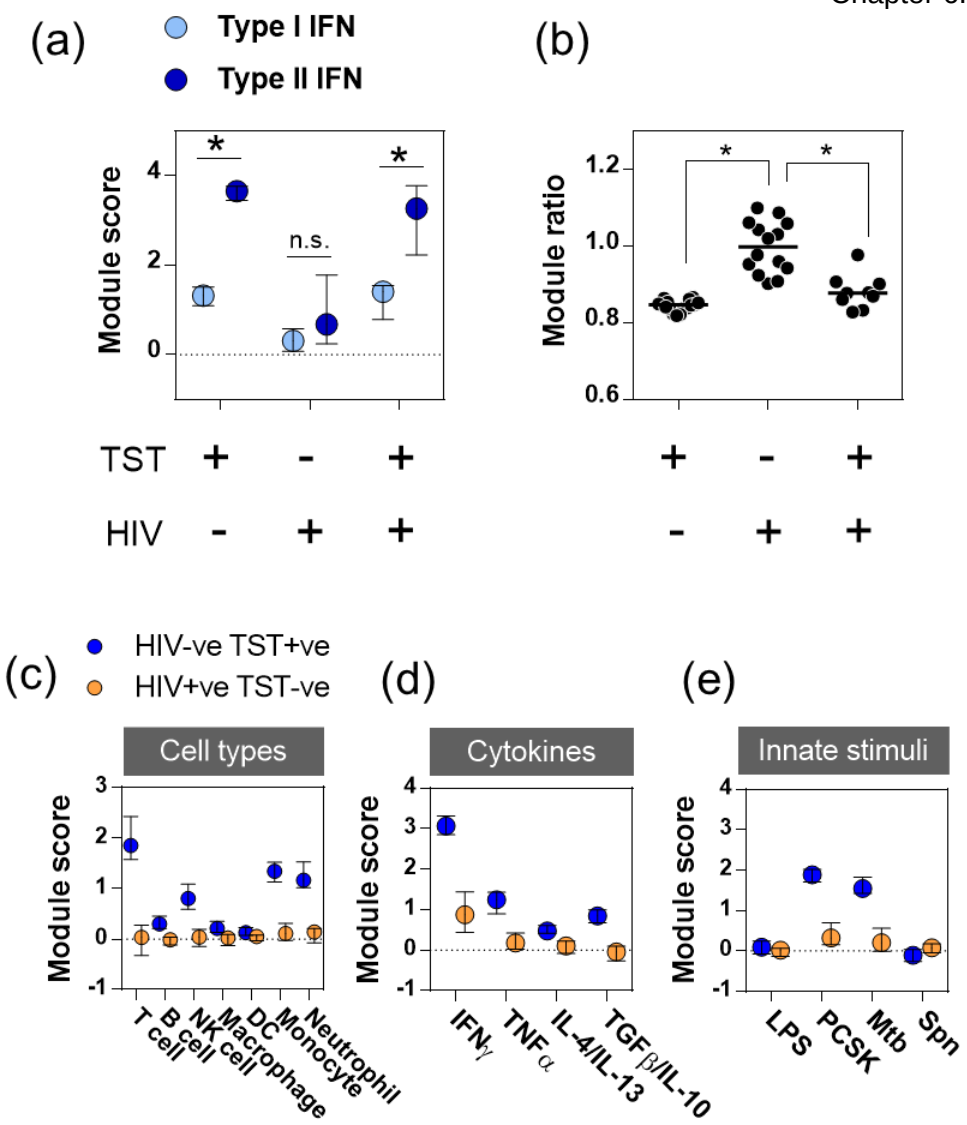

Figure 6.13: Modular analysis of the HIV-1⁺ anergic TST response demonstrates relative preservation of the type I IFN response.

Modular analysis of TST gene expression profiles from HIV-1⁻ TST⁺ and HIV-1⁺ TST⁻ samples. Module score represents the geometric mean expression of the module gene set in each TST gene expression profile, normalised to the saline control baseline, which is the median of the geometric mean module expression in all saline samples. Symbols represent group median module score and error bars represent interquartile range. The statistical significance of modular enrichment above the saline baseline was assessed using a Mann-Whitney test for differences in module expression between all TSTs and all salines (P<0.05). Mann-Whitney tests were also used to test for significant differences in module score between groups (* indicates P<0.05 between indicated groups). **(a)** Modular analysis of gene expression profiles using modules specific to type I and type II IFNs. All modules were significantly enriched above salines in all groups, but significant differences between type I and type II IFN expression were only observed for positive TSTs. **(b)** Ratio of type I IFN to type II IFN module scores. **(c)** All cell type modules were significantly enriched above salines in TST⁺ samples, but none were significantly enriched in anergic TSTs. **(d)** All cytokine modules were significantly enriched above salines in TST⁺ samples, but only the IFNγ module was significantly enriched in anergic TSTs. **(e)** PCSK and Mtb modules were significantly enriched above salines in TST⁺ samples, but only the PCSK module was significantly enriched in anergic TSTs.

6.5.5 HIV-1$^+$ TST anergy is molecularly distinct from healthy individual TST negativity

A previous investigation showed that healthy individual TST$^-$ biopsies contained detectable immune responses, which were qualitatively similar but quantitatively less than those in TST$^+$ samples (Tomlinson et al., 2011). I evaluated the differences between HIV-1$^+$ anergic TSTs and TST$^-$ samples from healthy volunteers. This showed that the HIV-1$^+$ anergic TST response was manifestly limited in comparison to healthy individual TST$^-$ samples (**Figure 6.14a, b**). This analysis also highlighted that a subset of the HIV-1$^+$ anergic response was less highly expressed in the HIV-1$^-$ TST$^-$ biopsies. Twenty-eight genes which were increased in the HIV-1$^+$ anergic group were not statistically significantly increased in expression in HIV-1$^-$ TST$^-$ samples in comparison to saline controls (**Figure 6.14a, b, c**). This list included multiple IFN response genes (**Figure 6.14d**).

These TSTs were also assessed via modular analysis. Statistically significant enrichment of most cytokine and cell type modules, as well as LPS and PCSK innate stimulus modules, was found in the HIV-1$^-$ TST$^-$ samples in comparison to salines (**Figure 6.15a, b, c**). As described above (**Figure 6.13**), only IFNγ and PCSK modules were significantly enriched in anergic TSTs, and the expression of these modules was much lower than in HIV-1$^-$ TST$^-$ samples (**Figure 6.15a, b, c**). This indicates that substantial cellular infiltration, cytokine activity and innate inflammation occur at the site of a negative TST in a healthy individual, but that these processes are absent in the context of HIV-1$^+$ anergy.

These assessments show that HIV-1$^+$ TST anergy in active TB patients is molecularly distinct from TST negativity in a healthy individual. This indicates that anergy is mechanistically different from TST negativity, and may involve a specific type I IFN response not detected in healthy individuals, in the absence of any other evident inflammation or cellular infiltration.

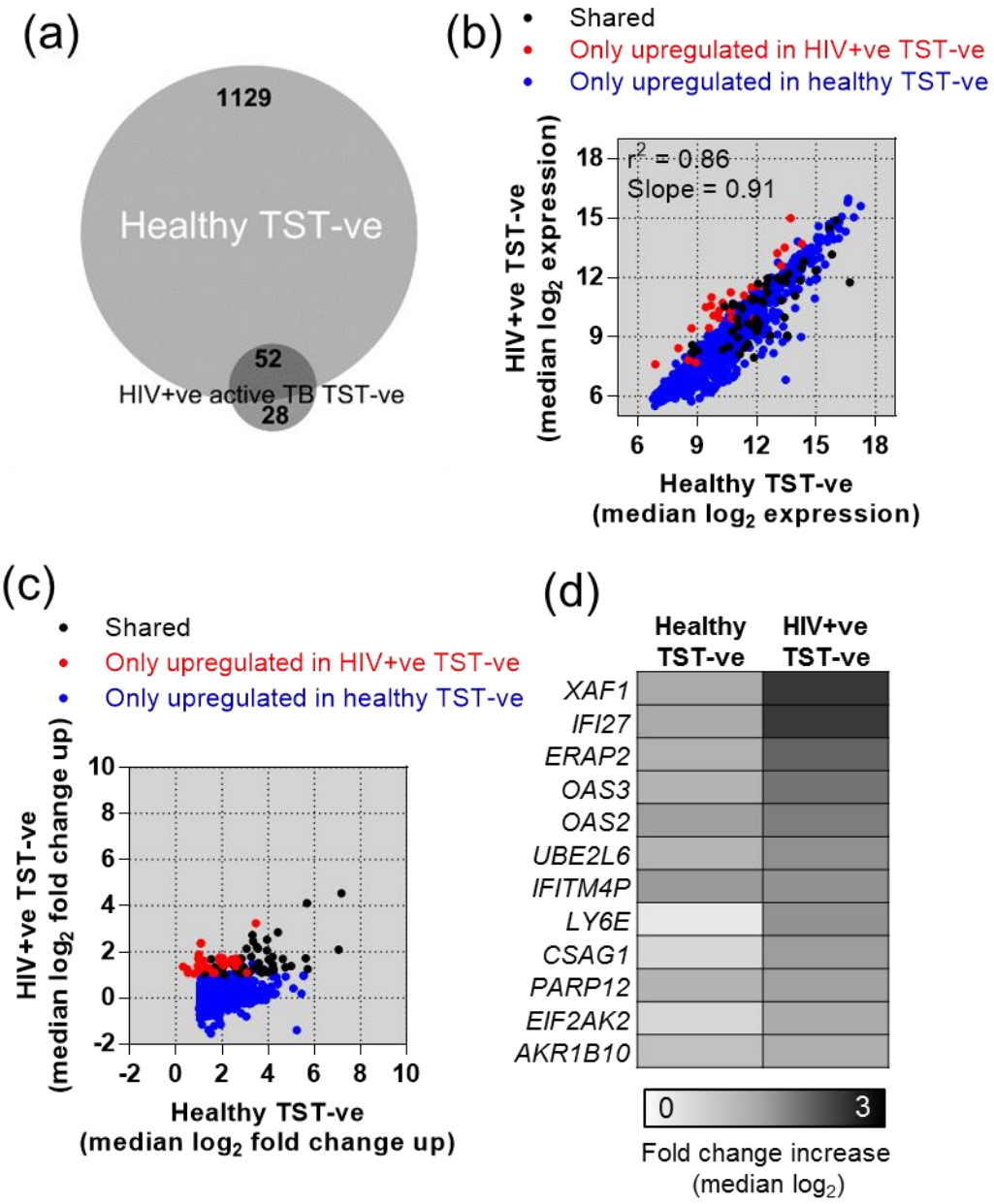

Figure 6.14: Comparison of HIV-1⁺ anergic TST samples from active TB patients with HIV-1⁻ TST⁻ samples from healthy individuals.

(a) Venn diagram demonstrating the overlap between genes significantly induced in healthy individual HIV-1⁻ TST⁻ vs. active TB HIV-1⁺ anergic biopsies (both in comparison to saline controls). **(b)** XY plot comparing median expression of all genes induced in either healthy individual HIV-1⁻ TST⁻ or active TB HIV-1⁺ anergic biopsies. Linear regression showed a significant positive correlation between the two groups, but limited covariance with a slope of substantially <1, suggesting reduced gene expression in HIV-1⁺ anergic biopsies. Genes which are significantly upregulated in either group are highlighted in blue and red. **(c)** XY plot comparing median fold-change induction compared to saline controls of all genes induced in either healthy individual HIV-1⁻ TST⁻ or active TB HIV-1⁺ anergic biopsies. **(d)** Heatmap showing expression of genes which are significantly increased in expression in HIV-1⁺ anergic TST biopsies but not in healthy individual HIV-1⁻ TST⁻ biopsies. All data presented are normalised microarray expression values.

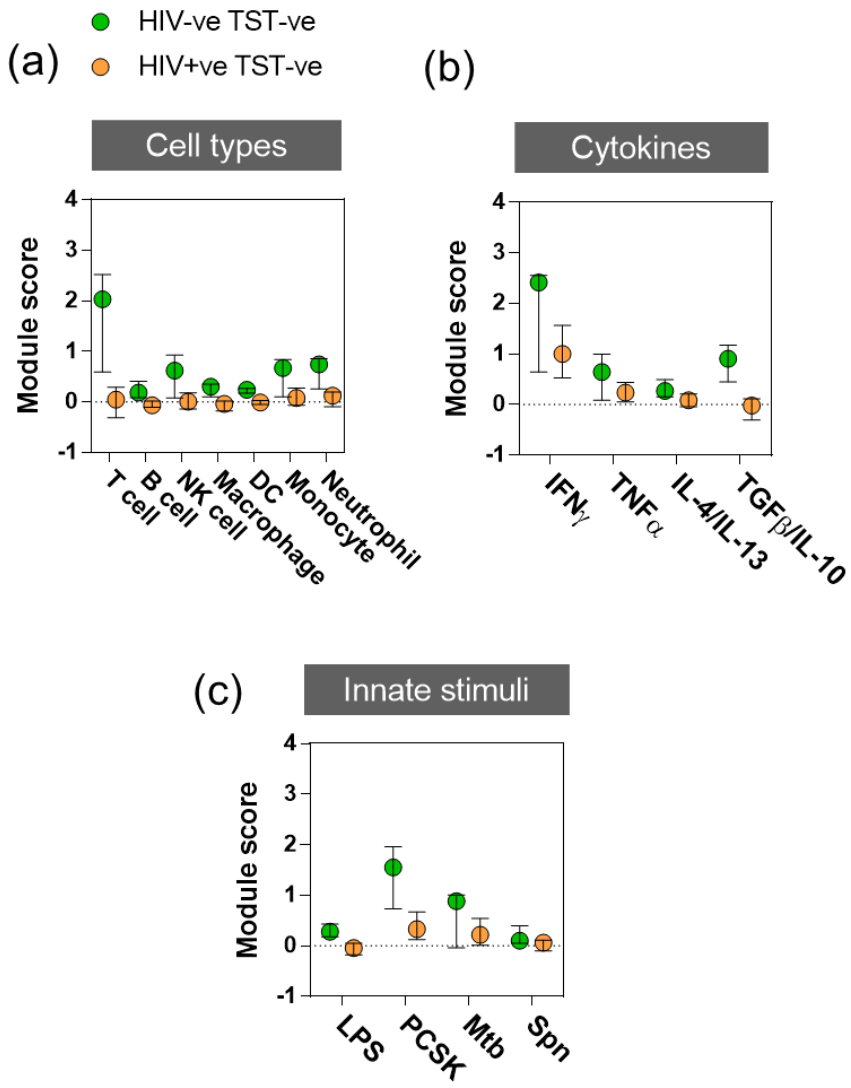

Figure 6.15: Modular analysis of gene expression profiles from HIV-1⁺ active TB patient anergic TSTs and healthy individual negative TSTs.

Modular analysis of TST gene expression profiles from HIV-1⁻ TST⁻ and HIV-1⁺ TST⁻ samples. Module score represents the geometric mean expression of the module gene set in each TST gene expression profile, normalised to the saline control baseline, which is the median of the geometric mean module expression in all saline samples. Symbols represent group median module score and error bars represent interquartile range. The statistical significance of modular enrichment above the saline baseline was assessed using a Mann-Whitney test for differences in module expression between all TSTs and all salines (P<0.05). Mann-Whitney tests were also used to test for significant differences in module score between groups. **(a)** All cell type modules were significantly enriched above salines in TST negative samples, but none were significantly enriched in anergic TSTs. **(b)** All cytokine modules except TNFα were significantly enriched above salines in TST negative samples, but only the IFNγ module was significantly enriched in anergic TSTs. **(c)** LPS and PCSK modules were significantly enriched above salines in TST negative samples, but only the PCSK module was significantly enriched in anergic TSTs.

6.5.6 TST gene expression is broadly conserved in HIV-1$^+$ TST$^+$ individuals but the immunoregulatory IL-10 response is specifically attenuated

I next investigated the TST$^+$ response in HIV-1$^+$ active TB patients (group C in **Table 6.3**). Significant ≥two-fold increases in expression of 1291 genes were observed above saline controls (**Figure 6.16a**), and this response was broadly concordant with the response in HIV-1$^-$ patients (**Figure 6.16b, c**). Specific comparison with the HIV-1$^-$ TST$^+$ response identified 44 genes which were statistically significantly attenuated in expression by ≥two-fold in HIV-1$^+$ TSTs (**Figure 6.16c**). TFBS enrichment analysis was used to assess the attenuated genes (**Figure 6.16d**). This showed enrichment for several factors: innate TFs such as RelA; STAT1, which is downstream of IFNγ signalling; and STAT3, which is downstream of signalling by the anti-inflammatory cytokine IL-10 (L. Williams et al., 2004).

I used modular analysis, as in previous sections, to specifically investigate if the activities of these pathways were altered in HIV-1$^+$TST$^+$ samples. Innate stimulus (downstream of RelA) and IFNγ (downstream of STAT1) module enrichment were preserved, as was enrichment of the module measuring activity of TGFβ and IL-10 in combination (**Figure 6.17b, c**). No differences were found in module expression in HIV-1$^+$ samples using the overall panel of modules, except for significantly reduced enrichment of the T cell-specific module (**Figure 6.17a**), as might be expected for a group of patients with a diminished peripheral CD4$^+$ T cell pool.

To measure the specific activity of IL-10, I used two IL-10-specific functional modules described in **Chapter 5 section 5.2.7**. IL-10 modular enrichment was significantly attenuated in HIV-1$^+$ TSTs (**Figure 6.18a**). As the enrichment for all other cytokine-induced modules tested was preserved, this suggested a specific deficit in IL-10. An independently published IL-10 module was used to confirm this finding (Teles et al., 2013). Enrichment for this module was much lower than that of my IL-10 modules (**Figure 6.18b**), which may reflect that the published module was generated from IL-10-stimulated PBMC rather than MDMs; the latter may be a more accurate model of a tissue-resident cell IL-10 response. Nonetheless, attenuation of IL-10 modular enrichment was also observed using this PBMC module (**Figure 6.18b**).

To further confirm this observation, a discrete assessment of modular enrichment was made using the gene set enrichment analysis (GSEA) algorithm (Subramanian et al., 2005). This algorithm is optimised for detecting differences in

module enrichment between two groups, as it involves ranking all genes in a dataset in order of their difference between the two groups to be compared. In a GSEA comparison of HIV-1$^-$ and HIV-1$^+$ TST$^+$ samples, significant relative enrichment of one IL-10 functional module was demonstrated in the HIV-1$^-$ group (**Figure 6.18c**), further confirming IL-10 functional deficiency at the site of inflammation in the HIV-1$^+$ TST$^+$ active TB patients.

As it has been shown that IL-10 responses to Mtb are attenuated *in vitro* in HIV-1 infected macrophages (Tomlinson et al., 2014; **Chapter 3**), this identification of functional deficiency of IL-10 activity in the HIV-1$^+$ TST response may represent an *in vivo* correlate of the *in vitro* observation. This suggests that an important immunoregulatory component of CMI to mycobacteria is deficient at the site of inflammation in HIV-1$^+$ patients with active TB.

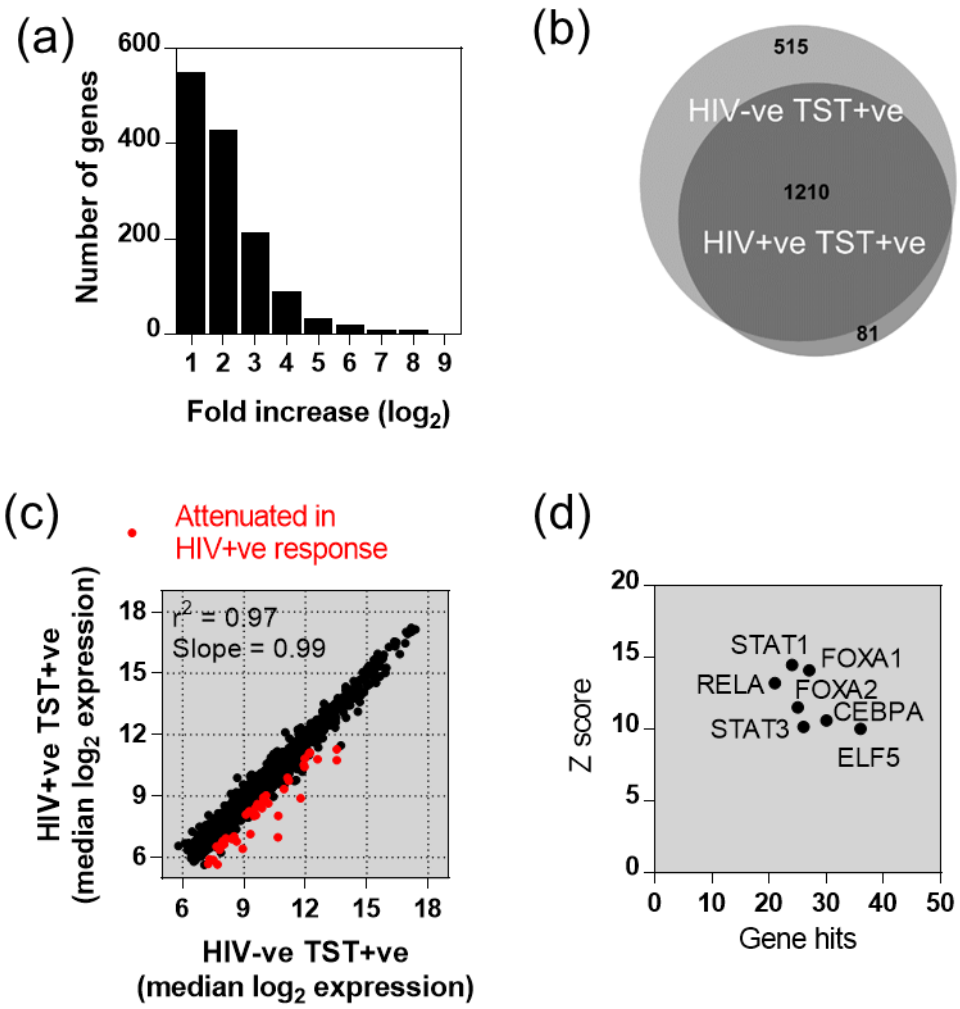

Figure 6.16: Gene expression profiling of positive TSTs from HIV-1$^+$ active TB patients.

(a) Frequency distribution of 1291 genes for which median expression was significantly increased by at least two-fold in HIV-1$^+$ TST$^+$ samples compared to saline controls. **(b)** Venn diagram demonstrating the overlap between genes significantly induced in active TB HIV-1$^-$ TST$^+$ vs. HIV-1$^+$ TST$^+$ samples (both in comparison to saline controls). **(c)** XY plot comparing median expression of all genes induced in either HIV-1$^-$ TST$^+$ or HIV-1$^+$ TST$^+$ biopsies. Linear regression showed a significant positive correlation between the two groups, with a slope of approximately 1, demonstrating broad conservation of the TST$^+$ response in HIV-1$^+$ active TB patients. Forty-four genes for which expression is significantly reduced by ≥ two-fold in HIV-1$^+$ TSTs are highlighted. Data presented are normalised microarray expression values. **(d)** oPOSSUM TFBS enrichment analysis of 10000bp upstream/downstream of the 44 attenuated genes. The X axis lists the number of genes enriched for a TFBS, and the Y axis displays significance by Z score.

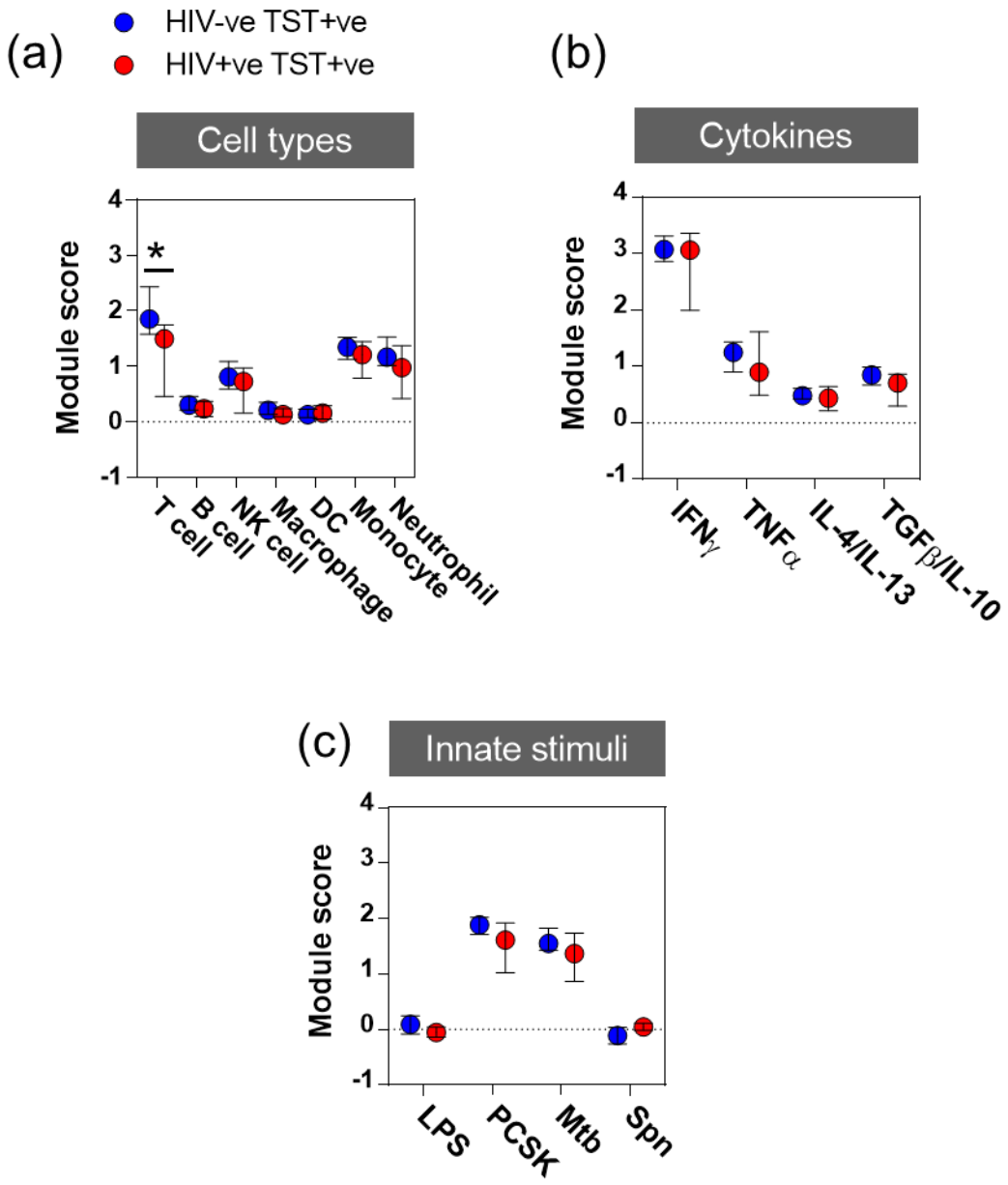

Figure 6.17: Modular analysis of gene expression profiles from HIV-1⁺ active TB patient positive TSTs.

Modular analysis of TST gene expression profiles from HIV-1⁻ TST⁺ and HIV-1⁺ TST⁺ samples. Module score represents the geometric mean expression of the module gene set in each TST gene expression profile, normalised to the saline control baseline, which is the median of the geometric mean module expression in all saline samples. Symbols represent group median module score and error bars represent interquartile range. The statistical significance of modular enrichment above the saline baseline was assessed using a Mann-Whitney test for differences in module expression between all TSTs and all saline (P<0.05). Mann-Whitney tests were also used to test for significant differences in module score between groups (* indicates P<0.05 between indicated groups). **(a)** All cell type modules were significantly enriched above salines in both groups. The T cell module was significantly more highly expressed in HIV-1⁻ TST⁺ samples. **(b)** All cytokine modules were significantly enriched above salines in both groups. **(c)** PCSK and Mtb modules were significantly enriched above salines in both groups.

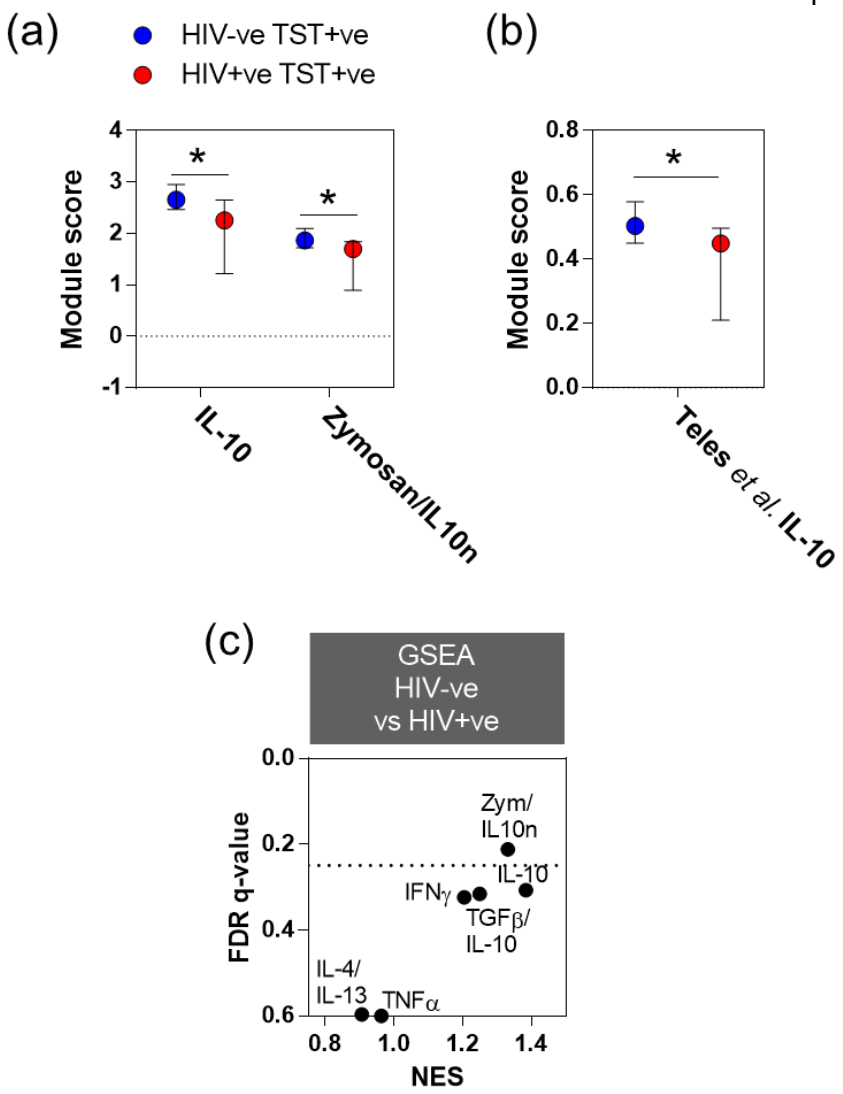

Figure 6.18: Attenuation of the IL-10 response in positive TSTs from HIV-1⁺ active TB patients.

Modular analysis of TST gene expression profiles from HIV-1⁻ TST⁺ and HIV-1⁺ TST⁺ samples. **(a, b)** Module score represents the geometric mean expression of the module gene set in each TST gene expression profile, normalised to the saline control baseline, which is the median of the geometric mean module expression in all saline samples. Symbols represent group median module score and error bars represent interquartile range. The statistical significance of modular enrichment above the saline baseline was assessed using a Mann-Whitney test for differences in module expression between all TSTs and all salines (P<0.05). Mann-Whitney tests were also used to test for significant differences in module score between groups (* indicates P<0.05 between indicated groups). **(a)** Expression of two IL-10 functional modules was significantly attenuated in HIV-1⁺ TST⁺ samples: an IL-10 inducible module (IL-10), a module made up of genes suppressed when IL-10 is neutralised in the context of zymosan-induced inflammation (zymosan/IL-10n). **(b)** Expression of an independently published IL-10 inducible module (Teles et al., 2013) was also attenuated in HIV-1⁺ TST⁺ samples. **(c)** Modular enrichment analysis of HIV-1⁻ TST⁺ biopsies compared to HIV-1⁺ TST⁺ samples performed using the GSEA algorithm. The dashed line indicates the threshold of statistical significance recommended for use for this algorithm. Although a number of modules were scored as enriched in HIV-1⁻ TST⁺ samples compared to HIV-1⁺ TST⁺ samples, only the zymosan/IL-10 n module was significantly enriched, and consequently assessed to be relatively attenuated in the HIV-1⁺ TSTs.

6.5.7 HIV-1$^+$ unmasking IRIS patients display accentuated Th2 responses in the TST

Within the HIV-1$^+$ active TB patient cohort, three patients were classified as undergoing an unmasking IRIS (group D in **Table 6.3**). Unmasking IRIS was defined as presentation with active TB within 2−8 weeks of commencing ARVs, consistent with published definitions (Haddow et al., 2009; Meintjes et al., 2008a). The immunopathology of unmasking IRIS remains incompletely understood (Lai et al., 2013), and so I used the TST samples collected from these patients as an opportunity to gain insights into anti-mycobacterial responses at the site of inflammation in IRIS.

All patients in this group had clinically positive TSTs (**Table 6.2**), and high histological inflammation scores (**Figure 6.3a, Figure 6.4**). IRIS TSTs showed statistically significant increases in expression of 2780 genes compared to saline controls (**Figure 6.19a**), representing an expanded response in comparison to HIV-1$^-$ TST$^+$ samples (**Figure 6.19b**). A direct comparison of all genes increased in IRIS or in HIV-1$^-$ TST$^+$ samples demonstrated that the responses were broadly concordant with significant correlation and covariance, but that 52 genes were statistically significantly increased ≥two-fold in expression in the IRIS group (**Figure 6.19c**). This gene list contained factors involved in driving Th2 immune responses, such as IL-13, IRF4, CCL26, CCL17 and CCL1 (Corren, 2013; Y. Gao et al., 2013; Gonzalo et al., 2007; Imai et al., 1999; Provost et al., 2013), and pathway enrichment analysis of this gene list showed overrepresentation for Th2 pathways such as IL-4 signalling and asthma (**Figure 6.19d**).

Upregulation of the Th2 response in IRIS patient TSTs was confirmed by modular analysis, which showed significantly increased enrichment for activity of the Th2 cytokines IL-4 and IL-13 in comparison to HIV-1$^-$ TST$^+$ samples (**Figure 6.20a**). All other cytokine-driven modules were similarly enriched between the groups, suggesting that Th1 responses driven by IFNγ or T-regulatory responses driven by TGFβ and IL-10 were not accentuated in the IRIS TSTs (**Figure 6.20b**). Additionally, T cell modular activity was not significantly enriched in IRIS TSTs above HIV-1$^-$ TST$^+$ samples (**Figure 6.20c**). Together, these observations suggest that the increase in Th2 activity in IRIS TSTs is not due to an overall broader T cell response than non-IRIS TSTs, but that a specific bias exists within a T cell response of similar magnitude. Activity of all

other modules tested was similar, with the exception of a significant but modest increase in DC module enrichment (**Figure 6.20a, c**); this could potentially also be involved in Th2 biasing, as a specific role for DCs in initiating this arm of immunity has recently been reported (Y. Gao et al., 2013). The Th2 bias in IRIS TSTs compared to HIV-1^- TST^+ samples was further confirmed in a separate modular assessment using the GSEA algorithm. This showed significant enrichment of the IL-4/IL-13 module in the IRIS samples (**Figure 6.20d**).

Th2-type inflammation was also evident in histological assessments of these samples. Upon H&E staining, infiltration of eosinophils, which are implicated in Th2 responses (Rothenberg and Hogan, 2006), was identified in all biopsy samples in the IRIS group, while it was only observed in 11% and 22% of the HIV-1^-TST^+ and HIV-1^+TST^+ groups respectively. Representative images of eosinophils present in IRIS biopsy sample H&E stains are shown in **Figure 6.21**.

Both gene expression and histological assessments at the site of inflammation in IRIS patients demonstrated a Th2 bias in the context of an otherwise typical TST^+ response. This may provide insight into the nature of the immunopathology which exacerbates TB disease in these patients.

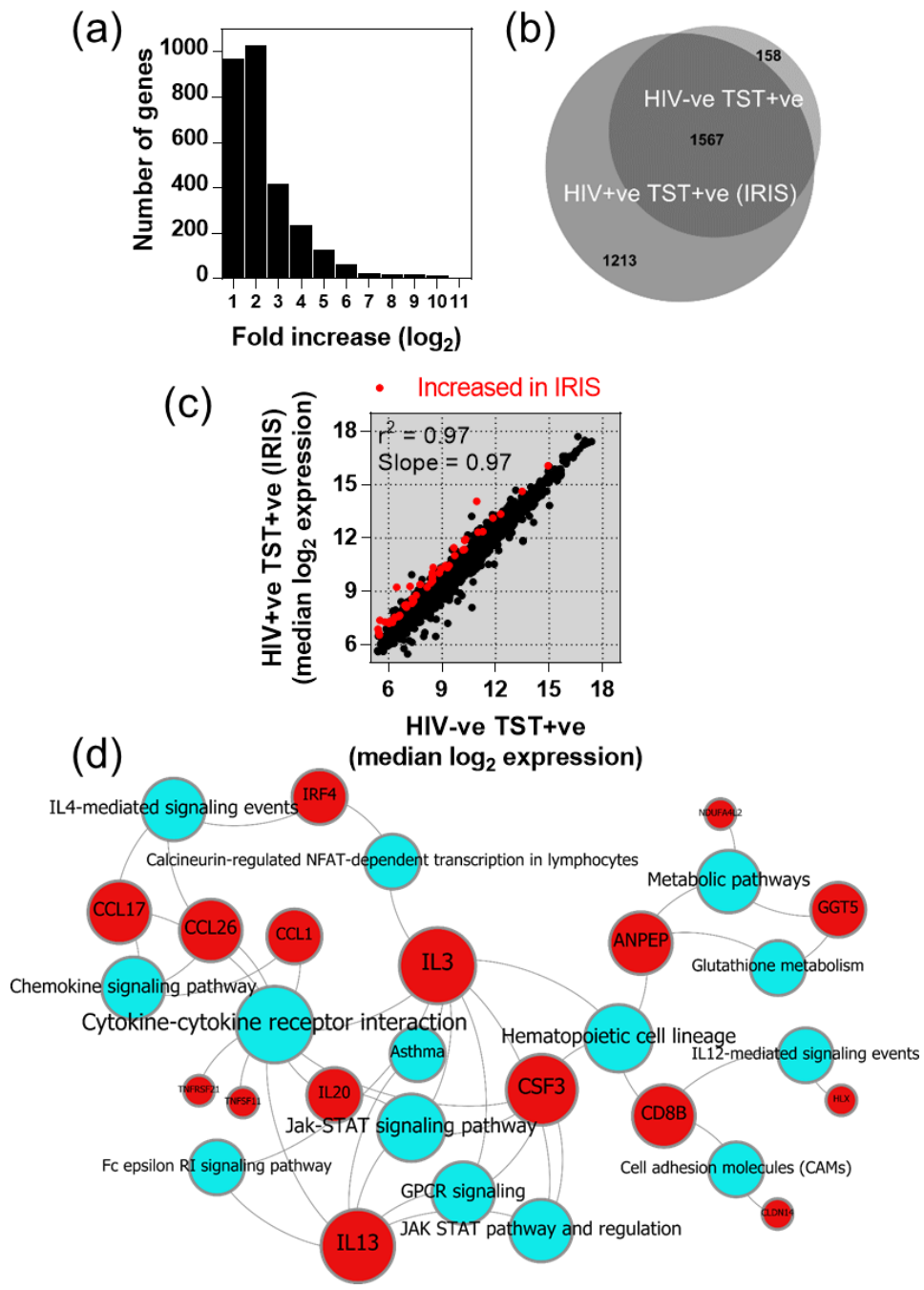

Figure 6.19: Gene expression profiling of positive TSTs from unmasking TB-IRIS patients.

(a) Frequency distribution of 2780 genes for which median expression was significantly increased by at least two-fold in HIV-1$^+$ TST$^+$ IRIS patient biopsies compared to saline controls. **(b)** Venn diagram demonstrating the overlap between genes significantly induced in active TB HIV-1$^-$ TST$^+$ vs. HIV-1$^+$ TST$^+$ IRIS biopsies (both in comparison to saline controls). **(c)** XY plot comparing median expression of all genes induced in either HIV-1$^-$ TST$^+$ or HIV-1$^+$ TST$^+$ IRIS biopsies. Linear regression showed a significant positive correlation between the two groups. Fifty-two genes for which expression is significantly increased by ≥ two-fold in IRIS biopsies are highlighted. Data presented are normalised microarray expression values. **(d)** Network visualisation of InnateDB (all curated databases) pathway enrichment analysis of the 52 genes for which expression was increased. All significantly enriched pathways in this gene set are shown (corrected P<0.05). Red nodes, pathways; blue nodes, genes; node size is correlated to number of network connections.

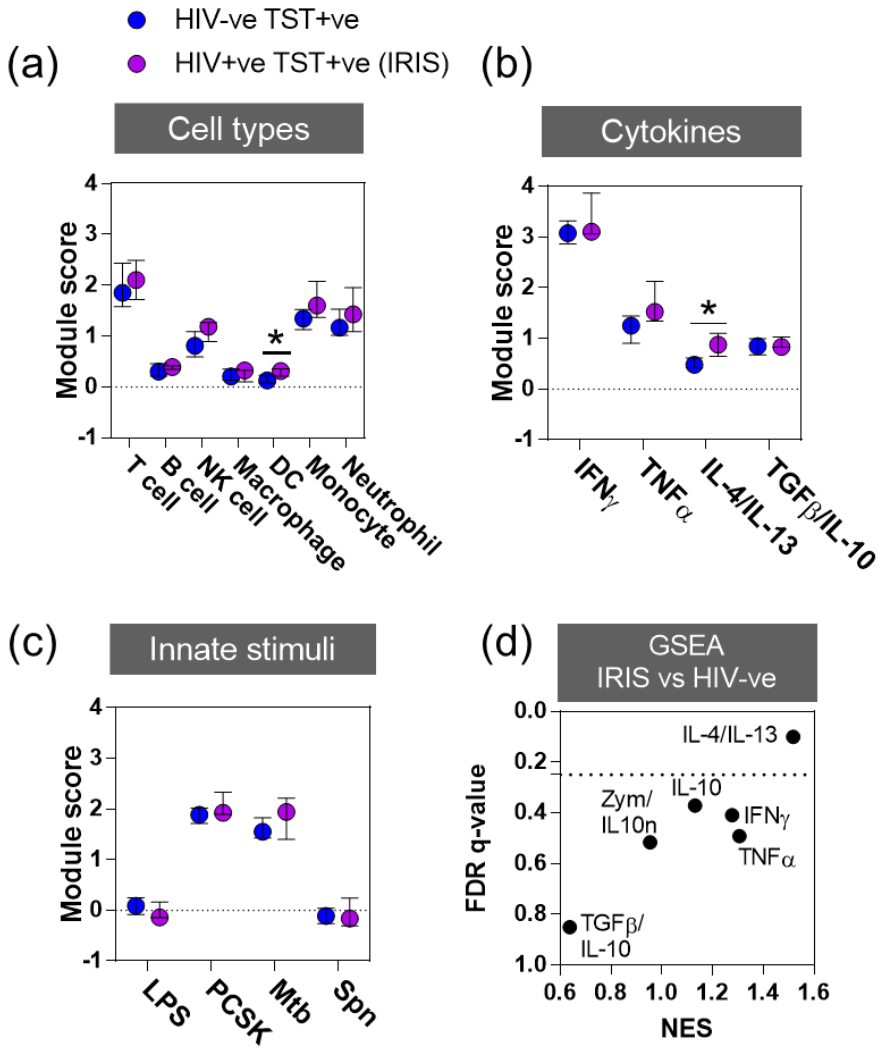

Figure 6.20: Modular analysis of gene expression profiles from unmasking TB-IRIS patients identifies increased Th2 responses.

Modular analysis of TST gene expression profiles from HIV-1$^-$ TST$^+$ and HIV-1$^+$ TST$^+$ (IRIS) samples. Module score represents the geometric mean expression of the module gene set in each TST gene expression profile, normalised to the saline control baseline, which is the median of the geometric mean module expression in all saline samples. Symbols represent group median module score and error bars represent interquartile range. The statistical significance of modular enrichment above the saline baseline was assessed using a Mann-Whitney test for differences in module expression between all TSTs and all salines (P<0.05). Mann-Whitney tests were also used to test for significant differences in module score between groups (* indicates P<0.05 between indicated groups). **(a)** All cell type modules were significantly enriched above salines in both groups. The DC module was significantly more highly expressed in HIV-1$^+$ TST$^+$ (IRIS) samples. **(b)** All cytokine modules were significantly enriched above salines in both groups. The IL-4/IL-13 module was significantly more highly expressed in HIV-1$^+$ TST$^+$ (IRIS) samples **(c)** PCSK and Mtb modules were significantly enriched above salines in both groups. **(d)** Modular enrichment analysis of HIV-1$^+$ TST$^+$ (IRIS) samples compared to HIV-1$^-$ TST$^+$ samples performed using the GSEA algorithm. The dashed line indicates the threshold of statistical significance recommended for use for this algorithm. Although a number of modules were scored as enriched in HIV-1$^+$ TST$^+$ (IRIS) samples compared to HIV-1$^-$ TST$^+$ samples, only the IL-4/IL-13 module was assessed as significantly enriched.

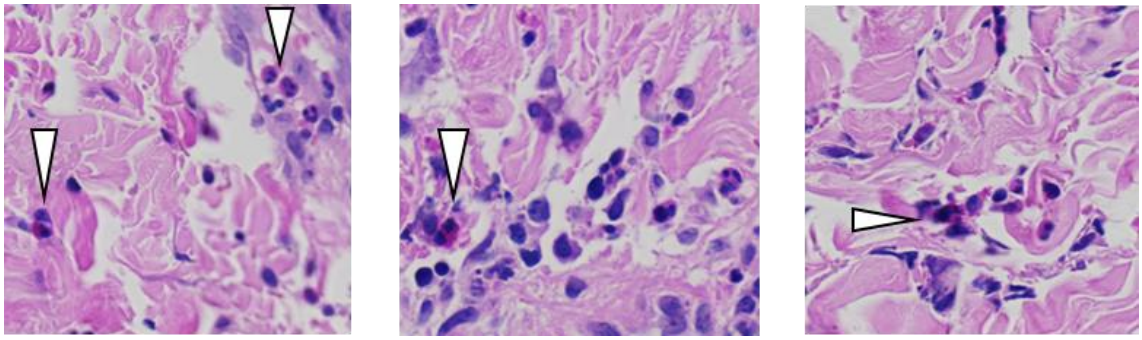

Figure 6.21: Eosinophilic infiltration in TST biopsies from IRIS patients.

Representative images of eosinophils from IRIS patient TST biopsy H&E stains. Each image is from a separate patient biopsy. Eosinophils, multinucleated cells staining highly positively for eosin (pink/purple), are indicated by white arrows.

6.5.8 Evidence for HIV-1 viral activity at the site of TST inflammation

Gene expression profiles of HIV-1^{+} active TB patient TSTs showed that HIV-1 was associated with multiple pathways of dysregulation compared to HIV-1^{-} TST responses. I was interested to determine whether HIV-1 was detectable at the TST site, as if so this might indicate that these phenotypes were a direct result of viral activity in the inflammatory milieu. This might include intracellular viral reservoirs in patients on ARVs, as the phenotypes described were not exclusive to patients with uncontrolled viral loads (VLs).

qRT-PCR for the HIV-1 LTR, a highly conserved viral sequence, was performed on TST RNA samples. This was detectable in a subset of TSTs (**Figure 6.22a**), which may either represent virus present in the TST tissue, or virus derived from blood contamination of the biopsy. In the latter scenario, it might be expected that HIV-1 LTR transcript would correlate with blood VL. A significant but weak positive correlation was found between the two measures (**Figure 6.22b**), although some patients with elevated VLs had undetectable TST virus, and one patient with a suppressed VL had a low level of TST viral transcript detectable. It is difficult to draw any conclusions from this data, as the weak correlation between TST LTR and VL is indicative that the LTR detectable may be derived from contaminating blood; further assessments are merited which would be less confounded by this issue, such as histological staining for HIV-1 proteins.

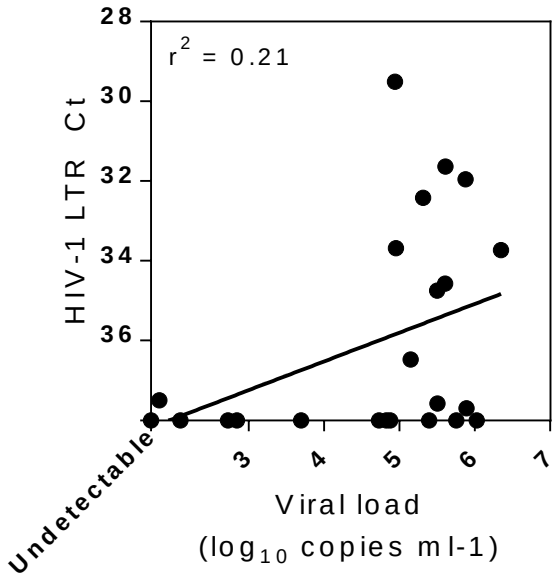

Figure 6.22: Investigating the presence of HIV-1 at the TST site.

qRT-PCR for the HIV-1 LTR demonstrates detectable HIV-1 transcript, expressed as HIV-1 LTR cycle threshold (ct) in which a lower value indicates higher levels of transcript, in a subset of biopsies, which showed a significant but weak positive correlation with peripheral blood HIV-1 viral load.

6.5.9 Molecular profiles of HIV-1 CMI dysregulation which are evident in the TST are not evident in the peripheral blood

Gene expression profiling of the immune response to TB *in vivo* has previously evaluated the peripheral blood, and insights into systemic immune activity have been gained via this method (Berry et al., 2010; Bloom et al., 2013, 2012; Cliff et al., 2013; Maertzdorf et al., 2012; Ottenhoff et al., 2012). I sought to assess whether the HIV-1-dysregulated phenotypes found in the TST were also evident in the peripheral blood. Cytokine-specific module expression was measured in peripheral blood gene expression profiles from samples which were collected contemporaneously with TST injection in the same patient cohort. Although all modules tested were statistically significantly enriched in TST^+ biopsy samples compared to saline controls, only a subset of modules were more highly expressed in active TB patient peripheral blood compared to healthy volunteer blood: IFNγ and type II IFN modules, and the IL-10 module (**Figure 6.23a−c**). This is hypothesised to reflect systemic immune activity resulting from active TB.

Some modules were differentially expressed in HIV-1^+ active TB peripheral blood compared to HIV-1^- patients. There was evidence for increased IFN signalling in HIV-1 infection, as the IFNγ, type I IFN and type II IFN modules were all significantly increased in expression in HIV-1^+ peripheral blood in comparison to HIV-1^- patients (**Figure 6.23a, b**). HIV-1^+ patients with anergic TSTs also had significant increased expression of the TNFα module, and significantly decreased expression of the TGFβ/IL-10 module (**Figure 6.23a**). These observations may be due to systemic immune activation in HIV-1^+ patients. Importantly, none of the phenotypes associated with HIV-1 infection in the TST were observed in the peripheral blood. Although type I IFN activity was increased in HIV-1+ patients, this was not specific to those with anergy (**Figure 6.23b**). Attenuation of IL-10 was not evident (**Figure 6.23c**). No IL-4/IL-13 (Th2) module expression was observed in any samples, including the IRIS patients ((**Figure 6.23a**). This suggests that these phenotypes are specific to the site of inflammation and are not evident in systemic immune activity as measured in the peripheral blood transcriptome.

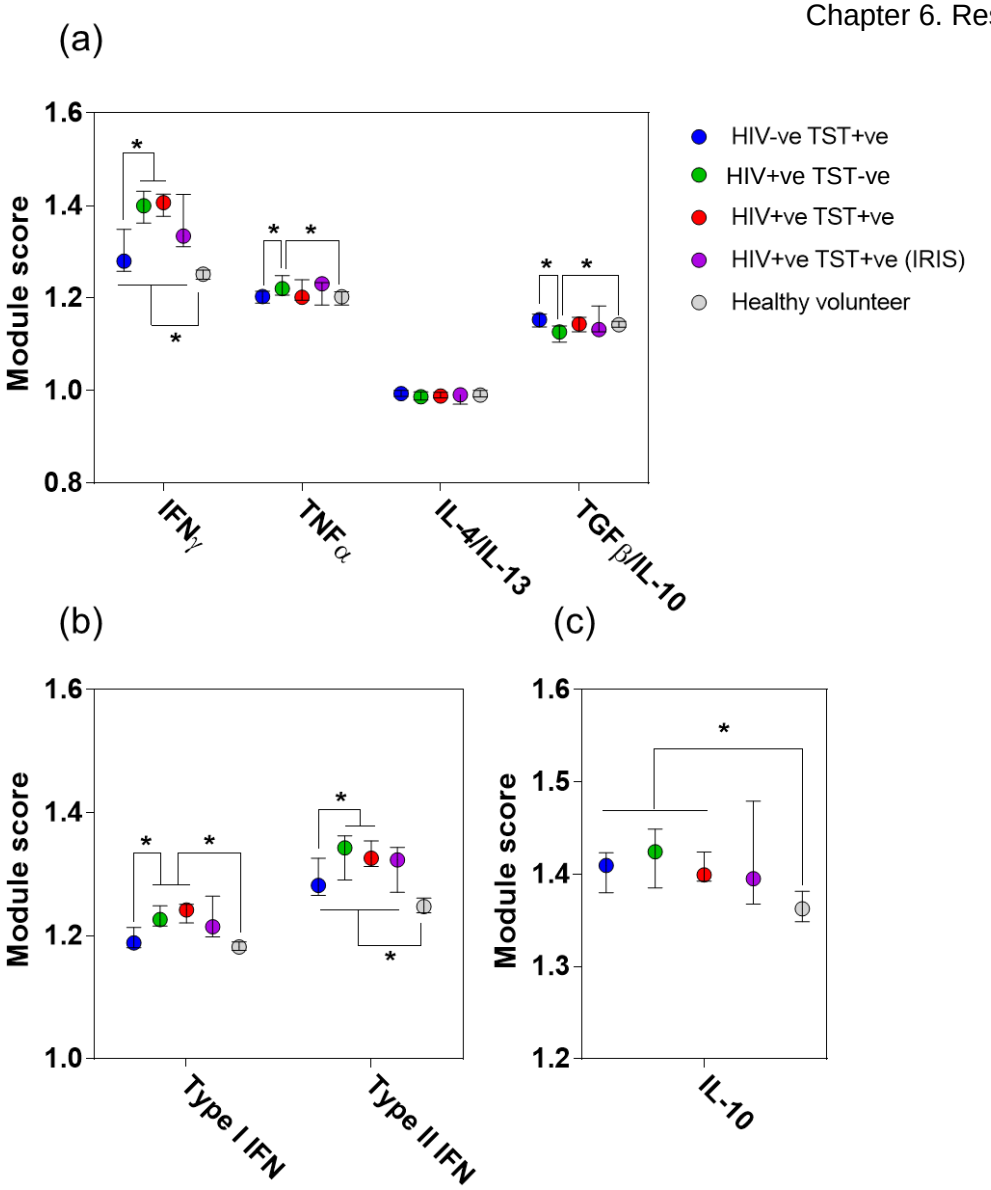

Figure 6.23: Modular analysis of peripheral blood transcriptional profiles from HIV-1⁻ and HIV-1⁺ active TB patients and healthy volunteers.

Modular analysis of peripheral blood gene expression profiles. Module score represents the geometric mean expression of the module gene set in each TST gene expression profile, normalised to the geometric mean expression of the entire genome. Symbols represent group median module score and error bars represent interquartile range. Mann-Whitney tests were also used to test for significant differences in module score between groups (* indicates $P<0.05$ between indicated groups). **(a)** The IFNγ module was significantly increased in expression in active TB patients compared to healthy volunteers, and significantly increased in expression in HIV-1⁺ patients compared to HIV-1⁻ patients. The TNFα module was significantly increased in HIV-1⁺ patients with anergic TSTs compared to HIV-1⁻ patients and healthy volunteers. The TGFβ/IL-10 module was significantly decreased in HIV-1⁺ patients with anergic TSTs compared to HIV-1⁻ patients and healthy volunteers. **(b)** The type I IFN module was significantly increased in expression in HIV-1⁺ patients compared to HIV-1⁻ patients and healthy volunteers. The type II IFN module was significantly increased in expression in active TB patients compared to healthy volunteers, and significantly increased in expression in HIV-1⁺ patients compared to HIV-1⁻ patients. **(c)** The IL-10 module was significantly increased in expression in active TB patients compared to healthy volunteers.

6.6 Chapter discussion

I have employed genome-wide transcriptional profiling of TST biopsy samples to gain insights into the function of CMI at the molecular level *in vivo*, and the pathways by which HIV-1 modulates this response. The TST^+ response was broadly consistent in active TB and in healthy individuals, but with some specific pathways upregulated which may represent active disease processes. Clinically negative TSTs were found to contain detectable responses, which were phenotypically divergent: healthy individual TST negativity displayed many features of the TST^+ response, while $HIV\text{-}1^+$ anergy showed a manifestly limited response with relative preservation of the type I IFN response. Positive TSTs from $HIV\text{-}1^+$ active TB patients had broad conservation of the TST response but with specific attenuation of activity of the anti-inflammatory cytokine IL-10. Finally, a Th2 response bias was identified in TSTs from $HIV\text{-}1^+$ unmasking IRIS patients.

Clinical TST responses in this cohort were broadly as expected. The frequency and disease correlates of anergic responses in $HIV\text{-}1^+$ individuals were consistent with previous reports in similar cohorts (Rangaka et al., 2007). Poor concordance was found between IGRA results and TST responses, which was again consistent with previous studies (Luetkemeyer et al., 2007; Rangaka et al., 2007). This observation highlights the potential value of studying anti-mycobacterial responses in a tissue setting, as the responses of peripheral blood cells are unlikely to be closely comparable. This is also shown by modular assessment of peripheral blood transcriptional profiles from these patients, in which the HIV-1-dysregulated phenotypes described in the TST were not evident by modular analysis.

Gene expression profiling of $HIV\text{-}1^-$ TST^+ samples from active TB patients confirmed the value of this approach in dissecting the CMI response at a systems level *in vivo*, consistent with the previous investigation in healthy volunteers (Tomlinson et al., 2011). A modular analysis strategy was used to gain further insights into the CMI response. Signatures of infiltration by a range of cell types were identified, and limited Th2 and T-regulatory responses were detected in the context of a dominant Th1 response. Importantly, Mtb-specific innate responses were enriched in comparison to those specific to other pathogens, confirming the utility of the TST as a model to study specific Mtb-induced inflammation.

Comparison of TST^+ samples from active TB patients with those from healthy individuals also lent confidence to utilising the TST as a challenge model in active TB patients, as it was not systematically confounded by active disease. However, the molecular resolution of the transcriptional approach allowed identification of a subset of genes with increased expression in active TB TSTs. Some of these have been implicated in TB pathogenesis, such as the matrix metalloproteinase MMP1 (Elkington et al., 2011) and anti-microbial peptides including a beta-defensin (Rivas-Santiago et al., 2006). This gene list was also enriched for inflammatory pathways such as integrin and complement activation. These observations suggest that although the TST response is broadly conserved in active TB, it may be used to gain disease-specific insights. Further such insights were gained from modular analysis showing decreased enrichment for the T cell-specific module, perhaps reflecting the relative lymphopenia which is observed in active TB patients (Beck et al., 1985).

Anergic TST responses, i.e. those in which patients fail to react to PPD despite having active TB and so presumably having Mtb antigenic memory, were found in 54% of the HIV-1^+ patients in this cohort, and similarly to previous reports (Cobelens et al., 2006), I found TST responsiveness to be an "all-or-nothing" phenomenon: i.e. responses were clearly positive (≥10mm induration) or completely negative, with no intermediate "weak" TST responses. This clinical observation presents the hypothesis that TST anergy in these individuals is due to a specific failure to generate any inflammation whatsoever, rather than being a diminishment in the inflammatory response due to immunosuppression. Gene expression profiling of HIV-1^+ anergic TSTs lent considerable support to this hypothesis. Comparison with TST^+ samples from HIV-1^- active TB patients showed a detectable but strikingly limited response in the anergic TSTs. This differed from observations in healthy individual TST^- samples, which despite being clinically identical to anergic responses contained a much broader gene expression response. Further comparisons between HIV-1^+ anergic TSTs and healthy individual negative TSTs confirmed that TST anergy was molecularly distinct from TST negativity. Anergic TSTs had little evidence of cellular infilitration or inflammatory activity, both of which were demonstrated in the healthy TST^- individuals. Further evaluations showed that the limited response in the HIV-1^+ anergic TSTs was dominated by a relatively preserved type I IFN response. This response was also present in its entirety in TST^+ samples. This confirms that type 1 IFN responses are evident at the tissue level in human anti-mycobacterial responses, consistent with previous reports derived from analysis of peripheral blood (Berry et al., 2010).

Interestingly, these can be invoked by PPD alone, which suggests that mycobacterial components without live bacterial replication are sufficient to induce a type I IFN response *in vivo*.

Observation of this type I IFN response in the absence of other inflammation in HIV-1$^+$ anergic TSTs raises two questions: firstly, what cells or mechanisms are generating this response, and secondly, what consequences might this phenotype have for TB pathogenesis in these individuals? As there appears to be an absence of any cellular influx in these samples, I hypothesise that the response is being generated by tissue-resident sentinel cells such as macrophages. In terms of the consequences for TB pathogenesis, there has recently been considerable interest and supportive assessment of the hypothesis that type I IFN is immunosuppressive and compromises control in tuberculosis and other mycobacterial infections (Manca et al., 2001; Mayer-Barber et al., 2011; Redford et al., 2014; Stanley et al., 2007; Teles et al., 2013). This suggests that this presence of this response in itself might be functionally implicated in the anergic failure to generate inflammation. At the site of disease, failure to generate an effective CMI response in HIV-1$^+$ individuals may lead to poor granulomatous organisation and uncontrolled bacillary replication (Lawn et al., 2002). This phenotype may be analogous to lepromatous lesions in leprosy, in which the failure of host immunity leads to uncontrolled bacillary replication and disease - a process which has been shown to be driven by type I IFN (Teles et al., 2013). My identification of type I IFN responses at the site of CMI anergy in HIV-1$^+$ individuals thus presents a novel hypothesis for the mechanism of anergy and associated poor clinical outcomes in these patients (Moreno et al., 1993), and lends further support to the notion that type I IFNs compromise control of mycobacteria *in vivo*.

Assessment of the site of inflammation in HIV-1$^+$ TST$^+$ active TB patients showed broadly typical TST responses in these individuals, with a specific deficiency in activity of the immunoregulatory cytokine IL-10. As it has been shown that human MDMs infected with HIV-1 *in vitro* display attenuated IL-10 responses to Mtb as a direct result of viral infection (Tomlinson et al., 2014, **Chapter 3**), this observation suggests that this phenomenon may also occur *in vivo*. A clear hypothesis for the mechanism of this phenotype within the TST is suggested by my experimental data - that IL-10 responses are inhibited in either tissue-resident macrophages or recruited monocyte-derived macrophages which are infected with HIV-1. Both my cellular module assessments and a previous report (Liang et al., 2013) indicate that recruitment of monocytes/APCs to

the TST is non-defective in HIV-1$^+$ individuals, meaning the latter scenario is plausible. However, if this is a specifically macrophage-driven phenomenon, 48 hours is likely to be an insufficient timeframe for differentiation of infiltrating monocytes into macrophages. Additionally, the burden of HIV-1 infection within the circulating monocyte population is thought to be extremely low (Spear et al., 1990). However, multiple reports have demonstrated HIV-1 infection in tissue macrophages *in vivo*, and so attenuated IL-10 responses generated by these cells as a mechanism for this phenotype is plausible (Cao et al., 1992; Jambo et al., 2014; Jarry et al., 1990; Koenig et al., 1986).

The potential consequences of attenuated IL-10 responses for TB pathogenesis *in vivo* in HIV-1$^+$ individuals are numerous. Previous *in vitro* data highlighted that deficiency in the innate immunoregulatory functions of IL-10 may lead to exacerbated pro-inflammatory responses, which have the potential to increase immunopathology and tissue damage (Tomlinson et al., 2014; **Chapter 4**). IL-10 also plays key roles in regulating apoptosis and promoting resolution of inflammation (Eslick et al., 2004; Ogawa et al., 2008; Zhou et al., 2001), and dysregulation of these processes could have consequences for the effective containment of Mtb within a protective fibrotic granuloma structure (Lin et al., 2014).

Finally, in HIV-1$^+$ active TB patients classified as undergoing an unmasking IRIS, I used gene expression profiling to identify a Th2 bias in the context of otherwise conserved CMI responses in the TST. Although this observation was made in a small patient cohort, it was statistically consistent and confirmed via both modular analysis of gene expression profiles and histopathological assessments.. Previous investigations of immunopathological mechanisms in IRIS have associated expanded polyfunctional T cell populations and hypercytokinaemia with the syndrome (Mahnke et al., 2012; Meintjes et al., 2008b; Tadokera et al., 2011), but I am aware of no previous reports specifically suggesting a role for Th2 responses. Some reports exist describing a systemic Th2 bias in HIV-1$^+$ individuals including in patients on HAART (Hagiwara et al., 1996; Meroni et al., 1996; Sindhu et al., 2006), which may contribute. Th2 responses represent an entirely distinct mode of immunity to the Th1 response which is classically protective in TB (Anthony et al., 2007; Jenkins et al., 2011; Voehringer et al., 2004), and so it may be suggested that this is a non-protective bias detected at the site of inflammation in IRIS. In support of this, corticosteroids have been shown to be effective in treating TB IRIS (Meintjes et al., 2012), and these agents are also widely used

clinically to treat Th2-associated conditions such as asthma. However, further confirmation of whether this phenotype exists *in vivo* in a wider cohort of patients is necessary before its potential consequences can be properly delineated.

Identification of these three dysregulated phenotypes at the site of anti-mycobacterial inflammation in HIV-1$^+$ active TB patients posed the question of whether virus could be detected in the TST samples, which might suggest that these phenotypes were due to some direct effects of the virus in the inflammatory context. Although viral transcript was detected in a subset of TST samples, it could not be definitively concluded that this was not due to bloodborne virus from contaminating blood. As such, there remains a lack of conclusive evidence as to whether HIV-1 is directly causing these phenotypes at the site of inflammation, or whether they are a result of some systemic effects of HIV-1 infection. Further assessments of whether HIV-1 infected cells are present in the TST reaction site are merited, for example by immunohistochemical staining of HIV-1 proteins, or by fluorescence *in situ* hybridisation for HIV-1 RNA, as has recently been successfully used to quantify infection in AMs *ex vivo* (Jambo et al., 2014).

To further investigate the phenotypes identified here, it may be informative to assess TST inflammation in similar patient cohorts at earlier and later time-points post-TST, as further temporal resolution might elucidate the mechanisms driving these phenotypes and characterise their consequences. For example, identifying at what stage post-TST the type I IFN response develops in HIV-1$^+$ anergy might be illustrative as to what cells generate this response and by what mechanism. Evaluation of TST inflammation in HIV-1$^+$ TST$^+$ samples at later time-points may assist in exploring the functional outcomes of IL-10 deficiency in terms of inflammation and resolution. Finally, confirmation of these phenotypes in samples from the site of TB disease is warranted, although methods for this which are sufficiently controlled to allow detailed cross-group comparisons need to be identified.

By using the TST as an *in vivo* human challenge model, I have identified multiple pathways through which HIV-1 may exert detrimental modulatory effects on anti-mycobacterial CMI. How does elucidating these phenotypes aid our ability to effectively combat active TB in HIV-1$^+$ individuals? Understanding the divergent nature of TB disease in this heterogeneous high-risk group may potentially aid diagnosis and treatment, particularly as strategies for targeted immunotherapeutics in human TB begin to be elucidated (Mayer-Barber et al., 2014; Tobin et al., 2012). Understanding

the fundamentals of immunopathogenesis in active TB, including in the context of HIV-1 co-infection, is essential if such strategies are to be widely employed successfully, and characterising anti-mycobacterial CMI *in vivo* is an important step forward in this regard.

Chapter 7. Discussion

7.1.1 Modulation of CMI by HIV-1

HIV-1 pathogenesis is characterised by immune and inflammatory dysfunction. The two key components of the CMI response, $CD4^+$ T cells and macrophages, are direct targets for infection by HIV-1. The effects that the virus has on these cells, as well as its other pleiotropic effects on immunity, has the potential to disrupt the function of this arm of the immune response. I have investigated how HIV-1 modulates CMI, firstly by using an *in vitro* model of human MDMs, and secondly by using an *in vivo* human challenge model, the TST.

7.1.2 Dysregulation of IL-10 responses by HIV-1

I have shown that HIV-1 infection of human MDMs *in vitro* inhibits production of the immunomodulatory cytokine IL-10 in response to innate immune stimulation, and that this is a consequence of integration by HIV-1 and expression of viral components. Importantly, IL-10 attenuation was also observed *in vivo*, in positive TST reactions from $HIV\text{-}1^+$ active TB patients. This suggests that this phenomenon is a novel host-virus interaction which may have physiologically significant consequences. Further confirmation of its role *in vivo*, elucidation of the mechanism which causes it and delineation of its consequences are priorities for further investigation. These will be necessary in evaluating any potential for targeting this phenotype therapeutically in HIV-1 associated co-infections.

The *in vitro* experiments presented here showed that IL-10 attenuation was context-specific and, of the cells tested, occurred only in monocyte-derived macrophages differentiated with M-CSF. This phenotype was confirmed *in vivo* in the TST via bioinformatic and modular evaluations of gene expression data, but although transcriptional profiling can provide highly multidimensional insights into immune responses, it does not facilitate direct identification of the cellular basis of a phenotype. Moreover, appropriate markers to evaluate IL-10 attenuation in paired histological samples were not available. Identification of the cell types *in vivo* wherein HIV-1 attenuates IL-10 responses therefore remains a priority. The most useful insights may be gained by studying mononuclear phagocytic cells from $HIV\text{-}1^+$ patients, and most importantly tissue-resident macrophages. It has recently been confirmed that alveolar macrophages (AMs) are infected with HIV-1 *in vivo* (Jambo et al., 2014), and so a key

investigation may be to obtain AMs from HIV-1$^+$ patients and evaluate their ability to mount IL-10 responses to Mtb and other clinically important pathogens.

Investigating site-of-disease samples may also be informative: it should be noted that substantially lower IL-10 levels in comparison to HIV-1$^-$ individuals have been measured in cerebrospinal fluid from TB meningitis cases (Simmons et al., 2006). Further investigations could utilise pleural fluid, BAL or other accessible site-of-disease samples to further confirm this phenotype. Systemically attenuated IL-10 levels in HIV-1$^+$ patients have not been reported; conversely, raised systemic IL-10 has been identified in HIV-1 infection (Arias et al., 2010; Brockman et al., 2009). However, this may be part of the generally raised cytokine levels which are associated with HIV-1 infection (Kedzierska and Crowe, 2001), and thus non-intuitively be originally due to a deficiency of early-response IL-10, causing a defective anti-inflammatory response and thus heightened inflammation. The model suggested by my *in vitro* data points to tissue-resident cells generating this phenotype early in the innate immune response, so it is conceivable that it will not be evident at steady state in the peripheral blood. This is also evidenced by assessment of peripheral blood transcriptional profiles from active TB patients, wherein expression of an IL-10 module was detected, but was not affected by HIV-1 co-infection.

As well as evaluating the presence of IL-10 attenuation by HIV-1 *in vivo*, further investigation of the mechanism of this phenotype is merited. I have shown that integration by HIV-1 is necessary for IL-10 attenuation, and have begun to delineate which viral proteins are involved. Further virological experiments should demonstrate which components of the virus are necessary and sufficient for this phenotype. This may also provide insight into the host pathways which are affected, but to this end I have identified a strong candidate in the PI3K pathway, and assessments of its function in HIV-1 infected MDMs may also assist in elucidating the mechanism of IL-10 attenuation. The experiments presented here indicate that HIV-1 inhibits IL-10 expression by modulating conserved innate immune signalling pathways involved in IL-10 induction, and so systems-level assessment of the activation of these pathways using phosphoproteomics may also be informative.

Identifying the consequences of attenuated IL-10 responses may inform our understanding of the immunopathogenesis of HIV-1 disease and associated co-infections. I have demonstrated that IL-10 attenuation potentiates HIV-1 replication in an inflammatory setting. Induction of HIV-1 replication by inflammatory pathways is

consistent with previous *in vitro* reports (Garrait et al., 1997; Hoshino et al., 2002; Poli et al., 1994, 1990; Ranjbar et al., 2009) and *in vivo* observations in TB disease (Collins et al., 2002; Nakata et al., 1997; Toossi et al., 2001a; Toossi et al., 2001b). As previous investigations have shown that IL-10 attenuation is associated with exacerbated pro-inflammatory responses (Tomlinson et al., 2014), this strongly supports the hypothesis that HIV-1 may attenuate IL-10 to promote its own replication in an inflammatory microenvironment, by eliminating IL-10-mediated immunosuppression. I have also shown that IL-10 neutralisation in the innate inflammatory response leads to increased recruitment of T cells, indicating a further pathway by which HIV-1 might promote its own propagation by inhibiting IL-10, via inducing recruitment of potential host cells. Investigating whether HIV-1 itself alters recruitment of T cells to inflammatory foci via IL-10 attenuation, and investigation of the relationship between this phenotype and cell-to-cell transfer of virus, may help confirm these hypotheses with regard to viral propagation.

To gain insight into the consequences of IL-10 attenuation for the function of the immune system, I carried out a series of experiments to investigate the role of IL-10 in modulating macrophage function. These experiments showed that IL-10 has a range of modulatory effects in the innate immune response, as opposed to being a purely immunosuppressive factor, and highlighted some key IL-10-regulated pathways which merit further investigation in the context of HIV-1 infection of macrophages. These included cell recruitment to inflammatory foci, as discussed above, and regulation of pro-inflammatory cytokine production, as previously investigated (Tomlinson et al., 2014). Exploration of two further pathways may also be informative.

Firstly, IL-10 regulates the production of secreted factors which control cell differentiation and polarisation. These include M-CSF and GM-CSF, which may regulate monocyte differentiation, and IL-12 p40, which regulates Th1 cell differentiation. Confirmation of whether attenuation of IL-10 by HIV-1 leads to dysregulation of these cell differentiation pathways may characterise effects of the virus on these key cells of cell-mediated immunity. Monocytes/macrophages and Th1 cells are the major constituents of the site of TB disease, the granuloma. Elucidating how HIV-1 modulates the phenotype of these cells, and hence the phenotype of the granuloma, may assist in identifying how HIV-1 exacerbates TB pathology during co-infection (Diedrich and Flynn, 2011; Lawn et al., 2002). To this end, evaluating the

outcomes of IL-10 attenuation and associated phenotypes using developed *in vitro* models of granulomata may be informative (Puissegur et al., 2004).

A second pathway regulated by IL-10 was apoptosis, consistent with previous reports describing IL-10 as an anti-apoptotic factor (Eslick et al., 2004; Zhou et al., 2001). Modulation of this function via HIV-1 attenuation could potentially contribute to macrophage cell death; this again could severely impact on granuloma function, and hence exacerbate TB disease in HIV-1$^+$ individuals. Increased cell death *in situ* has been observed in the pleural fluid of HIV-1$^+$ pleural TB patients in comparison to HIV-1$^-$ patients, particularly among mononuclear phagocytes (Hirsch et al., 2001), as has increased necrosis in pleural granulomata in HIV-1+ patients (Bezuidenhout et al., 2009). These observations suggest that exploration of the effects of HIV-1 on cell death *in vitro* is warranted, and any role of IL-10 in this.

As well as further exploring the consequences of IL-10 attenuation using *in vitro* models, the fact that this phenotype is evident in the TST challenge model provides a valuable *in vivo* opportunity to study its consequences. Characterising the TST response at later time-points in HIV-1$^-$ and HIV-1$^+$ TST$^+$ samples, for example at 1 week post-TST, may elucidate whether functional deficiency of IL-10 impairs resolution of inflammation – a described function of IL-10 (Aggarwal et al., 2014; Tabas, 2010). It may also be possible to utilize recently developed animal models of HIV-1 infection for further *in vivo* investigations, such as humanized mice (Calderon et al., 2013; Marsden et al., 2012; Sun et al., 2007) or macaque models of HIV-1/Mtb co-infection (Diedrich et al., 2010; Mattila et al., 2011).

7.1.3 Other axes of CMI dysregulation by HIV-1

In addition to identifying IL-10 attenuation by HIV-1 in an *in vivo* inflammatory setting, I used the TST human challenge model to identify two further phenotypes of HIV-1 dysregulation of CMI responses. Firstly, in HIV-1$^+$ patients with anergic TST responses, I showed that there was relative preservation of the type I IFN response in the absence of any other effective inflammation, and that this phenotype was molecularly distinct from negative TST responses in healthy individuals. This observation may help elucidate the mechanism of anti-mycobacterial anergy in HIV-1$^+$ individuals, particularly in the light of recent reports that type I IFN responses are damaging and immunosuppressive in mycobacterial disease (Mayer-Barber et al., 2014; Teles et al., 2013). To consider the effect this phenotype might have on TB

immunopathology, comparisons may be drawn with reports that the site of TB disease in severely immunosuppressed HIV-1$^+$ individuals is characterised by a paucity of CMI response (analogous to anergy) and a preponderance of replicating bacilli (de Noronha et al., 2008; Lawn et al., 2002; Nambuya et al., 1988). This suggests that anergy could promote TB disease via uncontrolled mycobacterial replication. Confirmation of whether type I IFN responses exist at disease sites, in a similar fashion to the TST model, may implicate them in this mechanism, along with *in vitro* evaluations of whether type I IFN can suppress CMI responses and mycobacterial killing. Consideration of how HIV-1 might mechanistically cause this anergic phenotype is also merited.

A second phenotype identified using the TST challenge model was that of exaggerated Th2 responses detectable at the site of CMI in HIV-1$^+$ patients classified as undergoing an unmasking IRIS. Further confirmation of this phenotype using the same model in further IRIS patients is warranted, as this finding was made in a limited cohort of patients. Additionally, it will be valuable to explore whether it is evident at the site of TB disease, if appropriate sampling opportunities are available. A mechanism is not clear for how HIV-1 would cause exaggerated Th2 responses, or how these would lead to exacerbated presentations of active TB in IRIS patients. If this phenotype is further confirmed *in vivo*, this may therefore be another potential avenue for investigation.

7.1.4 The impact of HIV-1 on TB disease

Two major models have emerged recently which have enhanced our understanding of the development and pathogenesis of mycobacterial disease. Firstly, the “Goldilocks effect”, in which either too little or too much inflammation can compromise protection and lead to immunopathogenesis. This is supported by evidence from the *M. marinum* zebrafish model, in which the magnitude of TNFα production can determine disease outcome (Roca and Ramakrishnan, 2013; Tobin et al., 2012), and from studies of human and mouse mycobacterial infections, in which a balance between inflammatory IL-1 or adaptive IFNγ responses and immunosuppressive type I IFN responses has been shown to be critical in mycobacterial control (Mayer-Barber et al., 2014; Teles et al., 2013). Secondly, although it has long been assumed that the function of the granuloma is central to Mtb control (Davis and Ramakrishnan, 2009), recent studies have demonstrated that the

dynamic and heterogeneous host/pathogen interactions which take place at the level of the single granuloma are critical in determining the clinical outcome of TB infection, particularly with regard to the granuloma stability and the degree of bacillary killing which occur in each lesion (Lin et al., 2014). Integrating these two models defines our current understanding of Mtb control and pathogenesis, in which the quantity and quality of inflammation at each site of infection has the potential to determine the systematic outcome of disease, via effects on bacterial killing and local tissue integrity.

By considering how the modulatory effects of HIV-1 on CMI described in this thesis might impact on this model, ways by which I have shown HIV-1 may compromise Mtb control are summarised (**Figure 7.1**). Dysregulation of IL-10 responses, in granulomata containing HIV-1-infected mononuclear phagocytes, may generate a nidus of exaggerated inflammation, which has the potential to compromise granuloma integrity, exacerbate symptoms and lead to excessive cell death. The exaggerated Th2 responses seen in IRIS patients may similarly contribute to exaggerated inappropriate inflammatory phenotypes which compromise granuloma function. Conversely, HIV-1 anergy at the site of disease, in which type I IFNs may potentially be implicated, may lead to active disease via the failure to generate an effective CMI response and subsequent uncontrolled bacillary replication. These stochastic events caused by HIV-1, which alter the functionality of individual granulomata, may convert sites of Mtb control to sites of uncontrolled replication and inflammation, and hence lead to development of clinical TB disease. Further work is required to confirm these proposed interactions and to delineate their mechanisms.

A body of previous data describes how the IL-10 response in TB is damaging, and compromises control of the pathogen by suppressing effective immune responses (Redford et al., 2011). Additionally, it is proposed that some of the immunosuppressive effects of type I IFN are in fact mediated by induction of IL-10 (Mayer-Barber et al., 2011; Teles et al., 2013). These findings are in conflict with the model presented here, as I propose that IL-10 deficiency is a pathway by which HIV-1 increases risk of TB disease. However, it should be pointed out that these observations have mainly been made out with the context of HIV-1 infection. The pleiotropic effects of HIV-1 on immunity may alter the outcomes of IL-10 deficiency. Additionally, another “Goldilocks effect” may be in evidence, wherein too much or too little IL-10 can lead to aberrant immune processes, and IL-10 attenuation by HIV-1 leads to the latter scenario.

TB disease clearly has an altered phenotype in HIV-1^{+} individuals, wherein profound loss of control of the pathogen is evident in disseminated disease and mycobacteraemia (Domoua et al., 1995; Elliott et al., 1993; Gilks et al., 1990; von Reyn et al., 2011), as well as in altered inflammatory phenotypes such as IRIS (Lawn et al., 2008). Modulation of CMI by HIV-1, which I have shown may include IL-10 attenuation, is likely to contribute to these processes. Further molecular characterisation of aberrant immune phenotypes in human tuberculosis *in vivo*, in HIV-1+ individuals and in other contexts, is necessary to fully elucidate the contribution of risk factors, genetics and immunology to this phenotypically heterogeneous disease.

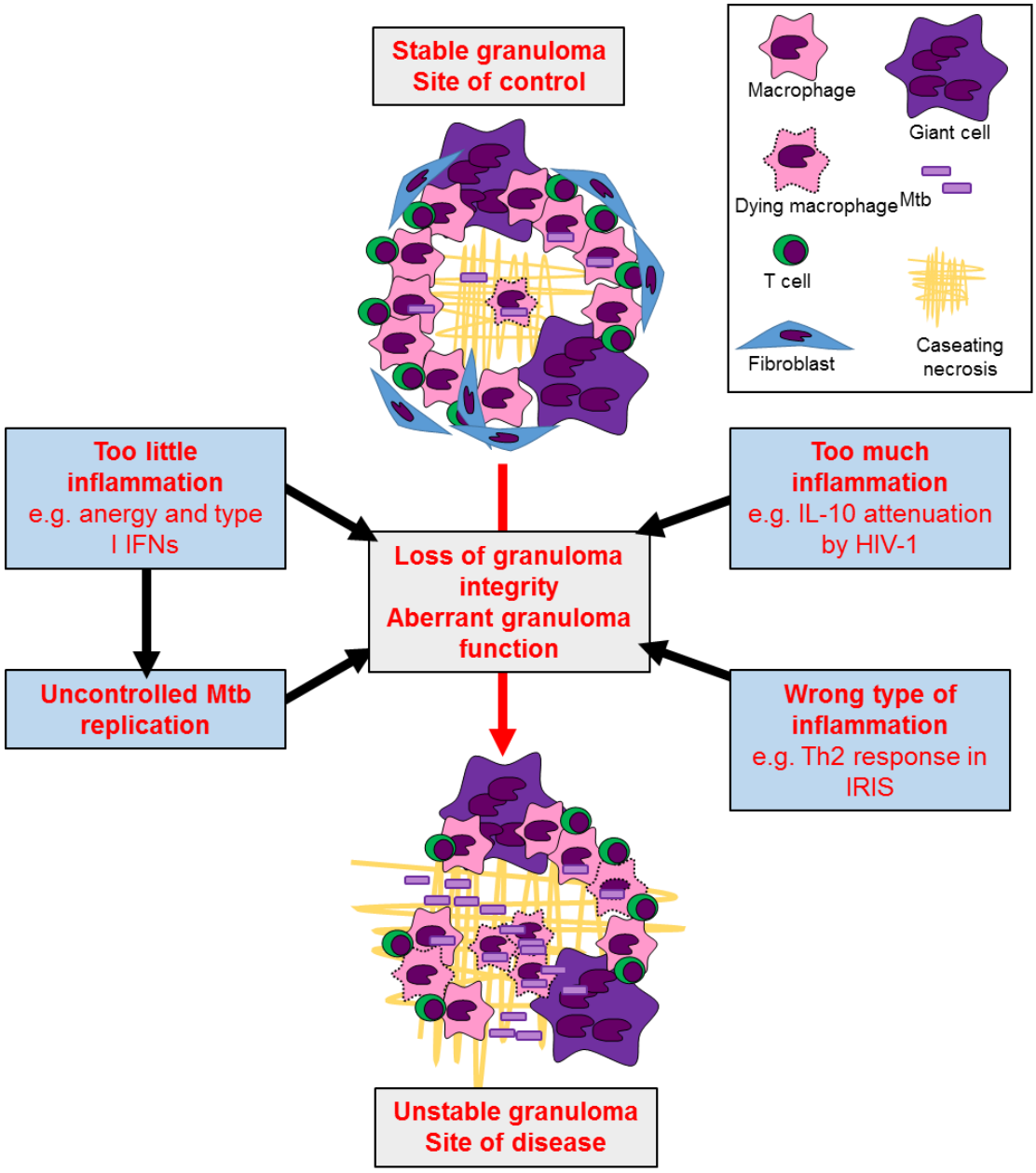

Figure 7.1: HIV-1 modulation of the CMI response to Mtb may contribute to granuloma instability.

Stable granulomata are hypothesised to be a site of an effective CMI response co-ordinated by macrophages, giant cells and T cells, in which mycobacteria and associated necrotic processes are contained by these cell types and recruited fibrotic processes (Ulrichs and Kaufmann, 2006). Progression to granuloma instability, in which there is uncontrolled mycobacterial replication and increased necrosis, is postulated to increase the risk of clinical TB disease (Lin et al., 2014). This schematic summarises the contribution of different inflammatory processes to granuloma deterioration, and wherein the effects of HIV-1 on CMI described in this thesis may contribute to this.

7.1.5 Potential for restoring functional CMI in HIV-1 infection

HIV-1 infected macrophages may represent a long-lived reservoir of viral infection (Gendelman et al., 1989; Groot et al., 2008). This indicates that HIV-1 modulation of CMI which results from macrophage infection may persist in the context of ART, hence potentially providing insight into immune and inflammatory dysfunction post-ARVs, such as IRIS. ARVs are highly effective in reducing mortality in HIV-1^+ patients (The HIV-CAUSAL Collaboration, 2010). In treating aspects of disease which persist despite their use (Palella et al., 2006) - or in the case of IRIS, because of it – understanding how HIV-1 modulates CMI may suggest potential therapeutics targeting immune processes dysregulated by the virus. These may also be therapeutic options in the context of ARV treatment failure. The mechanism of IL-10 attenuation, if elucidated, may be one such target. Exaggerated Th2 responses in IRIS, if confirmed to be pathogenic, are a clear opportunity for intervention due to the range of effective therapies available for treating Th2-mediated diseases such as allergy and asthma. In fact, as there is some evidence for using corticosteroids in the treatment of IRIS (Meintjes et al., 2012), it is possible that this pathway is already being targeted therapeutically.

7.1.6 Insights into the normal function of the cell-mediated immune system

Understanding pathological processes can provide insights into normal physiology, and the effects of HIV-1 on CMI described in this thesis provide some insights into the basic biology of this system. While investigating a mechanism by which HIV-1 might inhibit IL-10 but not pro-inflammatory cytokine production, a specific role was identified for the PI3K pathway in regulating IL-10 and not pro-inflammatory cytokine production. This may be a critical mechanism by which the host mounts appropriate immune responses to pathogenic and non-pathogenic microbes, as reported in the murine system (Ivanov and Roy, 2013), and as such further investigation is merited of how this pathway functions in human macrophages.

I have also specifically evaluated some functions of the cell-mediated immune system out with the context of HIV-1 infection. I used transcriptional profiling to explore how IL-10 regulates macrophage-mediated immune responses, showing that it might exert its most potent effects in modulating the innate response, while not inhibiting macrophage responses to IFNγ. This is in conflict with a prevalent concept in the field that IL-10 can inhibit protective IFNγ responses (O'Garra et al., 2013). Although a large

body of work exists describing the functions of IL-10, this highlights that many aspects of the biology of this immunomodulatory cytokine remain uncharacterised or controversial. Further work to clarify its precise functions is merited, particularly as it has been postulated to be a therapeutic target (O'Garra et al., 2008)

I also used transcriptional profiling to explore macrophage plasticity in the context of differentially polarised T cell responses, and showed that cytokines associated with Th1, Th2 and Treg responses could all produce large magnitudes of transcriptional changes in human MDMs. This corroborates recent reports demonstrating the broad diversity of macrophage activation states (Xue et al., 2014). One important limitation of these investigations is that they rely on the hypothesis that the transcriptome is an accurate barometer of cell state, when in fact there may be dissociation between the transcriptome and the functional proteome (Germain et al., 2011). Future systems biology approaches to understanding macrophage diversity, and furthermore, to understand immune responses *in vivo*, may be enhanced by integrating transcriptomic and proteomic approaches.

7.1.7 Summary of findings and further work

In this thesis, I have used *in vitro* and *in vivo* models to explore the effects of HIV-1 on the CMI response, and to gain insights into the normal function of this arm of the immune system. Using an *in vitro* MDM model, I have characterised a phenotype wherein HIV-1 attenuates innate immune production of the immunomodulatory cytokine IL-10. In work exploring the mechanism of this phenotype, I have determined that it is highly context-specific and likely to be due to a function of the viral accessory proteins. I have also identified that the PI3K pathway is involved in specifically regulating IL-10 production in human MDMs, suggesting that it might be a target for HIV-1 in mediating IL-10 attenuation. I have shown that HIV-1 may attenuate IL-10 in order to maximise its own replication in the advantageous inflammatory microenvironment, and have identified potential consequences of this phenotype for the immune response by studying the normal functions of IL-10 in regulating macrophage biology and innate immune responses.

By using transcriptional profiling to explore macrophage plasticity, I have developed methods for assessing the activity of different axes of the immune response in *in vivo* gene expression profiles. I have applied these while evaluating the effect of HIV-1 on CMI *in vivo* using a human challenge model, the TST, in active TB patients.

Using this model, I have gained insights into the function of CMI at the site of inflammation *in vivo* with molecular resolution, and have identified three dysregulated phenotypes associated with HIV-1 infection: IL-10 attenuation (corroborating my *in vitro* findings), a role for type I IFNs in anergy, and exaggerated Th2 responses in IRIS patients.

My findings suggest a range of potential future investigations. Further *in vitro* work to identify the mechanism of IL-10 attenuation by HIV-1 may identify a novel host-virus interaction. Further characterisation of the downstream consequences of this phenotype *in vitro*, in terms of its effects on cell differentiation, recruitment and apoptosis, will highlight its potentially physiologically relevant consequences. To this end, using macrophage/T cell co-culture systems or *in vitro* granuloma models may allow assessment of the effects of HIV-1 on CMI beyond the function of macrophages.

Using systems biology approaches to assess a human challenge model of CMI *in vivo* provided valuable insights into how HIV-1 dysregulates responses to mycobacteria. Further use of such approaches, both in expanding this challenge model to further timepoints and contexts, and in assessing samples obtained from the site of disease, will help to further confirm and explore these phenotypes. Such an approach may identify opportunities for using immunotherapeutics to mitigate the potent dysregulatory effects of HIV-1 on CMI, most importantly in the context of TB.

Chapter 8. Appendix I: Modules

Gene lists for modules developed in **Chapter 5** and/or used in **Chapter 6** are presented in this appendix. Modules 1–12 are those developed in **Chapter 5.**

Modules 13–19 were developed by Dr Gabriele Pollara (University College London). The strategy for deriving these modules is described as follows:

A semi-supervised bioinformatic approach was used to identify cell-type defining modules. A gene expression matrix of many cell types was derived from publicly available transcriptional profiling data repositories. For each cell type of interest, gene probes representing 3 putative markers that conventionally identify such cells were identified from the published literature. A correlation script in R identified the degree of co-correlation in gene expression between each marker probe and all other gene probes present in the expression matrix. The 1% of probes that were most co-correlated with the expression of each marker were identified, and modules were then derived from those highly co-correlated probes that were common to all 3 markers for each cell type.

(1) IFNγ module

Agilent Probe ID	RefSeq Accession number	Gene Symbol
A_23_P18452	NM_002416	CXCL9
A_23_P112026	NM_002164	IDO1
A_23_P81898	NM_006398	UBD
A_24_P303091	NM_001565	CXCL10
A_23_P1962	NM_004585	RARRES3
A_23_P7827	NM_001010919	FAM26F
A_32_P44394	NM_004833	AIM2
A_33_P3259393	NM_178232	HAPLN3
A_23_P39840	NM_006634	VAMP5
A_23_P72737	NM_003641	IFITM1
A_19_P00812190	NA	Q5D1D6
A_24_P48204	NM_003004	SECTM1
A_23_P32404	NM_002201	ISG20
A_23_P139123	NM_000062	SERPING1
A_33_P3407880	NM_144590	ANKRD22
A_23_P42353	NM_016135	ETV7
A_24_P270460	NM_005532	IFI27
A_24_P28722	NM_080657	RSAD2
A_24_P274270	NM_139266	STAT1
A_23_P121253	NM_003810	TNFSF10
A_32_P356316	NM_002119	HLA-DOA
A_23_P45871	NM_006820	IFI44L
A_32_P171061	NM_005170	ASCL2
A_33_P3276615	NM_030643	APOL4
A_32_P209960	NM_000246	CIITA
A_23_P85693	NM_004120	GBP2
A_23_P64721	NM_006018	HCAR3
A_23_P370682	NM_138456	BATF2
A_33_P3284933	NM_145659	IL27
A_24_P557479	NM_017523	XAF1
A_23_P210690	NM_021158	TRIB3
A_23_P156687	NM_001710	CFB
A_32_P453321	NM_001145636	C1orf228

Agilent Probe ID	RefSeq Accession number	Gene Symbol
A_24_P12690	NM_194294	IDO2
A_23_P18604	NM_015907	LAP3
A_33_P3424217	NM_001243962	HLA-DQB1
A_24_P687326	NR_024366	LINC00256A
A_23_P76529	NM_000889	ITGB7
A_33_P3402615	NM_201649	SLC6A9
A_33_P3393821	NM_001733	C1R
A_23_P65651	NM_004184	WARS
A_23_P116942	NM_002286	LAG3
A_33_P3376971	NM_024111	CHAC1
A_23_P105794	NM_033255	EPSTI1
A_23_P349966	NM_152913	TMEM130
A_33_P3401826	NM_207315	CMPK2
A_24_P387875	NM_002241	KCNJ10
A_24_P323148	NM_182573	LYPD5
A_23_P400378	NM_001077191	GPBAR1
A_24_P7594	NM_030641	APOL6
A_24_P245815	NM_020437	ASPHD2
A_33_P3369058	NM_198578	LRRK2
A_33_P3299279	NM_001014279	C5orf39
A_33_P3396139	NM_005214	CTLA4
A_23_P258493	NM_005573	LMNB1
A_23_P41470	NM_017631	DDX60
A_33_P3413905	NM_024866	ADM2
A_32_P108254	NM_017565	FAM20A
A_23_P17663	NM_002462	MX1
A_24_P274831	NM_153236	GIMAP7
A_23_P9883	NM_001079821	NLRP3
A_24_P340128	NM_178129	P2RY8
A_33_P3271635	NM_002121	HLA-DPB1
A_23_P42588	NM_018384	GIMAP5
A_23_P6535	NM_138433	KLHDC7B

(2) TNFα module

Agilent Probe ID	RefSeq Accession number	Gene Symbol
A_23_P119478	NM_005755	EBI3
A_33_P3398912	NM_017585	SLC2A6
A_33_P3303810	NM_005558	LAD1
A_33_P3227899	NR_015361	LOC440896
A_32_P87013	NM_000584	IL8
A_23_P76901	NM_015549	PLEKHG3
A_33_P3242623	NM_014331	SLC7A11
A_23_P106002	NM_020529	NFKBIA
A_23_P98350	NM_001165	BIRC3
A_23_P214222	NM_002356	MARCKS
A_33_P3226395	NR_024420	LOC389634
A_24_P56689	NM_003456	ZNF205
A_33_P3255131	NM_001100915	KCTD19
A_24_P941217	NA	SGPP2
A_23_P256948	NM_005098	MSC
A_23_P119042	NM_005601	NKG7

(3) IL-4/IL-13 module

Agilent Probe ID	RefSeq Accession number	Gene Symbol
A_23_P215484	NM_006072	CCL26
A_23_P55373	NM_001140	ALOX15
A_24_P125335	NM_005408	CCL13
A_23_P86470	NM_003956	CH25H
A_23_P254507	NM_139211	HOPX
A_23_P157795	NM_003798	CTNNAL1
A_23_P153390	NM_198492	CLEC4G
A_24_P73577	NM_170697	ALDH1A2
A_24_P313418	NM_002990	CCL22
A_32_P217750	NM_002183	IL3RA
A_23_P27795	NM_021102	SPINT2
A_33_P3258392	NM_001955	EDN1
A_24_P49190	NM_181655	C17orf58
A_33_P3354935	NM_172212	CSF1
A_23_P164773	NM_002002	FCER2
A_23_P139418	NM_198516	GALNTL4
A_23_P19624	NM_001718	BMP6
A_23_P339818	NM_183376	ARRDC4
A_33_P3245908	NM_001010863	C10orf128
A_33_P3422124	NM_181310	IL22RA2
A_23_P88626	NM_001150	ANPEP
A_23_P394986	NM_153836	CREG2
A_32_P86763	NM_004613	TGM2
A_33_P3287348	NM_004067	CHN2
A_24_P203056	NM_020993	BCL7A
A_23_P215956	NM_002467	MYC
A_23_P147711	NM_000906	NPR1
A_33_P3379775	NA	TLE1
A_23_P55749	NM_015719	COL5A3
A_23_P121499	NM_006005	WFS1
A_33_P3423979	NM_001166109	PALLD
A_23_P400716	NM_001010846	SHE

(4) TGFβ/IL-10 module

Agilent Probe ID	RefSeq Accession number	Gene Symbol
A_23_P131676	NM_020311	CXCR7
A_23_P144959	NM_004385	VCAN
A_23_P78543	NM_005498	AP1M2
A_23_P166408	NM_020530	OSM
A_23_P434809	NM_002964	S100A8
A_24_P413126	NM_020182	PMEPA1
A_23_P28815	NM_000782	CYP24A1
A_32_P65616	NM_000948	PRL
A_24_P118196	NM_001080393	GXYLT2
A_23_P79978	NM_020689	SLC24A3
A_23_P57709	NM_013363	PCOLCE2
A_24_P299685	NM_198389	PDPN
A_33_P3358099	NM_181449	CD300E
A_23_P21485	NM_017933	PID1
A_23_P87049	NM_003105	SORL1
A_24_P330518	NM_001218	CA12
A_23_P154037	NM_001159	AOX1
A_23_P404494	NM_002185	IL7R
A_33_P3236177	NM_001145	ANG
A_23_P79518	NM_000576	IL1B
A_19_P00318323	NR_015410	LINC00340
A_23_P99253	NM_004664	LIN7A
A_23_P33723	NM_004244	CD163
A_19_P00320881	NR_040025	LOC100505474
A_23_P134935	NM_001394	DUSP4
A_23_P136978	NM_014467	SRPX2
A_24_P277367	NM_002994	CXCL5

(5) IL-10 module

Agilent Probe ID	RefSeq Accession number	Gene Symbol
A_24_P59667	NM_000215	JAK3
A_23_P207058	NM_003955	SOCS3
A_23_P55270	NM_002988	CCL18
A_23_P404494	NM_002185	IL7R
A_23_P38795	NM_002029	FPR1
A_23_P434809	NM_002964	S100A8
A_32_P108254	NM_017565	FAM20A
A_23_P63209	NM_181755	HSD11B1
A_23_P12082	NM_001025199	CHI3L2
A_23_P62647	NM_003037	SLAMF1
A_23_P33723	NM_004244	CD163
A_23_P63390	NM_001017986	FCGR1B
A_23_P94338	NM_006209	ENPP2
A_23_P77493	NM_006086	TUBB3
A_33_P3381671	NA	LOC731424
A_23_P110473	NM_004536	NAIP
A_23_P79518	NM_000576	IL1B
A_33_P3413840	NM_001205019	GK
A_33_P3375934	NM_005746	NAMPT
A_23_P61371	NM_198282	TMEM173
A_23_P128974	NM_006399	BATF
A_23_P62115	NM_003254	TIMP1
A_24_P141214	NM_198194	STOM
A_23_P28485	NM_012198	GCA

Agilent Probe ID	RefSeq Accession number	Gene Symbol
A_23_P4662	NM_005178	BCL3
A_23_P98350	NM_001165	BIRC3
A_23_P134176	NM_001024465	SOD2
A_33_P3329013	NM_001050	SSTR2
A_23_P94552	NM_013390	TMEM2
A_32_P47754	NA	SLC2A14
A_23_P2492	NM_001734	C1S
A_23_P19226	NM_013352	DSE
A_23_P74001	NM_005621	S100A12
A_23_P102731	NM_175839	SMOX
A_24_P122921	NM_138621	BCL2L11
A_24_P261259	NM_004566	PFKFB3
A_23_P386478	NM_024873	TNIP3
A_24_P329795	NM_007021	C10orf10
A_32_P24585	NM_001017995	SH3PXD2B
A_23_P55649	NM_001462	FPR2
A_23_P112482	NM_004925	AQP3
A_23_P23048	NM_002965	S100A9
A_33_P3298587	NM_014963	SBNO2
A_23_P52647	NM_006795	EHD1
A_33_P3408918	NM_030754	SAA2
A_23_P74609	NM_015714	G0S2
A_23_P200728	NM_000569	FCGR3A

(6) Zymosan/IL-10 neutralisation module

Agilent Probe ID	RefSeq Accession number	Gene Symbol
A_23_P434809	NM_002964	S100A8
A_23_P38795	NM_002029	FPR1
A_23_P74001	NM_005621	S100A12
A_33_P3408918	NM_030754	SAA2
A_24_P335092	NM_000331	SAA1
A_23_P123853	NM_006274	CCL19
A_23_P386478	NM_024873	TNIP3
A_23_P41424	NM_022154	SLC39A8
A_23_P119042	NM_005601	NKG7
A_23_P77493	NM_006086	TUBB3
A_23_P206920	NM_001040114	MYH11
A_24_P133905	NM_005064	CCL23
A_24_P59667	NM_000215	JAK3
A_23_P61371	NM_198282	TMEM173
A_23_P12082	NM_001025199	CHI3L2
A_32_P108254	NM_017565	FAM20A
A_23_P208182	NM_033130	SIGLEC10
A_23_P150979	NM_058173	MUCL1
A_33_P3253394	NM_002287	LAIR1
A_23_P128974	NM_006399	BATF
A_24_P277367	NM_002994	CXCL5
A_23_P207058	NM_003955	SOCS3
A_23_P127584	NM_006169	NNMT
A_33_P3421351	NA	TRAF3IP3
A_33_P3358601	NM_001170820	IFITM10

Agilent Probe ID	RefSeq Accession number	Gene Symbol
A_23_P145965	NM_003596	TPST1
A_23_P127288	NM_000417	IL2RA
A_33_P3338121	NM_001017402	LAMB3
A_23_P211445	NM_016733	LIMK2
A_33_P3420035	NM_181489	ZNF445
A_23_P72117	NM_006714	SMPDL3A
A_33_P3242543	NM_000240	MAOA
A_23_P156687	NM_001710	CFB
A_24_P141214	NM_198194	STOM
A_19_P00318323	NR_015410	LINC00340
A_33_P3352578	NM_080387	CLEC4D
A_33_P3412975	NM_175875	SIX5
A_33_P3413840	NM_001205019	GK
A_33_P3350074	NM_001126121	SLC25A19
A_24_P299685	NM_198389	PDPN
A_23_P309701	NM_002828	PTPN2
A_23_P2492	NM_001734	C1S
A_23_P64650	NM_005726	TSFM
A_33_P3384432	NM_001178138	TFDP2
A_23_P256641	NM_012282	KCNE1L
A_33_P3215803	NM_001974	EMR1
A_23_P59045	NM_021052	HIST1H2AE
A_23_P7827	NM_001010919	FAM26F
A_24_P322474	NM_006202	PDE4A

(7) Type I IFN module

Agilent Probe ID	RefSeq Accession number	Gene Symbol
A_23_P24004	NM_001547	IFIT2
A_23_P52266	NM_001548	IFIT1
A_23_P139786	NM_003733	OASL
A_32_P9543	NM_145699	APOBEC3A
A_23_P132159	NM_017414	USP18
A_32_P54553	XM_036729	USP41
A_23_P53137	NM_000559	HBG1
A_23_P121106	NM_003865	HESX1
A_24_P66027	NM_004900	APOBEC3B
A_23_P23074	NM_006417	IFI44
A_23_P150609	NM_000612	IGF2
A_23_P127948	NM_001124	ADM
A_23_P166686	NM_016201	AMOTL2
A_23_P60146	NM_006207	PDGFRL
A_23_P87879	NM_001781	CD69
A_23_P321501	NM_182908	DHRS2
A_23_P59547	NM_001002010	NT5C3
A_23_P312851	NM_006928	PMEL
A_23_P6263	NM_002463	MX2
A_23_P20122	NM_024625	ZC3HAV1
A_23_P66798	NM_002276	KRT19
A_23_P52761	NM_002423	MMP7
A_24_P277657	NM_006877	GMPR
A_23_P29773	NM_014398	LAMP3
A_23_P72737	NM_003641	IFITM1
A_23_P64828	NM_002534	OAS1
A_24_P42136	NM_000224	KRT18
A_23_P200001	NM_144573	NEXN
A_23_P123672	NM_014290	TDRD7
A_23_P328740	NR_026875	NEURL3
A_23_P155514	NM_001622	AHSG
A_32_P231617	NM_014220	TM4SF1
A_23_P86470	NM_003956	CH25H
A_23_P153372	NM_032855	HSH2D
A_23_P154488	NM_033109	PNPT1
A_24_P7594	NM_030641	APOL6
A_24_P175187	NM_017654	SAMD9
A_24_P261259	NM_004566	PFKFB3
A_23_P38346	NM_024119	DHX58
A_23_P304171	NM_001145642	KIAA0226
A_23_P165624	NM_007115	TNFAIP6
A_23_P121011	NM_033027	CSRNP1
A_24_P239076	NM_020070	IGLL1
A_23_P200829	NM_015326	SRGAP2
A_24_P228796	NM_021123	GAGE7
A_23_P29922	NM_003265	TLR3
A_23_P15727	NM_021939	FKBP10
A_24_P12435	NM_181782	NCOA7
A_23_P59138	NM_002701	POU5F1
A_23_P215634	NM_001013398	IGFBP3
A_24_P576174	NM_018403	DCP1A
A_23_P42718	NM_004289	NFE2L3
A_23_P143845	NM_015508	TIPARP
A_24_P228130	NM_001001437	CCL3L3

Agilent Probe ID	RefSeq Accession number	Gene Symbol
A_23_P66948	NM_022751	FAM59A
A_23_P97700	NM_006472	TXNIP
A_23_P104318	NM_019058	DDIT4
A_24_P236251	NM_003836	DLK1
A_24_P23034	NM_021035	ZNFX1
A_23_P408285	NM_153026	PRICKLE1
A_23_P116942	NM_002286	LAG3
A_24_P68079	NM_014831	TRANK1
A_24_P183664	NM_014817	TRIL
A_23_P160025	NM_005531	IFI16
A_23_P75220	NM_031212	SLC25A28
A_23_P45087	NM_016220	ZNF107
A_23_P252928	NM_005367	MAGEA12
A_23_P94338	NM_006209	ENPP2
A_23_P423331	NM_032536	NTNG2
A_32_P108156	NR_001458	MIR155HG
A_23_P34628	NM_001514	GTF2B
A_23_P65442	NM_006084	IRF9
A_23_P48414	NM_003914	CCNA1
A_23_P26457	NM_000517	HBA2
A_24_P148717	NM_001295	CCR1
A_24_P258051	NM_032844	MASTL
A_23_P21838	NM_033133	CNP
A_23_P256504	NM_001633	AMBP
A_23_P84596	NM_016459	MZB1
A_23_P127584	NM_006169	NNMT
A_23_P62227	NM_025159	CXorf21
A_23_P115261	NM_000029	AGT
A_23_P398566	NM_173200	NR4A3
A_23_P23266	NA	BLZF1
A_23_P257834	NM_000477	ALB
A_32_P120895	NM_153374	LYSMD2
A_32_P157945	NM_004415	DSP
A_23_P61398	NM_001001852	PIM3
A_23_P118722	NM_001671	ASGR1
A_23_P89755	NM_016271	RNF138
A_32_P36235	NM_004907	IER2
A_23_P151710	NM_000956	PTGER2
A_23_P252106	NM_003821	RIPK2
A_32_P151800	NM_207418	FAM72D
A_23_P111132	NM_005345	HSPA1A
A_23_P109881	NM_002218	ITIH4
A_23_P203191	NM_000039	APOA1
A_23_P157299	NM_001129	AEBP1
A_23_P89941	NM_001800	CDKN2D
A_24_P214598	NM_152542	PPM1K
A_24_P274831	NM_153236	GIMAP7
A_24_P209455	NM_018326	GIMAP4
A_24_P896205	XR_132630	LOC645722
A_23_P337753	NM_138402	SP140L
A_23_P254741	NM_003102	SOD3
A_23_P374149	NM_015050	FTSJD2
A_23_P37375	NM_004755	RPS6KA5

(8) Type II IFN module

Agilent Probe ID	RefSeq Accession number	Gene Symbol
A_23_P18452	NM_002416	CXCL9
A_23_P81898	NM_006398	UBD
A_32_P209960	NM_000246	CIITA
A_23_P1962	NM_004585	RARRES3
A_24_P165864	NM_014879	P2RY14
A_24_P304071	NM_001547	IFIT2
A_23_P89431	NM_002982	CCL2
A_23_P125278	NM_005409	CXCL11
A_23_P207058	NM_003955	SOCS3
A_24_P125335	NM_005408	CCL13
A_23_P63390	NM_001017986	FCGR1B
A_23_P128974	NM_006399	BATF
A_24_P416997	NM_145641	APOL3
A_24_P59667	NM_000215	JAK3
A_23_P211445	NM_016733	LIMK2
A_23_P40453	NM_001236	CBR3
A_23_P38795	NM_002029	FPR1
A_23_P55270	NM_002988	CCL18
A_24_P941167	NM_030641	APOL6
A_23_P74278	NM_001037341	PDE4B
A_23_P153320	NM_000201	ICAM1
A_32_P56249	NR_038996	LOC100131733
A_23_P141555	NM_013351	TBX21
A_24_P322353	NM_024430	PSTPIP2

(9) LPS module

Agilent Probe ID	RefSeq Accession number	Gene Symbol
A_23_P253791	NM_004345	CAMP
A_23_P349966	NM_152913	TMEM130
A_23_P15727	NM_021939	FKBP10
A_23_P253602	NM_001721	BMX
A_23_P215634	NM_001013398	IGFBP3
A_23_P136683	NM_001243961	HLA-DQB1
A_24_P42136	NM_000224	KRT18
A_23_P78248	NM_015515	KRT23
A_23_P58266	NM_005980	S100P
A_24_P236251	NM_003836	DLK1
A_23_P46429	NM_001554	CYR61
A_23_P206760	NM_005143	HP
A_24_P201153	NM_201629	TJP2
A_32_P206839	NR_037631	LOC100288911
A_23_P252928	NM_005367	MAGEA12
A_24_P216361	NM_206956	PRAME
A_24_P941217	NA	SGPP2
A_23_P112982	NM_018711	SVOP
A_23_P59138	NM_002701	POU5F1
A_23_P319423	NM_003740	KCNK5
A_23_P254507	NM_139211	HOPX
A_23_P166297	NM_207627	ABCG1
A_23_P85783	NM_006623	PHGDH
A_23_P212508	NM_001063	TF
A_23_P257971	NM_001353	AKR1C1
A_23_P19517	NM_002224	ITPR3
A_23_P144916	NM_005110	GFPT2
A_23_P84596	NM_016459	MZB1
A_23_P30567	NM_001882	CRHBP
A_23_P256572	NM_000324	RHAG
A_32_P526255	NM_001145717	PNPLA1
A_23_P257834	NM_000477	ALB
A_23_P112482	NM_004925	AQP3
A_23_P2920	NM_001085	SERPINA3
A_23_P138541	NM_003739	AKR1C3
A_23_P157793	NM_001216	CA9
A_32_P141682	NM_001145127	EVPLL
A_23_P146456	NM_001333	CTSL2
A_23_P69586	NM_005245	FAT1
A_23_P50919	NM_006216	SERPINE2

(10) PCSK module

Agilent Probe ID	RefSeq Accession number	Gene Symbol
A_23_P82868	NM_000930	PLAT
A_23_P29773	NM_014398	LAMP3
A_23_P62647	NM_003037	SLAMF1
A_23_P112026	NM_002164	IDO1
A_23_P160720	NM_018664	BATF3
A_23_P51487	NM_018284	GBP3
A_23_P135271	NM_001497	B4GALT1
A_24_P126628	NM_015257	TMEM194A
A_24_P63522	NM_002130	HMGCS1
A_23_P207367	NM_003152	STAT5A
A_23_P94754	NM_005118	TNFSF15
A_24_P911676	NM_003107	SOX4

(11) Mtb module

Agilent Probe ID	RefSeq Accession number	Gene Symbol
A_23_P207456	NM_005623	CCL8
A_24_P133905	NM_005064	CCL23
A_23_P52207	NM_012342	BAMBI
A_24_P788878	NM_001007595	C2CD4B
A_23_P89431	NM_002982	CCL2
A_24_P277367	NM_002994	CXCL5
A_23_P25155	NM_020370	GPR84
A_23_P128808	NM_013345	GPR132
A_23_P78037	NM_006273	CCL7
A_24_P8371	NM_001124758	SPNS2
A_23_P25674	NM_001823	CKB
A_24_P280497	NM_001142641	FBRSL1
A_23_P329261	NM_000891	KCNJ2
A_23_P126735	NM_000572	IL10
A_23_P24004	NM_001547	IFIT2
A_23_P339818	NM_183376	ARRDC4
A_32_P9543	NM_145699	APOBEC3A
A_23_P108751	NM_001039492	FHL2

(12) Spn module

Agilent Probe ID	RefSeq Accession number	Gene Symbol
A_24_P252945	NM_032966	CXCR5
A_24_P399230	NM_175575	WFIKKN2
A_23_P407112	NM_145263	SPATA18
A_23_P52986	NM_152718	VWCE
A_23_P206359	NM_004360	CDH1
A_23_P218807	NM_017590	ZC3H7B
A_32_P52153	NR_038453	LOC728978
A_24_P404458	NM_170678	ITGB1BP3
A_23_P126103	NM_001902	CTH
A_23_P167983	NA	HIST1H2AC
A_24_P165423	NM_052960	RBP7
A_23_P309381	NM_001040874	HIST2H2AA4
A_23_P254944	NM_000853	GSTT1
A_24_P319374	NM_005814	GPA33
A_23_P16523	NM_004864	GDF15
A_23_P59045	NM_021052	HIST1H2AE
A_23_P428184	NM_021065	HIST1H2AD
A_24_P152649	NR_033748	LOC644189
A_24_P68631	NM_175065	HIST2H2AB

(13) T cell module

Agilent Probe ID	RefSeq Accession number	Gene Symbol
A_23_P10025	NM_006159	NELL2
A_23_P103361	NM_005356	LCK
A_23_P114299	NM_001504	CXCR3
A_23_P128993	NM_033423	GZMH
A_23_P1473	NM_005041	PRF1
A_23_P161280		SPOCK2
A_23_P28334	NM_003853	IL18RAP
A_23_P302018	NM_003328	TXK
A_23_P306941	NM_153615	RGL4
A_23_P340019	NM_178844	NLRC3
A_23_P34676	NM_198053	CD247
A_23_P37685		TMEM204
A_23_P44155	NM_198196	CD96
A_23_P8297		SCML4
A_23_P8424		PVRIG
A_23_P98173		PTPRCAP
A_24_P291278		LAX1
A_24_P673968		TTC22
A_24_P854492	NR_003491	MIAT

(14) Macrophage module

Agilent Probe ID	RefSeq Accession number	Gene Symbol
A_23_P140591		ABHD2
A_23_P256205	NM_014945	ABLIM3
A_23_P21758		ADAM28
A_23_P320304		AKR7L
A_23_P83098	NM_000689	ALDH1A1
A_23_P105184		ARAP1
A_24_P378202		ARL11
A_23_P379864		ASRGL1
A_23_P380614	NM_006045	ATP9A
A_23_P104996	NM_004183	BEST1
A_23_P7325	NM_004334	BST1
A_23_P76983	NM_025057	C14orf45
A_23_P163467	NM_207380	C15orf52
A_23_P368484	NM_207387	C17orf76
A_23_P142055		C19orf38
A_23_P153562	NM_001736	C5AR1
A_24_P283189		CD14
A_23_P33723	NM_004244	CD163
A_23_P209055	NM_001771	CD22
A_23_P26771	NM_006678	CD300C
A_23_P15369	NM_174892	CD300LB
A_24_P279307		CD300LF
A_23_P364437	NM_022124	CDH23
A_23_P137665	NM_001276	CHI3L1
A_23_P105571	NM_020244	CHPT1
A_23_P383986	NM_015892	CHST15
A_23_P128470	NM_138337	CLEC12A
A_24_P180654		CREB3L2
A_23_P217258		CYBB
A_23_P119266	NM_001375	DNASE2
A_23_P133506		DOK3
A_23_P79251	NM_014600	EHD3
A_23_P11764		EIF2C1
A_23_P165848		EMILIN1
A_23_P63390	NM_001017986	FCGR1B
A_23_P126298		FCGR3B
A_23_P67847	NM_024572	GALNT14
A_23_P8640	NM_001039966	GPER
A_23_P160226	NM_001039464	HEATR8
A_23_P210330	NM_014181	HSPC159
A_24_P318656	NM_000212	ITGB3
A_23_P501232		KCNAB2
A_24_P346762	NM_025182	KIAA1539
A_23_P125117		KLHDC8B
A_23_P86283	NM_006762	LAPTM5
A_23_P89187	NM_006148	LASP1
A_24_P348989	NM_006863	LILRA1
A_23_P142205	NM_006866	LILRA2
A_23_P107847		LILRA5
A_32_P95147		LOC100506190

Agilent Probe ID	RefSeq Accession number	Gene Symbol
A_23_P114414	NM_001031855	LONRF3
A_23_P112004	NM_012472	LRRC6
A_23_P388670	NM_000895	LTA4H
A_23_P70688	NM_004271	LY86
A_23_P250379		MAN2B2
A_23_P212061		MME
A_24_P184445	NM_002429	MMP19
A_23_P171296	NM_002436	MPP1
A_23_P148737	NM_004997	MYBPH
A_23_P360240	NM_138768	MYEOV
A_23_P143817	NM_053025	MYLK
A_24_P339664	NM_020170	NCLN
A_23_P381431		NPL
A_23_P88381	NM_001005743	NUMB
A_23_P372848	NM_002558	P2RX1
A_23_P24903	NM_176072	P2RY2
A_24_P243749	NM_002612	PDK4
A_23_P21485	NM_017933	PID1
A_24_P40165		PIGT
A_23_P151506	NM_016445	PLEK2
A_23_P6355		POM121L1P
A_23_P103011	NM_004914	RAB36
A_32_P393316	NM_001098531	RAPGEF3
A_32_P377577		SCAF1
A_32_P74391		SIRPD
A_24_P76831		SLC11A1
A_23_P325562	NM_006671	SLC1A7
A_23_P388900	NM_018420	SLC22A15
A_24_P208345	NM_033102	SLC45A3
A_32_P109653		SNCA
A_23_P7642		SPARC
A_23_P121533	NM_012445	SPON2
A_23_P94736	NM_175039	ST6GALNAC4
A_24_P122337	NM_080737	SYTL4
A_23_P75369		TCIRG1
A_23_P76402		TCTN1
A_23_P10873	NM_003263	TLR1
A_24_P17677		TLR6
A_24_P728604		TMEM114
A_23_P121196	NM_024334	TMEM43
A_23_P24784	NM_003282	TNNI2
A_23_P145965	NM_003596	TPST1
A_24_P239811	NM_183008	UBXN11
A_23_P201551	NM_006113	VAV3
A_24_P337700		VNN1
A_23_P217269	NM_007268	VSIG4
A_23_P105562	NM_000552	VWF
A_23_P215132	NM_014149	WDR91
A_23_P161156	NM_182755	ZNF438
A_24_P376787	NM_032752	ZNF496

(15) DC module

Agilent Probe ID	RefSeq Accession number	Gene Symbol
A_23_P500400	NM_080284	ABCA6
A_23_P202327		ADAM12
A_23_P115011	NM_019032	ADAMTSL4
A_23_P55373	NM_001140	ALOX15
A_23_P86570	NM_004034	ANXA7
A_24_P31275	NM_001678	ATP1B2
A_23_P49539	NM_001080519	BAHCC1
A_24_P203056	NM_020993	BCL7A
A_23_P24097		C10orf128
A_23_P155477	NM_016210	C3orf18
A_23_P345710	NM_152531	C3orf21
A_23_P58390	NM_152400	C4orf32
A_24_P123516		C5orf20
A_23_P39898		CALCRL
A_32_P4985	NM_015215	CAMTA1
A_23_P26965		CCL13
A_23_P26325	NM_002987	CCL17
A_24_P12065	NM_004354	CCNG2
A_23_P402670	NM_001763	CD1A
A_23_P351844	NM_001764	CD1B
A_23_P51767		CD1C
A_23_P201160		CD1E
A_23_P41217	NM_138806	CD200R1
A_23_P70095	NM_001025158	CD74
A_23_P113613	NM_022842	CDCP1
A_23_P83976	NM_145036	CEP112
A_23_P7212	NM_000204	CFI
A_23_P86470	NM_003956	CH25H
A_23_P338603	NM_001011667	CHCHD7
A_23_P33384		CIITA
A_23_P57784	NM_021101	CLDN1
A_23_P141508		CLEC10A
A_24_P360993		CLEC1A
A_23_P153390	NM_198492	CLEC4G
A_23_P157795	NM_003798	CTNNAL1
A_32_P104000	NM_173475	DCUN1D3
A_23_P20337		DPYSL2
A_23_P54291	NM_017434	DUOX1
A_24_P44453		DUOXA1
A_23_P3237		ELL3
A_23_P94338	NM_006209	ENPP2
A_24_P28578		EPS15
A_24_P205045	NM_015576	ERC2
A_24_P170983	NM_194312	ESPNL
A_23_P395609		FAM110B
A_23_P308150	NM_152424	FAM123B
A_23_P103765	NM_002001	FCER1A
A_23_P164773	NM_002002	FCER2
A_32_P164246	NM_033260	FOXQ1
A_23_P139418	NM_198516	GALNTL4
A_23_P146922	NM_000820	GAS6
A_23_P129144	NM_001018100	GCOM1

Agilent Probe ID	RefSeq Accession number	Gene Symbol
A_23_P166376		GGT5
A_23_P167005	NM_014373	GPR160
A_23_P154245		GPR35
A_24_P356601	NM_006460	HEXIM1
A_24_P354800		HLA-DOA
A_24_P243528		HLA-DPA1
A_24_P288836	NR_001435	HLA-DPB2
A_24_P239676		HLA-DQB1
A_24_P402222		HLA-DRB3
A_23_P99906	NM_199330	HOMER2
A_24_P305067		HOXB4
A_23_P126757	NM_023015	INTS3
A_23_P50591	NM_004823	KCNK6
A_23_P402157		KCTD17
A_23_P309619	NM_001145206	KIAA1671
A_32_P226646	XR_109259	LOC100129781
A_23_P145336		LOC100510687
A_23_P34452	NM_000427	LOR
A_23_P83857		MAOA
A_23_P85008		MAOB
A_23_P67042	NM_017947	MOCOS
A_23_P37205		NDRG2
A_24_P129277	NM_006092	NOD1
A_23_P147711	NM_000906	NPR1
A_23_P212779		PARM1
A_24_P27373		PLDN
A_23_P150807		PPFIBP2
A_24_P296772		PPP1R14A
A_24_P162911		PRKD3
A_32_P30345		RAB30
A_23_P50946	NM_005855	RAMP1
A_24_P36890	NM_002885	RAP1GAP
A_23_P425073	NM_002898	RBMS2
A_23_P113245		RBPJ
A_23_P256297		RRP1B
A_32_P227870		SLC30A4
A_23_P129433	NM_004594	SLC9A5
A_23_P156907	NM_018013	SOBP
A_23_P27795	NM_021102	SPINT2
A_23_P121061		STAC
A_24_P99046	NM_015000	STK38L
A_23_P149529	NM_002353	TACSTD2
A_23_P301372	NM_153365	TAPT1
A_23_P24751	NM_173810	TTC9C
A_23_P256445		VCPIP1
A_23_P218108		WDFY2
A_24_P179504	NM_144668	WDR66
A_23_P211926		WNT5A
A_23_P53588	NM_030775	WNT5B
A_23_P210608	NM_006526	ZNF217
A_23_P16652	NM_152791	ZNF555

(16) B cell module

Agilent Probe ID	RefSeq Accession number	Gene Symbol
A_23_P251686		ADRBK2
A_23_P373464	NM_002285	AFF3
A_23_P110151		ARHGAP24
A_23_P10232	NM_017935	BANK1
A_23_P97394	NM_003567	BCAR3
A_23_P218584		BCL11A
A_23_P139500	NM_030762	BHLHE41
A_23_P53763	NM_025113	C13orf18
A_23_P152858	NM_018405	C17orf79
A_23_P158470		C3orf54
A_23_P134477	NM_032350	C7orf50
A_23_P422851	NM_138375	CABLES1
A_23_P500741	NM_005187	CBFA2T3
A_23_P113572	NM_001770	CD19
A_23_P74575		CD1D
A_23_P351286		CD22
A_23_P107735	NM_001783	CD79A
A_23_P70670	NM_004233	CD83
A_23_P259189	NM_013943	CLIC4
A_23_P214208	NM_033181	CNR1
A_23_P40108	NM_001853	COL9A3
A_23_P360804	NM_020939	CPNE5
A_23_P14774	NM_004390	CTSH
A_23_P3237		ELL3
A_23_P201211	NM_031281	FCRL5
A_23_P67847	NM_024572	GALNT14
A_23_P153897	NM_052847	GNG7
A_23_P134734		GOLSYN
A_23_P30736	NM_002120	HLA-DOB
A_23_P30900		HLA-DQA1
A_23_P25194	NM_003806	HRK
A_23_P158817		IGHG1
A_23_P167168	NM_144646	IGJ
A_23_P117582	NM_130469	JDP2
A_23_P366453	NM_152688	KHDRBS2
A_23_P217528	NM_007250	KLF8
A_23_P70688	NM_004271	LY86
A_23_P5281		LYL1

Agilent Probe ID	RefSeq Accession number	Gene Symbol
A_23_P320739	NM_002397	MEF2C
A_23_P116371		MS4A1
A_23_P140434	NM_018728	MYO5C
A_23_P90130	NM_004851	NAPSA
A_23_P90125		NAPSB
A_23_P42746	NM_000265	NCF1
A_23_P30655	NM_004556	NFKBIE
A_23_P365614	NM_004557	NOTCH4
A_23_P53663	NM_002583	PAWR
A_23_P206532	NM_001031835	PHKB
A_23_P253321	NM_006228	PNOC
A_23_P408285	NM_153026	PRICKLE1
A_23_P130194	NM_006907	PYCR1
A_23_P97517		RALGPS2
A_23_P12363	NM_005012	ROR1
A_23_P169629	NM_005412	SHMT2
A_23_P76969	NM_015556	SIPA1L1
A_23_P160159	NM_003039	SLC2A5
A_23_P130735	NM_014037	SLC6A16
A_23_P209962	NM_024624	SMC6
A_23_P7697	NM_003100	SNX2
A_23_P203920	NM_005086	SSPN
A_23_P47282	NM_021978	ST14
A_23_P116533		SWAP70
A_23_P163697	NM_016524	SYT17
A_23_P357717	NM_021966	TCL1A
A_23_P53276	NM_003920	TIMELESS
A_23_P33420		TLR10
A_23_P85240	NM_016562	TLR7
A_23_P24716	NM_017870	TMEM132A
A_23_P91764	NM_052945	TNFRSF13C
A_23_P132536	NM_001042646	TRAK1
A_23_P168229	NM_030810	TXNDC5
A_23_P132956	NM_004181	UCHL1
A_23_P168306	NM_003931	WASF1
A_23_P134601	NM_057168	WNT16
A_23_P159027	NM_015461	ZNF521
A_23_P169978	NM_020747	ZNF608

(17) NK cell module

Agilent Probe ID	RefSeq Accession number	Gene Symbol
A_23_P128281	NM_007333	KLRC3
A_23_P348257	NM_014840	NUAK1
A_23_P259611	NM_016616	TXNDC3
A_23_P151046	NM_002259	KLRC1
A_23_P70359	NR_024277	NCRNA00241
A_23_P393777	NM_000953	PTGDR
A_23_P50678	NM_139355	MATK
A_23_P85453	NM_016382	CD244
A_23_P334218	NM_145647	WDR67
A_23_P1473	NM_005041	PRF1
A_23_P257895	NM_138957	MAPK1
A_23_P254507	NM_139211	HOPX
A_23_P219197	NM_134427	RGS3
A_23_P423331	NM_032536	NTNG2
A_23_P317683	NM_003274	TRAPPC10
A_23_P141394	NM_017983	WIPI1
A_23_P141429	NM_016428	ABI3
A_23_P28334	NM_003853	IL18RAP
A_23_P50799	NM_013939	OR10H2
A_23_P53081	NM_020896	OSBPL5
A_23_P152727	NM_014798	PLEKHM1
A_23_P142447	NM_012335	MYO1F
A_23_P28263	NM_021198	CTDSP1
A_23_P23443	NM_024329	EFHD2
A_23_P414913	NM_022343	GLIPR2
A_23_P121533	NM_012445	SPON2

(18) Monocyte module

Agilent Probe ID	RefSeq Accession number	Gene Symbol
A_23_P143120	NM_003183	ADAM17
A_23_P257971	NM_001353	AKR1C1
A_23_P259071	NM_001657	AREG
A_23_P68970	NM_014570	ARFGAP3
A_23_P97871		ARID5B
A_23_P211047	NM_206866	BACH1
A_23_P207564	NM_002984	CCL4
A_23_P138760	NM_013246	CLCF1
A_23_P7144	NM_001511	CXCL1
A_24_P257416	NM_002089	CXCL2
A_24_P251764		CXCL3
A_24_P217520		EREG
A_24_P382661		ETS2
A_32_P96000	NM_001004341	ETV3L
A_24_P4816	NM_031412	GABARAPL1
A_24_P100387		GK
A_23_P105442		GRASP
A_23_P19619	NM_002114	HIVEP1
A_23_P86330	NM_016545	IER5
A_23_P72096	NM_000575	IL1A
A_23_P79518	NM_000576	IL1B
A_23_P71037	NM_000600	IL6
A_32_P87013	NM_000584	IL8
A_23_P80635		IRAK2
A_23_P162300	NM_007199	IRAK3
A_32_P74409	NM_001145033	LOC387763
A_32_P219581		LOC440934
A_23_P35035		LPAR3
A_23_P78209	NM_002359	MAFG
A_23_P23947	NM_005204	MAP3K8

Agilent Probe ID	RefSeq Accession number	Gene Symbol
A_23_P214222	NM_002356	MARCKS
A_24_P278126	NM_002485	NBN
A_23_P106002	NM_020529	NFKBIA
A_24_P214754		NR3C1
A_24_P124624	NM_002543	OLR1
A_23_P71570		OSR2
A_23_P95755		PFKFB3
A_23_P61398	NM_001001852	PIM3
A_32_P89310	NM_001080475	PLEKHM3
A_23_P30254	NM_006622	PLK2
A_23_P90172	NM_014330	PPP1R15A
A_24_P77008		PTGS2
A_23_P121064	NM_002852	PTX3
A_23_P88849		RRAD
A_23_P4561		SERPINB8
A_23_P30687		SERPINB9
A_24_P359191	NM_003043	SLC6A6
A_23_P131846	NM_005985	SNAI1
A_24_P935819		SOD2
A_23_P156788	NM_003764	STX11
A_23_P74129		TMEM50A
A_24_P157926	NM_006290	TNFAIP3
A_23_P165624	NM_007115	TNFAIP6
A_24_P5856		TNFSF9
A_24_P89891	NM_005658	TRAF1
A_23_P167595	NM_003337	UBE2B
A_23_P215096		UBE2H
A_23_P371155		WTAP
A_23_P326160		ZC3H12A

(19) Neutrophil module

Agilent Probe ID	RefSeq Accession number	Gene Symbol
A_23_P250294	NM_016006	ABHD5
A_23_P206945		ACOX1
A_23_P110212	NM_001995	ACSL1
A_23_P127948	NM_001124	ADM
A_23_P106362	NM_020980	AQP9
A_24_P336577	NM_019099	C1orf183
A_23_P259506	NM_032412	C5orf32
A_23_P130515	NM_001815	CEACAM3
A_23_P152234	NM_144673	CMTM2
A_23_P77401	NM_018340	CPPED1
A_23_P157117	NM_182898	CREB5
A_23_P126218		CSF3R
A_23_P7144	NM_001511	CXCL1
A_23_P155057	NM_013385	CYTH4
A_23_P321201	NM_015213	DENND5A
A_23_P53198	NM_032564	DGAT2
A_23_P364580		DOCK4
A_23_P39925		DYSF
A_24_P154080	NM_001397	ECE1
A_23_P208768	NM_002000	FCAR
A_23_P214603	NM_005803	FLOT1
A_23_P55649	NM_001462	FPR2
A_23_P96556		GK
A_23_P61637	NM_002108	HAL

Agilent Probe ID	RefSeq Accession number	Gene Symbol
A_23_P79398		IL1R2
A_23_P209995		IL1RN
A_23_P17655		KCNJ15
A_23_P43380		KIAA1539
A_23_P217447		LAMP2
A_23_P30547	NM_005565	LCP2
A_23_P163380	NM_006441	MTHFS
A_23_P305060		NAMPT
A_23_P106463	NM_002537	OAZ2
A_24_P97342	NM_021935	PROK2
A_24_P250922	NM_000963	PTGS2
A_23_P137470	NM_020808	SIPA1L2
A_23_P29083		SLC19A1
A_23_P216004		SLC25A37
A_23_P134176	NM_001024465	SOD2
A_24_P351906		STEAP4
A_23_P394216		TECPR2
A_23_P60306		TLR4
A_23_P421423	NM_006291	TNFAIP2
A_23_P165624	NM_007115	TNFAIP6
A_23_P119102	NM_003370	VASP
A_23_P122724	NM_004665	VNN2
A_23_P214935		VNN3

Chapter 9. Appendix II: TST study case list

Anonymised demographic and clinical data for all active TB patients recruited into the TST study (**Chapter 6)** are presented in this Appendix. For the healthy volunteers, the relevant data can be found in the original publication (Tomlinson *et al.*, 2011).

Abbreviations used in tables: UIN, unique identification number; LDN, London; CPT, Cape Town; M, male; F, female; LN, lymph node; LLL, left lower lobe; MDR, multi-drug resistant; ARV, anti-retrovirals; Y, yes; N, no; CXR; chest x-ray; dx, diagnosis; TST, tuberculin skin test; N/A, not applicable.

UIN	CPT/ LDN	Gender	Age	Ethnicity	HIV-1 status	CD4 count (mm^{-3})	HIV-1 viral load (log_{10} copies ml^{-2})	Site of TB	TB diagnosis	ARVs	TST/ Saline	Induration (mm)	QuantiFERON result
A01	CPT	M	35	Black	Negative	N/A	N/A	Pulmonary (MDR)	Smear positive	N/A	TST	12	Positive
A02	CPT	M	34	White	Negative	N/A	N/A	Pulmonary (MDR)	Smear positive	N/A	TST	15	Positive
A05	CPT	M	29	Black	Negative	N/A	N/A	Pulmonary	Gene Xpert positive	N/A	TST	21	Positive
A06	CPT	M	66	Black	Negative	N/A	N/A	Pulmonary	Gene Xpert positive	N/A	TST	20	Positive
A07	CPT	F	40	Black	Negative	N/A	N/A	Pulmonary	Gene Xpert positive	N/A	TST	25	Positive
A09	CPT	M	45	Black	Negative	N/A	N/A	Pulmonary	Clinical dx on CXR	N/A	TST	15	Indeterminate
A10	CPT	F	27	Black	Negative	N/A	N/A	Pulmonary	Smear positive	N/A	TST	25	Positive
A11	CPT	M	30	Black	Negative	N/A	N/A	Pulmonary	Clinical dx on CXR	N/A	TST	16	Positive
A13	CPT	F	46	Black	Negative	N/A	N/A	Pulmonary	Gene Xpert positive	N/A	TST	25	Positive
L01	LDN	M	71	White	Negative	N/A	N/A	Mediastinal LN & LLL	Data not available	N/A	TST	13	Not done
L02	LDN	M	25	South Asian	Negative	N/A	N/A	Left knee joint	Data not available	N/A	TST	18	Not done
L03	LDN	F	51	Somalian	Negative	N/A	N/A	LN	Data not available	N/A	TST	25	Not done

UIN	CPT/ LDN	Gender	Age	Ethnicity	HIV-1 status	CD4 count (mm^{-3})	HIV-1 viral load (log_{10} copies ml^{-2})	Site of TB	TB diagnosis	ARVs	TST/ Saline	Induration (mm)	QuantiFERON result
L04	LDN	F	66	Asian	Negative	N/A	N/A	LN	Data not available	N/A	TST	26	Not done
L05	LDN	F	44	Afro-Caribbean	Negative	N/A	N/A	Abdominal LN	Data not available	N/A	TST	27	Not done
L12	LDN	M	30	Asian	Negative	N/A	N/A	Cervical and pulmonary LN	Data not available	N/A	TST	28	Not done
L13	LDN	M	36	South Asian	Negative	N/A	N/A	Mediastinal LN	Data not available	N/A	TST	23	Not done
B01	CPT	M	41	Black	Positive	34	Not done	Pulmonary	Culture positive	N	TST	15	Positive
B02	CPT	F	31	Black	Positive	10	6.34	Pulmonary & urinary tract	Smear positive	N	TST	0	Indeterminate
B03	CPT	F	35	Black	Positive	48	5.15	Pulmonary	Gene Xpert positive	N	TST	0	Positive
B05	CPT	M	38	Black	Positive	36	5.88	Pulmonary	Gene Xpert positive	Y	TST	17	Positive
B06	CPT	F	34	Black	Positive	31	5.50	Pulmonary	Smear positive	N	TST	0	Indeterminate
B07	CPT	M	44	Black	Positive	9	5.60	Pulmonary	Culture positive	N	TST	0	Negative
B09	CPT	M	58	Black	Positive	15	Not done	Pulmonary	Gene Xpert positive	N	TST	0	Indeterminate
B10	CPT	M	32	Black	Positive	16	5.39	Abdominal	Clinical dx on imaging	N	TST	0	Positive

UIN	CPT/ LDN	Gender	Age	Ethnicity	HIV-1 status	CD4 count (mm^{-3})	HIV-1 viral load (log_{10} copies ml^{-2})	Site of TB	TB diagnosis	ARVs	TST/ Saline	Induration (mm)	QuantiFERON result
B11	CPT	F	36	Black	Positive	2	4.94	Disseminated	Clinical dx	N	TST	0	Indeterminate
B13	CPT	M	41	Black	Positive	34	Not done	Pulmonary	Clinical dx on CXR	N	TST	0	Positive
C01	CPT	M	40	Cape coloured	Positive	170	2.84	Pulmonary	Smear positive	Y	TST	0	Positive
C03	CPT	F	26	Black	Positive	93	5.75	Pulmonary	Smear positive	N	TST	0	Negative
C05	CPT	F	36	Black	Positive	207	Not done	Disseminated	Smear positive	N	TST	0	Positive
C06	CPT	F	64	Black	Positive	207	6.02	Pulmonary	Gene Xpert positive	N	TST	10	Positive
C07	CPT	F	45	Black	Positive	294	1.70	Pulmonary	Gene Xpert positive	Y	TST	15	Negative
C09	CPT	M	23	Black	Positive	227	4.95	Pulmonary	Smear positive	N	TST	21	Positive
C10	CPT	F	30	Black	Positive	214	5.61	Pulmonary	Culture positive	Y	TST	16	Indeterminate
C11	CPT	F	51	Black	Positive	341	1.70	Pulmonary	Smear positive	Y	TST	15	Positive
C13	CPT	F	53	Black	Positive	54	3.69	Pulmonary	Gene Xpert positive	N	TST	0	Indeterminate
C16	CPT	F	40	Black	Positive	138	5.50	Pulmonary	Gene Xpert positive	N	TST	24	Positive
D01	CPT	M	37	Black	Positive	25	Not done	Miliary	Gene Xpert positive	Y	TST	0	Indeterminate

UIN	CPT/ LDN	Gender	Age	Ethnicity	HIV-1 status	CD4 count (mm^{-3})	HIV-1 viral load (log_{10} copies ml^{-2})	Site of TB	TB diagnosis	ARVs	TST/ Saline	Induration (mm)	QuantiFERON result
D02	CPT	F	35	Black	Positive	511	4.73	Pulmonary	Gene Xpert positive	N	TST	17	Positive
D03	CPT	F	37	Black	Positive	279	1.81	Pulmonary	Smear positive	Y	TST	24	Positive
D05	CPT	F	50	Black	Positive	128	5.31	Pulmonary	Smear positive	Y	TST	21	Positive
D06	CPT	F	19	Black	Positive	507	1.70	Pulmonary	Smear positive	Y	TST	26	Negative
D07	CPT	M	51	Black	Positive	3	2.09	Pulmonary	Smear positive	Y	TST	0	Indeterminate
D08	CPT	F	30	Black	Positive	46	1.66	Disseminated	Gene Xpert positive	Y	Saline	N/A	Indeterminate
C15	CPT	F	34	Black	Positive	287	2.46	Pulmonary	Clinical dx on CXR	N	Saline	N/A	Indeterminate
D04	CPT	M	39	Black	Positive	412	2.61	Pulmonary	Gene Xpert positive	Y	Saline	N/A	Positive
C12	CPT	M	53	Black	Positive	105	2.02	Pulmonary	Smear positive	N	Saline	N/A	Positive
A12	CPT	M	45	Black	Negative	N/A	N/A	Pulmonary	Smear positive	N/A	Saline	N/A	Positive
A04	CPT	M	54	Black	Negative	N/A	N/A	Pulmonary	Gene Xpert positive	N/A	Saline	N/A	Positive
A08	CPT	F	29	Cape coloured	Negative	N/A	N/A	Pulmonary	Smear positive	N/A	Saline	N/A	Positive
C04	CPT	M	47	Cape coloured	Positive	88	1.94	Pulmonary	Culture positive	N	Saline	N/A	Positive

Reference List

Abadi, J., Pirofski, L. a, 1999. Antibodies reactive with the cryptococcal capsular polysaccharide glucuronoxylomannan are present in sera from children with and without human immunodeficiency virus infection. J. Infect. Dis. 180, 915–919. doi:10.1086/314953

Abdool Karim, S.S., Churchyard, G.J., Karim, Q.A., Lawn, S.D., 2009. HIV infection and tuberculosis in South Africa: an urgent need to escalate the public health response. Lancet 374, 921–933. doi:10.1016/S0140-6736(09)60916-8

Abel, L., El-Baghdadi, J., Bousfiha, A.A., Casanova, J.-L., Schurr, E., 2014. Human genetics of tuberculosis: a long and winding road. Philos. Trans. R. Soc. B Biol. Sci. 369, 20130428. doi:10.1098/rstb.2013.0428

Aberdein, J.D., Cole, J., Bewley, M.A., Marriott, H.M., Dockrell, D.H., 2013. Alveolar macrophages in pulmonary host defence the unrecognized role of apoptosis as a mechanism of intracellular bacterial killing. Clin. Exp. Immunol. 174, 193–202. doi:10.1111/cei.12170

Abubakar, I., Lipman, M., Anderson, C., Davies, P., Zumla, A., 2011. Tuberculosis in the UK--time to regain control. BMJ 343, d4281–d4281. doi:10.1136/bmj.d4281

Ackermann, M., Strimmer, K., 2009. A general modular framework for gene set enrichment analysis. BMC Bioinformatics 10, 47. doi:10.1186/1471-2105-10-47

Aggarwal, B.B., 2003. Signalling pathways of the TNF superfamily: a double-edged sword. Nat. Rev. Immunol. 3, 745–756. doi:10.1038/nri1184

Aggarwal, N.R., Tsushima, K., Eto, Y., Tripathi, A., Mandke, P., Mock, J.R., Garibaldi, B.T., Singer, B.D., Sidhaye, V.K., Horton, M.R., King, L.S., D'Alessio, F.R., 2014. Immunological Priming Requires Regulatory T Cells and IL-10-Producing Macrophages To Accelerate Resolution from Severe Lung Inflammation. J. Immunol. Baltim. Md 1950. doi:10.4049/jimmunol.1400146

Aiken, C., Konner, J., Landau, N.R., Lenburg, M.E., Trono, D., 1994. Nef induces CD4 endocytosis: requirement for a critical dileucine motif in the membrane-proximal CD4 cytoplasmic domain. Cell 76, 853–864.

Ajami, B., Bennett, J.L., Krieger, C., McNagny, K.M., Rossi, F.M.V., 2011. Infiltrating monocytes trigger EAE progression, but do not contribute to the resident microglia pool. Nat. Neurosci. 14, 1142–1149. doi:10.1038/nn.2887

Akagawa, K.S., Komuro, I., Kanazawa, H., Yamazaki, T., Mochida, K., Kishi, F., 2006. Functional heterogeneity of colony-stimulating factor-induced human monocyte-derived macrophages. Respirol. Carlton Vic 11 Suppl, S32–36. doi:10.1111/j.1440-1843.2006.00805.x

Al-Muhsen, S., Casanova, J.-L., 2008. The genetic heterogeneity of mendelian susceptibility to mycobacterial diseases. J. Allergy Clin. Immunol. 122, 1043–1051; quiz 1052–1053. doi:10.1016/j.jaci.2008.10.037

Alavi-Majd, H., Khodakarim, S., Zayeri, F., Rezaei-Tavirani, M., Tabatabaei, S.M., Heydarpour-Meymeh, M., 2014. Assessment of gene set analysis methods based on microarray data. Gene 534, 383–389. doi:10.1016/j.gene.2013.08.063

Albacker, L.A., Yu, S., Bedoret, D., Lee, W.-L., Umetsu, S.E., Monahan, S., Freeman, G.J., Umetsu, D.T., DeKruyff, R.H., 2013. TIM-4, expressed by medullary macrophages, regulates respiratory tolerance by mediating phagocytosis of antigen-specific T cells. Mucosal Immunol. 6, 580–590. doi:10.1038/mi.2012.100

Ali, F., Lee, M.E., Iannelli, F., Pozzi, G., Mitchell, T.J., Read, R.C., Dockrell, D.H., 2003. Streptococcus pneumoniae-associated human macrophage apoptosis after bacterial internalization via complement and Fcgamma receptors correlates with intracellular bacterial load. J. Infect. Dis. 188, 1119–1131. doi:10.1086/378675

Alkhatib, G., Combadiere, C., Broder, C.C., Feng, Y., Kennedy, P.E., Murphy, P.M., Berger, E.A., 1996. CC CKR5: a RANTES, MIP-1alpha, MIP-1beta receptor as a fusion cofactor for macrophage-tropic HIV-1. Science 272, 1955–1958.

Allison, A.C., 1967. Cell-mediated immune responses to virus infections and virus-induced tumours. Br. Med. Bull. 23, 60–65.

Alonso, S., Pethe, K., Russell, D.G., Purdy, G.E., 2007. Lysosomal killing of Mycobacterium mediated by ubiquitin-derived peptides is enhanced by autophagy. Proc. Natl. Acad. Sci. 104, 6031–6036. doi:10.1073/pnas.0700036104

Altare, F., Durandy, A., Lammas, D., Emile, J.F., Lamhamedi, S., Le Deist, F., Drysdale, P., Jouanguy, E., Döffinger, R., Bernaudin, F., Jeppsson, O., Gollob, J.A., Meinl, E., Segal, A.W., Fischer, A., Kumararatne, D., Casanova, J.L., 1998a. Impairment of mycobacterial immunity in human interleukin-12 receptor deficiency. Science 280, 1432–1435.

Altare, F., Ensser, A., Breiman, A., Reichenbach, J., Baghdadi, J.E., Fischer, A., Emile, J.F., Gaillard, J.L., Meinl, E., Casanova, J.L., 2001. Interleukin-12 receptor beta1 deficiency in a patient with abdominal tuberculosis. J. Infect. Dis. 184, 231–236. doi:10.1086/321999

Altare, F., Lammas, D., Revy, P., Jouanguy, E., Döffinger, R., Lamhamedi, S., Drysdale, P., Scheel-Toellner, D., Girdlestone, J., Darbyshire, P., Wadhwa, M., Dockrell, H., Salmon, M., Fischer, A., Durandy, A., Casanova, J.L., Kumararatne, D.S., 1998b. Inherited interleukin 12 deficiency in a child with bacille Calmette-Guérin and Salmonella enteritidis disseminated infection. J. Clin. Invest. 102, 2035–2040. doi:10.1172/JCI4950

Aman, M.J., Tretter, T., Eisenbeis, I., Bug, G., Decker, T., Aulitzky, W.E., Tilg, H., Huber, C., Peschel, C., 1996. Interferon-alpha stimulates production of interleukin-10 in activated CD4+ T cells and monocytes. Blood 87, 4731–4736.

Andersen, J.L., Planelles, V., 2005. The role of Vpr in HIV-1 pathogenesis. Curr. HIV Res. 3, 43–51.

Andersen, P., Woodworth, J.S., 2014. Tuberculosis vaccines – rethinking the current paradigm. Trends Immunol. 35, 387–395. doi:10.1016/j.it.2014.04.006

Anderson, K.L., Smith, K.A., Conners, K., McKercher, S.R., Maki, R.A., Torbett, B.E., 1998. Myeloid development is selectively disrupted in PU.1 null mice. Blood 91, 3702–3710.

Anderson, L.W., Klevjer-Anderson, P., Liggitt, H.D., 1983. Susceptibility of blood-derived monocytes and macrophages to caprine arthritis-encephalitis virus. Infect. Immun. 41, 837–840.

Anthony, R.M., Rutitzky, L.I., Urban, J.F., Stadecker, M.J., Gause, W.C., 2007. Protective immune mechanisms in helminth infection. Nat. Rev. Immunol. 7, 975–987. doi:10.1038/nri2199

Antinori, A., Larussa, D., Cingolani, A., Lorenzini, P., Bossolasco, S., Finazzi, M.G., Bongiovanni, M., Guaraldi, G., Grisetti, S., Vigo, B., Gigli, B., Mariano, A., Nogare, E.R.D., Marco, M.D., Moretti, F., Corsi, P., Abrescia, N., Rellecati, P., Castagna, A., Mussini, C., Ammassari, A., Cinque, P., Monforte, A. d'Arminio, 2004. Prevalence, Associated Factors, and Prognostic Determinants of AIDS-Related Toxoplasmic Encephalitis in the Era of Advanced Highly Active Antiretroviral Therapy. Clin. Infect. Dis. 39, 1681–1691. doi:10.1086/424877

Antonelli, L.R.V., Mahnke, Y., Hodge, J.N., Porter, B.O., Barber, D.L., DerSimonian, R., Greenwald, J.H., Roby, G., Mican, J., Sher, A., Roederer, M., Sereti, I., 2010. Elevated frequencies of highly activated CD4+ T cells in HIV+ patients developing immune reconstitution inflammatory syndrome. Blood 116, 3818–3827. doi:10.1182/blood-2010-05-285080

Antoniv, T.T., Park-Min, K.-H., Ivashkiv, L.B., 2005. Kinetics of IL-10-induced gene expression in human macrophages. Immunobiology 210, 87–95. doi:10.1016/j.imbio.2005.05.003

Arias, J.F., Nishihara, R., Bala, M., Ikuta, K., 2010. High systemic levels of interleukin-10, interleukin-22 and C-reactive protein in Indian patients are associated with low in vitro replication of HIV-1 subtype C viruses. Retrovirology 7, 15. doi:10.1186/1742-4690-7-15

Astoul, E., Edmunds, C., Cantrell, D.A., Ward, S.G., 2001. PI 3-K and T-cell activation: limitations of T-leukemic cell lines as signaling models. Trends Immunol. 22, 490–496.

Auffray, C., Fogg, D., Garfa, M., Elain, G., Join-Lambert, O., Kayal, S., Sarnacki, S., Cumano, A., Lauvau, G., Geissmann, F., 2007. Monitoring of blood vessels and tissues by a population of monocytes with patrolling behavior. Science 317, 666–670. doi:10.1126/science.1142883

Avraham-Davidi, I., Yona, S., Grunewald, M., Landsman, L., Cochain, C., Silvestre, J.S., Mizrahi, H., Faroja, M., Strauss-Ayali, D., Mack, M., Jung, S., Keshet, E., 2013. On-site education of VEGF-recruited monocytes improves their performance as angiogenic and arteriogenic accessory cells. J. Exp. Med. 210, 2611–2625. doi:10.1084/jem.20120690

Awomoyi, A.A., Marchant, A., Howson, J.M.M., McAdam, K.P.W.J., Blackwell, J.M., Newport, M.J., 2002. Interleukin-10, polymorphism in SLC11A1 (formerly NRAMP1), and susceptibility to tuberculosis. J. Infect. Dis. 186, 1808–1814. doi:10.1086/345920

Azzam, R., Kedzierska, K., Leeansyah, E., Chan, H., Doischer, D., Gorry, P.R., Cunningham, A.L., Crowe, S.M., Jaworowski, A., 2006. Impaired complement-mediated phagocytosis by HIV type-1-infected human monocyte-derived macrophages involves a cAMP-dependent mechanism. AIDS Res. Hum. Retroviruses 22, 619–629. doi:10.1089/aid.2006.22.619

Baba, M., 2004. Inhibitors of HIV-1 gene expression and transcription. Curr. Top. Med. Chem. 4, 871–882.

Badley, A.D., Pilon, A.A., Landay, A., Lynch, D.H., 2000. Mechanisms of HIV-associated lymphocyte apoptosis. Blood 96, 2951–2964.

Bai, W., Liu, H., Ji, Q., Zhou, Y., Liang, L., Zheng, R., Chen, J., Liu, Z., Yang, H., Zhang, P., Kaufmann, S.H.E., Ge, B., 2014. TLR3 regulates mycobacterial RNA-induced IL-10 production through the PI3K/AKT signaling pathway. Cell. Signal. doi:10.1016/j.cellsig.2014.01.015

Bakri, Y., Sarrazin, S., Mayer, U.P., Tillmanns, S., Nerlov, C., Boned, A., Sieweke, M.H., 2005. Balance of MafB and PU.1 specifies alternative macrophage or dendritic cell fate. Blood 105, 2707–2716. doi:10.1182/blood-2004-04-1448

Balcewicz-Sablinska, M.K., Gan, H., Remold, H.G., 1999. Interleukin 10 Produced by Macrophages Inoculated with Mycobacterium avium Attenuates Mycobacteria-Induced Apoptosis by Reduction of TNF-α Activity. J. Infect. Dis. 180, 1230–1237. doi:10.1086/315011

Balcewicz-Sablinska, M.K., Keane, J., Kornfeld, H., Remold, H.G., 1998. Pathogenic Mycobacterium tuberculosis evades apoptosis of host macrophages by release of TNF-R2, resulting in inactivation of TNF-alpha. J. Immunol. Baltim. Md 1950 161, 2636–2641.

Balliet, J.W., Kolson, D.L., Eiger, G., Kim, F.M., McGann, K.A., Srinivasan, A., Collman, R., 1994. Distinct effects in primary macrophages and lymphocytes of the human immunodeficiency virus type 1 accessory genes vpr, vpu, and nef: mutational analysis of a primary HIV-1 isolate. Virology 200, 623–631. doi:10.1006/viro.1994.1225

Banerjee, A., Gugasyan, R., McMahon, M., Gerondakis, S., 2006. Diverse Toll-like receptors utilize Tpl2 to activate extracellular signal-regulated kinase (ERK) in hemopoietic cells. Proc. Natl. Acad. Sci. U. S. A. 103, 3274–3279. doi:10.1073/pnas.0511113103

Barnes, P.F., Lu, S., Abrams, J.S., Wang, E., Yamamura, M., Modlin, R.L., 1993. Cytokine production at the site of disease in human tuberculosis. Infect. Immun. 61, 3482–3489.

Barré-Sinoussi, F., Chermann, J.C., Rey, F., Nugeyre, M.T., Chamaret, S., Gruest, J., Dauguet, C., Axler-Blin, C., Vézinet-Brun, F., Rouzioux, C., Rozenbaum, W., Montagnier, L., 1983. Isolation of a T-lymphotropic retrovirus from a patient at risk for acquired immune deficiency syndrome (AIDS). Science 220, 868–871.

Barreto-de-Souza, V., Pacheco, G.J., Silva, A.R., Castro-Faria-Neto, H.C., Bozza, P.T., Saraiva, E.M., Bou-Habib, D.C., 2006. Increased Leishmania replication in HIV-1-infected macrophages is mediated by tat protein through cyclooxygenase-2 expression and prostaglandin E2 synthesis. J. Infect. Dis. 194, 846–854. doi:10.1086/506618

Beamer, G.L., Flaherty, D.K., Assogba, B.D., Stromberg, P., Gonzalez-Juarrero, M., de Waal Malefyt, R., Vesosky, B., Turner, J., 2008. Interleukin-10 promotes Mycobacterium tuberculosis disease progression in CBA/J mice. J. Immunol. Baltim. Md 1950 181, 5545–5550.

Bean, A.G., Roach, D.R., Briscoe, H., France, M.P., Korner, H., Sedgwick, J.D., Britton, W.J., 1999. Structural deficiencies in granuloma formation in TNF gene-targeted mice underlie the heightened susceptibility to aerosol Mycobacterium tuberculosis infection, which is not compensated for by lymphotoxin. J. Immunol. Baltim. Md 1950 162, 3504–3511.

Beck, J.S., Potts, R.C., Kardjito, T., Grange, J.M., 1985. T4 lymphopenia in patients with active pulmonary tuberculosis. Clin. Exp. Immunol. 60, 49–54.

Bedoret, D., Wallemacq, H., Marichal, T., Desmet, C., Quesada Calvo, F., Henry, E., Closset, R., Dewals, B., Thielen, C., Gustin, P., de Leval, L., Van Rooijen, N., Le Moine, A., Vanderplasschen, A., Cataldo, D., Drion, P.-V., Moser, M., Lekeux, P., Bureau, F., 2009. Lung interstitial macrophages alter dendritic cell functions to prevent airway allergy in mice. J. Clin. Invest. 119, 3723–3738. doi:10.1172/JCI39717

Begitt, A., Droescher, M., Meyer, T., Schmid, C.D., Baker, M., Antunes, F., Knobeloch, K.-P., Owen, M.R., Naumann, R., Decker, T., Vinkemeier, U., 2014. STAT1-cooperative DNA binding distinguishes type 1 from type 2 interferon signaling. Nat. Immunol. 15, 168–176. doi:10.1038/ni.2794

Behar, S.M., Martin, C.J., Booty, M.G., Nishimura, T., Zhao, X., Gan, H.-X., Divangahi, M., Remold, H.G., 2011. Apoptosis is an innate defense function of macrophages against Mycobacterium tuberculosis. Mucosal Immunol. doi:10.1038/mi.2011.3

Belge, K.-U., Dayyani, F., Horelt, A., Siedlar, M., Frankenberger, M., Frankenberger, B., Espevik, T., Ziegler-Heitbrock, L., 2002. The proinflammatory CD14+CD16+DR++ monocytes are a major source of TNF. J. Immunol. Baltim. Md 1950 168, 3536–3542.

Bell, E.B., Sparshott, S.M., Bunce, C., 1998. CD4+ T-cell memory, CD45R subsets and the persistence of antigen—a unifying concept. Immunol. Today 19, 60–64. doi:10.1016/S0167-5699(97)01211-5

Berg, D.J., Kühn, R., Rajewsky, K., Müller, W., Menon, S., Davidson, N., Grünig, G., Rennick, D., 1995a. Interleukin-10 is a central regulator of the response to LPS in murine models of endotoxic shock and the Shwartzman reaction but not endotoxin tolerance. J. Clin. Invest. 96, 2339–2347. doi:10.1172/JCI118290

Berg, D.J., Leach, M.W., Kühn, R., Rajewsky, K., Müller, W., Davidson, N.J., Rennick, D., 1995b. Interleukin 10 but not interleukin 4 is a natural suppressant of cutaneous inflammatory responses. J. Exp. Med. 182, 99–108.

Berger, G., Durand, S., Goujon, C., Nguyen, X.-N., Cordeil, S., Darlix, J.-L., Cimarelli, A., 2011. A simple, versatile and efficient method to genetically modify human monocyte-derived dendritic cells with HIV-1-derived lentiviral vectors. Nat. Protoc. 6, 806–816. doi:10.1038/nprot.2011.327

Berlato, C., Cassatella, M.A., Kinjyo, I., Gatto, L., Yoshimura, A., Bazzoni, F., 2002. Involvement of suppressor of cytokine signaling-3 as a mediator of the inhibitory effects of IL-10 on lipopolysaccharide-induced macrophage activation. J. Immunol. Baltim. Md 1950 168, 6404–6411.

Berry, M.P.R., Blankley, S., Graham, C.M., Bloom, C.I., O'Garra, A., 2013. Systems approaches to studying the immune response in tuberculosis. Curr. Opin. Immunol. 25, 579–587. doi:10.1016/j.coi.2013.08.003

Berry, M.P.R., Graham, C.M., McNab, F.W., Xu, Z., Bloch, S.A.A., Oni, T., Wilkinson, K.A., Banchereau, R., Skinner, J., Wilkinson, R.J., Quinn, C., Blankenship, D., Dhawan, R., Cush, J.J., Mejias, A., Ramilo, O., Kon, O.M., Pascual, V., Banchereau, J., Chaussabel, D., O'Garra, A., 2010. An interferon-inducible neutrophil-driven blood transcriptional signature in human tuberculosis. Nature 466, 973–977. doi:10.1038/nature09247

Bewley, M.A., Marriott, H.M., Tulone, C., Francis, S.E., Mitchell, T.J., Read, R.C., Chain, B., Kroemer, G., Whyte, M.K.B., Dockrell, D.H., 2011. A cardinal role for cathepsin d in co-ordinating the host-mediated apoptosis of macrophages and killing of pneumococci. PLoS Pathog. 7, e1001262. doi:10.1371/journal.ppat.1001262

Beyer, M., Mallmann, M.R., Xue, J., Staratschek-Jox, A., Vorholt, D., Krebs, W., Sommer, D., Sander, J., Mertens, C., Nino-Castro, A., Schmidt, S.V., Schultze, J.L., 2012. High-resolution transcriptome of human macrophages. PloS One 7, e45466. doi:10.1371/journal.pone.0045466

Bezuidenhout, J., Roberts, T., Muller, L., van Helden, P., Walzl, G., 2009. Pleural tuberculosis in patients with early HIV infection is associated with increased TNF-alpha expression and necrosis in granulomas. PloS One 4, e4228. doi:10.1371/journal.pone.0004228

Biggs, B.A., Hewish, M., Kent, S., Hayes, K., Crowe, S.M., 1995. HIV-1 infection of human macrophages impairs phagocytosis and killing of Toxoplasma gondii. J. Immunol. 154, 6132–6139.

Bigley, V., Haniffa, M., Doulatov, S., Wang, X.-N., Dickinson, R., McGovern, N., Jardine, L., Pagan, S., Dimmick, I., Chua, I., Wallis, J., Lordan, J., Morgan, C., Kumararatne, D.S., Doffinger, R., van der Burg, M., van Dongen, J., Cant, A., Dick, J.E., Hambleton, S., Collin, M., 2011. The human syndrome of dendritic cell, monocyte, B and NK lymphoid deficiency. J. Exp. Med. 208, 227–234. doi:10.1084/jem.20101459

Bild, A., Febbo, P.G., 2005. Application of a priori established gene sets to discover biologically important differential expression in microarray data. Proc. Natl. Acad. Sci. U. S. A. 102, 15278–15279. doi:10.1073/pnas.0507477102

Bilzer, M., Roggel, F., Gerbes, A.L., 2006. Role of Kupffer cells in host defense and liver disease. Liver Int. Off. J. Int. Assoc. Study Liver 26, 1175–1186. doi:10.1111/j.1478-3231.2006.01342.x

Biondo, C., Midiri, A., Messina, L., Tomasello, F., Garufi, G., Catania, M.R., Bombaci, M., Beninati, C., Teti, G., Mancuso, G., 2005. MyD88 and TLR2, but not TLR4, are required for host defense against Cryptococcus neoformans. Eur. J. Immunol. 35, 870–878. doi:10.1002/eji.200425799

Biswas, S.K., Lopez-Collazo, E., 2009. Endotoxin tolerance: new mechanisms, molecules and clinical significance. Trends Immunol. 30, 475–487. doi:10.1016/j.it.2009.07.009

Biswas, S.K., Mantovani, A., 2010. Macrophage plasticity and interaction with lymphocyte subsets: cancer as a paradigm. Nat. Immunol. 11, 889–896. doi:10.1038/ni.1937

Blacklaws, B.A., 2012. Small ruminant lentiviruses: immunopathogenesis of visna-maedi and caprine arthritis and encephalitis virus. Comp. Immunol. Microbiol. Infect. Dis. 35, 259–269. doi:10.1016/j.cimid.2011.12.003

Bloom, C.I., Graham, C.M., Berry, M.P.R., Rozakeas, F., Redford, P.S., Wang, Y., Xu, Z., Wilkinson, K.A., Wilkinson, R.J., Kendrick, Y., Devouassoux, G., Ferry, T., Miyara, M., Bouvry, D., Valeyre, D., Dominique, V., Gorochov, G., Blankenship, D., Saadatian, M., Vanhems, P., Beynon, H., Vancheeswaran, R., Wickremasinghe, M., Chaussabel, D., Banchereau, J., Pascual, V., Ho, L.-P., Lipman, M., O'Garra, A., 2013. Transcriptional blood signatures distinguish pulmonary tuberculosis, pulmonary sarcoidosis, pneumonias and lung cancers. PloS One 8, e70630. doi:10.1371/journal.pone.0070630

Bloom, C.I., Graham, C.M., Berry, M.P.R., Wilkinson, K.A., Oni, T., Rozakeas, F., Xu, Z., Rossello-Urgell, J., Chaussabel, D., Banchereau, J., Pascual, V., Lipman, M., Wilkinson, R.J., O'Garra, A., 2012. Detectable changes in the blood transcriptome are present after two weeks of antituberculosis therapy. PloS One 7, e46191. doi:10.1371/journal.pone.0046191

Bogunovic, M., Ginhoux, F., Helft, J., Shang, L., Hashimoto, D., Greter, M., Liu, K., Jakubzick, C., Ingersoll, M.A., Leboeuf, M., Stanley, E.R., Nussenzweig, M., Lira, S.A., Randolph, G.J., Merad, M., 2009. Origin of the lamina propria dendritic cell network. Immunity 31, 513–525. doi:10.1016/j.immuni.2009.08.010

Boisson-Dupuis, S., El Baghdadi, J., Parvaneh, N., Bousfiha, A., Bustamante, J., Feinberg, J., Samarina, A., Grant, A.V., Janniere, L., El Hafidi, N., Hassani, A., Nolan, D., Najib, J., Camcioglu, Y., Hatipoglu, N., Aydogmus, C., Tanir, G., Aytekin, C., Keser, M., Somer, A., Aksu, G., Kutukculer, N., Mansouri, D., Mahdaviani, A., Mamishi, S., Alcais, A., Abel, L., Casanova, J.-L., 2011. IL-12Rβ1 deficiency in two of fifty children with severe tuberculosis from Iran, Morocco, and Turkey. PloS One 6, e18524. doi:10.1371/journal.pone.0018524

Bond, E., Liang, F., Sandgren, K.J., Smed-Sörensen, A., Bergman, P., Brighenti, S., Adams, W.C., Betemariam, S.A., Rangaka, M.X., Lange, C., Wilkinson, R.J., Andersson, J., Loré, K., 2012. Plasmacytoid dendritic cells infiltrate the skin in positive tuberculin skin test indurations. J. Invest. Dermatol. 132, 114–123. doi:10.1038/jid.2011.246

Bonfield, T.L., Raychaudhuri, B., Malur, A., Abraham, S., Trapnell, B.C., Kavuru, M.S., Thomassen, M.J., 2003. PU.1 regulation of human alveolar macrophage differentiation requires granulocyte-macrophage colony-stimulating factor. Am. J. Physiol. Lung Cell. Mol. Physiol. 285, L1132–1136. doi:10.1152/ajplung.00216.2003

Boonstra, A., Rajsbaum, R., Holman, M., Marques, R., Asselin-Paturel, C., Pereira, J.P., Bates, E.E.M., Akira, S., Vieira, P., Liu, Y.-J., Trinchieri, G., O'Garra, A., 2006. Macrophages and myeloid dendritic cells, but not plasmacytoid dendritic cells, produce IL-10 in response to MyD88- and TRIF-dependent TLR signals, and TLR-independent signals. J. Immunol. Baltim. Md 1950 177, 7551–7558.

Bouhlel, M.A., Derudas, B., Rigamonti, E., Dièvart, R., Brozek, J., Haulon, S., Zawadzki, C., Jude, B., Torpier, G., Marx, N., Staels, B., Chinetti-Gbaguidi, G., 2007. PPARgamma activation primes human monocytes into alternative M2 macrophages with anti-inflammatory properties. Cell Metab. 6, 137–143. doi:10.1016/j.cmet.2007.06.010

Bour, S., Perrin, C., Akari, H., Strebel, K., 2001. The Human Immunodeficiency Virus Type 1 Vpu Protein Inhibits NF-κB Activation by Interfering with βTrCP-mediated Degradation of IκB. J. Biol. Chem. 276, 15920–15928. doi:10.1074/jbc.M010533200

Bourgarit, A., Carcelain, G., Martinez, V., Lascoux, C., Delcey, V., Gicquel, B., Vicaut, E., Lagrange, P.H., Sereni, D., Autran, B., 2006. Explosion of tuberculin-specific Th1-responses induces immune restoration syndrome in tuberculosis and HIV co-infected patients. AIDS Lond. Engl. 20, F1–7. doi:10.1097/01.aids.0000202648.18526.bf

Bourgarit, A., Carcelain, G., Samri, A., Parizot, C., Lafaurie, M., Abgrall, S., Delcey, V., Vicaut, E., Sereni, D., Autran, B., 2009. Tuberculosis-Associated Immune Restoration Syndrome in HIV-1-Infected Patients Involves Tuberculin-Specific CD4 Th1 Cells and KIR-Negative γδ T Cells. J. Immunol. 183, 3915–3923. doi:10.4049/jimmunol.0804020

Brenchley, J.M., Price, D.A., Schacker, T.W., Asher, T.E., Silvestri, G., Rao, S., Kazzaz, Z., Bornstein, E., Lambotte, O., Altmann, D., Blazar, B.R., Rodriguez, B., Teixeira-Johnson, L., Landay, A., Martin, J.N., Hecht, F.M., Picker, L.J., Lederman, M.M., Deeks, S.G., Douek, D.C., 2006. Microbial translocation is a cause of systemic immune activation in chronic HIV infection. Nat Med 12, 1365–1371. doi:10.1038/nm1511

Breuer, K., Foroushani, A.K., Laird, M.R., Chen, C., Sribnaia, A., Lo, R., Winsor, G.L., Hancock, R.E.W., Brinkman, F.S.L., Lynn, D.J., 2013. InnateDB: systems biology of innate immunity and beyond--recent updates and continuing curation. Nucleic Acids Res. 41, D1228–D1233. doi:10.1093/nar/gks1147

Brightbill, H.D., Plevy, S.E., Modlin, R.L., Smale, S.T., 2000. A prominent role for Sp1 during lipopolysaccharide-mediated induction of the IL-10 promoter in macrophages. J. Immunol. Baltim. Md 1950 164, 1940–1951.

Brockman, M.A., Kwon, D.S., Tighe, D.P., Pavlik, D.F., Rosato, P.C., Sela, J., Porichis, F., Le Gall, S., Waring, M.T., Moss, K., Jessen, H., Pereyra, F., Kavanagh, D.G., Walker, B.D., Kaufmann, D.E., 2009. IL-10 is up-regulated in multiple cell types during viremic HIV infection and reversibly inhibits virus-specific T cells. Blood 114, 346–356. doi:10.1182/blood-2008-12-191296

Brooks, D.G., Trifilo, M.J., Edelmann, K.H., Teyton, L., McGavern, D.B., Oldstone, M.B.A., 2006. Interleukin-10 determines viral clearance or persistence in vivo. Nat. Med. 12, 1301–1309. doi:10.1038/nm1492

Browne, S.K., Burbelo, P.D., Chetchotisakd, P., Suputtamongkol, Y., Kiertiburanakul, S., Shaw, P.A., Kirk, J.L., Jutivorakool, K., Zaman, R., Ding, L., Hsu, A.P., Patel, S.Y., Olivier, K.N., Lulitanond, V., Mootsikapun, P., Anunnatsiri, S., Angkasekwinai, N., Sathapatayavongs, B., Hsueh, P.-R., Shieh, C.-C., Brown, M.R., Thongnoppakhun, W., Claypool, R., Sampaio, E.P., Thepthai, C., Waywa, D., Dacombe, C., Reizes, Y., Zelazny, A.M., Saleeb, P., Rosen, L.B., Mo, A., Iadarola, M., Holland, S.M., 2012. Adult-onset immunodeficiency in Thailand and Taiwan. N. Engl. J. Med. 367, 725–734. doi:10.1056/NEJMoa1111160

Bulut, Y., Michelsen, K.S., Hayrapetian, L., Naiki, Y., Spallek, R., Singh, M., Arditi, M., 2005. Mycobacterium tuberculosis heat shock proteins use diverse Toll-like receptor pathways to activate pro-inflammatory signals. J. Biol. Chem. 280, 20961–20967. doi:10.1074/jbc.M411379200

Burdette, D.L., Vance, R.E., 2013. STING and the innate immune response to nucleic acids in the cytosol. Nat. Immunol. 14, 19–26. doi:10.1038/ni.2491

Bustamante, J., Arias, A.A., Vogt, G., Picard, C., Galicia, L.B., Prando, C., Grant, A.V., Marchal, C.C., Hubeau, M., Chapgier, A., de Beaucoudrey, L., Puel, A., Feinberg, J., Valinetz, E., Jannière, L., Besse, C., Boland, A., Brisseau, J.-M., Blanche, S., Lortholary, O., Fieschi, C., Emile, J.-F., Boisson-Dupuis, S., Al-Muhsen, S., Woda, B., Newburger, P.E., Condino-Neto, A., Dinauer, M.C., Abel, L., Casanova, J.-L., 2011. Germline CYBB mutations that selectively affect macrophages in kindreds with X-linked predisposition to tuberculous mycobacterial disease. Nat. Immunol. 12, 213–221. doi:10.1038/ni.1992

Cailhier, J.F., Partolina, M., Vuthoori, S., Wu, S., Ko, K., Watson, S., Savill, J., Hughes, J., Lang, R.A., 2005. Conditional macrophage ablation demonstrates that resident macrophages initiate acute peritoneal inflammation. J. Immunol. Baltim. Md 1950 174, 2336–2342.

Cailhier, J.F., Sawatzky, D.A., Kipari, T., Houlberg, K., Walbaum, D., Watson, S., Lang, R.A., Clay, S., Kluth, D., Savill, J., Hughes, J., 2006. Resident pleural macrophages are key orchestrators of neutrophil recruitment in pleural inflammation. Am. J. Respir. Crit. Care Med. 173, 540–547. doi:10.1164/rccm.200504-538OC

Calderon, V.E., Valbuena, G., Goez, Y., Judy, B.M., Huante, M.B., Sutjita, P., Johnston, R.K., Estes, D.M., Hunter, R.L., Actor, J.K., Cirillo, J.D., Endsley, J.J., 2013. A humanized mouse model of tuberculosis. PloS One 8, e63331. doi:10.1371/journal.pone.0063331

Cantu, E., Lederer, D.J., Meyer, K., Milewski, K., Suzuki, Y., Shah, R.J., Diamond, J.M., Meyer, N.J., Tobias, J.W., Baldwin, D.A., Van Deerlin, V.M., Olthoff, K.M., Shaked, A., Christie, J.D., CTOT Investigators, 2013. Gene set enrichment analysis identifies key innate immune pathways in primary graft dysfunction after lung transplantation. Am. J. Transplant. Off. J. Am. Soc. Transplant. Am. Soc. Transpl. Surg. 13, 1898–1904. doi:10.1111/ajt.12283

Cao, Y.Z., Dieterich, D., Thomas, P.A., Huang, Y.X., Mirabile, M., Ho, D.D., 1992. Identification and quantitation of HIV-1 in the liver of patients with AIDS. AIDS Lond. Engl. 6, 65–70.

Carballo, E., Lai, W.S., Blackshear, P.J., 1998. Feedback inhibition of macrophage tumor necrosis factor-alpha production by tristetraprolin. Science 281, 1001–1005.

Carey, A.J., Tan, C.K., Ulett, G.C., 2012. Infection-induced IL-10 and JAK-STAT: A review of the molecular circuitry controlling immune hyperactivity in response to pathogenic microbes. JAK-STAT 1, 159–167. doi:10.4161/jkst.19918

Carey, B., Trapnell, B.C., 2010. The molecular basis of pulmonary alveolar proteinosis. Clin. Immunol. Orlando Fla 135, 223–235. doi:10.1016/j.clim.2010.02.017

Carpenter, S., Ricci, E.P., Mercier, B.C., Moore, M.J., Fitzgerald, K.A., 2014. Post-transcriptional regulation of gene expression in innate immunity. Nat. Rev. Immunol. 14, 361–376. doi:10.1038/nri3682

Carrel, A., Ebeling, A.H., 1926. THE FUNDAMENTAL PROPERTIES OF THE FIBROBLAST AND THE MACROPHAGE : II. THE MACROPHAGE. J. Exp. Med. 44, 285–305.

Cassol, E., Alfano, M., Biswas, P., Poli, G., 2006. Monocyte-derived macrophages and myeloid cell lines as targets of HIV-1 replication and persistence. J. Leukoc. Biol. 80, 1018–1030. doi:10.1189/jlb.0306150

Celada, A., Gray, P.W., Rinderknecht, E., Schreiber, R.D., 1984. Evidence for a gamma-interferon receptor that regulates macrophage tumoricidal activity. J. Exp. Med. 160, 55–74.

Chahroudi, A., Silvestri, G., 2012. IRIS: the unfortunate rainbow of HIV. Blood 119, 2971–2972. doi:10.1182/blood-2012-01-403683

Chain, B., Bowen, H., Hammond, J., Posch, W., Rasaiyaah, J., Tsang, J., Noursadeghi, M., 2010. Error, reproducibility and sensitivity: a pipeline for data processing of Agilent oligonucleotide expression arrays. BMC Bioinformatics 11, 344. doi:10.1186/1471-2105-11-344

Chaisson, R.E., Moore, R.D., Richman, D.D., Keruly, J., Creagh, T., 1992. Incidence and natural history of Mycobacterium avium-complex infections in patients with advanced human immunodeficiency virus disease treated with zidovudine. The Zidovudine Epidemiology Study Group. Am. Rev. Respir. Dis. 146, 285–289. doi:10.1164/ajrccm/146.2.285

Chan, C.S., Ming-Lum, A., Golds, G.B., Lee, S.J., Anderson, R.J., Mui, A.L.-F., 2012. Interleukin-10 inhibits lipopolysaccharide-induced tumor necrosis factor-α translation through a SHIP1-dependent pathway. J. Biol. Chem. 287, 38020–38027. doi:10.1074/jbc.M112.348599

Chang, E.Y., Guo, B., Doyle, S.E., Cheng, G., 2007. Cutting edge: involvement of the type I IFN production and signaling pathway in lipopolysaccharide-induced IL-10 production. J. Immunol. Baltim. Md 1950 178, 6705–6709.

Chanteux, H., Guisset, A.C., Pilette, C., Sibille, Y., 2007a. LPS induces IL-10 production by human alveolar macrophages via MAPKinases- and Sp1-dependent mechanisms. Respir. Res. 8, 71. doi:10.1186/1465-9921-8-71

Chase, M.W., 1946. The cellular transfer of cutaneous hypersensitivity. J. Bacteriol. 51, 643.

Chattergoon, M.A., Latanich, R., Quinn, J., Winter, M.E., Buckheit, R.W., 3rd, Blankson, J.N., Pardoll, D., Cox, A.L., 2014. HIV and HCV Activate the Inflammasome in Monocytes and Macrophages via Endosomal Toll-Like Receptors without Induction of Type 1 Interferon. PLoS Pathog 10, e1004082. doi:10.1371/journal.ppat.1004082

Chaturvedi, S., Frame, P., Newman, S.L., 1995. Macrophages from Human Immunodeficiency Virus-Positive Persons Are Defective in Host Defense against Histoplasma Capsulatum. J. Infect. Dis. 171, 320–327. doi:10.1093/infdis/171.2.320

Chaussabel, D., Baldwin, N., 2014. Democratizing systems immunology with modular transcriptional repertoire analyses. Nat. Rev. Immunol. 14, 271–280. doi:10.1038/nri3642

Chaussabel, D., Quinn, C., Shen, J., Patel, P., Glaser, C., Baldwin, N., Stichweh, D., Blankenship, D., Li, L., Munagala, I., Bennett, L., Allantaz, F., Mejias, A., Ardura, M., Kaizer, E., Monnet, L., Allman, W., Randall, H., Johnson, D., Lanier, A., Punaro, M., Wittkowski, K.M., White, P., Fay, J., Klintmalm, G., Ramilo, O., Palucka, A.K., Banchereau, J., Pascual, V., 2008. A modular analysis framework for blood genomics studies: application to systemic lupus erythematosus. Immunity 29, 150–164. doi:10.1016/j.immuni.2008.05.012

Chen, B.K., Feinberg, M.B., Baltimore, D., 1997. The kappaB sites in the human immunodeficiency virus type 1 long terminal repeat enhance virus replication yet are not absolutely required for viral growth. J. Virol. 71, 5495–5504.

Chen, G., Shaw, M.H., Kim, Y.-G., Nuñez, G., 2009. NOD-Like Receptors: Role in Innate Immunity and Inflammatory Disease. Annu. Rev. Pathol. Mech. Dis. 4, 365–398. doi:10.1146/annurev.pathol.4.110807.092239

Chen, W., Jin, W., Hardegen, N., Lei, K.-J., Li, L., Marinos, N., McGrady, G., Wahl, S.M., 2003. Conversion of peripheral CD4+CD25- naive T cells to CD4+CD25+ regulatory T cells by TGF-beta induction of transcription factor Foxp3. J. Exp. Med. 198, 1875–1886. doi:10.1084/jem.20030152

Cheng, F., Lienlaf, M., Wang, H.-W., Perez-Villarroel, P., Lee, C., Woan, K., Rock-Klotz, J., Sahakian, E., Woods, D., Pinilla-Ibarz, J., Kalin, J., Tao, J., Hancock, W., Kozikowski, A., Seto, E., Villagra, A., Sotomayor, E.M., 2014. A Novel Role for Histone Deacetylase 6 in the Regulation of the Tolerogenic STAT3/IL-10 Pathway in APCs. J. Immunol. Baltim. Md 1950. doi:10.4049/jimmunol.1302778

Cher, D.J., Mosmann, T.R., 1987. Two types of murine helper T cell clone. II. Delayed-type hypersensitivity is mediated by TH1 clones. J. Immunol. Baltim. Md 1950 138, 3688–3694.

Chi, H., Barry, S.P., Roth, R.J., Wu, J.J., Jones, E.A., Bennett, A.M., Flavell, R.A., 2006. Dynamic regulation of pro- and anti-inflammatory cytokines by MAPK phosphatase 1 (MKP-1) in innate immune responses. Proc. Natl. Acad. Sci. U. S. A. 103, 2274–2279. doi:10.1073/pnas.0510965103

Chow, A., Brown, B.D., Merad, M., 2011a. Studying the mononuclear phagocyte system in the molecular age. Nat Rev Immunol 11, 788–798. doi:10.1038/nri3087

Chow, A., Lucas, D., Hidalgo, A., Méndez-Ferrer, S., Hashimoto, D., Scheiermann, C., Battista, M., Leboeuf, M., Prophete, C., van Rooijen, N., Tanaka, M., Merad, M., Frenette, P.S., 2011b. Bone marrow CD169+ macrophages promote the retention of hematopoietic stem and progenitor cells in the mesenchymal stem cell niche. J. Exp. Med. 208, 261–271. doi:10.1084/jem.20101688

Chu, C.Q., Field, M., Andrew, E., Haskard, D., Feldmann, M., Maini, R.N., 1992. Detection of cytokines at the site of tuberculin-induced delayed-type hypersensitivity in man. Clin. Exp. Immunol. 90, 522–529.

Chung, Y., Chang, S.H., Martinez, G.J., Yang, X.O., Nurieva, R., Kang, H.S., Ma, L., Watowich, S.S., Jetten, A., Tian, Q., Dong, C., 2009. Critical regulation of early Th17 cell differentiation by IL-1 signaling. Immunity 30, 576–587. doi:10.1016/j.immuni.2009.02.007

Cliff, J.M., Lee, J.-S., Constantinou, N., Cho, J.-E., Clark, T.G., Ronacher, K., King, E.C., Lukey, P.T., Duncan, K., Van Helden, P.D., Walzl, G., Dockrell, H.M., 2013. Distinct phases of blood gene expression pattern through tuberculosis treatment reflect modulation of the humoral immune response. J. Infect. Dis. 207, 18–29. doi:10.1093/infdis/jis499

Cobelens, F.G., Egwaga, S.M., van Ginkel, T., Muwinge, H., Matee, M.I., Borgdorff, M.W., 2006. Tuberculin skin testing in patients with HIV infection: limited benefit of reduced cutoff values. Clin. Infect. Dis. Off. Publ. Infect. Dis. Soc. Am. 43, 634–639. doi:10.1086/506432

Cohen, M.S., Chen, Y.Q., McCauley, M., Gamble, T., Hosseinipour, M.C., Kumarasamy, N., Hakim, J.G., Kumwenda, J., Grinsztejn, B., Pilotto, J.H.S., Godbole, S.V., Mehendale, S., Chariyalertsak, S., Santos, B.R., Mayer, K.H., Hoffman, I.F., Eshleman, S.H., Piwowar-Manning, E., Wang, L., Makhema, J., Mills, L.A., de Bruyn, G., Sanne, I., Eron, J., Gallant, J., Havlir, D., Swindells, S., Ribaudo, H., Elharrar, V., Burns, D., Taha, T.E., Nielsen-Saines, K., Celentano, D., Essex, M., Fleming, T.R., 2011a. Prevention of HIV-1 Infection with Early Antiretroviral Therapy. N. Engl. J. Med. 365, 493–505. doi:10.1056/NEJMoa1105243

Cohen, M.S., Hellmann, N., Levy, J.A., DeCock, K., Lange, J., 2008. The spread, treatment, and prevention of HIV-1: evolution of a global pandemic. J. Clin. Invest. 118, 1244–1254. doi:10.1172/JCI34706

Cohen, M.S., Shaw, G.M., McMichael, A.J., Haynes, B.F., 2011b. Acute HIV-1 Infection. N. Engl. J. Med. 364, 1943–1954. doi:10.1056/NEJMra1011874

Colditz, G.A., Brewer, T.F., Berkey, C.S., Wilson, M.E., Burdick, E., Fineberg, H.V., Mosteller, F., 1994. Efficacy of BCG vaccine in the prevention of tuberculosis. Meta-analysis of the published literature. JAMA J. Am. Med. Assoc. 271, 698–702.

Collins, K.R., Quiñones-Mateu, M.E., Toossi, Z., Arts, E.J., 2002a. Impact of tuberculosis on HIV-1 replication, diversity, and disease progression. AIDS Rev. 4, 165–176.

Collins, K.R., Quinones-Mateu, M.E., Wu, M., Luzze, H., Johnson, J.L., Hirsch, C., Toossi, Z., Arts, E.J., 2002b. Human Immunodeficiency Virus Type 1 (HIV-1) Quasispecies at the Sites of Mycobacterium tuberculosis Infection Contribute to Systemic HIV-1 Heterogeneity. J Virol 76, 1697–1706. doi: 10.1128/JVI.76.4.1697-1706.2002

Commins, S., Steinke, J.W., Borish, L., 2008. The extended IL-10 superfamily: IL-10, IL-19, IL-20, IL-22, IL-24, IL-26, IL-28, and IL-29. J. Allergy Clin. Immunol. 121, 1108–1111. doi:10.1016/j.jaci.2008.02.026

Conradie, F., Foulkes, A.S., Ive, P., Yin, X.M., Roussos, K., Glencross, D.K., Lawrie, D., Stevens, W., Montaner, L.J.D., Sanne, I., Azzoni, L., 2011. Natural Killer Cell Activation Distinguishes Mycobacterium tuberculosis-Mediated Immune Reconstitution Syndrome From Chronic HIV and HIV/MTB Coinfection. [Miscellaneous Article]. J. Acquir. Immune Defic. Syndr. Novemb. 1 58, 309–318. doi:10.1097/QAI.0b013e31822e0d15

Conticello, S.G., Harris, R.S., Neuberger, M.S., 2003. The Vif protein of HIV triggers degradation of the human antiretroviral DNA deaminase APOBEC3G. Curr. Biol. CB 13, 2009–2013.

Cooper, A.M., Dalton, D.K., Stewart, T.A., Griffin, J.P., Russell, D.G., Orme, I.M., 1993. Disseminated tuberculosis in interferon gamma gene-disrupted mice. J. Exp. Med. 178, 2243–2247.

Corbett, E.L., Marston, B., Churchyard, G.J., De Cock, K.M., 2006. Tuberculosis in sub-Saharan Africa: opportunities, challenges, and change in the era of antiretroviral treatment. Lancet 367, 926–937. doi:10.1016/S0140-6736(06)68383-9

Corren, J., 2013. Role of interleukin-13 in asthma. Curr. Allergy Asthma Rep. 13, 415–420. doi:10.1007/s11882-013-0373-9

Couper, K.N., Blount, D.G., Riley, E.M., 2008. IL-10: the master regulator of immunity to infection. J. Immunol. Baltim. Md 1950 180, 5771–5777.

Cretney, E., Xin, A., Shi, W., Minnich, M., Masson, F., Miasari, M., Belz, G.T., Smyth, G.K., Busslinger, M., Nutt, S.L., Kallies, A., 2011. The transcription factors Blimp-1 and IRF4 jointly control the differentiation and function of effector regulatory T cells. Nat. Immunol. 12, 304–311. doi:10.1038/ni.2006

Crowe, S.M., Carlin, J.B., Stewart, K.I., Lucas, C.R., Hoy, J.F., 1991. Predictive value of CD4 lymphocyte numbers for the development of opportunistic infections and malignancies in HIV-infected persons. J. Acquir. Immune Defic. Syndr. 4, 770–776.

Crowe, S.M., Vardaxis, N.J., Kent, S.J., Maerz, A.L., Hewish, M.J., McGrath, M.S., Mills, J., 1994. HIV infection of monocyte-derived macrophages in vitro reduces phagocytosis of Candida albicans. J. Leukoc. Biol. 56, 318–327.

Crozat, K., Guiton, R., Guilliams, M., Henri, S., Baranek, T., Schwartz-Cornil, I., Malissen, B., Dalod, M., 2010. Comparative genomics as a tool to reveal functional equivalences between human and mouse dendritic cell subsets. Immunol. Rev. 234, 177–198. doi:10.1111/j.0105-2896.2009.00868.x

Curtsinger, J.M., Schmidt, C.S., Mondino, A., Lins, D.C., Kedl, R.M., Jenkins, M.K., Mescher, M.F., 1999. Inflammatory Cytokines Provide a Third Signal for Activation of Naive CD4+ and CD8+ T Cells. J. Immunol. 162, 3256–3262.

Cyktor, J.C., Turner, J., 2011. Interleukin-10 and immunity against prokaryotic and eukaryotic intracellular pathogens. Infect. Immun. 79, 2964–2973. doi:10.1128/IAI.00047-11

Dai, X.-M., Ryan, G.R., Hapel, A.J., Dominguez, M.G., Russell, R.G., Kapp, S., Sylvestre, V., Stanley, E.R., 2002. Targeted disruption of the mouse colony-stimulating factor 1 receptor gene results in osteopetrosis, mononuclear phagocyte deficiency, increased primitive progenitor cell frequencies, and reproductive defects. Blood 99, 111–120.

Dalgleish, A.G., Beverley, P.C., Clapham, P.R., Crawford, D.H., Greaves, M.F., Weiss, R.A., 1984. The CD4 (T4) antigen is an essential component of the receptor for the AIDS retrovirus. Nature 312, 763–767.

Dalton, D.K., Pitts-Meek, S., Keshav, S., Figari, I.S., Bradley, A., Stewart, T.A., 1993. Multiple defects of immune cell function in mice with disrupted interferon-gamma genes. Science 259, 1739–1742.

Dannenberg, A.M., 1989. Immune mechanisms in the pathogenesis of pulmonary tuberculosis. Rev. Infect. Dis. 11 Suppl 2, S369–378.

Dannenberg, A.M., 1994. Roles of cytotoxic delayed-type hypersensitivity and macrophage-activating cell-mediated immunity in the pathogenesis of tuberculosis. Immunobiology 191, 461–473. doi:10.1016/S0171-2985(11)80452-3

Dannenberg, A.M., Meyer, O.T., Esterly, J.R., Kambara, T., 1968. The local nature of immunity in tuberculosis, illustrated histochemically in dermal BCG lesions. J. Immunol. Baltim. Md 1950 100, 931–941.

Das, A.T., Harwig, A., Berkhout, B., 2011. The HIV-1 Tat Protein Has a Versatile Role in Activating Viral Transcription. J. Virol. 85, 9506–9516. doi:10.1128/JVI.00650-11

Davies, L.C., Jenkins, S.J., Allen, J.E., Taylor, P.R., 2013. Tissue-resident macrophages. Nat. Immunol. 14, 986–995. doi:10.1038/ni.2705

Davies, L.C., Rosas, M., Smith, P.J., Fraser, D.J., Jones, S.A., Taylor, P.R., 2011. A quantifiable proliferative burst of tissue macrophages restores homeostatic macrophage populations after acute inflammation. Eur. J. Immunol. 41, 2155–2164. doi:10.1002/eji.201141817

Davis, J.M., Ramakrishnan, L., 2009. The role of the granuloma in expansion and dissemination of early tuberculous infection. Cell 136, 37–49. doi:10.1016/j.cell.2008.11.014

Dayton, A.I., Sodroski, J.G., Rosen, C.A., Goh, W.C., Haseltine, W.A., 1986. The trans-activator gene of the human T cell lymphotropic virus type III is required for replication. Cell 44, 941–947.

De Beaucoudrey, L., Samarina, A., Bustamante, J., Cobat, A., Boisson-Dupuis, S., Feinberg, J., Al-Muhsen, S., Jannière, L., Rose, Y., de Suremain, M., Kong, X.-F., Filipe-Santos, O., Chapgier, A., Picard, C., Fischer, A., Dogu, F., Ikinciogullari, A., Tanir, G., Al-Hajjar, S., Al-Jumaah, S., Frayha, H.H., AlSum, Z., Al-Ajaji, S., Alangari, A., Al-Ghonaium, A., Adimi, P., Mansouri, D., Ben-Mustapha, I., Yancoski, J., Garty, B.-Z., Rodriguez-Gallego, C., Caragol, I., Kutukculer, N., Kumararatne, D.S., Patel, S., Doffinger, R., Exley, A., Jeppsson, O., Reichenbach, J., Nadal, D., Boyko, Y., Pietrucha, B., Anderson, S., Levin, M., Schandené, L., Schepers, K., Efira, A., Mascart, F., Matsuoka, M., Sakai, T., Siegrist, C.-A., Frecerova, K., Blüetters-Sawatzki, R., Bernhöft, J., Freihorst, J., Baumann, U., Richter, D., Haerynck, F., De Baets, F., Novelli, V., Lammas, D., Vermylen, C., Tuerlinckx, D., Nieuwhof, C., Pac, M., Haas, W.H., Müller-Fleckenstein, I., Fleckenstein, B., Levy, J., Raj, R., Cohen, A.C., Lewis, D.B., Holland, S.M., Yang, K.D., Wang, X., Wang, X., Jiang, L., Yang, X., Zhu, C., Xie, Y., Lee, P.P.W., Chan, K.W., Chen, T.-X., Castro, G., Natera, I., Codoceo, A., King, A., Bezrodnik, L., Di Giovani, D., Gaillard, M.I., de Moraes-Vasconcelos, D., Grumach, A.S., da Silva Duarte, A.J., Aldana, R., Espinosa-Rosales, F.J., Bejaoui, M., Bousfiha, A.A., Baghdadi, J.E., Ozbek, N., Aksu, G., Keser, M., Somer, A., Hatipoglu, N., Aydogmus, C., Asilsoy, S., Camcioglu, Y., Gülle, S., Ozgur, T.T., Ozen, M., Oleastro, M., Bernasconi, A., Mamishi, S., Parvaneh, N., Rosenzweig, S., Barbouche, R., Pedraza, S., Lau, Y.L., Ehlayel, M.S., Fieschi, C., Abel, L., Sanal, O., Casanova, J.-L., 2010. Revisiting human IL-12Rβ1 deficiency: a survey of 141 patients from 30 countries. Medicine (Baltimore) 89, 381–402. doi:10.1097/MD.0b013e3181fdd832

De Cock, K.M., Soro, B., Coulibaly, I.M., Lucas, S.B., 1992. Tuberculosis and HIV infection in sub-Saharan Africa. JAMA J. Am. Med. Assoc. 268, 1581–1587.

De Noronha, A.L.L., Báfica, A., Nogueira, L., Barral, A., Barral-Netto, M., 2008. Lung granulomas from Mycobacterium tuberculosis/HIV-1 co-infected patients display decreased in situ TNF production. Pathol. Res. Pract. 204, 155–161. doi:10.1016/j.prp.2007.10.008

De Silva, T.I., Cotten, M., Rowland-Jones, S.L., 2008. HIV-2: the forgotten AIDS virus. Trends Microbiol. 16, 588–595. doi:10.1016/j.tim.2008.09.003

Deckert, M., Soltek, S., Geginat, G., Lütjen, S., Montesinos-Rongen, M., Hof, H., Schlüter, D., 2001. Endogenous interleukin-10 is required for prevention of a hyperinflammatory intracerebral immune response in Listeria monocytogenes meningoencephalitis. Infect. Immun. 69, 4561–4571. doi:10.1128/IAI.69.7.4561-4571.2001

Deeks, S.G., Kitchen, C.M.R., Liu, L., Guo, H., Gascon, R., Narváez, A.B., Hunt, P., Martin, J.N., Kahn, J.O., Levy, J., McGrath, M.S., Hecht, F.M., 2004. Immune activation set point during early HIV infection predicts subsequent CD4+ T-cell changes independent of viral load. Blood 104, 942–947. doi:10.1182/blood-2003-09-3333

Deeks, S.G., Tracy, R., Douek, D.C., 2013. Systemic Effects of Inflammation on Health during Chronic HIV Infection. Immunity 39, 633–645. doi:10.1016/j.immuni.2013.10.001

Del Prete, G., De Carli, M., Almerigogna, F., Giudizi, M.G., Biagiotti, R., Romagnani, S., 1993. Human IL-10 is produced by both type 1 helper (Th1) and type 2 helper (Th2) T cell clones and inhibits their antigen-specific proliferation and cytokine production. J. Immunol. Baltim. Md 1950 150, 353–360.

Delfino, D., Cianci, L., Lupis, E., Celeste, A., Petrelli, M.L., Curró, F., Cusumano, V., Teti, G., 1997. Interleukin-6 production by human monocytes stimulated with Cryptococcus neoformans components. Infect. Immun. 65, 2454–2456.

Delgado, M.A., Elmaoued, R.A., Davis, A.S., Kyei, G., Deretic, V., 2008. Toll-like receptors control autophagy. EMBO J. 27, 1110–1121. doi:10.1038/emboj.2008.31

Den Haan, J.M.M., Kraal, G., 2012. Innate immune functions of macrophage subpopulations in the spleen. J. Innate Immun. 4, 437–445. doi:10.1159/000335216

Deng, H., Liu, R., Ellmeier, W., Choe, S., Unutmaz, D., Burkhart, M., Di Marzio, P., Marmon, S., Sutton, R.E., Hill, C.M., Davis, C.B., Peiper, S.C., Schall, T.J., Littman, D.R., Landau, N.R., 1996. Identification of a major co-receptor for primary isolates of HIV-1. Nature 381, 661–666. doi:10.1038/381661a0

Denning, T.L., Campbell, N.A., Song, F., Garofalo, R.P., Klimpel, G.R., Reyes, V.E., Ernst, P.B., 2000. Expression of IL-10 receptors on epithelial cells from the murine small and large intestine. Int. Immunol. 12, 133–139.

Deregibus, M.C., Cantaluppi, V., Doublier, S., Brizzi, M.F., Deambrosis, I., Albini, A., Camussi, G., 2002. HIV-1-Tat Protein Activates Phosphatidylinositol 3-Kinase/ AKT-dependent Survival Pathways in Kaposi's Sarcoma Cells. J. Biol. Chem. 277, 25195–25202. doi:10.1074/jbc.M200921200

Derynck, R., Feng, X.-H., 1997. TGF-β receptor signaling. Biochim. Biophys. Acta BBA - Rev. Cancer 1333, F105–F150. doi:10.1016/S0304-419X(97)00017-6

Desmedt, M., Rottiers, P., Dooms, H., Fiers, W., Grooten, J., 1998. Macrophages Induce Cellular Immunity by Activating Th1 Cell Responses and Suppressing Th2 Cell Responses. J. Immunol. 160, 5300–5308.

Dhiman, R., Indramohan, M., Barnes, P.F., Nayak, R.C., Paidipally, P., Rao, L.V.M., Vankayalapati, R., 2009. IL-22 Produced by Human NK Cells Inhibits Growth of Mycobacterium tuberculosis by Enhancing Phagolysosomal Fusion. J. Immunol. 183, 6639–6645. doi:10.4049/jimmunol.0902587

Diedrich, C.R., Flynn, J.L., 2011. HIV-1/mycobacterium tuberculosis coinfection immunology: how does HIV-1 exacerbate tuberculosis? Infect. Immun. 79, 1407–1417. doi:10.1128/IAI.01126-10

Diedrich, C.R., Mattila, J.T., Klein, E., Janssen, C., Phuah, J., Sturgeon, T.J., Montelaro, R.C., Lin, P.L., Flynn, J.L., 2010. Reactivation of Latent Tuberculosis in Cynomolgus Macaques Infected with SIV Is Associated with Early Peripheral T Cell Depletion and Not Virus Load. PLoS ONE 5, e9611. doi:10.1371/journal.pone.0009611

Dinarello, C.A., 2009. Immunological and inflammatory functions of the interleukin-1 family. Annu. Rev. Immunol. 27, 519–550. doi:10.1146/annurev.immunol.021908.132612

Dinarello, C.A., 2010. IL-1: Discoveries, controversies and future directions. Eur. J. Immunol. 40, 599–606. doi:10.1002/eji.201040319

Dinu, I., Potter, J.D., Mueller, T., Liu, Q., Adewale, A.J., Jhangri, G.S., Einecke, G., Famulski, K.S., Halloran, P., Yasui, Y., 2007. Improving gene set analysis of microarray data by SAM-GS. BMC Bioinformatics 8, 242. doi:10.1186/1471-2105-8-242

Divangahi, M., Chen, M., Gan, H., Desjardins, D., Hickman, T.T., Lee, D.M., Fortune, S., Behar, S.M., Remold, H.G., 2009. Mycobacterium tuberculosis evades macrophage defenses by inhibiting plasma membrane repair. Nat. Immunol. 10, 899–906. doi:10.1038/ni.1758

Dockrell, D.H., Badley, A.D., Villacian, J.S., Heppelmann, C.J., Algeciras, A., Ziesmer, S., Yagita, H., Lynch, D.H., Roche, P.C., Leibson, P.J., Paya, C.V., 1998. The expression of Fas Ligand by macrophages and its upregulation by human immunodeficiency virus infection. J. Clin. Invest. 101, 2394–2405. doi:10.1172/JCI1171

Dockrell, D.H., Lee, M., Lynch, D.H., Read, R.C., 2001. Immune-mediated phagocytosis and killing of Streptococcus pneumoniae are associated with direct and bystander macrophage apoptosis. J. Infect. Dis. 184, 713–722. doi:10.1086/323084

Dockrell, D.H., Marriott, H.M., Prince, L.R., Ridger, V.C., Ince, P.G., Hellewell, P.G., Whyte, M.K.B., 2003. Alveolar macrophage apoptosis contributes to pneumococcal clearance in a resolving model of pulmonary infection. J. Immunol. Baltim. Md 1950 171, 5380–5388.

Doitsh, G., Cavrois, M., Lassen, K.G., Zepeda, O., Yang, Z., Santiago, M.L., Hebbeler, A.M., Greene, W.C., 2010. Abortive HIV infection mediates CD4 T cell depletion and inflammation in human lymphoid tissue. Cell 143, 789–801. doi:10.1016/j.cell.2010.11.001

Doitsh, G., Galloway, N.L.K., Geng, X., Yang, Z., Monroe, K.M., Zepeda, O., Hunt, P.W., Hatano, H., Sowinski, S., Muñoz-Arias, I., Greene, W.C., 2013. Cell death by pyroptosis drives CD4 T-cell depletion in HIV-1 infection. Nature advance online publication. doi:10.1038/nature12940

Domoua, K., N'Dhatz, M., Coulibaly, G., Traore, F., Konan, J.B., Lucas, S., Beaumel, A., De Cock, K.M., Dago-Akribi, A., Yapi, A., 1995. [Autopsy findings in 70 AIDS patients who died in a department of pneumology in Ivory Coast: impact of tuberculosis]. Médecine Trop. Rev. Corps Santé Colon. 55, 252–254.

Donato, R., Cannon, B.R., Sorci, G., Riuzzi, F., Hsu, K., Weber, D.J., Geczy, C.L., 2013. Functions of S100 Proteins. Curr. Mol. Med. 13, 24–57.

Dong, C., Davis, R.J., Flavell, R.A., 2002. MAP kinases in the immune response. Annu. Rev. Immunol. 20, 55–72. doi:10.1146/annurev.immunol.20.091301.131133

Dong, C., Zhao, G., Zhong, M., Yue, Y., Wu, L., Xiong, S., 2013. RNA sequencing and transcriptomal analysis of human monocyte to macrophage differentiation. Gene 519, 279–287. doi:10.1016/j.gene.2013.02.015

Dorman, S.E., Holland, S.M., 1998. Mutation in the signal-transducing chain of the interferon-gamma receptor and susceptibility to mycobacterial infection. J. Clin. Invest. 101, 2364–2369. doi:10.1172/JCI2901

Dorman, S.E., Picard, C., Lammas, D., Heyne, K., van Dissel, J.T., Baretto, R., Rosenzweig, S.D., Newport, M., Levin, M., Roesler, J., Kumararatne, D., Casanova, J.-L., Holland, S.M., 2004. Clinical features of dominant and recessive interferon γ receptor 1 deficiencies. The Lancet 364, 2113–2121. doi:10.1016/S0140-6736(04)17552-1

Douek, D.C., McFarland, R.D., Keiser, P.H., Gage, E.A., Massey, J.M., Haynes, B.F., Polis, M.A., Haase, A.T., Feinberg, M.B., Sullivan, J.L., Jamieson, B.D., Zack, J.A., Picker, L.J., Koup, R.A., 1998. Changes in thymic function with age and during the treatment of HIV infection. Nature 396, 690–695. doi:10.1038/25374

Douek, D.C., Roederer, M., Koup, R.A., 2009. Emerging concepts in the immunopathogenesis of AIDS. Annu. Rev. Med. 60, 471–484. doi:10.1146/annurev.med.60.041807.123549

Doyle, A.G., Herbein, G., Montaner, L.J., Minty, A.J., Caput, D., Ferrara, P., Gordon, S., 1994. Interleukin-13 alters the activation state of murine macrophages in vitro: comparison with interleukin-4 and interferon-gamma. Eur. J. Immunol. 24, 1441–1445. doi:10.1002/eji.1830240630

Dranoff, G., Crawford, A.D., Sadelain, M., Ream, B., Rashid, A., Bronson, R.T., Dickersin, G.R., Bachurski, C.J., Mark, E.L., Whitsett, J.A., 1994. Involvement of granulocyte-macrophage colony-stimulating factor in pulmonary homeostasis. Science 264, 713–716.

Driessler, F., Venstrom, K., Sabat, R., Asadullah, K., Schottelius, A.J., 2004. Molecular mechanisms of interleukin-10-mediated inhibition of NF-kappaB activity: a role for p50. Clin. Exp. Immunol. 135, 64–73.

Dubé, M., Bego, M.G., Paquay, C., Cohen, É.A., 2010. Modulation of HIV-1-host interaction: role of the Vpu accessory protein. Retrovirology 7, 114. doi:10.1186/1742-4690-7-114

Duffield, J.S., Forbes, S.J., Constandinou, C.M., Clay, S., Partolina, M., Vuthoori, S., Wu, S., Lang, R., Iredale, J.P., 2005. Selective depletion of macrophages reveals distinct, opposing roles during liver injury and repair. J. Clin. Invest. 115, 56–65. doi:10.1172/JCI22675

Dumonde, D.C., 1967. The Role of the Macrophage in Delayed Hypersensitivity. Br. Med. Bull. 23, 9–14.

Dupuis, S., Dargemont, C., Fieschi, C., Thomassin, N., Rosenzweig, S., Harris, J., Holland, S.M., Schreiber, R.D., Casanova, J.L., 2001. Impairment of mycobacterial but not viral immunity by a germline human STAT1 mutation. Science 293, 300–303. doi:10.1126/science.1061154

Ebert, R.H., Florey, H.W., 1939. The Extravascular Development of the Monocyte Observed In vivo. Br. J. Exp. Pathol. 20, 342–356.

Eckstein, D.A., Sherman, M.P., Penn, M.L., Chin, P.S., De Noronha, C.M., Greene, W.C., Goldsmith, M.A., 2001. HIV-1 Vpr enhances viral burden by facilitating infection of tissue macrophages but not nondividing CD4+ T cells. J. Exp. Med. 194, 1407–1419.

Edwards-Smith, C.J., Jonsson, J.R., Purdie, D.M., Bansal, A., Shorthouse, C., Powell, E.E., 1999. Interleukin-10 promoter polymorphism predicts initial response of chronic hepatitis C to interferon alfa. Hepatol. Baltim. Md 30, 526–530. doi:10.1002/hep.510300207

Eidsmo, L., Allan, R., Caminschi, I., van Rooijen, N., Heath, W.R., Carbone, F.R., 2009. Differential migration of epidermal and dermal dendritic cells during skin infection. J. Immunol. Baltim. Md 1950 182, 3165–3172. doi:10.4049/jimmunol.0802950

Ejrnaes, M., Filippi, C.M., Martinic, M.M., Ling, E.M., Togher, L.M., Crotty, S., von Herrath, M.G., 2006. Resolution of a chronic viral infection after interleukin-10 receptor blockade. J. Exp. Med. 203, 2461–2472. doi:10.1084/jem.20061462

Elcombe, S.E., Naqvi, S., Van Den Bosch, M.W.M., Mackenzie, K.F., Cianfanelli, F., Brown, G.D., Arthur, J.S.C., 2013. Dectin-1 Regulates IL-10 Production via a MSK1/2 and CREB Dependent Pathway and Promotes the Induction of Regulatory Macrophage Markers. PloS One 8, e60086. doi:10.1371/journal.pone.0060086

Elkington, P., Shiomi, T., Breen, R., Nuttall, R.K., Ugarte-Gil, C.A., Walker, N.F., Saraiva, L., Pedersen, B., Mauri, F., Lipman, M., Edwards, D.R., Robertson, B.D., D'Armiento, J., Friedland, J.S., 2011. MMP-1 drives immunopathology in human tuberculosis and transgenic mice. J. Clin. Invest. doi:10.1172/JCI45666

Elliott, A.M., Halwiindi, B., Hayes, R.J., Luo, N., Tembo, G., Machiels, L., Bem, C., Steenbergen, G., Pobee, J.O., Nunn, P.P., 1993. The impact of human immunodeficiency virus on presentation and diagnosis of tuberculosis in a cohort study in Zambia. J. Trop. Med. Hyg. 96, 1–11.

Elliott, J.H., Vohith, K., Saramony, S., Savuth, C., Dara, C., Sarim, C., Huffam, S., Oelrichs, R., Sophea, P., Saphonn, V., Kaldor, J., Cooper, D.A., Vun, M.C., French, M.A., 2009. Immunopathogenesis and Diagnosis of Tuberculosis and Tuberculosis-Associated Immune Reconstitution Inflammatory Syndrome during Early Antiretroviral Therapy. J. Infect. Dis. 200, 1736–1745. doi:10.1086/644784

Elssner, A., Carter, J.E., Yunger, T.M., Wewers, M.D., 2004. HIV-1 infection does not impair human alveolar macrophage phagocytic function unless combined with cigarette smoking. Chest 125, 1071–1076.

Eslick, J., Scatizzi, J.C., Albee, L., Bickel, E., Bradley, K., Perlman, H., 2004. IL-4 and IL-10 Inhibition of Spontaneous Monocyte Apoptosis Is Associated with Flip Upregulation. Inflammation 28, 139–145. doi:10.1023/B:IFLA.0000039560.00231.cd

Evans, D.T., Silvestri, G., 2013. Nonhuman primate models in AIDS research. [Miscellaneous Article]. Curr. Opin. HIV AIDS July 2013 8, 255–261. doi:10.1097/COH.0b013e328361cee8

Fabian, M.R., Sonenberg, N., Filipowicz, W., 2010. Regulation of mRNA Translation and Stability by microRNAs. Annu. Rev. Biochem. 79, 351–379. doi:10.1146/annurev-biochem-060308-103103

Fallah, M.P., Chelvarajan, R.L., Garvy, B., Bondada, S., 2011. Role of phosphoinositide 3-kinase-Akt signaling pathway in the age-related cytokine dysregulation in splenic macrophages stimulated via TLR-2 or TLR-4 receptors. Mech. Ageing Dev. doi:10.1016/j.mad.2011.05.003

Falvo, J.V., Ranjbar, S., Jasenosky, L.D., Goldfeld, A.E., 2011. Arc of a vicious circle: pathways activated by Mycobacterium tuberculosis that target the HIV-1 LTR. Am. J. Respir. Cell Mol. Biol. doi:10.1165/rcmb.2011-0186TR

Fauci, A.S., Mavilio, D., Kottilil, S., 2005. NK cells in HIV infection: Paradigm for protection or targets for ambush. Nat. Rev. Immunol. 5, 835–843. doi:10.1038/nri1711

Feng, Y., Broder, C.C., Kennedy, P.E., Berger, E.A., 1996. HIV-1 entry cofactor: functional cDNA cloning of a seven-transmembrane, G protein-coupled receptor. Science 272, 872–877.

Ferwerda, G., Girardin, S.E., Kullberg, B.-J., Le Bourhis, L., de Jong, D.J., Langenberg, D.M.L., van Crevel, R., Adema, G.J., Ottenhoff, T.H.M., Van der Meer, J.W.M., Netea, M.G., 2005. NOD2 and Toll-Like Receptors Are Nonredundant Recognition Systems of Mycobacterium tuberculosis. PLoS Pathog 1, e34. doi:10.1371/journal.ppat.0010034

Ferwerda, G., Meyer-Wentrup, F., Kullberg, B., Netea, M.G., Adema, G.J., 2008. Dectin-1 synergizes with TLR2 and TLR4 for cytokine production in human primary monocytes and macrophages. Cell. Microbiol. 10, 2058–2066. doi:10.1111/j.1462-5822.2008.01188.x

Finbloom, D.S., Winestock, K.D., 1995. IL-10 induces the tyrosine phosphorylation of tyk2 and Jak1 and the differential assembly of STAT1 alpha and STAT3 complexes in human T cells and monocytes. J. Immunol. Baltim. Md 1950 155, 1079–1090.

Finkel, T.H., Tudor-Williams, G., Banda, N.K., Cotton, M.F., Curiel, T., Monks, C., Baba, T.W., Ruprecht, R.M., Kupfer, A., 1995. Apoptosis occurs predominantly in bystander cells and not in productively infected cells of HIV- and SIV-infected lymph nodes. Nat. Med. 1, 129–134.

Fiorentino, D.F., Zlotnik, A., Mosmann, T.R., Howard, M., O'Garra, A., 1991. IL-10 inhibits cytokine production by activated macrophages. J. Immunol. Baltim. Md 1950 147, 3815–3822.

Fitzgerald-Bocarsly, P., Jacobs, E.S., 2010. Plasmacytoid dendritic cells in HIV infection: striking a delicate balance. J. Leukoc. Biol. 87, 609–620. doi:10.1189/jlb.0909635

Flannagan, R.S., Cosío, G., Grinstein, S., 2009. Antimicrobial mechanisms of phagocytes and bacterial evasion strategies. Nat. Rev. Microbiol. 7, 355–366. doi:10.1038/nrmicro2128

Flannagan, R.S., Jaumouillé, V., Grinstein, S., 2012. The cell biology of phagocytosis. Annu. Rev. Pathol. 7, 61–98. doi:10.1146/annurev-pathol-011811-132445

Flexner, C., 1998. HIV-protease inhibitors. N. Engl. J. Med. 338, 1281–1292. doi:10.1056/NEJM199804303381808

Flynn, J.L., 2006. Lessons from experimental Mycobacterium tuberculosis infections. Microbes Infect. Inst. Pasteur 8, 1179–1188. doi:10.1016/j.micinf.2005.10.033

Flynn, J.L., Chan, J., Triebold, K.J., Dalton, D.K., Stewart, T.A., Bloom, B.R., 1993. An essential role for interferon gamma in resistance to Mycobacterium tuberculosis infection. J. Exp. Med. 178, 2249–2254.

Foey, A.D., Feldmann, M., Brennan, F.M., 2001. CD40 ligation induces macrophage IL-10 and TNF-alpha production: differential use of the PI3K and p42/44 MAPK-pathways. Cytokine 16, 131–142. doi:10.1006/cyto.2001.0954

Fogg, D.K., Sibon, C., Miled, C., Jung, S., Aucouturier, P., Littman, D.R., Cumano, A., Geissmann, F., 2006. A clonogenic bone marrow progenitor specific for macrophages and dendritic cells. Science 311, 83–87. doi:10.1126/science.1117729

Forsman, A., Weiss, R.A., 2008. Why is HIV a pathogen? Trends Microbiol., 25 Years of HIV 16, 555–560. doi:10.1016/j.tim.2008.09.004

Fowles, R.E., Fajardo, I.M., Leibowitch, J.L., David, J.R., 1973. The enhancement of macrophage bacteriostasis by products of activated lymphocytes. J. Exp. Med. 138, 952–964.

François, F., Klotman, M.E., 2003. Phosphatidylinositol 3-Kinase Regulates Human Immunodeficiency Virus Type 1 Replication following Viral Entry in Primary CD4+ T Lymphocytes and Macrophages. J. Virol. 77, 2539–2549. doi:10.1128/JVI.77.4.2539-2549.2003

Fremond, C.M., Togbe, D., Doz, E., Rose, S., Vasseur, V., Maillet, I., Jacobs, M., Ryffel, B., Quesniaux, V.F.J., 2007. IL-1 receptor-mediated signal is an essential component of MyD88-dependent innate response to Mycobacterium tuberculosis infection. J. Immunol. Baltim. Md 1950 179, 1178–1189.

Fullmer, M.A., Shen, J.Y., Modlin, R.L., Rea, T.H., 1987. Immunohistological evidence of lymphokine production and lymphocyte activation antigens in tuberculin reactions. Clin. Exp. Immunol. 67, 383–390.

Gaba, A., Grivennikov, S.I., Do, M.V., Stumpo, D.J., Blackshear, P.J., Karin, M., 2012. Cutting Edge: IL-10–Mediated Tristetraprolin Induction Is Part of a Feedback Loop That Controls Macrophage STAT3 Activation and Cytokine Production. J. Immunol. 189, 2089–2093. doi:10.4049/jimmunol.1201126

Gallagher, P., Lowe, G., Fitzgerald, T., Bella, A., Greene, C., McElvaney, N., O'Neill, S., 2003. Association of IL-10 polymorphism with severity of illness in community acquired pneumonia. Thorax 58, 154–156. doi:10.1136/thorax.58.2.154

Gallegos, A.M., van Heijst, J.W.J., Samstein, M., Su, X., Pamer, E.G., Glickman, M.S., 2011. A gamma interferon independent mechanism of CD4 T cell mediated control of M. tuberculosis infection in vivo. PLoS Pathog. 7, e1002052. doi:10.1371/journal.ppat.1002052

Gan, H., Lee, J., Ren, F., Chen, M., Kornfeld, H., Remold, H.G., 2008. Mycobacterium tuberculosis blocks crosslinking of annexin-1 and apoptotic envelope formation on infected macrophages to maintain virulence. Nat. Immunol. 9, 1189–1197. doi:10.1038/ni.1654

Gantner, B.N., Simmons, R.M., Canavera, S.J., Akira, S., Underhill, D.M., 2003. Collaborative induction of inflammatory responses by dectin-1 and Toll-like receptor 2. J. Exp. Med. 197, 1107–1117. doi:10.1084/jem.20021787

Gao, D., Wu, J., Wu, Y.-T., Du, F., Aroh, C., Yan, N., Sun, L., Chen, Z.J., 2013. Cyclic GMP-AMP Synthase Is an Innate Immune Sensor of HIV and Other Retroviruses. Science 341, 903–906. doi:10.1126/science.1240933

Gao, F., Bailes, E., Robertson, D.L., Chen, Y., Rodenburg, C.M., Michael, S.F., Cummins, L.B., Arthur, L.O., Peeters, M., Shaw, G.M., Sharp, P.M., Hahn, B.H., 1999. Origin of HIV-1 in the chimpanzee Pan troglodytes troglodytes. Nature 397, 436–441. doi:10.1038/17130

Gao, F., Yue, L., White, A.T., Pappas, P.G., Barchue, J., Hanson, A.P., Greene, B.M., Sharp, P.M., Shaw, G.M., Hahn, B.H., 1992. Human infection by genetically diverse SIVSM-related HIV-2 in west Africa. Nature 358, 495–499. doi:10.1038/358495a0

Gao, Y., Nish, S.A., Jiang, R., Hou, L., Licona-Limón, P., Weinstein, J.S., Zhao, H., Medzhitov, R., 2013. Control of T helper 2 responses by transcription factor IRF4-dependent dendritic cells. Immunity 39, 722–732. doi:10.1016/j.immuni.2013.08.028

Garrait, V., Cadranel, J., Esvant, H., Herry, I., Morinet, P., Mayaud, C., Israël-Biet, D., 1997. Tuberculosis generates a microenvironment enhancing the productive infection of local lymphocytes by HIV. J. Immunol. Baltim. Md 1950 159, 2824–2830.

Gartner, S., Markovits, P., Markovitz, D.M., Betts, R.F., Popovic, M., 1986a. Virus isolation from and identification of HTLV-III/LAV-producing cells in brain tissue from a patient with AIDS. JAMA J. Am. Med. Assoc. 256, 2365–2371.

Gartner, S., Markovits, P., Markovitz, D.M., Kaplan, M.H., Gallo, R.C., Popovic, M., 1986b. The role of mononuclear phagocytes in HTLV-III/LAV infection. Science 233, 215–219.

Gautier, E.L., Shay, T., Miller, J., Greter, M., Jakubzick, C., Ivanov, S., Helft, J., Chow, A., Elpek, K.G., Gordonov, S., Mazloom, A.R., Ma'ayan, A., Chua, W.-J., Hansen, T.H., Turley, S.J., Merad, M., Randolph, G.J., Immunological Genome Consortium, 2012. Gene-expression profiles and transcriptional regulatory pathways that underlie the identity and diversity of mouse tissue macrophages. Nat. Immunol. 13, 1118–1128. doi:10.1038/ni.2419

Gazzinelli, R.T., Wysocka, M., Hieny, S., Scharton-Kersten, T., Cheever, A., Kühn, R., Müller, W., Trinchieri, G., Sher, A., 1996. In the absence of endogenous IL-10, mice acutely infected with Toxoplasma gondii succumb to a lethal immune response dependent on CD4+ T cells and accompanied by overproduction of IL-12, IFN-gamma and TNF-alpha. J. Immunol. 157, 798–805.

Geissmann, F., Jung, S., Littman, D.R., 2003. Blood monocytes consist of two principal subsets with distinct migratory properties. Immunity 19, 71–82.

Geissmann, F., Manz, M.G., Jung, S., Sieweke, M.H., Merad, M., Ley, K., 2010. Development of monocytes, macrophages, and dendritic cells. Science 327, 656–661. doi:10.1126/science.1178331

Geldmacher, C., Ngwenyama, N., Schuetz, A., Petrovas, C., Reither, K., Heeregrave, E.J., Casazza, J.P., Ambrozak, D.R., Louder, M., Ampofo, W., Pollakis, G., Hill, B., Sanga, E., Saathoff, E., Maboko, L., Roederer, M., Paxton, W.A., Hoelscher, M., Koup, R.A., 2010. Preferential infection and depletion of Mycobacterium tuberculosis-specific CD4 T cells after HIV-1 infection. J. Exp. Med. 207, 2869–2881. doi:10.1084/jem.20100090

Geldmacher, C., Zumla, A., Hoelscher, M., 2012. Interaction between HIV and Mycobacterium tuberculosis: HIV-1-induced CD4 T-cell depletion and the development of active tuberculosis. Curr. Opin. HIV AIDS 7, 268–275. doi:10.1097/COH.0b013e3283524e32

Gell, P.G.H., 1967. Delayed Hypersensitivity: Specific Cell-Mediated Immunity. Br. Med. Bull. 23, 1–2.

Gendelman, H.E., Orenstein, J.M., Baca, L.M., Weiser, B., Burger, H., Kalter, D.C., Meltzer, M.S., 1989. The macrophage in the persistence and pathogenesis of HIV infection. AIDS Lond. Engl. 3, 475–495.

Geng, Y., Shane, R.B., Berencsi, K., Gonczol, E., Zaki, M.H., Margolis, D.J., Trinchieri, G., Rook, A.H., 2000. Chlamydiapneumoniae Inhibits Apoptosis in Human Peripheral Blood Mononuclear Cells Through Induction of IL-10. J. Immunol. 164, 5522–5529. doi:10.4049/jimmunol.164.10.5522

Germain, R.N., Meier-Schellersheim, M., Nita-Lazar, A., Fraser, I.D.C., 2011. Systems Biology in Immunology - A Computational Modeling Perspective. Annu. Rev. Immunol. 29, 527–585. doi:10.1146/annurev-immunol-030409-101317

Gerszten, R.E., Garcia-Zepeda, E.A., Lim, Y.-C., Yoshida, M., Ding, H.A., Gimbrone, M.A., Luster, A.D., Luscinskas, F.W., Rosenzweig, A., 1999. MCP-1 and IL-8 trigger firm adhesion of monocytes to vascular endothelium under flow conditions. Nature 398, 718–723. doi:10.1038/19546

Geurtsen, J., Chedammi, S., Mesters, J., Cot, M., Driessen, N.N., Sambou, T., Kakutani, R., Ummels, R., Maaskant, J., Takata, H., Baba, O., Terashima, T., Bovin, N., Vandenbroucke-Grauls, C.M.J.E., Nigou, J., Puzo, G., Lemassu, A., Daffé, M., Appelmelk, B.J., 2009. Identification of mycobacterial alpha-glucan as a novel ligand for DC-SIGN: involvement of mycobacterial capsular polysaccharides in host immune modulation. J. Immunol. Baltim. Md 1950 183, 5221–5231. doi:10.4049/jimmunol.0900768

Ghisletti, S., Barozzi, I., Mietton, F., Polletti, S., De Santa, F., Venturini, E., Gregory, L., Lonie, L., Chew, A., Wei, C.-L., Ragoussis, J., Natoli, G., 2010. Identification and characterization of enhancers controlling the inflammatory gene expression program in macrophages. Immunity 32, 317–328. doi:10.1016/j.immuni.2010.02.008

Gibbs, J.H., Ferguson, J., Brown, R.A., Kenicer, K.J., Potts, R.C., Coghill, G., Swanson Beck, J., 1984. Histometric study of the localisation of lymphocyte subsets and accessory cells in human Mantoux reactions. J. Clin. Pathol. 37, 1227–1234.

Gilbert, P.B., McKeague, I.W., Eisen, G., Mullins, C., Guéye-NDiaye, A., Mboup, S., Kanki, P.J., 2003. Comparison of HIV-1 and HIV-2 infectivity from a prospective cohort study in Senegal. Stat. Med. 22, 573–593. doi:10.1002/sim.1342

Gilks, C.F., Brindle, R.J., Otieno, L.S., Bhatt, S.M., Newnham, R.S., Simani, P.M., Lule, G.N., Okelo, G.B., Watkins, W.M., Waiyaki, P.G., 1990. Extrapulmonary and disseminated tuberculosis in HIV-1-seropositive patients presenting to the acute medical services in Nairobi. AIDS Lond. Engl. 4, 981–985.

Gilleron, M., Quesniaux, V.F.J., Puzo, G., 2003. Acylation State of the Phosphatidylinositol Hexamannosides from Mycobacterium bovis Bacillus Calmette Guérin and Mycobacterium tuberculosis H37Rv and Its Implication in Toll-like Receptor Response. J. Biol. Chem. 278, 29880–29889. doi:10.1074/jbc.M303446200

Ginhoux, F., Greter, M., Leboeuf, M., Nandi, S., See, P., Gokhan, S., Mehler, M.F., Conway, S.J., Ng, L.G., Stanley, E.R., Samokhvalov, I.M., Merad, M., 2010. Fate mapping analysis reveals that adult microglia derive from primitive macrophages. Science 330, 841–845. doi:10.1126/science.1194637

Ginhoux, F., Jung, S., 2014. Monocytes and macrophages: developmental pathways and tissue homeostasis. Nat. Rev. Immunol. 14, 392–404. doi:10.1038/nri3671

Glazko, G.V., Emmert-Streib, F., 2009. Unite and conquer: univariate and multivariate approaches for finding differentially expressed gene sets. Bioinformatics 25, 2348–2354. doi:10.1093/bioinformatics/btp406

Glocker, E.-O., Kotlarz, D., Boztug, K., Gertz, E.M., Schäffer, A.A., Noyan, F., Perro, M., Diestelhorst, J., Allroth, A., Murugan, D., Hätscher, N., Pfeifer, D., Sykora, K.-W., Sauer, M., Kreipe, H., Lacher, M., Nustede, R., Woellner, C., Baumann, U., Salzer, U., Koletzko, S., Shah, N., Segal, A.W., Sauerbrey, A., Buderus, S., Snapper, S.B., Grimbacher, B., Klein, C., 2009. Inflammatory bowel disease and mutations affecting the interleukin-10 receptor. N. Engl. J. Med. 361, 2033–2045. doi:10.1056/NEJMoa0907206

Go, N.F., Castle, B.E., Barrett, R., Kastelein, R., Dang, W., Mosmann, T.R., Moore, K.W., Howard, M., 1990. Interleukin 10, a novel B cell stimulatory factor: unresponsiveness of X chromosome-linked immunodeficiency B cells. J. Exp. Med. 172, 1625–1631.

Goldman, D.L., Khine, H., Abadi, J., Lindenberg, D.J., Pirofski La, Niang, R., Casadevall, A., 2001. Serologic evidence for Cryptococcus neoformans infection in early childhood. Pediatrics 107, E66.

Goletti, D., Carrara, S., Vincenti, D., Giacomini, E., Fattorini, L., Garbuglia, A.R., Capobianchi, M.R., Alonzi, T., Fimia, G.M., Federico, M., Poli, G., Coccia, E., 2004. Inhibition of HIV-1 replication in monocyte-derived macrophages by Mycobacterium tuberculosis. J. Infect. Dis. 189, 624–633. doi:10.1086/381554

Gong, J.H., Zhang, M., Modlin, R.L., Linsley, P.S., Iyer, D., Lin, Y., Barnes, P.F., 1996. Interleukin-10 downregulates Mycobacterium tuberculosis-induced Th1 responses and CTLA-4 expression. Infect. Immun. 64, 913–918.

Gonzalez-Lombana, C., Gimblet, C., Bacellar, O., Oliveira, W.W., Passos, S., Carvalho, L.P., Goldschmidt, M., Carvalho, E.M., Scott, P., 2013. IL-17 Mediates Immunopathology in the Absence of IL-10 Following Leishmania major Infection. PLoS Pathog 9, e1003243. doi:10.1371/journal.ppat.1003243

González-Navajas, J.M., Lee, J., David, M., Raz, E., 2012. Immunomodulatory functions of type I interferons. Nat. Rev. Immunol. doi:10.1038/nri3133

Gonzalo, J.-A., Qiu, Y., Lora, J.M., Al-Garawi, A., Villeval, J.-L., Boyce, J.A., Martinez-A, C., Marquez, G., Goya, I., Hamid, Q., Fraser, C.C., Picarella, D., Cote-Sierra, J., Hodge, M.R., Gutierrez-Ramos, J.-C., Kolbeck, R., Coyle, A.J., 2007. Coordinated involvement of mast cells and T cells in allergic mucosal inflammation: critical role of the CC chemokine ligand 1:CCR8 axis. J. Immunol. Baltim. Md 1950 179, 1740–1750.

Gordon, M.A., Gordon, S.B., Musaya, L., Zijlstra, E.E., Molyneux, M.E., Read, R.C., 2007. Primary macrophages from HIV-infected adults show dysregulated cytokine responses to Salmonella, but normal internalization and killing. AIDS Lond. Engl. 21, 2399–2408. doi:10.1097/QAD.0b013e3282f25107

Gordon, S., 2008. Elie Metchnikoff: father of natural immunity. Eur. J. Immunol. 38, 3257–3264. doi:10.1002/eji.200838855

Gordon, S.B., Jarman, E.R., Kanyanda, S., French, N., Pridmore, A.C., Zijlstra, E.E., Molyneux, M.E., Read, R.C., 2005. Reduced interleukin-8 response to Streptococcus pneumoniae by alveolar macrophages from adults with HIV/AIDS. AIDS Lond. Engl. 19, 1197–1200.

Gordon, S.B., Molyneux, M.E., Boeree, M.J., Kanyanda, S., Chaponda, M., Squire, S.B., Read, R.C., 2001. Opsonic phagocytosis of Streptococcus pneumoniae by alveolar macrophages is not impaired in human immunodeficiency virus-infected Malawian adults. J. Infect. Dis. 184, 1345–1349. doi:10.1086/324080

Goujon, C., Moncorgé, O., Bauby, H., Doyle, T., Ward, C.C., Schaller, T., Hué, S., Barclay, W.S., Schulz, R., Malim, M.H., 2013. Human MX2 is an interferon-induced post-entry inhibitor of HIV-1 infection. Nature advance online publication. doi:10.1038/nature12542

Gracie, J.A., Robertson, S.E., McInnes, I.B., 2003. Interleukin-18. J. Leukoc. Biol. 73, 213–224.

Graham, N.M., Nelson, K.E., Solomon, L., Bonds, M., Rizzo, R.T., Scavotto, J., Astemborski, J., Vlahov, D., 1992. Prevalence of tuberculin positivity and skin test anergy in HIV-1-seropositive and -seronegative intravenous drug users. JAMA J. Am. Med. Assoc. 267, 369–373.

Gratchev, A., Kzhyshkowska, J., Kannookadan, S., Ochsenreiter, M., Popova, A., Yu, X., Mamidi, S., Stonehouse-Usselmann, E., Muller-Molinet, I., Gooi, L., Goerdt, S., 2008. Activation of a TGF-β-Specific Multistep Gene Expression Program in Mature Macrophages Requires Glucocorticoid-Mediated Surface Expression of TGF-β Receptor II. J. Immunol. 180, 6553 –6565.

Greter, M., Lelios, I., Pelczar, P., Hoeffel, G., Price, J., Leboeuf, M., Kündig, T.M., Frei, K., Ginhoux, F., Merad, M., Becher, B., 2012. Stroma-derived interleukin-34 controls the development and maintenance of langerhans cells and the maintenance of microglia. Immunity 37, 1050–1060. doi:10.1016/j.immuni.2012.11.001

Griffith, J.W., Sokol, C.L., Luster, A.D., 2014. Chemokines and chemokine receptors: positioning cells for host defense and immunity. Annu. Rev. Immunol. 32, 659–702. doi:10.1146/annurev-immunol-032713-120145

Gringhuis, S.I., den Dunnen, J., Litjens, M., van Het Hof, B., van Kooyk, Y., Geijtenbeek, T.B.H., 2007. C-type lectin DC-SIGN modulates Toll-like receptor signaling via Raf-1 kinase-dependent acetylation of transcription factor NF-kappaB. Immunity 26, 605–616. doi:10.1016/j.immuni.2007.03.012

Groot, F., Welsch, S., Sattentau, Q.J., 2008. Efficient HIV-1 transmission from macrophages to T cells across transient virological synapses. Blood 111, 4660–4663. doi:10.1182/blood-2007-12-130070

Grunig, G., Corry, D.B., Leach, M.W., Seymour, B.W.P., Kurup, V.P., Rennick, D.M., 1997. Interleukin-10 Is a Natural Suppressor of Cytokine Production and Inflammation in a Murine Model of Allergic Bronchopulmonary Aspergillosis. J. Exp. Med. 185, 1089–1100.

Guarda, G., Braun, M., Staehli, F., Tardivel, A., Mattmann, C., Förster, I., Farlik, M., Decker, T., Du Pasquier, R.A., Romero, P., Tschopp, J., 2011. Type I interferon inhibits interleukin-1 production and inflammasome activation. Immunity 34, 213–223. doi:10.1016/j.immuni.2011.02.006

Guilliams, M., Ginhoux, F., Jakubzick, C., Naik, S.H., Onai, N., Schraml, B.U., Segura, E., Tussiwand, R., Yona, S., 2014. Dendritic cells, monocytes and macrophages: a unified nomenclature based on ontogeny. Nat. Rev. Immunol. 14, 571–578. doi:10.1038/nri3712

Guilliams, M., Kleer, I.D., Henri, S., Post, S., Vanhoutte, L., Prijck, S.D., Deswarte, K., Malissen, B., Hammad, H., Lambrecht, B.N., 2013. Alveolar macrophages develop from fetal monocytes that differentiate into long-lived cells in the first week of life via GM-CSF. J. Exp. Med. doi:10.1084/jem.20131199

Gupta, A., Wood, R., Kaplan, R., Bekker, L.-G., Lawn, S.D., 2012. Tuberculosis incidence rates during 8 years of follow-up of an antiretroviral treatment cohort in South Africa: comparison with rates in the community. PloS One 7, e34156. doi:10.1371/journal.pone.0034156

Gutierrez, M.G., Master, S.S., Singh, S.B., Taylor, G.A., Colombo, M.I., Deretic, V., 2004. Autophagy Is a Defense Mechanism Inhibiting BCG and Mycobacterium tuberculosis Survival in Infected Macrophages. Cell 119, 753–766. doi:10.1016/j.cell.2004.11.038

Haase, A.T., 2005. Perils at mucosal front lines for HIV and SIV and their hosts. Nat. Rev. Immunol. 5, 783–792. doi:10.1038/nri1705

Haase, A.T., 2010. Targeting early infection to prevent HIV-1 mucosal transmission. Nature 464, 217–223. doi:10.1038/nature08757

Haddow, L.J., Dibben, O., Moosa, M.-Y.S., Borrow, P., Easterbrook, P.J., 2011. Circulating inflammatory biomarkers can predict and characterize tuberculosis-associated immune reconstitution inflammatory syndrome. AIDS Lond. Engl. 25, 1163–1174. doi:10.1097/QAD.0b013e3283477d67

Haddow, L.J., Easterbrook, P.J., Mosam, A., Khanyile, N.G., Parboosing, R., Moodley, P., Moosa, M.-Y.S., 2009. Defining Immune Reconstitution Inflammatory Syndrome: Evaluation of Expert Opinion versus 2 Case Definitions in a South African Cohort. Clin. Infect. Dis. 49, 1424–1432. doi:10.1086/630208

Hagiwara, E., Sacks, T., Leitman-Klinman, S.F., Klinman, D.M., 1996. Effect of HIV infection on the frequency of cytokine-secreting cells in human peripheral blood. AIDS Res. Hum. Retroviruses 12, 127–133.

Haniffa, M., Ginhoux, F., Wang, X.-N., Bigley, V., Abel, M., Dimmick, I., Bullock, S., Grisotto, M., Booth, T., Taub, P., Hilkens, C., Merad, M., Collin, M., 2009. Differential rates of replacement of human dermal dendritic cells and macrophages during hematopoietic stem cell transplantation. J. Exp. Med. 206, 371–385. doi:10.1084/jem.20081633

Hao, S., Baltimore, D., 2009. The stability of mRNA influences the temporal order of the induction of genes encoding inflammatory molecules. Nat. Immunol. 10, 281–288. doi:10.1038/ni.1699

Hardison, J.L., Wrightsman, R.A., Carpenter, P.M., Lane, T.E., Manning, J.E., 2006. The chemokines CXCL9 and CXCL10 promote a protective immune response but do not contribute to cardiac inflammation following infection with Trypanosoma cruzi. Infect. Immun. 74, 125–134. doi:10.1128/IAI.74.1.125-134.2006

Harrison, T.S., 2009. The burden of HIV-associated cryptococcal disease. AIDS Lond. Engl. 23, 531–532. doi:10.1097/QAD.0b013e328322ffc3

Hashimoto, D., Chow, A., Noizat, C., Teo, P., Beasley, M.B., Leboeuf, M., Becker, C.D., See, P., Price, J., Lucas, D., Greter, M., Mortha, A., Boyer, S.W., Forsberg, E.C., Tanaka, M., van Rooijen, N., García-Sastre, A., Stanley, E.R., Ginhoux, F., Frenette, P.S., Merad, M., 2013. Tissue-Resident Macrophages Self-Maintain Locally throughout Adult Life with Minimal Contribution from Circulating Monocytes. Immunity 38, 792–804. doi:10.1016/j.immuni.2013.04.004

Hayward, A.C., Darton, T., Van-Tam, J.N., Watson, J.M., Coker, R., Schwoebel, V., 2003. Epidemiology and control of tuberculosis in Western European cities. Int. J. Tuberc. Lung Dis. Off. J. Int. Union Tuberc. Lung Dis. 7, 751–757.

Heinz, S., Benner, C., Spann, N., Bertolino, E., Lin, Y.C., Laslo, P., Cheng, J.X., Murre, C., Singh, H., Glass, C.K., 2010. Simple combinations of lineage-determining transcription factors prime cis-regulatory elements required for macrophage and B cell identities. Mol. Cell 38, 576–589. doi:10.1016/j.molcel.2010.05.004

Hemelaar, J., 2012. The origin and diversity of the HIV-1 pandemic. Trends Mol. Med. 18, 182–192. doi:10.1016/j.molmed.2011.12.001

Herre, J., Marshall, A.S.J., Caron, E., Edwards, A.D., Williams, D.L., Schweighoffer, E., Tybulewicz, V., Sousa, C.R. e, Gordon, S., Brown, G.D., 2004. Dectin-1 uses novel mechanisms for yeast phagocytosis in macrophages. Blood 104, 4038–4045. doi:10.1182/blood-2004-03-1140

Hess, J., Ladel, C., Miko, D., Kaufmann, S.H., 1996. Salmonella typhimurium aroA- infection in gene-targeted immunodeficient mice: major role of CD4+ TCR-alpha beta cells and IFN-gamma in bacterial clearance independent of intracellular location. J. Immunol. 156, 3321–3326.

Hettinger, J., Richards, D.M., Hansson, J., Barra, M.M., Joschko, A.-C., Krijgsveld, J., Feuerer, M., 2013. Origin of monocytes and macrophages in a committed progenitor. Nat. Immunol. 14, 821–830. doi:10.1038/ni.2638

Heyworth, P.G., Cross, A.R., Curnutte, J.T., 2003. Chronic granulomatous disease. Curr. Opin. Immunol. 15, 578–584.

Higgins, D.M., Sanchez-Campillo, J., Rosas-Taraco, A.G., Lee, E.J., Orme, I.M., Gonzalez-Juarrero, M., 2009. Lack of IL-10 alters inflammatory and immune responses during pulmonary Mycobacterium tuberculosis infection. Tuberc. Edinb. Scotl. 89, 149–157. doi:10.1016/j.tube.2009.01.001

Hirsch, C.S., Toossi, Z., Johnson, J.L., Luzze, H., Ntambi, L., Peters, P., McHugh, M., Okwera, A., Joloba, M., Mugyenyi, P., Mugerwa, R.D., Terebuh, P., Ellner, J.J., 2001. Augmentation of apoptosis and interferon-gamma production at sites of active Mycobacterium tuberculosis infection in human tuberculosis. J. Infect. Dis. 183, 779–788. doi:10.1086/318817

Ho, D.D., Rota, T.R., Hirsch, M.S., 1986. Infection of monocyte/macrophages by human T lymphotropic virus type III. J. Clin. Invest. 77, 1712–1715. doi:10.1172/JCI112491

Hodge-Dufour, J., Marino, M.W., Horton, M.R., Jungbluth, A., Burdick, M.D., Strieter, R.M., Noble, P.W., Hunter, C.A., Puré, E., 1998. Inhibition of interferon γ induced interleukin 12 production: A potential mechanism for the anti-inflammatory activities of tumor necrosis factor. Proc. Natl. Acad. Sci. 95, 13806–13811. doi:10.1073/pnas.95.23.13806

Hoeffel, G., Wang, Y., Greter, M., See, P., Teo, P., Malleret, B., Leboeuf, M., Low, D., Oller, G., Almeida, F., Choy, S.H.Y., Grisotto, M., Renia, L., Conway, S.J., Stanley, E.R., Chan, J.K.Y., Ng, L.G., Samokhvalov, I.M., Merad, M., Ginhoux, F., 2012. Adult Langerhans cells derive predominantly from embryonic fetal liver monocytes with a minor contribution of yolk sac-derived macrophages. J. Exp. Med. 209, 1167–1181. doi:10.1084/jem.20120340

Hoffmann, M., Dutton, R.W., 1971. Immune response restoration with macrophage culture supernatants. Science 172, 1047–1048.

Hölscher, C., Mohrs, M., Dai, W.J., Köhler, G., Ryffel, B., Schaub, G.A., Mossmann, H., Brombacher, F., 2000. Tumor Necrosis Factor Alpha-Mediated Toxic Shock inTrypanosoma cruzi-Infected Interleukin 10-Deficient Mice. Infect. Immun. 68, 4075–4083. doi:10.1128/IAI.68.7.4075-4083.2000

Honda, Y., Rogers, L., Nakata, K., Zhao, B.-Y., Pine, R., Nakai, Y., Kurosu, K., Rom, W.N., Weiden, M., 1998. Type I Interferon Induces Inhibitory 16-kD CCAAT/ Enhancer Binding Protein (C/EBP)β, Repressing the HIV-1 Long Terminal Repeat in Macrophages: Pulmonary Tuberculosis Alters C/EBP Expression, Enhancing HIV-1 Replication. J. Exp. Med. 188, 1255 –1265. doi:10.1084/jem.188.7.1255

Hoppstädter, J., Diesel, B., Zarbock, R., Breinig, T., Monz, D., Koch, M., Meyerhans, A., Gortner, L., Lehr, C.-M., Huwer, H., Kiemer, A.K., 2010. Differential cell reaction upon Toll-like receptor 4 and 9 activation in human alveolar and lung interstitial macrophages. Respir. Res. 11, 124. doi:10.1186/1465-9921-11-124

Horwitz, D.A., Zheng, S.G., Gray, J.D., 2003. The role of the combination of IL-2 and TGF-β or IL-10 in the generation and function of CD4+ CD25+ and CD8+regulatory T cell subsets. J. Leukoc. Biol. 74, 471–478. doi:10.1189/jlb.0503228

Hoshino, Y., Nakata, K., Hoshino, S., Honda, Y., Tse, D.B., Shioda, T., Rom, W.N., Weiden, M., 2002. Maximal HIV-1 Replication in Alveolar Macrophages during Tuberculosis Requires both Lymphocyte Contact and Cytokines. J. Exp. Med. 195, 495 –505. doi:10.1084/jem.20011614

Hoshino, Y., Tse, D.B., Rochford, G., Prabhakar, S., Hoshino, S., Chitkara, N., Kuwabara, K., Ching, E., Raju, B., Gold, J.A., Borkowsky, W., Rom, W.N., Pine, R., Weiden, M., 2004. Mycobacterium tuberculosis-induced CXCR4 and chemokine expression leads to preferential X4 HIV-1 replication in human macrophages. J. Immunol. Baltim. Md 1950 172, 6251–6258.

Howard, M., Muchamuel, T., Andrade, S., Menon, S., 1993. Interleukin 10 protects mice from lethal endotoxemia. J. Exp. Med. 177, 1205–1208. doi:10.1084/jem.177.4.1205

Hrecka, K., Hao, C., Gierszewska, M., Swanson, S.K., Kesik-Brodacka, M., Srivastava, S., Florens, L., Washburn, M.P., Skowronski, J., 2011. Vpx relieves inhibition of HIV-1 infection of macrophages mediated by the SAMHD1 protein. Nature 474, 658–661. doi:10.1038/nature10195

Hsieh, C.-S., Macatonia, S.E., Tripp, C.S., Wolf, S.F., O'Garra, A., Murphy, K.M., 1993. Development of Th1 CD4 T Cells Through IL-12 Produced by Listeria-Induced Macrophages. Science, New Series 260, 547–549.

Hu, X., Paik, P.K., Chen, J., Yarilina, A., Kockeritz, L., Lu, T.T., Woodgett, J.R., Ivashkiv, L.B., 2006. IFN-gamma suppresses IL-10 production and synergizes with TLR2 by regulating GSK3 and CREB/AP-1 proteins. Immunity 24, 563–574. doi:10.1016/j.immuni.2006.02.014

Huang, Y., Erdmann, N., Peng, H., Herek, S., Davis, J.S., Luo, X., Ikezu, T., Zheng, J., 2006. TRAIL-Mediated Apoptosis in HIV-1-Infected Macrophages Is Dependent on the Inhibition of Akt-1 Phosphorylation. J. Immunol. 177, 2304–2313.

Hume, D.A., 2008. Macrophages as APC and the dendritic cell myth. J. Immunol. Baltim. Md 1950 181, 5829–5835.

Humphrey, J.H., 1967. Cell-mediated immunity--general perspectives. Br. Med. Bull. 23, 93–97.

Hung, C.-H., Thomas, L., Ruby, C.E., Atkins, K.M., Morris, N.P., Knight, Z.A., Scholz, I., Barklis, E., Weinberg, A.D., Shokat, K.M., Thomas, G., 2007. HIV-1 Nef Assembles a Src Family Kinase-ZAP-70/Syk-PI3K Cascade to Downregulate Cell-Surface MHC-I. Cell Host Microbe 1, 121–133. doi:10.1016/j.chom.2007.03.004

Hung, J.-H., Yang, T.-H., Hu, Z., Weng, Z., DeLisi, C., 2012. Gene set enrichment analysis: performance evaluation and usage guidelines. Brief. Bioinform. 13, 281–291. doi:10.1093/bib/bbr049

Hunter, C.A., Ellis-Neyes, L.A., Slifer, T., Kanaly, S., Grünig, G., Fort, M., Rennick, D., Araujo, F.G., 1997. IL-10 is required to prevent immune hyperactivity during infection with Trypanosoma cruzi. J. Immunol. Baltim. Md 1950 158, 3311–3316.

Hutchins, A.P., Diez, D., Miranda-Saavedra, D., 2013. The IL-10/STAT3-mediated anti-inflammatory response: recent developments and future challenges. Brief. Funct. Genomics 12, 489–498. doi:10.1093/bfgp/elt028

Hutchins, A.P., Poulain, S., Miranda-Saavedra, D., 2012. Genome-wide analysis of STAT3 binding in vivo predicts effectors of the anti-inflammatory response in macrophages. Blood 119, e110–119. doi:10.1182/blood-2011-09-381483

Ieong, M.H., Reardon, C.C., Levitz, S.M., Kornfeld, H., 2000. Human immunodeficiency virus type 1 infection of alveolar macrophages impairs their innate fungicidal activity. Am. J. Respir. Crit. Care Med. 162, 966–970.

Imai, T., Nagira, M., Takagi, S., Kakizaki, M., Nishimura, M., Wang, J., Gray, P.W., Matsushima, K., Yoshie, O., 1999. Selective recruitment of CCR4-bearing Th2 cells toward antigen-presenting cells by the CC chemokines thymus and activation-regulated chemokine and macrophage-derived chemokine. Int. Immunol. 11, 81–88.

Imam, N., Carpenter, C.C.J., Mayer, K.H., Fisher, A., Stein, M., Danforth, S.B., 1990. Hierarchical pattern of mucosal candida infections in HIV-seropositive women. Am. J. Med. 89, 142–146. doi:10.1016/0002-9343(90)90291-K

Imhof, B.A., Aurrand-Lions, M., 2004. Adhesion mechanisms regulating the migration of monocytes. Nat. Rev. Immunol. 4, 432–444. doi:10.1038/nri1375

Imperiali, F.G., Zaninoni, A., La Maestra, L., Tarsia, P., Blasi, F., Barcellini, W., 2001. Increased Mycobacterium tuberculosis growth in HIV-1-infected human macrophages: role of tumour necrosis factor-alpha. Clin. Exp. Immunol. 123, 435–442.

Ingersoll, M.A., Spanbroek, R., Lottaz, C., Gautier, E.L., Frankenberger, M., Hoffmann, R., Lang, R., Haniffa, M., Collin, M., Tacke, F., Habenicht, A.J.R., Ziegler-Heitbrock, L., Randolph, G.J., 2010. Comparison of gene expression profiles between human and mouse monocyte subsets. Blood 115, e10–19. doi:10.1182/blood-2009-07-235028

Irizarry, R.A., Wang, C., Zhou, Y., Speed, T.P., 2009. Gene set enrichment analysis made simple. Stat. Methods Med. Res. 18, 565–575. doi:10.1177/0962280209351908

Itoh, K., Hirohata, S., 1995. The role of IL-10 in human B cell activation, proliferation, and differentiation. J. Immunol. Baltim. Md 1950 154, 4341–4350.

Ivanov, S.S., Roy, C.R., 2013. Pathogen signatures activate a ubiquitination pathway that modulates the function of the metabolic checkpoint kinase mTOR. Nat. Immunol. 14, 1219–1228. doi:10.1038/ni.2740

Iwakura, Y., Ishigame, H., 2006. The IL-23/IL-17 axis in inflammation. J. Clin. Invest. 116, 1218–1222. doi:10.1172/JCI28508

Iwasaki, H., Takeuchi, O., Teraguchi, S., Matsushita, K., Uehata, T., Kuniyoshi, K., Satoh, T., Saitoh, T., Matsushita, M., Standley, D.M., Akira, S., 2011. The I[kappa]B kinase complex regulates the stability of cytokine-encoding mRNA induced by TLR-IL-1R by controlling degradation of regnase-1. Nat Immunol 12, 1167–1175. doi:10.1038/ni.2137

Iyer, S.S., Cheng, G., 2012. Role of interleukin 10 transcriptional regulation in inflammation and autoimmune disease. Crit. Rev. Immunol. 32, 23–63.

Izadpanah, A., Gallo, R.L., 2005. Antimicrobial peptides. J. Am. Acad. Dermatol. 52, 381–390. doi:10.1016/j.jaad.2004.08.026

Jacobson, M.A., Zegans, M., Pavan, P.R., O'Donnell, J.J., Sattler, F., Rao, N., Owens, S., Pollard, R., 1997. Cytomegalovirus retinitis after initiation of highly active antiretroviral therapy. The Lancet 349, 1443–1445. doi:10.1016/S0140-6736(96)11431-8

Jaffe, H.W., Bregman, D.J., Selik, R.M., 1983. Acquired immune deficiency syndrome in the United States: the first 1,000 cases. J. Infect. Dis. 148, 339–345.

Jakubzick, C., Gautier, E.L., Gibbings, S.L., Sojka, D.K., Schlitzer, A., Johnson, T.E., Ivanov, S., Duan, Q., Bala, S., Condon, T., van Rooijen, N., Grainger, J.R., Belkaid, Y., Ma'ayan, A., Riches, D.W.H., Yokoyama, W.M., Ginhoux, F., Henson, P.M., Randolph, G.J., 2013. Minimal differentiation of classical monocytes as they survey steady-state tissues and transport antigen to lymph nodes. Immunity 39, 599–610. doi:10.1016/j.immuni.2013.08.007

Jambo, K.C., Banda, D.H., Kankwatira, A.M., Sukumar, N., Allain, T.J., Heyderman, R.S., Russell, D.G., Mwandumba, H.C., 2014. Small alveolar macrophages are infected preferentially by HIV and exhibit impaired phagocytic function. Mucosal Immunol. doi:10.1038/mi.2013.127

Jarry, A., Cortez, A., René, E., Muzeau, F., Brousse, N., 1990. Infected cells and immune cells in the gastrointestinal tract of AIDS patients. An immunohistochemical study of 127 cases. Histopathology 16, 133–140.

Jenkins, S.J., Ruckerl, D., Cook, P.C., Jones, L.H., Finkelman, F.D., van Rooijen, N., MacDonald, A.S., Allen, J.E., 2011. Local Macrophage Proliferation, Rather than Recruitment from the Blood, Is a Signature of TH2 Inflammation. Science 332, 1284 –1288. doi:10.1126/science.1204351

Jenkins, S.J., Ruckerl, D., Thomas, G.D., Hewitson, J.P., Duncan, S., Brombacher, F., Maizels, R.M., Hume, D.A., Allen, J.E., 2013. IL-4 directly signals tissue-resident macrophages to proliferate beyond homeostatic levels controlled by CSF-1. J. Exp. Med. 210, 2477–2491. doi:10.1084/jem.20121999

Jiang, Y., Beller, D.I., Frendl, G., Graves, D.T., 1992. Monocyte chemoattractant protein-1 regulates adhesion molecule expression and cytokine production in human monocytes. J. Immunol. 148, 2423–2428.

Jouanguy, E., Altare, F., Lamhamedi, S., Revy, P., Emile, J.F., Newport, M., Levin, M., Blanche, S., Seboun, E., Fischer, A., Casanova, J.L., 1996. Interferon-gamma-receptor deficiency in an infant with fatal bacille Calmette-Guérin infection. N. Engl. J. Med. 335, 1956–1961. doi:10.1056/NEJM199612263352604

Jouanguy, E., Döffinger, R., Dupuis, S., Pallier, A., Altare, F., Casanova, J.L., 1999. IL-12 and IFN-gamma in host defense against mycobacteria and salmonella in mice and men. Curr. Opin. Immunol. 11, 346–351.

Jovanovic, D.V., Battista, J.A.D., Martel-Pelletier, J., Jolicoeur, F.C., He, Y., Zhang, M., Mineau, F., Pelletier, J.-P., 1998. IL-17 Stimulates the Production and Expression of Proinflammatory Cytokines, IL-β and TNF-α, by Human Macrophages. J. Immunol. 160, 3513–3521.

Jung, S.-B., Yang, C.-S., Lee, J.-S., Shin, A.-R., Jung, S.-S., Son, J.W., Harding, C.V., Kim, H.-J., Park, J.-K., Paik, T.-H., Song, C.-H., Jo, E.-K., 2006. The Mycobacterial 38-Kilodalton Glycolipoprotein Antigen Activates the Mitogen-Activated Protein Kinase Pathway and Release of Proinflammatory Cytokines through Toll-Like Receptors 2 and 4 in Human Monocytes. Infect. Immun. 74, 2686–2696. doi:10.1128/IAI.74.5.2686-2696.2006

Jung, Y.-J., Ryan, L., LaCourse, R., North, R.J., 2003. Increased interleukin-10 expression is not responsible for failure of T helper 1 immunity to resolve airborne Mycobacterium tuberculosis infection in mice. Immunology 109, 295–299.

Junt, T., Moseman, E.A., Iannacone, M., Massberg, S., Lang, P.A., Boes, M., Fink, K., Henrickson, S.E., Shayakhmetov, D.M., Di Paolo, N.C., van Rooijen, N., Mempel, T.R., Whelan, S.P., von Andrian, U.H., 2007. Subcapsular sinus macrophages in lymph nodes clear lymph-borne viruses and present them to antiviral B cells. Nature 450, 110–114. doi:10.1038/nature06287

Kagina, B.M.N., Abel, B., Scriba, T.J., Hughes, E.J., Keyser, A., Soares, A., Gamieldien, H., Sidibana, M., Hatherill, M., Gelderbloem, S., Mahomed, H., Hawkridge, A., Hussey, G., Kaplan, G., Hanekom, W.A., other members of the South African Tuberculosis Vaccine Initiative, 2010. Specific T cell frequency and cytokine expression profile do not correlate with protection against tuberculosis after bacillus Calmette-Guérin vaccination of newborns. Am. J. Respir. Crit. Care Med. 182, 1073–1079. doi:10.1164/rccm.201003-0334OC

Kaiser, F., Cook, D., Papoutsopoulou, S., Rajsbaum, R., Wu, X., Yang, H.-T., Grant, S., Ricciardi-Castagnoli, P., Tsichlis, P.N., Ley, S.C., O'Garra, A., 2009. TPL-2 negatively regulates interferon-β production in macrophages and myeloid dendritic cells. J. Exp. Med. 206, 1863–1871. doi:10.1084/jem.20091059

Kallenius, G., Koivula, T., Rydgard, K.J., Hoffner, S.E., Valentin, A., Asjo, B., Ljungh, C., Sharma, U., Svenson, S.B., 1992. Human immunodeficiency virus type 1 enhances intracellular growth of Mycobacterium avium in human macrophages. Infect. Immun. 60, 2453–2458.

Kalsdorf, B., Scriba, T.J., Wood, K., Day, C.L., Dheda, K., Dawson, R., Hanekom, W.A., Lange, C., Wilkinson, R.J., 2009. HIV-1 infection impairs the bronchoalveolar T-cell response to mycobacteria. Am. J. Respir. Crit. Care Med. 180, 1262–1270. doi:10.1164/rccm.200907-1011OC

Kane, M., Yadav, S.S., Bitzegeio, J., Kutluay, S.B., Zang, T., Wilson, S.J., Schoggins, J.W., Rice, C.M., Yamashita, M., Hatziioannou, T., Bieniasz, P.D., 2013. MX2 is an interferon-induced inhibitor of HIV-1 infection. Nature 502, 563–566. doi:10.1038/nature12653

Kang, P.B., Azad, A.K., Torrelles, J.B., Kaufman, T.M., Beharka, A., Tibesar, E., DesJardin, L.E., Schlesinger, L.S., 2005. The human macrophage mannose receptor directs Mycobacterium tuberculosis lipoarabinomannan-mediated phagosome biogenesis. J. Exp. Med. 202, 987–999. doi:10.1084/jem.20051239

Kanitakis, J., Morelon, E., Petruzzo, P., Badet, L., Dubernard, J.-M., 2011. Self-renewal capacity of human epidermal Langerhans cells: observations made on a composite tissue allograft. Exp. Dermatol. 20, 145–146. doi:10.1111/j.1600-0625.2010.01146.x

Kaplan, J.E., Hanson, D., Dworkin, M.S., Frederick, T., Bertolli, J., Lindegren, M.L., Holmberg, S., Jones, J.L., 2000. Epidemiology of Human Immunodeficiency Virus–Associated Opportunistic Infections in the United States in the Era of Highly Active Antiretroviral Therapy. Clin. Infect. Dis. 30, S5–S14. doi:10.1086/313843

Kapsenberg, M.L., 2003. Dendritic-cell control of pathogen-driven T-cell polarization. Nat. Rev. Immunol. 3, 984–993. doi:10.1038/nri1246

Karakousis, P.C., Moore, R.D., Chaisson, R.E., 2004. Mycobacterium avium complex in patients with HIV infection in the era of highly active antiretroviral therapy. Lancet Infect. Dis. 4, 557–565. doi:10.1016/S1473-3099(04)01130-2

Kassutto, S., Rosenberg, E.S., 2004. Primary HIV Type 1 Infection. Clin. Infect. Dis. 38, 1447–1453. doi:10.1086/420745

Katakura, T., Miyazaki, M., Kobayashi, M., Herndon, D.N., Suzuki, F., 2004. CCL17 and IL-10 as Effectors That Enable Alternatively Activated Macrophages to Inhibit the Generation of Classically Activated Macrophages. J. Immunol. 172, 1407–1413. doi:10.4049/jimmunol.172.3.1407

Kaufmann, S.H., 1999. Cell-mediated immunity: dealing a direct blow to pathogens. Curr. Biol. CB 9, R97–99.

Kaufmann, S.H.E., 1995. Immunity to intracellular microbial pathogens. Immunol. Today 16, 338–342. doi:10.1016/0167-5699(95)80151-0

Kaul, M., Garden, G.A., Lipton, S.A., 2001. Pathways to neuronal injury and apoptosis in HIV-associated dementia. Nature 410, 988–994. doi:10.1038/35073667

Kawai, T., Akira, S., 2006. Innate immune recognition of viral infection. Nat. Immunol. 7, 131–137. doi:10.1038/ni1303

Kawai, T., Akira, S., 2010. The role of pattern-recognition receptors in innate immunity: update on Toll-like receptors. Nat. Immunol. 11, 373–384. doi:10.1038/ni.1863

Keane, J., Balcewicz-Sablinska, M.K., Remold, H.G., Chupp, G.L., Meek, B.B., Fenton, M.J., Kornfeld, H., 1997. Infection by Mycobacterium tuberculosis promotes human alveolar macrophage apoptosis. Infect. Immun. 65, 298–304.

Keane, J., Gershon, S., Wise, R.P., Mirabile-Levens, E., Kasznica, J., Schwieterman, W.D., Siegel, J.N., Braun, M.M., 2001. Tuberculosis associated with infliximab, a tumor necrosis factor alpha-neutralizing agent. N. Engl. J. Med. 345, 1098–1104. doi:10.1056/NEJMoa011110

Keane, J., Remold, H.G., Kornfeld, H., 2000. Virulent Mycobacterium tuberculosis strains evade apoptosis of infected alveolar macrophages. J. Immunol. Baltim. Md 1950 164, 2016–2020.

Kedzierska, K., Crowe, S.M., 2001. Cytokines and HIV-1: interactions and clinical implications. Antivir. Chem. Chemother. 12, 133–150.

Keele, B.F., Jones, J.H., Terio, K.A., Estes, J.D., Rudicell, R.S., Wilson, M.L., Li, Y., Learn, G.H., Beasley, T.M., Schumacher-Stankey, J., Wroblewski, E., Mosser, A., Raphael, J., Kamenya, S., Lonsdorf, E.V., Travis, D.A., Mlengeya, T., Kinsel, M.J., Else, J.G., Silvestri, G., Goodall, J., Sharp, P.M., Shaw, G.M., Pusey, A.E., Hahn, B.H., 2009. Increased mortality and AIDS-like immunopathology in wild chimpanzees infected with SIVcpz. Nature 460, 515–519. doi:10.1038/nature08200

Kelly, E.K., Wang, L., Ivashkiv, L.B., 2010. Calcium-activated pathways and oxidative burst mediate zymosan-induced signaling and IL-10 production in human macrophages. J. Immunol. Baltim. Md 1950 184, 5545–5552. doi:10.4049/jimmunol.0901293

Kiemer, A.K., Senaratne, R.H., Hoppstädter, J., Diesel, B., Riley, L.W., Tabeta, K., Bauer, S., Beutler, B., Zuraw, B.L., 2009. Attenuated activation of macrophage TLR9 by DNA from virulent mycobacteria. J. Innate Immun. 1, 29–45. doi:10.1159/000142731

Kirchhoff, F., Greenough, T.C., Brettler, D.B., Sullivan, J.L., Desrosiers, R.C., 1995. Brief report: absence of intact nef sequences in a long-term survivor with nonprogressive HIV-1 infection. N. Engl. J. Med. 332, 228–232. doi:10.1056/NEJM199501263320405

Klein, I., Cornejo, J.C., Polakos, N.K., John, B., Wuensch, S.A., Topham, D.J., Pierce, R.H., Crispe, I.N., 2007. Kupffer cell heterogeneity: functional properties of bone marrow derived and sessile hepatic macrophages. Blood 110, 4077–4085. doi:10.1182/blood-2007-02-073841

Knipe, D.M., 2007. Fields Virology, 5th ed. Lippincott Williams & Wilkins.

Kobayashi, T., Matsuoka, K., Sheikh, S.Z., Elloumi, H.Z., Kamada, N., Hisamatsu, T., Hansen, J.J., Doty, K.R., Pope, S.D., Smale, S.T., Hibi, T., Rothman, P.B., Kashiwada, M., Plevy, S.E., 2011. NFIL3 Is a Regulator of IL-12 p40 in Macrophages and Mucosal Immunity. J. Immunol. 186, 4649–4655. doi:10.4049/jimmunol.1003888

Koenig, S., Gendelman, H.E., Orenstein, J.M., Dal Canto, M.C., Pezeshkpour, G.H., Yungbluth, M., Janotta, F., Aksamit, A., Martin, M.A., Fauci, A.S., 1986. Detection of AIDS virus in macrophages in brain tissue from AIDS patients with encephalopathy. Science 233, 1089–1093.

Kohl, N.E., Emini, E.A., Schleif, W.A., Davis, L.J., Heimbach, J.C., Dixon, R.A., Scolnick, E.M., Sigal, I.S., 1988. Active human immunodeficiency virus protease is required for viral infectivity. Proc. Natl. Acad. Sci. U. S. A. 85, 4686–4690.

Kohyama, M., Ise, W., Edelson, B.T., Wilker, P.R., Hildner, K., Mejia, C., Frazier, W.A., Murphy, T.L., Murphy, K.M., 2009. Role for Spi-C in the development of red pulp macrophages and splenic iron homeostasis. Nature 457, 318–321. doi:10.1038/nature07472

Koppensteiner, H., Banning, C., Schneider, C., Hohenberg, H., Schindler, M., 2012. Macrophage internal HIV-1 is protected from neutralizing antibodies. J. Virol. 86, 2826–2836. doi:10.1128/JVI.05915-11

Korber, B., Muldoon, M., Theiler, J., Gao, F., Gupta, R., Lapedes, A., Hahn, B.H., Wolinsky, S., Bhattacharya, T., 2000. Timing the ancestor of the HIV-1 pandemic strains. Science 288, 1789–1796.

Koziel, H., Eichbaum, Q., Kruskal, B.A., Pinkston, P., Rogers, R.A., Armstrong, M.Y., Richards, F.F., Rose, R.M., Ezekowitz, R.A., 1998. Reduced binding and phagocytosis of Pneumocystis carinii by alveolar macrophages from persons infected with HIV-1 correlates with mannose receptor downregulation. J. Clin. Invest. 102, 1332–1344. doi:10.1172/JCI560

Kramer, H.B., Lavender, K.J., Qin, L., Stacey, A.R., Liu, M.K.P., di Gleria, K., Simmons, A., Gasper-Smith, N., Haynes, B.F., McMichael, A.J., Borrow, P., Kessler, B.M., 2010. Elevation of intact and proteolytic fragments of acute phase proteins constitutes the earliest systemic antiviral response in HIV-1 infection. PLoS Pathog. 6, e1000893. doi:10.1371/journal.ppat.1000893

Krausgruber, T., Blazek, K., Smallie, T., Alzabin, S., Lockstone, H., Sahgal, N., Hussell, T., Feldmann, M., Udalova, I.A., 2011. IRF5 promotes inflammatory macrophage polarization and T(H)1-T(H)17 responses. Nat. Immunol. doi:10.1038/ni.1990

Kruijshaar, M.E., Abubakar, I., 2009. Increase in extrapulmonary tuberculosis in England and Wales 1999-2006. Thorax 64, 1090–1095. doi:10.1136/thx.2009.118133

Kühn, R., Löhler, J., Rennick, D., Rajewsky, K., Müller, W., 1993. Interleukin-10-deficient mice develop chronic enterocolitis. Cell 75, 263–274.

Kuritzkes, D.R., 2000. Neutropenia, Neutrophil Dysfunction, and Bacterial Infection in Patients with Human Immunodeficiency Virus Disease: The Role of Granulocyte Colony-Stimulating Factor. Clin. Infect. Dis. 30, 256–270. doi:10.1086/313642

Kusske, A.M., Rongione, A.J., Ashley, S.W., McFadden, D.W., Reber, H.A., 1996. Interleukin-10 prevents death in lethal necrotizing pancreatitis in mice. Surgery 120, 284–289. doi:10.1016/S0039-6060(96)80299-6

Kuwata, H., Watanabe, Y., Miyoshi, H., Yamamoto, M., Kaisho, T., Takeda, K., Akira, S., 2003. IL-10-inducible Bcl-3 negatively regulates LPS-induced TNF-alpha production in macrophages. Blood 102, 4123–4129. doi:10.1182/blood-2003-04-1228

Kwon, A.T., Arenillas, D.J., Worsley Hunt, R., Wasserman, W.W., 2012. oPOSSUM-3: advanced analysis of regulatory motif over-representation across genes or ChIP-Seq datasets. G3 Bethesda Md 2, 987–1002. doi:10.1534/g3.112.003202

Kyei, G.B., Dinkins, C., Davis, A.S., Roberts, E., Singh, S.B., Dong, C., Wu, L., Kominami, E., Ueno, T., Yamamoto, A., Federico, M., Panganiban, A., Vergne, I., Deretic, V., 2009. Autophagy pathway intersects with HIV-1 biosynthesis and regulates viral yields in macrophages. J. Cell Biol. 186, 255–268. doi:10.1083/jcb.200903070

Lacey, D.C., Achuthan, A., Fleetwood, A.J., Dinh, H., Roiniotis, J., Scholz, G.M., Chang, M.W., Beckman, S.K., Cook, A.D., Hamilton, J.A., 2012. Defining GM-CSF- and macrophage-CSF-dependent macrophage responses by in vitro models. J. Immunol. Baltim. Md 1950 188, 5752–5765. doi:10.4049/jimmunol.1103426

Laguette, N., Sobhian, B., Casartelli, N., Ringeard, M., Chable-Bessia, C., Ségéral, E., Yatim, A., Emiliani, S., Schwartz, O., Benkirane, M., 2011. SAMHD1 is the dendritic- and myeloid-cell-specific HIV-1 restriction factor counteracted by Vpx. Nature 474, 654–657. doi:10.1038/nature10117

Lai, R.P.J., Nakiwala, J.K., Meintjes, G., Wilkinson, R.J., 2013. The immunopathogenesis of the HIV tuberculosis immune reconstitution inflammatory syndrome. Eur. J. Immunol. 43, 1995–2002. doi:10.1002/eji.201343632

Lang, R., Patel, D., Morris, J.J., Rutschman, R.L., Murray, P.J., 2002a. Shaping gene expression in activated and resting primary macrophages by IL-10. J. Immunol. Baltim. Md 1950 169, 2253–2263.

Lang, R., Patel, D., Morris, J.J., Rutschman, R.L., Murray, P.J., 2002b. Shaping gene expression in activated and resting primary macrophages by IL-10. J. Immunol. Baltim. Md 1950 169, 2253–2263.

Lang, R., Rutschman, R.L., Greaves, D.R., Murray, P.J., 2002c. Autocrine deactivation of macrophages in transgenic mice constitutively overexpressing IL-10 under control of the human CD68 promoter. J. Immunol. Baltim. Md 1950 168, 3402–3411.

Langrish, C.L., Chen, Y., Blumenschein, W.M., Mattson, J., Basham, B., Sedgwick, J.D., McClanahan, T., Kastelein, R.A., Cua, D.J., 2005. IL-23 drives a pathogenic T cell population that induces autoimmune inflammation. J. Exp. Med. 201, 233–240. doi:10.1084/jem.20041257

Law, K.F., Jagirdar, J., Weiden, M.D., Bodkin, M., Rom, W.N., 1996. Tuberculosis in HIV-positive patients: cellular response and immune activation in the lung. Am. J. Respir. Crit. Care Med. 153, 1377–1384. doi:10.1164/ajrccm.153.4.8616569

Lawn, S.D., Butera, S.T., Shinnick, T.M., 2002. Tuberculosis unleashed: the impact of human immunodeficiency virus infection on the host granulomatous response to Mycobacterium tuberculosis. Microbes Infect. Inst. Pasteur 4, 635–646.

Lawn, S.D., Churchyard, G., 2009. Epidemiology of HIV-associated tuberculosis. Curr. Opin. HIV AIDS 4, 325–333. doi:10.1097/COH.0b013e32832c7d61

Lawn, S.D., Evans, A.J., Sedgwick, P.M., Acheampong, J.W., 1999. Pulmonary tuberculosis: radiological features in west Africans coinfected with HIV. Br. J. Radiol. 72, 339–344. doi:10.1259/bjr.72.856.10474493

Lawn, S.D., Pisell, T.L., Hirsch, C.S., Wu, M., Butera, S.T., Toossi, Z., 2001. Anatomically compartmentalized human immunodeficiency virus replication in HLA-DR+ cells and CD14+ macrophages at the site of pleural tuberculosis coinfection. J. Infect. Dis. 184, 1127–1133. doi:10.1086/323649

Lawn, S.D., Wilkinson, R.J., Lipman, M.C.I., Wood, R., 2008. Immune reconstitution and “unmasking” of tuberculosis during antiretroviral therapy. Am. J. Respir. Crit. Care Med. 177, 680–685. doi:10.1164/rccm.200709-1311PP

Lawn, S.D., Zumla, A.I., 2011. Tuberculosis. Lancet 378, 57–72. doi:10.1016/S0140-6736(10)62173-3

Lawrence, T., Natoli, G., 2011. Transcriptional regulation of macrophage polarization: enabling diversity with identity. Nat Rev Immunol 11, 750–761. doi:10.1038/nri3088

Le Bert, N., Chain, B.M., Rook, G., Noursadeghi, M., 2011. DC Priming by M. vaccae Inhibits Th2 Responses in Contrast to Specific TLR2 Priming and Is Associated with Selective Activation of the CREB Pathway. PLoS ONE 6, e18346. doi:10.1371/journal.pone.0018346

Lee, C.G., Homer, R.J., Zhu, Z., Lanone, S., Wang, X., Koteliansky, V., Shipley, J.M., Gotwals, P., Noble, P., Chen, Q., Senior, R.M., Elias, J.A., 2001. Interleukin-13 induces tissue fibrosis by selectively stimulating and activating transforming growth factor beta(1). J. Exp. Med. 194, 809–821.

Lee, P.P.W., Chan, K.-W., Jiang, L., Chen, T., Li, C., Lee, T.-L., Mak, P.H.S., Fok, S.F.S., Yang, X., Lau, Y.-L., 2008. Susceptibility to mycobacterial infections in children with X-linked chronic granulomatous disease: a review of 17 patients living in a region endemic for tuberculosis. Pediatr. Infect. Dis. J. 27, 224–230. doi:10.1097/INF.0b013e31815b494c

Leeansyah, E., Wines, B.D., Crowe, S.M., Jaworowski, A., 2007. The mechanism underlying defective Fcgamma receptor-mediated phagocytosis by HIV-1-infected human monocyte-derived macrophages. J. Immunol. Baltim. Md 1950 178, 1096–1104.

Lefford, M.J., McGregor, D.D., Mackaness, G.B., 1973. Immune Response to Mycobacterium tuberculosis in Rats. Infect. Immun. 8, 182–189.

Lehtonen, A., Ahlfors, H., Veckman, V., Miettinen, M., Lahesmaa, R., Julkunen, I., 2007. Gene expression profiling during differentiation of human monocytes to macrophages or dendritic cells. J. Leukoc. Biol. 82, 710–720. doi:10.1189/jlb.0307194

Leidl, L., Mayanja-Kizza, H., Sotgiu, G., Baseke, J., Ernst, M., Hirsch, C., Goletti, D., Toossi, Z., Lange, C., 2010. Relationship of immunodiagnostic assays for tuberculosis and numbers of circulating CD4+ T-cells in HIV infection. Eur. Respir. J. 35, 619–626. doi:10.1183/09031936.00045509

Leirião, P., del Fresno, C., Ardavín, C., 2012. Monocytes as effector cells: activated Ly-6C(high) mouse monocytes migrate to the lymph nodes through the lymph and cross-present antigens to CD8+ T cells. Eur. J. Immunol. 42, 2042–2051. doi:10.1002/eji.201142166

Lemaitre, B., Nicolas, E., Michaut, L., Reichhart, J.M., Hoffmann, J.A., 1996. The dorsoventral regulatory gene cassette spätzle/Toll/cactus controls the potent antifungal response in Drosophila adults. Cell 86, 973–983.

Lepelley, A., Louis, S., Sourisseau, M., Law, H.K.W., Pothlichet, J., Schilte, C., Chaperot, L., Plumas, J., Randall, R.E., Si-Tahar, M., Mammano, F., Albert, M.L., Schwartz, O., 2011. Innate Sensing of HIV-Infected Cells. PLoS Pathog 7, e1001284. doi:10.1371/journal.ppat.1001284

Leveton, C., Barnass, S., Champion, B., Lucas, S., De Souza, B., Nicol, M., Banerjee, D., Rook, G., 1989. T-cell-mediated protection of mice against virulent Mycobacterium tuberculosis. Infect. Immun. 57, 390–395.

Levitz, S.M., Tabuni, A., Kornfeld, H., Reardon, C.C., Golenbock, D.T., 1994. Production of tumor necrosis factor alpha in human leukocytes stimulated by Cryptococcus neoformans. Infect. Immun. 62, 1975–1981.

Levy, J.A., 2009. HIV pathogenesis: 25 years of progress and persistent challenges. AIDS Lond. Engl. 23, 147–160. doi:10.1097/QAD.0b013e3283217f9f

Li, C., Corraliza, I., Langhorne, J., 1999. A defect in interleukin-10 leads to enhanced malarial disease in Plasmodium chabaudi chabaudi infection in mice. Infect. Immun. 67, 4435–4442.

Li, H., Bar, K.J., Wang, S., Decker, J.M., Chen, Y., Sun, C., Salazar-Gonzalez, J.F., Salazar, M.G., Learn, G.H., Morgan, C.J., Schumacher, J.E., Hraber, P., Giorgi, E.E., Bhattacharya, T., Korber, B.T., Perelson, A.S., Eron, J.J., Cohen, M.S., Hicks, C.B., Haynes, B.F., Markowitz, M., Keele, B.F., Hahn, B.H., Shaw, G.M., 2010. High Multiplicity Infection by HIV-1 in Men Who Have Sex with Men. PLoS Pathog 6, e1000890. doi:10.1371/journal.ppat.1000890

Li, J., Pritchard, D.K., Wang, X., Park, D.R., Bumgarner, R.E., Schwartz, S.M., Liles, W.C., 2007. cDNA microarray analysis reveals fundamental differences in the expression profiles of primary human monocytes, monocyte-derived macrophages, and alveolar macrophages. J. Leukoc. Biol. 81, 328–335. doi:10.1189/jlb.0206124

Li, S., Rouphael, N., Duraisingham, S., Romero-Steiner, S., Presnell, S., Davis, C., Schmidt, D.S., Johnson, S.E., Milton, A., Rajam, G., Kasturi, S., Carlone, G.M., Quinn, C., Chaussabel, D., Palucka, A.K., Mulligan, M.J., Ahmed, R., Stephens, D.S., Nakaya, H.I., Pulendran, B., 2014. Molecular signatures of antibody responses derived from a systems biology study of five human vaccines. Nat. Immunol. 15, 195–204. doi:10.1038/ni.2789

Li, X.-D., Wu, J., Gao, D., Wang, H., Sun, L., Chen, Z.J., 2013. Pivotal Roles of cGAS-cGAMP Signaling in Antiviral Defense and Immune Adjuvant Effects. Science 341, 1390–1394. doi:10.1126/science.1244040

Liang, F., Bond, E., Sandgren, K.J., Smed-Sörensen, A., Rangaka, M.X., Lange, C., Koup, R.A., McComsey, G.A., Lederman, M.M., Wilkinson, R.J., Andersson, J., Loré, K., 2013. Dendritic cell recruitment in response to skin antigen tests in HIV-1-infected individuals correlates with the level of T-cell infiltration. AIDS Lond. Engl. 27, 1071–1080. doi:10.1097/QAD.0b013e32835ecaca

Lin, L., Hou, J., Ma, F., Wang, P., Liu, X., Li, N., Wang, J., Wang, Q., Cao, X., 2013. Type I IFN Inhibits Innate IL-10 Production in Macrophages through Histone Deacetylase 11 by Downregulating MicroRNA-145. J. Immunol. Baltim. Md 1950 191, 3896–3904. doi:10.4049/jimmunol.1203450

Lin, M.-T., Storer, B., Martin, P.J., Tseng, L.-H., Gooley, T., Chen, P.-J., Hansen, J.A., 2003. Relation of an interleukin-10 promoter polymorphism to graft-versus-host disease and survival after hematopoietic-cell transplantation. N. Engl. J. Med. 349, 2201–2210. doi:10.1056/NEJMoa022060

Lin, P.L., Ford, C.B., Coleman, M.T., Myers, A.J., Gawande, R., Ioerger, T., Sacchettini, J., Fortune, S.M., Flynn, J.L., 2014. Sterilization of granulomas is common in active and latent tuberculosis despite within-host variability in bacterial killing. Nat. Med. 20, 75–79. doi:10.1038/nm.3412

Lin, P.L., Rodgers, M., Smith, L., Bigbee, M., Myers, A., Bigbee, C., Chiosea, I., Capuano, S.V., Fuhrman, C., Klein, E., Flynn, J.L., 2009. Quantitative Comparison of Active and Latent Tuberculosis in the Cynomolgus Macaque Model. Infect. Immun. 77, 4631–4642. doi:10.1128/IAI.00592-09

Linnemann, T., Zheng, Y.-H., Mandic, R., Peterlin, B.M., 2002. Interaction between Nef and phosphatidylinositol-3-kinase leads to activation of p21-activated kinase and increased production of HIV. Virology 294, 246–255. doi:10.1006/viro.2002.1365

Liu, H., Shi, B., Huang, C.-C., Eksarko, P., Pope, R.M., 2008. Transcriptional diversity during monocyte to macrophage differentiation. Immunol. Lett. 117, 70–80. doi:10.1016/j.imlet.2007.12.012

Liu, P., Cheng, H., Roberts, T.M., Zhao, J.J., 2009. Targeting the phosphoinositide 3-kinase pathway in cancer. Nat. Rev. Drug Discov. 8, 627–644. doi:10.1038/nrd2926

Lokken, K.L., Mooney, J.P., Butler, B.P., Xavier, M.N., Chau, J.Y., Schaltenberg, N., Begum, R.H., Müller, W., Luckhart, S., Tsolis, R.M., 2014. Malaria Parasite Infection Compromises Control of Concurrent Systemic Non-typhoidal Salmonella Infection via IL-10-Mediated Alteration of Myeloid Cell Function. PLoS Pathog 10, e1004049. doi:10.1371/journal.ppat.1004049

London, A., Cohen, M., Schwartz, M., 2013. Microglia and monocyte-derived macrophages: functionally distinct populations that act in concert in CNS plasticity and repair. Front. Cell. Neurosci. 7, 34. doi:10.3389/fncel.2013.00034

Loo, Y.-M., Gale, M., 2011. Immune signaling by RIG-I-like receptors. Immunity 34, 680–692. doi:10.1016/j.immuni.2011.05.003

Luban, J., 2012. Innate Immune Sensing of HIV-1 by Dendritic Cells. Cell Host Microbe 12, 408–418. doi:10.1016/j.chom.2012.10.002

Lucas, T., Waisman, A., Ranjan, R., Roes, J., Krieg, T., Müller, W., Roers, A., Eming, S.A., 2010. Differential roles of macrophages in diverse phases of skin repair. J. Immunol. Baltim. Md 1950 184, 3964–3977. doi:10.4049/jimmunol.0903356

Luetkemeyer, A.F., Charlebois, E.D., Flores, L.L., Bangsberg, D.R., Deeks, S.G., Martin, J.N., Havlir, D.V., 2007. Comparison of an interferon-gamma release assay with tuberculin skin testing in HIV-infected individuals. Am. J. Respir. Crit. Care Med. 175, 737–742. doi:10.1164/rccm.200608-1088OC

Luo, W., Friedman, M.S., Shedden, K., Hankenson, K.D., Woolf, P.J., 2009. GAGE: generally applicable gene set enrichment for pathway analysis. BMC Bioinformatics 10, 161. doi:10.1186/1471-2105-10-161

Lupo, P., Chang, Y.C., Kelsall, B.L., Farber, J.M., Pietrella, D., Vecchiarelli, A., Leon, F., Kwon-Chung, K.J., 2008. The presence of capsule in Cryptococcus neoformans influences the gene expression profile in dendritic cells during interaction with the fungus. Infect. Immun. 76, 1581–1589. doi:10.1128/IAI.01184-07

Ma, W., Lim, W., Gee, K., Aucoin, S., Nandan, D., Kozlowski, M., Diaz-Mitoma, F., Kumar, A., 2001. The p38 mitogen-activated kinase pathway regulates the human interleukin-10 promoter via the activation of Sp1 transcription factor in lipopolysaccharide-stimulated human macrophages. J. Biol. Chem. 276, 13664–13674. doi:10.1074/jbc.M011157200

Maartens, G., Wilkinson, R.J., 2007. Tuberculosis. Lancet 370, 2030–2043. doi:10.1016/S0140-6736(07)61262-8

Mackaness, G.B., 1964. The immunological basis of acquired cellular resistance. J. Exp. Med. 120, 105–120.

Mackaness, G.B., 1967. The Relationship of Delayed Hypersensitivity to Acquired Cellular Resistance. Br. Med. Bull. 23, 52–54.

Maddocks, S., Scandurra, G.M., Nourse, C., Bye, C., Williams, R.B., Slobedman, B., Cunningham, A.L., Britton, W.J., 2009. Gene expression in HIV-1/Mycobacterium tuberculosis co-infected macrophages is dominated by M. tuberculosis. Tuberc. Edinb. Scotl. 89, 285–293. doi:10.1016/j.tube.2009.05.003

Maddon, P.J., Dalgleish, A.G., McDougal, J.S., Clapham, P.R., Weiss, R.A., Axel, R., 1986. The T4 gene encodes the AIDS virus receptor and is expressed in the immune system and the brain. Cell 47, 333–348.

Maeda, N., Nigou, J., Herrmann, J.-L., Jackson, M., Amara, A., Lagrange, P.H., Puzo, G., Gicquel, B., Neyrolles, O., 2003. The cell surface receptor DC-SIGN discriminates between Mycobacterium species through selective recognition of the mannose caps on lipoarabinomannan. J. Biol. Chem. 278, 5513–5516. doi:10.1074/jbc.C200586200

Maertzdorf, J., Weiner, J., 3rd, Mollenkopf, H.-J., TBornotTB Network, Bauer, T., Prasse, A., Müller-Quernheim, J., Kaufmann, S.H.E., 2012. Common patterns and disease-related signatures in tuberculosis and sarcoidosis. Proc. Natl. Acad. Sci. U. S. A. 109, 7853–7858. doi:10.1073/pnas.1121072109

Magnusson, M., Bentzon, M.W., 1958. Preparation of purified tuberculin RT 23. Bull. World Health Organ. 19, 829–843.

Mahnke, Y.D., Greenwald, J.H., Dersimonian, R., Roby, G., Antonelli, L.R.V., Sher, A., Roederer, M., Sereti, I., 2012. Selective expansion of polyfunctional pathogen-specific CD4+ T cells in HIV-1-infected patients with immune reconstitution inflammatory syndrome. Blood. doi:10.1182/blood-2011-09-380840

Mak, K.S., Funnell, A.P.W., Pearson, R.C.M., Crossley, M., 2011. PU.1 and Haematopoietic Cell Fate: Dosage Matters. Int. J. Cell Biol. 2011, e808524. doi:10.1155/2011/808524

Manca, C., Tsenova, L., Bergtold, A., Freeman, S., Tovey, M., Musser, J.M., Barry, C.E., Freedman, V.H., Kaplan, G., 2001. Virulence of a Mycobacterium tuberculosis clinical isolate in mice is determined by failure to induce Th1 type immunity and is associated with induction of IFN-alpha /beta. Proc. Natl. Acad. Sci. U. S. A. 98, 5752–5757. doi:10.1073/pnas.091096998

Mangan, P.R., Harrington, L.E., O'Quinn, D.B., Helms, W.S., Bullard, D.C., Elson, C.O., Hatton, R.D., Wahl, S.M., Schoeb, T.R., Weaver, C.T., 2006. Transforming growth factor-β induces development of the TH17 lineage. Nature 441, 231–234. doi:10.1038/nature04754

Mangeat, B., Turelli, P., Caron, G., Friedli, M., Perrin, L., Trono, D., 2003. Broad antiretroviral defence by human APOBEC3G through lethal editing of nascent reverse transcripts. Nature 424, 99–103. doi:10.1038/nature01709

Mantovani, A., Sica, A., Sozzani, S., Allavena, P., Vecchi, A., Locati, M., 2004. The chemokine system in diverse forms of macrophage activation and polarization. Trends Immunol. 25, 677–686. doi:10.1016/j.it.2004.09.015

Marais, S., Wilkinson, K.A., Lesosky, M., Coussens, A.K., Deffur, A., Pepper, D.J., Schutz, C., Ismail, Z., Meintjes, G., Wilkinson, R.J., 2014. Neutrophil-associated central nervous system inflammation in tuberculous meningitis immune reconstitution inflammatory syndrome. Clin. Infect. Dis. Off. Publ. Infect. Dis. Soc. Am. doi:10.1093/cid/ciu641

Margolis, L., Shattock, R., 2006. Selective transmission of CCR5-utilizing HIV-1: the "gatekeeper" problem resolved? Nat Rev Micro 4, 312–317. doi:10.1038/nrmicro1387

Markowitz, N., Hansen, N.I., Wilcosky, T.C., Hopewell, P.C., Glassroth, J., Kvale, P.A., Mangura, B.T., Osmond, D., Wallace, J.M., Rosen, M.J., Reichman, L.B., 1993. Tuberculin and anergy testing in HIV-seropositive and HIV-seronegative persons. Pulmonary Complications of HIV Infection Study Group. Ann. Intern. Med. 119, 185–193.

Marlink, R., Kanki, P., Thior, I., Travers, K., Eisen, G., Siby, T., Traore, I., Hsieh, C.C., Dia, M.C., Gueye, E.H., Et, A., 1994. Reduced rate of disease development after HIV-2 infection as compared to HIV-1. Science 265, 1587–1590. doi:10.1126/science.7915856

Marsden, M.D., Kovochich, M., Suree, N., Shimizu, S., Mehta, R., Cortado, R., Bristol, G., An, D.S., Zack, J.A., 2012. HIV latency in the humanized BLT mouse. J. Virol. 86, 339–347. doi:10.1128/JVI.06366-11

Martinez, F.O., Gordon, S., 2014. The M1 and M2 paradigm of macrophage activation: time for reassessment. F1000prime Rep. 6, 13. doi:10.12703/P6-13

Martinez, F.O., Gordon, S., Locati, M., Mantovani, A., 2006. Transcriptional profiling of the human monocyte-to-macrophage differentiation and polarization: new molecules and patterns of gene expression. J. Immunol. Baltim. Md 1950 177, 7303–7311.

Martinez, F.O., Helming, L., Milde, R., Varin, A., Melgert, B.N., Draijer, C., Thomas, B., Fabbri, M., Crawshaw, A., Ho, L.P., Hacken, N.H.T., Jiménez, V.C., Kootstra, N.A., Hamann, J., Greaves, D.R., Locati, M., Mantovani, A., Gordon, S., 2013. Genetic programs expressed in resting and IL-4 alternatively activated mouse and human macrophages: similarities and differences. Blood 121, e57–e69. doi:10.1182/blood-2012-06-436212

Matthews, K., Ntsekhe, M., Syed, F., Scriba, T., Russell, J., Tibazarwa, K., Deffur, A., Hanekom, W., Mayosi, B.M., Wilkinson, R.J., Wilkinson, K.A., 2012. HIV-1 infection alters CD4+ memory T-cell phenotype at the site of disease in extrapulmonary tuberculosis. Eur. J. Immunol. 42, 147–157. doi:10.1002/eji.201141927

Mattila, J.T., Diedrich, C.R., Lin, P.L., Phuah, J., Flynn, J.L., 2011. Simian immunodeficiency virus-induced changes in T cell cytokine responses in cynomolgus macaques with latent Mycobacterium tuberculosis infection are associated with timing of reactivation. J. Immunol. Baltim. Md 1950 186, 3527–3537. doi:10.4049/jimmunol.1003773

Mayer-Barber, K.D., Andrade, B.B., Barber, D.L., Hieny, S., Feng, C.G., Caspar, P., Oland, S., Gordon, S., Sher, A., 2011. Innate and adaptive interferons suppress IL-1α and IL-1β production by distinct pulmonary myeloid subsets during Mycobacterium tuberculosis infection. Immunity 35, 1023–1034. doi:10.1016/j.immuni.2011.12.002

Mayer-Barber, K.D., Andrade, B.B., Oland, S.D., Amaral, E.P., Barber, D.L., Gonzales, J., Derrick, S.C., Shi, R., Kumar, N.P., Wei, W., Yuan, X., Zhang, G., Cai, Y., Babu, S., Catalfamo, M., Salazar, A.M., Via, L.E., Barry Iii, C.E., Sher, A., 2014. Host-directed therapy of tuberculosis based on interleukin-1 and type I interferon crosstalk. Nature advance online publication. doi:10.1038/nature13489

Mazzolini, J., Herit, F., Bouchet, J., Benmerah, A., Benichou, S., Niedergang, F., 2010. Inhibition of phagocytosis in HIV-1-infected macrophages relies on Nef-dependent alteration of focal delivery of recycling compartments. Blood 115, 4226–4236. doi:10.1182/blood-2009-12-259473

McNab, F.W., Ewbank, J., Rajsbaum, R., Stavropoulos, E., Martirosyan, A., Redford, P.S., Wu, X., Graham, C.M., Saraiva, M., Tsichlis, P., Chaussabel, D., Ley, S.C., O'Garra, A., 2013. TPL-2-ERK1/2 signaling promotes host resistance against intracellular bacterial infection by negative regulation of type I IFN production. J. Immunol. Baltim. Md 1950 191, 1732–1743. doi:10.4049/jimmunol.1300146

McQuiston, T.J., Williamson, P.R., 2011. Paradoxical roles of alveolar macrophages in the host response to Cryptococcus neoformans. J. Infect. Chemother. Off. J. Jpn. Soc. Chemother. doi:10.1007/s10156-011-0306-2

Means, T.K., Wang, S., Lien, E., Yoshimura, A., Golenbock, D.T., Fenton, M.J., 1999. Human Toll-Like Receptors Mediate Cellular Activation by Mycobacterium tuberculosis. J. Immunol. 163, 3920–3927.

Medzhitov, R., 2009. Approaching the asymptote: 20 years later. Immunity 30, 766–775. doi:10.1016/j.immuni.2009.06.004

Medzhitov, R., Horng, T., 2009. Transcriptional control of the inflammatory response. Nat. Rev. Immunol. 9, 692–703. doi:10.1038/nri2634

Medzhitov, R., Preston-Hurlburt, P., Janeway, C.A., 1997. A human homologue of the Drosophila Toll protein signals activation of adaptive immunity. Nature 388, 394–397. doi:10.1038/41131

Medzhitov, R., Preston-Hurlburt, P., Janeway, C.A., 1997. A human homologue of the Drosophila Toll protein signals activation of adaptive immunity. Nature 388, 394–397.

Meintjes, G., Lawn, S.D., Scano, F., Maartens, G., French, M.A., Worodria, W., Elliott, J.H., Murdoch, D., Wilkinson, R.J., Seyler, C., John, L., van der Loeff, M.S., Reiss, P., Lynen, L., Janoff, E.N., Gilks, C., Colebunders, R., 2008a. Tuberculosis-associated immune reconstitution inflammatory syndrome: case definitions for use in resource-limited settings. Lancet Infect. Dis. 8, 516–523. doi:10.1016/S1473-3099(08)70184-1

Meintjes, G., Scriven, J., Marais, S., 2012. Management of the immune reconstitution inflammatory syndrome. Curr. HIV/AIDS Rep. 9, 238–250. doi:10.1007/s11904-012-0129-5

Meintjes, G., Wilkinson, K.A., Rangaka, M.X., Skolimowska, K., van Veen, K., Abrahams, M., Seldon, R., Pepper, D.J., Rebe, K., Mouton, P., van Cutsem, G., Nicol, M.P., Maartens, G., Wilkinson, R.J., 2008b. Type 1 helper T cells and FoxP3-positive T cells in HIV-tuberculosis-associated immune reconstitution inflammatory syndrome. Am. J. Respir. Crit. Care Med. 178, 1083–1089. doi:10.1164/rccm.200806-858OC

Meraz, M.A., White, J.M., Sheehan, K.C., Bach, E.A., Rodig, S.J., Dighe, A.S., Kaplan, D.H., Riley, J.K., Greenlund, A.C., Campbell, D., Carver-Moore, K., DuBois, R.N., Clark, R., Aguet, M., Schreiber, R.D., 1996. Targeted disruption of the Stat1 gene in mice reveals unexpected physiologic specificity in the JAK-STAT signaling pathway. Cell 84, 431–442.

Meroni, L., Trabattoni, D., Balotta, C., Riva, C., Gori, A., Moroni, M., Luisa Villa, M., Clerici, M., Galli, M., 1996. Evidence for type 2 cytokine production and lymphocyte activation in the early phases of HIV-1 infection. AIDS Lond. Engl. 10, 23–30.

Meyaard, L., Otto, S.A., Jonker, R.R., Mijnster, M.J., Keet, R.P., Miedema, F., 1992. Programmed death of T cells in HIV-1 infection. Science 257, 217–219.

Mildner, A., Jung, S., 2014. Development and function of dendritic cell subsets. Immunity 40, 642–656. doi:10.1016/j.immuni.2014.04.016

Millar, A.B., Miller, R.F., Foley, N.M., Meager, A., Semple, S.J.G., Rook, G.A.W., 1991. Production of Tumor Necrosis Factor-α by Blood and Lung Mononuclear Phagocytes from Patients with Human Immunodeficiency Virus-related Lung Disease. Am. J. Respir. Cell Mol. Biol. 5, 144–148. doi:10.1165/ajrcmb/5.2.144

Mills, C.D., Kincaid, K., Alt, J.M., Heilman, M.J., Hill, A.M., 2000. M-1/M-2 macrophages and the Th1/Th2 paradigm. J. Immunol. Baltim. Md 1950 164, 6166–6173.

Mishra, B.B., Moura-Alves, P., Sonawane, A., Hacohen, N., Griffiths, G., Moita, L.F., Anes, E., 2010. Mycobacterium tuberculosis protein ESAT-6 is a potent activator of the NLRP3/ASC inflammasome. Cell. Microbiol. 12, 1046–1063. doi:10.1111/j.1462-5822.2010.01450.x

Mohammadi, P., Desfarges, S., Bartha, I., Joos, B., Zangger, N., Muñoz, M., Günthard, H.F., Beerenwinkel, N., Telenti, A., Ciuffi, A., 2013. 24 Hours in the Life of HIV-1 in a T Cell Line. PLoS Pathog 9, e1003161. doi:10.1371/journal.ppat.1003161

Mohr, H., Gravemann, U., Müller, T.H., 2009. Inactivation of pathogens in single units of therapeutic fresh plasma by irradiation with ultraviolet light. Transfusion (Paris) 49, 2144–2151. doi:10.1111/j.1537-2995.2009.02234.x

Moir, S., Fauci, A.S., 2008. Pathogenic mechanisms of B-lymphocyte dysfunction in HIV disease. J. Allergy Clin. Immunol. 122, 12–21. doi:10.1016/j.jaci.2008.04.034

Monari, C., Kozel, T.R., Paganelli, F., Pericolini, E., Perito, S., Bistoni, F., Casadevall, A., Vecchiarelli, A., 2006. Microbial immune suppression mediated by direct engagement of inhibitory Fc receptor. J. Immunol. Baltim. Md 1950 177, 6842–6851.

Monroe, K.M., Yang, Z., Johnson, J.R., Geng, X., Doitsh, G., Krogan, N.J., Greene, W.C., 2014. IFI16 DNA sensor is required for death of lymphoid CD4 T cells abortively infected with HIV. Science 343, 428–432. doi:10.1126/science.1243640

Moore, K.W., de Waal Malefyt, R., Coffman, R.L., O'Garra, A., 2001. Interleukin-10 and the interleukin-10 receptor. Annu. Rev. Immunol. 19, 683–765. doi:10.1146/annurev.immunol.19.1.683

Moore, R.D., Chaisson, R.E., 1996. Natural History of Opportunistic Disease in an HIV-Infected Urban Clinical Cohort. Ann. Intern. Med. 124, 633–642. doi:10.7326/0003-4819-124-7-199604010-00003

Moorjani, H., Craddock, B., Morrison, S.A., Steigbigel, R., 1996. Impairment of Phagosome-Lysosome Fusion in HIV-1-Infected Macrophages. [Miscellaneous Article]. J. Acquir. Immune Defic. Syndr. 13, 18–22.

Mootha, V.K., Lindgren, C.M., Eriksson, K.-F., Subramanian, A., Sihag, S., Lehar, J., Puigserver, P., Carlsson, E., Ridderstråle, M., Laurila, E., Houstis, N., Daly, M.J., Patterson, N., Mesirov, J.P., Golub, T.R., Tamayo, P., Spiegelman, B., Lander, E.S., Hirschhorn, J.N., Altshuler, D., Groop, L.C., 2003. PGC-1alpha-responsive genes involved in oxidative phosphorylation are coordinately downregulated in human diabetes. Nat. Genet. 34, 267–273. doi:10.1038/ng1180

Moreira, L.O., El Kasmi, K.C., Smith, A.M., Finkelstein, D., Fillon, S., Kim, Y.-G., Núñez, G., Tuomanen, E., Murray, P.J., 2008. The TLR2-MyD88-NOD2-RIPK2 signalling axis regulates a balanced pro-inflammatory and IL-10-mediated anti-inflammatory cytokine response to Gram-positive cell walls. Cell. Microbiol. 10, 2067–2077. doi:10.1111/j.1462-5822.2008.01189.x

Moreno, S., Baraia-Etxaburu, J., Bouza, E., Parras, F., Pérez-Tascón, M., Miralles, P., Vicente, T., Alberdi, J.C., Cosín, J., López-Gay, D., 1993. Risk for developing tuberculosis among anergic patients infected with HIV. Ann. Intern. Med. 119, 194–198.

Moretta, L., Bottino, C., Pende, D., Mingari, M.C., Biassoni, R., Moretta, A., 2002. Human natural killer cells: their origin, receptors and function. Eur. J. Immunol. 32, 1205–1211. doi:10.1002/1521-4141(200205)32:5<1205::AID-IMMU1205>3.0.CO;2-Y

Morrow, C.D., Park, J., Wakefield, J.K., 1994. Viral gene products and replication of the human immunodeficiency type 1 virus. Am. J. Physiol. 266, C1135–1156.

Moser, M., 2001. Regulation of Th1/Th2 development by antigen-presenting cells in vivo. Immunobiology 204, 551–557. doi:10.1078/0171-2985-00092

Mosmann, T.R., Cherwinski, H., Bond, M.W., Giedlin, M.A., Coffman, R.L., 1986. Two types of murine helper T cell clone. I. Definition according to profiles of lymphokine activities and secreted proteins. J. Immunol. Baltim. Md 1950 136, 2348–2357.

Mosser, D.M., Edwards, J.P., 2008. Exploring the full spectrum of macrophage activation. Nat Rev Immunol 8, 958–969. doi:10.1038/nri2448

Mukherjee, S., Chen, L.-Y., Papadimos, T.J., Huang, S., Zuraw, B.L., Pan, Z.K., 2009. Lipopolysaccharide-driven Th2 Cytokine Production in Macrophages Is Regulated by Both MyD88 and TRAM. J. Biol. Chem. 284, 29391–29398. doi:10.1074/jbc.M109.005272

Müller, M., Wandel, S., Colebunders, R., Attia, S., Furrer, H., Egger, M., 2010. Immune reconstitution inflammatory syndrome in patients starting antiretroviral therapy for HIV infection: a systematic review and meta-analysis. Lancet Infect. Dis. 10, 251–261. doi:10.1016/S1473-3099(10)70026-8

Murphy, J., Summer, R., Wilson, A.A., Kotton, D.N., Fine, A., 2008. The prolonged life-span of alveolar macrophages. Am. J. Respir. Cell Mol. Biol. 38, 380–385. doi:10.1165/rcmb.2007-0224RC

Murray, P.J., 2005a. The primary mechanism of the IL-10-regulated antiinflammatory response is to selectively inhibit transcription. Proc. Natl. Acad. Sci. U. S. A. 102, 8686–8691. doi:10.1073/pnas.0500419102

Murray, P.J., 2006. Understanding and exploiting the endogenous interleukin-10/STAT3-mediated anti-inflammatory response. Curr. Opin. Pharmacol. 6, 379–386. doi:10.1016/j.coph.2006.01.010

Murray, P.J., Wynn, T.A., 2011. Protective and pathogenic functions of macrophage subsets. Nat Rev Immunol 11, 723–737. doi:10.1038/nri3073

Muthumani, K., Hwang, D.S., Choo, A.Y., Mayilvahanan, S., Dayes, N.S., Thieu, K.P., Weiner, D.B., 2005. HIV-1 Vpr inhibits the maturation and activation of macrophages and dendritic cells in vitro. Int. Immunol. 17, 103–116. doi:10.1093/intimm/dxh190

Mwandumba, H.C., Bertel Squire, S., White, S.A., Nyirenda, M.H., Kampondeni, S.D., Rhoades, E.R., Zijlstra, E.E., Molyneux, M.E., Russell, D.G., 2008. Association between sputum smear status and local immune responses at the site of disease in HIV-infected patients with pulmonary tuberculosis. Tuberc. Edinb. Scotl. 88, 58–63. doi:10.1016/j.tube.2007.06.003

Nagata, S., 2007. Autoimmune diseases caused by defects in clearing dead cells and nuclei expelled from erythroid precursors. Immunol. Rev. 220, 237–250. doi:10.1111/j.1600-065X.2007.00571.x

Naif, H.M., Li, S., Alali, M., Sloane, A., Wu, L., Kelly, M., Lynch, G., Lloyd, A., Cunningham, A.L., 1998. CCR5 expression correlates with susceptibility of maturing monocytes to human immunodeficiency virus type 1 infection. J. Virol. 72, 830–836.

Naik, S.H., Perié, L., Swart, E., Gerlach, C., van Rooij, N., de Boer, R.J., Schumacher, T.N., 2013. Diverse and heritable lineage imprinting of early haematopoietic progenitors. Nature 496, 229–232. doi:10.1038/nature12013

Naik, S.H., Sathe, P., Park, H.-Y., Metcalf, D., Proietto, A.I., Dakic, A., Carotta, S., O'Keeffe, M., Bahlo, M., Papenfuss, A., Kwak, J.-Y., Wu, L., Shortman, K., 2007. Development of plasmacytoid and conventional dendritic cell subtypes from single precursor cells derived in vitro and in vivo. Nat Immunol 8, 1217–1226. doi:10.1038/ni1522

Nair, M.G., Du, Y., Perrigoue, J.G., Zaph, C., Taylor, J.J., Goldschmidt, M., Swain, G.P., Yancopoulos, G.D., Valenzuela, D.M., Murphy, A., Karow, M., Stevens, S., Pearce, E.J., Artis, D., 2009. Alternatively activated macrophage-derived RELM-{alpha} is a negative regulator of type 2 inflammation in the lung. J. Exp. Med. 206, 937–952. doi:10.1084/jem.20082048

Naito, M., Hasegawa, G., Takahashi, K., 1997. Development, differentiation, and maturation of Kupffer cells. Microsc. Res. Tech. 39, 350–364. doi:10.1002/(SICI)1097-0029(19971115)39:4<350::AID-JEMT5>3.0.CO;2-L

Nakata, K., Rom, W.N., Honda, Y., Condos, R., Kanegasaki, S., Cao, Y., Weiden, M., 1997. Mycobacterium tuberculosis enhances human immunodeficiency virus-1 replication in the lung. Am. J. Respir. Crit. Care Med. 155, 996–1003. doi:10.1164/ajrccm.155.3.9117038

Naldini, L., Blömer, U., Gallay, P., Ory, D., Mulligan, R., Gage, F.H., Verma, I.M., Trono, D., 1996. In vivo gene delivery and stable transduction of nondividing cells by a lentiviral vector. Science 272, 263–267.

Nambuya, A., Sewankambo, N., Mugerwa, J., Goodgame, R., Lucas, S., 1988. Tuberculous lymphadenitis associated with human immunodeficiency virus (HIV) in Uganda. J. Clin. Pathol. 41, 93–96.

Narayan, O., Cork, L.C., 1985. Lentiviral Diseases of Sheep and Goats: Chronic Pneumonia Leukoencephalomyelitis and Arthritis. Rev. Infect. Dis. 7, 89–98. doi:10.1093/clinids/7.1.89

Narayan, O., Wolinsky, J.S., Clements, J.E., Strandberg, J.D., Griffin, D.E., Cork, L.C., 1982. Slow Virus Replication: the Role of Macrophages in the Persistence and Expression of Visna Viruses of Sheep and Goats. J. Gen. Virol. 59, 345–356. doi:10.1099/0022-1317-59-2-345

Narayanan, A., Kehn-Hall, K., Bailey, C., Kashanchi, F., 2011. Analysis of the roles of HIV-derived microRNAs. Expert Opin. Biol. Ther. 11, 17–29. doi:10.1517/14712598.2011.540564

Nathan, C., Ding, A., 2010. Nonresolving inflammation. Cell 140, 871–882. doi:10.1016/j.cell.2010.02.029

Nathan, C.F., Murray, H.W., Wiebe, M.E., Rubin, B.Y., 1983. Identification of interferon-gamma as the lymphokine that activates human macrophage oxidative metabolism and antimicrobial activity. J. Exp. Med. 158, 670–689.

Nathan, C.F., Remold, H.G., David, J.R., 1973. Characterization of a lymphocyte factor which alters macrophage functions. J. Exp. Med. 137, 275–290.

Natoli, G., Monticelli, S., 2014. Macrophage Activation: Glancing into Diversity. Immunity 40, 175–177. doi:10.1016/j.immuni.2014.01.004

Nau, G.J., Richmond, J.F.L., Schlesinger, A., Jennings, E.G., Lander, E.S., Young, R.A., 2002. Human macrophage activation programs induced by bacterial pathogens. Proc. Natl. Acad. Sci. U. S. A. 99, 1503–1508. doi:10.1073/pnas.022649799

Nègre, D., Mangeot, P.E., Duisit, G., Blanchard, S., Vidalain, P.O., Leissner, P., Winter, A.J., Rabourdin-Combe, C., Mehtali, M., Moullier, P., Darlix, J.L., Cosset, F.L., 2000. Characterization of novel safe lentiviral vectors derived from simian immunodeficiency virus (SIVmac251) that efficiently transduce mature human dendritic cells. Gene Ther. 7, 1613–1623. doi:10.1038/sj.gt.3301292

Neil, S.J.D., Zang, T., Bieniasz, P.D., 2008. Tetherin inhibits retrovirus release and is antagonized by HIV-1 Vpu. Nature 451, 425–430. doi:10.1038/nature06553

Nelson, D.R., Lauwers, G.Y., Lau, J.Y., Davis, G.L., 2000. Interleukin 10 treatment reduces fibrosis in patients with chronic hepatitis C: a pilot trial of interferon nonresponders. Gastroenterology 118, 655–660.

Netea, M.G., Sutmuller, R., Hermann, C., Van der Graaf, C.A.A., Van der Meer, J.W.M., van Krieken, J.H., Hartung, T., Adema, G., Kullberg, B.J., 2004. Toll-like receptor 2 suppresses immunity against Candida albicans through induction of IL-10 and regulatory T cells. J. Immunol. Baltim. Md 1950 172, 3712–3718.

Newport, M.J., Huxley, C.M., Huston, S., Hawrylowicz, C.M., Oostra, B.A., Williamson, R., Levin, M., 1996. A mutation in the interferon-gamma-receptor gene and susceptibility to mycobacterial infection. N. Engl. J. Med. 335, 1941–1949. doi:10.1056/NEJM199612263352602

Nicol, M.Q., Mathys, J.-M., Pereira, A., Ollington, K., Ieong, M.H., Skolnik, P.R., 2008. Human Immunodeficiency Virus Infection Alters Tumor Necrosis Factor Alpha Production via Toll-Like Receptor-Dependent Pathways in Alveolar Macrophages and U1 Cells. J. Virol. 82, 7790–7798. doi:10.1128/JVI.00362-08

Niemand, C., Nimmesgern, A., Haan, S., Fischer, P., Schaper, F., Rossaint, R., Heinrich, P.C., Müller-Newen, G., 2003. Activation of STAT3 by IL-6 and IL-10 in primary human macrophages is differentially modulated by suppressor of cytokine signaling 3. J. Immunol. Baltim. Md 1950 170, 3263–3272.

North, R.J., 1998. Mice incapable of making IL-4 or IL-10 display normal resistance to infection with Mycobacterium tuberculosis. Clin. Exp. Immunol. 113, 55–58. doi:10.1046/j.1365-2249.1998.00636.x

Noursadeghi, M., Katz, D.R., Miller, R.F., 2006a. HIV-1 infection of mononuclear phagocytic cells: the case for bacterial innate immune deficiency in AIDS. Lancet Infect. Dis. 6, 794–804. doi:10.1016/S1473-3099(06)70656-9

Noursadeghi, M., Tsang, J., Miller, R.F., Straschewski, S., Kellam, P., Chain, B.M., Katz, D.R., 2009. Genome-wide innate immune responses in HIV-1-infected macrophages are preserved despite attenuation of the NF-kappa B activation pathway. J. Immunol. Baltim. Md 1950 182, 319–328.

Noursadeghi, M., Ustianowski, A., Elgalib, A., Miller, R., 2006b. Bacterial Disease in HIV-Infected Patients. JAIDS J. Acquir. Immune Defic. Syndr. 41, 532–535. doi:10.1097/01.qai.0000209912.17695.e5

Nowak, E.C., Weaver, C.T., Turner, H., Begum-Haque, S., Becher, B., Schreiner, B., Coyle, A.J., Kasper, L.H., Noelle, R.J., 2009. IL-9 as a mediator of Th17-driven inflammatory disease. J. Exp. Med. 206, 1653–1660. doi:10.1084/jem.20090246

O'Garra, A., Barrat, F.J., Castro, A.G., Vicari, A., Hawrylowicz, C., 2008. Strategies for use of IL-10 or its antagonists in human disease. Immunol. Rev. 223, 114–131. doi:10.1111/j.1600-065X.2008.00635.x

O'Garra, A., Murphy, K.M., 2009. From IL-10 to IL-12: how pathogens and their products stimulate APCs to induce T(H)1 development. Nat. Immunol. 10, 929–932. doi:10.1038/ni0909-929

O'Garra, A., Redford, P.S., McNab, F.W., Bloom, C.I., Wilkinson, R.J., Berry, M.P.R., 2013. The immune response in tuberculosis. Annu. Rev. Immunol. 31, 475–527. doi:10.1146/annurev-immunol-032712-095939

O'Leary, S., O'Sullivan, M.P., Keane, J., 2011. IL-10 blocks phagosome maturation in mycobacterium tuberculosis-infected human macrophages. Am. J. Respir. Cell Mol. Biol. 45, 172–180. doi:10.1165/rcmb.2010-0319OC

Obermoser, G., Presnell, S., Domico, K., Xu, H., Wang, Y., Anguiano, E., Thompson-Snipes, L., Ranganathan, R., Zeitner, B., Bjork, A., Anderson, D., Speake, C., Ruchaud, E., Skinner, J., Alsina, L., Sharma, M., Dutartre, H., Cepika, A., Israelsson, E., Nguyen, P., Nguyen, Q.-A., Harrod, A.C., Zurawski, S.M., Pascual, V., Ueno, H., Nepom, G.T., Quinn, C., Blankenship, D., Palucka, K., Banchereau, J., Chaussabel, D., 2013. Systems scale interactive exploration reveals quantitative and qualitative differences in response to influenza and pneumococcal vaccines. Immunity 38, 831–844. doi:10.1016/j.immuni.2012.12.008

Odegaard, J.I., Ricardo-Gonzalez, R.R., Goforth, M.H., Morel, C.R., Subramanian, V., Mukundan, L., Red Eagle, A., Vats, D., Brombacher, F., Ferrante, A.W., Chawla, A., 2007. Macrophage-specific PPARgamma controls alternative activation and improves insulin resistance. Nature 447, 1116–1120. doi:10.1038/nature05894

Ogawa, Y., Duru, E.A., Ameredes, B.T., 2008. Role of IL-10 in the resolution of airway inflammation. Curr. Mol. Med. 8, 437–445.

Okabe, Y., Medzhitov, R., 2014. Tissue-specific signals control reversible program of localization and functional polarization of macrophages. Cell 157, 832–844. doi:10.1016/j.cell.2014.04.016

Okoye, A., Meier-Schellersheim, M., Brenchley, J.M., Hagen, S.I., Walker, J.M., Rohankhedkar, M., Lum, R., Edgar, J.B., Planer, S.L., Legasse, A., Sylwester, A.W., Piatak, M., Lifson, J.D., Maino, V.C., Sodora, D.L., Douek, D.C., Axthelm, M.K., Grossman, Z., Picker, L.J., 2007. Progressive CD4+ central memory T cell decline results in CD4+ effector memory insufficiency and overt disease in chronic SIV infection. J. Exp. Med. 204, 2171–2185. doi:10.1084/jem.20070567

Okulicz, J.F., Grandits, G.A., Dolan, M.J., Marconi, V.C., Wortmann, G., Landrum, M.L., 2012. Spontaneous virologic suppression in HIV controllers is independent of delayed-type hypersensitivity test responsiveness. AIDS Res. Ther. 9, 10. doi:10.1186/1742-6405-9-10

Oliveira, D.L., Freire-de-Lima, C.G., Nosanchuk, J.D., Casadevall, A., Rodrigues, M.L., Nimrichter, L., 2010. Extracellular vesicles from Cryptococcus neoformans modulate macrophage functions. Infect. Immun. 78, 1601–1609. doi:10.1128/IAI.01171-09

Ott, D.E., 2008. Cellular proteins detected in HIV-1. Rev. Med. Virol. 18, 159–175. doi:10.1002/rmv.570

Ottenhoff, T.H.M., Dass, R.H., Yang, N., Zhang, M.M., Wong, H.E.E., Sahiratmadja, E., Khor, C.C., Alisjahbana, B., van Crevel, R., Marzuki, S., Seielstad, M., van de Vosse, E., Hibberd, M.L., 2012. Genome-wide expression profiling identifies type 1 interferon response pathways in active tuberculosis. PloS One 7, e45839. doi:10.1371/journal.pone.0045839

Ouellet, D.L., Vigneault-Edwards, J., Létourneau, K., Gobeil, L.-A., Plante, I., Burnett, J.C., Rossi, J.J., Provost, P., 2013. Regulation of host gene expression by HIV-1 TAR microRNAs. Retrovirology 10, 86. doi:10.1186/1742-4690-10-86

Ouyang, P., Rakus, K., van Beurden, S., Westphal, A., Davison, A., Gatherer, D., Vanderplasschen, A., 2013. Interleukin-10s encoded by viruses: a remarkable example of independent acquisitions of a cellular gene by viruses and its subsequent evolution in the viral genome. J. Gen. Virol. doi:10.1099/vir.0.058966-0

Ozinsky, A., Underhill, D.M., Fontenot, J.D., Hajjar, A.M., Smith, K.D., Wilson, C.B., Schroeder, L., Aderem, A., 2000. The repertoire for pattern recognition of pathogens by the innate immune system is defined by cooperation between toll-like receptors. Proc. Natl. Acad. Sci. U. S. A. 97, 13766–13771. doi:10.1073/pnas.250476497

Pace, J.L., Russell, S.W., Schreiber, R.D., Altman, A., Katz, D.H., 1983. Macrophage activation: priming activity from a T-cell hybridoma is attributable to interferon-gamma. Proc. Natl. Acad. Sci. U. S. A. 80, 3782–3786.

Pacheco, A.G., Cardoso, C.C., Moraes, M.O., 2008. IFNG +874T/A, IL10 -1082G/A and TNF -308G/A polymorphisms in association with tuberculosis susceptibility: a meta-analysis study. Hum. Genet. 123, 477–484. doi:10.1007/s00439-008-0497-5

Paladino, N., Fainboim, H., Theiler, G., Schroder, T., Munoz, A.E., Flores, A.C., Galdame, O., Fainboim, L., 2006. Gender Susceptibility to Chronic Hepatitis C Virus Infection Associated with Interleukin 10 Promoter Polymorphism. J. Virol. 80, 9144–9150. doi:10.1128/JVI.00339-06

Palella, F.J., Baker, R.K., Moorman, A.C., Chmiel, J.S., Wood, K.C., Brooks, J.T., Holmberg, S.D., 2006. Mortality in the Highly Active Antiretroviral Therapy Era: Changing Causes of Death and Disease in the HIV Outpatient Study. JAIDS J. Acquir. Immune Defic. Syndr. 43, 27–34. doi:10.1097/01.qai.0000233310.90484.16

Paludan, S.R., Bowie, A.G., 2013. Immune Sensing of DNA. Immunity 38, 870–880. doi:10.1016/j.immuni.2013.05.004

Park-Min, K.-H., Antoniv, T.T., Ivashkiv, L.B., 2005. Regulation of macrophage phenotype by long-term exposure to IL-10. Immunobiology 210, 77–86. doi:10.1016/j.imbio.2005.05.002

Patel, N.R., Swan, K., Li, X., Tachado, S.D., Koziel, H., 2009. Impaired M. tuberculosis-mediated apoptosis in alveolar macrophages from HIV+ persons: potential role of IL-10 and BCL-3. J. Leukoc. Biol. 86, 53–60. doi:10.1189/jlb.0908574

Patel, N.R., Zhu, J., Tachado, S.D., Zhang, J., Wan, Z., Saukkonen, J., Koziel, H., 2007. HIV impairs TNF-alpha mediated macrophage apoptotic response to Mycobacterium tuberculosis. J. Immunol. Baltim. Md 1950 179, 6973–6980.

Pathak, S., Wentzel-Larsen, T., Asjö, B., 2010. Effects of in vitro HIV-1 infection on mycobacterial growth in peripheral blood monocyte-derived macrophages. Infect. Immun. 78, 4022–4032. doi:10.1128/IAI.00106-10

Pazin, M.J., Sheridan, P.L., Cannon, K., Cao, Z., Keck, J.G., Kadonaga, J.T., Jones, K.A., 1996. NF-kappa B-mediated chromatin reconfiguration and transcriptional activation of the HIV-1 enhancer in vitro. Genes Dev. 10, 37–49.

Penttilä, T., Haveri, A., Tammiruusu, A., Vuola, J.M., Lahesmaa, R., Puolakkainen, M., 2008. Chlamydia pneumoniae infection in IL-10 knock out mice: accelerated clearance but severe pulmonary inflammatory response. Microb. Pathog. 45, 25–29. doi:10.1016/j.micpath.2008.02.004

Perkins, N.D., Agranoff, A.B., Pascal, E., Nabel, G.J., 1994. An interaction between the DNA-binding domains of RelA(p65) and Sp1 mediates human immunodeficiency virus gene activation. Mol. Cell. Biol. 14, 6570–6583.

Perkins, N.D., Edwards, N.L., Duckett, C.S., Agranoff, A.B., Schmid, R.M., Nabel, G.J., 1993. A cooperative interaction between NF-kappa B and Sp1 is required for HIV-1 enhancer activation. EMBO J. 12, 3551–3558.

Pfeffer, K., Matsuyama, T., Kündig, T.M., Wakeham, A., Kishihara, K., Shahinian, A., Wiegmann, K., Ohashi, P.S., Krönke, M., Mak, T.W., 1993. Mice deficient for the 55 kd tumor necrosis factor receptor are resistant to endotoxic shock, yet succumb to L. monocytogenes infection. Cell 73, 457–467.

Phair, J., Muñoz, A., Detels, R., Kaslow, R., Rinaldo, C., Saah, A., 1990. The risk of Pneumocystis carinii pneumonia among men infected with human immunodeficiency virus type 1. Multicenter AIDS Cohort Study Group. N. Engl. J. Med. 322, 161–165. doi:10.1056/NEJM199001183220304

Picard, C., Fieschi, C., Altare, F., Al-Jumaah, S., Al-Hajjar, S., Feinberg, J., Dupuis, S., Soudais, C., Al-Mohsen, I.Z., Génin, E., Lammas, D., Kumararatne, D.S., Leclerc, T., Rafii, A., Frayha, H., Murugasu, B., Wah, L.B., Sinniah, R., Loubser, M., Okamoto, E., Al-Ghonaium, A., Tufenkeji, H., Abel, L., Casanova, J.-L., 2002. Inherited interleukin-12 deficiency: IL12B genotype and clinical phenotype of 13 patients from six kindreds. Am. J. Hum. Genet. 70, 336–348. doi:10.1086/338625

Pierre, P., Turley, S.J., Gatti, E., Hull, M., Meltzer, J., Mirza, A., Inaba, K., Steinman, R.M., Mellman, I., 1997. Developmental regulation of MHC class II transport in mouse dendritic cells. Nature 388, 787–792. doi:10.1038/42039

Platanias, L.C., 2005. Mechanisms of type-I- and type-II-interferon-mediated signalling. Nat. Rev. Immunol. 5, 375–386. doi:10.1038/nri1604

Poli, G., Kinter, A., Justement, J.S., Kehrl, J.H., Bressler, P., Stanley, S., Fauci, A.S., 1990. Tumor necrosis factor alpha functions in an autocrine manner in the induction of human immunodeficiency virus expression. Proc. Natl. Acad. Sci. U. S. A. 87, 782–785.

Poli, G., Kinter, A.L., Fauci, A.S., 1994. Interleukin 1 induces expression of the human immunodeficiency virus alone and in synergy with interleukin 6 in chronically infected U1 cells: inhibition of inductive effects by the interleukin 1 receptor antagonist. Proc. Natl. Acad. Sci. U. S. A. 91, 108–112.

Pollard, J.W., 2009. Trophic macrophages in development and disease. Nat. Rev. Immunol. 9, 259–270. doi:10.1038/nri2528

Popovic, M., Sarngadharan, M.G., Read, E., Gallo, R.C., 1984. Detection, isolation, and continuous production of cytopathic retroviruses (HTLV-III) from patients with AIDS and pre-AIDS. Science 224, 497–500.

Pouliot, P., Turmel, V., Gélinas, E., Laviolette, M., Bissonnette, E.Y., 2005. Interleukin-4 production by human alveolar macrophages. Clin. Exp. Allergy J. Br. Soc. Allergy Clin. Immunol. 35, 804–810. doi:10.1111/j.1365-2222.2005.02246.x

Poulter, L.W., Seymour, G.J., Duke, O., Janossy, G., Panayi, G., 1982. Immunohistological analysis of delayed-type hypersensitivity in man. Cell. Immunol. 74, 358–369.

Powell, M.J., Thompson, S.A., Tone, Y., Waldmann, H., Tone, M., 2000. Posttranscriptional regulation of IL-10 gene expression through sequences in the 3'-untranslated region. J. Immunol. Baltim. Md 1950 165, 292–296.

Pozio, E., Rezza, G., Boschini, A., Pezzotti, P., Tamburrini, A., Rossi, P., Di Fine, M., Smacchia, C., Schiesari, A., Gattei, E., Zucconi, R., Ballarini, P., 1997. Clinical cryptosporidiosis and human immunodeficiency virus (HIV)-induced immunosuppression: findings from a longitudinal study of HIV-positive and HIV-negative former injection drug users. J. Infect. Dis. 176, 969–975.

Pranada, A.L., Metz, S., Herrmann, A., Heinrich, P.C., Müller-Newen, G., 2004. Real Time Analysis of STAT3 Nucleocytoplasmic Shuttling. J. Biol. Chem. 279, 15114–15123. doi:10.1074/jbc.M312530200

Prinz, M., Priller, J., Sisodia, S.S., Ransohoff, R.M., 2011. Heterogeneity of CNS myeloid cells and their roles in neurodegeneration. Nat. Neurosci. 14, 1227–1235. doi:10.1038/nn.2923

Provost, V., Larose, M.-C., Langlois, A., Rola-Pleszczynski, M., Flamand, N., Laviolette, M., 2013. CCL26/eotaxin-3 is more effective to induce the migration of eosinophils of asthmatics than CCL11/eotaxin-1 and CCL24/eotaxin-2. J. Leukoc. Biol. jlb.0212074. doi:10.1189/jlb.0212074

Puissegur, M.-P., Botanch, C., Duteyrat, J.-L., Delsol, G., Caratero, C., Altare, F., 2004. An in vitro dual model of mycobacterial granulomas to investigate the molecular interactions between mycobacteria and human host cells. Cell. Microbiol. 6, 423–433. doi:10.1111/j.1462-5822.2004.00371.x

Quesniaux, V.J., Nicolle, D.M., Torres, D., Kremer, L., Guérardel, Y., Nigou, J., Puzo, G., Erard, F., Ryffel, B., 2004. Toll-Like Receptor 2 (TLR2)-Dependent-Positive and TLR2-Independent-Negative Regulation of Proinflammatory Cytokines by Mycobacterial Lipomannans. J. Immunol. 172, 4425–4434. doi:10.4049/jimmunol.172.7.4425

Ramakrishnan, L., 2012. Revisiting the role of the granuloma in tuberculosis. Nat. Rev. Immunol. 12, 352–366. doi:10.1038/nri3211

Rambaut, A., Posada, D., Crandall, K.A., Holmes, E.C., 2004. The causes and consequences of HIV evolution. Nat. Rev. Genet. 5, 52–61. doi:10.1038/nrg1246

Randolph, G.J., Angeli, V., Swartz, M.A., 2005. Dendritic-cell trafficking to lymph nodes through lymphatic vessels. Nat. Rev. Immunol. 5, 617–628. doi:10.1038/nri1670

Rangaka, M.X., Wilkinson, K.A., Seldon, R., Van Cutsem, G., Meintjes, G.A., Morroni, C., Mouton, P., Diwakar, L., Connell, T.G., Maartens, G., Wilkinson, R.J., 2007. Effect of HIV-1 infection on T-Cell-based and skin test detection of tuberculosis infection. Am. J. Respir. Crit. Care Med. 175, 514–520. doi:10.1164/rccm.200610-1439OC

Ranjbar, S., Boshoff, H.I., Mulder, A., Siddiqi, N., Rubin, E.J., Goldfeld, A.E., 2009. HIV-1 replication is differentially regulated by distinct clinical strains of Mycobacterium tuberculosis. PloS One 4, e6116. doi:10.1371/journal.pone.0006116

Ranjbar, S., Jasenosky, L.D., Chow, N., Goldfeld, A.E., 2012. Regulation of Mycobacterium tuberculosis-Dependent HIV-1 Transcription Reveals a New Role for NFAT5 in the Toll-Like Receptor Pathway. PLoS Pathog 8, e1002620. doi:10.1371/journal.ppat.1002620

Rasaiyaah, J., Noursadeghi, M., Kellam, P., Chain, B., 2009. Transcriptional and functional defects of dendritic cells derived from the MUTZ-3 leukaemia line. Immunology 127, 429–441. doi:10.1111/j.1365-2567.2008.03018.x

Rasaiyaah, J., Tan, C.P., Fletcher, A.J., Price, A.J., Blondeau, C., Hilditch, L., Jacques, D.A., Selwood, D.L., James, L.C., Noursadeghi, M., Towers, G.J., 2013. HIV-1 evades innate immune recognition through specific cofactor recruitment. Nature 503, 402–405. doi:10.1038/nature12769

Rathinam, V.A.K., Vanaja, S.K., Fitzgerald, K.A., 2012. Regulation of inflammasome signaling. Nat. Immunol. 13, 333–332. doi:10.1038/ni.2237

Ratner, L., Haseltine, W., Patarca, R., Livak, K.J., Starcich, B., Josephs, S.F., Doran, E.R., Rafalski, J.A., Whitehorn, E.A., Baumeister, K., Ivanoff, L., Petteway, S.R., Pearson, M.L., Lautenberger, J.A., Papas, T.S., Ghrayeb, J., Chang, N.T., Gallo, R.C., Wong-Staal, F., 1985. Complete nucleotide sequence of the AIDS virus, HTLV-III. Nature 313, 277–284. doi:10.1038/313277a0

Ravindran, R., Foley, J., Stoklasek, T., Glimcher, L.H., McSorley, S.J., 2005. Expression of T-bet by CD4 T cells is essential for resistance to Salmonella infection. J. Immunol. Baltim. Md 1950 175, 4603–4610.

Reboldi, A., Dang, E.V., McDonald, J.G., Liang, G., Russell, D.W., Cyster, J.G., 2014. 25-Hydroxycholesterol suppresses interleukin-1–driven inflammation downstream of type I interferon. Science 345, 679–684. doi:10.1126/science.1254790

Redford, P.S., Boonstra, A., Read, S., Pitt, J., Graham, C., Stavropoulos, E., Bancroft, G.J., O'Garra, A., 2010. Enhanced protection to Mycobacterium tuberculosis infection in IL-10-deficient mice is accompanied by early and enhanced Th1 responses in the lung. Eur. J. Immunol. 40, 2200–2210. doi:10.1002/eji.201040433

Redford, P.S., Mayer-Barber, K.D., McNab, F.W., Stavropoulos, E., Wack, A., Sher, A., O'Garra, A., 2014. Influenza A virus impairs control of Mycobacterium tuberculosis coinfection through a type I interferon receptor-dependent pathway. J. Infect. Dis. 209, 270–274. doi:10.1093/infdis/jit424

Redford, P.S., Murray, P.J., O'Garra, A., 2011. The role of IL-10 in immune regulation during M. tuberculosis infection. Mucosal Immunol. doi:10.1038/mi.2011.7

Reid, D.M., Gow, N.A.R., Brown, G.D., 2009. Pattern recognition: recent insights from Dectin-1. Curr. Opin. Immunol. 21, 30–37. doi:10.1016/j.coi.2009.01.003

Reiling, N., Hölscher, C., Fehrenbach, A., Kröger, S., Kirschning, C.J., Goyert, S., Ehlers, S., 2002. Cutting Edge: Toll-Like Receptor (TLR)2- and TLR4-Mediated Pathogen Recognition in Resistance to Airborne Infection with Mycobacterium tuberculosis. J. Immunol. 169, 3480–3484. doi:10.4049/jimmunol.169.7.3480

Rep, M.H., Schrijver, H.M., van Lopik, T., Hintzen, R.Q., Roos, M.T., Adèr, H.J., Polman, C.H., van Lier, R.A., 1999. Interferon (IFN)-beta treatment enhances CD95 and interleukin 10 expression but reduces interferon-gamma producing T cells in MS patients. J. Neuroimmunol. 96, 92–100.

Rhodes, D.R., Kalyana-Sundaram, S., Mahavisno, V., Barrette, T.R., Ghosh, D., Chinnaiyan, A.M., 2005. Mining for regulatory programs in the cancer transcriptome. Nat. Genet. 37, 579–583. doi:10.1038/ng1578

Riemann, M., Endres, R., Liptay, S., Pfeffer, K., Schmid, R.M., 2005. The IkappaB protein Bcl-3 negatively regulates transcription of the IL-10 gene in macrophages. J. Immunol. Baltim. Md 1950 175, 3560–3568.

Riley, J.K., Takeda, K., Akira, S., Schreiber, R.D., 1999. Interleukin-10 Receptor Signaling through the JAK-STAT Pathway REQUIREMENT FOR TWO DISTINCT RECEPTOR-DERIVED SIGNALS FOR ANTI-INFLAMMATORY ACTION. J. Biol. Chem. 274, 16513–16521. doi:10.1074/jbc.274.23.16513

Ringnér, M., 2008. What is principal component analysis? Nat. Biotechnol. 26, 303–304. doi:10.1038/nbt0308-303

Rivas-Santiago, B., Sada, E., Tsutsumi, V., Aguilar-León, D., Contreras, J.L., Hernández-Pando, R., 2006. β-Defensin Gene Expression during the Course of Experimental Tuberculosis Infection. J. Infect. Dis. 194, 697–701. doi:10.1086/506454

Robbins, S.H., Walzer, T., Dembélé, D., Thibault, C., Defays, A., Bessou, G., Xu, H., Vivier, E., Sellars, M., Pierre, P., Sharp, F.R., Chan, S., Kastner, P., Dalod, M., 2008. Novel insights into the relationships between dendritic cell subsets in human and mouse revealed by genome-wide expression profiling. Genome Biol. 9, R17. doi:10.1186/gb-2008-9-1-r17

Roca, F.J., Ramakrishnan, L., 2013. TNF dually mediates resistance and susceptibility to mycobacteria via mitochondrial reactive oxygen species. Cell 153, 521–534. doi:10.1016/j.cell.2013.03.022

Rodig, S.J., Meraz, M.A., White, J.M., Lampe, P.A., Riley, J.K., Arthur, C.D., King, K.L., Sheehan, K.C., Yin, L., Pennica, D., Johnson, E.M., Schreiber, R.D., 1998. Disruption of the Jak1 gene demonstrates obligatory and nonredundant roles of the Jaks in cytokine-induced biologic responses. Cell 93, 373–383.

Roers, A., Siewe, L., Strittmatter, E., Deckert, M., Schlüter, D., Stenzel, W., Gruber, A.D., Krieg, T., Rajewsky, K., Müller, W., 2004. T cell-specific inactivation of the interleukin 10 gene in mice results in enhanced T cell responses but normal innate responses to lipopolysaccharide or skin irritation. J. Exp. Med. 200, 1289–1297. doi:10.1084/jem.20041789

Roeth, J.F., Collins, K.L., 2006. Human immunodeficiency virus type 1 Nef: adapting to intracellular trafficking pathways. Microbiol. Mol. Biol. Rev. MMBR 70, 548–563. doi:10.1128/MMBR.00042-05

Rojas, M., Olivier, M., Gros, P., Barrera, L.F., García, L.F., 1999. TNF-α and IL-10 Modulate the Induction of Apoptosis by Virulent Mycobacterium tuberculosis in Murine Macrophages. J. Immunol. 162, 6122–6131.

Rosas, M., Davies, L.C., Giles, P.J., Liao, C.-T., Kharfan, B., Stone, T.C., O'Donnell, V.B., Fraser, D.J., Jones, S.A., Taylor, P.R., 2014. The Transcription Factor Gata6 Links Tissue Macrophage Phenotype and Proliferative Renewal. Science 344, 645–648. doi:10.1126/science.1251414

Rothenberg, M.E., Hogan, S.P., 2006. The eosinophil. Annu. Rev. Immunol. 24, 147–174. doi:10.1146/annurev.immunol.24.021605.090720

Rothfuchs, A.G., Bafica, A., Feng, C.G., Egen, J.G., Williams, D.L., Brown, G.D., Sher, A., 2007. Dectin-1 interaction with Mycobacterium tuberculosis leads to enhanced IL-12p40 production by splenic dendritic cells. J. Immunol. Baltim. Md 1950 179, 3463–3471.

Rudick, R.A., Ransohoff, R.M., Peppler, R., VanderBrug Medendorp, S., Lehmann, P., Alam, J., 1996. Interferon beta induces interleukin-10 expression: relevance to multiple sclerosis. Ann. Neurol. 40, 618–627. doi:10.1002/ana.410400412

Rusinova, I., Forster, S., Yu, S., Kannan, A., Masse, M., Cumming, H., Chapman, R., Hertzog, P.J., 2013. INTERFEROME v2.0: an updated database of annotated interferon-regulated genes. Nucleic Acids Res. 41, D1040–D1046. doi:10.1093/nar/gks1215

Russell, D.G., 2007. Who puts the tubercle in tuberculosis? Nat. Rev. Microbiol. 5, 39–47. doi:10.1038/nrmicro1538

Russell, D.G., Cardona, P.-J., Kim, M.-J., Allain, S., Altare, F., 2009. Foamy macrophages and the progression of the human tuberculosis granuloma. Nat. Immunol. 10, 943–948. doi:10.1038/ni.1781

Russell, D.G., VanderVen, B.C., Lee, W., Abramovitch, R.B., Kim, M., Homolka, S., Niemann, S., Rohde, K.H., 2010. Mycobacterium tuberculosis Wears What It Eats. Cell Host Microbe 8, 68–76. doi:10.1016/j.chom.2010.06.002

Sabiiti, W., May, R.C., Pursall, E.R., 2012. Experimental models of cryptococcosis. Int. J. Microbiol. 2012, 626745. doi:10.1155/2012/626745

Sakai, S., Mayer-Barber, K.D., Barber, D.L., 2014. Defining features of protective CD4 T cell responses to Mycobacterium tuberculosis. Curr. Opin. Immunol., Host pathogens * Immune senescence 29, 137–142. doi:10.1016/j.coi.2014.06.003

Sakata, A., Ida, E., Tominaga, M., Onoue, K., 1987. Arachidonic acid acts as an intracellular activator of NADPH-oxidase in Fc gamma receptor-mediated superoxide generation in macrophages. J. Immunol. Baltim. Md 1950 138, 4353–4359.

Sakula, A., 1982. Robert Koch: centenary of the discovery of the tubercle bacillus, 1882. Thorax 37, 246–251. doi:10.1136/thx.37.4.246

Salazar-Gonzalez, J.F., Salazar, M.G., Keele, B.F., Learn, G.H., Giorgi, E.E., Li, H., Decker, J.M., Wang, S., Baalwa, J., Kraus, M.H., Parrish, N.F., Shaw, K.S., Guffey, M.B., Bar, K.J., Davis, K.L., Ochsenbauer-Jambor, C., Kappes, J.C., Saag, M.S., Cohen, M.S., Mulenga, J., Derdeyn, C.A., Allen, S., Hunter, E., Markowitz, M., Hraber, P., Perelson, A.S., Bhattacharya, T., Haynes, B.F., Korber, B.T., Hahn, B.H., Shaw, G.M., 2009. Genetic identity, biological phenotype, and evolutionary pathways of transmitted/founder viruses in acute and early HIV-1 infection. J. Exp. Med. 206, 1273–1289. doi:10.1084/jem.20090378

Sandler, N.G., Bosinger, S.E., Estes, J.D., Zhu, R.T.R., Tharp, G.K., Boritz, E., Levin, D., Wijeyesinghe, S., Makamdop, K.N., del Prete, G.Q., Hill, B.J., Timmer, J.K., Reiss, E., Yarden, G., Darko, S., Contijoch, E., Todd, J.P., Silvestri, G., Nason, M., Norgren Jr, R.B., Keele, B.F., Rao, S., Langer, J.A., Lifson, J.D., Schreiber, G., Douek, D.C., 2014. Type I interferon responses in rhesus macaques prevent SIV infection and slow disease progression. Nature 511, 601–605. doi:10.1038/nature13554

Saraiva, M., Christensen, J.R., Tsytsykova, A.V., Goldfeld, A.E., Ley, S.C., Kioussis, D., O'Garra, A., 2005. Identification of a macrophage-specific chromatin signature in the IL-10 locus. J. Immunol. Baltim. Md 1950 175, 1041–1046.

Saraiva, M., Christensen, J.R., Veldhoen, M., Murphy, T.L., Murphy, K.M., O'Garra, A., 2009. Interleukin-10 production by Th1 cells requires interleukin-12-induced STAT4 transcription factor and ERK MAP kinase activation by high antigen dose. Immunity 31, 209–219. doi:10.1016/j.immuni.2009.05.012

Saraiva, M., O'Garra, A., 2010. The regulation of IL-10 production by immune cells. Nat. Rev. Immunol. 10, 170–181. doi:10.1038/nri2711

Sarrazin, H., Wilkinson, K.A., Andersson, J., Rangaka, M.X., Radler, L., van Veen, K., Lange, C., Wilkinson, R.J., 2009. Association between tuberculin skin test reactivity, the memory CD4 cell subset, and circulating FoxP3-expressing cells in HIV-infected persons. J. Infect. Dis. 199, 702–710. doi:10.1086/596735

Sasaki, Y., Nomura, A., Kusuhara, K., Takada, H., Ahmed, S., Obinata, K., Hamada, K., Okimoto, Y., Hara, T., 2002. Genetic Basis of Patients with Bacille Calmette-Guérin Osteomyelitis in Japan: Identification of Dominant Partial Interferon-γ Receptor 1 Deficiency as a Predominant Type. J. Infect. Dis. 185, 706–709. doi:10.1086/339011

Satoh, T., Takeuchi, O., Vandenbon, A., Yasuda, K., Tanaka, Y., Kumagai, Y., Miyake, T., Matsushita, K., Okazaki, T., Saitoh, T., Honma, K., Matsuyama, T., Yui, K., Tsujimura, T., Standley, D.M., Nakanishi, K., Nakai, K., Akira, S., 2010. The Jmjd3-Irf4 axis regulates M2 macrophage polarization and host responses against helminth infection. Nat. Immunol. 11, 936–944. doi:10.1038/ni.1920

Satpathy, A.T., Wu, X., Albring, J.C., Murphy, K.M., 2012. Re(de)fining the dendritic cell lineage. Nat. Immunol. 13, 1145–1154. doi:10.1038/ni.2467

Schäfer, G., Jacobs, M., Wilkinson, R.J., Brown, G.D., 2009. Non-opsonic recognition of Mycobacterium tuberculosis by phagocytes. J. Innate Immun. 1, 231–243. doi:10.1159/000173703

Schaljo, B., Kratochvill, F., Gratz, N., Sadzak, I., Sauer, I., Hammer, M., Vogl, C., Strobl, B., Müller, M., Blackshear, P.J., Poli, V., Lang, R., Murray, P.J., Kovarik, P., 2009. Tristetraprolin is required for full anti-inflammatory response of murine macrophages to IL-10. J. Immunol. Baltim. Md 1950 183, 1197–1206. doi:10.4049/jimmunol.0803883

Scheller, J., Chalaris, A., Schmidt-Arras, D., Rose-John, S., 2011. The pro- and anti-inflammatory properties of the cytokine interleukin-6. Biochim. Biophys. Acta BBA - Mol. Cell Res., Including the Special Section: 11th European Symposium on Calcium 1813, 878–888. doi:10.1016/j.bbamcr.2011.01.034

Scheynius, A., Klareskog, L., Forsum, U., 1982. In situ identification of T lymphocyte subsets and HLA-DR expressing cells in the human skin tuberculin reaction. Clin. Exp. Immunol. 49, 325–330.

Schmid, M.A., Kingston, D., Boddupalli, S., Manz, M.G., 2010. Instructive cytokine signals in dendritic cell lineage commitment. Immunol. Rev. 234, 32–44. doi:10.1111/j.0105-2896.2009.00877.x

Schneider, W.M., Chevillotte, M.D., Rice, C.M., 2014. Interferon-stimulated genes: a complex web of host defenses. Annu. Rev. Immunol. 32, 513–545. doi:10.1146/annurev-immunol-032713-120231

Schopman, N.C.T., Willemsen, M., Liu, Y.P., Bradley, T., van Kampen, A., Baas, F., Berkhout, B., Haasnoot, J., 2012. Deep sequencing of virus-infected cells reveals HIV-encoded small RNAs. Nucleic Acids Res. 40, 414–427. doi:10.1093/nar/gkr719

Schraml, B.U., van Blijswijk, J., Zelenay, S., Whitney, P.G., Filby, A., Acton, S.E., Rogers, N.C., Moncaut, N., Carvajal, J.J., Reis e Sousa, C., 2013. Genetic tracing via DNGR-1 expression history defines dendritic cells as a hematopoietic lineage. Cell 154, 843–858. doi:10.1016/j.cell.2013.07.014

Schreiber, T., Ehlers, S., Heitmann, L., Rausch, A., Mages, J., Murray, P.J., Lang, R., Hölscher, C., 2009. Autocrine IL-10 induces hallmarks of alternative activation in macrophages and suppresses antituberculosis effector mechanisms without compromising T cell immunity. J. Immunol. Baltim. Md 1950 183, 1301–1312. doi:10.4049/jimmunol.0803567

Schroder, K., Tschopp, J., 2010. The inflammasomes. Cell 140, 821–832. doi:10.1016/j.cell.2010.01.040

Schulz, C., Gomez Perdiguero, E., Chorro, L., Szabo-Rogers, H., Cagnard, N., Kierdorf, K., Prinz, M., Wu, B., Jacobsen, S.E.W., Pollard, J.W., Frampton, J., Liu, K.J., Geissmann, F., 2012. A lineage of myeloid cells independent of Myb and hematopoietic stem cells. Science 336, 86–90. doi:10.1126/science.1219179

Schutz, C., Meintjes, G., Almajid, F., Wilkinson, R.J., Pozniak, A., 2010. Clinical management of tuberculosis and HIV-1 co-infection. Eur. Respir. J. 36, 1460–1481. doi:10.1183/09031936.00110210

Scott, E.W., Simon, M.C., Anastasi, J., Singh, H., 1994. Requirement of transcription factor PU.1 in the development of multiple hematopoietic lineages. Science 265, 1573–1577.

Seddiki, N., Sasson, S.C., Santner-Nanan, B., Munier, M., van Bockel, D., Ip, S., Marriott, D., Pett, S., Nanan, R., Cooper, D.A., Zaunders, J.J., Kelleher, A.D., 2009. Proliferation of weakly suppressive regulatory CD4+ T cells is associated with over-active CD4+ T-cell responses in HIV-positive patients with mycobacterial immune restoration disease. Eur. J. Immunol. 39, 391–403. doi:10.1002/eji.200838630

Segal, E., Shapira, M., Regev, A., Pe'er, D., Botstein, D., Koller, D., Friedman, N., 2003. Module networks: identifying regulatory modules and their condition-specific regulators from gene expression data. Nat. Genet. 34, 166–176. doi:10.1038/ng1165

Selwyn, P.A., Sckell, B.M., Alcabes, P., Friedland, G.H., Klein, R.S., Schoenbaum, E.E., 1992. High risk of active tuberculosis in HIV-infected drug users with cutaneous anergy. JAMA J. Am. Med. Assoc. 268, 504–509.

Shen, Y.-M.P., Frenkel, E.P., 2004. Thrombosis and a hypercoagulable state in HIV-infected patients. Clin. Appl. Thromb. Off. J. Int. Acad. Clin. Appl. Thromb. 10, 277–280.

Shi, C., Pamer, E.G., 2011. Monocyte recruitment during infection and inflammation. Nat Rev Immunol 11, 762–774. doi:10.1038/nri3070

Shibata, Y., Berclaz, P.Y., Chroneos, Z.C., Yoshida, M., Whitsett, J.A., Trapnell, B.C., 2001. GM-CSF regulates alveolar macrophage differentiation and innate immunity in the lung through PU.1. Immunity 15, 557–567.

Shibata, Y., Foster, L.A., Kurimoto, M., Okamura, H., Nakamura, R.M., Kawajiri, K., Justice, J.P., Van Scott, M.R., Myrvik, Q.N., Metzger, W.J., 1998. Immunoregulatory roles of IL-10 in innate immunity: IL-10 inhibits macrophage production of IFN-gamma-inducing factors but enhances NK cell production of IFN-gamma. J. Immunol. Baltim. Md 1950 161, 4283–4288.

Shioda, T., Levy, J.A., Cheng-Mayer, C., 1991. Macrophage and T cell-line tropisms of HIV-1 are determined by specific regions of the envelope gp120 gene. Nature 349, 167–169. doi:10.1038/349167a0

Shoemaker, J., Saraiva, M., O'Garra, A., 2006. GATA-3 directly remodels the IL-10 locus independently of IL-4 in CD4+ T cells. J. Immunol. Baltim. Md 1950 176, 3470–3479.

Shoham, S., Huang, C., Chen, J.M., Golenbock, D.T., Levitz, S.M., 2001. Toll-like receptor 4 mediates intracellular signaling without TNF-alpha release in response to Cryptococcus neoformans polysaccharide capsule. J. Immunol. Baltim. Md 1950 166, 4620–4626.

Shouval, D.S., Biswas, A., Goettel, J.A., McCann, K., Conaway, E., Redhu, N.S., Mascanfroni, I.D., Al Adham, Z., Lavoie, S., Ibourk, M., Nguyen, D.D., Samsom, J.N., Escher, J.C., Somech, R., Weiss, B., Beier, R., Conklin, L.S., Ebens, C.L., Santos, F.G.M.S., Ferreira, A.R., Sherlock, M., Bhan, A.K., Müller, W., Mora, J.R., Quintana, F.J., Klein, C., Muise, A.M., Horwitz, B.H., Snapper, S.B., 2014. Interleukin-10 Receptor Signaling in Innate Immune Cells Regulates Mucosal Immune Tolerance and Anti-Inflammatory Macrophage Function. Immunity 40, 706–719. doi:10.1016/j.immuni.2014.03.011

Siegal, F.P., Kadowaki, N., Shodell, M., Fitzgerald-Bocarsly, P.A., Shah, K., Ho, S., Antonenko, S., Liu, Y.J., 1999. The nature of the principal type 1 interferon-producing cells in human blood. Science 284, 1835–1837.

Siegal, F.P., Lopez, C., Hammer, G.S., Brown, A.E., Kornfeld, S.J., Gold, J., Hassett, J., Hirschman, S.Z., Cunningham-Rundles, C., Adelsberg, B.R., 1981. Severe acquired immunodeficiency in male homosexuals, manifested by chronic perianal ulcerative herpes simplex lesions. N. Engl. J. Med. 305, 1439–1444. doi:10.1056/NEJM198112103052403

Siewe, L., Bollati-Fogolin, M., Wickenhauser, C., Krieg, T., Müller, W., Roers, A., 2006. Interleukin-10 derived from macrophages and/or neutrophils regulates the inflammatory response to LPS but not the response to CpG DNA. Eur. J. Immunol. 36, 3248–3255. doi:10.1002/eji.200636012

Sigal, A., Kim, J.T., Balazs, A.B., Dekel, E., Mayo, A., Milo, R., Baltimore, D., 2011. Cell-to-cell spread of HIV permits ongoing replication despite antiretroviral therapy. Nature advance online publication. doi:10.1038/nature10347

Sigurdardottir, B., Thormar, H., 1964. ISOLATION OF A VIRAL AGENT FROM THE LUNGS OF SHEEP AFFECTED WITH MAEDI. J. Infect. Dis. 114, 55–60.

Simmons, C.P., Thwaites, G.E., Quyen, N.T.H., Torok, E., Hoang, D.M., Chau, T.T.H., Mai, P.P., Lan, N.T.N., Dung, N.H., Quy, H.T., Bang, N.D., Hien, T.T., Farrar, J., 2006. Pretreatment Intracerebral and Peripheral Blood Immune Responses in Vietnamese Adults with Tuberculous Meningitis: Diagnostic Value and Relationship to Disease Severity and Outcome. J. Immunol. 176, 2007–2014.

Simonney, N., Dewulf, G., Herrmann, J.-L., Gutierrez, M.C., Vicaut, E., Boutron, C., Leportier, M., Lafaurie, M., Abgrall, S., Sereni, D., Autran, B., Carcelain, G., Bourgarit, A., Lagrange, P.H., 2008. Anti-PGL-Tb1 responses as an indicator of the immune restoration syndrome in HIV-TB patients. Tuberc. Edinb. Scotl. 88, 453–461. doi:10.1016/j.tube.2008.01.006

Sindhu, S., Toma, E., Cordeiro, P., Ahmad, R., Morisset, R., Menezes, J., 2006. Relationship of in vivo and ex vivo levels of TH1 and TH2 cytokines with viremia in HAART patients with and without opportunistic infections. J. Med. Virol. 78, 431–439. doi:10.1002/jmv.20558

Sing, A., Roggenkamp, A., Geiger, A.M., Heesemann, J., 2002. Yersinia enterocolitica Evasion of the Host Innate Immune Response by V Antigen-Induced IL-10 Production of Macrophages Is Abrogated in IL-10-Deficient Mice. J. Immunol. 168, 1315–1321. doi:10.4049/jimmunol.168.3.1315

Singh, S.B., Davis, A.S., Taylor, G.A., Deretic, V., 2006. Human IRGM Induces Autophagy to Eliminate Intracellular Mycobacteria. Science 313, 1438–1441. doi:10.1126/science.1129577

Smallie, T., Ricchetti, G., Horwood, N.J., Feldmann, M., Clark, A.R., Williams, L.M., 2010. IL-10 inhibits transcription elongation of the human TNF gene in primary macrophages. J. Exp. Med. 207, 2081–2088. doi:10.1084/jem.20100414

Sobell, H.M., 1985. Actinomycin and DNA transcription. Proc. Natl. Acad. Sci. U. S. A. 82, 5328–5331.

Sonnenberg, P., Glynn, J.R., Fielding, K., Murray, J., Godfrey-Faussett, P., Shearer, S., 2005. How soon after infection with HIV does the risk of tuberculosis start to increase? A retrospective cohort study in South African gold miners. J. Infect. Dis. 191, 150–158. doi:10.1086/426827

Spear, G.T., Ou, C.Y., Kessler, H.A., Moore, J.L., Schochetman, G., Landay, A.L., 1990. Analysis of lymphocytes, monocytes, and neutrophils from human immunodeficiency virus (HIV)-infected persons for HIV DNA. J. Infect. Dis. 162, 1239–1244.

Stacey, A.R., Norris, P.J., Qin, L., Haygreen, E.A., Taylor, E., Heitman, J., Lebedeva, M., DeCamp, A., Li, D., Grove, D., Self, S.G., Borrow, P., 2009. Induction of a striking systemic cytokine cascade prior to peak viremia in acute human immunodeficiency virus type 1 infection, in contrast to more

modest and delayed responses in acute hepatitis B and C virus infections. J. Virol. 83, 3719–3733. doi:10.1128/JVI.01844-08

Stacey, M.A., Marsden, M., Wang, E.C.Y., Wilkinson, G.W.G., Humphreys, I.R., 2011. IL-10 restricts activation-induced death of NK cells during acute murine cytomegalovirus infection. J. Immunol. Baltim. Md 1950 187, 2944–2952. doi:10.4049/jimmunol.1101021

Stanley, E., Lieschke, G.J., Grail, D., Metcalf, D., Hodgson, G., Gall, J.A., Maher, D.W., Cebon, J., Sinickas, V., Dunn, A.R., 1994. Granulocyte/macrophage colony-stimulating factor-deficient mice show no major perturbation of hematopoiesis but develop a characteristic pulmonary pathology. Proc. Natl. Acad. Sci. U. S. A. 91, 5592–5596.

Stanley, S.A., Johndrow, J.E., Manzanillo, P., Cox, J.S., 2007. The Type I IFN response to infection with Mycobacterium tuberculosis requires ESX-1-mediated secretion and contributes to pathogenesis. J. Immunol. Baltim. Md 1950 178, 3143–3152.

Stein, M., Keshav, S., Harris, N., Gordon, S., 1992. Interleukin 4 potently enhances murine macrophage mannose receptor activity: a marker of alternative immunologic macrophage activation. J. Exp. Med. 176, 287–292.

Steinman, R.M., Lustig, D.S., Cohn, Z.A., 1974. Identification of a novel cell type in peripheral lymphoid organs of mice. 3. Functional properties in vivo. J. Exp. Med. 139, 1431–1445.

Steinman, R.M., Witmer, M.D., 1978. Lymphoid dendritic cells are potent stimulators of the primary mixed leukocyte reaction in mice. Proc. Natl. Acad. Sci. U. S. A. 75, 5132–5136.

Stetson, D.B., Medzhitov, R., 2006. Type I Interferons in Host Defense. Immunity 25, 373–381. doi:10.1016/j.immuni.2006.08.007

Stevenson, M., 2003. HIV-1 pathogenesis. Nat Med 9, 853–860. doi:10.1038/nm0703-853

Stoecklin, G., Tenenbaum, S.A., Mayo, T., Chittur, S.V., George, A.D., Baroni, T.E., Blackshear, P.J., Anderson, P., 2008. Genome-wide analysis identifies interleukin-10 mRNA as target of tristetraprolin. J. Biol. Chem. 283, 11689–11699. doi:10.1074/jbc.M709657200

Stout, R.D., Jiang, C., Matta, B., Tietzel, I., Watkins, S.K., Suttles, J., 2005. Macrophages sequentially change their functional phenotype in response to changes in microenvironmental influences. J. Immunol. Baltim. Md 1950 175, 342–349.

Stout, R.D., Suttles, J., 2004. Functional plasticity of macrophages: reversible adaptation to changing microenvironments. J. Leukoc. Biol. 76, 509–513. doi:10.1189/jlb.0504272

Strebel, K., 2013. HIV accessory proteins versus host restriction factors. Curr. Opin. Virol., Virus replication in animals and plants 3, 692–699. doi:10.1016/j.coviro.2013.08.004

Stremlau, M., Owens, C.M., Perron, M.J., Kiessling, M., Autissier, P., Sodroski, J., 2004. The cytoplasmic body component TRIM5α restricts HIV-1 infection in Old World monkeys. Nature 427, 848–853. doi:10.1038/nature02343

Strowig, T., Henao-Mejia, J., Elinav, E., Flavell, R., 2012. Inflammasomes in health and disease. Nature 481, 278–286. doi:10.1038/nature10759

Stuart, L.M., Ezekowitz, R.A.B., 2005. Phagocytosis: elegant complexity. Immunity 22, 539–550. doi:10.1016/j.immuni.2005.05.002

Stumpo, R., Kauer, M., Martin, S., Kolb, H., 2003. IL-10 induces gene expression in macrophages: partial overlap with IL-5 but not with IL-4 induced genes. Cytokine 24, 46–56. doi:10.1016/S1043-4666(03)00270-9

Subramanian, A., Tamayo, P., Mootha, V.K., Mukherjee, S., Ebert, B.L., Gillette, M.A., Paulovich, A., Pomeroy, S.L., Golub, T.R., Lander, E.S., Mesirov, J.P., 2005. Gene set enrichment analysis: a knowledge-based approach for interpreting genome-wide expression profiles. Proc. Natl. Acad. Sci. U. S. A. 102, 15545–15550. doi:10.1073/pnas.0506580102

Sullivan, B.M., Jobe, O., Lazarevic, V., Vasquez, K., Bronson, R., Glimcher, L.H., Kramnik, I., 2005. Increased susceptibility of mice lacking T-bet to infection with Mycobacterium tuberculosis correlates with increased IL-10 and decreased IFN-gamma production. J. Immunol. Baltim. Md 1950 175, 4593–4602.

Sun, Z., Denton, P.W., Estes, J.D., Othieno, F.A., Wei, B.L., Wege, A.K., Melkus, M.W., Padgett-Thomas, A., Zupancic, M., Haase, A.T., Garcia, J.V., 2007. Intrarectal transmission, systemic infection, and

CD4+ T cell depletion in humanized mice infected with HIV-1. J. Exp. Med. 204, 705–714. doi:10.1084/jem.20062411

Sunseri, N., O'Brien, M., Bhardwaj, N., Landau, N.R., 2011. Human immunodeficiency virus type 1 modified to package Simian immunodeficiency virus Vpx efficiently infects macrophages and dendritic cells. J. Virol. 85, 6263–6274. doi:10.1128/JVI.00346-11

Swann, S.A., Williams, M., Story, C.M., Bobbitt, K.R., Fleis, R., Collins, K.L., 2001. HIV-1 Nef blocks transport of MHC class I molecules to the cell surface via a PI 3-kinase-dependent pathway. Virology 282, 267–277. doi:10.1006/viro.2000.0816

Tabas, I., 2010. Macrophage death and defective inflammation resolution in atherosclerosis. Nat. Rev. Immunol. 10, 36–46. doi:10.1038/nri2675

Tachado, S.D., Li, X., Bole, M., Swan, K., Anandaiah, A., Patel, N.R., Koziel, H., 2010. MyD88-dependent TLR4 signaling is selectively impaired in alveolar macrophages from asymptomatic HIV+ persons. Blood 115, 3606–3615. doi:10.1182/blood-2009-10-250787

Tachado, S.D., Zhang, J., Zhu, J., Patel, N., Koziel, H., 2005. HIV impairs TNF-alpha release in response to Toll-like receptor 4 stimulation in human macrophages in vitro. Am. J. Respir. Cell Mol. Biol. 33, 610–621. doi:10.1165/rcmb.2004-0341OC

Tadokera, R., Meintjes, G., Skolimowska, K.H., Wilkinson, K.A., Matthews, K., Seldon, R., Chegou, N.N., Maartens, G., Rangaka, M.X., Rebe, K., Walzl, G., Wilkinson, R.J., 2011. Hypercytokinaemia accompanies HIV-tuberculosis immune reconstitution inflammatory syndrome. Eur. Respir. J. Off. J. Eur. Soc. Clin. Respir. Physiol. 37, 1248–1259. doi:10.1183/09031936.00091010

Takeda, K., Kaisho, T., Akira, S., 2003. Toll-like receptors. Annu. Rev. Immunol. 21, 335–376. doi:10.1146/annurev.immunol.21.120601.141126

Takeda, K., Tanaka, T., Shi, W., Matsumoto, M., Minami, M., Kashiwamura, S., Nakanishi, K., Yoshida, N., Kishimoto, T., Akira, S., 1996. Essential role of Stat6 in IL-4 signalling. Nature 380, 627–630. doi:10.1038/380627a0

Takeuchi, O., Akira, S., 2010. Pattern recognition receptors and inflammation. Cell 140, 805–820. doi:10.1016/j.cell.2010.01.022

Tameris, M.D., Hatherill, M., Landry, B.S., Scriba, T.J., Snowden, M.A., Lockhart, S., Shea, J.E., McClain, J.B., Hussey, G.D., Hanekom, W.A., Mahomed, H., McShane, H., 2013. Safety and efficacy of MVA85A, a new tuberculosis vaccine, in infants previously vaccinated with BCG: a randomised, placebo-controlled phase 2b trial. The Lancet 381, 1021–1028. doi:10.1016/S0140-6736(13)60177-4

Tamoutounour, S., Guilliams, M., Montanana Sanchis, F., Liu, H., Terhorst, D., Malosse, C., Pollet, E., Ardouin, L., Luche, H., Sanchez, C., Dalod, M., Malissen, B., Henri, S., 2013. Origins and Functional Specialization of Macrophages and of Conventional and Monocyte-Derived Dendritic Cells in Mouse Skin. Immunity 39, 925–938. doi:10.1016/j.immuni.2013.10.004

Tan, J.C., Indelicato, S.R., Narula, S.K., Zavodny, P.J., Chou, C.C., 1993. Characterization of interleukin-10 receptors on human and mouse cells. J. Biol. Chem. 268, 21053–21059.

Tanaka, N., Hoshino, Y., Gold, J., Hoshino, S., Martiniuk, F., Kurata, T., Pine, R., Levy, D., Rom, W.N., Weiden, M., 2005. Interleukin-10 induces inhibitory C/EBPbeta through STAT-3 and represses HIV-1 transcription in macrophages. Am. J. Respir. Cell Mol. Biol. 33, 406–411. doi:10.1165/rcmb.2005-0140OC

Tascon, R.E., Stavropoulos, E., Lukacs, K.V., Colston, M.J., 1998. Protection against Mycobacterium tuberculosis infection by CD8+ T cells requires the production of gamma interferon. Infect. Immun. 66, 830–834.

Taylor, P.R., Martinez-Pomares, L., Stacey, M., Lin, H.-H., Brown, G.D., Gordon, S., 2005. Macrophage receptors and immune recognition. Annu. Rev. Immunol. 23, 901–944. doi:10.1146/annurev.immunol.23.021704.115816

Teixeira-Coelho, M., Guedes, J., Ferreirinha, P., Howes, A., Pedrosa, J., Rodrigues, F., Lai, W.S., Blackshear, P.J., O Garra, A., Castro, A.G., Saraiva, M., 2013. Differential post-transcriptional regulation of IL-10 by TLR2 and TLR4-activated macrophages. Eur. J. Immunol. doi:10.1002/eji.201343734

Teles, R.M.B., Graeber, T.G., Krutzik, S.R., Montoya, D., Schenk, M., Lee, D.J., Komisopoulou, E., Kelly-Scumpia, K., Chun, R., Iyer, S.S., Sarno, E.N., Rea, T.H., Hewison, M., Adams, J.S., Popper, S.J.,

Relman, D.A., Stenger, S., Bloom, B.R., Cheng, G., Modlin, R.L., 2013. Type I interferon suppresses type II interferon-triggered human anti-mycobacterial responses. Science 339, 1448–1453. doi:10.1126/science.1233665

Terwilliger, E., Burghoff, R., Sia, R., Sodroski, J., Haseltine, W., Rosen, C., 1988. The art gene product of human immunodeficiency virus is required for replication. J. Virol. 62, 655–658.

The HIV-CAUSAL Collaboration *, 2010. The effect of combined antiretroviral therapy on the overall mortality of HIV-infected individuals. [Miscellaneous Article]. AIDS January 2 2010 24, 123–137. doi:10.1097/QAD.0b013e3283324283

Thormar, H., 2013. The origin of lentivirus research: Maedi-visna virus. Curr. HIV Res. 11, 2–9.

Thwaites, G.E., Bang, N.D., Dung, N.H., Quy, H.T., Oanh, D.T.T., Thoa, N.T.C., Hien, N.Q., Thuc, N.T., Hai, N.N., Lan, N.T.N., Lan, N.N., Duc, N.H., Tuan, V.N., Hiep, C.H., Chau, T.T.H., Mai, P.P., Dung, N.T., Stepniewska, K., White, N.J., Hien, T.T., Farrar, J.J., 2004. Dexamethasone for the Treatment of Tuberculous Meningitis in Adolescents and Adults. N. Engl. J. Med. 351, 1741–1751. doi:10.1056/NEJMoa040573

Tobin, D.M., Roca, F.J., Oh, S.F., McFarland, R., Vickery, T.W., Ray, J.P., Ko, D.C., Zou, Y., Bang, N.D., Chau, T.T.H., Vary, J.C., Hawn, T.R., Dunstan, S.J., Farrar, J.J., Thwaites, G.E., King, M.-C., Serhan, C.N., Ramakrishnan, L., 2012. Host genotype-specific therapies can optimize the inflammatory response to mycobacterial infections. Cell 148, 434–446. doi:10.1016/j.cell.2011.12.023

Tomlinson, G., Chimalapati, S., Lapp, T., Pollard, T., Cohen, J., Camberlein, E., Stafford, S., Periselneris, J., Aldridge, C., Vollmer, W., Picard, C., Casanova, J.L., Noursadeghi, M., Brown, J., In press. TLR-mediated inflammatory responses to Streptococcus pneumoniae are highly dependent on surface expression of bacterial lipoproteins. J. Immunol.

Tomlinson, G.S., Bell, L.C.K., Walker, N.F., Tsang, J., Brown, J.S., Breen, R., Lipman, M., Katz, D.R., Miller, R.F., Chain, B.M., Elkington, P.T.G., Noursadeghi, M., 2014. HIV-1 Infection of Macrophages Dysregulates Innate Immune Responses to Mycobacterium tuberculosis by Inhibition of Interleukin-10. J. Infect. Dis. 209, 1055–1065. doi:10.1093/infdis/jit621

Tomlinson, G.S., Booth, H., Petit, S.J., Potton, E., Towers, G.J., Miller, R.F., Chain, B.M., Noursadeghi, M., 2012. Adherent Human Alveolar Macrophages Exhibit a Transient Pro-Inflammatory Profile That Confounds Responses to Innate Immune Stimulation. PLoS ONE 7, e40348. doi:10.1371/journal.pone.0040348

Tomlinson, G.S., Cashmore, T.J., Elkington, P.T.G., Yates, J., Lehloenya, R.J., Tsang, J., Brown, M., Miller, R.F., Dheda, K., Katz, D.R., Chain, B.M., Noursadeghi, M., 2011. Transcriptional profiling of innate and adaptive human immune responses to mycobacteria in the tuberculin skin test. Eur. J. Immunol. 41, 3253–3260. doi:10.1002/eji.201141841

Toossi, Z., Johnson, J.L., Kanost, R.A., Wu, M., Luzze, H., Peters, P., Okwera, A., Joloba, M., Mugyenyi, P., Mugerwa, R.D., Aung, H., Ellner, J.J., Hirsch, C.S., 2001. Increased replication of HIV-1 at sites of Mycobacterium tuberculosis infection: potential mechanisms of viral activation. J. Acquir. Immune Defic. Syndr. 1999 28, 1–8.

Toossi, Z., Mayanja-Kizza, H., Hirsch, C.S., Edmonds, K.L., Spahlinger, T., Hom, D.L., Aung, H., Mugyenyi, P., Ellner, J.J., Whalen, C.W., 2001. Impact of tuberculosis (TB) on HIV-1 activity in dually infected patients. Clin. Exp. Immunol. 123, 233–238.

Toossi, Z., Nicolacakis, K., Xia, L., Ferrari, N.A., Rich, E.A., 1997. Activation of latent HIV-1 by Mycobacterium tuberculosis and its purified protein derivative in alveolar macrophages from HIV-infected individuals in vitro. J. Acquir. Immune Defic. Syndr. Hum. Retrovirology Off. Publ. Int. Retrovirology Assoc. 15, 325–331.

Torre, D., Gennero, L., Baccino, F.M., Speranza, F., Biondi, G., Pugliese, A., 2002. Impaired macrophage phagocytosis of apoptotic neutrophils in patients with human immunodeficiency virus type 1 infection. Clin. Diagn. Lab. Immunol. 9, 983–986.

Torrelles, J.B., Azad, A.K., Henning, L.N., Carlson, T.K., Schlesinger, L.S., 2008. Role of C-type lectins in mycobacterial infections. Curr. Drug Targets 9, 102–112.

Torrelles, J.B., Azad, A.K., Schlesinger, L.S., 2006. Fine discrimination in the recognition of individual species of phosphatidyl-myo-inositol mannosides from Mycobacterium tuberculosis by C-type lectin pattern recognition receptors. J. Immunol. Baltim. Md 1950 177, 1805–1816.

Towers, G.J., Noursadeghi, M., 2014. Interactions between HIV-1 and the Cell-Autonomous Innate Immune System. Cell Host Microbe 16, 10–18. doi:10.1016/j.chom.2014.06.009

Tran, H.T.T., Van den Bergh, R., Loembé, M.M., Worodria, W., Mayanja-Kizza, H., Colebunders, R., Mascart, F., Stordeur, P., Kestens, L., De Baetselier, P., Raes, G., TB-IRIS study group, 2013. Modulation of the complement system in monocytes contributes to tuberculosis-associated immune reconstitution inflammatory syndrome. AIDS Lond. Engl. 27, 1725–1734. doi:10.1097/QAD.0b013e328361648b

Trapani, J.A., Dawson, M., Apostolidis, V.A., Browne, K.A., 1994. Genomic organization of IFI16, an interferon-inducible gene whose expression is associated with human myeloid cell differentiation: correlation of predicted protein domains with exon organization. Immunogenetics 40, 415–424.

Trentin, L., Garbisa, S., Zambello, R., Agostini, C., Caenazzo, C., Di Francesco, C., Cipriani, A., Francavilla, E., Semenzato, G., 1992. Spontaneous production of interleukin-6 by alveolar macrophages from human immunodeficiency virus type 1-infected patients. J. Infect. Dis. 166, 731–737.

Trifari, S., Kaplan, C.D., Tran, E.H., Crellin, N.K., Spits, H., 2009. Identification of a human helper T cell population that has abundant production of interleukin 22 and is distinct from TH-17, TH1 and TH2 cells. Nat. Immunol. 10, 864–871. doi:10.1038/ni.1770

Trunz, B.B., Fine, P., Dye, C., 2006. Effect of BCG vaccination on childhood tuberculous meningitis and miliary tuberculosis worldwide: a meta-analysis and assessment of cost-effectiveness. Lancet 367, 1173–1180. doi:10.1016/S0140-6736(06)68507-3

Tsai, C.-A., Chen, J.J., 2009. Multivariate analysis of variance test for gene set analysis. Bioinformatics 25, 897–903. doi:10.1093/bioinformatics/btp098

Tsang, J., Chain, B.M., Miller, R.F., Webb, B.L.J., Barclay, W., Towers, G.J., Katz, D.R., Noursadeghi, M., 2009. HIV-1 infection of macrophages is dependent on evasion of innate immune cellular activation. AIDS Lond. Engl. 23, 2255–2263. doi:10.1097/QAD.0b013e328331a4ce

Turner, J., Gonzalez-Juarrero, M., Ellis, D.L., Basaraba, R.J., Kipnis, A., Orme, I.M., Cooper, A.M., 2002. In vivo IL-10 production reactivates chronic pulmonary tuberculosis in C57BL/6 mice. J. Immunol. Baltim. Md 1950 169, 6343–6351.

Tuttle, D.L., Harrison, J.K., Anders, C., Sleasman, J.W., Goodenow, M.M., 1998. Expression of CCR5 increases during monocyte differentiation and directly mediates macrophage susceptibility to infection by human immunodeficiency virus type 1. J. Virol. 72, 4962–4969.

Uhlin, M., Andersson, J., Zumla, A., Maeurer, M., 2012. Adjunct Immunotherapies for Tuberculosis. J. Infect. Dis. jis197. doi:10.1093/infdis/jis197

Ulrichs, T., Kaufmann, S.H.E., 2006. New insights into the function of granulomas in human tuberculosis. J. Pathol. 208, 261–269. doi:10.1002/path.1906

UNAIDS, 2013. 2013 UNAIDS Report on the global AIDS epidemic.

Unanue, E.R., 1976. Secretory function of mononuclear phagocytes: a review. Am. J. Pathol. 83, 396–418.

Underhill, D.M., Ozinsky, A., 2002. Phagocytosis of microbes: complexity in action. Annu. Rev. Immunol. 20, 825–852. doi:10.1146/annurev.immunol.20.103001.114744

Underhill, D.M., Ozinsky, A., Hajjar, A.M., Stevens, A., Wilson, C.B., Bassetti, M., Aderem, A., 1999. The Toll-like receptor 2 is recruited to macrophage phagosomes and discriminates between pathogens. Nature 401, 811–815. doi:10.1038/44605

Van Furth, R., Cohn, Z.A., 1968. The origin and kinetics of mononuclear phagocytes. J. Exp. Med. 128, 415–435.

Van Furth, R., Cohn, Z.A., Hirsch, J.G., Humphrey, J.H., Spector, W.G., Langevoort, H.L., 1972. The mononuclear phagocyte system: a new classification of macrophages, monocytes, and their precursor cells. Bull. World Health Organ. 46, 845–852.

Varol, C., Landsman, L., Fogg, D.K., Greenshtein, L., Gildor, B., Margalit, R., Kalchenko, V., Geissmann, F., Jung, S., 2007. Monocytes give rise to mucosal, but not splenic, conventional dendritic cells. J. Exp. Med. 204, 171–180. doi:10.1084/jem.20061011

Vecchiarelli, A., Dottorini, M., Pietrella, D., Monari, C., Retini, C., Todisco, T., Bistoni, F., 1994. Role of human alveolar macrophages as antigen-presenting cells in Cryptococcus neoformans infection. Am. J. Respir. Cell Mol. Biol. 11, 130–137.

Vecchiarelli, A., Retini, C., Monari, C., Tascini, C., Bistoni, F., Kozel, T.R., 1996. Purified capsular polysaccharide of Cryptococcus neoformans induces interleukin-10 secretion by human monocytes. Infect. Immun. 64, 2846–2849.

Vecchiarelli, A., Retini, C., Pietrella, D., Monari, C., Tascini, C., Beccari, T., Kozel, T.R., 1995. Downregulation by cryptococcal polysaccharide of tumor necrosis factor alpha and interleukin-1 beta secretion from human monocytes. Infect. Immun. 63, 2919–2923.

Veldhoen, M., Uyttenhove, C., van Snick, J., Helmby, H., Westendorf, A., Buer, J., Martin, B., Wilhelm, C., Stockinger, B., 2008. Transforming growth factor-[beta] "reprograms" the differentiation of T helper 2 cells and promotes an interleukin 9-producing subset. Nat Immunol 9, 1341–1346. doi:10.1038/ni.1659

Velmurugan, K., Chen, B., Miller, J.L., Azogue, S., Gurses, S., Hsu, T., Glickman, M., Jacobs, W.R., Porcelli, S.A., Briken, V., 2007. Mycobacterium tuberculosis nuoG is a virulence gene that inhibits apoptosis of infected host cells. PLoS Pathog. 3, e110. doi:10.1371/journal.ppat.0030110

Verver, S., Warren, R.M., Munch, Z., Vynnycky, E., van Helden, P.D., Richardson, M., van der Spuy, G.D., Enarson, D.A., Borgdorff, M.W., Behr, M.A., Beyers, N., 2004. Transmission of tuberculosis in a high incidence urban community in South Africa. Int. J. Epidemiol. 33, 351–357. doi:10.1093/ije/dyh021

Vigerust, D.J., Egan, B.S., Shepherd, V.L., 2005. HIV-1 Nef mediates post-translational down-regulation and redistribution of the mannose receptor. J. Leukoc. Biol. 77, 522–534. doi:10.1189/jlb.0804454

Villagra, A., Cheng, F., Wang, H.-W., Suarez, I., Glozak, M., Maurin, M., Nguyen, D., Wright, K.L., Atadja, P.W., Bhalla, K., Pinilla-Ibarz, J., Seto, E., Sotomayor, E.M., 2009. The histone deacetylase HDAC11 regulates the expression of interleukin 10 and immune tolerance. Nat. Immunol. 10, 92–100. doi:10.1038/ni.1673

Voehringer, D., Shinkai, K., Locksley, R.M., 2004. Type 2 immunity reflects orchestrated recruitment of cells committed to IL-4 production. Immunity 20, 267–277.

Von Reyn, C.F., Kimambo, S., Mtei, L., Arbeit, R.D., Maro, I., Bakari, M., Matee, M., Lahey, T., Adams, L.V., Black, W., Mackenzie, T., Lyimo, J., Tvaroha, S., Waddell, R., Kreiswirth, B., Horsburgh, C.R., Pallangyo, K., 2011. Disseminated tuberculosis in human immunodeficiency virus infection: ineffective immunity, polyclonal disease and high mortality. Int. J. Tuberc. Lung Dis. Off. J. Int. Union Tuberc. Lung Dis. 15, 1087–1092. doi:10.5588/ijtld.10.0517

Wain-Hobson, S., Sonigo, P., Danos, O., Cole, S., Alizon, M., 1985. Nucleotide sequence of the AIDS virus, LAV. Cell 40, 9–17.

Wajant, H., Pfizenmaier, K., Scheurich, P., 2003. Tumor necrosis factor signaling. Cell Death Differ. 10, 45–65. doi:10.1038/sj.cdd.4401189

Wakeham, J., Wang, J., Magram, J., Croitoru, K., Harkness, R., Dunn, P., Zganiacz, A., Xing, Z., 1998. Lack of both types 1 and 2 cytokines, tissue inflammatory responses, and immune protection during pulmonary infection by Mycobacterium bovis bacille Calmette-Guérin in IL-12-deficient mice. J. Immunol. Baltim. Md 1950 160, 6101–6111.

Walenkamp, A.M., Chaka, W.S., Verheul, A.F., Vaishnav, V.V., Cherniak, R., Coenjaerts, F.E., Hoepelman, I.M., 1999. Cryptococcus neoformans and its cell wall components induce similar cytokine profiles in human peripheral blood mononuclear cells despite differences in structure. FEMS Immunol. Med. Microbiol. 26, 309–318.

Walker, N.F., Clark, S.O., Oni, T., Andreu, N., Tezera, L., Singh, S., Saraiva, L., Pedersen, B., Kelly, D.L., Tree, J.A., D'Armiento, J.M., Meintjes, G., Mauri, F.A., Williams, A., Wilkinson, R.J., Friedland, J.S., Elkington, P.T., 2012. Doxycycline and HIV infection suppress tuberculosis-induced matrix metalloproteinases. Am. J. Respir. Crit. Care Med. 185, 989–997. doi:10.1164/rccm.201110-1769OC

Walker, N.F., Meintjes, G., Wilkinson, R.J., 2013. HIV-1 and the immune response to TB. Future Virol. 8, 57–80. doi:10.2217/fvl.12.123

Wang, Y., Rice, A.P., 2006. Interleukin-10 inhibits HIV-1 LTR-directed gene expression in human macrophages through the induction of cyclin T1 proteolysis. Virology 352, 485–492. doi:10.1016/j.virol.2006.05.013

Wang, Y., Szretter, K.J., Vermi, W., Gilfillan, S., Rossini, C., Cella, M., Barrow, A.D., Diamond, M.S., Colonna, M., 2012. IL-34 is a tissue-restricted ligand of CSF1R required for the development of Langerhans cells and microglia. Nat. Immunol. 13, 753–760. doi:10.1038/ni.2360

Weber-Nordt, R.M., Meraz, M.A., Schreiber, R.D., 1994. Lipopolysaccharide-dependent induction of IL-10 receptor expression on murine fibroblasts. J. Immunol. Baltim. Md 1950 153, 3734–3744.

Weber-Nordt, R.M., Riley, J.K., Greenlund, A.C., Moore, K.W., Darnell, J.E., Schreiber, R.D., 1996. Stat3 Recruitment by Two Distinct Ligand-induced, Tyrosine-phosphorylated Docking Sites in the Interleukin-10 Receptor Intracellular Domain. J. Biol. Chem. 271, 27954–27961. doi:10.1074/jbc.271.44.27954

Wehle, K., Schirmer, M., Dünnebacke-Hinz, J., Küpper, T., Pfitzer, P., 1993. Quantitative differences in phagocytosis and degradation of Pneumocystis carinii by alveolar macrophages in AIDS and non-HIV patients in vivo. Cytopathol. Off. J. Br. Soc. Clin. Cytol. 4, 231–236.

Weichhart, T., Costantino, G., Poglitsch, M., Rosner, M., Zeyda, M., Stuhlmeier, K.M., Kolbe, T., Stulnig, T.M., Hörl, W.H., Hengstschläger, M., Müller, M., Säemann, M.D., 2008. The TSC-mTOR signaling pathway regulates the innate inflammatory response. Immunity 29, 565–577. doi:10.1016/j.immuni.2008.08.012

Weichhart, T., Säemann, M.D., 2008. The PI3K/Akt/mTOR pathway in innate immune cells: emerging therapeutic applications. Ann. Rheum. Dis. 67, iii70–iii74. doi:10.1136/ard.2008.098459

Weiden, M., Tanaka, N., Qiao, Y., Zhao, B.Y., Honda, Y., Nakata, K., Canova, A., Levy, D.E., Rom, W.N., Pine, R., 2000. Differentiation of Monocytes to Macrophages Switches the Mycobacterium tuberculosis Effect on HIV-1 Replication from Stimulation to Inhibition: Modulation of Interferon Response and CCAAT/Enhancer Binding Protein ß Expression. J. Immunol. 165, 2028 –2039.

Wessells, J., Baer, M., Young, H.A., Claudio, E., Brown, K., Siebenlist, U., Johnson, P.F., 2004. BCL-3 and NF-kappaB p50 attenuate lipopolysaccharide-induced inflammatory responses in macrophages. J. Biol. Chem. 279, 49995–50003. doi:10.1074/jbc.M404246200

West, A.P., Brodsky, I.E., Rahner, C., Woo, D.K., Erdjument-Bromage, H., Tempst, P., Walsh, M.C., Choi, Y., Shadel, G.S., Ghosh, S., 2011. TLR signalling augments macrophage bactericidal activity through mitochondrial ROS. Nature 472, 476–480. doi:10.1038/nature09973

Westphalen, K., Gusarova, G.A., Islam, M.N., Subramanian, M., Cohen, T.S., Prince, A.S., Bhattacharya, J., 2014. Sessile alveolar macrophages communicate with alveolar epithelium to modulate immunity. Nature advance online publication. doi:10.1038/nature12902

WHO, 2013a. WHO | Consolidated guidelines on the use of antiretroviral drugs for treating and preventing HIV infection.

WHO, 2013b. Global tuberculosis report 2013.

Williams, L., Bradley, L., Smith, A., Foxwell, B., 2004. Signal transducer and activator of transcription 3 is the dominant mediator of the anti-inflammatory effects of IL-10 in human macrophages. J. Immunol. Baltim. Md 1950 172, 567–576.

Williams, L., Jarai, G., Smith, A., Finan, P., 2002. IL-10 expression profiling in human monocytes. J. Leukoc. Biol. 72, 800–809.

Williams, L.M., Sarma, U., Willets, K., Smallie, T., Brennan, F., Foxwell, B.M.J., 2007. Expression of constitutively active STAT3 can replicate the cytokine-suppressive activity of interleukin-10 in human primary macrophages. J. Biol. Chem. 282, 6965–6975. doi:10.1074/jbc.M609101200

Williams, S.A., Chen, L.-F., Kwon, H., Fenard, D., Bisgrove, D., Verdin, E., Greene, W.C., 2004. Prostratin antagonizes HIV latency by activating NF-kappaB. J. Biol. Chem. 279, 42008–42017. doi:10.1074/jbc.M402124200

Williams, S.A., Kwon, H., Chen, L.-F., Greene, W.C., 2007. Sustained induction of NF-kappa B is required for efficient expression of latent human immunodeficiency virus type 1. J. Virol. 81, 6043–6056. doi:10.1128/JVI.02074-06

Wing, E.J., Remington, J.S., 1977. Cell-mediated immunity and its role in resistance to infection. West. J. Med. 126, 14–31.

Witmer-Pack, M.D., Hughes, D.A., Schuler, G., Lawson, L., McWilliam, A., Inaba, K., Steinman, R.M., Gordon, S., 1993. Identification of macrophages and dendritic cells in the osteopetrotic (op/op) mouse. J. Cell Sci. 104 (Pt 4), 1021–1029.

Wolf, D., Witte, V., Laffert, B., Blume, K., Stromer, E., Trapp, S., Paola, Schürmann, A., Baur, A.S., 2001. HIV-1 Nef associated PAK and PI3-Kinases stimulate Akt-independent Bad-phosphorylation to induce anti-apoptotic signals. Nat. Med. 7, 1217–1224. doi:10.1038/nm1101-1217

Wolk, K., Kunz, S., Witte, E., Friedrich, M., Asadullah, K., Sabat, R., 2004. IL-22 Increases the Innate Immunity of Tissues. Immunity 21, 241–254. doi:10.1016/j.immuni.2004.07.007

Wynn, T.A., Chawla, A., Pollard, J.W., 2013. Macrophage biology in development, homeostasis and disease. Nature 496, 445–455. doi:10.1038/nature12034

Wynn, T.A., Ramalingam, T.R., 2012. Mechanisms of fibrosis: therapeutic translation for fibrotic disease. Nat. Med. 18, 1028–1040. doi:10.1038/nm.2807

Xie, N., Cui, H., Banerjee, S., Tan, Z., Salomao, R., Fu, M., Abraham, E., Thannickal, V.J., Liu, G., 2014. miR-27a Regulates Inflammatory Response of Macrophages by Targeting IL-10. J. Immunol. Baltim. Md 1950. doi:10.4049/jimmunol.1400203

Xue, J., Schmidt, S.V., Sander, J., Draffehn, A., Krebs, W., Quester, I., De Nardo, D., Gohel, T.D., Emde, M., Schmidleithner, L., Ganesan, H., Nino-Castro, A., Mallmann, M.R., Labzin, L., Theis, H., Kraut, M., Beyer, M., Latz, E., Freeman, T.C., Ulas, T., Schultze, J.L., 2014. Transcriptome-Based Network Analysis Reveals a Spectrum Model of Human Macrophage Activation. Immunity 40, 274–288. doi:10.1016/j.immuni.2014.01.006

Yadav, M., Schorey, J.S., 2006. The beta-glucan receptor dectin-1 functions together with TLR2 to mediate macrophage activation by mycobacteria. Blood 108, 3168–3175. doi:10.1182/blood-2006-05-024406

Yasukawa, H., Ohishi, M., Mori, H., Murakami, M., Chinen, T., Aki, D., Hanada, T., Takeda, K., Akira, S., Hoshijima, M., Hirano, T., Chien, K.R., Yoshimura, A., 2003. IL-6 induces an anti-inflammatory response in the absence of SOCS3 in macrophages. Nat. Immunol. 4, 551–556. doi:10.1038/ni938

Yauch, L.E., Mansour, M.K., Shoham, S., Rottman, J.B., Levitz, S.M., 2004. Involvement of CD14, toll-like receptors 2 and 4, and MyD88 in the host response to the fungal pathogen Cryptococcus neoformans in vivo. Infect. Immun. 72, 5373–5382. doi:10.1128/IAI.72.9.5373-5382.2004

Yi, A.-K., Yoon, J.-G., Yeo, S.-J., Hong, S.-C., English, B.K., Krieg, A.M., 2002. Role of mitogen-activated protein kinases in CpG DNA-mediated IL-10 and IL-12 production: central role of extracellular signal-regulated kinase in the negative feedback loop of the CpG DNA-mediated Th1 response. J. Immunol. Baltim. Md 1950 168, 4711–4720.

Yona, S., Kim, K.-W., Wolf, Y., Mildner, A., Varol, D., Breker, M., Strauss-Ayali, D., Viukov, S., Guilliams, M., Misharin, A., Hume, D.A., Perlman, H., Malissen, B., Zelzer, E., Jung, S., 2013. Fate mapping reveals origins and dynamics of monocytes and tissue macrophages under homeostasis. Immunity 38, 79–91. doi:10.1016/j.immuni.2012.12.001

Zaragoza, O., Rodrigues, M.L., De Jesus, M., Frases, S., Dadachova, E., Casadevall, A., 2009. The capsule of the fungal pathogen Cryptococcus neoformans. Adv. Appl. Microbiol. 68, 133–216. doi:10.1016/S0065-2164(09)01204-0

Zhang, M., Gong, J., Iyer, D.V., Jones, B.E., Modlin, R.L., Barnes, P.F., 1994. T cell cytokine responses in persons with tuberculosis and human immunodeficiency virus infection. J. Clin. Invest. 94, 2435–2442. doi:10.1172/JCI117611

Zhou, J.H., Broussard, S.R., Strle, K., Freund, G.G., Johnson, R.W., Dantzer, R., Kelley, K.W., 2001. IL-10 inhibits apoptosis of promyeloid cells by activating insulin receptor substrate-2 and phosphatidylinositol 3'-kinase. J. Immunol. Baltim. Md 1950 167, 4436–4442.

Zhu, T., Mo, H., Wang, N., Nam, D.S., Cao, Y., Koup, R.A., Ho, D.D., 1993. Genotypic and phenotypic characterization of HIV-1 patients with primary infection. Science 261, 1179–1181.

Ziegler-Heitbrock, L., Ancuta, P., Crowe, S., Dalod, M., Grau, V., Hart, D.N., Leenen, P.J.M., Liu, Y.-J., MacPherson, G., Randolph, G.J., Scherberich, J., Schmitz, J., Shortman, K., Sozzani, S., Strobl, H., Zembala, M., Austyn, J.M., Lutz, M.B., 2010. Nomenclature of monocytes and dendritic cells in blood. Blood 116, e74–80. doi:10.1182/blood-2010-02-258558

Zigmond, E., Bernshtein, B., Friedlander, G., Walker, C.R., Yona, S., Kim, K.-W., Brenner, O., Krauthgamer, R., Varol, C., Müller, W., Jung, S., 2014. Macrophage-Restricted Interleukin-10 Receptor Deficiency, but Not IL-10 Deficiency, Causes Severe Spontaneous Colitis. Immunity 40, 720–733. doi:10.1016/j.immuni.2014.03.012

Zigmond, E., Jung, S., 2013. Intestinal macrophages: well educated exceptions from the rule. Trends Immunol. 34, 162–168. doi:10.1016/j.it.2013.02.001

Zink, A.R., Sola, C., Reischl, U., Grabner, W., Rastogi, N., Wolf, H., Nerlich, A.G., 2003. Characterization of Mycobacterium tuberculosis complex DNAs from Egyptian mummies by spoligotyping. J. Clin. Microbiol. 41, 359–367.

Zinsser, H., 1921. Studies on the Tuberculin Reaction and on Specific Hypersensitiveness in Bacterial Infection. J. Exp. Med. 34, 495–524. doi:10.1084/jem.34.5.495

Zizzo, G., Cohen, P.L., 2013. IL-17 Stimulates Differentiation of Human Anti-Inflammatory Macrophages and Phagocytosis of Apoptotic Neutrophils in Response to IL-10 and Glucocorticoids. J. Immunol. Baltim. Md 1950. doi:10.4049/jimmunol.1203017

Zufferey, R., Nagy, D., Mandel, R.J., Naldini, L., Trono, D., 1997. Multiply attenuated lentiviral vector achieves efficient gene delivery in vivo. Nat. Biotechnol. 23, 871–875.

Zumla, A., Raviglione, M., Hafner, R., Fordham von Reyn, C., 2013. Tuberculosis. N. Engl. J. Med. 368, 745–755. doi:10.1056/NEJMra1200894